ANNUAL REPORTS ON NMR SPECTROSCOPY

Volume 13

ANNUAL REPORTS ON

NMR SPECTROSCOPY

This Page Intentionally Left Blank

ANNUAL REPORTS ON
NMR SPECTROSCOPY

Edited by

G. A. WEBB

Department of Chemistry, University of Surrey, Guildford, Surrey, England

VOLUME 13

1982

ACADEMIC PRESS

A Subsidiary of Harcourt Brace Jovanovich, Publishers

London New York
Paris San Diego San Francisco São Paulo
Sydney Tokyo Toronto

ACADEMIC PRESS INC. (LONDON) LTD.
24–28 Oval Road,
London, NW1 7DX

U.S. Edition Published by

ACADEMIC PRESS INC.
111 Fifth Avenue
New York, New York 10003

British Library Cataloguing in Publication Data

Annual reports on NMR spectroscopy.—13
1. Nuclear magnetic resonance spectroscopy
541.2'8 QD96.N8

ISBN 0-12-505313-4
ISSN 0066-4103

Printed in Great Britain by J. W. Arrowsmith Ltd.
Bristol BS3 2NT

LIST OF CONTRIBUTORS

K. BOCK, *Department of Organic Chemistry, The Technical University of Denmark, DK-2800 Lyngby, Denmark.*

R. T. BOERÉ, *Department of Chemistry, The University of Western Ontario, London, Ontario, Canada.*

R. W. BRIGGS, *Department of Chemistry, University of Arkansas, Fayetteville, Arkansas 72701, USA.*

T. A. CRABB, *Department of Chemistry, Portsmouth Polytechnic, Portsmouth, Hampshire PO1 3QL, UK.*

J. F. HINTON, *Department of Chemistry, University of Arkansas, Fayetteville, Arkansas 72701, USA.*

R. G. KIDD, *Department of Chemistry, The University of Western Ontario, London, Ontario, Canada.*

K. R. METZ, *Department of Chemistry, University of Arkansas, Fayetteville, Arkansas 72701, USA.*

H. THØGERSON, *Department of Organic Chemistry, The Technical University of Denmark, DK-2800 Lyngby, Denmark.*

This Page Intentionally Left Blank

PREFACE

The continuing growth of the use of NMR spectroscopy in chemistry is clearly reflected both in the disparate nature of the areas covered in Volume 13 of Annual Reports and in the amount of information contained in each report presented.

Drs Bock and Thøgerson have reviewed the NMR of carbohydrates which is an area showing considerable expansion since it was last reviewed in Volume 5A. Recent developments in the NMR of alkaloids are covered by Professor Crabb who builds on his previous reports in Volumes 6A and 8. For the first time in this series I am happy to include reports from Professor Hinton and Drs Metz and Briggs on Thallium NMR, and from Professor Kidd and Dr Boeré on rotational correlation times in nuclear magnetic relaxation.

It is a pleasure to be able to express my thanks to all of the contributors for the careful preparation, and prompt submission, of their manuscripts. These efforts, in no small way, facilitate the continuing success of Annual Reports on NMR Spectroscopy.

University of Surrey,
Guildford, Surrey,
England

G. A. WEBB
March 1982

This Page Intentionally Left Blank

CONTENTS

Nuclear Magnetic Resonance Spectroscopy in the Study of Mono- and Oligosaccharides

KLAUS BOCK AND HENNING THØGERSON

Nuclear Magnetic Resonance of Alkaloids

TREVOR A. CRABB

Thallium NMR Spectroscopy

J. F. HINTON, K. R. METZ AND R. W. BRIGGS

Rotational Correlation Times in Nuclear Magnetic Relaxation

RENÉ T. BOERÉ AND R. GARTH KIDD

Nuclear Magnetic Resonance Spectroscopy in the Study of Mono- and Oligosaccharides

KLAUS BOCK AND HENNING THØGERSEN

Department of Organic Chemistry, The Technical University of Denmark, DK-2800 Lyngby, Denmark

I. INTRODUCTION

Since this subject was last reviewed in this series[1] the importance of NMR spectroscopy in the study of carbohydrates has increased tremendously. This has occurred primarily because the introduction of pulsed Fourier transform (FT) NMR spectrometers has made the measurement of ^{13}C NMR spectral parameters easy, which is particularly important for the study of carbohydrates in aqueous solutions. Furthermore, pulsed NMR instruments have increased the sensitivity of ^{1}H NMR spectra by several orders of magnitude and facilitated the measurement of relaxation times and nuclear Overhauser enhancement (NOE) factors. Computer control of the spectrometers has made new experiments possible such as two-dimensional NMR spectra, and simplified other experiments. Magnet technology has improved and 500 MHz ^{1}H NMR spectrometers are commercially available with the associated high dispersion and sensitivity, and today multinuclear spectrometers are routine tools in many chemical laboratories.

This review covers the period 1973–1980, particularly the last part of the period. It is primarily concerned with a description of how to assign NMR parameters and how to use these values in the study of carbohydrates. Special emphasis is given to the ^{1}H NMR parameters because the application of ^{13}C NMR spectroscopy in the study of monosaccharides and oligo- and polysaccharides has recently been reviewed.[2–5]

The NMR parameters of nucleotides, nucleosides and aminoglycoside antibiotics are not discussed in the present review. The NMR parameters of the former compounds have been discussed extensively in a recent review.[6]

No attempt has been made to cover all applications in which NMR data have been used to establish carbohydrate structures or to study carbohydrates in solution. The yearly reports from The Chemical Society on carbohydrate chemistry[7] and nuclear magnetic resonance spectroscopy[8] are excellent references in this respect. Several general reviews on NMR spectroscopy of carbohydrates have appeared during the period.[9–11] A

description of how NMR parameters are obtained is beyond the scope of the present review, but readers are referred to general monographs.[12–15]

II. ASSIGNMENT TECHNIQUES

The assignment of the NMR signals is a necessary prerequisite for the application of NMR spectroscopy in structural investigations of carbohydrates. Since assignment techniques have been described in many reviews and monographs (e.g. references 12, 13), special emphasis is given to the problems associated with the assignment of signals in the NMR spectra of carbohydrates and their derivatives. The assignment techniques for ^{1}H NMR data and ^{13}C NMR data are described separately.

A. ^{1}H NMR assignments

The following points will be discussed:

1. Comparison with model compounds
2. Isotopic substitution
3. Double resonance experiments
4. Relaxation experiments
5. Two-dimensional spectroscopy
6. Paramagnetic shift reagents
7. Protonation shifts
8. Miscellaneous

1. Comparison with model compounds

With modern high field NMR spectrometers the ^{1}H NMR spectra of most monosaccharides can be analysed on a first-order basis. Mutarotated mixtures of carbohydrates in aqueous (D_2O) solutions give well resolved spectra when measured on a high field spectrometer.

The ^{1}H chemical shifts and coupling constants for the most predominant anomers of aldohexoses and aldopentoses and the corresponding methylglycosides together with those of the most common methyldeoxyhexopyranosides and methyl-2-acetamido-2-deoxyhexopyranosides are given in Section IV. Assignment techniques based on comparison with model compounds are important when analysing spectra of complex oligosaccharides.[16,17] Difficulties will often arise because the protons are located at the surface of the molecules (in contrast to the ^{13}C nuclei) making interunit shielding and deshielding effects important.[18]

De Bruyn, Ānteunis and coworkers have in a series of papers[19–26] described the 300 MHz ^{1}H NMR spectra in D_2O of a series of mono- and oligosaccharides. They conclude that shift increments can be used in the

identification of individual proton resonances and to assess the position of glycosidic linkages.

The chemical shifts of protected carbohydrate derivatives (e.g. acetates) have been discussed in previous reviews[9–11] and follow the general rules for ^{1}H NMR chemical shifts.[27] The chemical shifts of common protecting groups used in carbohydrate chemistry are given in reference 11.

When comparing ^{1}H chemical shifts with literature data it is important, particularly in aqueous solutions, to measure the spectra at the same temperature and in the same solvent.

2. *Isotopic substitution*

If the molecules of interest contains spin $\frac{1}{2}$ nuclei other than protons (e.g. ^{19}F, ^{31}P or ^{13}C (enriched)) heteronuclear spin–spin couplings will appear in the ^{1}H NMR spectrum. This can be valuable in the assignment of the proton spectra, particularly if heteronuclear decoupling facilities are available. A recent review has discussed results obtained for fluorinated carbohydrate derivatives.[28]

Deuterium substitution in carbohydrates causes the substituted proton to disappear in the ^{1}H NMR spectrum and also reduces the spin–spin couplings by approximately a factor of six. The result of this substitution is generally that spin–spin couplings, to all neighbouring protons from the site where the deuterium substitution has taken place, are removed. The reduced couplings can of course be removed by deuterium decoupling.

Figure 1 shows the ^{1}H NMR spectrum of octa-*O*-acetyl-*β*-D-gentiobiose together with two deuterated derivatives which clearly illustrates the points discussed above.

Protons which are neighbouring to the substituted site will in addition to the reduction of spin–spin couplings also experience an isotope effect and resonate at lower frequencies, as demonstrated recently.[29] The preparation of deuterated derivatives normally requires several more or less laborious synthetic steps,[30] but a convenient method for the preparation of glycosides labelled with deuterium on hydroxy-bearing carbon atoms has recently been developed as described in Section II.B.2.

3. *Double resonance experiments*

(a) *Homonuclear decoupling* (^1H–$\{^1H\}$ *experiments*). Homonuclear decoupling is probably the single most widely used experiment to assist in the assignment of proton spectra. With computer-controlled FT instruments this experiment can be performed in the difference mode, as described by Gibbons *et al.*,[31] and applied in the analysis of the spectra of oligosaccharides.[17]

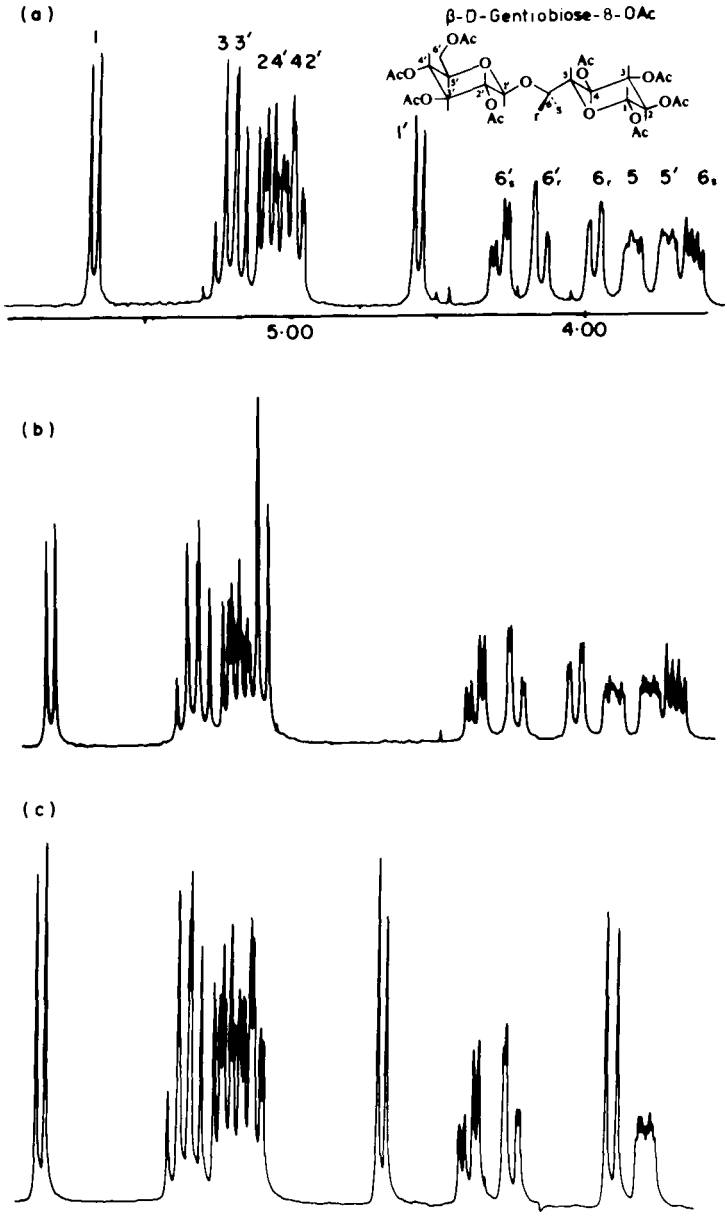

FIG. 1. Partial ^{1}H 270 MHz spectrum of octa-*O*-acetyl-*β*-D-gentiobiose and deuterated derivatives in deuteriochloroform. (a) Spectrum of normal compound. (b) Spectrum of [1′-^{2}H] derivative. (c) Spectrum of [6$_r$,6$_s$-^{2}H$_2$] derivative.

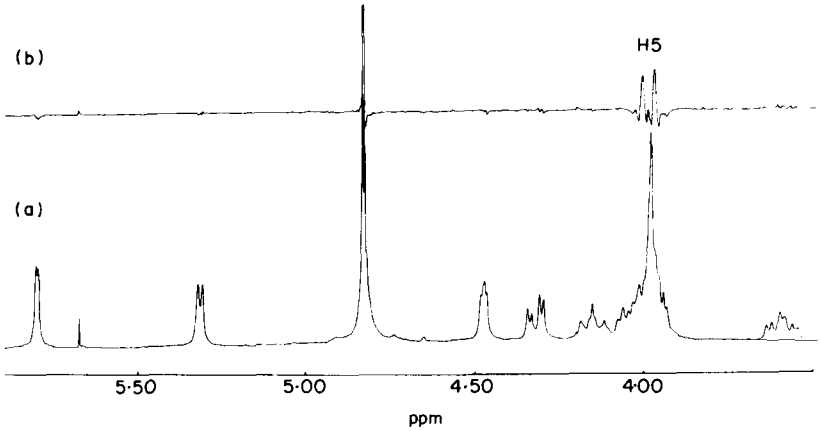

FIG. 2. Partial 270 MHz ^{1}H spectrum of *p*-trifluoroacetamidophenyl-3-*O*-(3,6-dideoxy-α-D-*ribo*-hexopyranosyl)-α-D-mannopyranoside in D_2O at 310 K. (a) Normal spectrum. (b) Difference decoupling experiment with saturation of the H-6 resonances at 1·2 ppm. The chemical shift of H-5 is easily determined from the experiment and it is also seen that H-5 and H-4 are spin–spin coupled with a large coupling constant (10 Hz).

This is illustrated in Fig. 2 which shows how this technique makes it possible to obtain both chemical shift and coupling information from a "hidden resonance".

The only limitation to this experiment is that Block–Siegert shifts are induced when the chemical shift difference between the saturated proton(s) and the observed proton(s) becomes too small. This makes it more difficult to interpret the difference spectrum.

A recent version of a multi-homodecoupling experiment, the two-dimensional scalar coupling experiment (SECSY), has been developed by Ernst *et al.*[32]

In this experiment the data points are collected in a data matrix as a function of t_1 and t_2, where t_1 and t_2 are the times in a $90°-t_1-90°-\mathrm{FID}(t_2)$ pulse sequence. The data are then Fourier-transformed with respect to both directions in the data matrix. The results can then be displayed as shown in reference 33. A modification of the pulse sequence, i.e. $90°-t_1-90°-t_1-\mathrm{FID}(t_2)$, where the half echo is sampled, results after data manipulation in a spectrum, as shown in Fig. 3.

Figure 3 shows the SECSY experiment at 400 MHz of a disaccharide, methyl-2-*O*-(α-D-mannopyranosyl)-α-D-mannopyranoside. Figure 3(b) shows the two-dimensional scalar coupled spectrum as a contour diagram with the normal spectrum appearing along the horizontal line in the middle. Resonances which are spin–spin coupled give rise to signals off this line and are connected by parallel lines (as shown in Fig. 3(b)), i.e. the high

frequency H-1 is spin–spin coupled to H-2 resonating at 3·85 ppm and H-1 resonating at 4·90 ppm is spin–spin coupled to H-2 resonating at 3·95 ppm. This is a very powerful experiment in the analysis of the spectra of complex oligosaccharides and makes it possible to perform "homodecoupling" experiments without the use of a homodecoupler, i.e. avoiding the problems with off-resonance effects and other difficulties associated with this experiment. The disadvantage is that the experiment is rather time consuming in acquisition, processing and plotting time and normally requires *c.* 20 h of instrument time.

(b) *INDOR experiments.* INDOR experiments[34] have been used extensively in the spectral analysis of carbohydrate derivatives in continous wave experiments.[20–26] It is also possible to perform these experiments on FT instruments[35] by applying selective pulses[36] to the resonance lines. An example of the application of this technique in the analysis of the ^{1}H NMR spectrum of methylhepta-*O*-acetyl-*β*-D-cellobioside is shown in Fig. 4 using the difference technique. In order to obtain good results it is important to have a very stable magnetic field, which may be obtained with a superconducting magnet.

(c) *Nuclear Overhauser experiments.* Nuclear Overhauser experiments[37,38] have become a useful tool in the assignment of ^{1}H NMR spectra of complex oligosaccharides,[16,18,39,40] particularly when performed in the difference mode.[41] In Fig. 5 is shown the result of saturation of H-1 in methylhepta-*O*-acetyl-*β*-D-cellobioside. Protons H-3′ and H-5′ have their signals enhanced because of the 1–3 diaxial relationship to H-1′; also H-4 is enhanced due to its closeness in space to H-1′ in the preferred conformation of the oligosaccharide. H-6b is also enhanced because H-6a has the same chemical shift as H-1. H-4′ experiences a negative NOE because it is very strongly relaxed by H-5′, H-3′ and H-2′, all of which are relaxed by the saturated H-1′. This second-order effect has been discussed in detail by Noggle and Schirmer.[37]

The numerical values of the enhancements can furthermore be used in a conformational analysis of oligosaccharides.[40] However, the NOE values are dependent not only on the correlation times of the molecules (T_c) (i.e. dependent on the size of the molecule, the viscosity of the solution and the temperature) but also on the applied magnetic field strength, as shown in Fig. 6. For a 0·1 M sample of a heptasaccharide in D_2O at 300 K the NOE values are zero for some atoms at 400 MHz, but positive at, for example, 270 MHz. Larger molecules, i.e. polysaccharides, may show negative enhancements, as illustrated in Fig. 7.

For larger molecules spin diffusion[42] may be a problem and the transient method[43] may be preferred. Alternatively, a two-dimensional FT

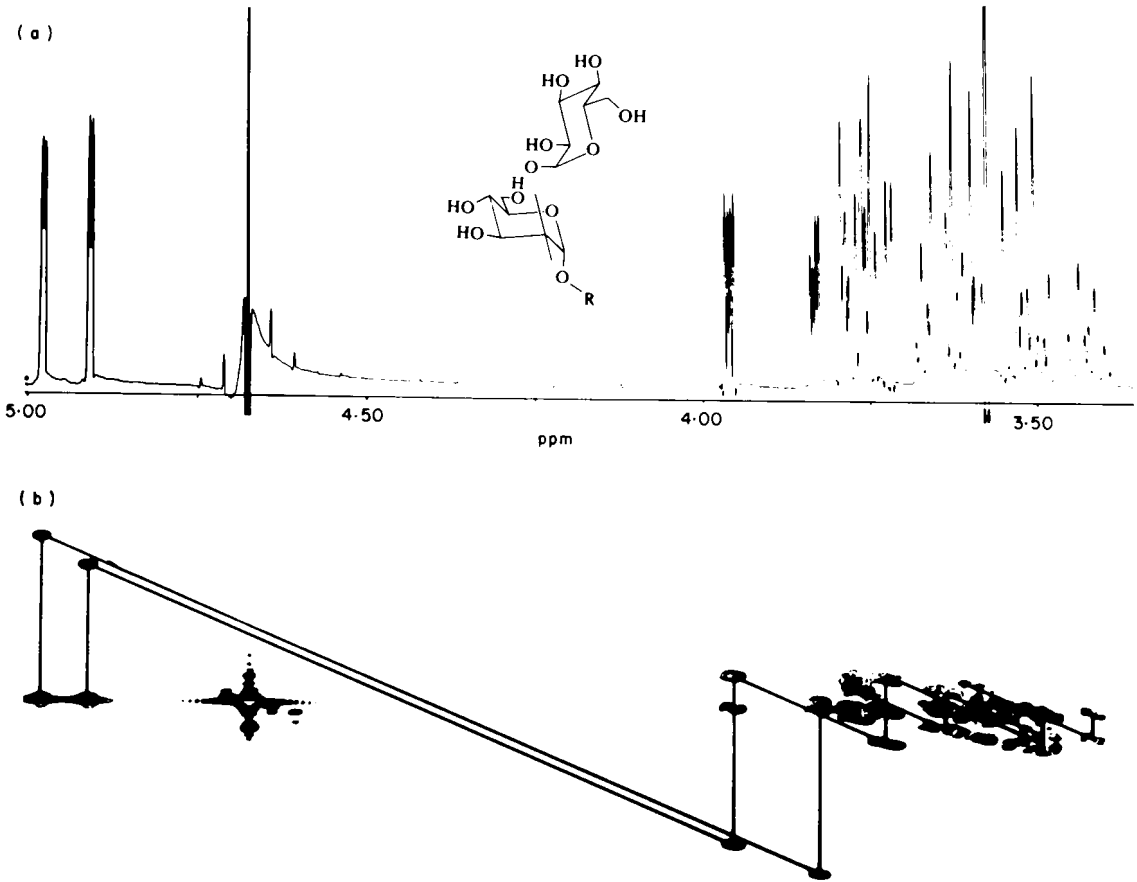
(a)
HO
HO
OH
HO
O
O
H
O
HO
O
HO
O
R
5·00
4·50
4·00
3·50
ppm
(b)

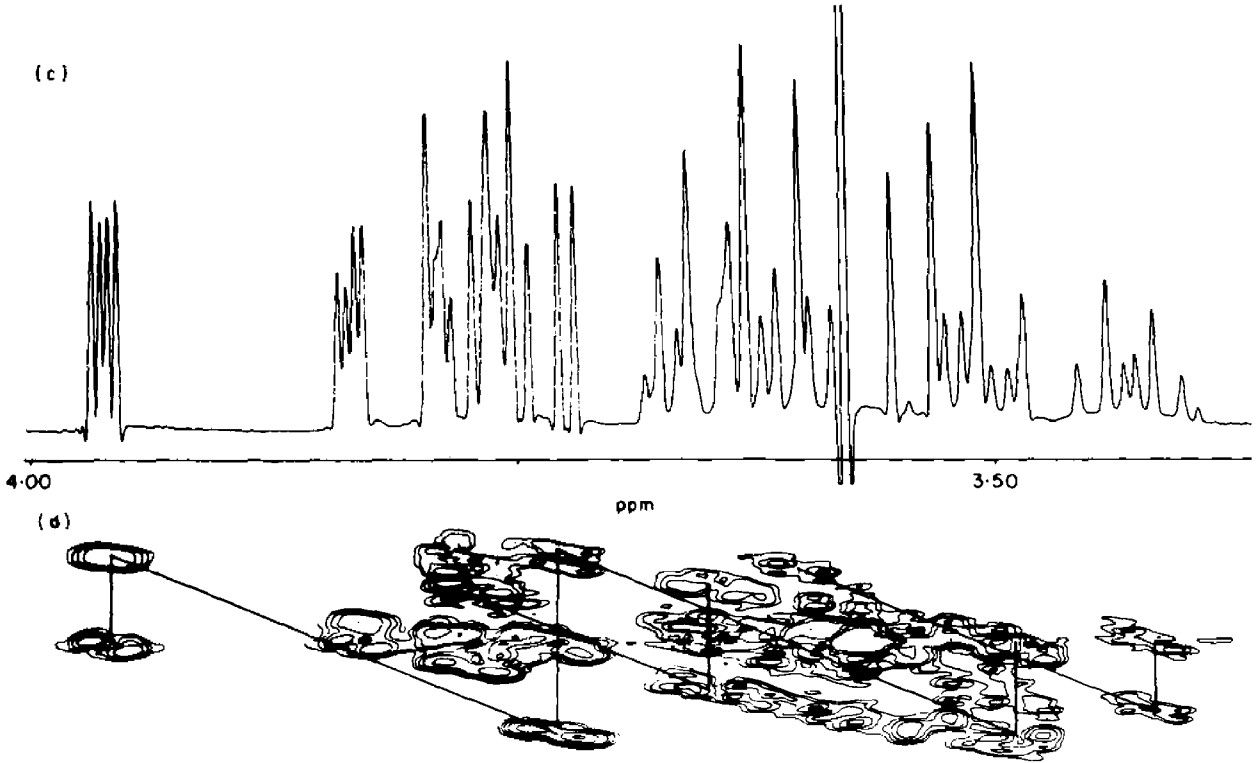

FIG. 3. Partial 400 MHz ^{1}H spectrum of 8-methoxycarbonyloctyl-2-*O*-(α-D-manno-pyranosyl)-α-D-mannopyranoside in D_2O at 300 K. (a) Normal one-dimensional spectrum. (b) Contour diagram of a two-dimensional SECSY experiment. The normal spectrum, seen from the top, is displayed along the centre line. The spin–spin connectivities are indicated on parallel diagonal lines. Thus H-2 resonating at 3·95 ppm is coupled to H-1 at 4·90 ppm and H-3 at 3·74 ppm. (c) Enlargement of part of the normal spectrum. (d) Enlargement of part of the contour diagram.

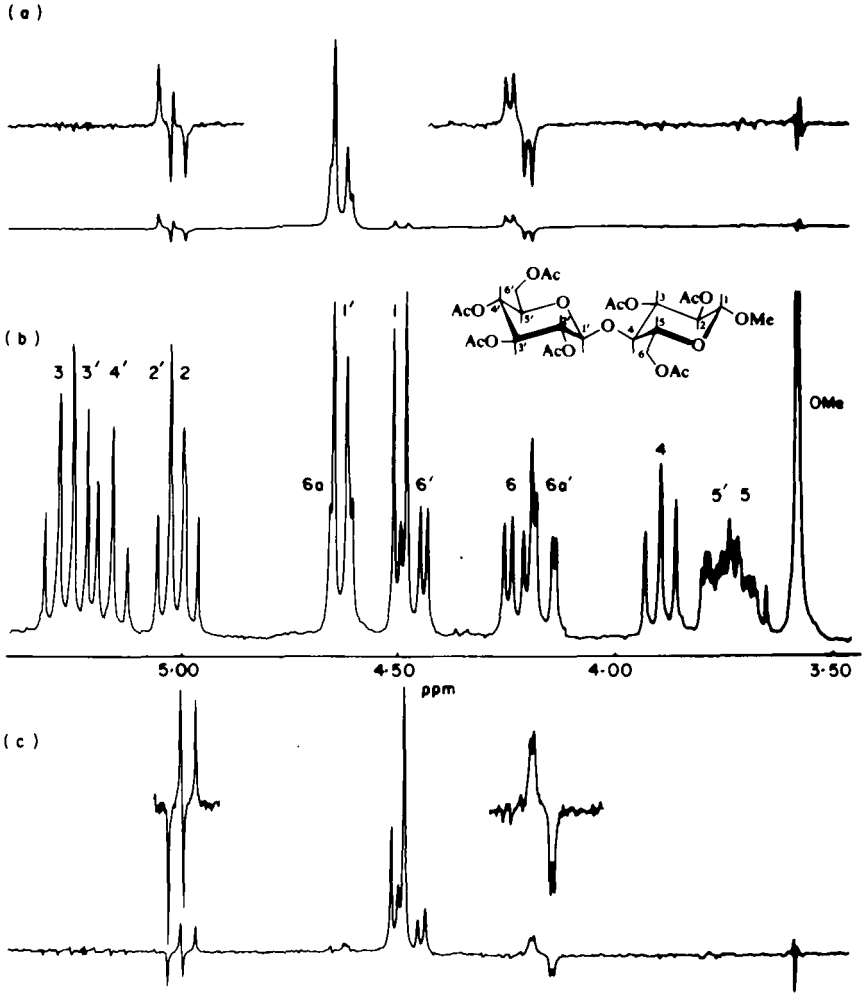

FIG. 4. Partial 270 MHz ^{1}H spectrum of methylhepta-*O*-acetyl-β-D-cellobioside in deuteriochloroform. The normal spectrum is displayed in (b). (a) Fourier transform INDOR experiment with selective inversion of the high frequency part of the H-1 (and H-6a) resonances. Typical INDOR responses are seen for H-2′ and H-6. (c) Same experiment with selective inversion of the low frequency part of H-1 and low frequency part of H-6′. Typical INDOR responses are seen for H-2 and H-6a′.

experiment may eliminate the problems arising from spin diffusion. The two-dimensional NOE experiment described by Ernst *et al.*[44,45] eliminates these problems because this is an experiment with no decoupling field, by analogy with the SECSY experiment described above. Furthermore, the two-dimensional dipolar-coupled (2-D-NOE) experiment has the

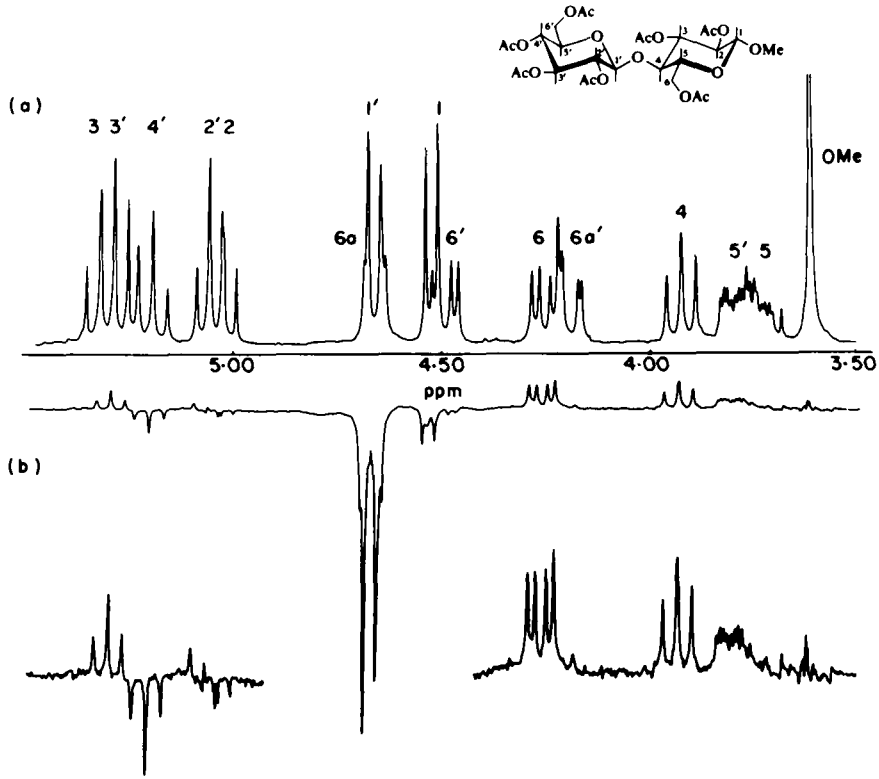

FIG. 5. Partial 270 MHz ^{1}H spectrum of methylhepta-*O*-acetyl-*β*-D-cellobioside in deuteriochloroform. (a) Normal spectrum. (b) Difference NOE experiment with saturation of H-1′ (and also H-6a due to chemical shift equivalence). Positive enhancements are observed for H-3′, H-5′, H-2′, H-4 and H-6 and negative enhancements for H-4′ and H-2.

advantage that off-resonance saturation[40,46] is avoided because the decoupler is not used, and it is thus more easy to measure NOEs for hidden or close-lying lines. The disadvantage is that it is not as easy to quantify these results compared to the results obtained in the one-dimensional experiments. This experiment has been used on an oligosaccharide in the conformational analysis of a blood-group determinant.[40]

4. *Relaxation experiments*

The advent of pulsed FT instruments has, in addition to the enhanced sensitivity in the spectra, made it possible to perform relaxation experiments and to determine, in particular, T_1 data from ^{1}H NMR spectra.[47,48] Using the inversion–recovery method (180°–T–90°–FID–delay) it is possible to detect "hidden resonances".[49] This technique is very useful in the analysis

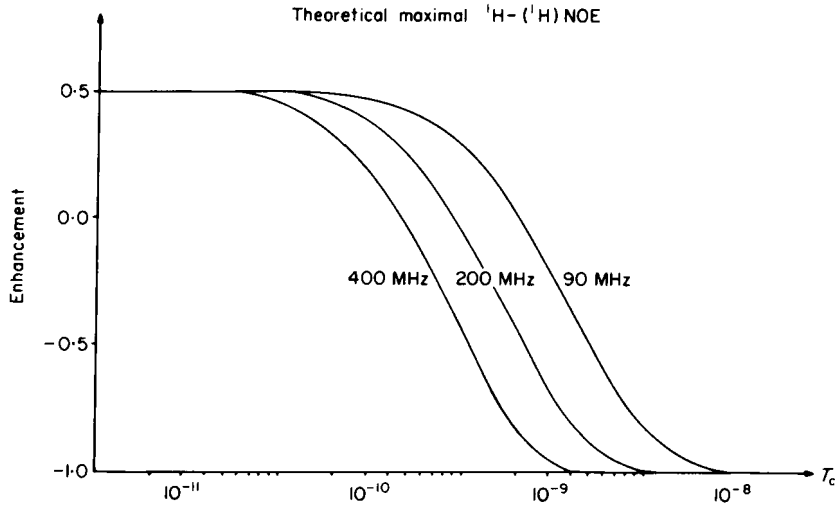

FIG. 6. Magnetic field dependence (400, 200 and 90 MHz) of the NOE as a function of the correlation time (T_c). The curves are calculated as described in reference 39.

of the spectra of complex oligosaccharides in aqueous solution, where most of the protons resonate in the region between 3·6 and 4·3 ppm. Resonances from hydroxymethyl groups will always relax faster due to the two geminal protons and can easily be determined in a partially relaxed spectrum, as shown in Fig. 8. It is possible simultaneously to perform a partially relaxed spectrum and a homo-decoupling experiment[50] as shown in Fig. 8(c). H-5 in the β-D-glcNAc unit is here saturated and it is seen that the H-5–H-6 couplings disappear from the spectrum. The limitation to this experiment is that it is difficult to change the relative ratio of the T_1 values upon which the success of the experiment is dependent.

Another type of relaxation experiment, the spin–echo experiment, which can be used to determine T_2 values in non-spin–spin coupled systems, allows one to measure individual spectra of small molecules in the presence of large molecules.[51] This has been illustrated by Hall and Sukumar[52] in the area of carbohydrates. They obtained the spectrum of D-xylose even though it is present in a mixture of cyclodextrin and dextran T10.

5. *Two-dimensional spectroscopy*

Two-dimensional *J*-resolved spectroscopy[53,54] separates signals with different chemical shifts from their coupling constants if no second-order effects are present. The chemical shifts are observed along one frequency

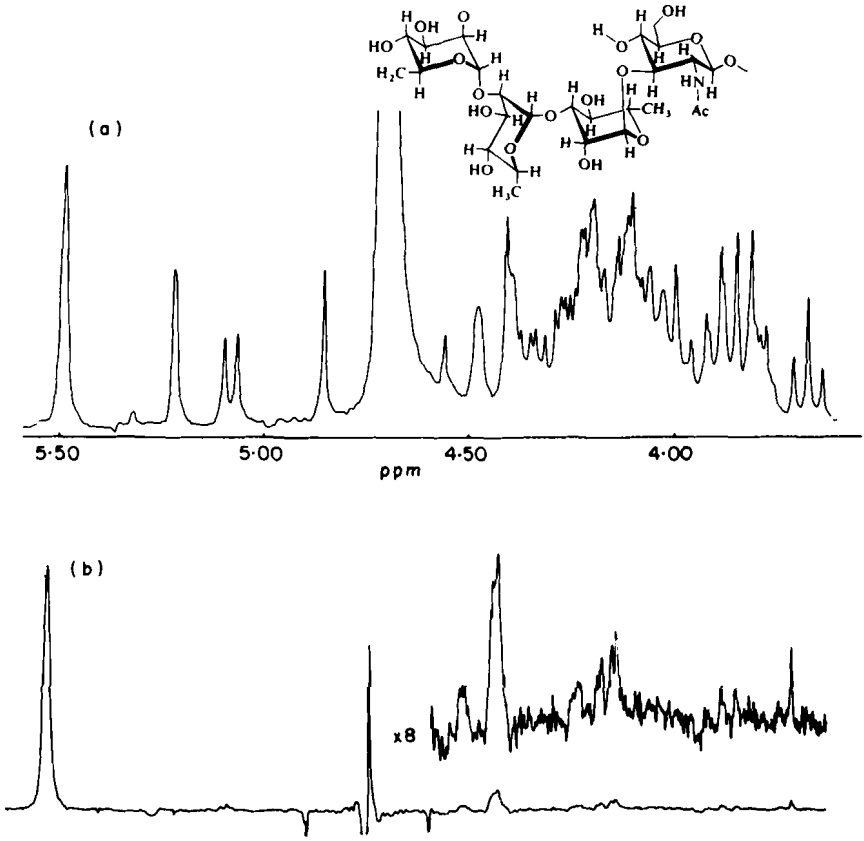

FIG. 7. Partial 270 MHz ^{1}H spectrum of the *O*-specific polysaccharide from *Shigella flexneri* which contains the repeating tetrasaccharide → 2-(α-L-Rham)-1 → 2-(α-L-Rham)-1 → 3(α-L-Rham)-1 → 3(β-D-glcNAc)-1 →. (a) Normal spectrum in D_2O at 310 K. (b) Difference NOE experiment with saturation of the H-1 resonances at 5·50 ppm. The observed enhancements are observed for, for example, the H-2 resonances at 4·40 and 4·45 ppm respectively. The enhancements are observed with the same phase as the reference signal at 5·50 ppm, i.e. a negative NOE.

axis and the associated spin–spin couplings along the other frequency axis. This technique has made it possible to perform a much more complete analysis of the overlapping signals in oligosaccharides between 3·6 and 4·3 ppm. In combination with the SECSY experiment mentioned above, these two experiments are important tools in the assignment of spectra of complex oligosaccharides. Several carbohydrate examples have been discussed in the literature.[55–57]

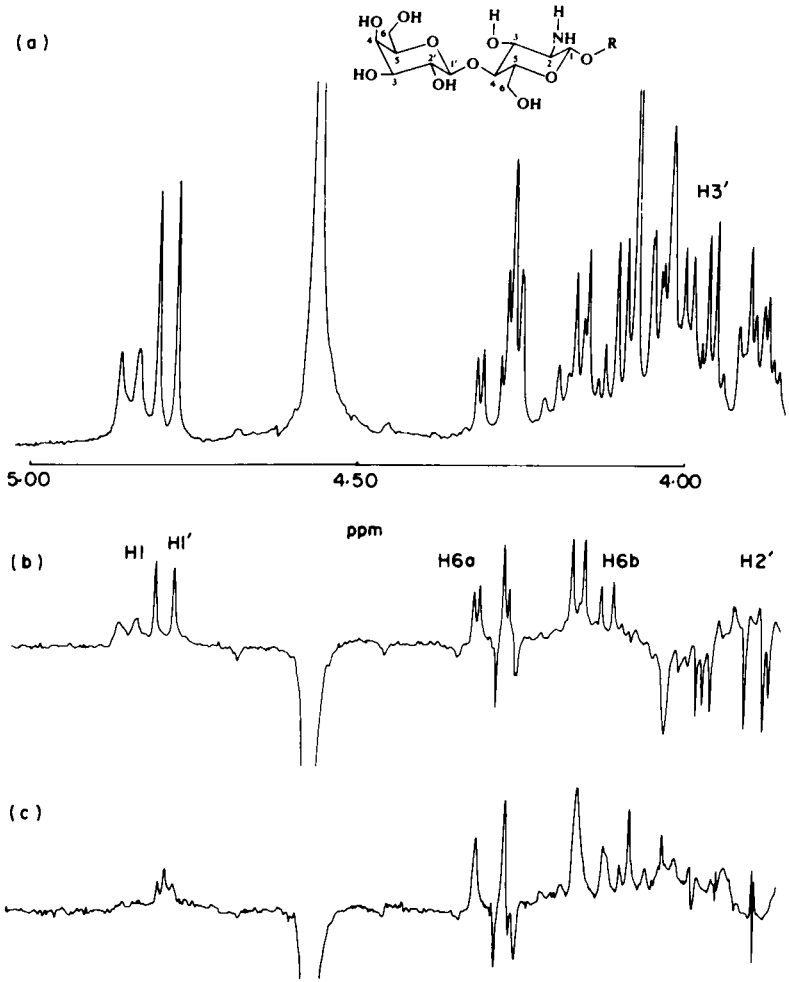

FIG. 8. Partial 270 MHz ^{1}H spectrum of 8-methoxycarbonyloctyl-4-*O*-(β-D-galactopyranosyl)-2-acetamido-3-deoxy-β-D-glucopyranoside in D_2O at 340 K. (a) Normal spectrum. (b) Partially relaxed spectrum, where the fast relaxing H-6 resonances from the β-D-glcNAc unit are positive and the slowly relaxing H-2 and H-3 protons from the β-D-gal unit are appearing negative. (c) Partially relaxed spectrum using the same delay between the 180° and 90° pulses as in (b) but with simultaneous homodecoupling of H-5 of the β-D-glcNAc unit. The disappearance of the H-5–H-6 couplings are clearly seen.

6. *Paramagnetic shift reagents*

Paramagnetic shift reagents have not been used very extensively in the assignment of carbohydrates and their derivatives, mainly due to the difficulty in determining the site of complexation of these reagents with

TABLE I

Proton magnetic resonance parameters for kanamycin A.[a]

Deoxystreptamine unit (B)

Parameter	δ_1	J_{12}	$J_{12'}$	δ_2	$J_{22'}$	J_{23}	$J_{2'3}$	δ_3	J_{34}	δ_4	J_{45}	δ_5	J_{56}	δ_6	J_{16}
Base	3·162	4·0	12·5	2·225	13·0	4·0	12·5	3·154	9·5	3·588	9·3	3·923	9·3	3·515	9·4
Salt	3·872	4·3	12·5	2·813	13·0	4·3	12·5	3·880	9·5	4·117	9·3	4·224	9·3	4·040	9·5

3-Aminoglucose unit (A)

Parameter	δ_1	J_{12}	δ_2	J_{23}	δ_3	J_{34}	δ_4	J_{45}	δ_5	J_{56}	$J_{56'}$	δ_6	$J_{66'}$	$\delta_{6'}$
Base	5·305	3·8	3·762	10·4	3·267	10·0	3·594	10·2	4·179	3·4	3·4	4·03	—	4·01
Salt	5·400	3·7	4·215	11·0	3·775	10·0	3·957	10·5	4·201	2·1	5·0	4·095	12·0	4·036

6-Aminoglucose unit (C)

Parameter	δ_1	J_{12}	δ_2	J_{23}	δ_3	J_{34}	δ_4	J_{45}	δ_5	J_{56}	$J_{56'}$	δ_6	$J_{66'}$	$\delta_{6'}$
Base	5·595	3·9	3·851	9·8	3·961	9·5	3·569	10·0	4·034	2·0	8·0	3·257	14·0	3·029
Salt	5·812	3·8	3·940	10·0	4·040	9·5	3·646	10·0	4·285	3·0	8·0	3·692	13·5	3·445

[a] In D_2O at 300 K. The δ values are in parts per million using 1% acetone as internal reference (2·480 ppm), the first-order couplings are in hertz. The subscript numbers indicate the position in the structural unit as indicated in [1]. Data are from reference 18.

multifunctional carbohydrate compounds.[11,58] However, some examples are given in references 59–64.

7. *Protonation shifts*

Compounds with substituents which can be protonated or deprotonated (e.g. amino groups or carboxylic acids) have chemical shifts which are dependent on the pH. When spectral data are reported for this type of compound it is therefore important to specify the pH of the solution. The data in Table I for kanamycin A ([1] and [2]) illustrates the big changes that may occur with pH even though the conformation of the molecule is virtually unchanged.[18]

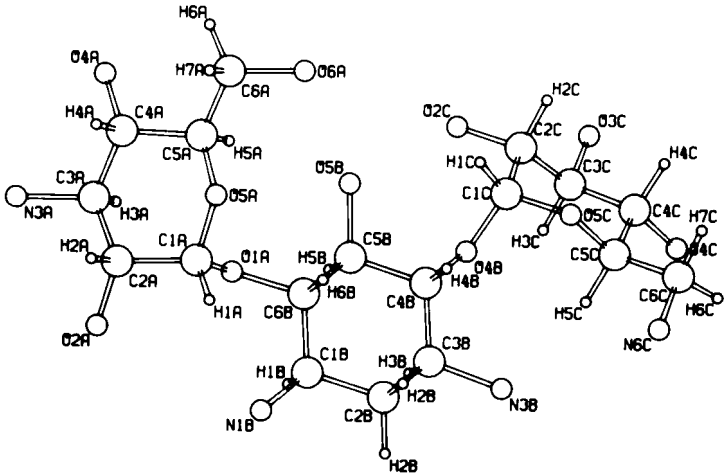

[1] Kanamycin

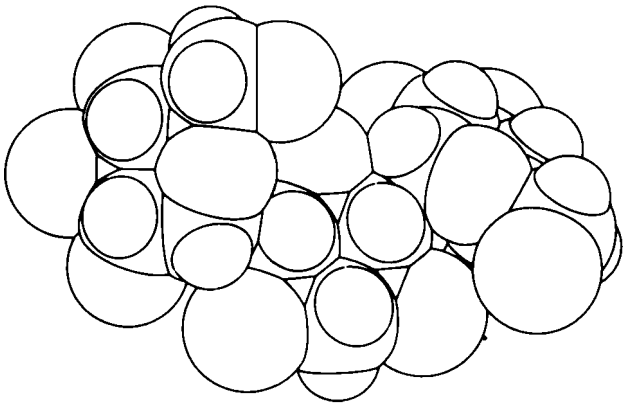

[2] Kanamycin (space-filling model)

8. Miscellaneous

Solvent-induced shifts can be useful in the assignment of ^{1}H NMR spectra even though it is not possible to predict the result of changing the solvent from, say, deuteriochloroform to deuteriobenzene. Many of these solvent-induced shifts appear to arise from favoured solvation of specific sites of the solute molecule. Thus, the chemical shifts of acetate methyl resonances and the protons on the carbon atom where the acetate group is positioned are substantially altered when deuteriobenzene is the solvent.[65]

Bendall *et al.*[66] have described a multinuclear multipulse sequence which allows the measurement of the protons coupled to ^{13}C in a ^{1}H NMR spectrum with elimination of the signals from protons bonded to ^{12}C nuclei.

B. ^{13}C NMR assignments

The following points are discussed in this section:

1. Comparison with model compounds
2. Isotopic substitution
3. Correlation with proton spectra
4. Relaxation experiments
5. Paramagnetic reagents
6. Protonation shifts
7. Miscellaneous

1. Comparison with model compounds

Comparison with model compounds, for the assignment of ^{13}C chemical shift data, has been used more frequently than for ^{1}H NMR data, particularly in publications prior to 1976 (e.g. references 67, 68). This has led to a number of general rules for the assignment of signals in carbohydrate derivatives.[2,3,5,69] Complex rules have been described[70] for the influence of axial or equatorial substituents on the ^{13}C chemical shifts of α-, β- and γ-carbon atoms. Because the pyranose and furanose derivatives of carbohydrates contain several mutually interacting substituents these rules have, in some cases, led to erroneous assignments. The use of model compounds in the assignment of the ^{13}C NMR signals of oligo- and polysaccharides is much more justified[3–5] than in ^{1}H NMR spectroscopy. Table II clearly shows how the ^{13}C chemical shifts of terminal L-fucose units in a number of complex oligosaccharides only vary significantly for the anomeric carbon atom. Even though carbon atoms usually constitute the molecular skeleton, and thus their shieldings are less sensitive than those of protons to interunit interactions, such effects may in special cases lead to unexpected shieldings[16] (Section III. B) and thus to erroneous assignments.

TABLE II

^{13}C chemical shifts[a] of 6-deoxy-α-L-galactopyranoside derivatives.

Compound, R =	C-1	C-2	C-3	C-4	C-5	C-6
Methyl	100·40	68·87	70·53	72·74	67·38	16·24
2-D-Galactose	100·13	69·20	70·46	72·78	67·58	16·25
A-Trisaccharide	99·17	68·66	70·60	72·84	67·57	16·16
B-Trisaccharide	99·33	68·67	70·37	72·84	67·46	16·21
H-Trisaccharide	100·32	68·96	70·32	72·66	67·34	16·05
Lew. B	100·36	69·11	70·28	72·76	67·01	16·06
Lew. B	98·69	68·78	70·06	72·86	67·86	16·25
Lew. A	98·91	68·75	70·08	72·86	67·66	16·25
Standard deviation	0·71	0·20	0·20	0·07	0·25	0·09
Maximum deviation	1·44	0·54	0·54	0·20	0·85	0·19

[a] Data taken from reference 16. In D_2O at 67·89 MHz, with dioxane as internal reference (67·40 ppm.).

The ^{13}C chemical shifts of a series of simple mono- and oligosaccharides, their methylglycosides, and acetylated hexopyranose derivatives are given in Section IV.

2. Isotopic substitution

The assignment of ^{13}C NMR spectra is greatly facilitated if compounds substituted in known positions with deuterium or carbon-13 are available. In *C*-deuterated molecules the carbon atom usually gives no signal due to (a) saturation (longer spin–lattice relaxation time), (b) coupling to deuterium and (c) quadropolar broadening of the signal. The last point is particularly important in asymmetric carbohydrate derivatives. Furthermore, the β-carbon atom may be assigned due to a small low frequency deuterium-induced isotope shift.[71–74] On the other hand, derivatives enriched with ^{13}C in specific positions give rise to intense signals in the spectra and thus provide an unambiguous assignment. In addition, ^{13}C–^{13}C couplings may be visible in the spectra of ^{13}C-enriched compounds and these, together with isotope-induced shifts, may assist in the assignment of carbon atoms in positions α or β to the ^{13}C-enriched site.[75–80]

The presence of magnetic nuclei, such as ^{19}F and ^{31}P, leads to spin–spin coupling with neighbouring carbon atoms and these ^{13}C signals may therefore be readily assigned.[81–85] If no information about the size of the heteronuclear couplings is available, it is often useful to perform triple resonance experiments. This is illustrated in Fig. 9, where a ^{13}C NMR

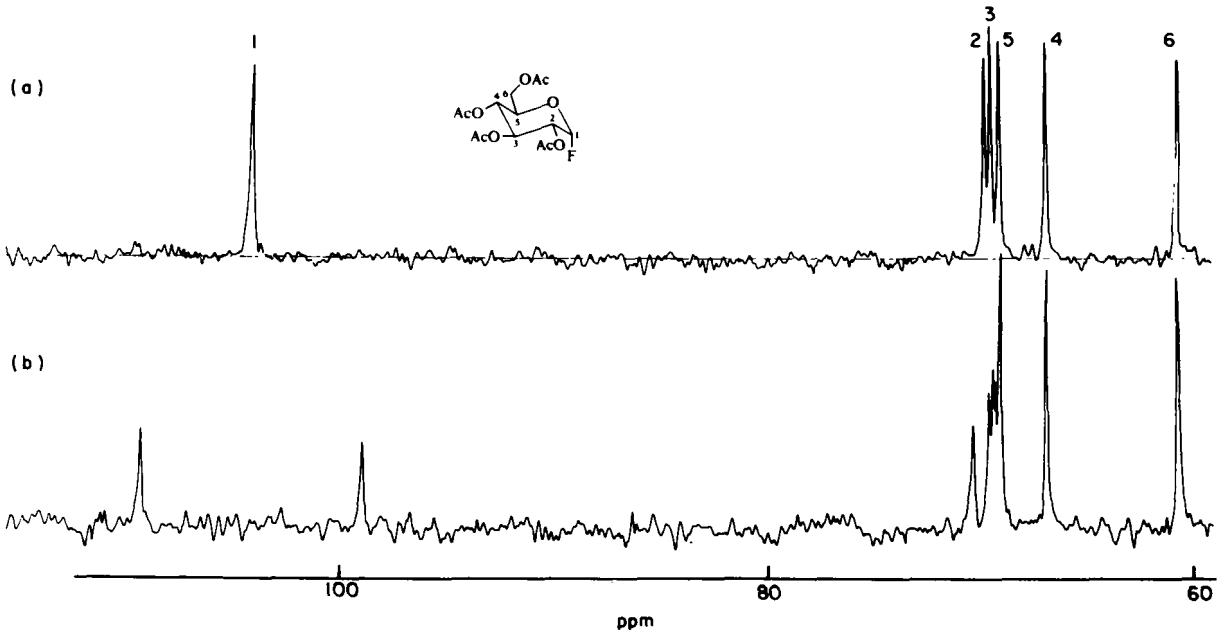

FIG. 9. Partial 22·63 MHz ^{13}C spectrum of 2,3,4,6-tetra-*O*-acetyl-α-D-glucopyranosyl fluoride in deuteriochloroform. The normal spectrum with the ^{13}C–^{19}F couplings is shown in (b). (a) The same spectrum with simultaneous decoupling of both the protons and the fluorine resonances.

spectrum of acetofluoroglucose is obtained with simultaneous irradiation of the proton and fluorine atoms in the molecule.

O-Deuteration of hydroxyl groups or *N*-deuteration of amino groups is readily carried out by exchange with D_2O. The associated deuterium isotope shifts are measurable under appropriate conditions and thus this method is very useful in the assignment of spectra of carbohydrate derivatives.[86–91] The experiment is most conveniently done by obtaining a spectrum in 100% D_2O solution and then in a 95% H_2O (5% D_2O for lock) solution and measuring the difference in chemical shifts. The capillary technique[89] is not easy to perform on a superconducting high field instrument, because the capillary tends to destroy the homogeneity of the magnetic field, and it is therefore not possible to obtain the necessary resolution.

3. *Correlation with proton spectra*

^{13}C–^{1}H couplings are obtained from proton-coupled ^{13}C NMR spectra, usually measured by the "gated technique".[12–14] Because the one-bond couplings are large (125–200 Hz), the ^{13}C multiplets may overlap and make identification of the multiplicity difficult. In an off-resonance decoupled spectrum[12–14] the C–H couplings are reduced and the overlap of signals therefore less likely. Both types of spectra show unambiguously how many protons are attached to each carbon atom. In addition to these one-bond couplings,[92–95] fully proton-coupled spectra obtained with good resolution show well resolved two- and three-bond couplings, which are useful for the assignment of signals to some carbon atoms. Two- and three-bond couplings have been discussed in several papers[76,94,96–100] and summarized in a recent review.[101] In Fig. 10 is shown a fully proton-coupled spectrum of methyl α-L-fucopyranoside in D_2O, where the multiplicity of the individual signals is easily observed. The assignment of these long range couplings is done using a very selective decoupling field in the ^{1}H NMR spectrum.[102] The problem of non-first-order behaviour in these fully coupled ^{13}C NMR spectra has been discussed.[103]

Selective irradiation in the proton spectrum with a much stronger field ($\gamma B_2/2\pi \equiv 1000$ Hz) is the most straightforward method for assigning ^{13}C signals. By this technique one proton is irradiated with a single frequency causing the carbon to which it is bound to appear as a singlet in the ^{13}C spectrum while most other carbon atoms give off-resonance decoupled multiplets (Fig. 11). This technique requires a fully assigned proton spectrum with well dispersed signals (separated by ~10 Hz) and is therefore most successful on high field instruments. The same technique can be applied in the assignment of the ^{1}H NMR spectra provided that the ^{13}C signals are previously assigned. This is of particular interest when assigning

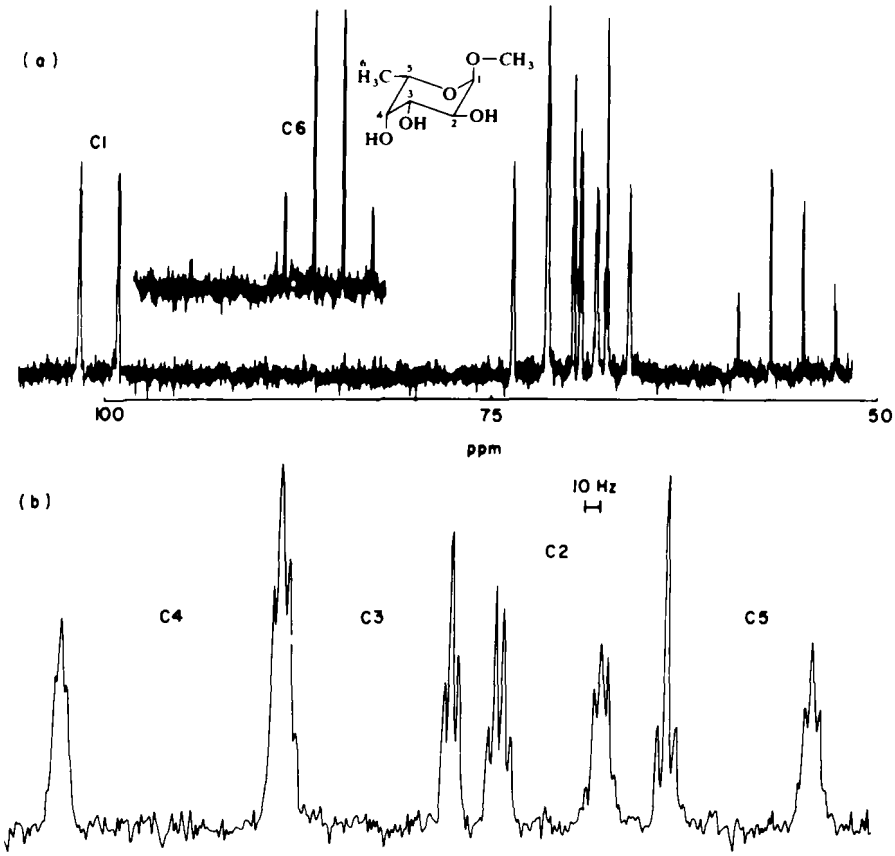

FIG. 10. 67·89 MHz ^{13}C spectrum of methyl-6-deoxy-α-L-galactopyranoside (α-L-fucopyranoside) in D_2O at 310 K. (a) Normal proton-coupled ^{13}C spectrum. (b) Expansion of the resonances between 65 and 75 ppm. The multiplicities of the carbon atoms 2, 3, 4 and 5 are easily determined from the spectrum.

the overlapping signals between 3·80 and 4·30 ppm in oligosaccharides in aqueous solutions (Fig. 11(c)).

Correlations between the chemical shifts of the proton and carbon atoms may also be obtained through heteronuclear, two-dimensional NMR experiments.[104,105]

4. *Relaxation experiments*

The relaxation rates of the carbon atoms in most mono- and oligosaccharides are dominated by the intramolecular dipole–dipole mechanism.[106,107] For protonated carbon atoms, the relaxation primarily gives

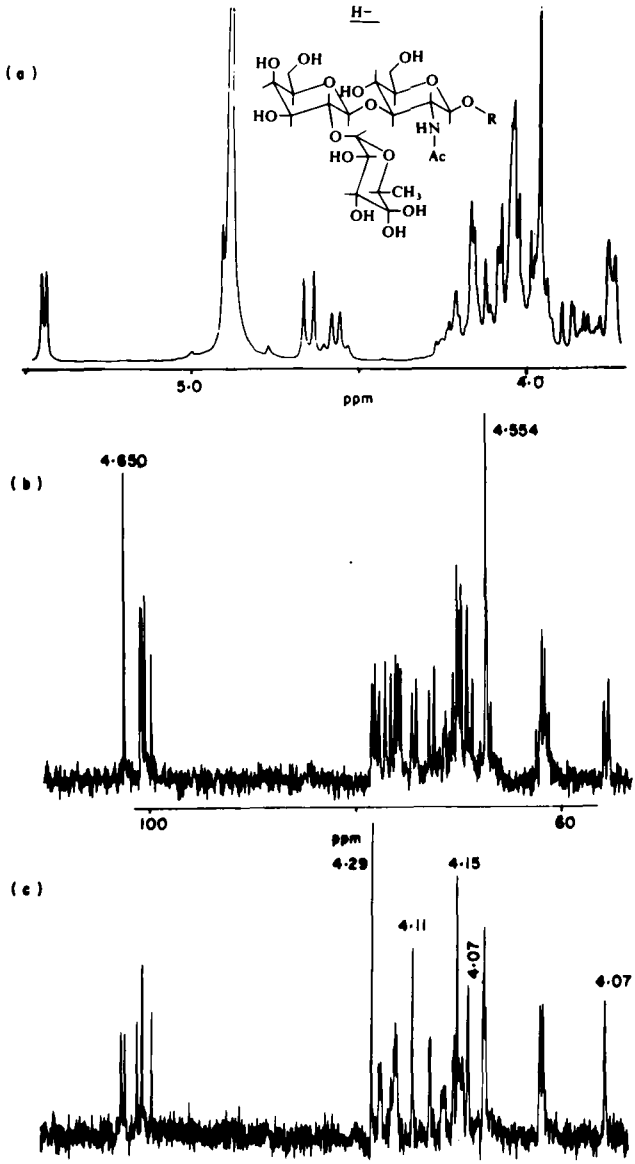

FIG. 11. ^{1}H and ^{13}C spectra of blood-group determinant H$^-$: (α-L-Fuc)-1 → 2-(β-D-gal)-1 → 3-(β-D-glcNAc)-1 → OR. (a) Partial ^{1}H spectrum at 270 MHz in D_2O at 310 K. (b) Partial ^{13}C spectrum at 67·89 MHz with selective proton irradiation ($\gamma B_2/2\pi \approx 1000$ Hz) at 4·554 ppm in the ^{1}H spectrum. The value above the high frequency anomeric carbon atom indicates the ^{1}H chemical shift of the attached proton. (c) As in (b) but with selective proton irradiation at 4·29 ppm. The values above the carbon resonances indicate the ^{1}H chemical shifts of the protons attached to these carbon atoms.

information about molecular motion[108,109] in addition to the trivial distinction between C, CH, CH_2 and CH_3 groups. This technique is therefore most useful for the identification of carbon atoms belonging to the same unit in an oligosaccharide which may be undergoing an isotropic motion.[110–112]

Recently a pulse sequence has been published[113,114] which can be used for the assignment of ^{13}C resonances from overlapping C, CH, CH_2 and CH_3 groups.

5. Paramagnetic shift reagents

Paramagnetic shift reagents (notably europium, gadolinium and cupric complexes) cause large changes in the shielding and line width and their use in assigning carbon signals has been discussed in general terms by several authors.[12,13] Paramagnetic shift reagents have been used in the study of ^{13}C NMR data of carbohydrate derivatives.[58,115–118]

6. Protonation shifts

The carbon chemical shifts of carbohydrate derivatives which contain groups which can be protonated or deprotonated (e.g. amino and carboxyl groups) are strongly dependent on the pH of the sample solution. The spectra of such compounds should therefore always be measured with control of pH. Comparison of ^{13}C NMR spectra of aminodeoxy sugars measured at low and high pH, i.e. with protonated or free amino groups, may be used for the assignment of carbon atoms α and β to the amino group.[9,14,16,119] Similar but smaller effects are observed in the spectra of aldonic or uronic acids.[89,90,120]

Derivatives with only hydroxyl groups may also show ^{13}C chemical shifts which are pH dependent, as illustrated in Fig. 12.

7. Miscellaneous

Freeman *et al.*[121] have recently shown that two-dimensional FT double quantum coherence experiments give AB subspectra from the ^{13}C satellites; such experiments may become a very important tool in the analysis of decoupled carbon spectra.

III. APPLICATIONS

A. ^{1}H NMR data

1. Structural determination

^{1}H NMR spectroscopy in combination with ^{13}C NMR spectroscopy is the most powerful tool available for the structural analysis of carbohydrates.

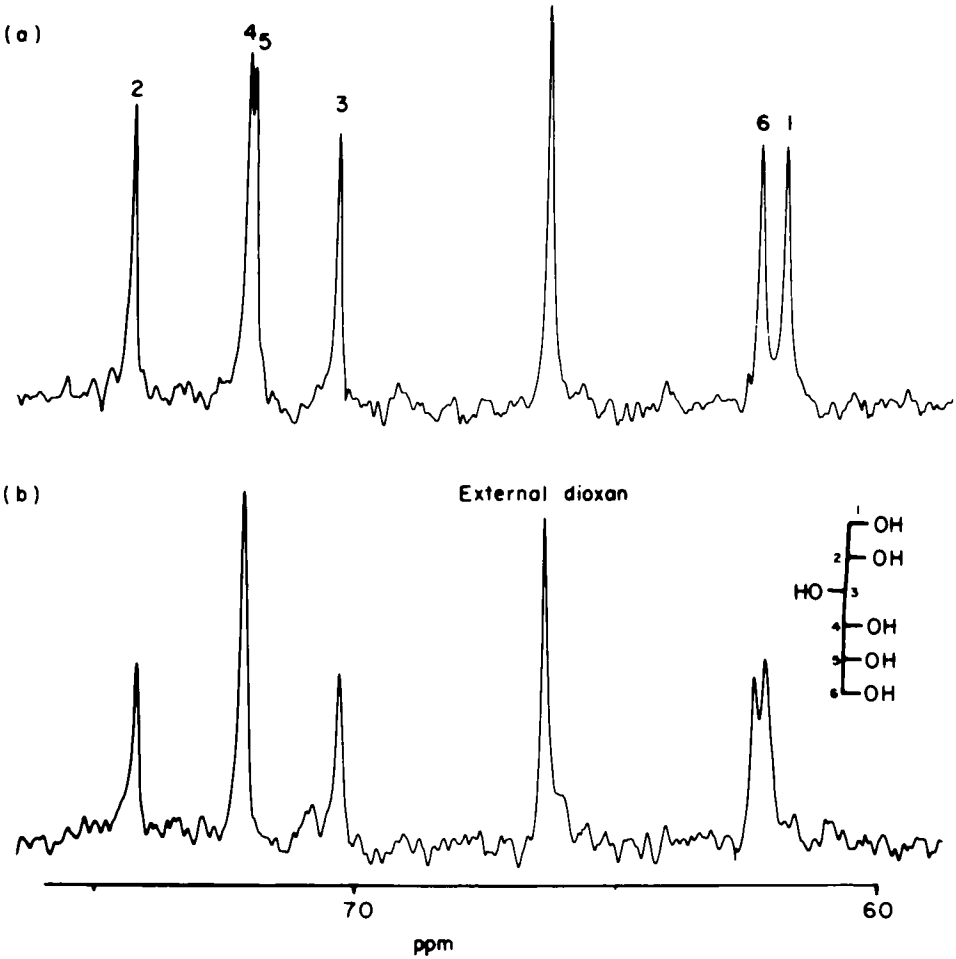

FIG. 12. 22·63 MHz proton noise-decoupled ^{13}C spectrum of D-glucitol at 300 K with external D_2O for lock and external dioxane as reference. (a) Normal spectrum in H_2O. (b) Same as in (a) but in 12 N H_2SO_4. It is clearly seen that the C-1 signal is shifted more to low frequency than is the C-6 signal.

The literature contains numerous examples and it is impossible to mention all of them here. The following therefore considers the more general aspects of the problems associated with the structural analysis of carbohydrates and their derivatives.

The dependence of the ^1H chemical shifts with respect to carbohydrate structures has been discussed in detail in reviews[9–11,122] and papers.[19–26,123] Chemical shifts have been used to determine the composition of muta-

rotated mixtures of hexoses and pentoses as described in a review.[124] Angyal and Wheen have recently shown[125] that D,L-glyceraldehyde, D-erythrose and D-threose in a syrupy state exist mainly as mixtures of dimers. Their aqueous solutions also contain some dimers but the components are mainly present in furanose or hydrated aldehyde forms. All solutions contain >1% of the aldehyde form. The proportion of the individual forms has been determined by ^{1}H NMR spectroscopy at various temperatures.

The ketoses have no anomeric protons, which can facilitate the analysis of mutarotated mixtures. This problem is therefore best solved by ^{13}C NMR spectroscopy.[126] But when only a small amount of a compound is available, as for most biologically important molecules, ^{1}H NMR data can give information about the mutarotation of, for example, *N*-acetylneuraminic acid.[127] The ^{1}H chemical shift of the equatorial H-3 in 16 anomeric ketosides of *N*-acetylneuraminic acid in D_2O shows a characteristic dependence of the anomeric configuration ($\delta = 2{\cdot}72 \pm 0{\cdot}05$ ppm for the α-anomer and $\delta = 2{\cdot}32 \pm 0{\cdot}08$ ppm for the β-anomer).[128]

Dissolution of carbohydrates in $(CF_3CO)_2O$ is accompanied by the trifluoroacetylation of hydroxyl groups, resulting in a high frequency shift of the protons of the sugars, which gives well resolved ^{1}H NMR spectra.[129] Similarly, the addition of trichloromethyl isocyanate in deuteriochloroform to solutions of alchohols or amines results in the formation of trichloromethylcarbamide esters or urea derivatives and thus high frequency shifts of the protons positioned on the carbon atoms carrying the hydroxyl or amino groups.[130,131]

Application of resolution enhancement in FT ^{1}H NMR spectroscopy is a powerful tool in the structural determination of, for example, deoxy sugars.[132] This technique has been described in general terms in a review,[133] and has also been used in a study of oligosaccharides.[134]

In addition to chemical shifts the ^{1}H spin–spin couplings play a dominant role in structural studies of carbohydrates. Several papers have therefore been devoted to the description of appropriate equations which may be used to predict vicinal couplings in carbohydrates and their derivatives.[135–138] Altona and Haasnoot[139] have determined the effects of relative orientation and electronegativity on $^3J(aa)$, $^3J(ea)$, and $^3J(ee)$ couplings. The effects are well predicted by a simple set of additivity constants valid for pyranose rings in carbohydrates. The proposed set of parameters has been used to calculate 327 couplings in a variety of pyranosides and related structures. Comparison with experimental data shows that, for a selected group of 305 couplings, couplings in molecules which are conformationally pure and undeformed can be predicted with an accuracy of 0·27 Hz. A statistical breakdown of $\Delta J(aa)$ and $\Delta J(ea)$ along each C—C bond in the pyranose system reveals an unexpected degree of geometrical homogeneity.

A similar study has been conducted[140] in conjunction with conformational analysis of the sugar rings in nucleosides and nucleotides in solution. The relation between vicinal ^{1}H NMR proton–proton couplings, obtained using the generalized Karplus equation, and the pseudorotational properties of the sugar ring has been re-investigated and compared with earlier studies.

A general study of the relationship between proton–proton vicinal couplings and the substituent electronegativity has been published.[141] A similar study for geminal couplings has also been published.[142,143]

Jankowski has shown that vicinal ^{1}H–^{1}H couplings can be correlated with ^{13}C–^{1}H one-bond couplings and these values used as a correction term to a Karplus equation.[144]

Coupling along H—C—O—H fragments has been discussed in two papers.[145,146] An unexpected long range coupling has been noticed in L-idofuranose derivatives, which is thought to proceed by a direct "through space" rather than an indirect "through bond" path.[147]

The non-selective spin–lattice relaxation rates of a series of furanose derivatives have been determined.[148] Substantial differences in relaxation rates are found for epimeric pairs of substances. This information can be used as structural evidence in these types of compounds where chemical shifts and couplings often yield unsatisfactory results. A more general discussion of the application of proton spin–lattice relaxation rates to the structural analysis of carbohydrates has been given.[11,48,49]

An approach to the structural analysis of oligosaccharides by ^{1}H NMR spectroscopy has been described by Bradbury and Collins,[149] who measured the chemical shifts of the glycosidic protons of oligosaccharides in D_2O. These shifts are to some degree diagnostic of both the nature of the sugar and the type of linkage, but do not determine the sequence of sugar residues. To solve this problem the aldose or ketose is first treated with cyanide to produce a terminal carboxylic acid. Then Gd^{3+} is added, which is bound to the carboxyl group, causing a line broadening of the proton resonances and a decrease in the spin–lattice relaxation times of the glycosidic protons. These effects fall off progressively along the oligosaccharide chain, hence allowing the sequence to be determined. The method, which is illustrated for maltotriose, has been used at the milligram level and may be applicable up to pentasaccharides. Difficulties occur in the treatment of non-reducing sugars or with certain sugar residues, which contain carboxylic groups themselves or residues, which bind Gd^{3+} on three adjacent hydroxyl groups with a particular stereochemistry. The possible usefulness of this technique in ^{13}C NMR spectroscopy has also been considered.

High field NMR instruments facilitate the interpretation of the ^{1}H NMR spectra of oligosaccharides in D_2O.[19–26] Application of FT NMR techniques, as described in Section II, has made it possible to analyse completely the ^{1}H NMR spectra of tetrasaccharides[16–18,150] and thus to carry out a complete structural analysis of these compounds.

2. *Conformational analysis*

The conformation of mono- and oligosaccharides can be determined from (a) chemical shifts, (b) couplings (c) relaxation data and (d) NOE results.

Numerous papers[7] have discussed the conformational analysis of carbohydrate derivatives during the period 1973–80 and the results are summarized in reviews[9–11,151–154].

The conformational aspects of idopyranose derivatives have been studied by Paulsen and Friedman,[155,156] who also showed[157] that 5-benzyloxycarbonylamino-5,6-dideoxy-β-L-idopyranose exists predominantly in the $^4C_1$ (L) conformation. This corresponds to the $^1C_4$ (D) conformation in the D series. Angyal and Kondo have also published[158] a conformational study of the 4,6-*O*-benzylidene acetals of methyl-α-D-idopyranoside. In $CDCl_3$ solution the methyl-4,6-*O*-(*R*)-benzylidene-α-D-idopyranoside adopts the $^4C_1$ (D) conformation, having the phenyl group axial, whereas methyl-α-D-idopyranoside in D_2O exists as a mixture of the two chair forms. Several other compounds having three or more axially attached O atoms have been studied.[158]

1,5-Anhydro pentitols have been investigated[152,159] with respect to their conformation in solution by comparison with the corresponding pentose derivatives. Thus 1,2,3,4-tetra-*O*-benzoyl-β-D-xylopyranose in acetone-d_6 at room temperature exists as a 1:1 mixture of the $^4C_1$ and $^1C_4$ (D) conformers, but crystallizes in the all-axial form ($^1C_4$). 1,5-Anhydro-2,3,4-tri-*O*-benzoylxylitol, which lacks the anomeric effect when compared to the xylose derivative mentioned above, shows in solution a ratio of $^4C_1$ to $^1C_4$ conformers of 81:19 and crystallizes in the all-equatorial form ($^4C_1$).

1,6-Anhydrohexoses have been investigated with respect to their conformations in solution. An analysis of the ^1H spin–spin couplings of the eight isomeric 1,6-anhydro-β-D-hexopyranoses in DMSO-d_6 and the corresponding tri-*O*-acetates in $CDCl_3$ has been published.[136] Comparison of the experimental vicinal couplings with the theoretical values calculated from torsion angles obtained from Dreiding models proves that the $^1C_4$ (D) conformation is preferred in the whole series, and that the pyranose ring is flattened to some extent due to the interaction of substituents in 2, 3 and 4 positions.

A similar study has been conducted[160] measuring the non-selective spin–lattice relaxation rates (R_1 values) for all of the ring protons of the eight isomeric tri-*O*-acetyl-1,6-anhydro-β-D-hexopyranoses as 0·1 M solutions in benzene-d_6. The effect on the proton R_1 values of a change in solvent, concentration, temperature and proton impurities is documented and ^{13}C R_1 values are given to show that the first three sets of variations are due to changes in the motional correlation times of the molecules. The proton relaxation data can be fitted by a regressional analysis to a single

set of interproton relaxation contributions, the numerical values of which accord with a $^1C_4$ (D) conformation for the pyranose ring, somewhat distorted by the 1,6-anhydro ring and the substituents on atoms 2, 3 and 4.

The conformation of 2,3- and 3,4-anhydro derivatives of 1,6-anhydro-β-D-hexopyranoses,[161] 2,3-anhydro-4-deoxyhexopyranosides[162] and benzyl-4-*O*-(aldopentopyranosyl)-2,3-anhydro-β-D-ribopyranosides[163] has been investigated and the results indicate that all of the compounds exist in half-chair conformations. Similarly the conformations of 3,4-unsaturated[164] and 2,3-unsaturated[165] carbohydrate derivatives have been shown by ^{1}H NMR data to be predominantly in half-chair or sofa conformations.

A complete analysis of the ^{1}H NMR spectra of acetylated glycals[166] and D-arabinal and D-xylal[167] has been carried out. The conformation of these compounds, as determined from the proton couplings, is interpreted in terms of a rapid equilibrium between the two possible dihydropyran half-chair conformations. A computer treatment of all observed couplings has been carried out to obtain optimized values for the populations and coupling characteristics of the two alternative conformations.

A conformational analysis of 2,3,4-tri-*O*-acetyl-D-xylono-1,5-lactone has been described[168] by using ^{1}H NMR data. The possible contribution of attractive 1,3- and 1,4-interactions between the electropositive lactone ring oxygen and the *endo*-acetoxy groups at C-3 and C-4 to the conformational stability is discussed.

The conformations of 1,2-*O*-alkylidene-α-D-hexopyranoses has been investigated[169] by ^{1}H NMR spectroscopy and compared with *X*-ray results. The assignments are corroborated by ^{1}H NOE experiments. A similar study of 1,2-acylspiroorthoesters of 3,4,6-tri-*O*-acetyl-α-D-glucopyranoses has been published.[170] Nashed *et al.*[171] have shown by ^{1}H NMR that 1,2-oxazolines exist in modified $^0S_2$ conformations.

Conformational analysis based on ^{1}H NMR results and comparison with X-ray data has appeared on anhydro hexopyranosides[172,173] and α-D-galactooctopyranose derivatives.[174]

Studies on the C-5 to C-6 rotamer population of the hydroxymethyl group has been published by several groups.[166,175–177] The rotameric behaviour of methoxy groups in some aldopyranoses[178] and barriers to hindered rotation around *N*-glycoside bonds[179,180] have been discussed.

Conformational analysis of acyclic carbohydrate derivatives has been described in a study of 1-amino-1-deoxypentitols,[181] and dithioacetals.[182–184] ^{1}H NMR spectra of chloroform-*d* solutions of eight penta-*O*-acetyldimethylacetals and the corresponding diethyldithioacetals at 250 MHz furnish a complete set of chemical shifts and couplings that can be interpreted in terms of conformational composition at room temperature. The galacto- and manno- derivatives adopt planar, extended conformations, whereas the other six stereoisomers all adopt one or more

non-extended (sickle) conformations. The results are interpreted on the basis of the avoidance of parallel 1,3-interactions of substituents. Similar studies have been published for phenylhydrazones[185] and peracetylated hexononitriles.[186]

Conformational analysis of furanosides or 2,5-anhydro pentoses has been investigated in detail by several groups.[140,187–189] Angyal[190] has described the ^{1}H NMR spectra of most of the methyl aldofuranosides and has analysed the data with respect to the conformation of the glycosides. In the D series the β-pentofuranosides are in the $^3T_2$ form with the methoxy group quasi-axial and the side chain quasi-equatorial. The α-D-pento furanosides are mixtures of two twist forms or assume an envelope conformation.

^{1}H chemical shifts, spin–lattice relaxation rates and NOE factors are the parameters which are important in a conformational analysis of oligosaccharides in solution. Berry *et al.*[191] have discussed the use of proton spin–lattice relaxation rates as a measure of aglycone–sugar interaction and Lemieux *et al.*[192] have discussed the influence of the *exo* anomeric effect on the conformation around the glycosidic centre. Detailed studies of the conformation of branched oligosaccharides related to blood-group determinants have been published.[16,18,40] An extension of this work to a study of linear oligosaccharides and a polysaccharide has also appeared recently.[39]

A conformational analysis by ^{1}H NMR spectroscopy of amylose and related model compounds in DMSO-d_6 has also been published.[146]

3. *Solution properties*

At low temperatures, and in a narrow pH range, the hydroxyl proton resonance spectra of a range of mono-, di- and oligosaccharides in dilute aqueous solutions have been resolved.[193] The signals broaden rapidly on raising the temperature and on changing the pH of the solution. Optimum conditions for obtaining maximal resolution are described and attempts are made to assign the resonances to specific hydroxyl groups. In all cases the anomeric hydroxyl protons occur at highest frequency and the pH value for optimum resolution of these resonances is always lower than that for the other protons. Similar work has been published by Bociek and Franks,[194] who describe exchange phenomena for the anomeric hydroxyl protons of D-glucose in detail. Residence times are of the order of 10 ms^{-1} in the accessible temperature range, with the exchange being slowest for the α-anomer.

The anomeric equilibrium of D-glucose in acidic and basic media has been deduced from the ^{1}H NMR data.[195] The results show that the α-anomer is more abundant in acidic media and the β-anomer more abundant in basic media. These results are discussed in terms of hydrogen bonding.

Hydrogen bonding has also been discussed in a comparative study of the ^{1}H NMR data of aqueous solutions of D-glucose of different concentrations.[196]

The structure of dehydroascorbic acid in solution has been investigated[197] together with its methanol complex.[198] This complex has been shown by ^{1}H and ^{13}C NMR spectroscopy to be a 2-methoxy derivative (*exo* and *endo*) of dehydroascorbic acid in its bicyclic hydrated form.

Several papers have been published on the complexation of carbohydrate derivatives and metal ions.[58–65] Taga *et al.* have discussed the lanthanide-[199] and calcium-[200] induced shifts in the ^{1}H NMR spectra of glyceric acid, gluconic acid and lactobionic acid in D_2O. Complexes between epi-inositol or anhydro hexoses and various lanthanides have also been studied.[201] The proton spectra of some 3,6-anhydro-D-galactose[202] and methylated disaccharide[203] derivatives in the presence of europium shift reagents have been published.

Alfoldi *et al.* have published the ^{1}H NMR spectra of aldoses in D_2O in the presence of molybdate ions[204] and alkali metal sucrates,[205] and borax complexes of D-glucose[206] have been studied.

Stoddard *et al.* have used dynamic ^{1}H NMR spectroscopy in a study of the complexation of chiral crown ethers with different anions.[207–209]

Stopped flow ^{1}H NMR methods have been used to study the conformational changes induced in concanavalin A by Mn^{2+} and Ca^{2+} and methyl-α-D-mannopyranoside.[210]

Finally, Perkin *et al.*[211] have analysed the high resolution proton and carbon spectra of D-glucose, 2-acetamido-D-glucose and related compounds in aqueous media. The implications of systematic errors from assuming first-order conditions for the ^{1}H NMR spectra of sugars are discussed in relation to measuring the shift changes of sugar–enzyme complexes.

B. ^{13}C NMR data

1. Identity of mono- or oligosaccharides

Because ^{13}C chemical shifts are very sensitive to structural changes these data are important for the identification of carbohydrates and their derivatives. The identity of the shift data of an unknown structure with those of a known compound can prove the identity in structure, except for the absolute configuration. Assignment of ^{13}C NMR parameters is not necessary in this application, but the experimental conditions, e.g. solvent, temperature and concentration, have to be identical. ^{13}C chemical shifts of mono- and oligosaccharides and their derivatives have been published in several reviews[2–5] and papers[212–219] and some are given in Section IV.

This has been used in the study of equilibrium mixtures for different types of reactions of monosaccharides[220–223] and their derivatives.[224–236] The progress of a reaction can be monitored[224,230] and reaction intermediates detected[231] by the addition of authentic samples to the reaction mixtures.

2. *Structure determination*

A ^{13}C chemical shift change, as a result of *C*-substitution, is an important parameter for structural elucidation of carbohydrate derivatives. These shift changes, which are sensitive to substitution, reflect the influence of electronegativity and polarizability.[2,3,5] Examples are given in Tables XIV and XV in Section IV.

Elucidation of the anomeric configuration is not possible from the ^{13}C chemical shift alone. However, for pairs of furanoses the signal of the anomeric carbon atom of the compound with a *trans* orientation of the substituents at C-1 and C-2 appears at a higher frequency than the one with a *cis* orientation.[237] The best method for determining the anomeric configuration of pyranoses is from the one-bond coupling for the anomeric carbon atom ($^1J_{C1,H1}$).[5,92,93,94,101,238] The difference in the couplings for the two anomeric configurations is generally about 10 Hz with the value for the equatorial ^{13}C–H coupling being the larger. The one-bond coupling is solvent dependent,[239] so comparison has to be made in the same solvent. For 5-thio-D-galactose a difference of only 1–3 Hz is reported.[240] Assignment of the anomeric configuration for pyranoses has been accomplished from a study of the chemical shifts of carbons other than C-1, particularly C-3 and C-5.[241]

Change of ring size from furanoses and other five-membered rings to the configurationally related six-membered rings is accompanied by an increase in carbon nuclear shielding.[2,126,242] This rule is also valid for lactones.[120] Open chain derivatives show resonances at lower frequencies than those of the corresponding cyclic compounds.[2]

The chemical shift of the quarternary carbon atom of five-membered isopropylidene derivatives, when fused to a furanose ring, is 111·4–115·7 ppm, whereas when fused to a pyranose ring or in a monocyclic derivative the chemical shift is 108·5–111·4 ppm. The shifts of the quarternary carbon atoms in six- or seven-membered isopropylidene derivatives are 97·1–99·5 and 101–102 ppm, respectively.[243,244] Similar data are found for benzylidene derivatives.[245] Information about the ring size of the isopropylidene derivatives is also obtained from the chemical shifts of the methyl groups.[243] The signals from epoxides can readily be assigned from their large (180–190 Hz) one-bond couplings.[246]

Alkylation of oxygen causes rather large high frequency shifts of the α-carbon atoms.[2,3,5,67,68,242,247-254] Similar effects are observed upon glycosidation to oligosaccharides.[3,5] These chemical shift changes give valuable information about the structure of oligosaccharides.[16,255-261] Formation of cyclic acetals also results in a high frequency shift of the furanose or pyranose carbon atoms.[2,262-270]

Acylation of oxygen leads to smaller (1·5–4 ppm) high frequency shifts of the α-carbon atom. However, this decrease in shielding is accompanied by a low frequency shift (1–5 ppm) of the β-carbon atom, so the total effect of several acetyl groups may be difficult to predict. Several papers describe these effects.[164,261,271-277]

The structure of isotopically labelled (e.g. ^{2}H, ^{13}C) compounds in an unknown position may be determined from isotope-induced shifts, as discussed in Section II.B.2, or from couplings.[278] ^{13}C isotope enrichment can also be determined from the peak area or intensity by comparison with a reference peak in the same compound or in another substance.[279]

Valuable information about the stereochemistry of quaternary carbon atoms in branched chain carbohydrates can be obtained from chemical shifts or long range ^{13}C–^{1}H couplings.[280-285] Similarly, ^{13}C chemical shifts of acetals of pyruvic acid[269,270] and of benzylidene acetals[267,268] can be used in the determination of the stereochemistry of the acetal carbon atoms.

The stereochemistry of aglycones has been determined from the ^{13}C chemical shifts of glucopyranosides,[252] and rates of inversion of glucosylbromides have been correlated with the ^{13}C chemical shifts.[70]

3. *Conformational analysis*

^{13}C chemical shifts and ^{13}C–^{1}H couplings have been used in the conformational analysis of carbohydrates.

Perlin and Cyr[99] have published an extensive study of the conformation of furanoses based on the couplings between ^{13}C-1 and ^{13}C-2 and the protons of the five-membered ring. The conformation of pentopyranoses has also been investigated through one-bond ^{13}C–^{1}H couplings.[93]

The conformation of alditols has been investigated by the use of chemical shift relationships.[285-287] Examination of the chemical shifts of the primary carbon atom show that if the conformation in the near vicinity is mainly extended ("linear"), chemical shifts of 64·2–64·6 ppm are observed, whereas a non-linear conformation gives shifts of 63·4–64·1 ppm.[287]

The conformation of the glycosidic linkage in oligosaccharides has been investigated by ^{13}C chemical shifts and long range ^{13}C–^{1}H and ^{13}C–^{13}C couplings.[5] Chemical shifts have been used to determine the conformation of glycosidic bonds, as discussed by several authors.[16,258,288,289] The carbon atom of the aglyconic unit, which is glycosylated, is normally observed

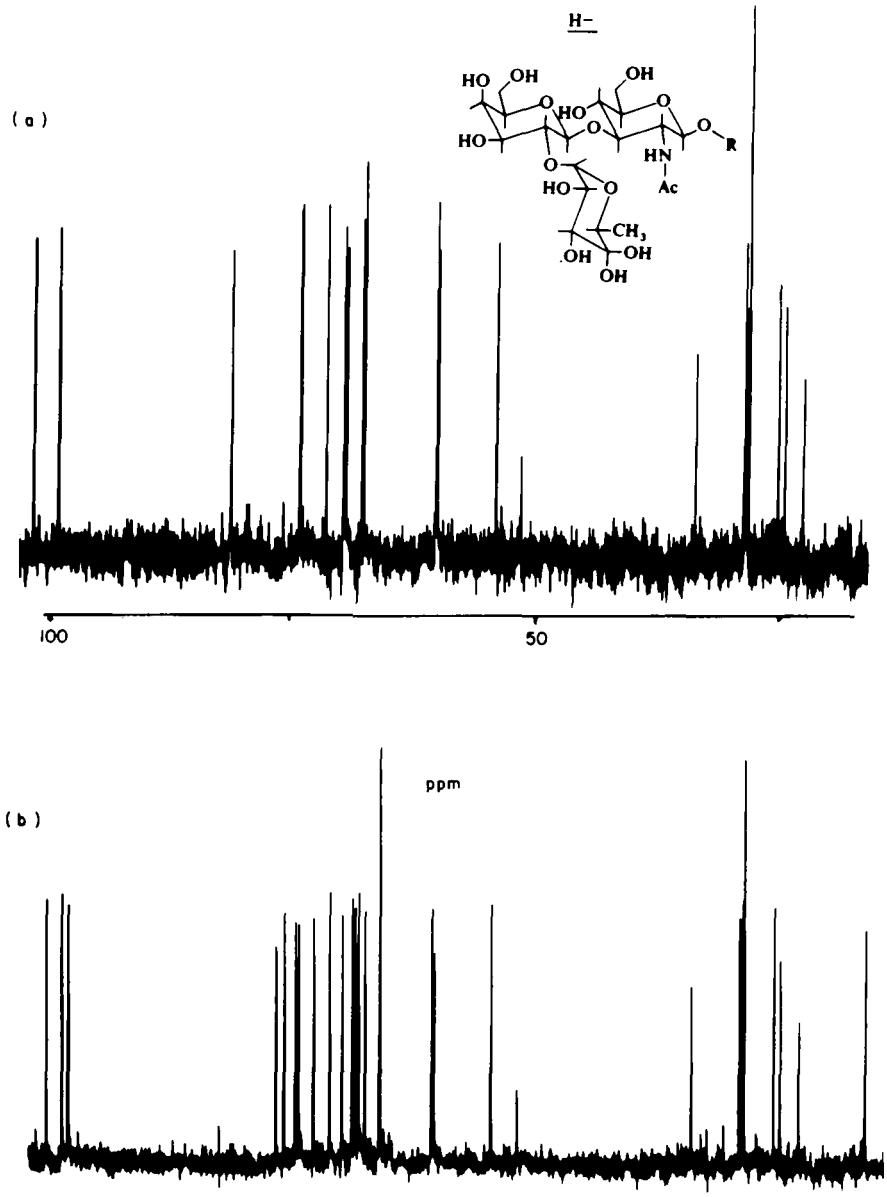

FIG. 13. 67·89 ^{13}C spectrum of blood-group determinants in D_2O at 310 K. (a) Spectrum of 8-methoxycarbonyloctyl 3-*O*-(β-D-galactopyranosyl)-2-acetamido-β-D-glucopyranoside. (b) Spectrum of H-trisaccharide, i.e. an α-L-fucosyl unit added to the 2-position of the β-D-galactopyranose unit. It is clearly seen that the aglyconic carbon atom is shifted to low frequency in this trisaccharide compared to the corresponding disaccharide shown in (a).

towards higher frequency.[3-5] If the interaction between the carbohydrate units becomes severe, a shielding increase may occur due to small valence or bond angle deformations.[16] An example is shown in Fig. 13.

A more accurate determination of the conformation of the glycosidic linkage is obtained by measurement of $^3J_{^{13}C-^1H}$ couplings.[5,16,40,290,291] The two glycosidic torsion angles (ϕ, ψ) can be determined from a Karplus-type relationship between the torsion angle and the size of the coupling.[96-101,292,293]

By this method the conformation of methyl-β-D-cellobioside has been determined for a compound where all protons on carbon atoms carrying a free hydroxyl group are substituted with a deuterium atom. This simplifies the coupled ^{13}C NMR spectrum so the important ^{13}C–O–C–^{1}H couplings are easily determined.[291] Use of ^{13}C–^{13}C couplings also facilitates the determination of the glycosidic conformation.[290]

In a specific application ^{13}C chemical shifts have been used for the estimation of fractional charges on the carbon atoms in β-D-maltose.[294] These results have been correlated with the theoretical calculation of conformers by potential energy functions.

4. *Solution properties*

Excellent information about molecular motion is obtained from ^{13}C spin–lattice relaxation times as discussed in Section II.B.4. If NT_1 is constant for protonated carbon atoms, where N is the number of directly bonded protons, the molecular motion can be considered to be isotropic, provided that the relaxation mechanism is purely dipolar.[5,107,110] It has been shown that the side chain in *N*-acetylneuraminic acid undergoes isotropic motion, except for the C-9 atom.[295] A model involving an intramolecular hydrogen bond network is supported by the relaxation data.

The spin–lattice relaxation times can also be used to estimate different degrees of mobility within the same molecule.[5,108-112,296]

The complexation of monosaccharides with borates,[297-299] molybdate[300] and calcium ions[301,302] has been analysed from ^{13}C chemical shifts. Complexation with paramagnetic reagents has been described in Section II.B.5.[115-118]

The effect of pH on the chemical shifts has been studied[9,4,16,119,289,302,303] and the pK_a values and differences in acid strength of the α/β anomeric forms have been determined for D-glucose, D-mannose and D-fructose.[303]

C. Nuclei other than ^{1}H and ^{13}C

1. *^{3}H NMR*

Elvidge and coworkers have published[304] a detailed study of the six possible isomers of mono ^{3}H-labelled D-glucose. ^{3}H NMR spectra allow

TABLE III

^{3}H Chemical shifts[a] of tritiated D-glucose derivatives compared with the ^{1}H chemical shifts[b] of D-glucose.

Proton	^{3}H	^{1}H	^{3}H–^{1}H difference	^{3}H	^{1}H	^{3}H–^{1}H difference
1	5·15	5·09	0·06	4·57	4·51	0·06
2	3·49	3·41	0·08	3·20	3·13	0·07
3	3·66	3·61	0·05	3·44	3·37	0·07
4	*c.*3·40	3·29		3·36	3·30	0·06
5	3·77	3·72	0·05	3·41	3·35	0·06
6	3·71	3·63	0·08	3·67	3·60	0·07
6	3·79	3·72	0·07	3·84	3·76	0·08

[a] Data taken from reference 304.
[b] Data taken from Table IV, measured at 400 MHz.

a complete assignment of the NMR spectrum of D-glucose in dilute solution. The data are in good accord with the directly measured results obtained at 400 MHz as shown in Table III.

2. *^{15}N NMR*

The application of ^{15}N FT NMR spectroscopy in the study of amino sugars was reviewed by Coxon in 1977.[305] Coxon also published the first natural abundance ^{15}N spectra of carbohydrate derivatives in 1974,[306] together with data for the ^{15}N-enriched samples of 6-deoxy-1,2–3,4-di-*O*-isopropylidene-6[^{15}N]-phtalimido-α-D-galactopyranose and 6-deoxy-1,2-3,5-di-*O*-isopropylidene-6[^{15}N]-phtalimido-α-D-glucofuranose. A full account of the work, including ^{15}N–^{13}C couplings and a study of the complexation of these derivatives with Cu^{2+}, has appeared.[307]

Botto and Roberts have reported the ^{15}N chemical shift data obtained from natural abundance 2-amino-2-deoxy-D-hexopyranose, hydrochlorides and their acetamido derivatives.[308]

^{15}N and ^{13}C NMR spectroscopy have furthermore been used in a structural study of bis(methyl-2-*O*-acetyl-4,6-*O*-benzylidene-3-deoxy-α-D-altropyranosid-3-yl)amine. The configuration and conformation of the compound have been determined and its unusually large $^1J_{^{15}N-^1H}$ value discussed.[309]

Similarly, ^{15}N and ^{13}C NMR spectroscopy have been used to determine the pK_a values of an amino sugar, apramycin.[310]

3. *^{19}F NMR*

The use of ^{19}F NMR spectroscopy in carbohydrate chemistry has been discussed extensively in a recent review.[28]

Hadfield *et al.*[311] have recently described the synthesis of 4-amino-4,6-dideoxy-6-fluoro-α-D-galactopyranosyl-4-amino-4,6-dideoxy-6-fluoro-α-D-galactopyranoside. The ^{19}F NMR spectra of the salts of this compound reveal an unexpected conformation about the C-5—C-6 bond, due to the dipolar attraction between the C-6—F and C-4—N^+ bonds.

^{19}F and also ^{31}P NMR spectroscopy have been measured on reaction mixtures of 1,6-anhydro-2,3,4-tri-*O*-benzyl-β-D-glucopyranose and PF_5 with different mole ratios in the temperature range of −40 to −80 °C. The PF_4O, PF_6^-, POF_3 and sugar–PF_5 complex species are determined by ^{19}F and ^{31}P NMR[312] and a polymerization mechanism of the anhydro sugar with PF_5 has been discussed.

The enhanced sensitivity of ^{19}F FT NMR spectroscopy over the continuous wave technique has made it a powerful tool in the analysis of fluorinated carbohydrate derivatives.[313]

4. *^{31}P NMR*

Several reports on the application of ^{31}P NMR spectroscopy in carbohydrate chemistry have appeared;[314–317] however, most of the data in the literature are concerned with the study of nucleosides, which is beyond the scope of this review.

5. *Miscellaneous*

^{11}B NMR has been used in a study of the complexation of carbohydrate derivatives with benzene boronic acid.[318]

^{17}O NMR has been applied in a study of hydration of monosaccharides.[319] Gorin and Mazurek have reported the ^{17}O NMR spectra of 18 hydroxyether and acetate derivatives of monosaccharides. Most of the compounds were prepared by isotopic exchange with $H_2{}^{17}O$.[320]

Laszlo and coworkers have studied the complexation of carbohydrates and sodium through ^{23}Na NMR data in two papers.[321,322]

Haines has assigned the ^{29}Si chemical shifts of some trimethylsilyl derivatives of methyl-α-D-glucopyranoside. Double resonance spectra taken in the presence of $Pr(dpm)_3$ enable the ^{19}Si and ^{1}H signals to be connected and the ^{19}Si assignments are completed from selective deuteration data. The lanthanide-induced effects on the ^{29}Si and ^{1}H signals in the TMS groups are discussed.[323,324]

Hall and coworkers have described the heteronuclear couplings between ^{13}C and ^{119}Sn, ^{199}Hg and ^{205}Tl respectively in carbohydrate derivatives,[325–327] and Gagnaire *et al.*[328] the ^{13}C–^{13}C couplings in uniformly ^{13}C-enriched carbohydrates. Finally, Mazurek *et al.* have described ^{13}C–^{11}B couplings for borate complexes of carbohydrates.[329]

IV. TABLES

TABLE IV

^{1}H chemical shifts[a] and couplings[b] (in parenthesis) of D-aldohexoses.[c]

Compound	H-1	H-2	H-3	H-4	H-5	H-6	H-6′
D-*Hexopyranoses*							
α-glu	5·09	3·41	3·61	3·29	3·72	3·72	3·63
	(3·6)	(9·5)	(9·5)	(9·5)		(2·8)	(5·7, 12·8)
β-glu	4·51	3·13	3·37	3·30	3·35	3·75	3·60
	(7·8)	(9·5)	(9·5)	(9·5)		(2·8)	(5·7, 12·8)
α-gal	5·16	3·72	3·77	3·90	4·00	3·70	– 3·62
	(3·8)	(10·0)	(3·8)	(1·0)		(6·4)	(6·4)
β-gal	4·48	3·41	3·56	3·84	3·61	3·70	– 3·62
	(8·0)	(10·0)	(3·8)	(1·0)		(3·8)	(7·8)
α-man	5·05	3·79	3·72	3·52	3·70	3·74	3·63
	(1·8)	(3·8)	(10·0)	(9·8)		(2·8)	(6·8, 12·2)
β-man	4·77	3·85	3·53	3·44	3·25	3·74	3·60
	(1·5)	(3·8)	(10·0)	(9·8)		(2·8)	(6·8, 12·2)
β-all	4·76	3·30	4·05	3·51	3·66	3·76	3·57
	(8·5)	(3·3)	(3·2)	(9·5)		(2·4)	(6·0, 12·8)
β-gul	4·76	3·52	3·95	3·70	3·92	3·62	– 3·58
	(8·3)	(3·6)	(3·6)	(0·8)		(6·0)	(6·0)

[a] Measured at 400 MHz in D_2O at 296 K relative to internal acetone (2·12 ppm).
[b] Observed first-order couplings (±0·2 Hz).
[c] Data taken from reference 330.

TABLE V

^{1}H chemical shifts[a] and couplings[b] (in parenthesis) of D-aldopentoses.[c]

Compound	H-1	H-2	H-3	H-4	H-5e	H-5a
D-*Pentopyranoses*						
β-xyl	4·47	3·14	3·33	3·51	3·82	3·22
	(7·8)	(9·2)	(9·0)		(5·6)	(10·5, 11·4)
α-xyl	5·09	3·42	3·48	3·52	3·58	3·57
	(3·6)	(9·0)	(9·0)		(7·5)	(7·5)
β-ara	5·12	3·70	3·77	3·89	3·54	3·91
	(3·6)	(9·3)	(9·8)		(2·5)	(1·7, 13·5)
α-ara	4·40	3·40	3·55	3·83	3·78	3·57
	(7·8)	(9·8)	(3·6)		(1·8)	(1·3, 13·0)
α-rib	4·75	3·71	3·83	3·77	3·82	3·50
	(2·1)	(3·0)	(3·0)		(5·3)	(2·6, 12·4)
β-rib	4·81	3·41	3·98	3·77	3·72	3·57
	(6·5)	(3·3)	(3·2)		(4·4)	(8·8, 11·4)
α-lyx	4·89	3·69	3·78	3·73	3·71	3·58
	(4·9)	(3·6)	(7·8)		(3·8)	(7·2, 12·1)
β-lyx	4·74	3·81	3·53	3·73	3·84	3·15
	(1·1)	(2·7)	(8·5)		(5·1)	(9·1, 11·7)

[a] Measured at 400 MHz in D_2O at 296 K relative to internal acetone (2·12 ppm).
[b] Observed first-order couplings (±0·2 Hz).
[c] Data taken from reference 330.

TABLE VI

^{1}H chemical shifts[a] and couplings[b] (in parenthesis) for methyl-D-hexosides in D_2O.[c]

Compound	H-1	H-2	H-3	H-4	H-5	H-6	H-6′	OMe
D-*Hexopyranosides*								
α-glu	4·70	3·46	3·56	3·29	3·54	3·77	3·66	3·31
	(4·0)	(10·0)	(10·0)	(10·0)		(2·8, 12·8)	(5·8)	
β-glu	4·27	3·15	3·38	3·27	3·36	3·82	3·62	3·46
	(8·2)	(9·6)	(9·6)	(9·6)		(2·4, 12·8)	(6·4)	
α-gal	4·73	3·72	3·68	3·86	3·78	3·67[d]	3·61[d]	3·31
	(3·0)	(9·8)	(2·3)	(1·0)		(8·2, 12·0)[d]	(4·6)[d]	
β-gal	4·20	3·39	3·53	3·81	3·57	3·69	3·64	3·45
	(8·0)	(10·0)	(3·8)	(0·8)		(7·6, 11·2)	(4·4)	
α-man	4·66	3·82	3·65	3·53	3·51	3·79	3·65	3·30
	(1·6)	(3·5)	(10·0)	(10·0)		(1·9, 12·0)	(5·8)	
β-man	4·47	3·88	3·53	3·46	3·27	3·83	3·63	3·44
	(0·9)	(3·2)	(10·0)	(10·0)		(2·2, 12·2)	(6·7)	

[a] Measured at 400 MHz in D_2O at 296 K relative to internal acetone (2·12 ppm).
[b] Observed first-order couplings.
[c] Data taken from reference 330.
[d] Values obtained through ABX analyses.

TABLE VII

^{1}H chemical shifts[a] and couplings[b] (in parenthesis) for methyldeoxy-D-aldopyranosides in D_2O.[c]

Compound	H-1	H-2e	H-2a	H-3	H-4	H-5	H-6	H-6′	OMe
D-*Hexopyranosides*									
α-2-deoxyglu	4·81	2·23	1·59	3·73	3·25	3·51	3·75	3·65	3·26
	(1·0, 3·8)	(14·0, 2·4)	(12·0)	(9·9)	(9·9)		(2·3, 12·2)	(5·8)	
β-2-deoxyglu	4·54	2·15	1·36	3·62	3·15	3·28	3·84	3·63	3·42
	(2·0, 10·0)	(13·0, 5·0)	(12·0)	(9·5)	(9·9)		(2·2, 12·3)	(6·0)	
α-6-deoxygal	4·64	3·67		3·70	3·68	3·92	1·11		3·28
	(2·8)	(m)[d]		(m)[d]	(1·0)	(6·3)			
β-6-deoxygal	4·19	3·36		3·52	3·62	3·69	1·15		3·44
	(8·2)	(10·0)		(3·6)	(0·8)	(6·6)			
α-6-deoxyglu	4·64	3·47		3·51	3·04	3·61	1·17		3·30
	(3·6)	(9·2)		(9·5)	(9·6)	(6·3)			
β-6-deoxyglu	4·25	3·15		3·33	3·04	3·38	1·19		3·44
	(8·2)	(9·8)		(9·5)	(9·5)	(6·6)			
α-6-deoxyman	4·59	3·82		3·60	3·33	3·56	1·19		3·29
	(1·6)	(3·5)		(9·5)	(9·5)	(6·2)			
β-6-deoxyman	4·43	3·87		3·48	3·26	3·29	1·21		3·42
	(0·9)	(3·3)		(9·2)	(m)[d]	(m)[d]			

[a] Measured at 400 MHz in D_2O at 296 K relative to internal acetone (2·12 ppm).
[b] Observed first-order couplings.
[c] Data taken from reference 330.
[d] (m) = unresolved multiplet.

TABLE VIII

^{1}H chemical shifts[a] and couplings[b] (in parenthesis) for methyl-D-pentosides in D_2O.[c]

Compound	H-1	H-2	H-3	H-4	H-5e	H-5a	OMe
D-*Pentopyranosides*							
α-ara	4·16	3·43	3·57	3·85	3·82	3·57	3·44
	(8·0)	(10·0)	(3·9)		(2·8, 13·8)	(1·0)	
β-ara	4·72	3·74	3·72	3·89	3·55	3·77	3·30
	(2·8)	(10·0)	(3·0)		(2·3, 13·0)	(1·0)	
α-lyx	4·58	3·77	3·68	3·76	3·69	3·42	3·32
	(3·2)	(3·8)	(4·0)		(4·8, 12·0)	(9·0)	
β-lyx	4·51	3·14	3·60	3·75	3·89	3·23	3·37
	(2·2)	(3·8)	(7·5)		(4·0, 12·5)	(7·5)	
α-rib	4·51	3·70	3·86	3·72	3·47	3·68	3·35
	(3·0)	(3·2)	(3·2)				
β-rib	4·52	3·51	3·91	3·79	3·74	3·61	3·37
	(5·1)	(3·4)	(3·4)		(3·5, 12·5)	(7·0)	
α-xyl	4·67	3·44	3·53	3·47	3·59	3·39	3·30
	(3·4)	(10·0)			(5·0, 11·0)	(11·0)	
β-xyl	4·21	3·14	3·33	3·51	3·88	3·21	3·44
	(7·9)	(9·5)	(9·5)		(5·5, 12·3)	(11·0)	

[a] Measured at 400 MHz in D_2O at 296 K relative to internal acetone (2·12 ppm).
[b] Observed first-order couplings.
[c] Data taken from reference 330.

TABLE IX

^{1}H chemical shifts[a] and couplings[b] (in parenthesis) for 2-deoxy-2-*N*-acetamido-D-hexopyranosides.[c]

Compound	H-1	H-2	H-3	H-4	H-5	H-6	H-6′
Methyl-α-	4·67	4·05	3·75	3·91	3·79	3·67	3·62
D-GalNAc	(3·6)	(10·8)	(3·2)	(0·8)		(6·0)	(6·0)
Methyl-β-	4·29	3·78	3·61	3·84	3·52	3·71	3·66
D-GalNAc	(8·4)	(10·5)	(3·2)	(0·8)		(7·7, 11·9)	(4·2)
Methyl-β-	4·39	3·61	3·47	3·32	3·32	3·80	3·65
D-GlcNAc	(8·4)	(9·6)	(9·2)	(9·2)		(1·6, 12·0)	(4·8)

[a] Measured at 400 MHz in D_2O at 310 K relative to internal acetone (2·12 ppm).
[b] Observed first-order coupling constants.
[c] Data taken from reference 330.

TABLE X

^{13}C chemical shifts for some aldoses.[a]

Compound	C-1	C-2	C-3	C-4	C-5	C-6
D-*Hexopyranoses*						
α-all	93·7	67·9	72·0	66·9	67·7	61·6
β-all	94·3	72·2	72·0	67·7	74·4	62·1
α-alt	94·7	71·2	71·1	66·0	72·0	61·6
β-alt	92·6	71·6	71·3	65·2	75·0	62·5
α-gal	93·2	69·4	70·2	70·3	71·4	62·2
β-gal	97·3	72·9	73·8	69·7	76·0	62·0
α-glu	92·9	72·5	73·8	70·6	72·3	61·6
β-glu	96·7	75·1	76·7	70·6	76·8	61·7
α-gul	93·6	65·5	71·6	70·2	67·2	61·7
β-gul	94·6	69·9	72·0	70·2	74·6	61·8
β-ido	93·9	71·1[b]	68·8[b]	70·6[b]	75·6[b]	62·1
α-ido	93·6	73·6[b]	72·7[b]	70·6[b]	73·6[b]	59·4
α-man	95·0	71·7	71·3	68·0	73·4	62·1
β-man	94·6	72·3	74·1	67·8	77·2	62·1
α-tal	95·5	71·7	66·0	70·6	72·0	62·4
β-tal	95·0	72·5[b]	69·6[b]	69·4	76·5	62·2
D-*Pentopyranoses*						
α-ara	97·6	72·9	73·5	69·6	67·2	
β-ara	93·4	69·5	69·5	69·5	63·4	
α-lyx	94·9	71·0	71·4	68·4	63·9	
β-lyx	95·0	70·9	63·5	67·4	65·0	
α-rib	94·3	70·8	70·1	68·1	63·8	
β-rib	94·7	71·9	69·7	68·2	63·8	
α-xyl	93·1	72·5	73·9	70·4	61·9	
β-xyl	97·5	75·1	76·8	70·2	66·1	
D-*Hexofuranoses*						
α-all	96·8	72·4	[c]	84·3	70·2	63·1
β-all	101·6	76·1	73·3	83·0	71·7	63·3
α-alt	102·2	82·4	76·9	84·3	72·5	63·3
β-alt	96·2	77·5	76·0	82·1	73·4	63·3
α-gal	95·8	77·1	75·1	81·6	[c]	63·3
β-gal	101·8	82·2	76·6	82·8	71·5	63·6
β-glu	103·7	81·8[b]	[c]	82·1[b]	[c]	[c]
α-gul	97·3	[c]	[c]	80·4	[c]	62·6
β-gul	101·4	78·1	[c]	80·3	[c]	63·2
α-ido	102·5	78·6	75·6[b]	82·2	70.3[b]	63·4
β-ido	96·3	77·0	75.9[b]	81·6	71·7[b]	63·4
α-tal	101·8	76·1	72·7	82·7	71·6	63·7
β-tal	97·3	71·6	72·0	83·3	[c]	63·8
D-*Pentofuranoses*						
α-ara	101·9	82·3	76·5	83·8	62·0	
β-ara	96·0	77·1	75·1	82·2	62·0	
α-lyx	101·5	77·8	71·9	80·7	61·9	

TABLE X (*continued*)

^{13}C chemical shifts for some aldoses.[a]

Compound	C-1	C-2	C-3	C-4	C-5	C-6
α-rib	97·1	71·7	70·8	83·8	62·1	
β-rib	101·7	76·0	71·2	83·3	63·3	
D,L-*Erythrose*						
α-furanose	96·8	72·4	70·6	72·9		
β-furanose	102·4	77·7	71·7	72·4		
hydrate	90·8	74·9	73·0	64·0		
D,L-*Threose*						
α-furanose	103·4	82·0	76·4	74·3		
β-furanose	97·9	77·5	76·2	71·8		
hydrate	91·1	74·6	72·2	64·4		
D,L-*Glyceraldehyde*						
hydrate	91·2	75·5	63·4			
Glycolaldehyde						
hydrate	91·2	66·0				
Formaldehyde						
hydrate	83·3					

[a] Data taken from reference 2.
[b] Assignments may be reversed.
[c] Not resolved.

TABLE XI

^{13}C chemical shifts for some methyl aldosides.[a]

Compound	C-1	C-2	C-3	C-4	C-5	C-6	OMe
D-*Hexopyranosides*							
α-all	100·0	68·3	72·1	68·0	67·3	61·7	56·3
β-all	101·9	72·2	71·4	68·0	74·8	62·2	58·0
α-alt	101·1	70·0	70·0	64·8	70·0	61·3	55·4
β-alt	100·4	70·7	70·2	65·6	75·6	61·7	57·7
α-gal	100·1	69·2	70·5	70·2	71·6	62·2	56·0
β-gal	104·5	71·7	73·8	69·7	76·0	62·0	58·1
α-glu	100·0	72·2	74·1	70·6	72·5	61·6	55·9
β-glu	104·0	74·1	76·8	70·6	76·8	61·8	58·1
α-gul	100·4	65·5	71·4	70·4	67·3	62·0	56·3
β-gul	102·6	69·1	72·3	70·5	74·9	62·1	58·1
α-ido	101·5	70·9	71·8	70·3	70·8	60·2	55·8
α-man	101·9	71·2	71·8	68·0	73·7	62·1	55·9
β-man	101·3	70·6	73·3	67·1	76·6	61·4	56·9
α-tal	102·2	70·7	66·2	70·3	72·1	62·3	55·6
D-*Pentopyranosides*							
α-ara	107·0	73·9	75·6	71·5	69·3		60·0
β-ara	103·0	72·1	70·1	71·4	65·7		58·1
α-lyx	102·0	70·4	71·6	67·7	63·3		55·9
α-rib	100·4	69·2	70·4	67·4	60·8		56·7
β-rib	103·1	71·0	68·6	68·6	63·9		57·0
α-xyl	100·6	72·3	74·3	70·4	62·0		56·0
β-xyl	105·1	74·0	76·9	70·4	66·3		58·3
D-*Hexofuranosides*							
α-all	103·8	72·3	69·9	85·9	72·7	63·5	56·6
β-all	109·0	75·6	72·7	83·4	73·8	63·9	56·4
α-gal	103·8	78·2	76·2	83·1	74·5	64·1	57·2
β-gal	109·9	81·3	78·4	84·7	71·7	63·6	55·6
α-glu	104·0	77·7	76·6	78·8	70·7	64·2	57·0
β-glu	110·0	80·6	75·8	82·3	70·7	64·7	56·3
α-man	109·7	77·9	72·5	80·5	70·6	64·5	57·2
β-man	103·6	73·1	71·2[b]	80·7	71·0[b]	64·4	56·8
D-*Pentofuranosides*							
α-ara	109·2	81·8	77·5	84·9	62·4		56·0
β-ara	103·1	77·4	75·7	82·9	62·4		56·3
α-lyx	109·2	77·0	72·2	81·4	61·5		56·9
β-lyx	103·3	73·2	71·0	82·1	62·7		56·7
α-rib	103·1	71·1	69·8	84·6	61·9		55·5
β-rib	108·0	74·3	70·9	83·0	62·9		55·3
α-xyl	103·0	77·8	76·2	79·3	61·6		56·7
β-xyl	109·7	81·0	76·0	83·6	62·2		56·4
D-*Tetrofuranosides*							
α-ery	103·6	72·8	69·9	73·6			56·7
β-ery	109·6	76·4	71·4	72·6			56·6
α-thr	109·4	80·5	76·4	73·7			55·5
β-thr	103·8	77·4	75·8	72·0			56·2

[a] Data taken from reference 2.
[b] Assignment may be reversed.

TABLE XII

^{13}C chemical shifts for some ketoses and their methyl glycosides.[a]

Compound	C-1	C-2	C-3	C-4	C-5	C-6	OMe
D-*Hexopyranoses*							
α-fru	65·9	—	70·9	71·3	—	—	
β-fru	64·7	99·1	68·4	70·5	70·0	64·1	
α-psi	64·0	98·4	66·4	72·6	66·7	58·8	
β-psi	64·8	99·2	71·2	65·9	69·8	65·0	
α-sor	64·5	98·5	71·4	74·8	70·3	62·7	
α-tag	64·8	99·0	70·7	71·8	67·2	63·1	
β-tag	64·4	99·1	64·6	70·7	70·1	61·0	
D-*Hexofuranoses*							
α-fru	63·8	105·5	82·9	77·0	82·2	61·9	
β-fru	63·6	102·6	76·4	75·4	81·6	63·2	
α-psi	64·2	104·0	71·2	71·2	83·6	62·2	
β-psi	63·3	106·4	75·5	71·8	83·6	63·7	
α-sor	64·3	102·5	77·0	76·2	78·6	61·6	
α-tag	—	105·7	77·6	71·9	80·0	—	
β-tag	63·5	103·3	71·7	71·8	80·9	61·9	
D-*Hexopyranosides*							
β-fru	61·8	101·4	69·3	70·5	70·0	64·7	49·3
α-psi	61·1	100·7	67·3	72·1	66·7	58·9	49·1
β-psi	57·7	102·6	69·7	65·7	69·9	65·4	48·7
α-sor	61·2	100·9	72·0	74·5	70·1	63·0	49·2
α-tag	61·0	102·4	69·6	71·7	66·8	63·4	48·5
β-tag	61·7	101·4	65·5	71·5[b]	70·4[b]	61·1	49·3
D-*Hexofuranosides*							
α-fru	58·7	109·1	81·0	78·2	84·0	62·1	49·1
β-fru	60·0	104·7	77·7	75·9	82·1	63·6	49·8
α-sor	60·7	104·2	80·0	76·5	78·8	61·6	49·9
β-sor	57·7	109·9	80·3	77·2	83·4	62·1	49·3
α-tag	58·8	108·7	75·2	71·9	80·6	60·8	49·6
β-tag	60·3	105·3	73·4	71·7	82·0	61·9	49·8

[a] Data taken from reference 2.
[b] Assignment may be reversed.

TABLE XIII

^{13}C chemical shifts for some aromatic glycosides.[a]

Compound	C-1	C-2	C-3	C-4	C-5	C-6
Phenyl-D-glucopyranosides						
α	97·9	72·0	73·3	70·2	73·9	61·1
β	103·1	75·8	79·5	72·4	79·3	63·6
α *p*-NO_2	100·5	74·1	76·9	72·5	75·8	63·5
β *p*-NO_2	102·7	76·0	80·1	72·4	79·3	63·5
β *m*-NO_2	103·6	76·1	80·0	72·6	79·2	63·6
β *o*-NO_2	103·3	76·0	80·1	72·4	79·5	63·5
Phenyl-D-galactopyranosides						
β	104·0	73·6	76·4	71·3	78·3	63·7
α *p*-NO_2	100·8	75·5	71·2	70·5	72·1	63·0
β *p*-NO_2	103·4	73·2	76·1	71·1	78·6	63·5
β *m*-NO_2	104·2	73·3	76·1	71·1	78·7	63·5
β *o*-NO_2	104·1	73·2	76·3	71·1	78·7	63·5
Phenyl-D-mannopyranosides						
α *p*-NO_2	101·5	73·4	72·5	69·5	78·0	63·8

[a] Data taken from reference 2.

TABLE XIV

^{13}C chemical shifts for some peracetylated pyranoses and furanoses.[a]

Compound	C-1	C-2	C-3	C-4	C-5	C-6
D-*Hexopyranoses*						
β-all	90·1	68·2	68·2	65·8	71·2	61·9
α-alt	90·2	68·2	66·4	64·4	66·4	62·1
α-gal	89·5	67·2	67·2	66·2	68·5	61·0
β-gal	91·8	67·8	70·6	66·8	71·5	61·0
α-glu	89·2	69·4	70·0	68·1	70·0	61·1
β-glu	91·8	70·5	72·8	68·1	72·8	61·7
β-gul	89·7	67·3[b]	67·1[b]	67·1[b]	71·1	61·3
α-ido	90·4	65·9	66·2	65·9	66·2	61·8
α-man	90·4	68·6	68·2	65·4	70·5	62·0
α-tal	91·4	65·2[b]	66·3[b]	65·3[b]	68·8[b]	61·5
D-*Pentopyranoses*						
α-ara	92·2	68·2	69·9	67·3	63·8	
β-ara	90·4	67·3	68·7	66·9	62·9	
α-lyx	90·7	68·2	68·2	66·6	61·9	
α-rib	88·7	67·1	65·6	66·5	59·3	
β-rib	90·7	67·1	66·0	66·0	62·5	
α-xyl	88·9	69·2	69·2	68·8	60·5	
β-xyl	91·7	69·3	70·8	68·1	62·5	
D-*Pentofuranoses*						
α-ara	99·4	80·6	76·9	82·4	63·1	
β-ara	93·7	75·4	74·8	79·7	64·5	
α-lyx	98·0	75·0	70·6	77·0	62·4	
β-lyx	93·2	70·5	68·5	77·7	62·8	
α-rib	94·1	70·0	69·8	81·6	63·3	
β-rib	98·1	74·1	70·5	79·2	63·6	
α-xyl	92·8	75·3	73·8	75·4	61·6	
β-xyl	98·9	79·4	74·3	79·9	62·3	

[a] Data taken from reference 2.
[b] Assignment may be reversed.

TABLE XV

^{13}C chemical shifts for some tetra-*O*-acetyl-D-glycopyranosyl derivatives.[a]

Compound	C-1	C-2	C-3	C-4	C-5	C-6	Me
D-*Gluco derivatives*							
α-azide	86·1	69·7	69·8	68·1	70·1	61·7	
β-azide	87·3	70·3	72·2	67·6	73·6	61·4	
α-bromide	86·5	70·4[b]	72·0[b]	67·0	70·0[b]	60·8	
α-chloride	89·5	70·2[b]	70·3[b]	66·8[b]	68·8[b]	60·4	
β-chloride	87·1	72·4	73·0	67·2	74·9	61·2	
β-cyanide	66·8	69·4	73·3	67·8	77·3	61·8	114·5
α-fluoride	103·5	69·9	69·1	67·1	69·6	61·0	
β-fluoride	105·7	70·6	71·4	67·0	71·5	61·3	
α-*O*-methyl	96·3	70·4	69·7	68·2	66·8	61·5	55·6
β-*O*-methyl	101·1	70·9	72·5	68·1	71·4	61·6	56·6
α-*O*-phenyl	94·3	70·5	70·1	68·4	68·1	61·7	
β-*O*-phenyl	98·8	71·1	71·8	68·2	72·5	61·8	
α-*N*-phenyl	80·1	65·8	71·0	68·5	72·1	61·7	
β-*N*-phenyl	84·0	70·4	72·1	68·7	72·8	62·0	
α-*S*-ethyl	81·8	70·8[b]	70·6	68·7	67·6[b]	62·0	
β-*S*-ethyl	83·2	69·6[b]	73·4[b]	68·2[b]	75·6[b]	61·9	
α-*S*-methyl	83·0	71·0[b]	70·7[b]	68·9[b]	67·7[b]	62·1	12·4
β-*S*-methyl	82·3	68·7[b]	72·5[b]	68·0[b]	75·5[b]	61·8	
α-*O*-methyl benzoate	96·8	71·8	70·3	69·4	67·5	62·9	55·4
Methyl-D-glycopyranosides							
β-all	99·3	68·9	68·2	66·1	70·0	62·1	56·0
α-alt	98·2	64·6[b]	66·6[b]	64·1[b]	68·9[b]	62·2	55·0
α-gal	96·5	67·6	67·6	67·0	65·7	61·2	54·8
β-gal	101·5	68·5	70·2	66·8	70·6	61·0	56·6
α-man	98·1	69·1	68·8	65·8	68·0	62·1	54·9
α-ara	101·9	69·3	70·4	67·9	63·2		56·6
β-ara	97·6	68·4	69·3	67·2	60·3		55·4
α-lyx	98·4	69·3	68·2	66·6	59·4		54·9
α-rib	97·5	67·5	67·4	66·1	57·9		56·2
β-rib	99·4	68·3	66·0	66·9	61·1		55·7
α-xyl	96·4	70·5	69·1	68·8	57·7		54·7
β-xyl	101·0	70·2	71·0	68·3	61·3		55·8

[a] Data taken from reference 2.
[b] Assignment may be reversed.

TABLE XVI

^{13}C chemical shifts for some oligosaccharides.[a]

Compound	C-1	C-2	C-3	C-4	C-5	C-6
Sucrose	92·9	72·0	73·6	70·2	73·3	61·1
	63·3	104·4	77·4	75·0	82·2	63·4
α,α-Trehalose	94·0	72·0	73·5	70·6	73·0	61·5
β,β-Trehalose	100·7	74·2	77·3	71·1	77·3	62·5
α,β-Trehalose	100·9	72·4	73·8	70·4	73·6	61·6
	103·6	74·1	76·4	70·4	77·0	62·0
α-Lactose	103·6	72·0	73·5	69·5	76·2	62·0
	92·7	72·2	72·4	79·3	71·0	61·0
β-Lactose	103·7	72·0	73·5	69·5	76·2	62·0
	96·6	74·8	75·3	79·2	75·6	61·1
α-Cellobiose	103·3	74·1	76·5	70·4	76·8	61·6
	92·7	72·3	72·3	79·6	71·0	61·1
β-Cellobiose	103·3	74·1	76·5	70·4	76·8	61·6
	96·6	74·9	75·3	79·5	75·6	61·1
α-Maltose	101·1	73·2	74·3	70·8	74·0	62·0
	93·2	72·7	74·5	78·9	71·4	62·0
β-Maltose	101·1	73·1	74·3	70·8	74·0	62·0
	97·2	75·4	77·5	78·6	76·0	62·2
α-Nigerose	99·8	72·8	74·1	71·3	72·8	61·8
	93·1	71·3	80·8	70·6	72·2	61·8
β-Nigerose	99·8	72·8	74·1	71·3	72·8	61·8
	97·0	74·1	83·2	70·6	76·6	61·8
α-Laminaribiose	103·9	74·8	77·1	71·2	77·1	62·4
	93·4	72·2	84·2	69·6	72·4	62·4
β-Laminaribiose	103·9	74·8	77·1	71·2	77·1	62·4
	97·2	74·8	86·7	69·6	77·1	62·4
α-Kojibiose	97·5	73·1	74·4	71·1	73·1	62·0
	90·8	77·1	73·1	71·1	73·1	62·0
β-Kojibiose	99·0	73·1	74·4	71·1	73·1	62·0
	97·5	79·9	75·8	71·1	77·1	62·0
α-Sophorose	105·1	74·9	77·2	71·1	77·2	62·4
	93·1	82·1	73·2	71·1	72·5	62·4
β-Sophorose	103·9	74·9	77·2	71·1	77·2	62·4
	95·8	82·8	77·2	71·1	77·2	62·4
α-Isomaltose	99·4	73·3	75·0	71·3	73·8	62·5
	93·8	73·3	75·0	71·3	71·3	67·4
β-Isomaltose	99·4	73·3	75·0	71·3	73·8	62·5
	97·7	75·9	77·7	71·3	75·9	67·4
α-Gentiobiose	103·8	74·5	77·1	71·1	77·1	62·5
	93·3	72·9	74·5	71·1	71·8	70·2
β-Gentiobiose	103·8	74·5	77·1	71·1	77·1	62·5
	97·2	75·5	77·1	71·1	76·1	70·2

[a] Data taken from references 5 and 251.

ACKNOWLEDGMENT

One of the authors (K.B.) wishes to thank Professor R. U. Lemieux, Edmonton, Canada for access to 400 MHz facilities and for stimulating discussions during the period where this paper was prepared.

REFERENCES

1. T. D. Inch, in *Annual Reports on NMR Spectroscopy*, Vol. 5A (ed. G. Webb), Academic Press, London, 1972, p. 305.
2. K. Bock and C. Pedersen, *Advan. Carbohyd. Chem. Biochem.*, in press.
3. P. A. J. Gorin, *Advan. Carbohyd. Chem. Biochem.*, 1980, **38**, 13.
4. H. Sugiyama, *Heterocycles*, 1978, **11**, 615.
5. B. Coxon, *Dev. Food Carbohyd.*, 1980, **2**, 351.
6. D. B. Davis, *Progr. NMR Spectrosc.*, 1978, **12**, 135.
7. *Specialist Periodical Report on Carbohydrate Chemistry*, Vols 1–11, The Chemical Society, London, 1968–80.
8. *Specialist Periodical Report on Nuclear Magnetic Resonance Spectroscopy*, Vols 1–10, The Chemical Society, London, 1972–81.
9. G. Kotowycz and R. U. Lemieux, *Chem. Rev.*, 1973, **73**, 669.
10. B. Coxon, *Advan. Carbohyd. Chem. Biochem.*, 1972, **27**, 7.
11. L. D. Hall, in *The Carbohydrates*, Vol. 1B, 1980, p. 1299 (ed. W. Pigman and D. Horton), Academic Press, New York, 1980.
12. F. W. Wehrli and T. Wirthlin, *Interpretation of Carbon-13 NMR Spectra*, Heyden, London, 1976.
13. M. L. Martin, J.-J. Delpuech, *Practical NMR Spectroscopy*, Heyden, London, 1980.
14. E. Breitmaier and W. Voelter, *13-C NMR Spectroscopy*, Verlag Chemie, Weinheim, 1974.
15. J. B. Stothers, *Carbon-13 NMR Spectroscopy*, Academic Press, New York, 1972.
16. R. U. Lemieux, K. Bock, L. T. J. Delbaere, S. Koto and V. S. Rao, *Canad. J. Chem.*, 1980, **58**, 631.
17. J. Dabrowski, P. Hanfland and H. Egge, *Biochemistry*, 1980, **19**, 5652.
18. R. U. Lemieux and K. Bock, *Jap. J. Antibiotics*, 1979, **32**, s163.
19. A. De Bruyn, M. Anteunis and J. van Beeumen, *Bull. Soc. Chem. Belg.*, 1977, **86**, 259.
20. A. De Bruyn and M. Anteunis, *Bull. Soc. Chem. Belg.*, 1975, **84**, 799.
21. A. De Bruyn and M. Anteunis, *Bull. Soc. Chem. Belg.*, 1975, **84**, 721.
22. A. De Bruyn and M. Anteunis, *Bull. Soc. Chem. Belg.*, 1975, **84**, 831.
23. A. De Bruyn, M. Anteunis, M. Claeyssens and E. Saman, *Bull. Soc. Chem. Belg.*, 1975, **85**, 605.
24. A. De Bruyn and M. Anteunis, *Bull. Soc. Chem. Belg.*, 1975, **84**, 1201.
25. M. Anteunis, A. De Bruyn and G. Verhegge, *Carbohyd. Res.*, 1975, **44**, 101.
26. A. De Bruyn, M. Anteunis, J. van Beeumen and G. Verhegge, *Bull. Soc. Chem. Belg.*, 1975, **84**, 407.
27. L. M. Jackman and S. Sternhell, *Applications of Nuclear Magnetic Resonance Spectroscopy in Organic Chemistry*, 2nd edn, Pergamon, Oxford, 1969.
28. A. A. E. Penglis, *Advan. Carbohyd. Chem. Biochem.*, 1980, **38**, 195.
29. L. D. Hall, K. F. Wong, W. E. Hull and J. D. Stevens, *J. Chem. Soc. Chem. Commun.*, 1979, 953.
30. A. S. Serianni and R. Barker, *Canad. J. Chem.*, 1979, **57**, 3160.
31. W. A. Gibbons, C. F. Beyer, J. Dadok, R. F. Speicher and H. R. Wyssbrod, *Biochemistry*, 1975, **14**, 420.
32. W. P. Aue, E. Bartholdi and R. R. Ernst, *J. Chem. Phys.*, 1976, **64**, 2229.
33. K. Nagayama, A. Kumar, K. Wuthrich and R. R. Ernst, *J. Magn. Reson.*, 1978, **40**, 321.
34. V. J. Kowalewski, *Progr. NMR Spectrosc.*, 1969, **5**, 1.

35. K. Bock, R. Burton and L. D. Hall, *Canad. J. Chem.*, 1976, **54**, 3526.
36. K. Bock, R. Burton and L. D. Hall, *Canad. J. Chem.*, 1977, **55**, 1045.
37. J. H. Noggle and R. E. Schirmer, *The Nuclear Overhauser Effect*, Academic Press, New York, 1971.
38. J. K. Saunders and J. W. Easton, in *High Resolution NMR: Theory and Chemical Applications*, Academic Press, New York, 1980, p. 271.
39. K. Bock, D. Bundle and S. Josephson, *J. Chem. Soc. Perkin II*, 1982, 59.
40. H. Thøgersen, R. U. Lemieux, K. Bock and B. Meyer, *Canad. J. Chem.*, 1982, **60**, 44.
41. R. Richarz and K. Wúthrich, *J. Magn. Reson.*, 1978, **30**, 147.
42. A. Kalk and H. J. C. Berendsen, *J. Magn. Reson.*, 1976, **24**, 343.
43. F. Heatley, L. Athker and R. T. Brown, *J. Chem. Soc. Perkin I*, 1980, 919.
44. B. H. Meier and R. R. Ernst, *J. Amer. Chem. Soc.*, 1979, **101**, 6441.
45. J. Jeener, B. H. Meier, P. Bachmann and R. R. Ernst, *J. Chem. Phys.*, 1979, **71**, 4546.
46. J. H. Noggle, *J. Amer. Chem. Soc.*, 1980, **102**, 2230.
47. R. L. Vold and R. R. Vold, *Progr. NMR Spectrosc.*, 1978, **12**, 79.
48. L. D. Hall, *Chem. Soc. Rev.*, 1975, **4**, 401.
49. L. D. Hall, *Advan. Carbohyd. Chem. Biochem.*, 1974, **29**, 11.
50. K. Bock, B. Meyer and J. Thiem, *Angew. Chem.*, 1978, **90**, 472.
51. F. F. Brown, I. D. Cambell, P. W. Kuchel and D. L. Rabenstein, *Fed. Eur. Biochem. Soc. Letters*, 1977, **82**, 12.
52. L. D. Hall and S. Sukumar, *J. Magn. Reson.*, 1980, **38**, 559.
53. W. P. Aue, J. Karhan and R. R. Ernst, *J. Chem. Phys.*, 1976, **64**, 4226.
54. K. Nagayama, P. Bachmann, K. Wuthrich and R. R. Ernst, *J. Magn. Reson.*, 1978, **31**, 133.
55. L. D. Hall, S. Sukumar and G. R. Sullivan, *J. Chem. Soc. Chem. Commun.*, 1979, 292.
56. L. D. Hall, G. A. Morris and S. Sukumar, *J. Amer. Chem. Soc.*, 1980, **102**, 1745.
57. L. D. Hall and S. Sukumar, *J. Amer. Chem. Soc.*, 1979, **101**, 3120.
58. P. McArdle, J. O. Wood, E. E. Lee and M. J. Conneely, *Carbohyd. Res.*, 1979, **69**, 39.
59. L. D. Hall and C. M. Preston, *Carbohyd. Res.*, 1975, **41**, 53.
60. I. A. Armitage, L. D. Hall, A. G. Marshall and L. G. Werbelow, *J. Amer. Chem. Soc.*, 1973, **95**, 1437.
61. H. R. Rackwitz and Z. Shahrokh, *Carbohyd. Res.*, 1981, **88**, 233.
62. S. D. Gero, D. Horton, A. M. Sepulchre and J. D. Wander, *Tetrahedron*, 1973, **29**, 2963.
63. S. D. Gero, D. Horton, A. M. Sepulchre and J. D. Wander, *J. Org. Chem.*, 1975, **40**, 1061.
64. D. Horton and J. D. Wander, *Carbohyd. Res.*, 1975, **39**, 141.
65. D. Horton and J. H. Lauterbach, *Carbohyd. Res.*, 1975, **43**, 9.
66. M. R. Bendall, D. T. Pegg, D. M. Doddrell and J. Field, *J. Amer. Chem. Soc.*, 1981, **103**, 934.
67. A. S. Perlin, B. Casu and H. J. Koch, *Canad. J. Chem.*, 1970, **48**, 2596.
68. D. E. Dorman and J. D. Roberts, *J. Amer. Chem. Soc.*, 1970, **92**, 1355.
69. D. K. Dalling and D. M. Grant, *J. Amer. Chem. Soc.*, 1967, **89**, 6612.
70. H. Paulsen, A. Richter, V. Sinnwell and W. Stenzel, *Carbohyd. Res.*, 1978, **64**, 339.
71. P. A. J. Gorin, *Canad. J. Chem.*, 1974, **52**, 458.
72. P. A. J. Gorin and M. Mazurek, *Canad. J. Chem.*, 1975, **53**, 1212.
73. H. J. Koch and R. S. Stuart, *Carbohyd. Res.*, 1978, **67**, 341.
74. E. Breitmaier and U. Hollstein, *Org. Magn. Reson.*, 1976, **8**, 573.
75. R. Barker and T. E. Walker, in *Methods in Carbohydrate Chemistry*, Vol. VIII (eds R. L. Whistler and M. L. Wolfrom), Academic Press, New York, 1980, p. 151.
76. T. E. Walker, R. E. London, T. W. Whaley, R. Barker and N. A. Matwiyoff, *J. Amer. Chem. Soc.*, 1976, **98**, 5807.

77. T. E. Walker, R. E. London, R. Barker and N. A. Matwiyoff, *Carbohyd. Res.*, 1978, **60**, 9.
78. T. E. Walker and R. Barker, *Carbohyd. Res.*, 1978, **64**, 266.
79. A. S. Serianni, E. L. Clark and R. Barker, *Carbohyd. Res.*, 1979, **72**, 79.
80. G. Excoffier, D. Y. Gagnaire and F. R. Taravel, *Carbohyd. Res.*, 1977, **56**, 229.
81. K. Bock and C. Pedersen, *Acta Chem. Scand. B*, 1975, **29**, 682.
82. V. Wray, *J. Chem. Soc. Perkin Trans. II*, 1976, 1598.
83. G. Adiwadjaja, B. Meyer, H. Paulsen and J. Thiem, *Tetrahedron*, 1979, **35**, 373.
84. J. V. O'Conner, H. A. Nunez and R. Barker, *Biochemistry*, 1979, **18**, 500.
85. T. A. W. Koerner, R. J. Voll, L. W. Cary and E. S. Younathan, *Biochemistry*, 1980, **19**, 2795.
86. S.-C. Ho, H. J. Koch and R. S. Stuart, *Carbohyd. Res.*, 1978, **64**, 251.
87. D. Gagnaire and M. Vincendon, *J. Chem. Soc. Chem. Commun.*, 1977, 509.
88. D. Gagnaire, D. Mancier and M. Vincendon, *Org. Magn. Reson.*, 1978, **11**, 344.
89. P. E. Pfeffer, K. M. Valentine and F. W. Parrish, *J. Amer. Chem. Soc.*, 1979, **101**, 1265.
90. P. E. Pfeffer, F. W. Parrish and J. Unruh, *Carbohyd. Res.*, 1980, **84**, 13.
91. K. Bock, D. Gagnaire and M. Vignon, *Compt. Rend. Acad. Sci. (Paris) C*, 1979, **289**, 345.
92. K. Bock and C. Pedersen, *J. Chem. Soc. Perkin Trans. II*, 1974, 293.
93. K. Bock and C. Pedersen, *Acta Chem. Scand. B*, 1975, **29**, 258.
94. J. A. Schwarcz and A. S. Perlin, *Canad. J. Chem.*, 1972, **50**, 3667.
95. H. Paulsen, V. Sinnwell, and W. Greve, *Carbohyd. Res.*, 1976, **49**, 27.
96. R. U. Lemieux, T. L. Nagabhushan and B. Paul, *Canad. J. Chem.*, 1972, **50**, 773.
97. J. A. Schwarcz, N. Cyr and A. S. Perlin, *Canad. J. Chem.*, 1975, **53**, 1872.
98. R. G. S. Ritchie, N. Cyr and A. S. Perlin, *Canad. J. Chem.*, 1976, **54**, 2301.
99. N. Cyr and A. S. Perlin, *Canad. J. Chem.*, 1979, **57**, 2504.
100. G. T. Andrews, I. J. Colquhoun, B. R. Doggett, W. McFarlane, B. E. Stacey and M. R. Taylor, *J. Chem. Soc. Chem. Commun.*, 1979, 89.
101. P. E. Hansen, *Progr. NMR Spectrosc.*, 1981, **14**, 175.
102. K. Bock and C. Pedersen, *J. Magn. Reson.*, 1977, **25**, 227.
103. A. J. Jones, G. A. Jenkins and M. L. Hefferman, *Austral. J. Chem.*, 1980, **33**, 1275.
104. R. Freeman and G. A. Morris, *J. Chem. Soc. Chem. Commun.*, 1978, 684.
105. L. D. Hall and G. A. Morris, *Carbohyd. Res.*, 1980, **82**, 175.
106. A. Allerhand, D. Doddrell and R. Komoroski, *J. Chem. Phys.*, 1971, **55**, 189.
107. K. Bock and L. D. Hall, *Carbohyd. Res.*, 1975, **40**, C3.
108. M. F. Czarniecki and E. R. Thornton, *J. Amer. Chem. Soc.*, 1977, **99**, 8279.
109. J. M. Berry, L. D. Hall and K. F. Wong, *Carbohyd. Res.*, 1977, **56**, C16.
110. A. Allerhand and D. Doddrell, *J. Amer. Chem. Soc.*, 1971, **93**, 2777.
111. A. Neszmelyi, K. Tori and G. Lukacs, *J. Chem. Soc. Chem. Commun.*, 1977, 613.
112. P. A. J. Gorin and M. Mazurek, *Carbohyd. Res.*, 1979, **72**, C1.
113. C. LeCoco and J.-Y. Lallemand, *J. Chem. Soc. Chem. Commun.*, 1981, 150.
114. D. M. Doddrell and D. T. Pegg, *J. Amer. Chem. Soc.*, 1980, **102**, 6388.
115. B. Casu, G. Gatti, N. Cyr and A. S. Perlin, *Carbohyd. Res.*, 1975, **41**, C6.
116. S. Hanessian and G. Patil, *Tetrahedron Letters*, 1978, 1031.
117. B. Coxon, *Ann. N.Y. Acad. Sci.*, 1973, 952.
118. A. P. G. Kieboom, A. Sinnema, J. M. van Der Torn and H. von Bekkum, *Rec. Trav. Chim. Pays-Bas*, 1977, **96**, 35.
119. K. F. Koch, J. A. Rhoades, E. W. Hagaman and E. Wenkert, *J. Amer. Chem. Soc.*, 1974, **96**, 3300.
120. K. Bock and C. Pedersen, unpublished results.
121. A. Bax, R. Freeman, T. A. Frenkiel and M. H. Levitt, *J. Magn. Reson.*, 1981, **43**, 478.

122. D. R. Bundle and R. U. Lemieux, in *Methods in Carbohydrate Chemistry*, Vol. 7 (eds R. L. Whistler and M. L. Wolfrom), Academic Press, New York, 1976, p. 79.
123. A. DeBruyn, M. Anteunis, R. DeGusseen and G. G. S. Dutton, *Carbohyd. Res.*, 1976, **47**, 158.
124. S. J. Angyal, in *Asymmetry in Carbohydrates*, Marcel Dekker, New York, 1979, p. 15.
125. S. J. Angyal and R. G. Wheen, *Austral. J. Chem.*, 1980, **33**, 1001.
126. A. S. Perlin, P. Herve Du Penhoat and H. S. Isbell, in *Carbohydrates in Solution*, ACS Chemistry Series no. 117, American Chemical Society, New York, 1973, p. 39.
127. H. Friebolin, M. Supp, R. Brossmer, G. Keilich and D. Ziegler, *Angew. Chem.*, 1980, **92**, 200.
128. U. Dabrowski, H. Friebolin, R. Brossmer and M. Supp, *Tetrahedron Letters*, 1979, 4637.
129. M. Ranganatgan and P. Balaram, *Org. Magn. Reson.*, 1980, **13**, 220.
130. V. W. Goodlett, *Anal. Chem.*, 1965, **37**, 431.
131. P. A. Garegg and H. Hultberg, *Carbohyd. Res.*, 1981, **93**, C10.
132. A. G. Ferrige and J. C. Lindon, *Spectrosc. Letters*, 1980, **13**, 339.
133. J. C. Lindon and A. G. Ferrige, *Progr. NMR Spectrosc.*, 1980, **14**, 27.
134. G. Gatti, B. Casu, G. Torri and J. Vercelotti, *Carbohyd. Res.*, 1979, **68**, C3.
135. A. DeBruyn and M. Anteunis, *Org. Magn. Reson.*, 1976, **8**, 228.
136. M. Budesinsky, T. Trnka and M. Cerny, *Collect. Czech. Chem. Commun.*, 1979, **44**, 1949.
137. L. G. Vorantsova and A. F. Bochov, *Org. Magn. Reson.*, 1974, **6**, 654.
138. L. G. Vorantsova and A. F. Bochov, *Org. Magn. Reson.*, 1975, **7**, 313.
139. C. Altona and C. A. G. Haasnoot, *Org. Magn. Reson.*, 1980, **13**, 417.
140. C. A. G. Haasnoot, F. A. A. M. DeLeeuw, H. P. M. Deleeuw and C. Altona, *Org. Magn. Reson.*, 1981, **15**, 43.
141. C. A. G. Haasnoot, F. A. A. M. Deleeuw and C. Altona, *Tetrahedron*, 1980, **36**, 2783.
142. R. Davies and J. Hudec, *J. Chem. Soc. Perkin Trans. II*, 1975, 1395.
143. R. Davies, *J. Chem. Soc. Perkin Trans. II*, 1975, 1400.
144. K. Jankowski, *Org. Magn. Reson.*, 1977, **10**, 50.
145. Y. Kondo and K. Kitamura, *Agric. Biol. Chem. (Japan)*, 1977, **41**, 907; Y. Kondo and K. Kitamura, *Canad. J. Chem.*, 1977, **55**, 141.
146. M. St Jaques, P. R. Sundararajan, K. J. Taylor and R. H. Marchessault, *J. Amer. Chem. Soc.*, 1976, **98**, 4386.
147. H. Hoenig, I. Macher and H. Weidmann, *Tetrahedron Letters*, 1979, 2579.
148. K. Bock, L. D. Hall and C. Pedersen, *Canad. J. Chem.*, 1980, **58**, 1923.
149. J. Bradbury and J. G. Collins, *Carbohyd. Res.*, 1979, **71**, 15.
150. J. F. G. Vliegenthart, H. van Halbeek and L. Dorland, *Pure Appl. Chem.*, 1981, **53**, 45.
151. P. L. Durette, D. Horton and J. D. Wander, in *Carbohydrates in Solution*, ACS Chemistry Series no. 117, American Chemical Society, New York, 1973, p. 147.
152. H. Paulsen, P. Luger and F. R. Heiker, in *The Anomeric Effect*, ACS Symposium Series no. 87, American Chemical Society, New York, 1979, p. 63.
153. L. D. Hall, K. F. Wong and W. Schittenhelm, in *Sucrochemistry*, ACS Symposium Series no. 41, American Chemical Society, New York, 1977, p. 22.
154. V. S. R. Rao, *J. Indian Inst. Sci.*, 1974, **56**, 253.
155. H. Paulsen and M. Friedmann, *Chem. Ber.*, 1972, **105**, 705.
156. H. Paulsen and M. Friedmann, *Chem. Ber.*, 1972, **105**, 718.
157. H. Paulsen and M. Friedmann, *Chem. Ber.*, 1972, **105**, 731.
158. S. J. Angyal and Y. Kondo, *Carbohyd. Res.*, 1980, **81**, 35.
159. P. Luger, G. Kothe, K. Vangehr, H. Paulsen and F. R. Heiker, *Carbohyd. Res.*, 1979, **68**, 207.
160. K. Bock, L. D. Hall and C. Pedersen, *Canad. J. Chem.*, 1980, **58**, 1916.
161. M. Budesinsky, M. Cerny, T. Trnka and S. Vasickova, *Collect. Czech. Chem. Commun.*, 1979, **44**, 1965.

162. M. Chmielewski, J. Mieczkowski, W. Priebe, A. Zamojski and H. Adamowicz, *Tetrahedron*, 1978, **34**, 3325.
163. A. DeBruyn, R. van Rijsbergen, M. Anteunis, M. Claeyssens and F. Deleyn, *Bull. Soc. Chim. Belg.*, 1978, **87**, 783.
164. M. Chmielewski, A. Banaszek, A. Zamojski and H. Adamowitz, *Carbohyd. Res.*, 1980, **83**, 3.
165. J. Thiem, J. Schwentner, E. Schuettpelz and J. Kopf, *Chem. Ber.*, 1979, **112**, 1023.
166. M. Rico and J. Santoro, *Org. Magn. Reson.*, 1976, **8**, 49.
167. J. Santoro, *An. Quim.*, 1978, **74**, 538.
168. C. R. Nelson, *Carbohyd. Res.*, 1979, **68**, 55.
169. C. Foces-Foces, A. Alemany, M. Bernabe and M. Martin-Lomas, *J. Org. Chem.*, 1980, **45**, 3502.
170. R. Lemieux and O. Hindsgaul, *Carbohyd. Res.*, 1980, **82**, 195.
171. M. A. Nashed, C. W. Slife, M. Kiso and L. Anderson, *Carbohyd. Res.*, 1980, **82**, 237.
172. P. Koell, H. Komander and J. Kopf, *Chem. Ber.*, 1980, **113**, 3919.
173. P. Koell, F. S. Tayman and K. Heyns, *Chem. Ber.*, 1979, **112**, 2305.
174. K. G. Pachler, E. B. Rathbone, G. R. Woolard and M. Woudenberg, *Carbohyd. Res.*, 1980, **79**, 29.
175. R. U. Lemieux and J. T. Brewer, in *Carbohydrates in Solution*, ACS Chemistry Series no. 117, American Chemical Society, New York, 1973, p. 121.
176. A. DeBruyn and M. Anteunis, *Carbohyd. Res.*, 1976, **47**, 311.
177. L. Evelyn and L. D. Hall, *Carbohyd. Res.*, 1976, **47**, 285.
178. A. DeBruyn, M. Anteunis and P. Kovac, *Collect. Czech. Chem. Commun.*, 1977, **42**, 3057.
179. W. Depmeier, H. Von Voithenberg, J. C. Jochims and K. H. Klaska, *Chem. Ber.*, 1978, **111**, 2010.
180. J. C. Jochims, H. Von Voithenberg and G. Wegner, *Chem. Ber.*, 1978, **111**, 1693.
181. M. Blanc-Muesser, J. Defaye and D. Horton, *Carbohyd. Res.*, 1979, **68**, 175.
182. M. Blanc-Muesser, J. Defaye and D. Horton, *J. Org. Chem.*, 1978, **43**, 3053.
183. A. Ducruix, D. Horton, C. Pascard, J. D. Wander and T. Prange, *J. Chem. Res. (S)*, 1978, 470.
184. M. Blanc-Muesser, J. Defaye and D. Horton, *Carbohyd. Res.*, 1980, **87**, 71.
185. J. Alfoldi, R. Palovcik, C. Peciar and K. Linek, *Chem. Zvesti*, 1978, **32**, 238.
186. L. M. Sweeting, B. Coxon and R. Varma, *Carbohyd. Res.*, 1979, **72**, 43.
187. A. Rockenbauer, J. Hemela, G. Toth and A. Gerecs, *Magy. Kem. Foly.*, 1977, **83**, 442.
188. E. J. Freyne, R. A. Dammisse, J. A. Lepoivre and F. C. Alderweireldt, *J. Carbohyd., Nucleosides, Nucleotides*, 1980, **7**, 263.
189. W. Z. Antkowiak and W. J. Krzyzosiak, *Bull. Acad. Pol. Sci. Ser. Sci. Chim.*, 1977, **25**, 421.
190. S. J. Angyal, *Carbohyd. Res.*, 1979, **77**, 37.
191. J. M. Berry, L. D. Hall, D. G. Welder and K. F. Wong, in *The Anomeric Effect*, ACS Symposium Series no. 87, American Chemical Society, New York, 1979, p. 30.
192. R. U. Lemieux, S. Koto and D. Voisin, in *The Anomeric Effect*, ACS Symposium Series no. 87, American Chemical Society, New York, 1979, p. 17.
193. M. C. R. Symons, J. A. Benbow and J. M. Harvey, *Carbohyd. Res.*, 1980, **83**, 9.
194. S. Bociek and F. Franks, *J. Chem. Soc., Faraday Trans. I*, 1979, **75**, 262.
195. H. Sugiyama and T. Usui, *Agric. Biol. Chem. (Japan)*, 1980, **55**, 3001.
196. M. D. Adamenkova, V. I. Ermakov and V. V. Makhlyarchuk, *Vestn. Mosk. Univ., Ser. 2, Khim.*, 1980, **21**, 199.
197. J. Hvoslef and B. Pedersen, *Acta Chem. Scand. B*, 1979, **33**, 503.
198. J. Hvoslef and B. Pedersen, *Acta Chem. Scand. B*, 1980, **34**, 285.
199. T. Taga, Y. Kuroda and M. Ohashi, *Bull. Chem. Soc. Jpn*, 1978, **51**, 2278.

200. T. Taga, Y. Kuroda and K. Osaki, *Bull. Chem. Soc. Jpn*, 1977, **50**, 3079.
201. H. Grasdalen, T. Anthonsen, O. Harbitz, B. Larsen and O. Smidsroed, *Acta Chem. Scand. A*, 1978, **32**, 31.
202. K. Izumi, *Carbohyd. Res.*, 1978, **62**, 368.
203. D. G. Streefkerk and A. M. Stephen, *Carbohyd. Res.*, 1977, **57**, 25.
204. J. Alfoldi, L. Petrus and B. Vojtech, *Collect. Czech. Chem. Commun.*, 1978, **43**, 1476.
205. L. Poncini, *Indian J. Chem. A*, 1980, **19**, 1035.
206. A. DeBruyn and M. Anteunis, *Acta Cienc. Indica*, 1976, **2**, 1.
207. D. A. Laidler, J. F. Stoddard and J. B. Wolstenholme, *Tetrahedron Letters*, 1979, 465.
208. R. B. Pettman and J. F. Stoddard, *Tetrahedron Letters*, 1979, 461.
209. R. B. Pettman and J. F. Stoddard, *Tetrahedron Letters*, 1979, 457.
210. J. J. Grimaldi and B. D. Sykes, *J. Biol. Chem.*, 1975, **250**, 1618.
211. S. J. Perkins, L. N. Johnson, D. C. Phillips and R. A. Dwek, *Carbohyd. Res.*, 1977, **59**, 19.
212. R. C. Beier, B. P. Mundy and G. A. Strobel, *Canad. J. Chem.*, 1980, **58**, 2800.
213. J. P. Utille and P. J. A. Vottero, *Carbohyd. Res.*, 1980, **85**, 289.
214. H. C. Jarrell, T. F. Conway, P. Moyna and I. C. P. Smith, *Carbohyd. Res.*, 1979, **76**, 45.
215. J. Alfoldi, C. Peciar, P. Kocis and J. Hirsch, *Chem. Zvesti*, 1980, **34**, 679.
216. D. Gagnaire, F. R. Taravel and M. Vignon, *Carbohyd. Res.*, 1976, **51**, 157.
217. J. Cerbulis, P. E. Pfeffer and H. M. Jarrel, Jr, *Carbohyd. Res.*, 1978, **65**, 311.
218. A. Heyraud, M. Rinaudo, M. Vignon and M. Vincendon, *Biopolymers*, 1979, **18**, 167.
219. B. Capon, D. S. Rycroft and J. W. Thomson, *Carbohyd. Res.*, 1979, **70**, 145.
220. W. Funcke, C. von Sonntag and C. Triantaphylides, *Carbohyd. Res.*, 1979, **75**, 305.
221. B. T. Grindley and V. Gulasekharam, *J. Chem. Soc. Chem. Commun.*, 1978, 1073.
222. S. J. Angyal, G. S. Bethell, D. E. Cowley and V. A. Pickles, *Austral. J. Chem.*, 1976, **29**, 1239.
223. C. F. Midelfort, R. K. Gupta and H. P. Meloche, *J. Biol. Chem.*, 1977, **252**, 3486.
224. T. C. Crawford, G. C. Andrews, H. Faubl and G. N. Chmurny, *J. Amer. Chem. Soc.*, 1980, **102**, 2220.
225. A. S. Serianni, J. Pierce and R. Barker, *Biochemistry*, 1979, **18**, 1192.
226. Y. Takeda, *Carbohyd. Res.*, 1979, **77**, 9.
227. R. Cherniak, R. G. Jones and D. S. Gupta, *Carbohyd. Res.*, 1979, **75**, 39.
228. W. Funcke and C. von Sonntag, *Carbohyd. Res.*, 1979, **69**, 247.
229. M. Chmielewski and R. L. Whistler, *Carbohyd. Res.*, 1979, **69**, 259.
230. K. Bock, C. Pedersen and H. Thøgersen, *Acta Chem. Scand. B*, 1981, **35**, 441.
231. R. M. Blazer and T. W. Whaley, *J. Amer. Chem. Soc.*, 1980, **102**, 5082.
232. W. Funcke, A. Klemer and E. Meissner, *Justus Liebigs Ann. Chem.*, 1978, 2088.
233. W. Funcke, *Justus Liebigs Ann. Chem.*, 1978, 2099.
234. W. Funcke, C. Von Sonntag and A. Klemer, *Carbohyd. Res.*, 1979, **71**, 315.
235. A. Klemer and W. Funcke, *Justus Liebigs Ann. Chem.*, 1979, 1682.
236. A. S. Serianni, H. A. Nunez and R. Barker, *J. Org. Chem.*, 1980, **45**, 3329.
237. R. G. S. Ritchie, N. Cyr, B. Korsch, H. J. Koch and A. S. Perlin, *Canad. J. Chem.*, 1975, **53**, 1424.
238. A. S. Perlin and B. Casu, *Tetrahedron Letters*, 1969, 2921.
239. K. Bock and C. Pedersen, *Carbohyd. Res.*, 1979, **71**, 319.
240. J. E. N. Shin and A. S. Perlin, *Carbohyd. Res.*, 1979, **76**, 165.
241. C. Laffite, A. M. N. Phuoc Du, F. Winternitz, R. Wylde and F. Pratviel-Sosa, *Carbohyd. Res.*, 1978, **67**, 105.
242. A. S. Perlin, *Int. Rev. Sci. Org. Chem.*, 1976, **7**, 1.
243. J. G. Buchanan, M. E. Chacon-Fuertes, A. R. Edgar, S. J. Moorehouse, D. I. Rawson and R. H. Wightman, *Tetrahedron Letters*, 1980, 1793.
244. G. Aslani-Shotorbani, J. G. Buchanan, A. R. Edgar, D. Henderson and P. Shahidi, *Tetrahedron Letters*, 1980, 1791.

245. T. B. Grindley and V. Gulasekharam, *Carbohyd. Res.*, 1979, **74**, 7.
246. K. S. Kim, D. M. Vyas and W. A. Szarek, *Carbohyd. Res.*, 1979, **72**, 25.
247. P. A. J. Gorin and M. Mazurek, *Carbohyd. Res.*, 1976, **48**, 171.
248. J. Haverkamp, J. P. C. M. van Dongen and J. F. G. Vliegenthart, *Tetrahedron*, 1973, **29**, 3431.
249. J. Haverkamp, J. P. C. M. van Dongen and J. F. G. Vliegenthart, *Carbohyd. Res.*, 1974, **33**, 319.
250. J. Haverkamp, M. J. A. De Bie and J. F. G. Vliegenthart, *Carbohyd. Res.*, 1975, **39**, 201.
251. T. Usui, N. Yamaoka, K. Matsuda, K. Tuzimura, H. Sugiyama and S. Seto, *J. Chem. Soc. Perkin Trans. I*, 1973, 2425.
252. S. Seo, Y. Tomita, K. Tori and Y. Yoshimura, *J. Amer. Chem. Soc.*, 1978, **100**, 3331.
253. J. Alfoldi, P. Kocis and R. Toman, *Chem. Zvesti*, 1980, 514.
254. A. Liptak, P. Nanasi, A. Neszmelyi and H. Wagner, *Tetrahedron*, 1980, **36**, 1261.
255. Y. Inoue and R. Chujo, *Carbohyd. Res.*, 1978, **60**, 367.
256. D. D. Cox, E. K. Metzner, L. W. Cary and E. J. Reist, *Carbohyd. Res.*, 1978, **67**, 23.
257. A. S. Shaskov, N. P. Arbetsky, V. A. Derevitskaya and N. K. Kochetkov, *Carbohyd. Res.*, 1979, **71**, 218.
258. J. C. Gast, G. H. Atalla and R. D. McKelvey, *Carbohyd. Res.*, 1980, **84**, 137.
259. P. Kovac, J. Hirsch, A. S. Shashkov, A. I. Usov and S. V. Yarotskii, *Carbohyd. Res.*, 1980, **85**, 177.
260. F. R. Seymour, R. D. Knapp, J. E. Zweig and S. H. Bishop, *Carbohyd. Res.*, 1979, **72**, 57.
261. H. Komura, A. Matsuno, Y. Ishido, K. Kushida and K. Aoki, *Carbohyd. Res.*, 1978, **65**, 271.
262. W. Voelter, E. Breitmaier, E. B. Rathbone and A. M. Stephen, *Tetrahedron*, 1973, **29**, 3845.
263. W. A. Szarek, A. Zamojski, A. R. Gibson, D. M. Vyas and J. K. N. Jones, *Canad. J. Chem.*, 1976, **54**, 3783.
264. A. S. Shashkov, A. I. Shienok, M. Islomov, A. F. Sviridov and O. S. Chizhov, *Bioorg. Khim.*, 1977, **3**, 1021.
265. A. Liptak, P. Nanasi, A. Neszmelyi and H. Wagner, *Carbohyd. Res.*, 1980, **86**, 133.
266. E. Conway, R. D. Guthrie, S. D. Gero, G. Lukacs and A.-M. Sepulchre, *J. Chem. Soc. Perkin Trans. II*, 1974, 542.
267. A. Liptak, P. Fugedi, P. Nanasi and A. Neszmelyi, *Tetrahedron*, 1979, **35**, 1111.
268. A. Neszmelyi, A. Liptak and P. Nanasi, *Carbohyd. Res.*, 1977, **58**, C7.
269. P. J. Garegg, B. Lindberg and I. Kvarnstrom, *Carbohyd. Res.*, 1979, **77**, 71.
270. P. J. Garegg, P.-E. Jansson, B. Lindberg, F. Lindh, J. Lonngren, I. Kvarnstrom and W. Nimmich, *Carbohyd. Res.*, 1980, **78**, 127.
271. Y. Terui, K. Tori and N. Tsuji, *Tetrahedron Letters*, 1976, 621.
272. M. R. Vignon and P. J. A. Vottero, *Tetrahedron Letters*, 1976, 2445.
273. M. R. Vignon and P. J. A. Vottero, *Carbohyd. Res.*, 1977, **53**, 197.
274. K. Yoshimoto, Y. Itatani and Y. Tsuda, *Chem. Pharm. Bull.*, 1980, **28**, 2065.
275. K. Yoshimoto, Y. Itatani, K. Shibata and Y. Tsuda, *Chem. Pharm. Bull.*, 1980, **28**, 208.
276. P. E. Pfeffer, K. M. Valentine, B. G. Moyer and D. L. Gustine, *Carbohyd. Res.*, 1979, **73**, 1.
277. V. Pozsgay and A. Neszmelyi, *Carbohyd. Res.*, 1980, **80**, 196.
278. L. J. Altman, R. E. O'Brien, S. K. Gupta and H. R. Schulten, *Carbohyd. Res.*, 1980, **87**, 189.
279. V. H. Kollman, R. E. London, J. L. Hanners, C. T. Gregg and T. W. Whaley, *J. Labelled Compd. Radiopharm.*, 1979, **16**, 833.
280. P. M. Collins and V. R. N. Munasinghe, *Carbohyd. Res.*, 1978, **62**, 19.
281. J.-C. Depezay, A. Dureault and M. Saniere, *Carbohyd. Res.*, 1980, **83**, 273.

282. M. Miljkovic, M. Gligorijevic, T. Satoh, D. Glisin and R. G. Pitcher, *J. Org. Chem.*, 1974, **39**, 3847.
283. K. Sato, M. Matsuzawa, K. Ajisaka and J. Yoshimura, *Bull. Chem. Soc. Jpn.*, 1980, **53**, 189.
284. A. M. Sepulchre, B. Septe, G. Lukacs, S. D. Gero, W. Voelter and E. Breitmaier, *Tetrahedron*, 1974, **30**, 905.
285. G. W. Schnarr, D. M. Vyas and W. A. Szarek, *J. Chem. Soc. Perkin Trans. I*, 1979, 496.
286. S. J. Angyal and R. Le Fur, *Carbohyd. Res.*, 1980, **84**, 201.
287. H. Thøgersen, PhD thesis, The Technical University of Denmark, Lyngby, 1980.
288. S. Koto, S. Inada and S. Zen, *Chem. Letters*, 1980, 403.
289. A. A. Pavia, S. N. Ung-Chhun and J.-M. Lacombe, *Nouv. J. Chem.*, 1981, **5**, 101.
290. D. Y. Gagnaire, F. R. Taravel and M. R. Vignon, *Nouv. J. Chim.*, 1977, **1**, 423.
291. G. K. Hamer, F. Balza, N. Cyr and A. S. Perlin, *Canad. J. Chem.*, 1978, **56**, 3109.
292. K. Bock and C. Pedersen, *Acta Chem. Scand. B*, 1977, **31**, 354.
293. H. Thøgersen, unpublished results.
294. K. Rasmussen, *Acta Chem. Scand. A*, 1980, **34**, 155.
295. M. F. Czarniecki and E. R. Thornton, *J. Amer. Chem. Soc.*, 1977, **99**, 8273.
296. P. D. Hoagland, P. E. Pfeffer and K. M. Valentine, *Carbohyd. Res.*, 1979, **74**, 135.
297. P. A. J. Gorin and M. Mazurek, *Carbohyd. Res.*, 1973, **27**, 325.
298. P. A. J. Gorin and M. Mazurek, *Canad. J. Chem.*, 1973, **51**, 3277.
299. W. Voelter, C. Burvenich and E. Breitmaier, *Angew. Chem.*, 1972, **84**, 589.
300. J. Alfoldi, V. Bilik and P. Ladislav, *Collect. Czech. Chem. Commun.*, 1980, **45**, 123.
301. M. F. Czarniecki and E. R. Thornton, *Biochem. Biophys. Res. Commun.*, 1977, **74**, 553.
302. L. W. Jaques, J. B. Macaskill and W. Weltner, Jr, *J. Chem. Phys.*, 1979, **83**, 1412.
303. G. De Wit, A. P. G. Kieboom and H. Van Bekkum, *Rec. Trav. Chim. Pays-Bas*, 1979, **98**, 355.
304. J. A. Elvidge, J. R. Jones, R. B. Mane, V. M. A. Chambers, E. A. Evans and D. C. Warrell, *J. Labelled Compd. Radiopharm.*, 1978, **15**, 141.
305. B. Coxon, *Pure Appl. Chem.*, 1977, **49**, 1151.
306. B. Coxon, *Carbohyd. Res.*, 1974, **35**, C1.
307. B. Coxon and R. C. Reynolds, *Carbohyd. Res.*, 1980, **78**, 1.
308. R. E. Botto and J. D. Roberts, *J. Org. Chem.*, 1977, **42**, 2247.
309. B. Coxon and L. Hough, *Carbohyd. Res.*, 1979, **73**, 47.
310. J. W. Pascal and D. E. Dorman, *Org. Magn. Reson.*, 1978, **11**, 632.
311. A. F. Hadfield, L. Hough and A. C. Richardson, *Carbohyd. Res.*, 1980, **80**, 123.
312. T. Uryu, K. Ito, K. Kobayashi and K. Matsuzaki, *Makromol. Chem.*, 1979, **180**, 1509.
313. K. Bock and C. Pedersen, *Acta Chem. Scand. B*, 1976, **30**, 727.
314. V. I. Gorbach, V. V. Isakov, Y. G. Kulesh, P. A. Lukayanov, T. F. Soloveva and Y. S. Ovodov, *Bioorg. Khim.*, 1980, **6**, 81.
315. D. A. Predvoditelev, M. K. Grachev, M. V. Galakhov and E. E. Nifantev, *Zhur. Obshch. Khim.*, 1979, **49**, 285.
316. E. E. Nifantev, D. A. Predvoditelev, M. K. Grachev and V. A. Shin, *Dokl. Akad. Nauk. SSSR*, 1977, **235**, 595.
317. A. J. R. Castello, T. Glonek and T. C. Myers, *Carbohyd. Res.*, 1976, **46**, 159.
318. G. R. Kennedy and M. J. How, *Carbohyd. Res.*, 1973, **28**, 13.
319. M. J. Tait, A. Suggett, F. Franks, S. Ablett and P. A. Quickenden, *J. Solution Chem.*, 1972, **1**, 131.
320. P. A. J. Gorin and M. Mazurek, *Carbohyd. Res.*, 1978, **67**, 479.
321. J. Grandjean and P. Laszlo, *Helv. Chim. Acta*, 1977, **60**, 259.
322. C. Detellier, J. Grandjean and P. Laszlo, *J. Amer. Chem. Soc.*, 1976, **98**, 3375.
323. R. K. Harris and R. C. Rao, *Org. Magn. Reson.*, 1977, **9**, 432.

324. D. J. Gale, A. H. Haines and R. K. Harris, *Org. Magn. Reson.*, 1975, **7**, 635.
325. V. G. Gibb and L. D. Hall, *Carbohyd. Res.*, 1977, **55**, 239.
326. V. G. Gibb and L. D. Hall, *Carbohyd. Res.*, 1978, **63**, C1.
327. L. D. Hall, P. R. Steiner and D. C. Miller, *Canad. J. Chem.*, 1979, **57**, 38.
328. D. Gagnaire, H. Reutenauer and F. Taravel, *Org. Magn. Reson.*, 1979, **12**, 679.
329. M. Mazurek, T. M. Mallard and P. A. J. Gorin, *Org. Magn. Reson.*, 1977, **9**, 193.
330. K. Bock, unpublished results.

This Page Intentionally Left Blank

Nuclear Magnetic Resonance of Alkaloids

TREVOR A. CRABB

Department of Chemistry, Portsmouth Polytechnic, Hampshire, UK

I. INTRODUCTION

This review is designed to update the two previous reviews contained in Volume 6A and Volume 8 of this series[1,2] and presents selected examples of the NMR spectra of alkaloids (and of model systems) taken from the literature (mid-1977 to early 1981). The organization and intention are essentially the same as described before.[1,2]

Chemical shifts (ppm to high frequency from internal TMS unless otherwise stated) and coupling constants or splittings (Hz) are given with many of the structural formulae, and unless indicated otherwise relate to measurements made on solutions in $CDCl_3$. Asterisks signify possible reversal of shift assignments.

A collection of ^{13}C NMR spectral data on alkaloids and amines covering the literature through 1977 is available.[3]

II. ISOQUINOLINE ALKALOIDS

The ^{13}C NMR spectra of isoquinoline alkaloids have been reviewed[4] with the literature covered to mid-1979.

A. Simple isoquinoline alkaloids

^{13}C shifts and long range (^{13}C–^{1}H) couplings of isoquinoline are given in [1][5] and ^{13}C shifts of a number of simple isoquinolines in [2]–[8].[6] The

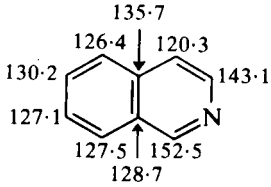

[1]

$J_{C(1)-H(8)} = 4{\cdot}7$
$J_{C(1)-H(3)} = 10{\cdot}5$
$J_{C(3)-H(4)} = 3{\cdot}6$
$J_{C(3)-H(1)} = 12{\cdot}5$
$J_{C(4)-H(3)} = 8{\cdot}9$
$J_{C(8)-H(1)} = 3{\cdot}4$
$J_{C(4)-H(5)} = 3{\cdot}2$
$J_{C(5)-H(4)} = 5{\cdot}1$
$J_{C(5)-H(7)} = 5{\cdot}9$
$J_{C(6)-H(8)} = 8{\cdot}3$
$J_{C(7)-H(5)} = 8{\cdot}4$
$J_{C(8)-H(6)} = 6{\cdot}0$

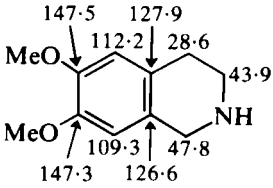

[2]

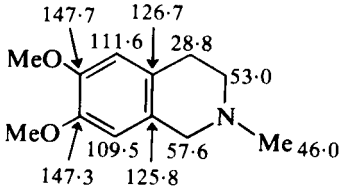

[3]

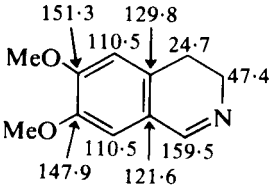

[4]

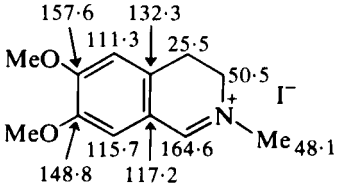

[5]

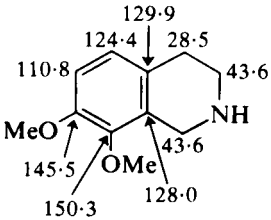

[6]

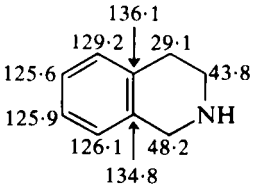

[7]

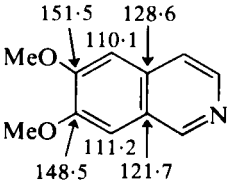

[8]

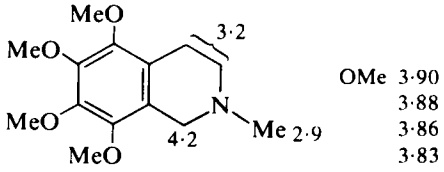

[9] Weberine

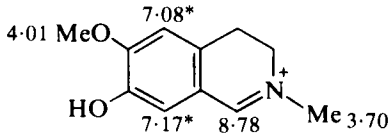

[10] Pycnarrhine (in CD_3OD)

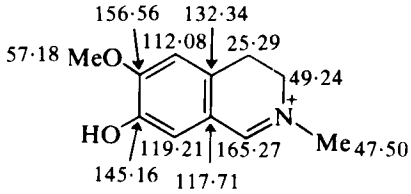

[11] (in D_2O)

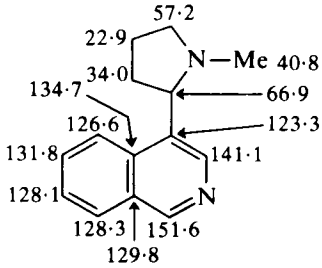

[12]

shifts of 6,7-dimethoxyisoquinoline [8] are calculated from shift values obtained from a comparison of benzene and veratrole. Comparisons within the set [2]–[8] indicate methoxy substituent effects and *N*-methylation effects on ^{13}C shifts.

The ^{1}H NMR spectra of a range of simple mono-, di-, tri- and tetramethoxyisoquinoline alkaloids (e.g. weberine [9]) have been described.[7] The ^{1}H and ^{13}C NMR shifts of pycnarrhine are given in [10] and [11][8] and the ^{13}C shifts of 4-(1-methyl-2-pyrrolidinyl)isoquinoline, a model for the 4-pyrrolidinylisoquinoline alkaloids, in [12][9].

B. Benzylisoquinoline alkaloids

Replacement of the 6,7-methoxy group in papaverine [13] and in 1-(*p*-methoxybenzyl)-6,7-dimethoxyisoquinoline [14] by the methylenedioxy group as in 1-(*p*-methoxybenzyl)-6,7-methylenedioxyisoquinoline [15] results in shielding of C(5), C(6), C(7) and C(8) and deshielding of C(4a) and C(8a). These shift changes are also shown by the tetrahydroisoquinolines [16] and [17].[10] ^{13}C shift changes resulting from *N*-methylation are illustrated by comparison of papaverine [13] and its methiodide [18][10] and of laudanosine [19] and its methiodide [20].[11]

The low frequency *N*Me signal in the ^{1}H NMR spectrum of [20] is assigned by NOE measurements to that *trans* to the 1-benzyl group. Since quaternization of laudanosine [19] with $^{13}CH_3I$ gives the major ^{13}C enriched *N*Me signal to low frequency, the quaternization is shown to proceed *trans* to the benzyl group.[12]

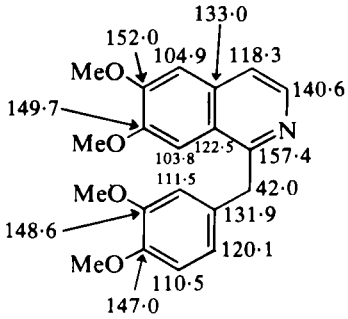

[13] Papaverine $J_{C(4)-H(3)} = 8$
$J_{C(4)-H(5)} = 4{\cdot}9$
$J_{C(3)-H(4)} = 3{\cdot}1$

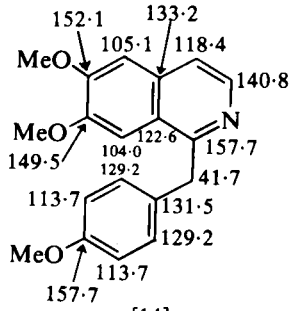

[14]

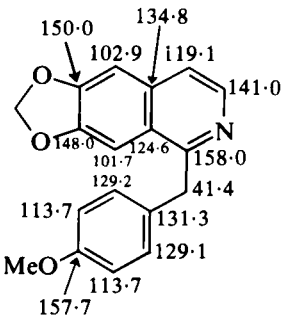

[15]

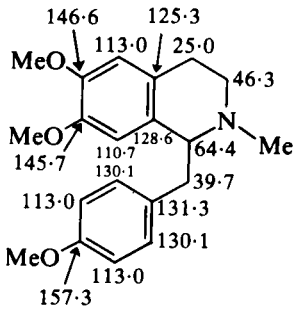

[16]

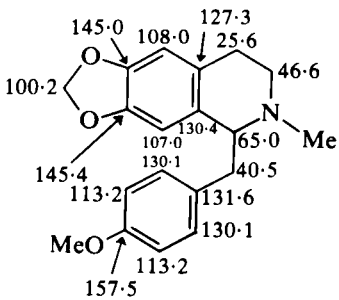

[17]

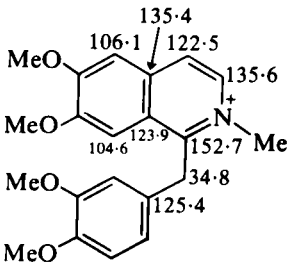

[18]

The low frequency shift (0·93 ppm) of 8-H and the high frequency shift (0·42 ppm) of 5-H observed[13] on addition of CD_3ONa to a DMSO solution of sevanine [21] shows the C(7) location of the hydroxy group. ^1H shifts have been recorded[13] for macrostomine [22].

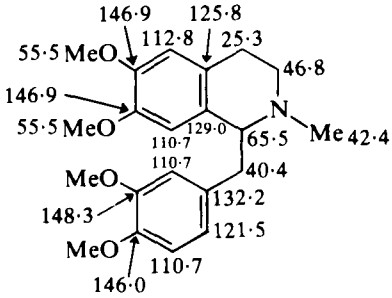

[19] Laudanosine

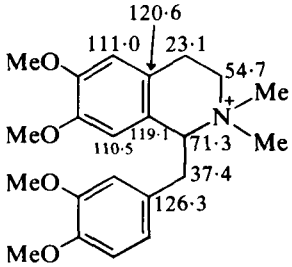

[20]

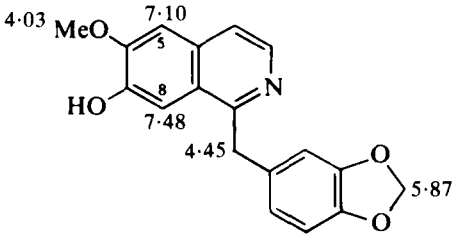

Ar-H 6·72 (s, 3H)
7·45 (d, 1H)
8·23 (d, 1H)

[21] Sevanine (in $CDCl_3$–CD_3OD)

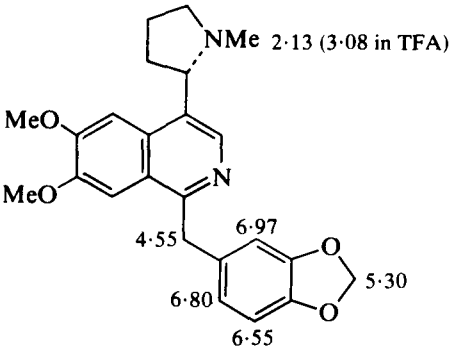

Ar-H 7·35
7·87
8·72
OMe 3·47
3·55

[22] Macrostomine (C_6D_6)

C. Aporphine, oxo-aporphine and proaporphine alkaloids

1. Aporphines

A collection of ^1H and ^{13}C NMR data of aporphines, dehydroaporphines, phenanthrenes and miscellaneous aporphinoids is available.[14]

It has been pointed out[11] that the non-aromatic ^{13}C shifts of the aporphines are very different from those of the benzylisoquinolines (compare nuciferine [23] and laudanosine [19]). In addition the C(1) methoxy group protons in the aporphines absorb to higher frequency of the other methoxy

group protons (see glaucine [24]) and the shift is very marked in the case of isocorydine [25][11] which possesses the C(11)—OH. The effects of replacement of the dimethoxy group in [24] by a methylenedioxy group as in nantenine [26] on the aromatic carbon signals shows shielding of the *ortho* carbons and deshielding of the *meta* carbons.[11] ^{13}C shifts for apormorphine are given in [27][15] and for boldine and ocoteine in [28] and [29].[16] Comparison of ^{13}C shifts in ocoteine [29] and glaucine [24] show the expected marked differences in ring A shifts. The low frequency shift of

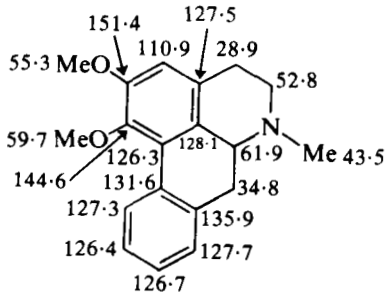

[23] Nuciferine

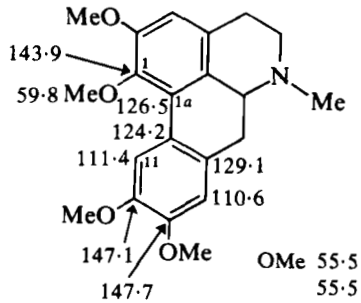

[24] Glaucine

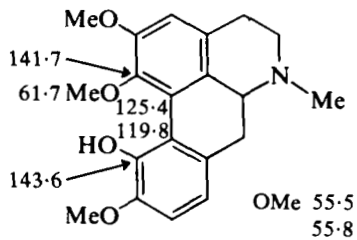

[25] Isocorydine

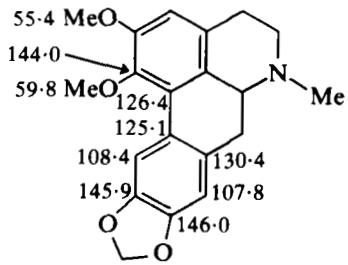

[26] Nantenine

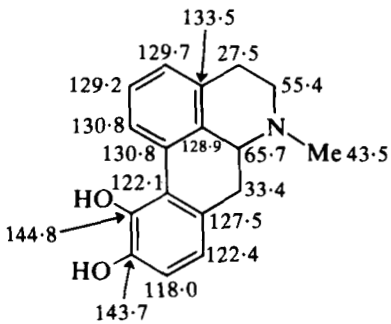

[27] Apomorphine (in TFA)

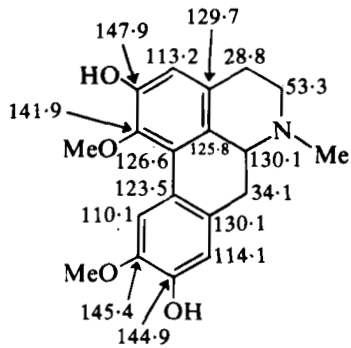

[28] Boldine

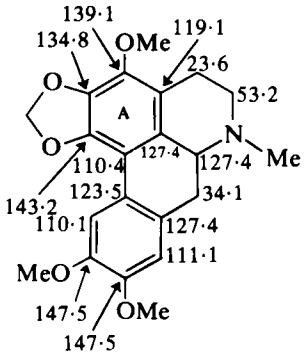

[29] Ocoteine

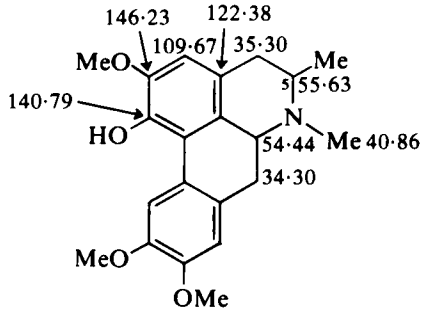

[30]

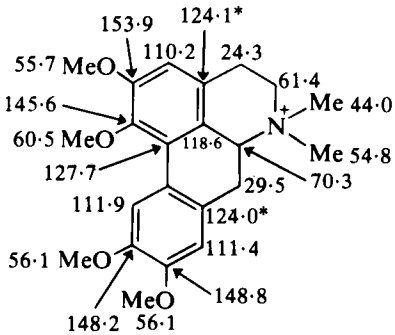

[31] Glaucine methiodide (in $CDCl_3$–MeOD)

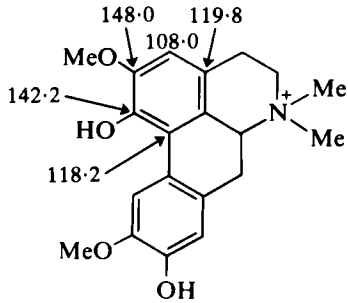

[32] Laurifoline methochloride in ($CDCl_3$–MeOD)

C(1a) is particularly marked. Substitution at C(5) in the aporphines as in [30] causes low frequency shifts of NMe and of C(6a).[17]

^{13}C shifts of a variety of quaternary aporphine alkaloids are shown in [31]–[34][16] and in [35],[8] and illustrate the deshielding of C(5) and C(6a) and the shielding of C(1b), C(3a), C(7) and C(7a) resulting from quaternization. Comparison of the spectrum of glaucine methiodide [31] with that of xantoplanine methiodide [33] shows the normally encountered shift changes *ortho* and *para* to OH in ring D consequent upon replacement of OMe by OH. Replacement of the more hindered OMe in glaucine methiodide [31] by OH as in laurifoline methochloride [32], however, causes large shielding effects on C(1a), C(2) and C(3a).[16] Comparison of ring A ^{13}C shifts in [31] and dicentrine methiodide [34] shows that the normal shift changes (see [16] and [17]) resulting from replacement of a dimethoxy unit by a methylene dioxy group are not observed in the more crowded systems (the *para* C(3a) is also shielded and the *ortho* positions are more strongly shielded in [34] than in [31]).[16]

^{1}H NMR data on a range of aporphines are available.[18] The high frequency shift of 11-H in xylopine [36][19] is typical of such a structure and the couplings involving the 6a-proton indicate its axial orientation. The low frequency shift of two of the methoxy group protons in *N*-methylhernagine [37] indicate MeO substitution at C(1) and C(11). The observation of low frequency shifts of the aromatic proton signals (δ 6·91 (d), 6·78 (d) and 6·85 (s) in DMSO-d_6) in the spectrum of [37] on the addition of KOH to the DMSO-d_6 solution by 0·45, 0·59 and 0·25 ppm respectively indicate the location of the OH group at C(10).[20]

The difference in ^{1}H NMR parameters consequent upon a change in C(7) stereochemistry is illustrated by the spectra of oliveroline [38] and

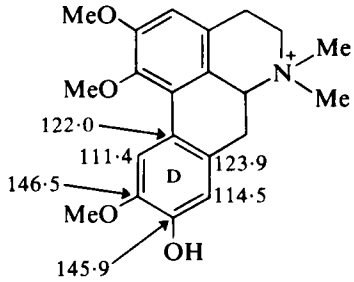

[33] Xantoplanine methiodide (in $CDCl_3$–MeOD)

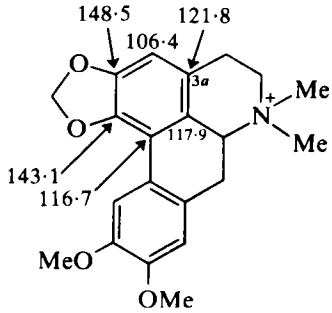

[34] Dicentrine methiodide

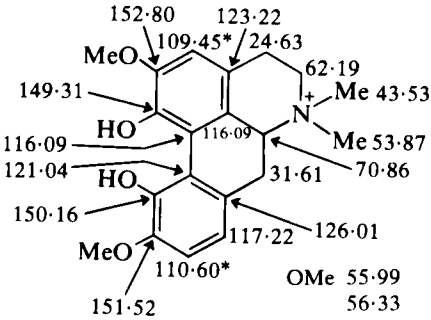

[35] Magnoflorine (in CD_3OD)

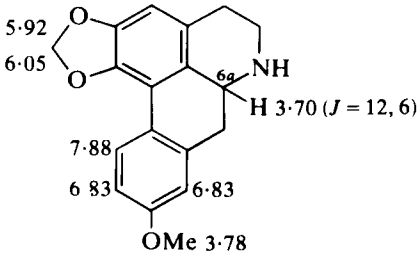

[36] Xylopine

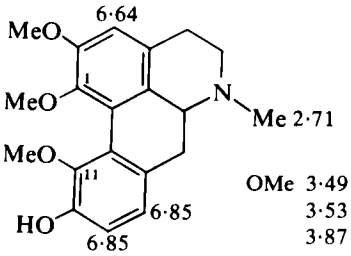

[37] *N*-Methylhernagine

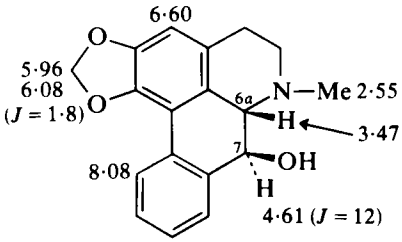

[38] Oliveroline

ushinsunine [39].[21] The difference in chemical shift between the 6a- and 7-protons ($\Delta_{6a\text{-}H,7\text{-}H}$) is *c.* 1·14 ppm in oliveroline type compounds whereas in the 7-*O*-methyl series (see oliverine [40][22]) $\Delta_{6a\text{-}H,7\text{-}H}$ is *c.* 0·64 ppm. Marked differences in the ^{1}H NMR parameters of *N*-oxyoliveroline [41] and of *N*-oxy-*N*-methylpachypodanthine [42] presumably result from the increase in non-bonded interactions in [42]. The ^{1}H NMR spectrum of [42] also provides evidence for solvation by a water molecule.[22]

^{1}H NMR parameters of a variety of 4-hydroxylated aporphines are available.[23–26] The 4-proton is shown to be pseudo-equatorial in 4-hydroxynornantenine [43] but pseudo-axial in the *O,N*-diacetyl derivative

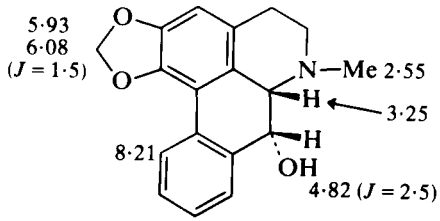

[39] Ushinsunine

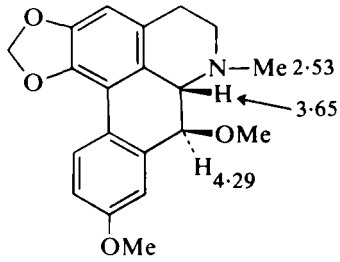

[40] Oliverine

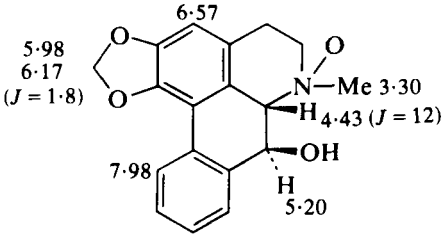

[41] *N*-Oxyoliveroline

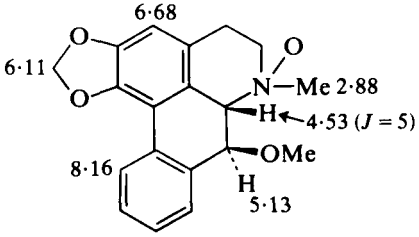

[42] *N*-Oxy-*N*-methylpachypodanthine

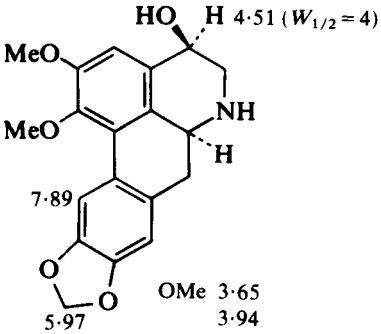

[43] 4(*S*)-Hydroxy-6a(*S*)-nornantenine

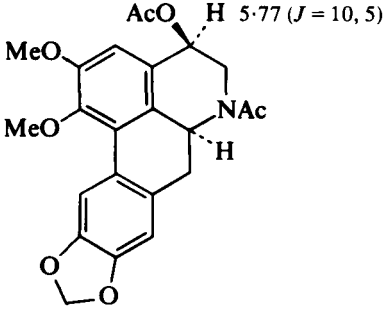

[44]

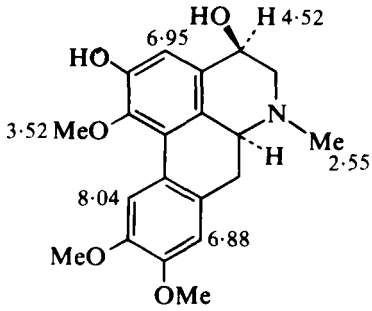

[45] Srilankine

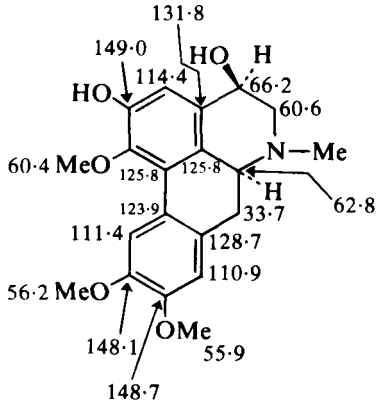

[46] Srilankine

[44] by the magnitudes of the vicinal coupling constants involving the C(4) protons.[23] The 3-proton shift is *c.* 0·30 ppm to higher frequency in srilankine [45][24] and in 4-episteporphine[25] than in aporphines lacking a 4-hydroxy substituent. ^{1}H NMR spectra of 4-alkoxy aporphines are available.[26] The ^{13}C NMR shifts of srilankine are shown in [46].[24]

2. *Oxo-aporphines*

^{13}C NMR shifts of oxo-*O*-methylpukateine [47],[27] *O*-methylmoscatoline [48][27] and oxoglaucine [49],[27] and ^{1}H NMR shifts for oxo-*O*-methylpukateine [50],[28] 11-hydroxy-1,2-methylenedioxyoxoaporphine [51],[28] splendidine [52],[29] subsessiline [53],[30] liriodendronine [54],[31] *O,N*-dimethylliriodendronine [55],[31] arosine [56][32] and arosinine [57][32] are given with the structures.

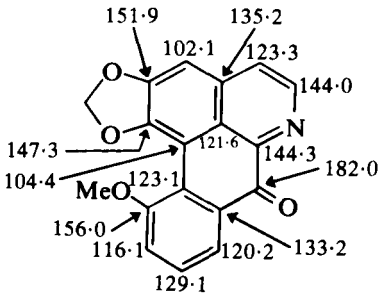

[47] Oxo-*O*-methylpukateine

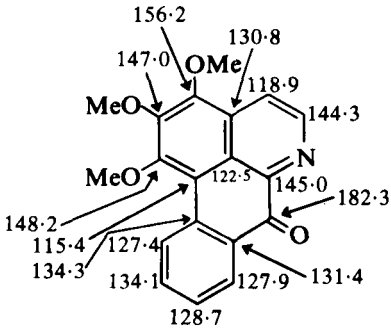

[48] *O*-Methylmoscatoline

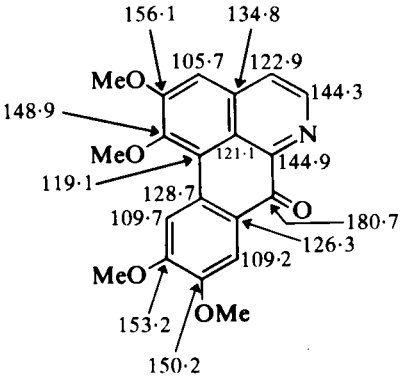

[49] Oxoglaucine

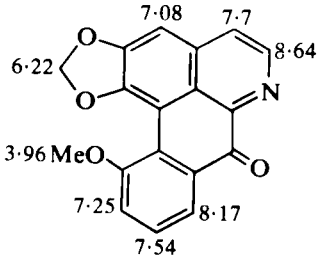

[50] Oxo-*O*-methylpukateine

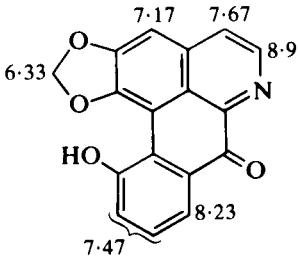

[51] 11-Hydroxy-1,2-methylenedioxyoxoaporphine

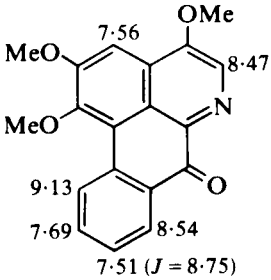

OMe 4·01
4·10
4·21

[52] Splendidine

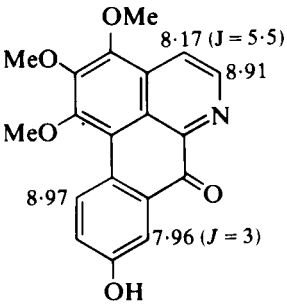

OMe 4·05
4·09
4·15

[53] Subsessiline

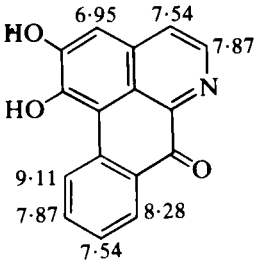

[54] Liriodendronine (in TFA-d_1)

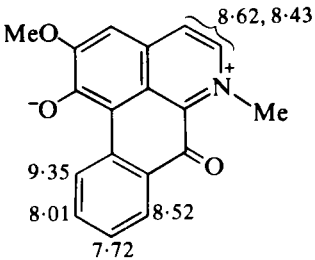

[55] *O,N*-Dimethylliriodendronine (in TFA-d_1)

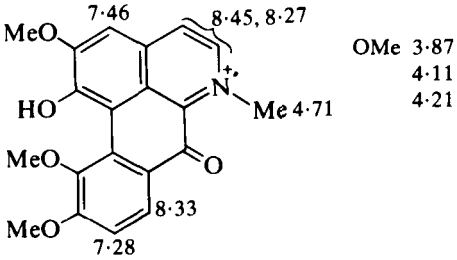

[56] Arosine (in $CDCl_3$/TFA-d_1)

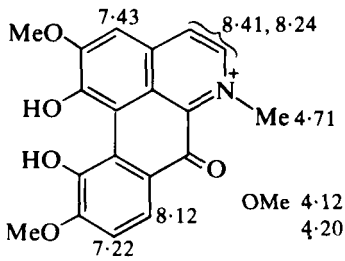

[57] Arosinine (in $CDCl_3$/TFA-d_1)

3. *Proaporphines*

Details of the ^{13}C NMR spectra of a range of proaporphines have been published[33] and [58] and [59] are provided as illustrations.

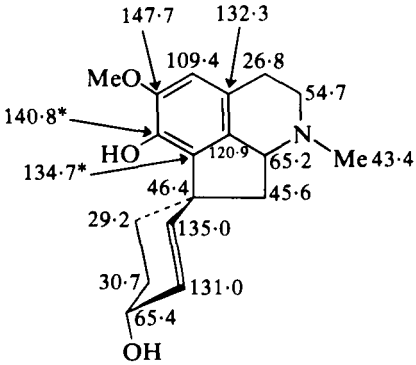

[58] (in DMSO-d_6)

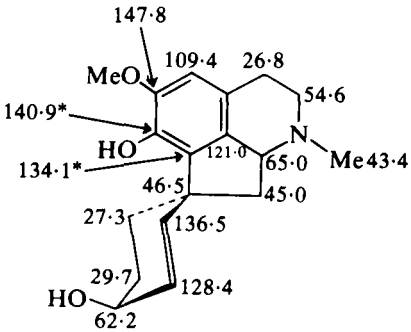

[59] (in DMSO-d_6)

D. Bisbenzylisoquinolines and benzylisoquinoline–aporphine dimers

1. *Bisbenzylisoquinolines*

^{13}C NMR shifts of cycleanine [60][34] and of isochondodendrine [61][10] have been published. The shielding of two *ortho* aromatic protons (10-H, 11-H) of ring C′ (δ 5·79, 6·25) suggests the conformation [62] for cycleanine in which these protons are shielded by the aromatic ring B′. In this conformation the 7-OMe in ring B is shielded by the aromatic C′ ring.[34] ^1H NMR data on a number of new bisbenzylisoquinoline alkaloids have been published.[35–38] Among these thalirugidine [63] exemplifies the low frequency shifts of the 8 and 8′ aromatic ring protons.[35]

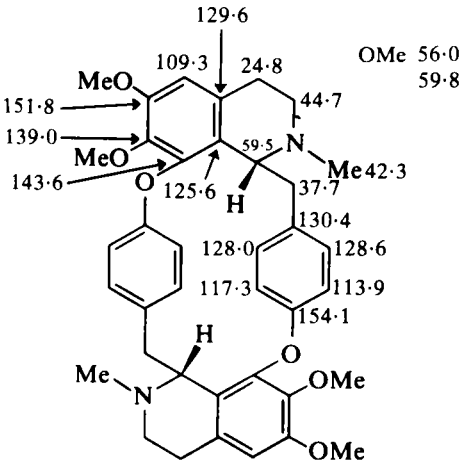

[60] Cycleanine

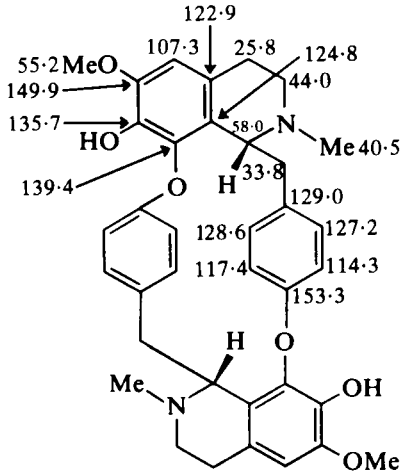

[61] Isochondodendrine

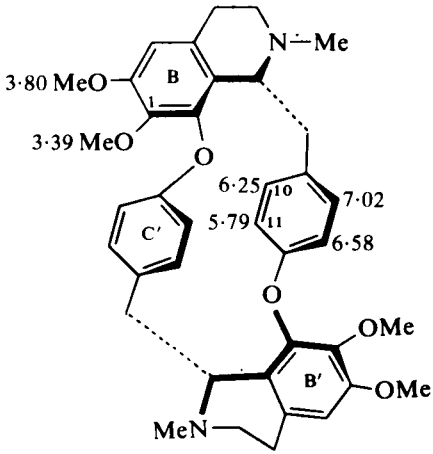

[62] Cycleanine

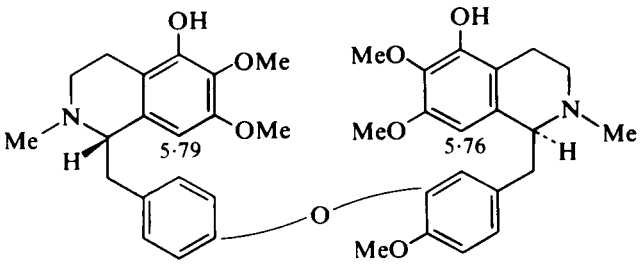

NMe	2·48
	2·51
OMe	3·61
	3·63
	3·85
	3·81
	3·81
ArH	6·6–7·2

[63] Thalirugidine

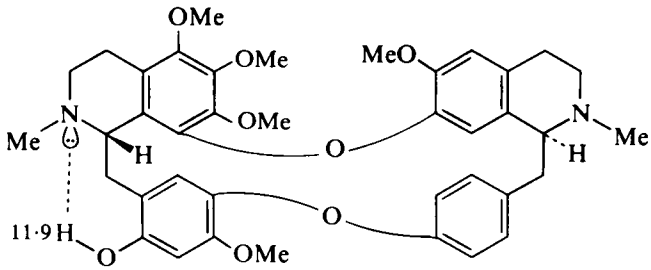

[64] Thalibrunine (in acetone-d_6)

NMe	2·46
	2·56
OMe	3·15
	3·38
	3·73
	3·79
	3·82
ArH	5·89 (s)
	6·37 (s)
	6·46 (s)
	6·64 (s)
	6·16 (dd)
	6·36 (dd)
	7·16 (dd)
	7·37 (dd)

On the basis of singlet absorption for the aromatic protons of the trisubstituted benzene ring and of the high frequency absorption of the OH proton the structure of thalibrunine has been revised to [64].[38]

2. *Benzylisoquinoline–aporphine dimers*

The absence of the high frequency 11-proton signal in the spectra of kalashine [65][39] and khyberine [66][40] is diagnostic of the position of the ether linkage. Proton shifts for thalirevolutine and for thalilutine are given in [67] and [68].[41]

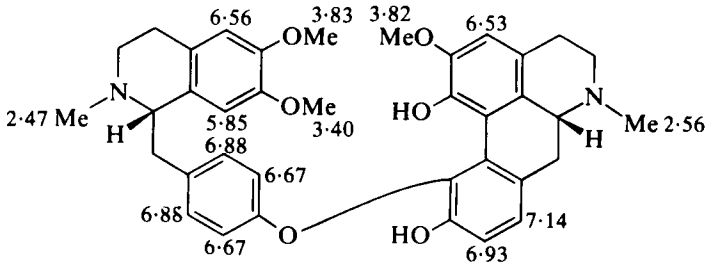

[65] Kalashine

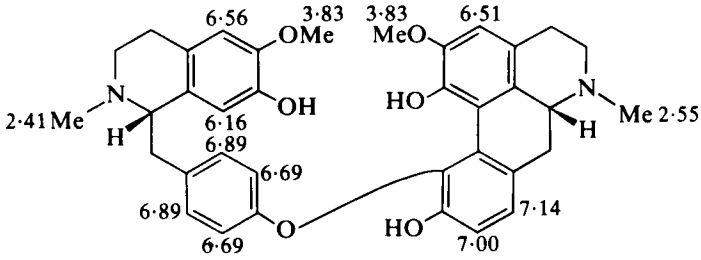

[66] Khyberine

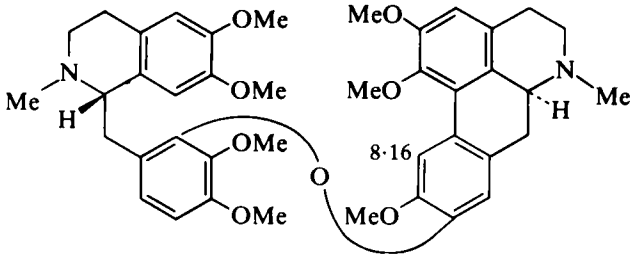

NMe 2·36
2·43
OMe 3·59
3·66
3·78
3·80
3·87
3·87
3·96
ArH 6·18
6·42
6·52
6·57
6·75
6·75

[67] Thalirevolutine

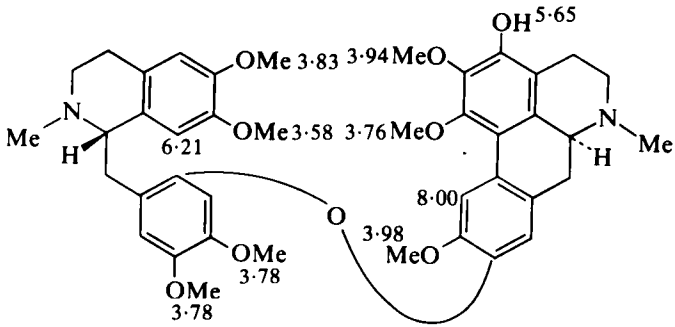

NMe 2·48
2·49
ArH 6·53
6·56
6·58
6·63

[68] Thalilutine

E. Cularines

The ^{13}C shifts of cularine are shown in [69][11] and the conformation is in accord with the dependency of ^{3}J couplings on C—C—C—H dihedral angle.[42]

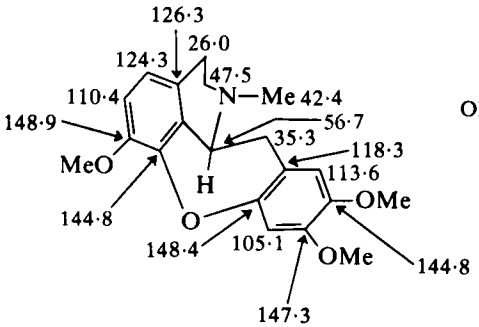

OMe 55·8
56·0
56·0

[69] Cularine

F. Protoberberines

The ^{13}C NMR spectra of quinolizidine derivatives including the protoberberines have been reviewed and the diagnostic importance of the C(6) shift in determining the nature of the ring fusion discussed.[43] This is illustrated by the ^{13}C NMR spectra of corydaline [70] and mesocorydaline [71][6] as well as by examples included in the previous review.[2]

The ^{13}C NMR spectra of *O*-acetylcapaurine [72], *O,O*-diacetylcapaurimine and capaurimine di-*p*-bromobenzoate at low temperatures show signals for *cis* and for *trans* forms and at −80 °C *O*-acetylcapaurine is shown to exist as a *c.* 3·4 : 1 mixture of *trans*:*cis* forms.[44]

^{1}H NMR parameters are available for a range of tetrahydroprotoberberines[45–47] illustrated by thalictricavine [73][45] and [74].[46] Features of the

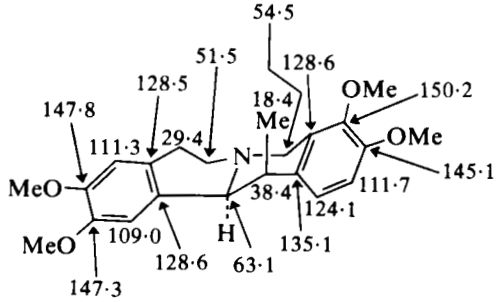

[70] Corydaline

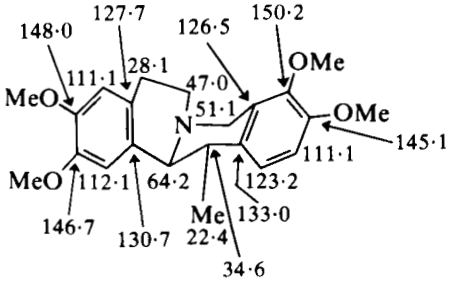

[71] Mesocorydaline

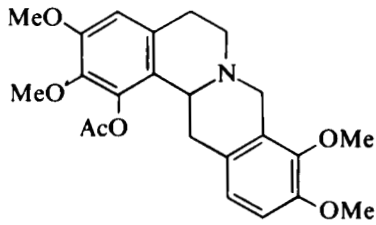

[72] *O*-Acetylcapaurine

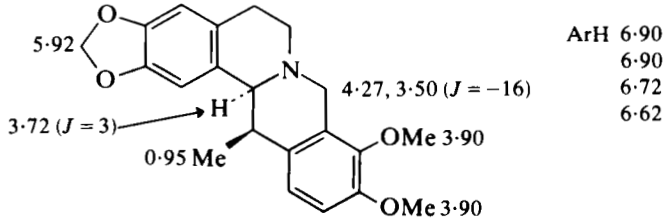

[73] Thalictricavine

spectra of 4-hydroxylated tetrahydroprotoberberines[48,49] are represented by [75] and [76],[48] which show the high frequency shift of the 4-proton in the pseudo-equatorially C(5)—OH substituted isomer [76]. In [76] the 5-proton is relatively deshielded as a result of its near 1,3-*syn* axial relationship to the nitrogen lone pair.

The ^{13}C NMR spectra of the berbine *N*-oxides [77] and [78] show the low frequency shift of C(6) in the *cis* isomer [78].[50]

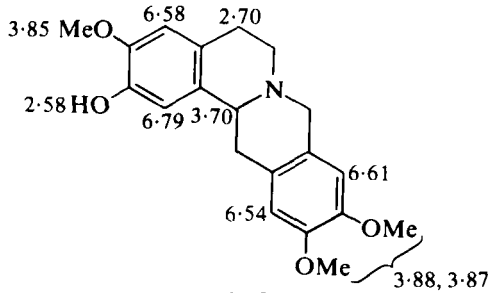

[74]

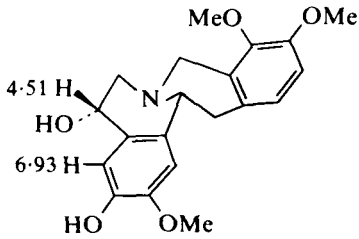

[75]

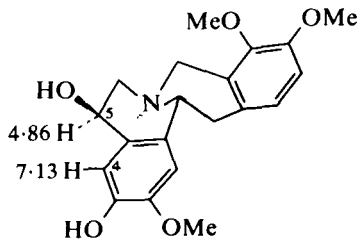

[76]

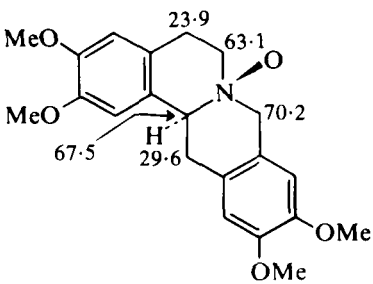

[77] *trans*-Xylopinine-*N*-oxide

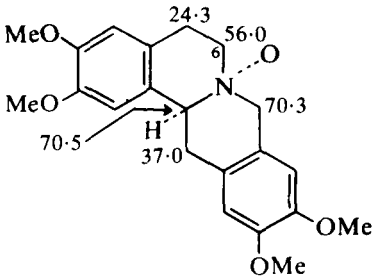

[78] *cis*-Xylopinine-*N*-oxide

^{1}H shifts for the 8,13-dioxo-14-hydroxyberbine and for the derived aporhoeadine are given in [79] and [80][51] and for compounds derived from berberidic acid in [81]–[83].[52] The deshielding of the peri proton by the carbonyl group is seen in [81] and [82], and [82] shows a complex pattern

for the lactam methylene and the 8-proton in contrast to the two singlet absorptions for the analogous set of protons in [81]. ^{1}H NMR parameters typical of protopines are provided by [84].[53]

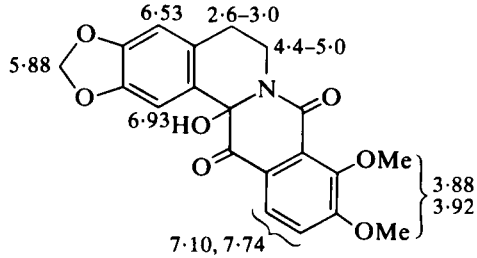

[79]

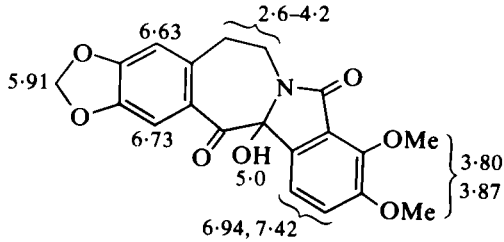

[80] Aporhoeadane

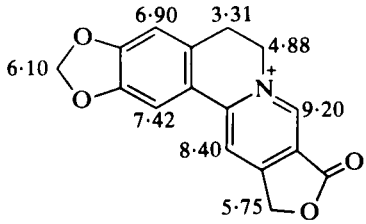

[81] (in TFA)

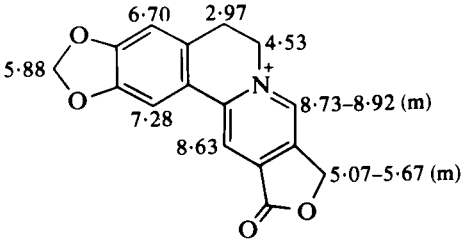

[82] (in TFA)

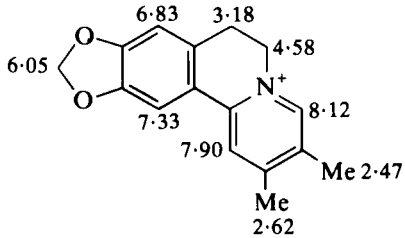

[83] (in TFA)

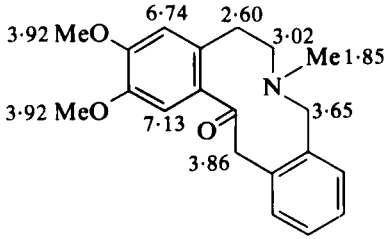

[84]

G. Spirobenzylisoquinolines

The ^{13}C shifts of fumaritine *N*-oxide [85] and those of fumaritine [86][54] are displayed. The conformation depicted in [87] for fumaritine *N*-oxide is suggested by NOE measurements. In alkaline D_2O the 13-methylene protons of [87] absorb at δ3·90 and 3·34 (J_{gem} −15·5 Hz).[54] The ^1H NMR spectrum of parviflorine is shown in [88].[55] J_{gem} for the NCH_2O protons in 1,3-oxazolidines of the type [89] is −7 Hz.[56]

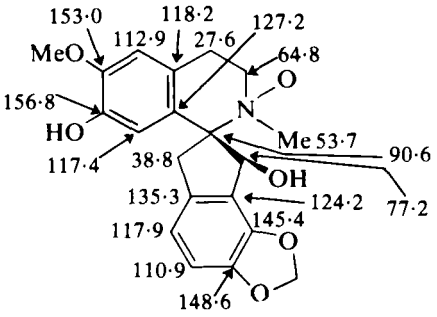

[85] Fumaritine *N*-oxide (in D_2O + NaOD)

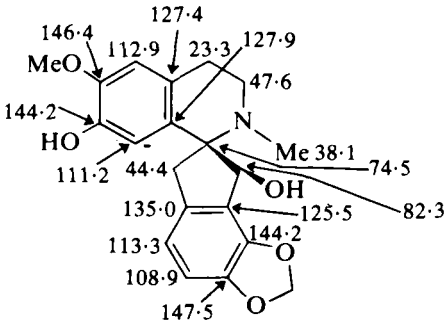

[86] Fumaritine

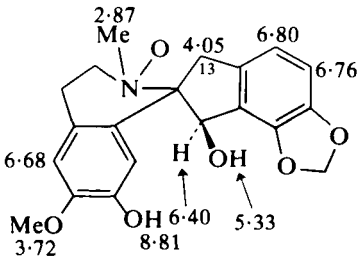

[87] Fumaritine-*N*-oxide (in DMSO)

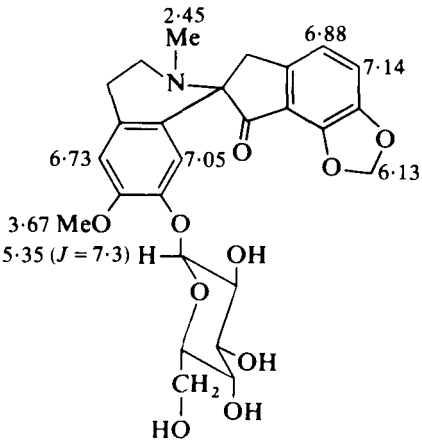

[88] Parviflorine (in pyridine-d_5)

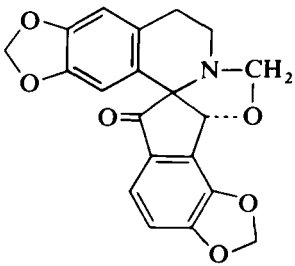

[89]

H. Benzophenanthridines

Following the establishment of the structure [90] for chelirubine the ^{1}H NMR shifts may now be assigned as shown.[57] This structure also permits rationalization of the chemical shift changes of the C(9) and C(11) protons between dihydrosanguinarine derivatives [91] and dihydrochelirubine [92] with the low frequency shift of 9-H and the high frequency shift of 11-H in the spectrum of [92] resulting from the C(10)-placed methoxy group.[57] ^{1}H NMR shifts for dihydrochelerythrine [93], bocconoline [94],[58] luguine [95][59] and corynolamine [96][60] illustrate features of the spectra of these compounds.

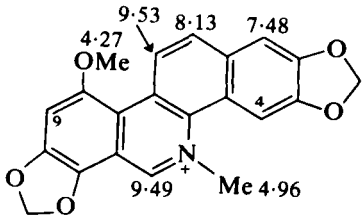

OCH_2O 6·24
6·44
4-H, 9-H, 7·61, 7·87

[90] Chelirubine chloride (in TFA)

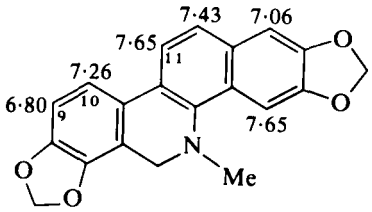

[91] Dihydrosanguinarine derivative

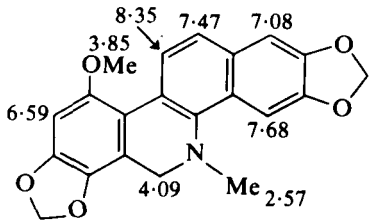

[92] Dihydrochelirubine

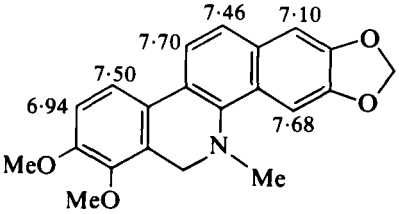

[93] Dihydrochelerythrine

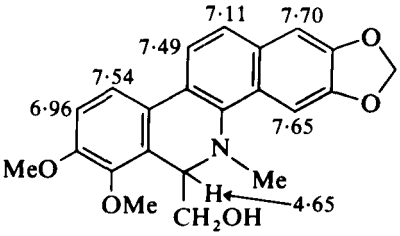

3·47 (J = −10.5, 5·0)
3·09 (J = −10·5, 10·5)

[94] Bocconoline

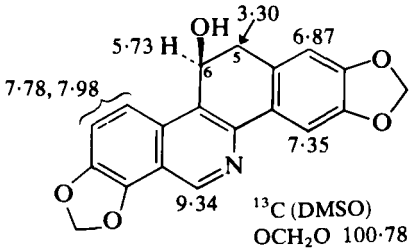

[95] Luguine (in $CDCl_3$/TFA-d_1)

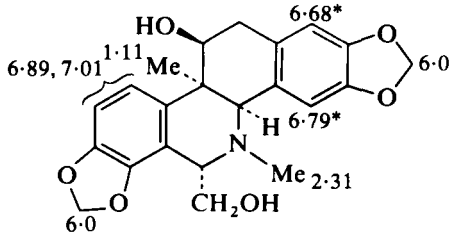

[96] Corynolamine

^{13}C shifts for corynoline [97] and corynoline-11-*O* sulphate [98] show lower frequency shifts for C(1a), C(6a) and C(10a) in the sulphate.[61] ^{1}H shifts for three isomers of 12-hydroxycorynoline are given with [99].[62] The 11β-OH,12β-OH isomer shows coupling between 11-H and 4b-H (4b-H δ3·28, $J = 2$ Hz).[62] A twist half-chair conformation for ring C in chelidonine [100] has been proposed[63] on the basis of the couplings between the C(11) and C(12) protons.

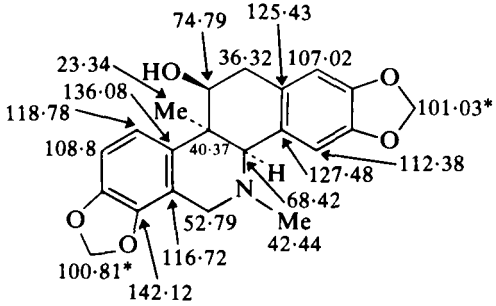

[97] Corynoline (in DMSO-d_6)

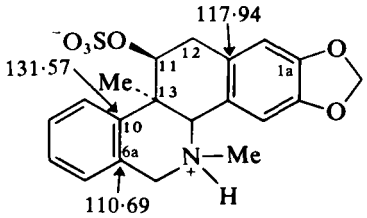

[98] Corynoline-11-*O*-sulphate (in DMSO-d_6)

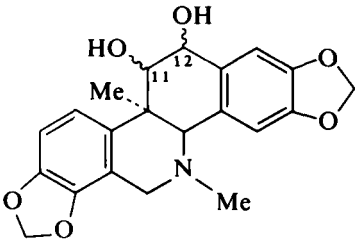

[99]

11α-*OH*, 12α-OH:δ4·72($J = 5$)
4·44($J = 5$)

11α-OH, 12β-OH:δ4·36($J = 7·5$)
4·32($J = 7·5$)

11β-OH, 12β-OH:δ4·59($J = 5$)(12-H)
3·90($J = 5, 2$)(11-H)

O—CH_2—O 5·99, 5·55(J = 1·4)
O—CH_2—O 5·93, 5·92(J = 1·5)

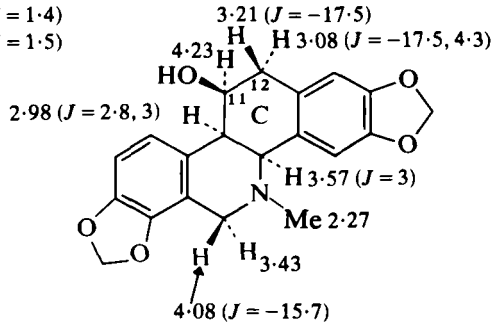

[100] Chelidonine

I. Phthalideisoquinolines (including rhoeadine type)

^{13}C shifts of the stereoisomeric pairs of phthalidoisoquinoline alkaloids α- and β-hydrastine and corlumine and adlumine are shown in [101]–[104].[6] In [102] and [104] C(3) and C(4) absorb at higher frequency than in [101] and [103]. C(1′) shifts are also diagnostic of stereochemistry.[6] The

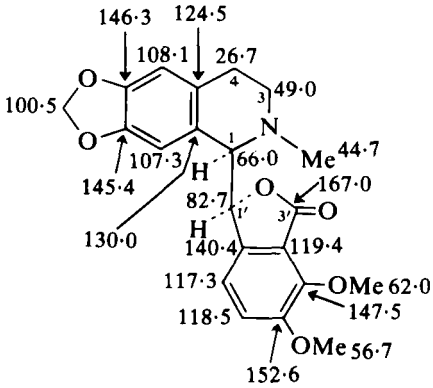

[101] β-Hydrastine

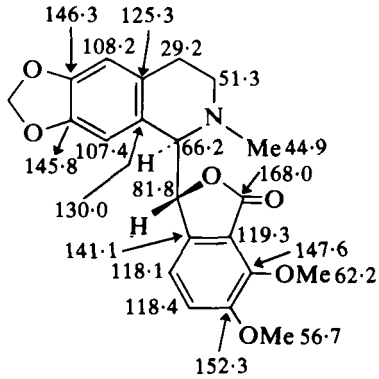

[102] α-Hydrastine

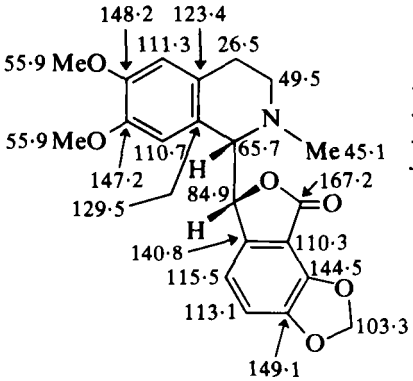

$J_{C(1)-H}$ = 133·8
$J_{C(3)-H}$ = 133·5
$J_{C(4)-H}$ = 128·3
$J_{C(1')-H}$ = 155·2

[103] Corlumine

^{1}H and ^{13}C NMR of fumschleicherine are summarized in [105] and [106] together with the ^{1}H NMR of fumaramine [107] for comparison purposes.[64] NOE measurements between the aromatic proton at δ 7·71 and the NMe protons establish the *E*-configuration of the double bond in dehydrobicuculline [108].[65]

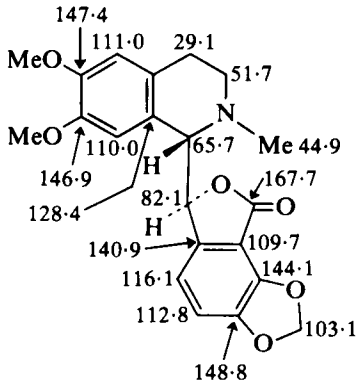

OMe	55·6
	55·9
$J_{C(1)-H}$	= 132·3
$J_{C(3)-H}$	= 136·0
$J_{C(4)-H}$	= 127·9
$J_{C(1')-H}$	= 155·2

[104] Adlumine

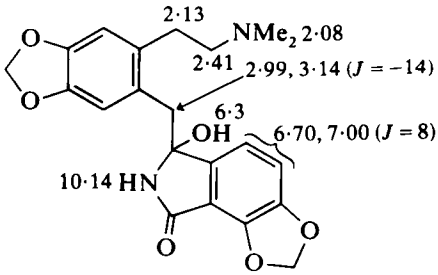

O–CH$_2$–O	5·86
	6·07
Ar—H	6·61
	6·62

[105] Fumschleicherine (in DMSO-d_6)

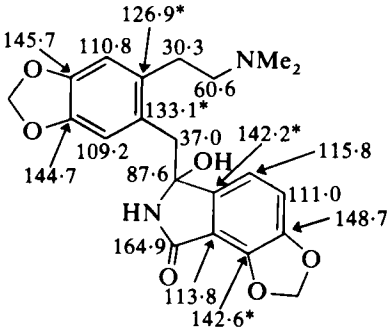

[106] (in DMSO-d_6)

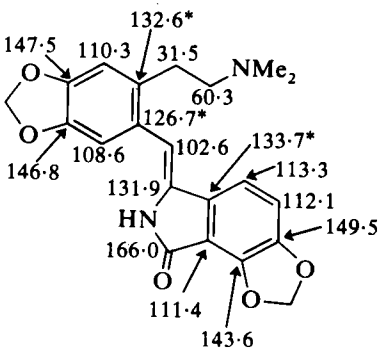

[107] Fumaramine

^{1}H NMR parameters for a selection of rhoeadine type alkaloids are given in [109], [110],[66] [111],[67] [112][68] and [113].[69] The open chain derivative [113] shows a value of J_{vic} intermediate between values of J_{vic} across the ring fusion for *cis* and *trans* compounds (cf. 9 Hz in [109], 2 Hz in [111]).

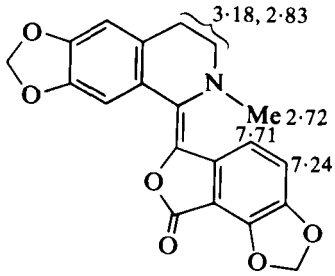

Ar–H 7·20 (s)
6·62 (s)
O–CH$_2$–O 6·18
5·96

[108] Dehydrobicuculline

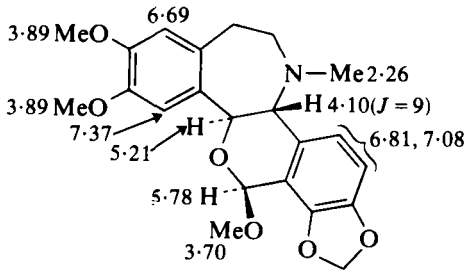

5·94, 6·05 (J = 1·3)

[109] Glaudine

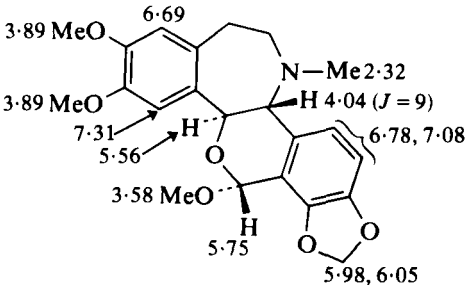

[110] Epiglaudine

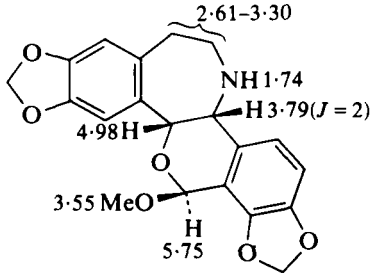

O–CH$_2$–O 5·95
6·09

[111] Papaverrubine

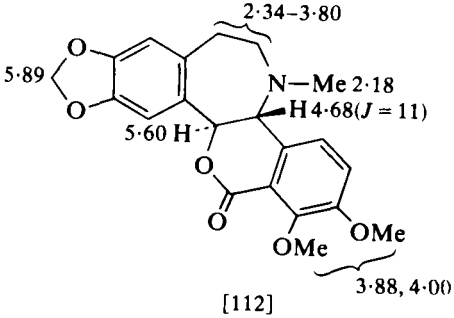

[112]

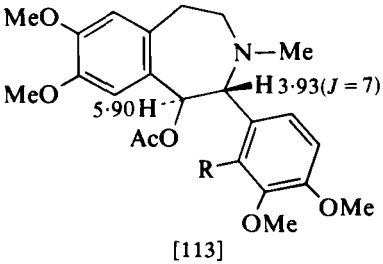

[113]

J. Colchicine alkaloids

The complete assignment of ^{13}C shifts in colchicine has been determined in DMSO-d_6 [114][70] and in $CDCl_3$ solution [115][71] and this has resulted in the correction of some previous assignments.[72]

^{13}C shifts of the tropolone ring permit a ready differentiation between the normal and iso-colchicine series (see demecolcine (normal [116] and iso-demecolcine (iso) [117]).[73] The ^{1}H NMR spectra of the same compounds [118] and [119] show a smaller chemical shift difference between 11-H and 12-H in the iso series than in the normal series.[73,74]

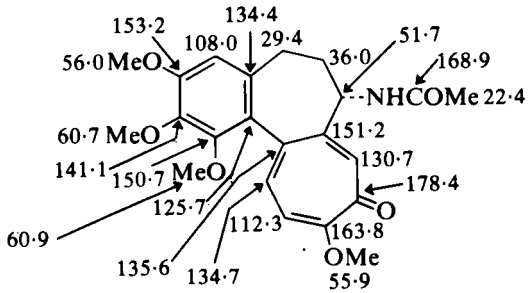

[114] Colchicine (in DMSO-d_6)

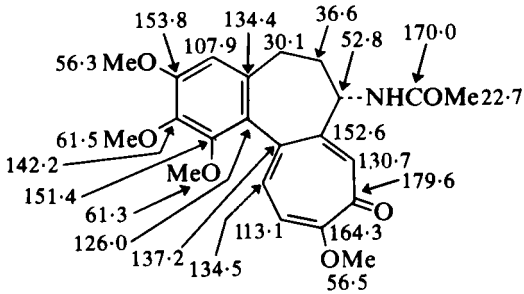

[115] Colchicine

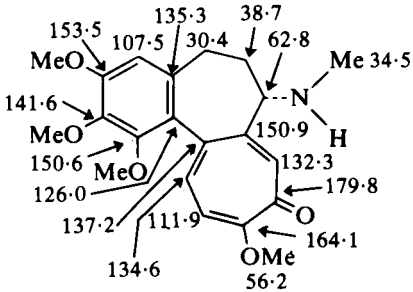

[116] Demecolcine

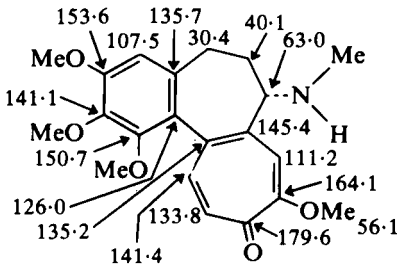

[117] Isodemecolcine

^{13}C shifts permit a reassignment of structure to "epoxycolchicine" [120][75] and ^{1}H shifts suggest the structure [121] for a product obtained by treatment of colchicine with acetic anhydride.[76]

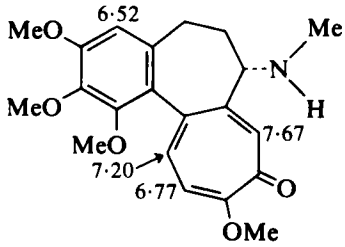

[118] Demecolcine

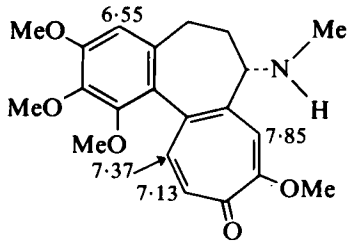

[119] Isodemecolcine

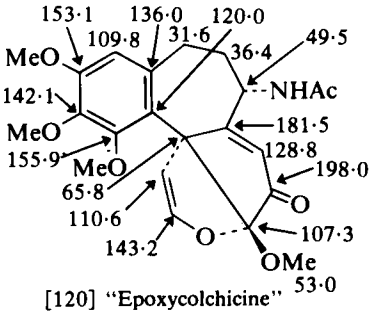

[120] "Epoxycolchicine"

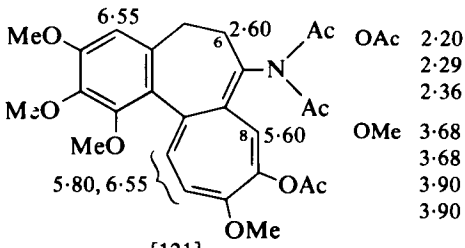

[121]

K. Emetine-type alkaloids

^{1}H NMR shifts for emetine and isomers are given in [122]–[125][77] and ^{13}C shifts for alangimarckine [126] and its epimer [127][78] show the lower frequency shifts of C(1), C(2) and C(1′) in [126] (see ochrolifuanine A and B shifts – structures [546] and [547] in reference 2).

From a knowledge of the ^{13}C shifts of the ethyl group carbons in [128] and [129][79] the *cis* → *trans* isomerization [130] → [131] can be followed.[80]

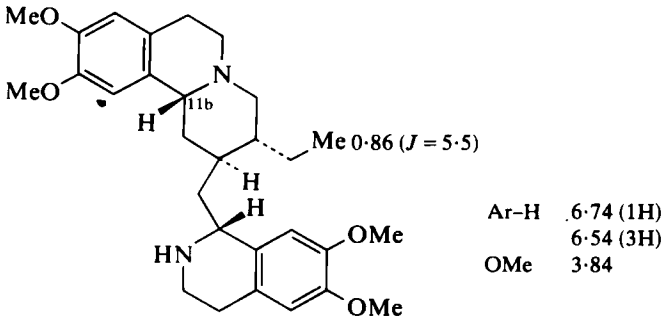

[122] 11b-Epiemetine

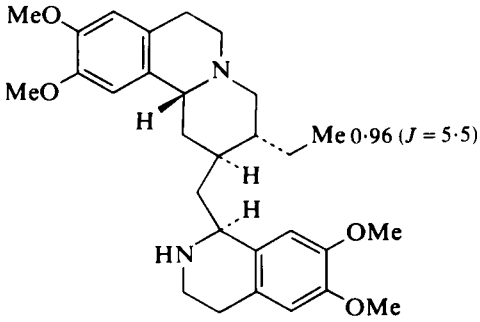

Ar–H 6·68
OMe 3·87

[123] 11b-Epiisoemetine

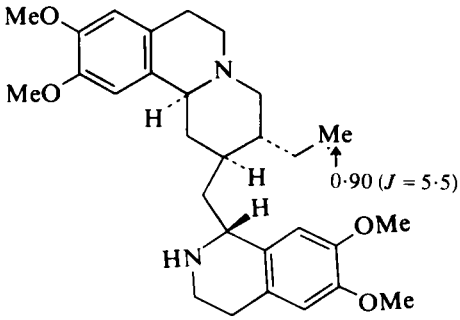

Ar–H	6·73 (1H)
	6·54 (2H)
	6·47 (1H)
OMe	3·83 (3OMe)
	3·80

[124] Emetine

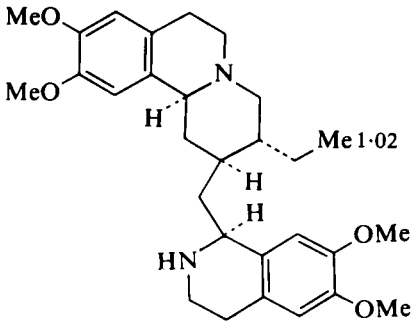

Ar–H	6·77 (1H)
	6·63 (3H)
OMe	3·88

[125] Isoemetine

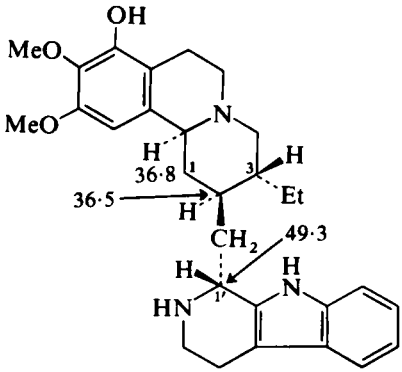

^{1}H NMR (in DMSO): OMe 3·64
3·72

[126] Alangimarckine

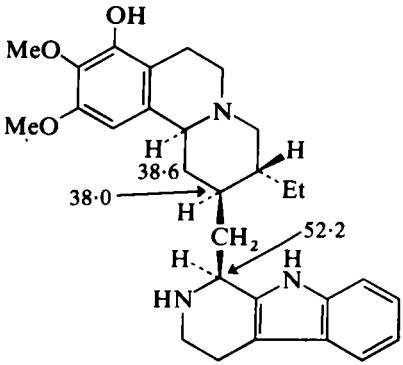

^{1}H NMR (in DMSO): OMe 3·48
3·64

[127]

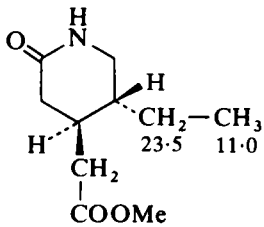

[128]

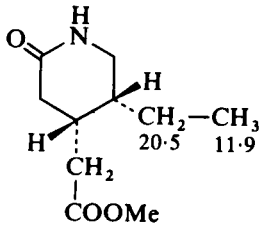

[129]

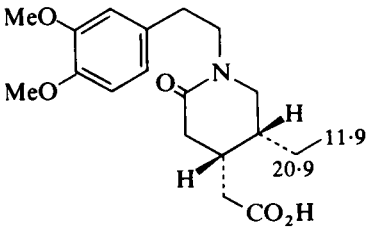

[130]

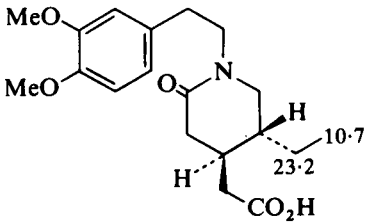

[131]

L. Other isoquinoline alkaloids including pavines

^{13}C NMR shifts for argemonine are given in [132].[11] The aromatic proton shifts in caryachine [133] and in [134][81] are in accord with substituent parameters developed earlier[82] and with solvent-induced changes (DMSO to $CDCl_3$) consonant with literature values.[1] ^{1}H NMR shifts are given for quettamine [135], dihydrosecoquettamine [136] and secoquettamine [137][83] and for peshawarine [138].[84]

A ^{13}C NMR procedure has been described[85] for a rapid quantitative estimation of ephedra alkaloids.

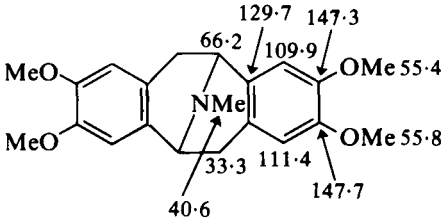

[132] Argemonine

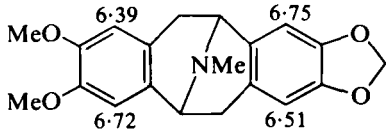

[133] Caryachine (in DMSO-d_6)

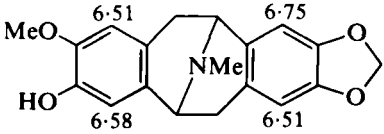

[134] (in DMSO-d_6)

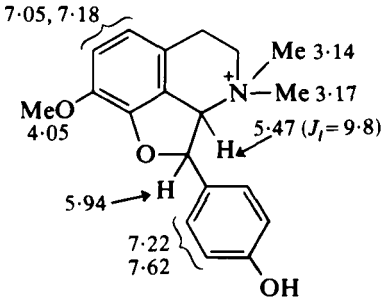

[135] Quettamine (in TFA-d)

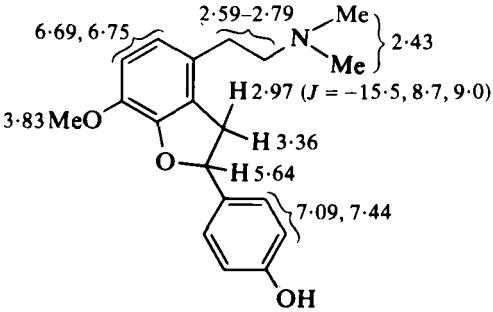

[136] Dihydrosecoquettamine

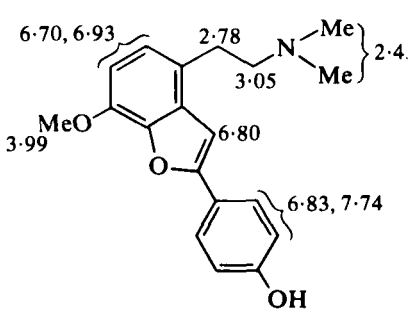

[137] Secoquettamine

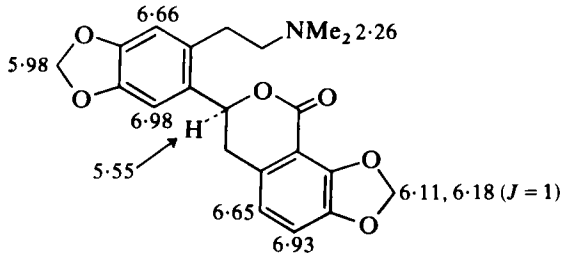

[138] Peshawarine

III. AMARYLLIDACEAE ALKALOIDS

The ^{1}H NMR spectra of clivacetine [139],[86] 3-epitazettadiol [140], tazettadiol [141], deoxypretazettine [142], deoxytazettine [143],[87] carinatine [144],[88] a synthetic analogue of the galanthan group [145],[89] a sceletium-type alkaloid [146][90] and of some apogalanthamine analogues [147] and [148][91] illustrate some of the spectral features of alkaloids of the Amaryllidaceae.

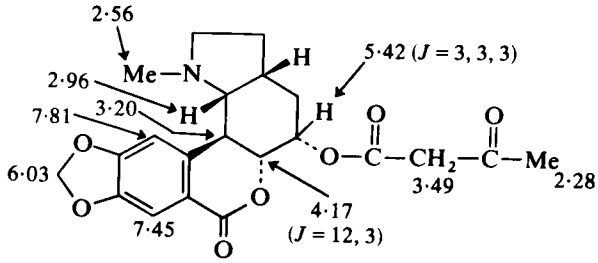

[139] Clivacetine

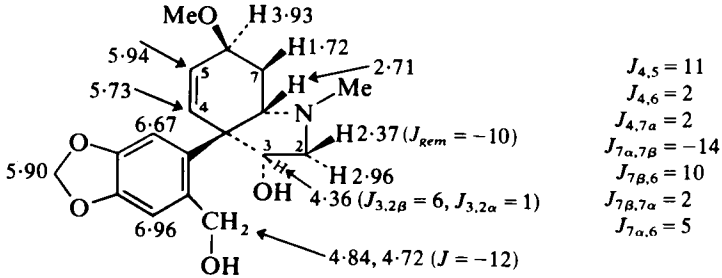

[140] 3-Epitazettadiol

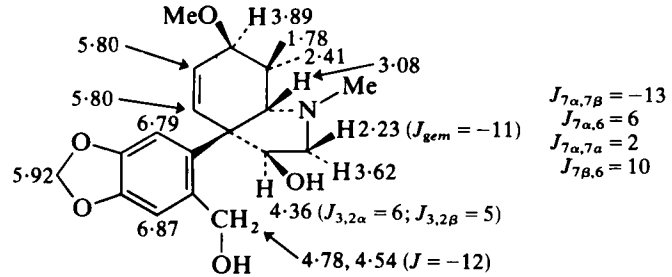

[141] Tazettadiol

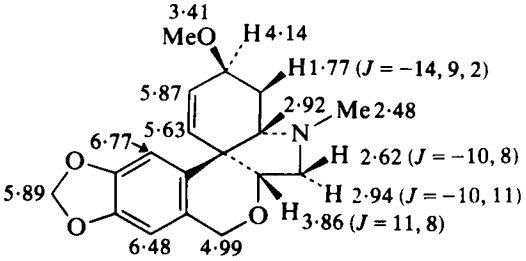

[142] Deoxypretazettine

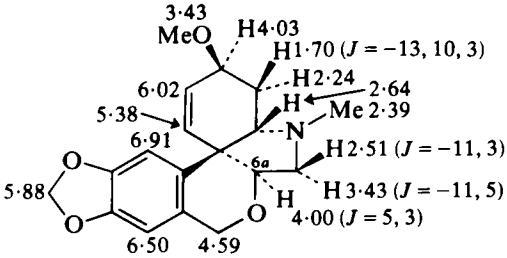

[143] Deoxytazettine

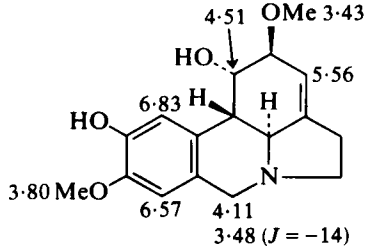

[144] Carinatine

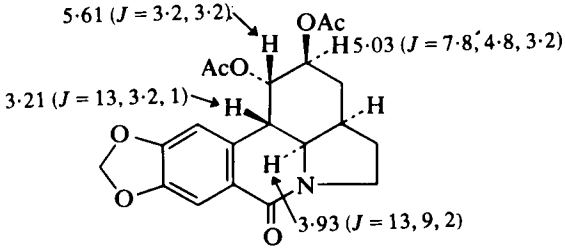

[145]

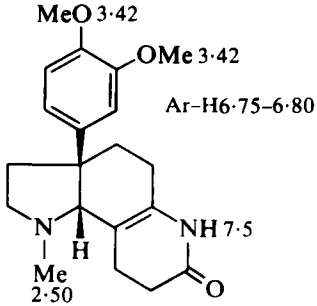

[146]

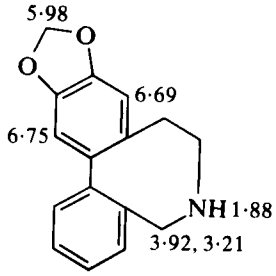

[147]

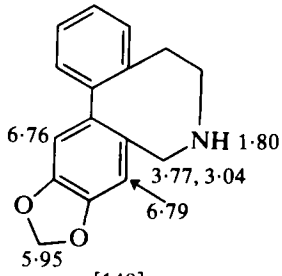

[148]

IV. ERYTHRINA, DIBENZ[*d,f*]AZONINE AND CEPHALOTAXINE ALKALOIDS

The relationship between 14-H chemical shifts and stereochemistry in erythrinane derivatives outlined in a previous review[1] has been extended[92–95] to 1-bromo- and other 1-, 2-, 3- and 7-substituted derivatives.

α-substituents at the 1-position in *cis*-erythrinanes normally deshield 14-H. This is not observed in [149] (cf. shift in [150]) and the value of $J_{1,6}$ of 11·5 Hz (in DMSO-d_6) in this compound indicates an equatorial bromine. Thus in 1,2-disubstituted *cis*-erythrinanes stereochemical decisions must not be based on 14-H shifts.[92] In the β-bromoketone [151] the conformation is solvent dependent. Thus in DMSO-d_6 the compound adopts the equatorial bromo conformation [152] and shows deshielding of 14-H as a result of the close approach to 1- and 3-H_{ax}. In $CDCl_3$ [151] adopts the axial bromo conformation [153] and 14-H absorbs "normally".[93]

The influence of the axial OH and OAc in the oxides [154] and [155] on the chemical shifts of 14-H is marked.[94]

Differences in 14-H chemical shift are seen in the spectra of the *trans*-erythrinane [156] and the ring-enlarged derivative [157].[95]

Comparison of the ^{13}C NMR spectra of [158] and [159] show that C(14) is not influenced by the steric compression shift. The C(5) shift is also rather similar in both compounds.[96] Differences in C(1) to C(3) shifts are

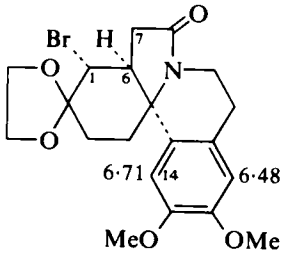

[149]

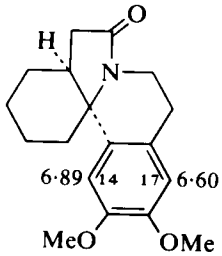

[150]

14-H 6·90 (in DMSO-d_6)
17-H 6·68 (in DMSO-d_6)

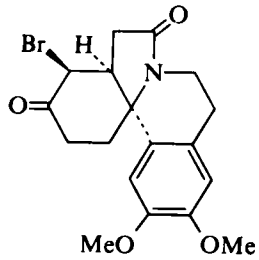

[151]

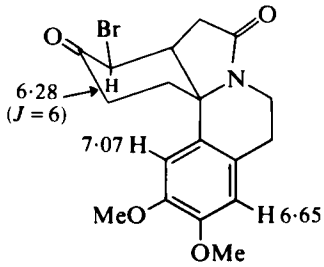

[152] (in DMSO-d_6)

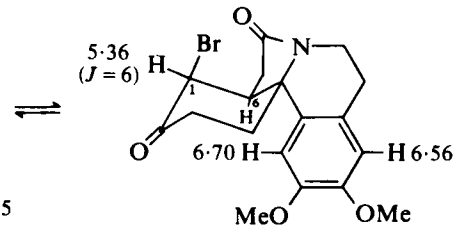

[153]

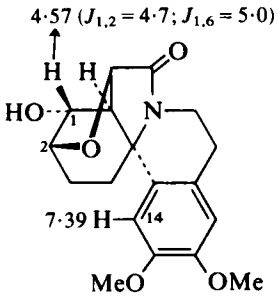

[154]

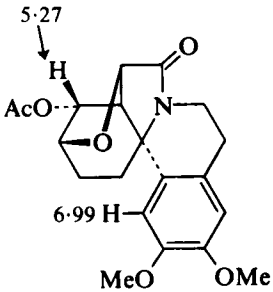

[155]

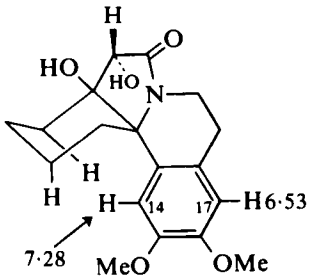

[156]

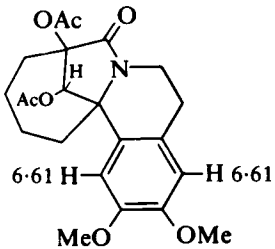

[157]

noted in [160] and [161] and in [162]–[163] the effect of the angular substituent on shifts is marked.[97]

The ^{1}H NMR spectra of a number of alkaloids exemplified by erysopinophorine [164][98] have been reported[98–100] and some parameters for the homoerythrinane phellibilidine [165][101] and of the synthetic C-homo erythrina derivative [166][102] are given. Some ^{13}C shifts for the dibenz[*d*,*f*]azonine derivative [167] have been published.[103]

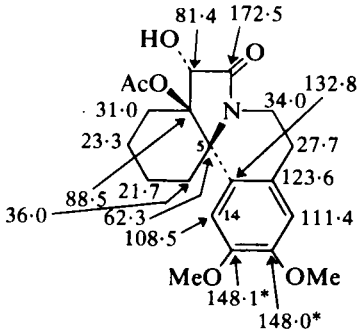

[158]

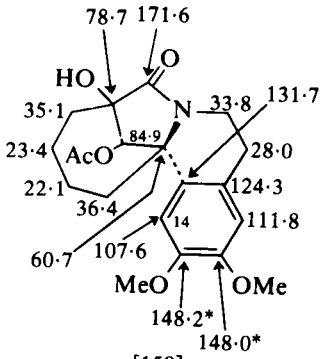

[159]

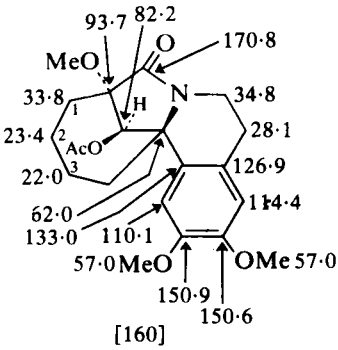

[160]

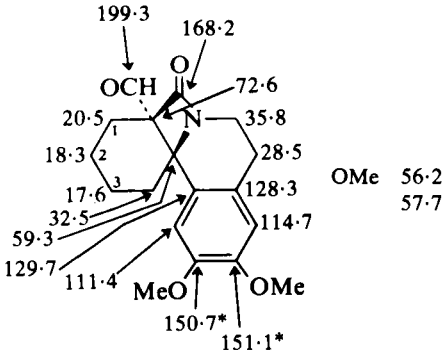

[161]

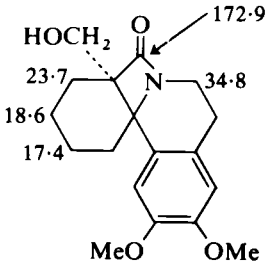

[162]

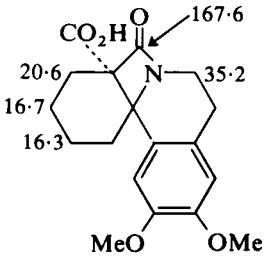

[163]

^{13}C shifts for a range of *Cephalotaxus* alkaloids are given in [168]–[172][104] and ^{1}H NMR shifts for harringtonine[105] and for the acyl C(2) epimer in [173] and [174] respectively.[105]

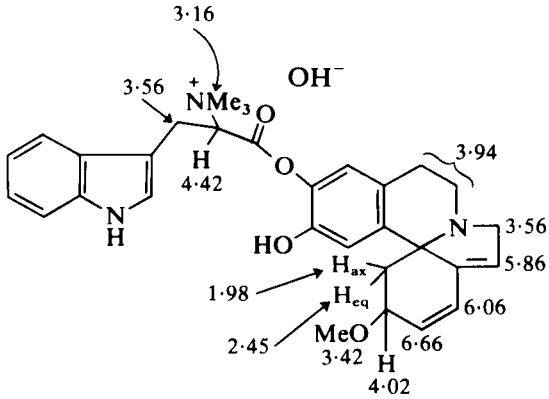

[164] Erysopinophorine (in D_2O)

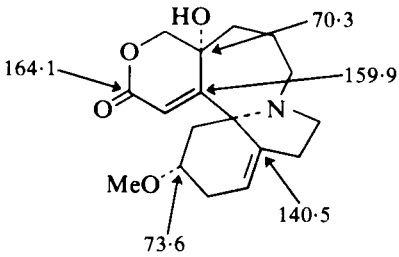

[165] Phellibilidine

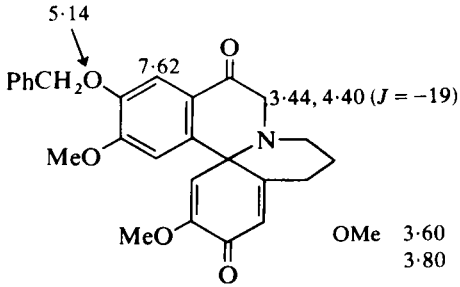

[166]

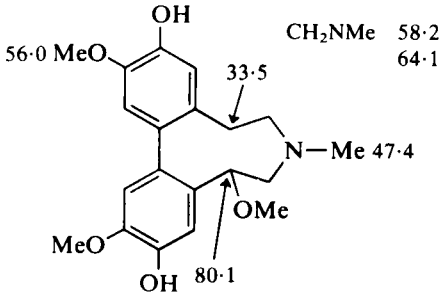

[167]

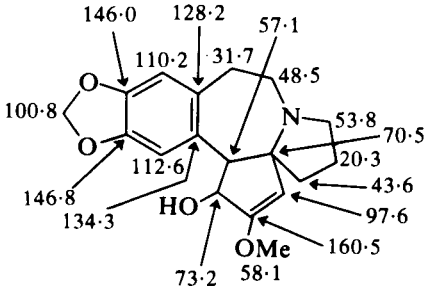

[168] Cephalotaxine

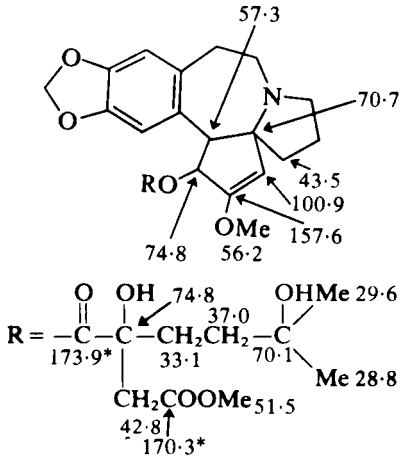

[169] Harringtonine

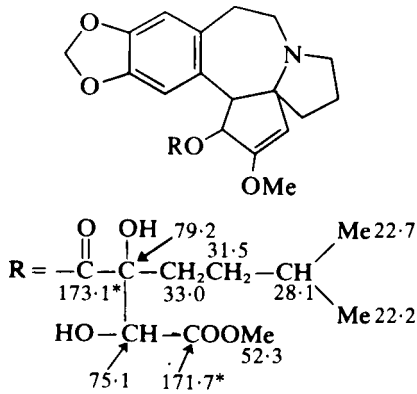

[170] Isoharringtonine

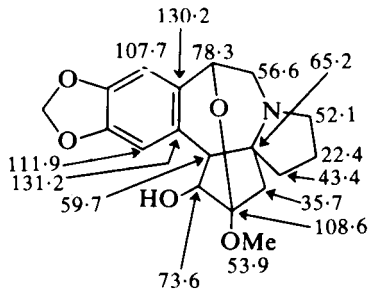

[171] Drupacine

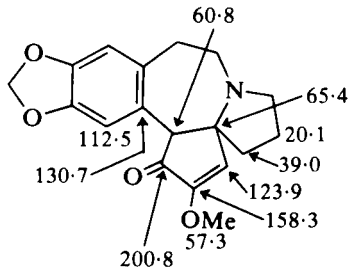

[172] Cephalotaxinone

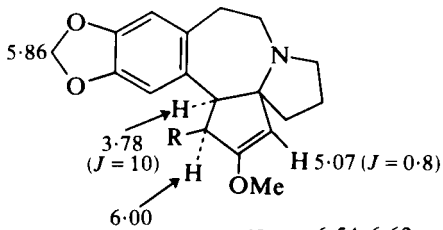

Ar–H	6·54, 6·62
OMe, COOMe	3·58, 3·69

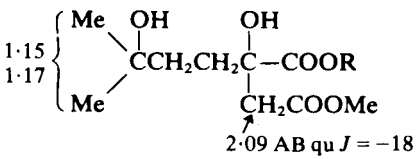

[173] Harringtonine

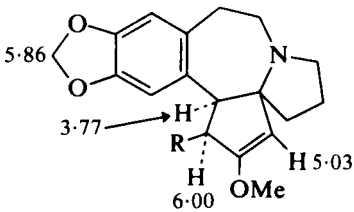

Ar–H	6·62, 6·62
OMe, COOMe	3·65, 3·67

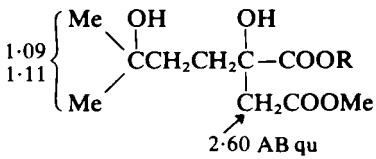

[174] *C*(2)-Acylepiharringtonine

V. MORPHINE ALKALOIDS

^{1}H NMR shifts for thebaine methochloride (in D_2O) are given in [175].[106]

The ^{1}H NMR spectra of 14β-carboxymethyl-8β-hydroxy-8,14-dihydrothebaine lactone [176] and 8β,14β-epoxyethano-8,14-dihydrothebaine [177] demonstrate the "acylation shift" of 0·46 ppm of 8-H between the lactone and the ether and the low frequency shift of 7-H typical of enol ethers of the morphine series.[107] The isomers [178] and [179] are readily differentiated on the basis of the value of $J_{5,6}$ (5-H: δ 4·61 (J = 6) in [178] and δ 4·50 (J = 2·2) in [178]).[107]

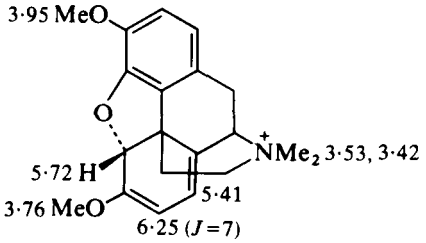

[175] Thebaine methochloride (in D_2O)

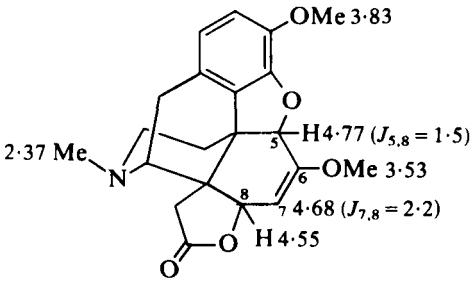

[176]

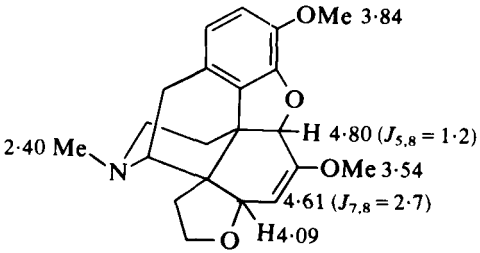

[177]

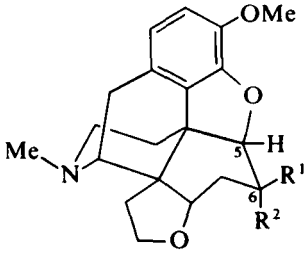

[178] R^1 = OH, R^2 = H
[179] R^1 = H, R^2 = OH

In the ^{1}H NMR spectrum of the codeine derivative [180] the value of $J_{7,8\beta}$ of 4·8 Hz indicates a dihedral angle $\phi_{7,8}$ of 40–50° consonant with a deformation of ring C.[108] In a rearranged derivative [181] 5-H absorbs to higher frequency of the aromatic protons (δ 6·62) as a result of its position in the plane of the aromatic ring and interaction with the phenolic OH.[108]

Coupling constants in the 9,17-secocodeine [182] are similar to those for codeine[1] and indicate 6-H to be axial.[109] NMR studies (particularly ^{13}C shifts of C(5), C(6) and C(7)) show an equilibrium in $CDCl_3$ solution between the 5,6-dehydromorphinan [183] and its Michael addition product [184].[110]

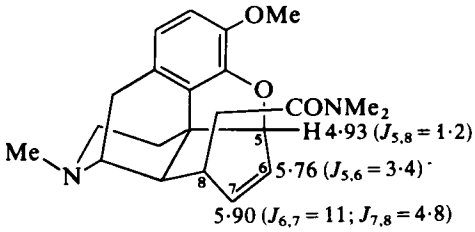

[180]

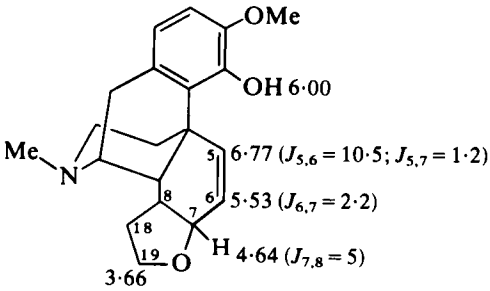

[181]

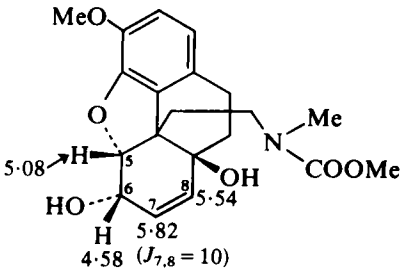

$J_{5,6} = 5{\cdot}5$
$J_{6,7} = 2{\cdot}0$
$J_{6,8} = 3{\cdot}5$
$J_{6,OH} = 10{\cdot}0$

[182]

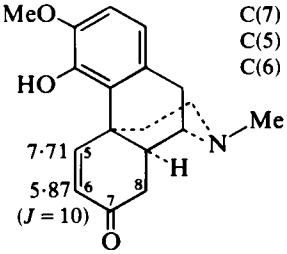

^{13}C NMR:
C(7) 199·2
C(5) 158·8
C(6) 125·9

[183]

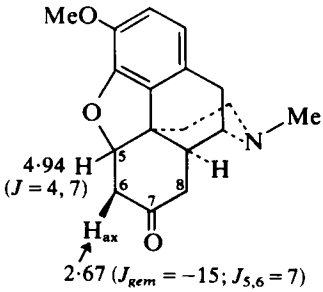

^{13}C NMR
C(7) 206·9
C(5) 90·0
C(6) 45·1

[184]

^{13}C shifts for ocobotrine and *O*-methylpallidinine are given in [185] and [186][111] and ^{1}H shifts for 1,2-dehydroreticulinium chloride and *N*-norsalutaridine in [187][112] and [188].[113]

The C(3) stereochemistry in [189] and [190] is reflected in the C(7)-Me proton shifts[114] and in the ^{1}H NMR spectrum of the benzomorphan [191] the absorption for the C(9)-Me at $\delta 1{\cdot}37$ indicates the β-isomer since α- and β-C(9)-Me groups in such compounds absorb at $\delta 0{\cdot}8$ and $\delta 1{\cdot}3$ respectively.[115] The structure of the morphinanedione relative [192] is based on 360 MHz NMR data, particularly on the observation of coupling between 5-H and one of the protons at C(4).[116]

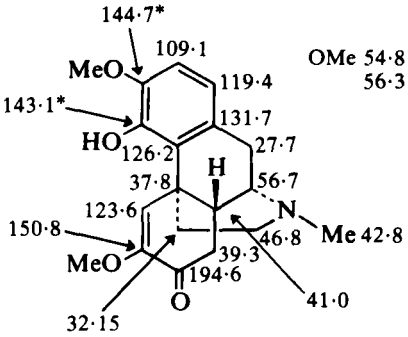

[185] Ocobotrine

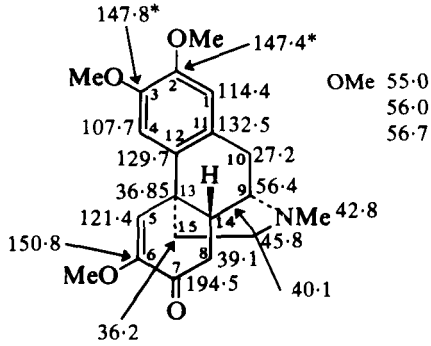

[186] *O*-Methylpallidinine

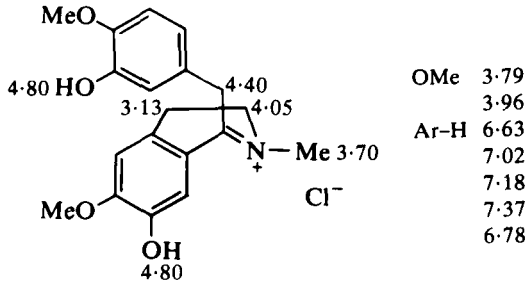

[187] 1,2-Dehydroreticulinium chloride (in CD_3OD)

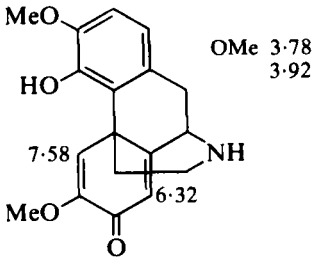

[188] *N*-Norsalutaridine

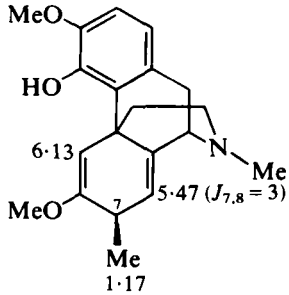

[189]

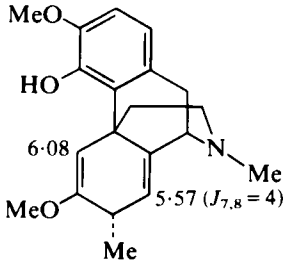

[190]

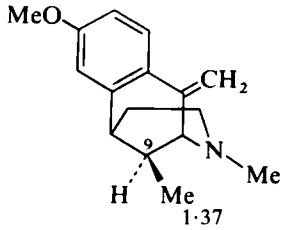

[191]

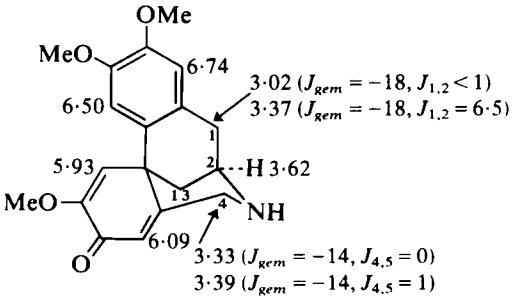

OMe 3·70
3·73
3·89

13–H 1·91 (J_{gem} = −12·5, $J_{1,13}$ = 1·5, $J_{2,13}$ = 4·0)
13–H′ 2·37 ($J_{2,13}$ = 1·8)

[192]

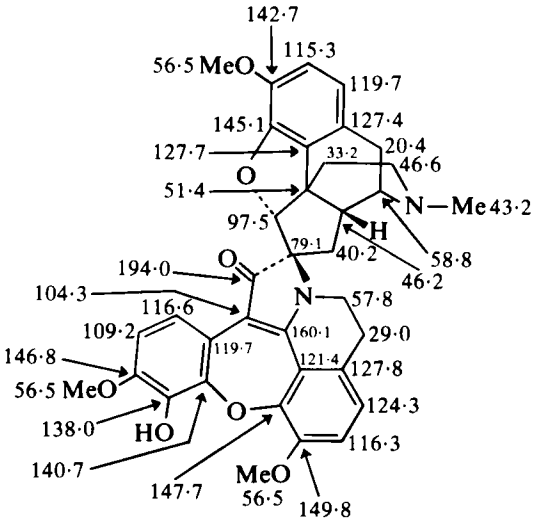

[193] Cancentrine

^{13}C NMR shifts of cancentrine [193], 10-oxocancentrine [194] and 9,10-dihydrocancentrine methine-*O*-methyl ether [195] are given[117] and ^{1}H NMR parameters for cancentrine and 10-oxocancentrine in [196] and [197].[117] The C(20)-O*Me* in [195] absorbs at δ 61·5 consistent with its sterically crowded position.

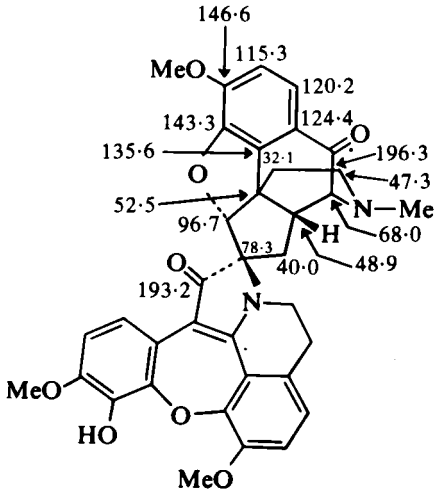

[194] 10-Oxocancentrine

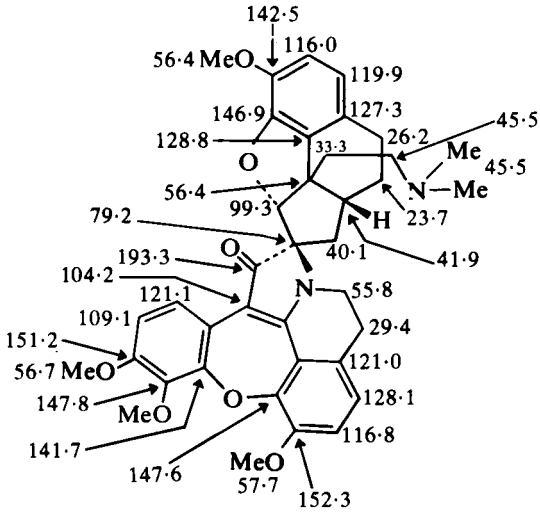

[195] 9,10-Dihydrocancentrine methine-*O*-methyl ether

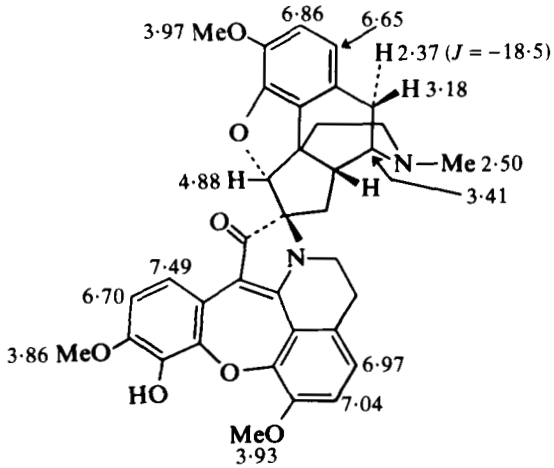

[196] Cancentrine

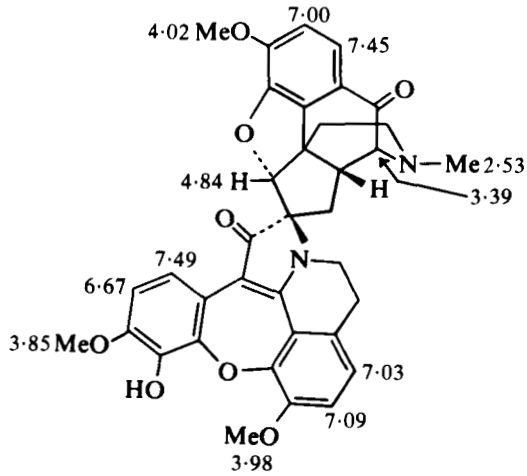

[197] 10-Oxocancentrine

VI. PYRROLIZIDINE AND PYRROLE ALKALOIDS

Since the last review in this series[2] ^{13}C NMR shifts for a range of pyrrolizidine alkaloids have been reported. Comparison of the ^{13}C chemical shifts in monocrotaline [198] and its *N*-oxide [199] and in retronecine [201] and its *N*-oxide [202] shows the expected deshielding of C(5), C(3) and C(8) on *N*-oxidation (C(5) is less deshielded than C(3) and C(8) as a result of the γ-shielding effect of the C(7)-O). *N*-methylation produces

comparable shifts to *N*-oxidation (see [200] and [203]).[118] On the basis of the *N*-oxide shifts the values of 74·6 and 96·4 are assigned to C(7) and C(8) in monocrotaline *N*-oxide [199] and this suggests[118] reversal of the assignments in the published values[119] for europine *N*-oxide [204] (the reported[119] C(9) shift of 77·9 for europine *N*-oxide is probably in error since the C(9) shift in lasiocarpine [205] is 62·3[120]). The shifts shown in [204] incorporate the suggested corrections.[118,120] The C(7) and C(8) shifts reported[121] for senecionine [206] have been reversed.[118]

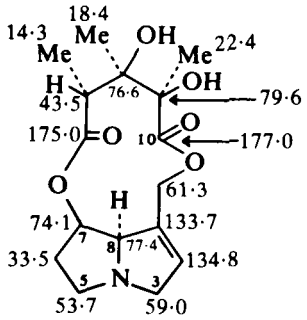

[198] Monocrotaline (in pyridine-d_5)

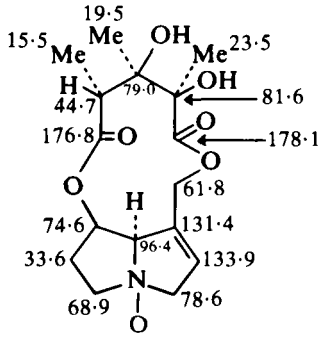

[199] Monocrotaline *N*-oxide (in D_2O)

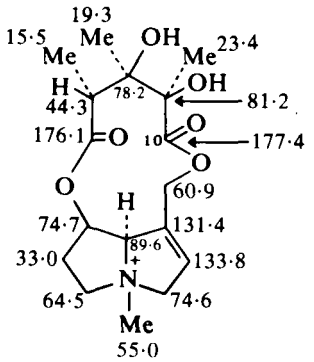

[200] Monocrotaline methiodide (in D_2O)

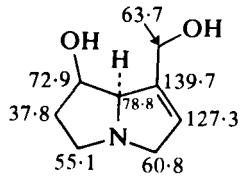

[201] Retronecine (in D_2O)

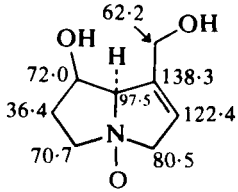

[202] Retronecine *N*-oxide (in D_2O)

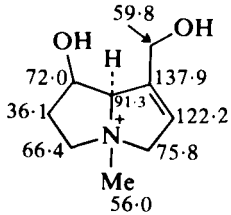

[203] Retronecine methiodide (in D_2O)

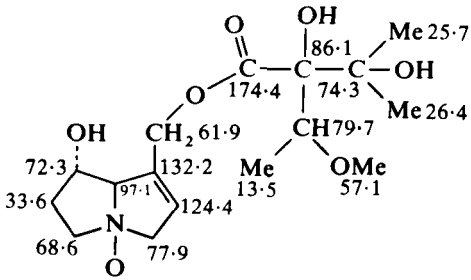

[204] Europine *N*-oxide (in D_2O)

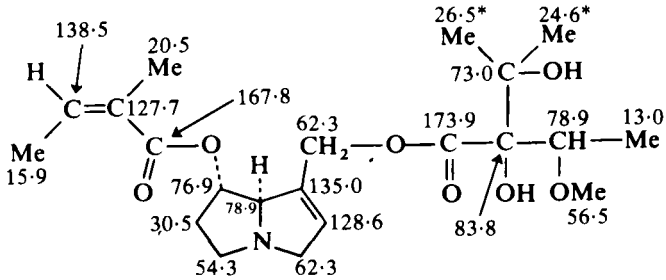

[205] Lasiocarpine

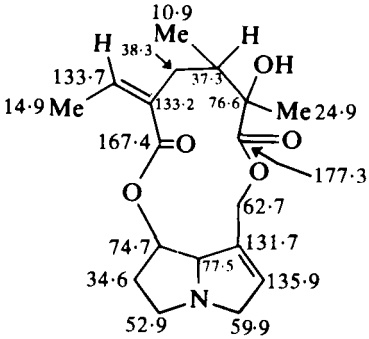

[206] Senecionine

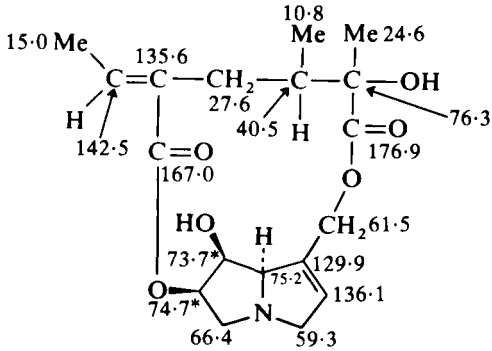

[207] Madurensine

^{13}C shifts for madurensine [207],[120] retrorsine [208],[120] swazine [209],[122] isoline [210],[122] hygrophylline [211],[122] bulgarsenine [212] and doronenine [213][123] are provided with the structures.

^{1}H NMR data are given for senecionine [214],[121] europine *N*-oxide [215],[119] parsonine [216],[124] ligularidine [217],[125] petasinine [218] and petasinoside [219],[126] yamataimine [220][127] and [221].[128]

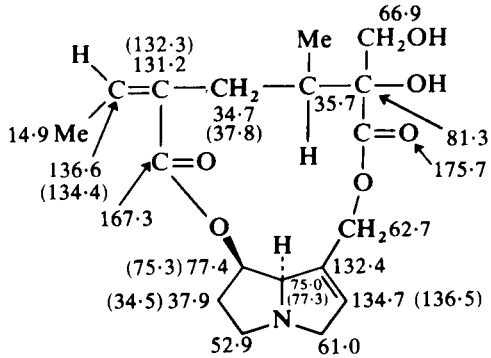

[208] Retrorsine (values in parentheses taken from reference 122)

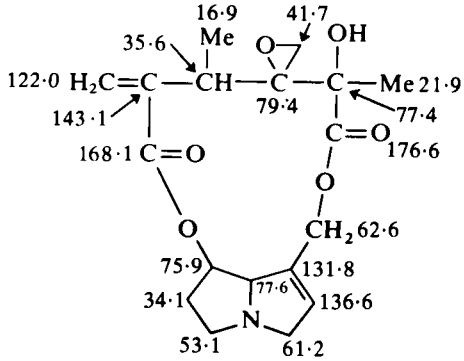

[209] Swazine

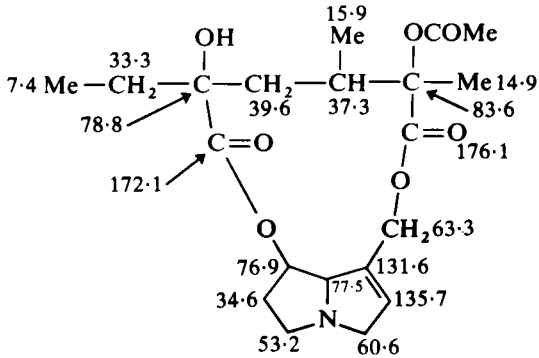

[210] Isoline

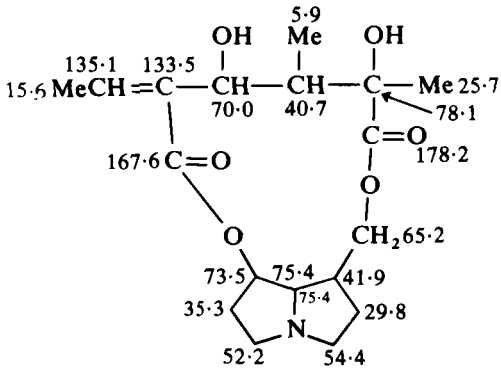

[211] Hygrophylline

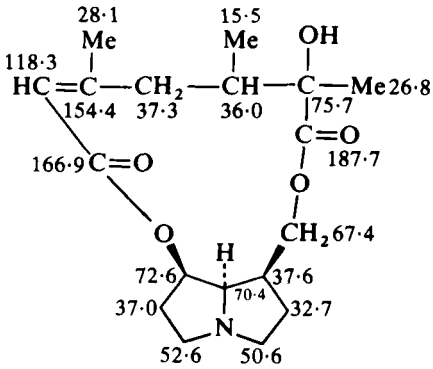

[212] Bulgarsenine

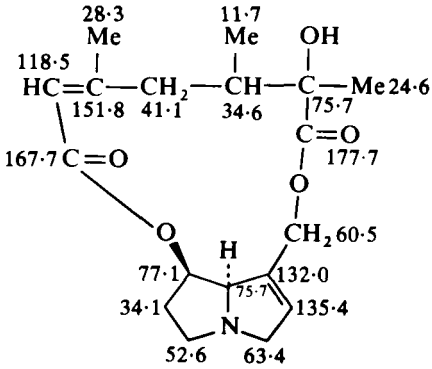

[213] Doronenine

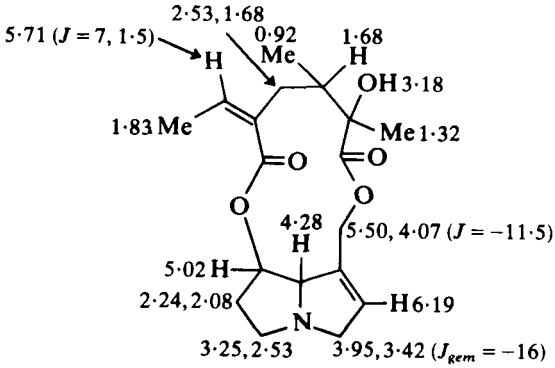

[214] Senecionine

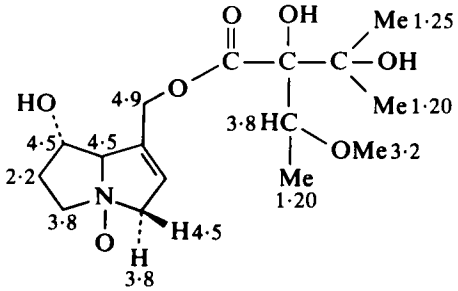

[215] Europine *N*-oxide (in D_2O)

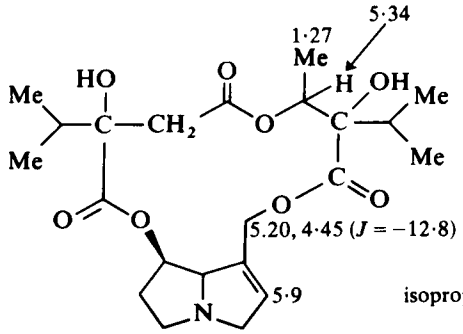

[216] Parsonine

isopropyl Me	0·84, 0·98, 0·98, 1·04
isopropyl CH	1·79, 1·93

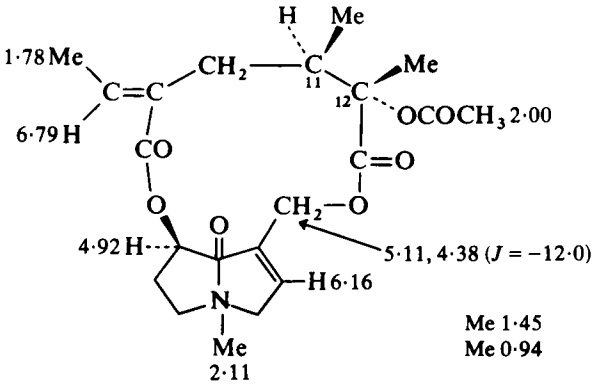

[217] Ligularidine

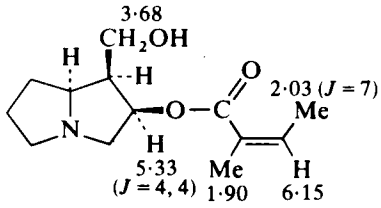

[218] Petasinine

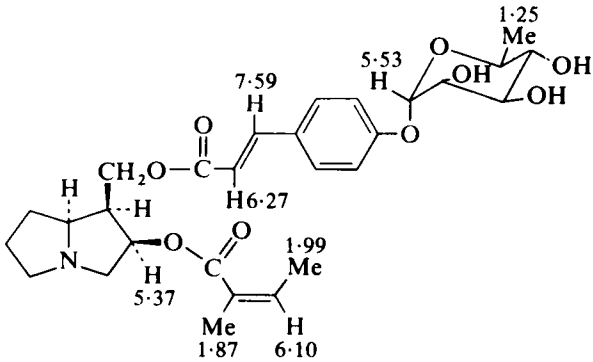

[219] Petasinoside

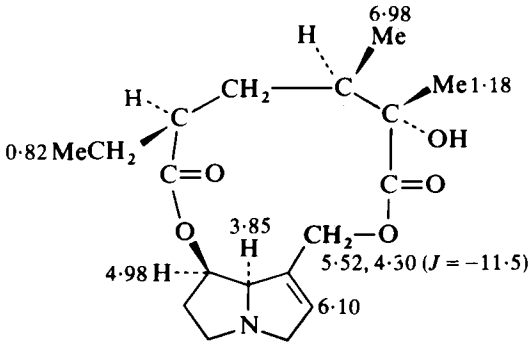

[220] Yamataimine

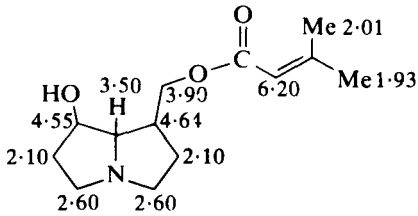

[221] (in CD_3OD)

The ^{1}H NMR spectra of 3-oxo-dehydroheliotridine and of the related isosenaetnine are summarized in [222][129] and [223][130] respectively. The chemical shifts of a 14- and of a 19-proton in the ^{1}H NMR spectra of the isomeric acylpyrroles [224] and [225][131] result from differing stereochemistry with respect to the 11-carbonyl group (effect on 14-H) and from the acetoxy function (effect on 19-H).

^{13}C and ^{1}H NMR parameters for roxburghilin/odorine[132,133] are given in [226] and [227]. The ^{13}C NMR spectrum of [226] in $CDCl_3$ solution shows evidence for both C(2) epimers.[132] ^{1}H NMR parameters for the relation odorinol [228][133] are provided.

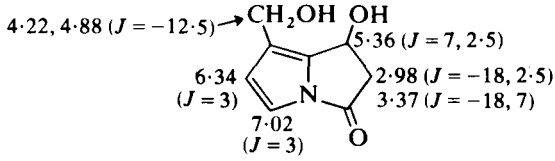

[222] 3-Oxo-dehydroheliotridine

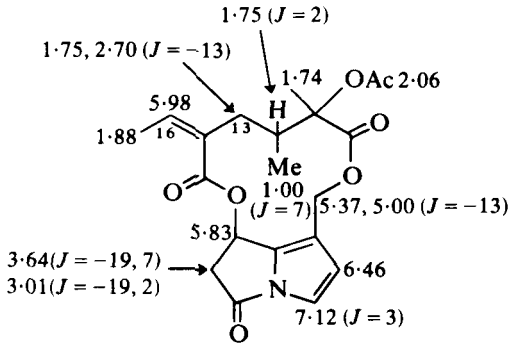

[223] Isosenaetnine

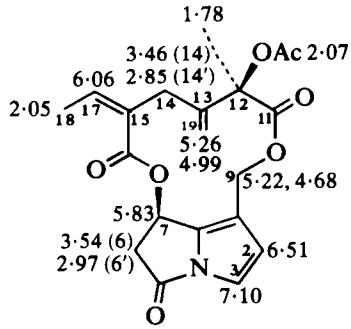

[224]

$J_{2,3} = 3{\cdot}5$
$J_{6,6'} = -19$
$J_{6,7} = 6{\cdot}5$
$J_{6',7} = 2$
$J_{7,9'} \simeq 0{\cdot}5$
$J_{9,9'} = -14$
$J_{14,14'} = -17$
$J_{14,17} = 1{\cdot}0$
$J_{14,18} = 1{\cdot}5$
$J_{14,19'} \simeq 0{\cdot}5$
$J_{14',17} \simeq 0{\cdot}5$
$J_{14',18} = 1{\cdot}5$
$J_{14',19'} = 1{\cdot}5$
$J_{14',19} = 2$

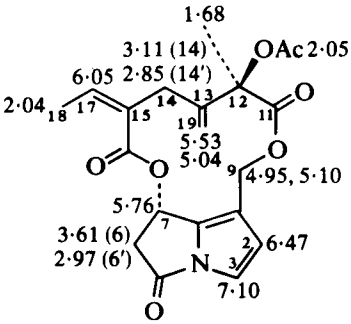

[225]

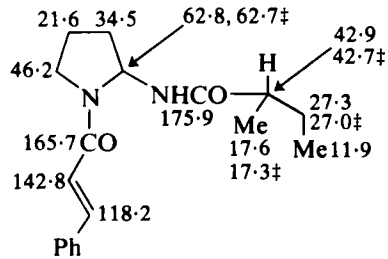

Ar 134·8(s)
129·9(d)
128·8(d)
128·8(d)
128·3(d)
128·3(d)

[226] Roxburghilin/odorine (‡both C(2) epimers present $CDCl_3$ solution)

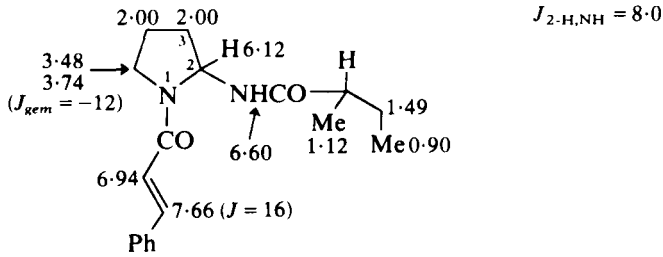

[227]

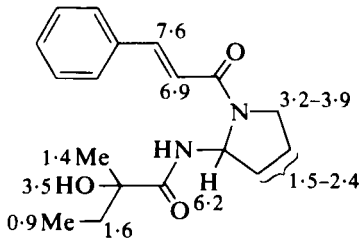

[228] Odorinol

VII. INDOLIZIDINE ALKALOIDS

^{13}C and ^{1}H NMR parameters for an indolizidine alkaloid isolated from an Ecuadoran frog (*Dendrobates tricolor*) are given in [229] and [230].[134] In the ^{13}C NMR spectrum of dendrocrepine [231] recorded at 25 °C the phenyl group gives rise to six resonances due to restricted rotation of the phenyl group. (Four resonances are observed at 57 °C.) A similar effect is observed in the low temperature ^{13}C NMR spectrum of the related 2,6-dimethyl-1-phenylcyclohexanol [232].[135]

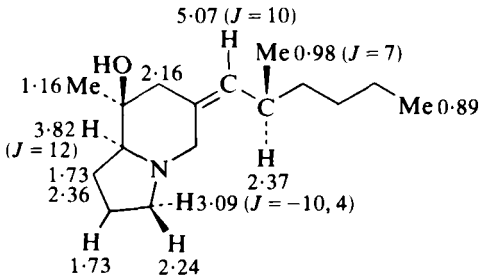

[229]

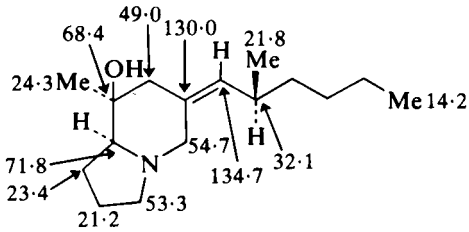

[230]

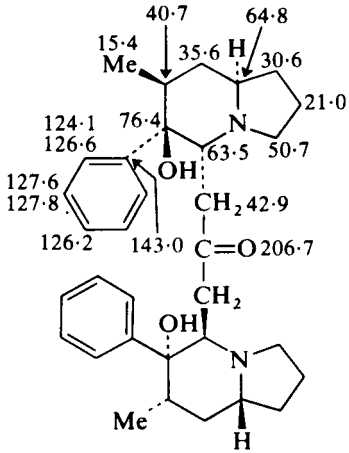

^{13}C NMR at 57 °C:
Ar 143·1 C1′
127·8 *m*
126·3 *p*
125·9 *o*

[231] Dendrocrepine

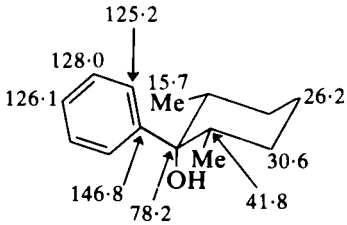

[232]

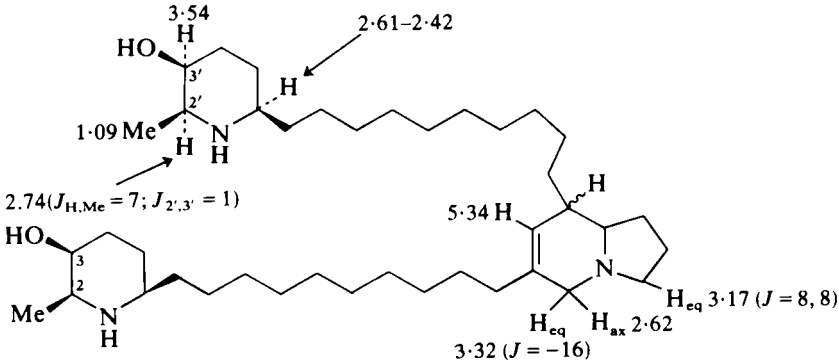

[233] Juliprosopine

^{1}H and ^{13}C NMR parameters for juliprosopine are given in [233] and [234].[136] (See also spectaline [283] in Section IX.)

The ^{1}H NMR spectrum of vinceten is summarized in [235].[137] Comparison of the chemical shifts in [236]–[238] shows the effect of C(12) hydroxylation on the 1-proton shifts.[137]

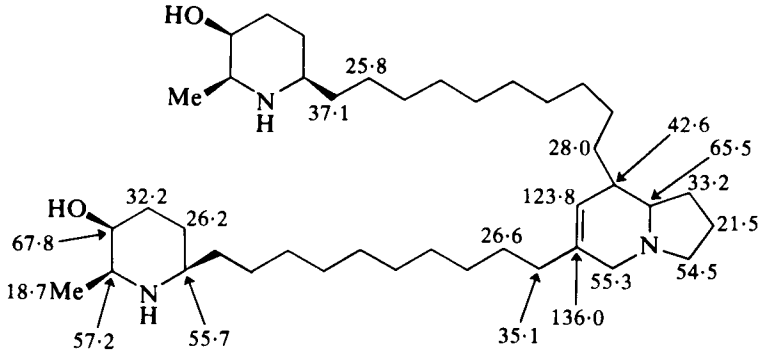

[234].

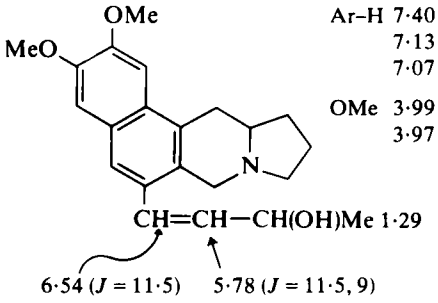

[235] Vinceten

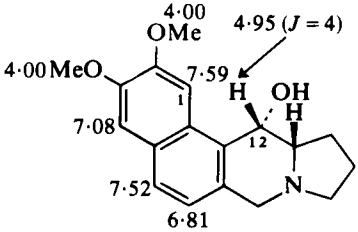

[236]

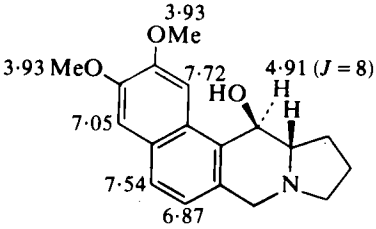

[237]

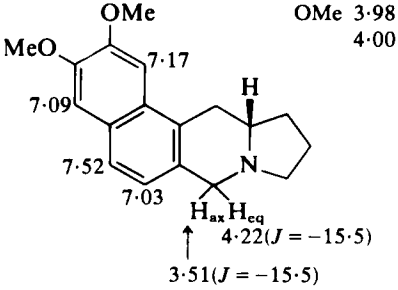

[238]

VIII. QUINOLIZIDINE ALKALOIDS

The ^{13}C shift of C(6) in benzo[*a*]quinolizidines [239] provides a reliable indication of the *cis/trans* ring fusion[138–140] (see also protoberberines, Section II.F of this review and previous review[2]). The chemical shift of the 4-proton in 4-phenylquinolizidines is well known as a probe in the determination of the *cis/trans* nature of the quinolizidine ring fusion (Section VIII.C in previous review[2]) and additional examples are provided by [240] and [241],[141,142] by 7-methyl-4-phenylquinolizidin-2-ones,[143] by lasubine-I [242] and lasubine-II [243][144] and by various nupharidine derivatives [244].[145] ^{13}C and ^{1}H NMR shifts for the nuphar indolizidine [245][146] and ^{1}H shifts for nupharopumiline [246][147] are available. ^{13}C shifts for myrtine

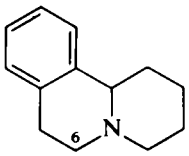

[239]

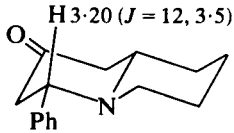

[240]

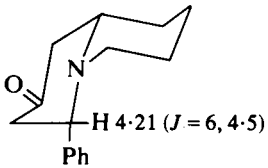

[241]

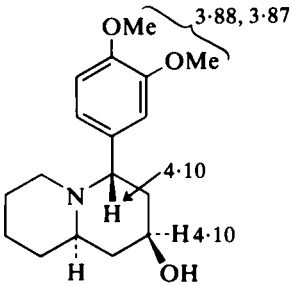

Ar–H	6·86
	6·86
	6·83
^{13}C NMR: Ar	120·5
	111·8
	110·6
C(4)	135·5
OMe	148·6
	147·7

[242] Lasubine-I

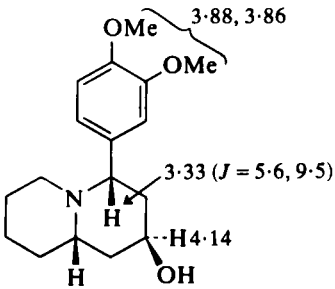

Ar–H	6·84
	6·84
	6·92

[243] Lasubine-II

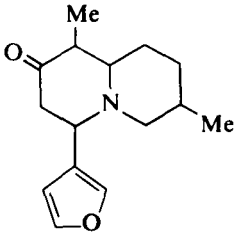

[244]

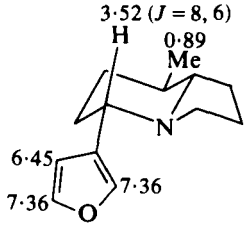

^{13}C NMR: 18·2(q)
20·2(t)
29·2(t)
34·1(t)
34·4(t)
36·5(d)
53·3(t)
60·0(d)
71·6(d)
139·7(d)
143·1(d)

[245] Nuphar indolizidine

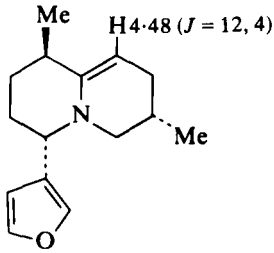

Me 0·93
1·03

[246] Nupharopumiline

[247][148] and 4-epimyrtine [248][149] indicate the stereochemical dependence of these shifts.

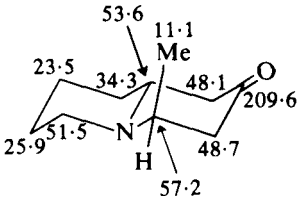

[247] Myrtine

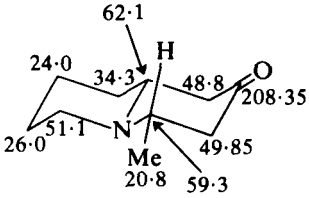

[248] 4-Epimyrtine

In the monocations of sparteine-N_{16}-oxide [249] and of 2-phenylsparteine-N_{16}-oxide the bridge proton absorbs at very high frequency (δ 18·2–18·8).[150] ^{1}H NMR shifts for chamaetin [250][151] and of methyl 12-cytisineacetate [251][152] are provided with the structures.

The axial orientation of the N-oxide function in the lupin alkaloid 5,17-dehydromatrine N-oxide is established[153] from a comparison of the ^{1}H chemical shifts of 11-H in 5,17-dehydromatrine [252] (δ 4·15) and in the oxide (δ 5·13) with those in matrine (δ 3·81) and in matrine N-oxide

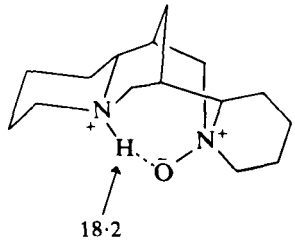

[249] Monocation of sparteine-N_{16}-oxide

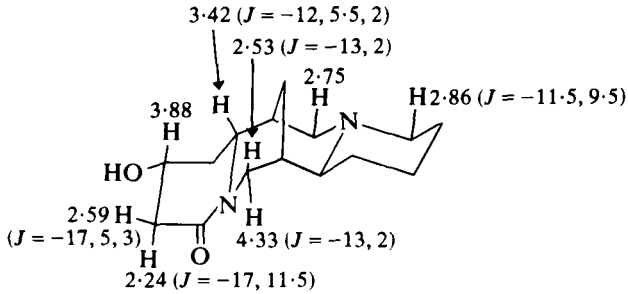

[250] Chamaetin (in CD_3COCD_3/CD_3OD)

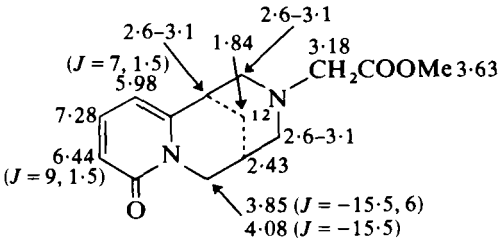

[251] Methyl 12-cytisineacetate

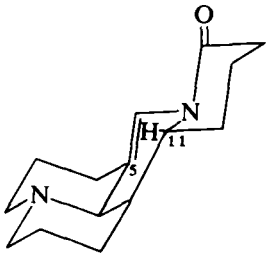

[252] 5,17-Dehydromatrine

(δ5·12). ^{1}H and ^{13}C shifts for 5α,9α-dihydroxymatrine are given in [253] and [254],[154] and those for sophoranol (5α-hydroxymatrine) in [255] and [256].[155]

Comparison of the ^{13}C shifts of sophoridine [257], sophoridine-*N*-oxide [258] and of an isomeric *N*-oxide [259] permit the assignments shown.[156] The similar difference in chemical shift between C(2) and C(10) in [257] and [258] suggests similar *trans*-fused quinolizidine systems, whereas the low frequency shift of C(10) in the spectrum of [259] indicates the *cis*-quinolizidine system. In the ^{1}H NMR spectra of [257] and [258] there is no absorption below δ4·00 whereas the *cis*-quinolizidine [259] shows C(17)

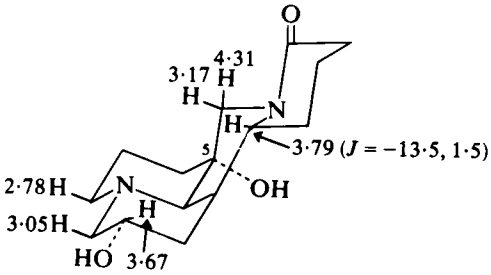

[253] 5α,9α-Dihydroxymatrine

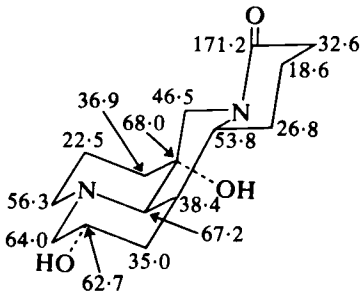

[254]

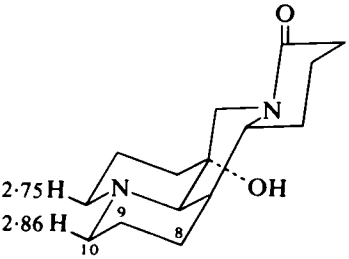

[255] Sophoranol

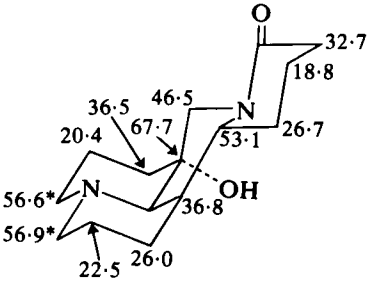

[256]

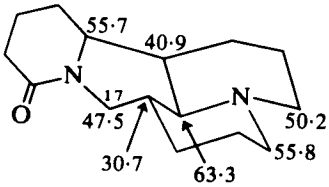

[257] Sophorodine

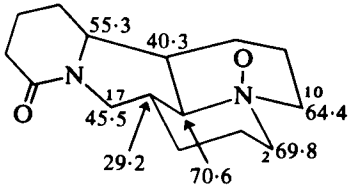

[258] Sophorodine *N*-oxide

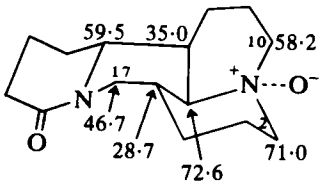

[259]

^{1}H NMR:
C(17)H$_2$ 4·08 (J = −13·5, 7·5)
3·14 (J = −13·5, 8·0)

methylene absorption at $\delta 4{\cdot}08$ and $3{\cdot}14$. ^{1}H NMR parameters for a stereoisomer of sophocarpine are shown in [260].[157]

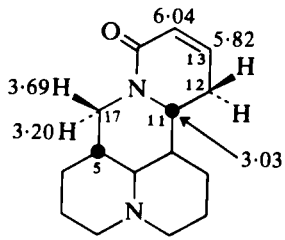

$J_{12\alpha,13} = 3{\cdot}5$
$J_{12\beta,13} = 5{\cdot}0$
$J_{17\alpha,17\beta} = -13{\cdot}5$
$J_{17\beta,5\beta} = 5{\cdot}0$
$J_{17\alpha,5\beta} = 11{\cdot}0$
$J_{13,14} = 10{\cdot}5$

[260] (in C_6D_6)

Comparison of the ^{1}H chemical shifts of 6-H and 6′-H in the spectra of thionuphlutine [261] and of its two isomeric sulphoxides [262] and [263][158] permits assignment of the sulphoxide stereochemistry.

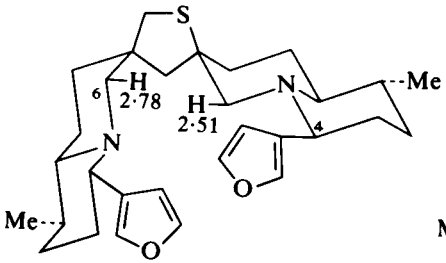

[261] Thionuphlutine

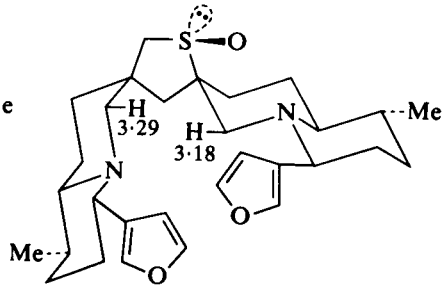

[262]

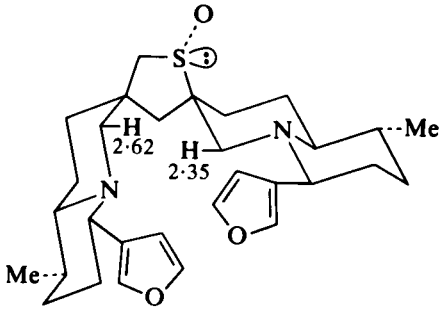

[263]

The C(13) epimers [264] and [265] are differentiated by the couplings involving the 13-protons – 13-H: $\delta 4{\cdot}52$ ($J = 2, 6$) in [264], $\delta 4{\cdot}50$ ($J = 3, 10$) in [265].[159]

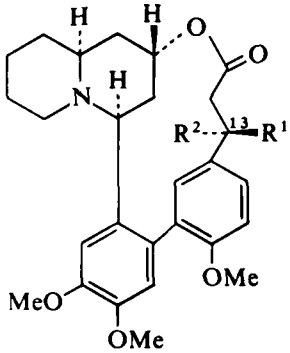

[264] R^1 = OMe, R^2 = H
[265] R^1 = H, R^2 = OMe

NMR characteristics of porantheridine are given in [266].[160] Propyleine has been shown to be an interconverting mixture of [267] and [268] with [268] as the major component. The protonated olefinic carbon absorbs at higher frequency in [267] than in [268], showing its proximity to the methyl group.[161]

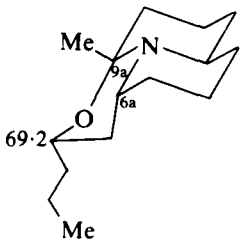

^{13}C NMR:	^{1}H NMR:
49·4(d)	$J_{6a,7ax}$ = 11
48·4(d)	$J_{6a,6eq} = J_{6a,7eq}$ = 2·5
40·1(t)	
39·25(t)	9a-Me 1·5
34·2(t)	6a-H 2·96
30·9(t)	3′-Me 0·93
27·4(t)	
23·8(q)	
19·8(t)	
19·4(t)	
18·0(t)	
14·2(q)	

[266] Porantheridine

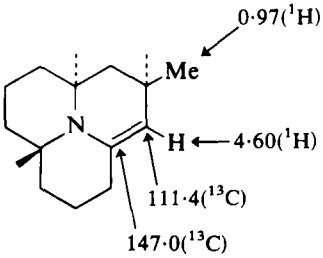

[267]

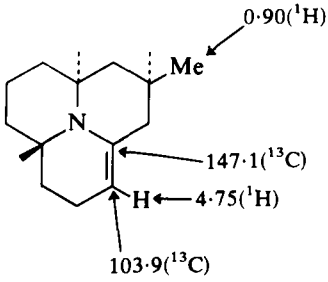

[268]

^{1}H NMR shifts for some benzopyridoquinolizidine bases are shown in [269] and [270].[162]

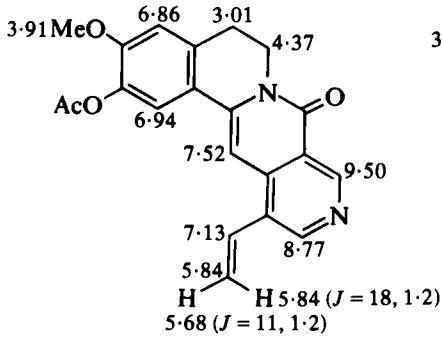

[269]

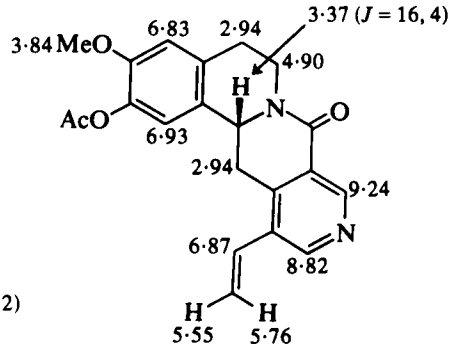

[270]

IX. PIPERIDINE AND PYRIDINE ALKALOIDS

A. Tropane alkaloids

The enantiomorphic composition of cocaine may be determined by the tris-*d*-trifluoroacetylcamphorate-induced separation of proton shifts.[163] ^{1}H NMR data on 3α-tigloyloxynortropan-6β-ol [271],[164] 3α-senecioyloxytropan-6β-ol [272] and 6β-angeloyloxytropan-3α-ol [273][165] are displayed. The shifts at δ 5·58, 1·92 and 2·18 in [272] and at δ 6·05, 1·93 and 2·03, in [273] are typical of senecioyl and angeloyl moieties respectively.[166] ^{1}H NMR shifts for related systems are available.[167]

The C(5′) or C(1′) signal (δ 59·28) in the ^{13}C NMR spectrum of scopolamine [274] in a ^{15}N-enriched sample shows $J_{^{13}C,^{15}N}$ 2·9 Hz.[168]

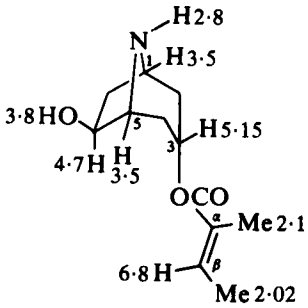

[271] 3α-Tigloyloxynortropan-6β-ol

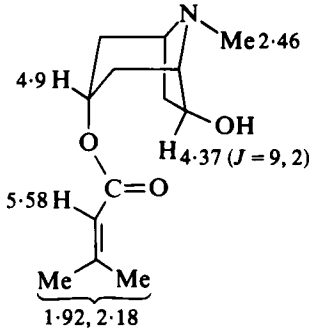

[272] 3α-Senecoyltropan-6β-ol

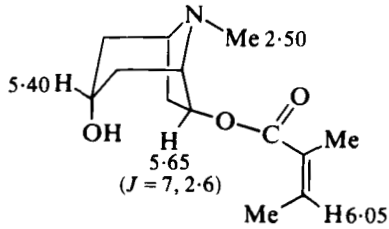

Me 1·93
2·03

[273] 6β-Angeloyloxytropan-3α-ol

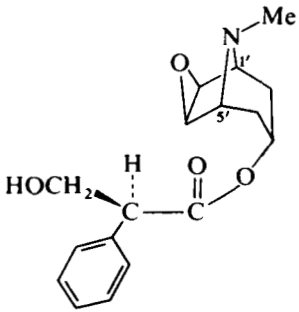

[274] Scopolamine

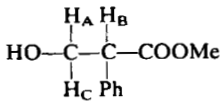

δ_A 3·76 $J_{AB} = 5{\cdot}38 \pm 0{\cdot}12$
δ_B 3·82 $J_{BC} = 9{\cdot}05 \pm 0{\cdot}11$
δ_C 4·10 $J_{AC} = -11{\cdot}24 \pm 0{\cdot}13$

[275] Tropic acid methyl ester

A detailed ^{1}H NMR study of tropic acid and derivatives has been made[169] and some data for tropic acid methyl ester are given in [275].

The ^{13}C NMR spectrum of *N*-benzoylphysoperuvine is given in [276][170] and the ^{1}H NMR spectrum of an intermediate in the synthesis of cocaine in [277].[171]

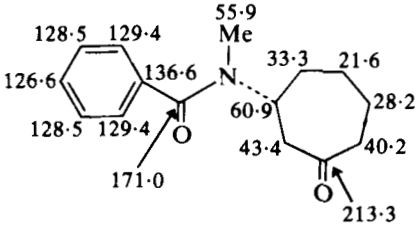

[276] *N*-Benzoylphysoperuvine

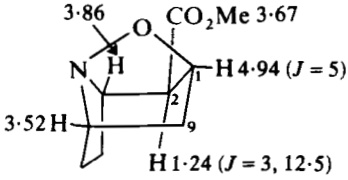

[277]

B. Other alkaloids containing the piperidine moiety

^{1}H NMR data for the simply substituted piperidine alkaloids spectaline [278],[172] the related spectalinine,[173] *N*-methylpseudoconhydrine [279],[174] and the pair of epimers D,L-allosedamine [280] and D,L-sedamine [281][175]

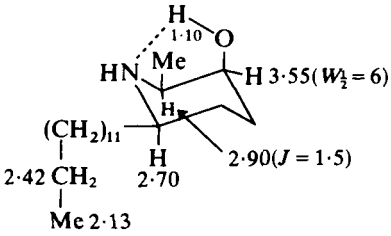

[278] Spectaline

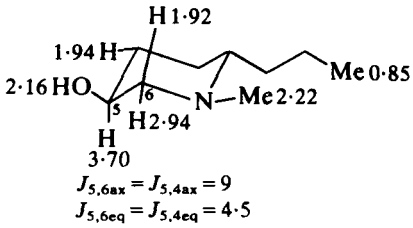

[279] *N*-Methylpseudoconhydrine

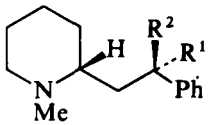

[280] R^1 = OH, R^2 = H, Allosedamine
[281] R^1 = H, R^2 = OH, Sedamine

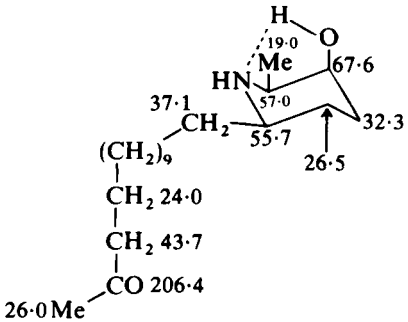

[282] Spectaline

are available. In the spectra of [280] and [281] the benzylic proton absorbs at δ5·04 (J = 4, 10) and at δ4·84 (J = 2·5, 9·5) respectively.[175] The ^{13}C NMR spectrum of spectaline is summarized in [282].[172]

A careful analysis of the ^{1}H NMR spectra of wisanine [283] and of an isomer [284] establishes the structures shown.[176] Comparison of the ^{1}H NMR spectra of *trans*- and *cis*-2-methoxy-4,5-methylenedioxycinnamoylpiperidine, [285] and [286] respectively, with that of an alkaloid from *Piper peepuloides* establishes the structure of the alkaloid as [286].[177] ^{1}H NMR and ^{13}C NMR spectra of pipermethystine are shown in [287] and [288][178] and the ^{13}C NMR spectrum of piplartine dimer A in [289].[179]

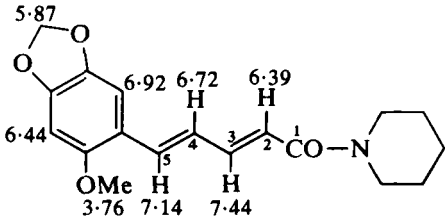

$J_{2,3}$ = 14·7
$J_{2,4}$ = 0·2
$J_{2,5}$ = 0
$J_{3,4}$ = 11·2
$J_{3,5}$ = 0·2
$J_{4,5}$ = 15·7

[283] Wisanine

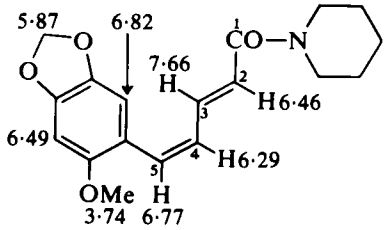

$J_{2,3} = 14{\cdot}7$
$J_{2,4} = 0{\cdot}4$
$J_{2,5} = 0$
$J_{3,4} = 11{\cdot}6$
$J_{3,5} = 0{\cdot}6$
$J_{4,5} = 11{\cdot}6$

[284]

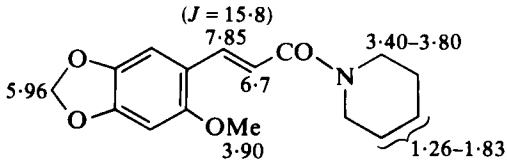

Ar–H 6·50
6·96

[285]

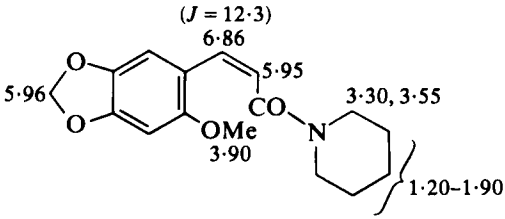

Ar–H 6·52
6·96

[286]

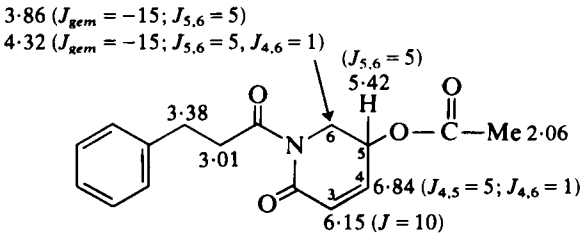

[287] Pipermethystine

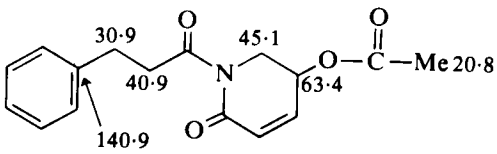

[288]

C=O 163·8
169·9
175·3

C=C 126·1(d)
and Ar 127·6(d)
128·4(d)
128·8(d)
140·2(d)

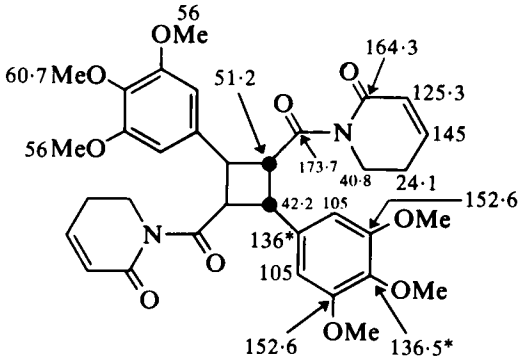

[289]

Spectral data for rohitukine [290][180] and tecomanine [291][181] are provided. Comparison of the ^{13}C NMR spectra of xylostosidine [292] and sweroside [293] shows differences in the C(3), C(4), C(6) and C(11) shifts consonant with structure [292] for the monoterpene alkaloid.[182] In addition the 360 MHz ^{1}H NMR spectrum of xylostosidine [294] shows the *cis* arrangement of the 5- and 7-protons by the values of $J_{5,6ax}$ and $J_{6ax,7}$.[182]

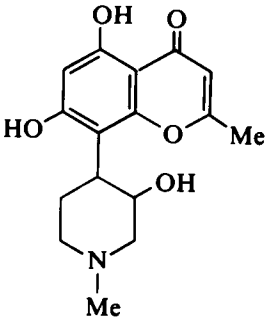

^{13}C NMR (in pyridine-d_5)		^{1}H NMR (in pyridine-d_5)
19·9q	101·5d	1·57dd, J = 12(1H)
25·4t	108·5d	2·14m (1H)
38·2d	155·9s	2·21s, (3H)
46·2q	156·2s	2·27s, (3H)
56·8t	161·4s	2·36d, J = 12(2H)
62·5t	168·8s	2·99d, J = 12(2H)
69·9d	183·2s	3·16dt, J = 12, <2(1H)
		3·63dt, J = 12, <2(1H)
		4·44d, J < 2(1H)
		6·17s, (1H)
		6·79s, (1H)

[290] Rohitukine

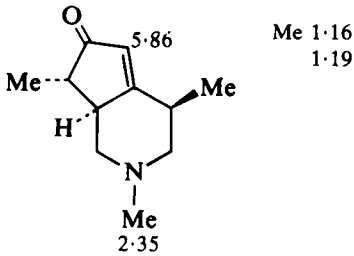

[291] Tecomanine

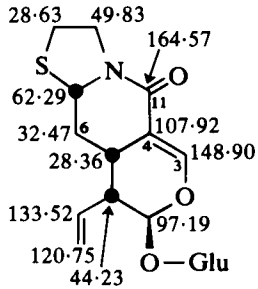

[292] Xylostosidine (in CD_3OD)

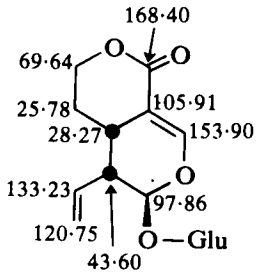

[293] Sweroside (in CD_3OD)

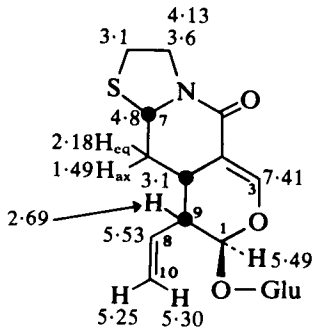

$J_{3,5} = 2{\cdot}7$
$J_{8,10} = 17$
$J_{8,9} = J_{8,10'} = 10$
$J_{1,9} = 1{\cdot}9$
$J_{10,10'} = 2$
$J_{5,9} = 5{\cdot}5$
$J_{6ax,6eq} = -12{\cdot}5$
$J_{5,6eq} = J_{7,6eq} = 3{\cdot}5$
$J_{5,6ax} = 13$
$J_{6ax,7} = 11$

[294] Xylostosidine (in CD_3OD)

The configuration of the sulphoxide group in the loxylostosidines A [295] and B [296][183] may be assigned from a comparison of the C(6) shifts with that in xylostosidine [292]. The small γ-effect ($-4{\cdot}64$ ppm) in [295] indicates a *trans* arrangement between C(6) and the oxygen atom of the sulphoxide group (cf. $-8{\cdot}12$ ppm (*syn*-γ-effect) in [296]). In addition the ^{1}H NMR spectra of the sulphoxides show a deshielding of C(6)-H_{eq} in [295]

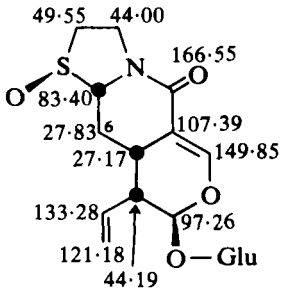

[295] Loxylostosidine A (in CD_3OD)

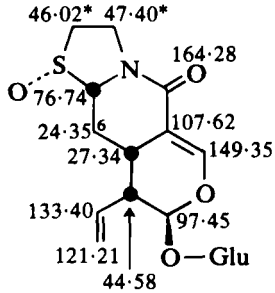

[296] Loxylostosidine B (in CD_3OD)

by 0·33 ppm whereas C(6)-H_{ax} in [296] is shifted to high frequency by 0·23 ppm and C(6)-H_{eq} is unchanged (all shifts relative to [292]).[183]

The ^{13}C NMR spectra of the compounds [297] and [298] obtained by synthesis shows[184] that the structure [297] proposed for cannivonine cannot be correct.

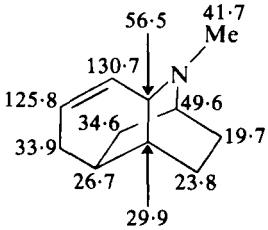

[297]

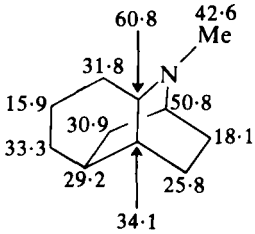

[298]

C. Pyridine alkaloids

The structure of melochinone [299] is assigned largely on the basis of a comparison of the ^{13}C NMR spectrum with those of 3-methoxy-2-methyl-4(1*H*)-pyridone [300] and 5-methoxy-2-methyl-4(1*H*)-pyridone [301].[185]

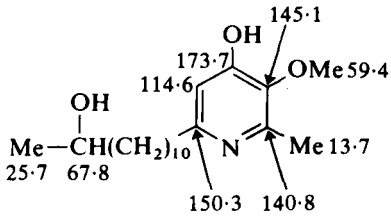

[299] Melochinine

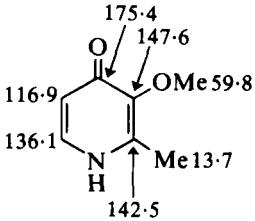

[300] (in CD_3OD)

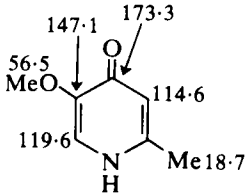

[301] (in CD_3OD)

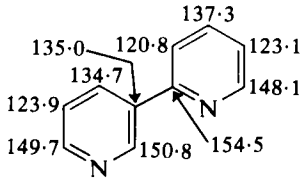

[302] α,β-Dipyridyl

Differences in the ^{13}C NMR shifts in α,β-dipyridyl [302] and in the perchlorate [303][186] are similar to those observed on protonation of pyridine. Shifts for α,α-dipyridyl [304] and for β,β-dipyridyl [305] are provided for comparison purposes.[186] ^{13}C shifts for 5-fluoronicotinic acid sodium salt are given in [306][187] and comparison of shifts for anabasine and 5-fluoroanabasine may be made by reference to [307] and [308].[187]

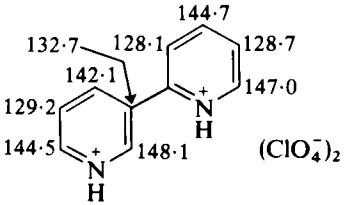

[303] α,β-Dipyridyl diperchlorate (in D_2O)

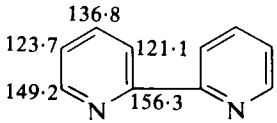

[304]

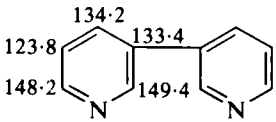

[305]

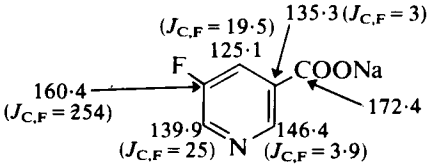

[306] 5-Fluoronicotinic acid sodium salt (in D_2O)

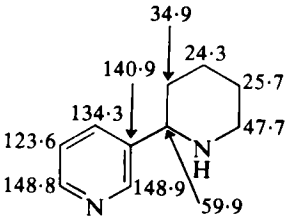

[307] Anabasine

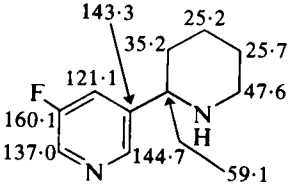

[308] 5-Fluoroanabasine

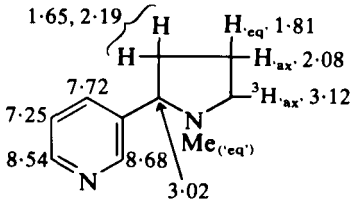

[309] Nicotine (neat liquid)

Tritium NMR chemical shifts for nicotine are given in [309].[188] In the ^{13}C NMR spectrum of *N*-methylnicotinium iodide the *cis*-methyl resonance (δ 46·5) appears to low frequency of the *trans*-methyl (δ 51·1) (cf. ^{1}H NMR spectrum: *cis*-Me δ2·94, *trans*-Me δ 3·27).[189]

^{1}H and ^{13}C NMR parameters for some alkaloids based on the 2,7-naphthyridine nucleus are given in [310]–[313][190,191] and in [314] and [315].[192]

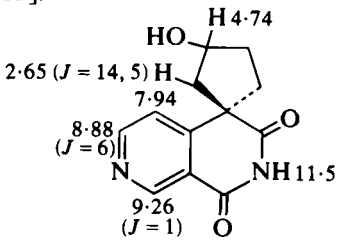

[310] Sesbanine (in $CDCl_3$–CD_3OD)

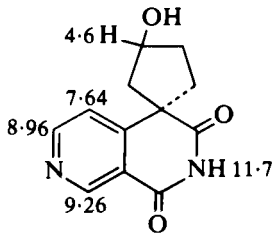

[311] 10-Episesbanine (in DMSO-d_6)

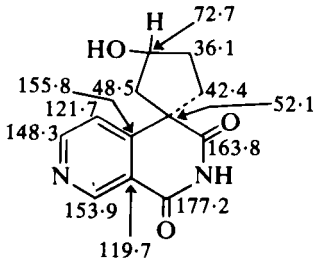

[312] Sesbanine (in DMSO-d_6)

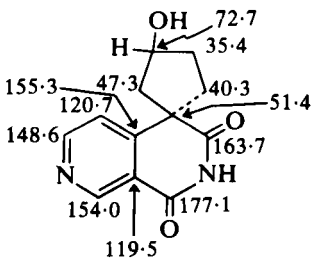

[313] 10-Episesbanine (in DMSO-d_6)

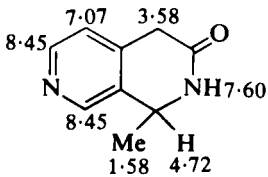

[314] Jasminidine

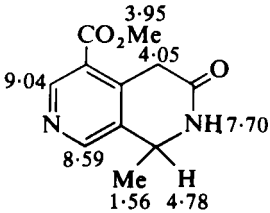

[315] Jasminine

Details of the ^{1}H NMR spectra of alatamine [316] and of wilfordine [317] are now available[193] (see Section IX.C in reference 2).

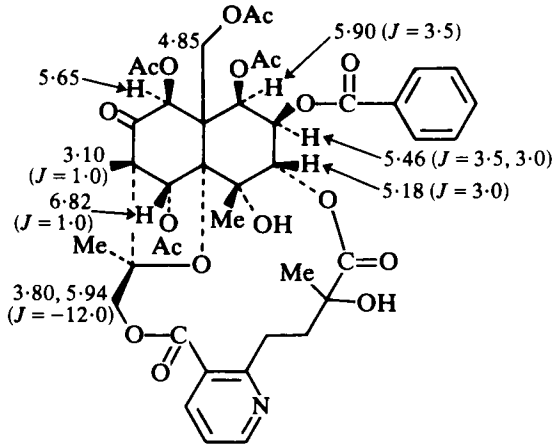

[316] Alatamine

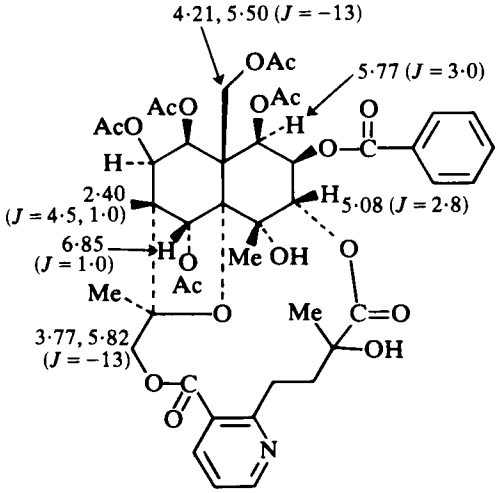

[317] Wilfordine

In the ^{1}H NMR spectra of the cathedulins and derivatives [318]–[320], 6-H_{ax} is increasingly deshielded with successive hydrolytic removal of the ester groups at C(8) and C(15). In the conversion [320] → [321], however, this trend is reversed and in addition the 15-methylene protons also become

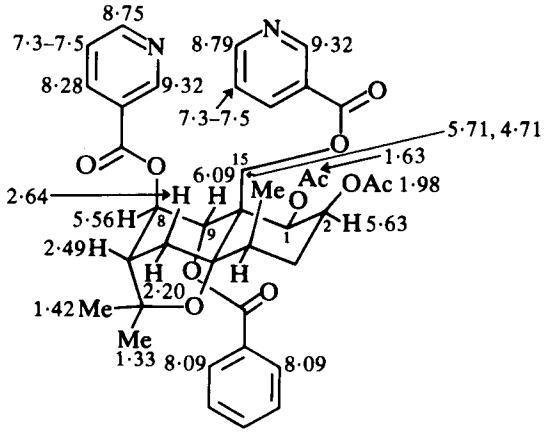

[318] Cathedulin E2

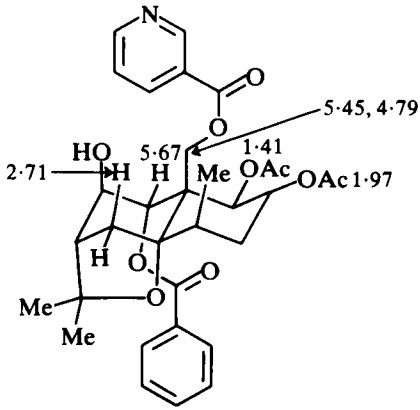

[319] Cathedulin E8

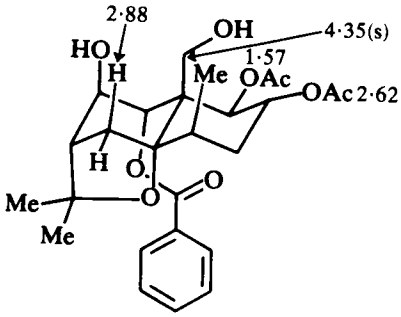

[320]

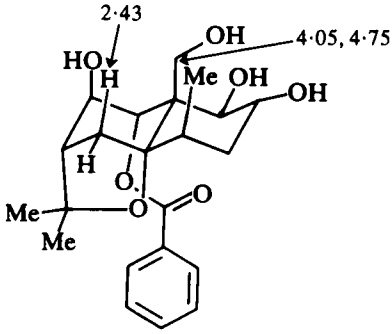

[321]

markedly non-equivalent. This suggests a change in the hydrogen-bonding preference of 15-OH away from 8-OH towards 2-OH.[194] The 1-acetate methyl protons in [318], [319] and [320] are shielded relative to the 2-acetate methyl protons, possibly as a result of the presence of the neighbouring 9-axial benzoate group.[194]

^{1}H and ^{13}C NMR parameters for cathedulin K2 are given in [322] and [323] together with data for the model compounds dimethyl evoninate [324] and evonine [325].[195]

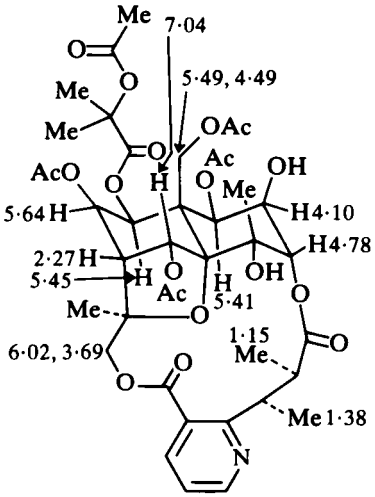

[322] Cathedulin K2

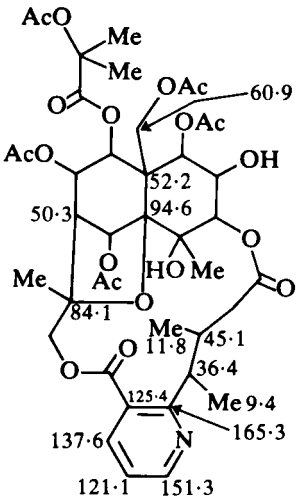

[323] Cathedulin K2

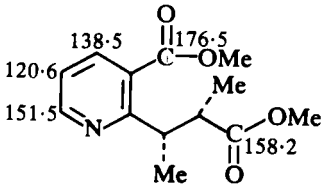

C—Me	40·2, 40·4
OMe	51·2, 52·3
Me	15·2, 17·9

[324] Dimethyl evoninate

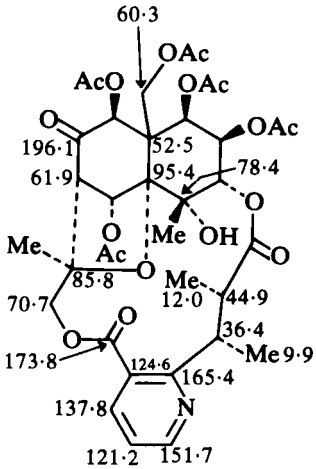

[325] Evonine

^{1}H NMR chemical shift differences in cathedulin E3 [326] have been interpreted in terms of the orientation of the cathate bridge shown in [326].[196] In this conformation one of the 15-protons lies in the shielding zone of the syringate related aromatic ring (δ 3·92, cf. δ 5·58 for the other 15-proton); 19″-H is deshielded by the ester carbonyl attached to the same ring (δ 7·43, cf. δ 6·96 for the other aromatic proton); one of the 16″-H protons lies in the plane of the pyridine ring and is deshielded (δ 6·42, cf. δ 4·89 for the other 16″-proton) and one of the methoxy groups lies in the shielding zone of the pyridine ring (δ 3·10, cf. δ 4·10 for the other OMe protons) as does the 2-acetyl methyl group (δ 1·35).

The ^{13}C NMR spectrum of cathedulin E3 is summarized in [327].[196]

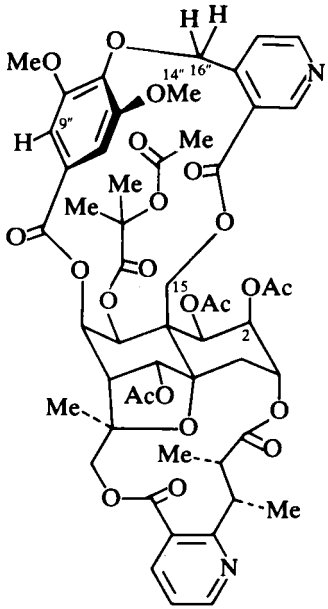

[326] Cathedulin E3

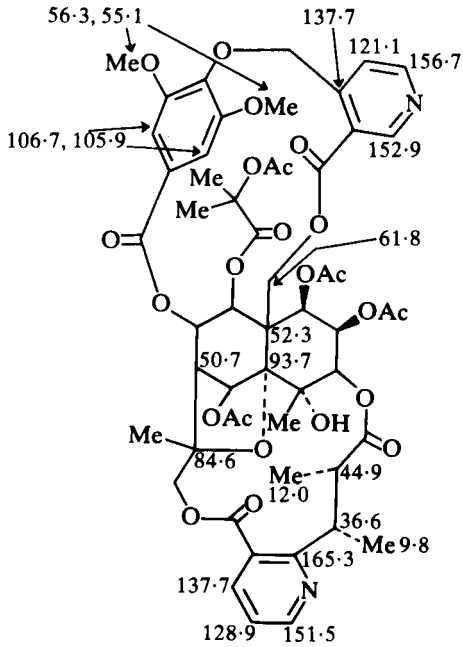

[327] Cathedulin E3

X. QUINOLINE, ACRIDONE AND QUINAZOLINE ALKALOIDS

^{1}H NMR spectra of dihydroquinine and dihydroquinidinine are given in [328] and [329][197] and ^{13}C shifts of pumiliotoxin C hydrochloride in [330].[198]

The ^{13}C NMR spectra of 25 quinoline alkaloids and related compounds have been published[199] and some of these are depicted below [331]–[335].

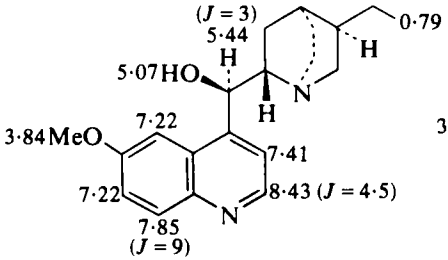

[328] Dihydroquinine

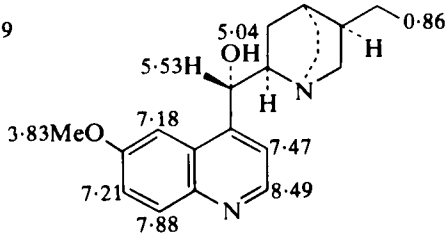

[329] Dihydroquinidine

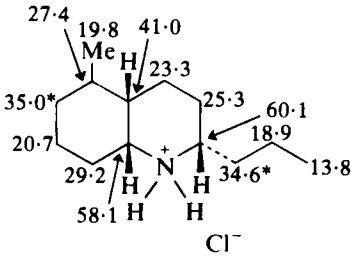

[330] Pumiliotoxin C hydrochloride

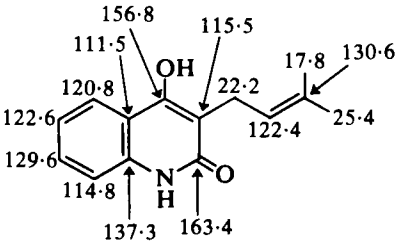

[331]

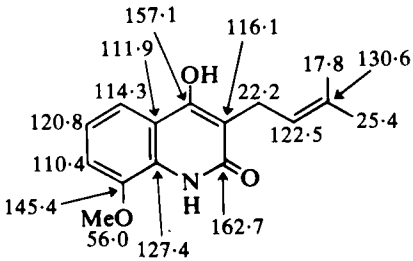

[332]

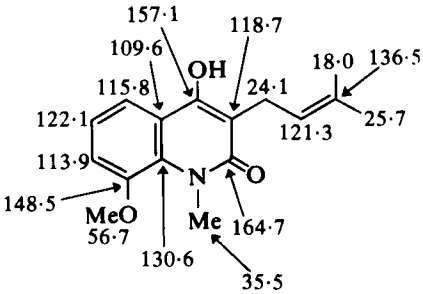

[333]

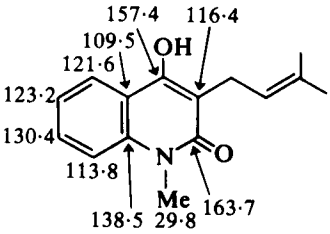

[334]

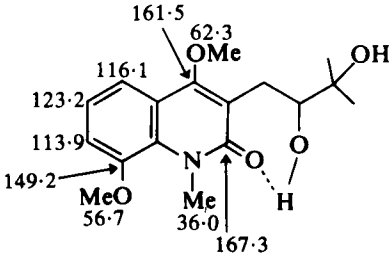

[335] Balfourolone

Of diagnostic importance is the high frequency shift of the *N*Me resonance in 8-methoxy derivatives ([333] → [334]) and the C(2) shift in the hydrogen bonded structure [335] (cf. [333]).[199]

The ^{13}C NMR spectrum of 3,3-diisopentenyl-*N*-methyl-2,4-quinoldione is depicted in [351].[200]

The ^{1}H NMR spectra of a variety of quinolones are summarized in [337],[201] [338],[202] [339],[203] [340] and [341].[204]

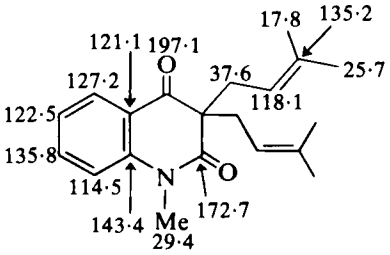

[336]

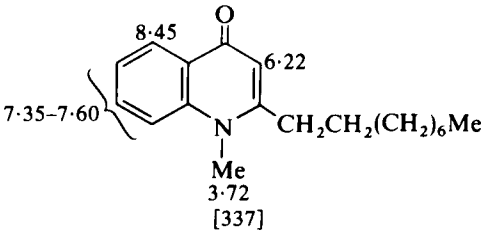

[337]

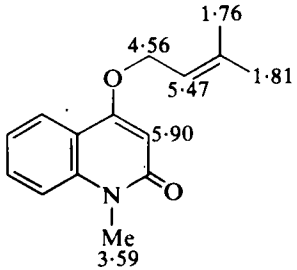

[338] Revenine

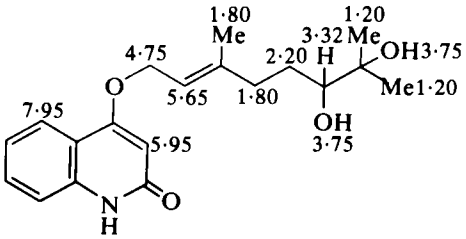

[339] Bucharaine (in CD_3OD)

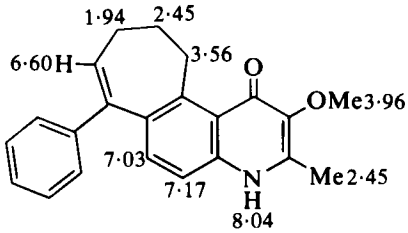

[340] Melochinone

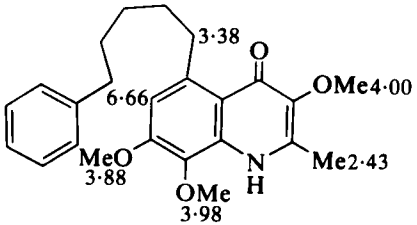

[341] Melovinone

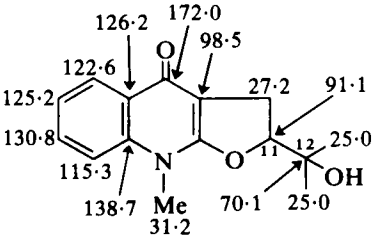

[342] Isoplatydesmine

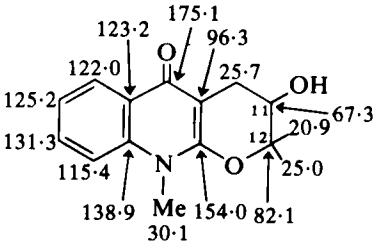

[343] Ribalinine

The ^{13}C NMR spectra of a variety of furoquinolines and pyranoquinolines are summarized in [342]–[346],[199] [347],[205] [348] and [349].[206] The furo- and pyrano- compounds isoplatydesmine [342] and ribalinine [343] may be distinguished by differences in C(11) and C(12) shifts (see also araliopsine [344] and ψ-ribalinine [345]). The linear and angular systems (e.g. [343] and [345]) differ in the chemical shift of the carbon of the carbonyl group.[199]

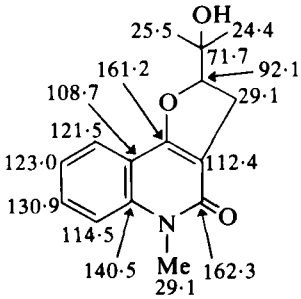

[344] Araliopsine

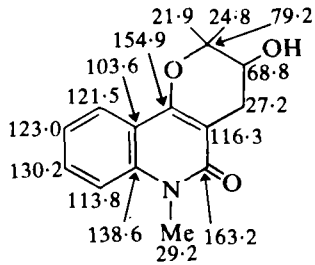

[345] ψ-Ribalinine

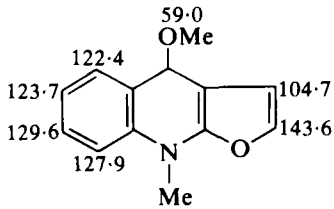

[346] Dictamnine

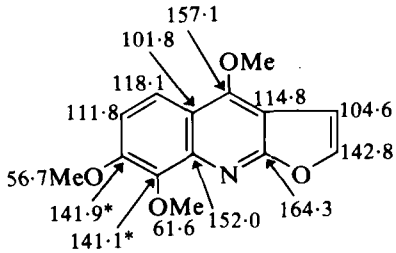

[347] Skimmianine

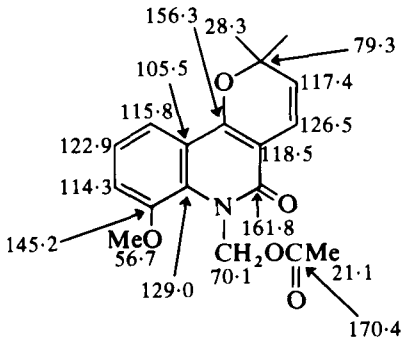

[348] Zanthophylline

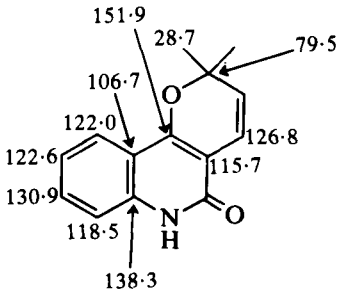

[349] Flindersine

^{1}H NMR shifts for furoquinolines and pyranoquinolines are given for skimmianine [350],[205] glycarpine [351],[207] pteledimerine [352],[208] geibalansine [353],[209] veprisine [354][210] and 8-methoxyflindersine [355].[211]

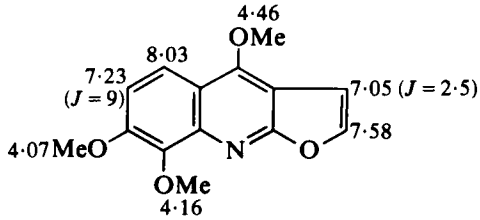

[350] Skimmianine

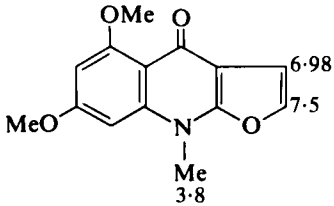

OMe	4·4
Ar—H	7·0
	7·28

[351] Glycarpine

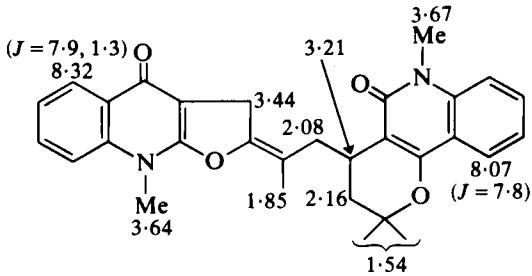

[352] Pteledimerine

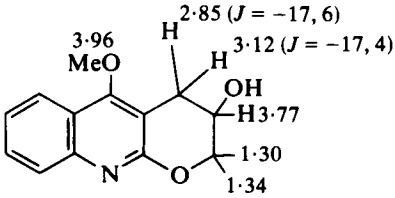

[353] Geibalansine (in DMSO-d_6)

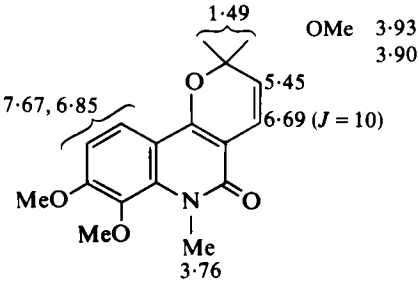

[354] Veprisine

NMR parameters for some acridones are given in [356]–[360],[212] [361],[213] [362] and [363],[214] for some camptothecins in [364][215] and [365][216] and for a new 4-quinazolone alkaloid in [366].[217]

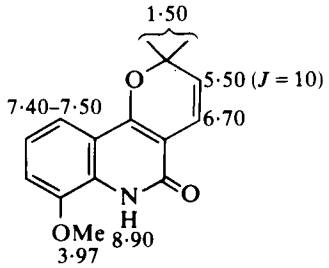

[355] 8-Methoxyflindersine

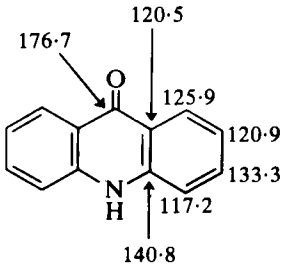

[356]

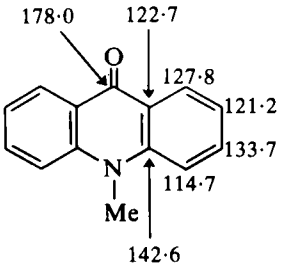

[357]

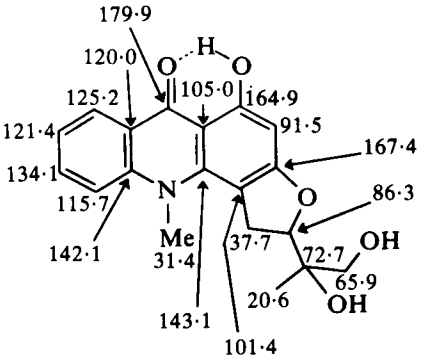

[358]

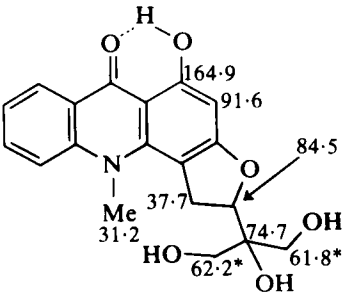

[359]

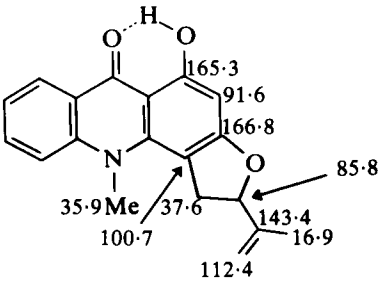

[360]

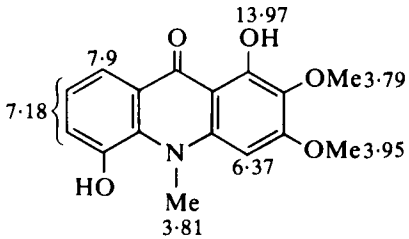

[361]

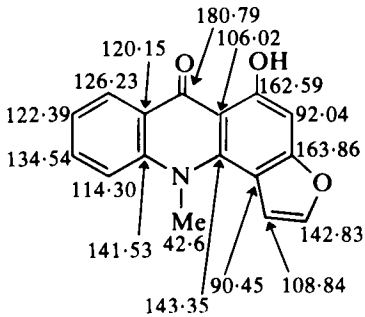

[362] (in DMSO-d_6)

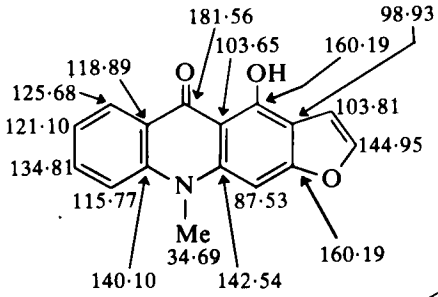

[363] (in DMSO-d_6)

Ar—H 7·70(s)
8·40(s)
7·14–8·33(4H, m)

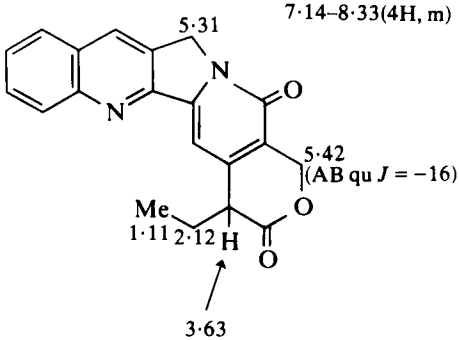

[364] 20-Deoxycamptothecin

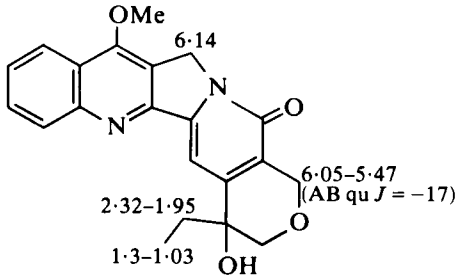

[365] 7-Methoxycamptothecin (in TFA)

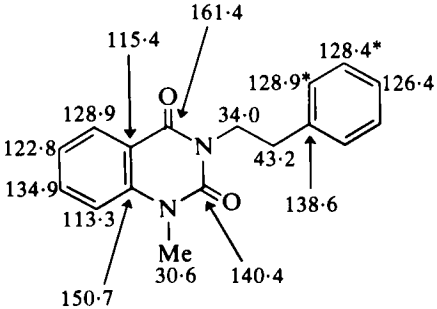

[366]

XI. IMIDAZOLE ALKALOIDS

Pilocarpine [367] and isopilocarpine [368] may be differentiated by the chemical shift of the methylene group carbon (between the lactone and imidazole rings) and of the methylene group carbons of the ethyl group on the lactone ring.[218]

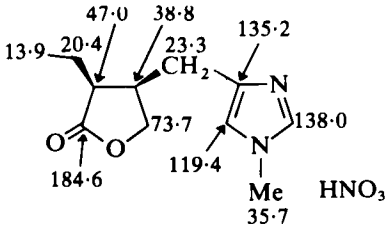

[367] Pilocarpine nitrate (in D_2O)

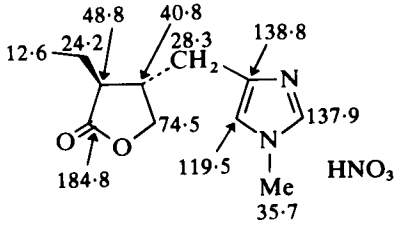

[368] Isopilocarpine nitrate (in D_2O)

XII. INDOLE ALKALOIDS

A. Simple indoles, carbazoles, carbolines and physostygmine-type alkaloids

NMR parameters for a number of naturally occurring halogenated indoles are available (for example 2,3,7-trichloroindole [369],[219] 1-methyl-2,3,6-tribromoindole [370], 1-methyl-2,3,5-tribromoindole [371] and [372][220]

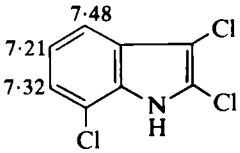

[369]

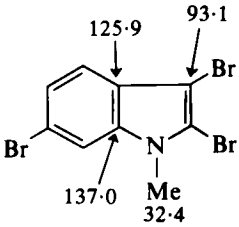

C—Br	115·7
	116·8
Ar	112·7
	120·2
	134·3

[370]

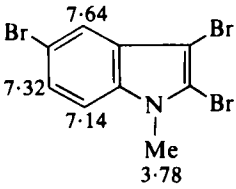

[371]

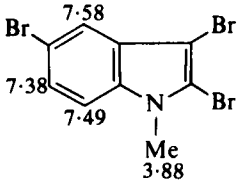

[372] (in CD_3COCD_3)

and 6-chlorohyellazole [373][221]). The ^{1}H NMR spectrum of 1-methyl-2,3,5-tribromoindole shows a high frequency shift of 7-H on changing

solvent from chloroform [371] to acetone [372].[220] The ^{13}C NMR spectrum of 3,6-bis(γ,γ-dimethylalkyl)indole (^{1}H NMR spectrum summarized in

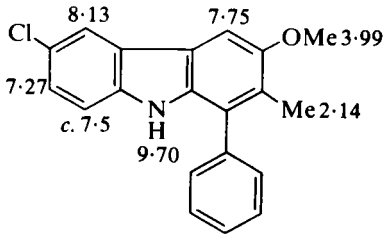

[373] 6-Chlorohyellazole (in acetone-d_6)

^{13}C NMR:

152·6(s)
137·5(s)
136·8(s)
133·6(s)
129·5(d)(2C)
128·9(d)(2C)
127·5(d)
125·5(s)
125·3(s)
124·5(d)
124·0(s)(2C)
119·5(s)
119·3(d)
111·4(d)
99·9(d)
56·1(g)
13·7(g)

[374]) confirms the substitution at C(3), (C(2) 123·3, C(3) 110·3 – cf. 3-methylindole C(2) 122·7, C(3) 111·4).[222] ^{13}C shifts for borrecapine are in accord with [375].[223] The ^{1}H NMR spectrum of melosatin B [376][224] shows the high frequency shift of the benzylic C(4) methylene resulting from the peri C(3) carbonyl. ^{1}H NMR shifts are also available for melosatin A (6,7-dimethoxy derivative of [376] – 5-H, δ 6·37)[224] and for melosatin

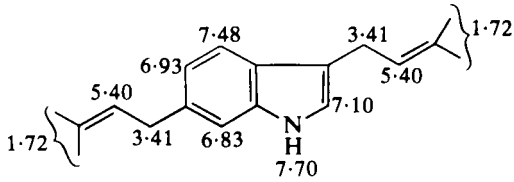

[374]

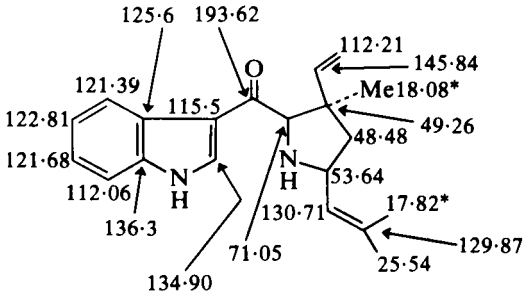

[375] Borrecapine

C (7-methoxy derivative of [376]-5-H, δ6·84; 6-H, δ7·06).[225] The angular structure for mupamine [377] is shown by the high frequency shift of 1-H.[226] ^{1}H NMR shifts for ellipticine [378] and the 5-carboxaldehyde

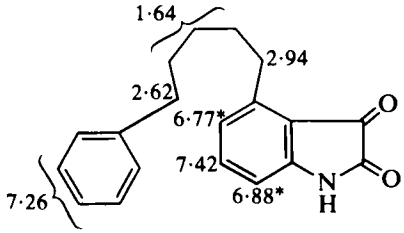

[376] Melosatin B

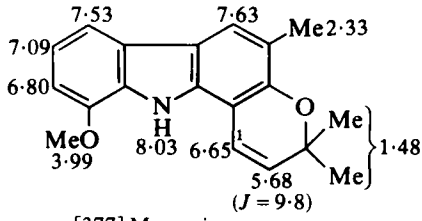

[377] Mupamine

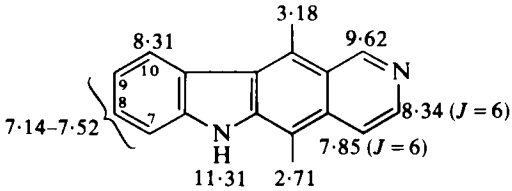

[378] Ellipticine (in DMSO-d_6)

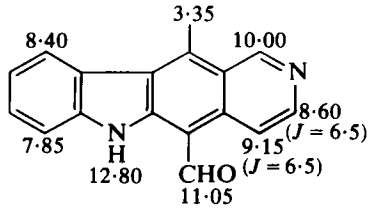

[379] 17-Oxo-ellipticine (in DMSO-d_6)

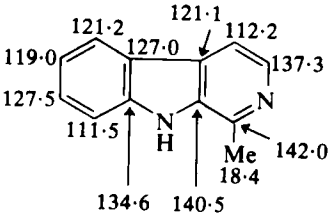

[380] Harmane (in DMSO-d_6)

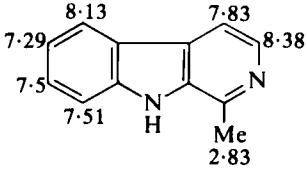

[381] (in DMSO-d_6)

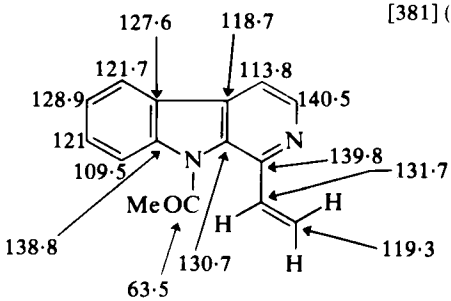

[382]

derivative [379][227] are displayed. The ^{1}H NMR spectrum of 7-hydroxyellipticine shows δ 8-H 7·06, 9-H 7·12, 10-H 7·86.[228]

^{13}C and ^{1}H shifts for harmane are given in [380] and [381].[229] Shifts for harmalol and harmaline are also available.[229] ^{13}C shifts for *N*-methoxy-1-vinyl-β-carboline are given in [382] and the ^{1}H NMR spectrum shows δ7·71 (J = 17, 10·6), δ 5·64 (J = 10·6) and δ 6·60 (J = 17) characteristic of the vinyl group.[230] NMR shifts for some other carbolines are given in [383],[231] [384][232] and [385]–[387].[233]

The results of detailed NMR studies of flustramine A are summarized in [388] and [389].[234] Differences in ^{1}H NMR parameters for racemic and

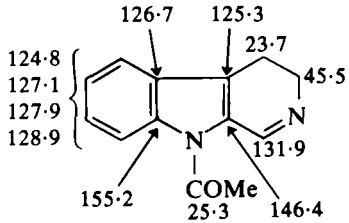

[383]

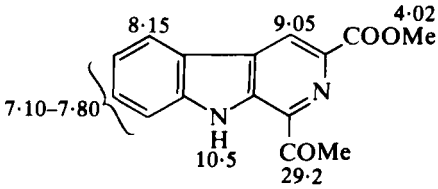

[384]

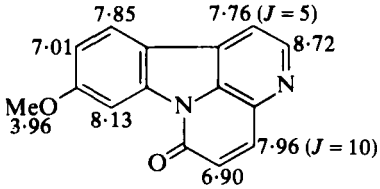

[385] 8-Methoxycanthin-6-one

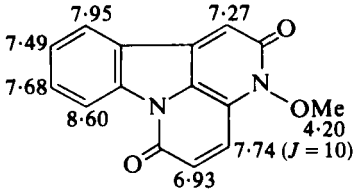

[386] 3-Methoxycanthin-2,6-dione

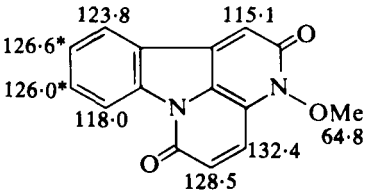

[387]

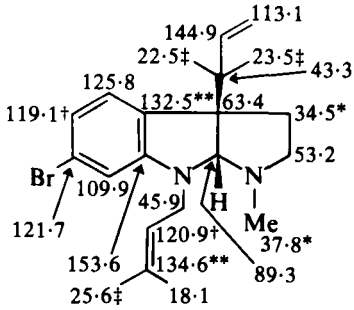

[388]

meso-folicanthine [390] (racemic isomer: N_b-Me 2·40, N_a-Me 3·00, *N*CH*N* 4·36; *meso* isomer: *N*-Me 2·40, *N*CH*N* 3·6–4·6) have been noted.[235]

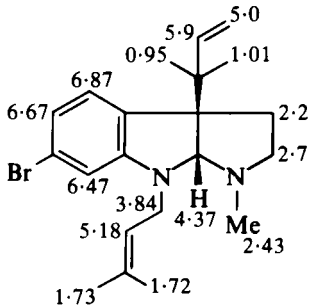

[389] Flustramine A

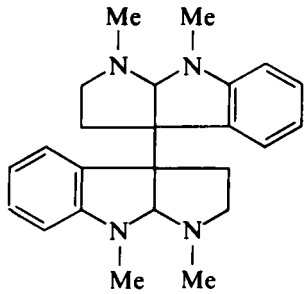

[390] Folicanthine

B. Mould metabolites

More ^{1}H NMR data on tryptoquivalines (see [344] in Section XII.B of reference 2) are available[236–238] and the spectrum of tryptoquivaline L is summarized in [391].[238]

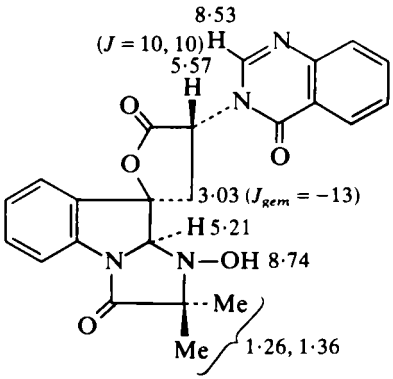

[391] Tryptoquivaline L (in DMSO-d_6)

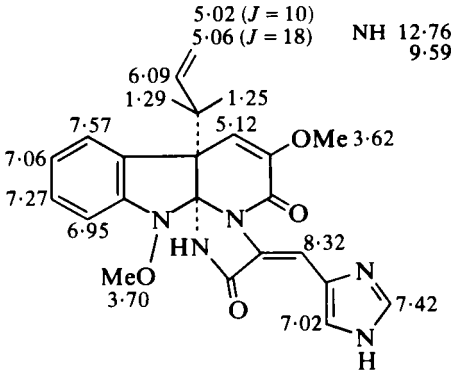

[392] Oxaline

The results of detailed NMR studies of oxaline and neoxaline are given in [392]–[395].[239] The values of the proton–proton vicinal coupling constants involving 9-H in the spectrum of neoxaline [393] suggest an equatorial orientation of the hydroxy group.[239] ^{1}H NMR data on paraherquamide and ditryptophenaline are summarized in [396][240] and [397].[241] In the ^{13}C NMR spectrum of cryptoechinuline G [398], C(3) absorbs at

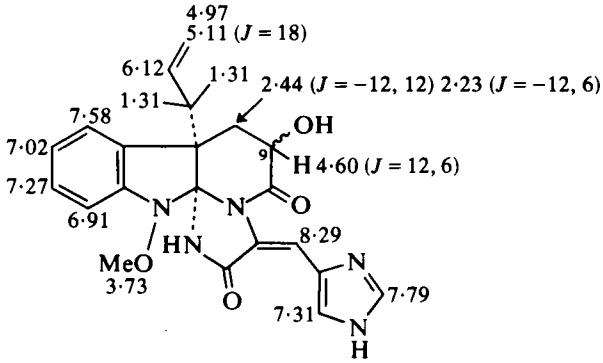

[393] Neoxaline

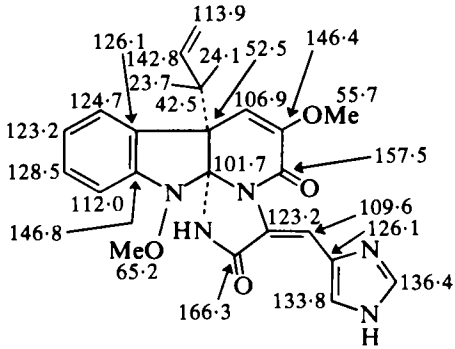

[394] Oxaline

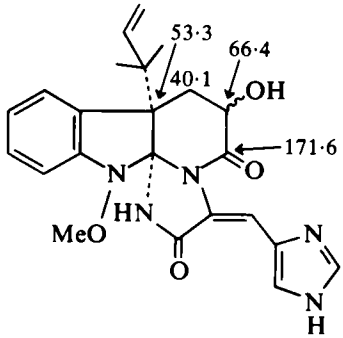

[395] Neoxaline

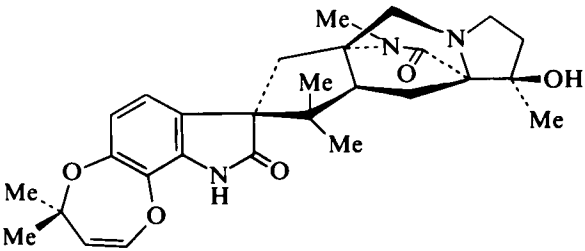

[396] Paraherquamide

Me	0·86
	1·10
	1·45
	1·45
	1·65
	3·03
	1·85 (J = 15)(1H)
	2·55 (J = 11)(1H)
	2·67 (J = 15)(1H)
	3·58 (J = 11)(1H)
	4·87 (J = 8)(1H)
	6·30 (J = 8)(1H)
	6·64 (J = 8)(1H)
	6·78 (J = 8)(1H)
OH, NH	2·58, 8·33

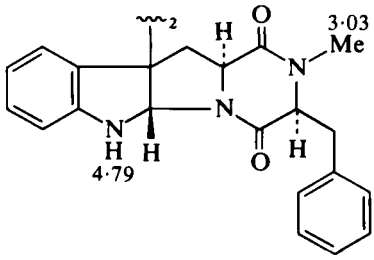

1·59 (J = 12, 12)
2·05 (J = 12, 5)
3·21 (J = 14, 5)
3·55 (J = 14, 4)
3·65 (J = 12, 5)
4·25 (br.m.)
4·89 (s)
6·5–6·9 (m, 2H)
6·95–7·3 (m, 4H)
7·4–7·7 (m, 3H)

[397] Ditryptophenaline

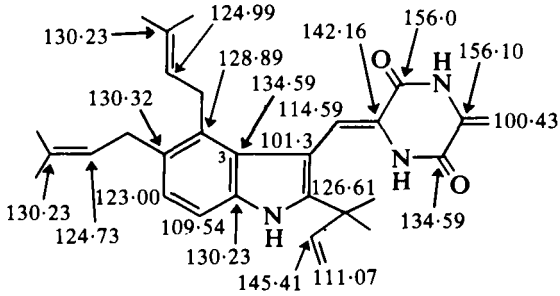

[398] Cryptoechinuline G

c. δ 101·3, whereas in similar metabolites unsubstituted at C(4), it absorbs at δ 103–104.[242] ^{13}C shifts for aflavinine are given in [399][243] and NMR data on paspalinine in [400]–[401].[244] In the ^{13}C NMR spectrum of paspalinine the singlet at δ 76·0 (C(13)) replaces the doublet at δ 39·2 present in the spectrum of paspalicine (structure as [401] but lacking angular C(13)-OH) and the ^{1}H NMR spectrum of paspalicine shows allylic coupling between 11-H and 13-H which is absent in the spectrum of paspalinine [400].[244] In the ^{13}C NMR spectrum of aflatrem (structure as in [401] but

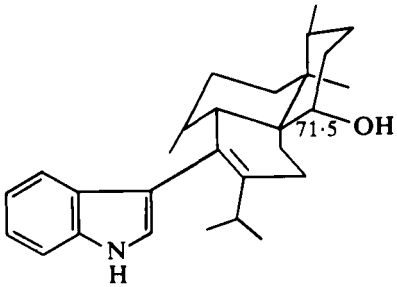

141·1	121·8
135·9	121·3
127·6	119·6
125·5	119·4
	118·6
	111·0
43·7	27·6
42·4	25·7
38·5	25·4
31·3	21·9
31·0	20·8
30·1	20·5
29·1	18·1
	15·7

[399] Aflavinine

with α,α-dimethylalkyl substituent at C(4')), the indolylmethylene carbon absorbs at δ 29·1 (cf. δ 27·3 in paspalinine) as a result of the presence of the C(4') substituent.[245] ^{13}C NMR shifts for penitrem A are given in [402] and $J_{C,H}$ and $J_{C,C}$ values are available.[246]

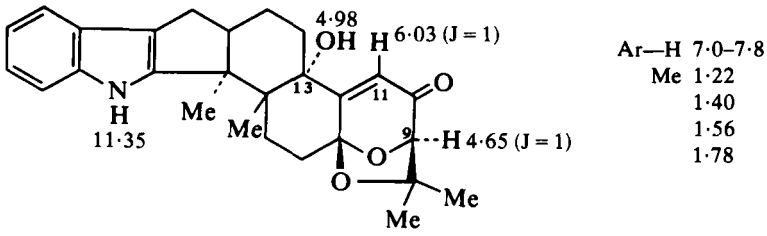

[400] Paspalinine (in pyridine-d_5)

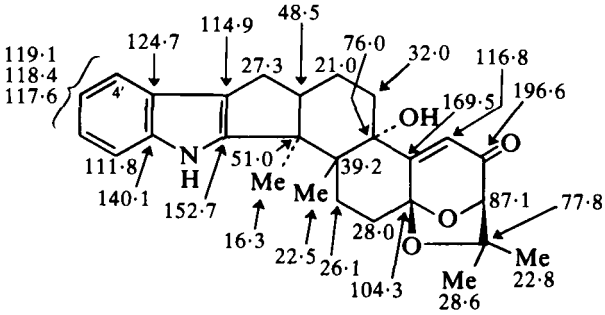

[401] Paspalinine (in DMSO-d_6)

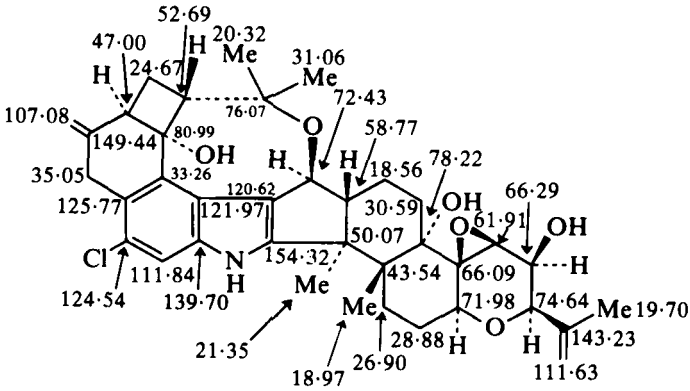

[402] Penitrem A (in CD_3COCD_3)

C. Indolo[*a*]quinolizidines (including corynantheine type), heteroyohimbines, yohimbines and oxindole alkaloids

1. ^{15}N *NMR of* Rauwolfia *alkaloids*

^{15}N shifts (to high frequency of external anhydrous liquid ammonia) for the indolo[*a*]quinolizidines [403] and [404] and in yohimbine [405], reserpine [406] and isoreserpine [407] show shielding of the nitrogen in the *cis* C/D compounds. This has been explained in terms of a hyperconjugative interaction between the antiperiplanar C—H bonds and the nitrogen lone pair in the *trans*-fused structures which increase the C—N π bond character resulting in a deshielding of the nitrogen.[247]

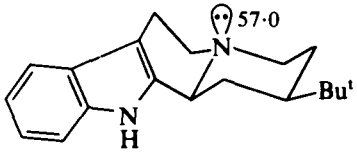

[403]

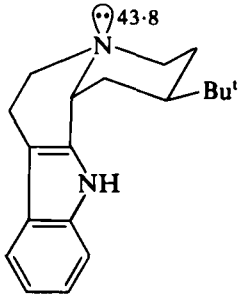

[404]

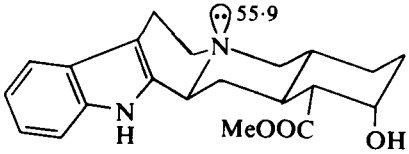

[405] Yohimbine

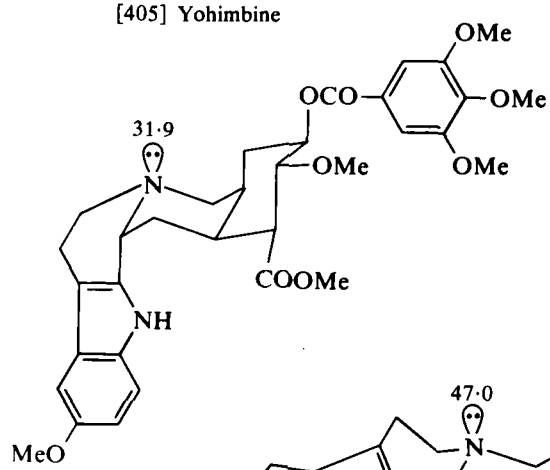

[406]
Reserpine (in DMSO)

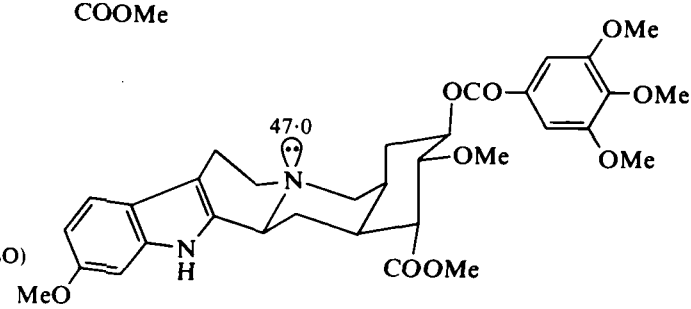

[407] Isoreserpine

2. Indolo[a]*quinolizidines (including corynantheine-type alkaloids)*

The ^{13}C shifts of C(6) and C(4) in octahydroindolo[2,3-*a*] quinolizine given with structure [363] in reference 2 (Section XII.D) should be reversed. The interchange of shifts mentioned in the text[2] should have referred to a 2-*t*-butyl derivative.

The ^{13}C NMR spectrum of deplancheine is summarized in [408].[248] The ^{1}H NMR spectrum of the unnatural *Z*-isomer[249] shows a very high frequency absorption (δ 3·9, $J = -12$) for the 21eq-proton (no aliphatic protons absorb to high frequency of δ 3·6 in deplancheine).

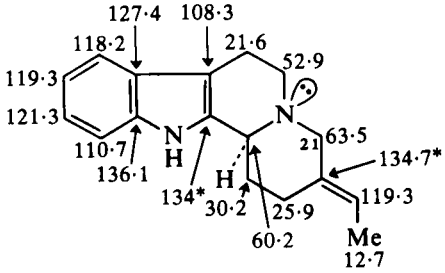

[408] Deplancheine

The conformation of geissoschizine [409][250] has been supported by the 270 MHz ^{1}H NMR data[251] depicted in [409]. The ^{13}C NMR spectrum of geissoschizine reported previously (see structure [382] in reference 2) has been discussed in terms of the same conformation.[252]

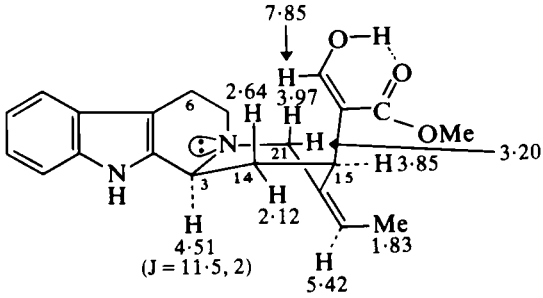

$J_{3\alpha,14\beta} = 11{\cdot}5$
$J_{3\alpha,14\alpha} = 2$
$J_{14\alpha,14\beta} = -13$
$J_{14\beta,15\alpha} = 6{\cdot}5$
$J_{14\alpha,15\alpha} = 11{\cdot}5$
$J_{15\alpha,21\alpha} = 1$
$J_{18,21\beta} = 2$
$J_{19,21\beta} = 2$
$J_{21\alpha,21\beta} = -12{\cdot}5$

[409] Geissoschizine

^{13}C NMR spectra of a variety of 1,2,3,4,6,7,12,12b-octahydroindolo[2,3-*a*]quinolizine derivatives have been reported.[253–255] The double bond stereochemistry in the pair of compounds [410] and [411][253] is reflected in the differences in C(15) and C(21) shifts. The stereochemistry of the

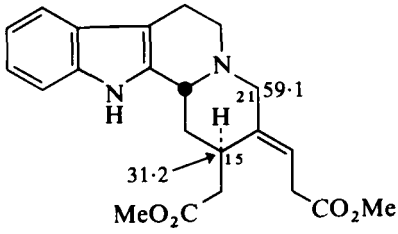

[410]

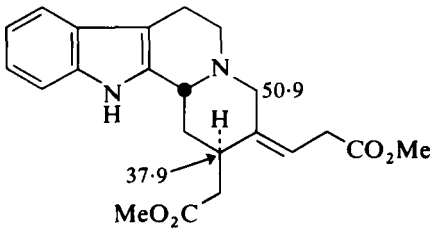

[411]

four stereoisomeric indolo[2,3-*a*]quinolizidines may readily be differentiated by ^{13}C NMR shift changes. Thus the *trans* C/D junction in [412] and [414] (normal and allo series respectively) is indicated by the C(3) and C(6) shifts. The change from the 15,20-diequatorially substituted isomer [412] to the 15eq,20ax-disubstituted isomer [414] is reflected in the shifts of C(19) and C(14) (reciprocal γ-effects). The depicted shifts in the epi-allo compound [415] show the *cis*-C/D ring junction with an equatorial 15-substituent and an axial 20-substituent but the intermediate values for the

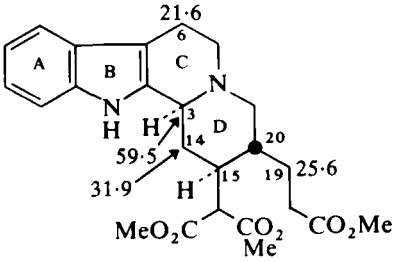

[412]

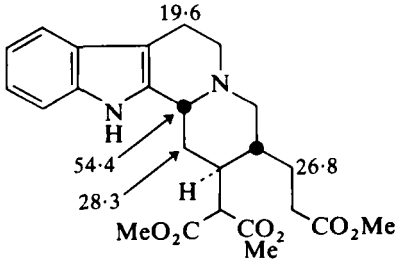

[413]

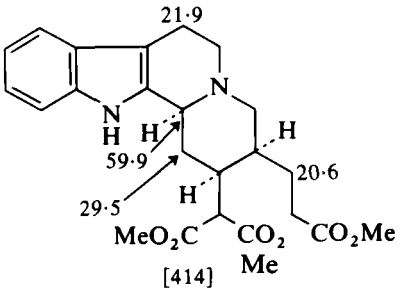

[414]

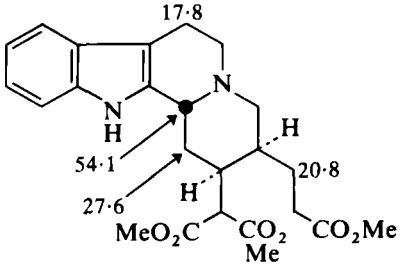

[415]

pseudo-compound [413] suggest an equilibrium between the *cis*-C/D-15,20-diequatorial conformation and a *trans*-C/D conformer with a non-chair D ring.[253]

The C(16) configuration in sitsirikine [416] cannot be based on C(17) methylene ^{1}H NMR parameters since 300 MHz data show no appreciable difference between the C(17) proton chemical shifts for sitsirikine (δ3·97,

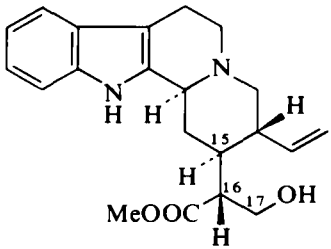

[416] Sitsirikine

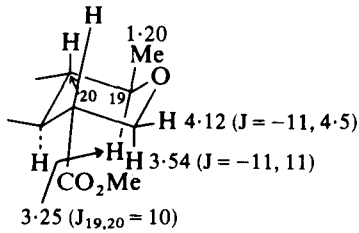

[417] Cyclositsirikine

$J = -11$, 8; δ3·76, $J = -11$, 6·5) and 16-episitsirikine (δ3·92, $J = -11$, 8; δ3·71, $J = -11$, 3·5).[256] The stereochemistry of sitsirikine was, however, established[256] by analysis of the ^{1}H NMR spectrum of cyclositsirikine [417] obtained by oxymercuration of [416]. ^{13}C NMR parameters of the quaternary alkaloid diploceline are shown in [418].[229]

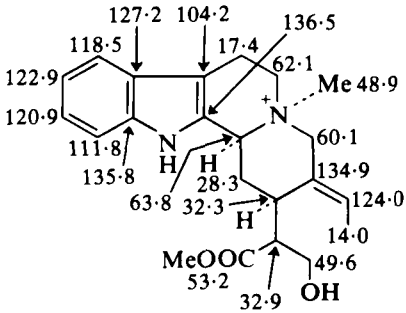

[418] Diploceline (in DMSO-d_6)

3. *Heteroyohimbine and yohimbine alkaloids*

The 400 MHz NMR spectra[257] of the eight basic heteroyohimbine alkaloids – tetrahydroalstonine [419], akuammigine [420], rauniticine [421], 3-isorauniticine [422], ajmalicine [423], 19-epiajmalicine [424], 3-isoajmalicine [425] and 3-iso-19-epiajmalicine [426] – are summarized with the structures. 270 MHz spectral data of four of these, [419], [421], [423] and [424], have also been reported.[251] With the exception of akuammigine [420] only half-chair C ring, chair D ring and half-chair E ring conformations were considered[257] and the spectroscopic results are largely in accord with these restrictions. Both sets of authors interpret the results

5ax-H 2·54
14ax-H 1·52
20eq-H 1·68
21ax-H 2·72

Geminal couplings:
$J_{5ax,5eq} = -12{\cdot}5$
$J_{6ax,6eq} = -15$
$J_{14ax,14eq} = -12$
$J_{21ax,21eq} = -12$

Vicinal couplings:
$J_{3,14\alpha} = 3$
$J_{3,14\beta} = 12$
$J_{5\alpha,6\alpha} = 4$
$J_{5\alpha,6\beta} = 11$
$J_{5\beta,6\alpha} < 1$
$J_{5\beta,6\beta} = 6$
$J_{14\alpha,15} = 4$
$J_{14\beta,15} = 12$
$J_{15,20} = 4$
$J_{18,19} = 6{\cdot}5$
$J_{19,20} = 12$
$J_{20,21\alpha} = 5$
$J_{20,21\beta} = 3$

Long range couplings:
$J_{15,17} = 0{\cdot}5$

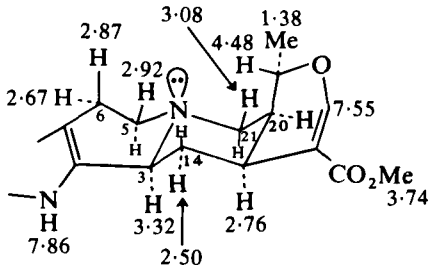

[419] Tetrahydroalstonine

for rauniticine as indicating a predominance of the *trans*-C/D conformation but the boat E ring for rauniticine has been proposed[251] on the basis of the value for $J_{19\alpha,20\alpha}$ of 7 Hz. The values of $J_{14\beta,15}$ 12 Hz, $J_{19,20}$ 6 Hz, $J_{20,21\alpha}$ for 5 Hz for akuammigine [420] have been taken to provide evidence

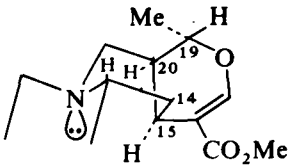

[420c]

[420] Akuammigine

Vicinal couplings:
$J_{3,14\alpha} \sim 9$
$J_{3,14\beta} \sim 4$
$J_{5\alpha,6\alpha} = 6$
$J_{5\alpha,6\beta} < 1$
$J_{5\beta,6\alpha} = 12$
$J_{5\beta,6\beta} = 4$
$J_{14\alpha,15} = 6$
$J_{14\beta,15} = 12$
$J_{15,20} \sim 6$
$J_{18,19} = 7$
$J_{19,20} = 6$
$J_{20,21\alpha} = 5$
$J_{20,21\beta} = 7$

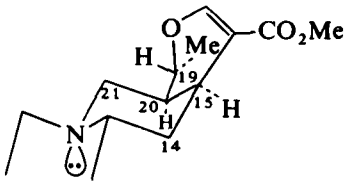

[420a]

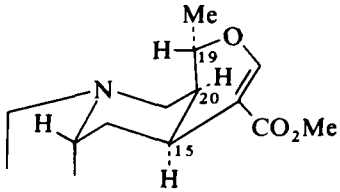

[420b]

3-H 3·48
5α-H 2·65
5β-H 3·00
14α-H 2·13
14β-H 3·04
15-H 2·74
20-H 1·86
21α-H 2·98
21α-H 2·62

Geminal couplings:
$J_{5\alpha,5\beta} = -12$
$J_{6\alpha,6\beta} = -15$
$J_{14\alpha,14\beta} = -12$
$J_{21\alpha,21\beta} = -12$

Long range coupling:
$J_{15,17} < 0{\cdot}3$

for the third conformation [420c] in the [420a] ⇌ [420b] equilibrium. The low frequency shift (δ 25·7) for C(15) in the ^{13}C NMR spectrum of this alkaloid has been attributed to an interaction between the nitrogen lone pair and the C(15) methylene in [420c].[257]

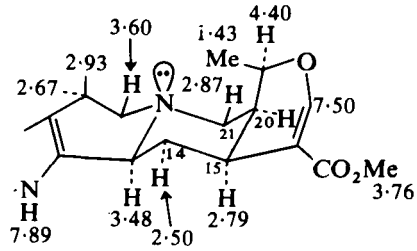

[421] Rauniticine

5ax-H 2·65
14ax-H 1·83
20eq-H 2·22
21eq-H 2·77

Geminal couplings:
$J_{5\alpha,5\beta} = -12$
$J_{6\alpha,6\beta} = -15$
$J_{14\alpha,14\beta} = -12$
$J_{21\alpha,21\beta} = -12{\cdot}5$

Vicinal couplings:
$J_{3,14\alpha} = 3$
$J_{3,14\beta} = 12$
$J_{5\alpha,6\beta} = 12$
$J_{5\beta,6\alpha} < 1$
$J_{5\beta,6\beta} = 6$
$J_{14\alpha,15} = 4$
$J_{14\beta,15} = 12$
$J_{15,20} = 4$
$J_{18,19} = 7$
$J_{19,20} = 6$
$J_{20,21\alpha} = 5$
$J_{20,21\beta} = 3$

Long range coupling:
$J_{15,17} = 0{\cdot}5$

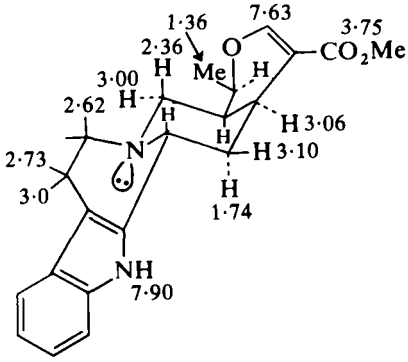

[422] 3-Isorauniticine

3ax-H 3·12
5eq-H 3·1
19-H 4·14
20-H 2·29

Geminal couplings:
$J_{5\alpha,5\beta} = -11$
$J_{6\alpha,6\beta} = -15$
$J_{14\alpha,14\beta} = -12$
$J_{21\alpha,21\beta} = -11{\cdot}5$

Vicinal couplings:
$J_{3,14\alpha} = 12$
$J_{3,14\beta} = 3$
$J_{5\alpha,6\beta} < 1$
$J_{5\beta,6\alpha} = 11$
$J_{5\beta,6\beta} = 4{\cdot}5$
$J_{14\alpha,15} = 4$
$J_{14\beta,15} = 2$
$J_{15,20} = 1$
$J_{18,19} = 6$
$J_{19,20} = 1$
$J_{20,21\alpha} = 4$
$J_{20,21\beta} = 11{\cdot}5$

Long range coupling:
$J_{15,17} = 1$

5ax-H 2·68
14ax-H 1·32
21ax-H 2·25

Geminal couplings:
$J_{5\alpha,5\beta} = -12$
$J_{6\alpha,6\beta} = -16$
$J_{14\alpha,14\beta} = -12$
$J_{21\alpha,21\beta} = -12$

Vicinal couplings:
$J_{3,14\alpha} = 3$
$J_{3,14\beta} = 12$
$J_{5\alpha,6\alpha} = 4$
$J_{5\alpha,6\beta} = 11$
$J_{5\beta,6\alpha} < 1$
$J_{5\beta,6\beta} = 6$
$J_{14\alpha,15} = 3$
$J_{14\beta,15} = 12$
$J_{15,20} = 12$
$J_{18,19} = 6$
$J_{19,20} = 3$
$J_{20,21\alpha} = 12$
$J_{20,21\beta} = 3$

Long range coupling:
$J_{15,17} = 1·5$

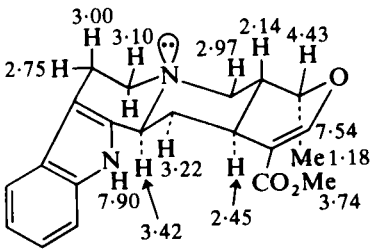

[423] Ajmalicine

21ax-H 2·20
$J_{19,20} = 12$

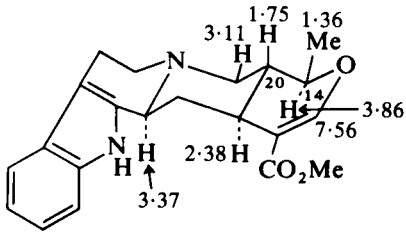

[424] 19-Epiajmalicine

14ax-H 1·70
21ax-H 2·56

Geminal couplings:
$J_{6\alpha,6\beta} = -16$
$J_{14\alpha,14\beta} = -12$
$J_{21\alpha,21\beta} = -12$

Vicinal couplings:
$J_{3,14\alpha} = 2$
$J_{3,14\beta} = 4$
$J_{5\alpha,6\alpha} = 8$
$J_{5\alpha,6\beta} < 1$
$J_{5\beta,6\alpha} = 10$
$J_{5\beta,6\beta} = 4$
$J_{14\alpha,15} = 2$
$J_{14\beta,15} = 12$
$J_{15,20} = 12$
$J_{18,19} = 6$
$J_{19,20} = 3$
$J_{20,21\alpha} = 12$
$J_{20,21\beta} = 3$

Long range coupling:
$J_{15,17} = 1$

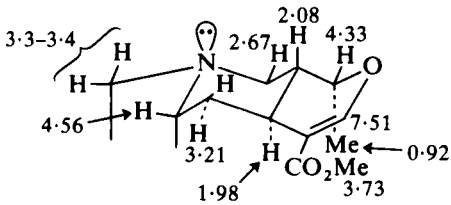

[425] 3-Isoajmalicine

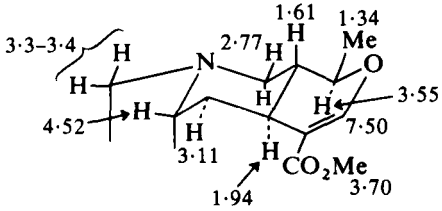

[426] 3-Iso-19-epiajmalicine

14ax-H 1·59
21ax-H 2·48

Geminal couplings:
$J_{6\alpha,6\beta} = -16$
$J_{14\alpha,14\beta} = -12$
$J_{21\alpha,21\beta} = -12$

Vicinal couplings:
$J_{3,14\alpha} = 2$
$J_{3,14\beta} = 4$
$J_{5\alpha,6\alpha} = 8$
$J_{5\alpha,6\beta} < 1$
$J_{5\beta,6\alpha} = 10$
$J_{5\beta,6\beta} = 4$
$J_{14\alpha,15} = 2$
$J_{15,20} = 12$
$J_{18,19} = 6{\cdot}5$
$J_{19,20} = 12$
$J_{20,21\alpha} = 12$
$J_{20,21\beta} = 3$

Long range coupling:
$J_{15,17} = 1$

Comparison of the ^{13}C NMR spectrum of an alkaloid from *Uncaria attenuata* with that of 3-isorauniticine (provided in [374] in reference 2) suggests the 14β-hydroxy-3-isorauniticine structure [427].[258]

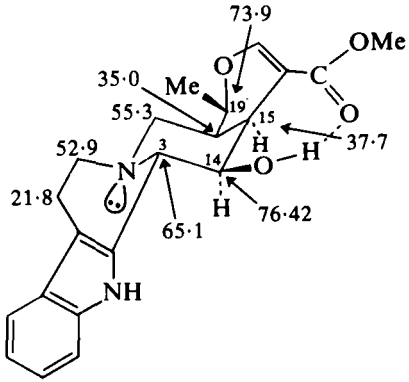

[427] 14β-Hydroxy-3-isorauniticine

^{1}H NMR parameters for 21-cyanoakuammigine are given in [428][259] and suggest a conformation of the type [420a]. Similar data are available for 21-cyanotetrahydroalstonine.[259] The spectrum of 19-epinaucleidinal

differs from that of naucleidinal shown in [429] by shifts of 18-H δ1·00; 19-H δ4·86; and 20-H δ2·65 and by $J_{18,19}$ = 7·0, $J_{19,20}$ = 4·0 and $J_{20,21}$ = 0·5 Hz.[260]

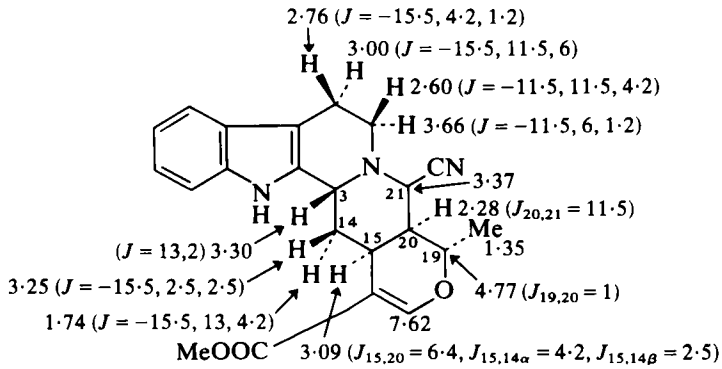

[428] 21-Cyanoakuammigine

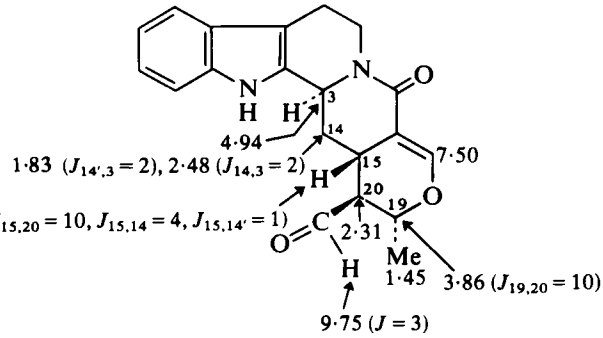

[429] Naucleidinal

Comparison of the ^{13}C NMR spectrum of 5β-carboxamidoyohimbine [430] with that of yohimbine and pseudoyohimbine (structures [368] and [369] in reference 2) together with the high frequency (δ4·23) absorption of the 3-proton suggests a *cis*-C/D ring fusion with a boat-type ring D.[261]

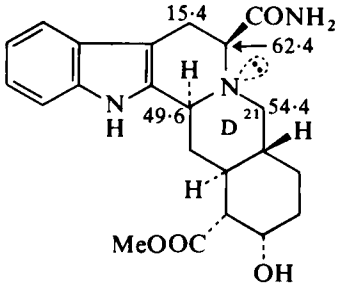

[430]

4. Oxindole alkaloids

To extend the collection of NMR data on oxindole alkaloids,[2] the spectra of palmirine [431][262] and cyclopiamine B [432][263] are provided.

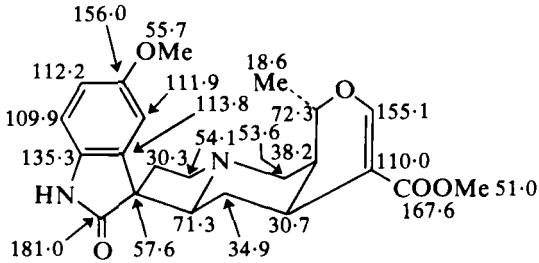

[431] Palmirine

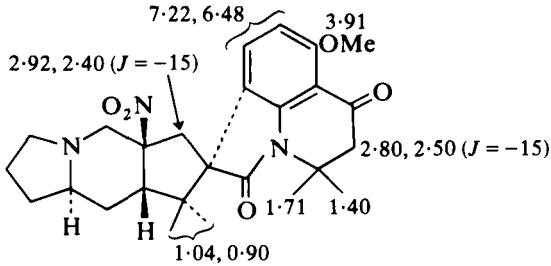

[432] Cyclopiamine B

D. Strychnine and related alkaloids

1. Compounds possessing the heptacyclic structure

The suggestion[2] of an incorrect analysis of the signals arising from $C(17)H_2$—$C(18)H_2$ moiety in the 250 MHz NMR spectrum of strychnine (provided in [413] in reference 2) has been confirmed.[264,265] The spectrum of strychnine in pyridine shows an increase in the chemical shift difference between the C(6) methylene protons (C(17) in [413] in reference 2) so that the intensities of the weak outer lines (neglected in the original analysis) increases. This permits an evaluation of a normal $J_{6\alpha,6\beta}$ value of −12·8 Hz.[265] A reversal of the shifts of the C(5) and C(21) methylene protons reported in [413] of reference 2 has also been suggested[264] and these are shown in [433] together with coupling constant data on which boat D, chair F and chair E ring conformations [433a] and [433b] were assigned. Of particular importance in this study[264] is the elucidation of the long range couplings ($J_{21\alpha,19}$ and $J_{15,8\alpha}$).

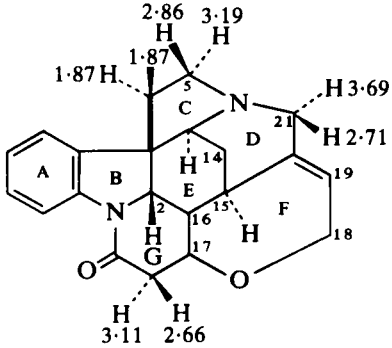

[433]

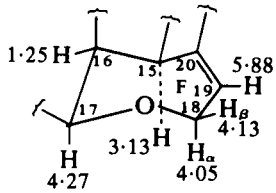

[433a]

$J_{19,18\beta} = 6{\cdot}9$
$J_{19,18\alpha} = 5{\cdot}7$
$J_{19,15\alpha} = 2{\cdot}5$
$J_{15,16} = 3{\cdot}1$
$J_{15,18\alpha} = 2{\cdot}5$
$J_{16,17} = 3{\cdot}1$

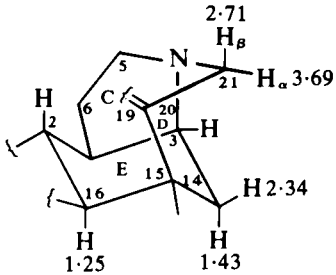

[433b]

$J_{21\alpha,19} = 1{\cdot}2$
$J_{21\alpha,5\alpha} = 1{\cdot}7$
$J_{2,16} = 10{\cdot}5$
$J_{21\alpha,21\beta} = -14{\cdot}8$

The ^{13}C NMR spectra of strychnine and strychnine hydrochloride have been reported[264,266,267] and that for strychnine shown in [434][264] shows some alternative assignments to those in structure [420] in reference 2. In

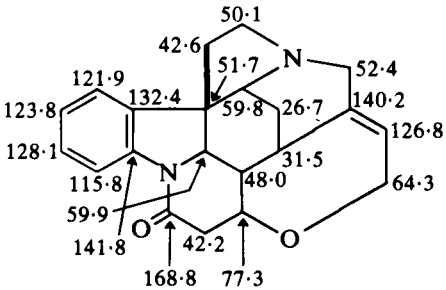

[434] Strychnine

the spectrum of the hydrochloride [435][264] C(19) and C(20) are markedly affected relative to the free base [434]. The spectrum of strychnine in 70% aqueous perchloric acid in which both nitrogen atoms are protonated is

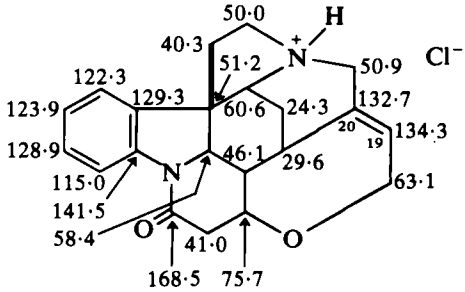

[435] Strychnine hydrochloride (in DMSO-d_6)

shown in [436].[268] ^{13}C shifts for some strychnine sulphonic acids in 70% aqueous perchloric acid solution are given in [437]–[439].[268] In the ^{1}H NMR spectrum of 15-hydroxystrychnine, 17-H is deshielded (δ 4·76) relative to the absorption of 17-H (δ 4·27) in strychnine [433a] (1,3-*syn*-axial relationship) and 16-H absorbs at δ 1·45 (cf. δ 1·25 in strychnine [433a]).[269]

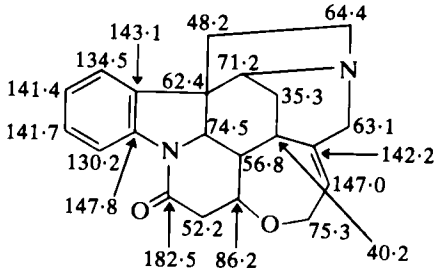

[436] Strychnine (in 70% aq. $HClO_4$)

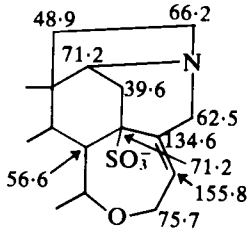

[437] (in 70% aq. $HClO_4$)

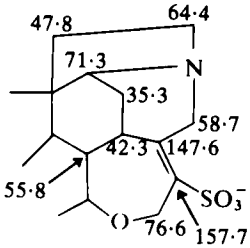

[438] (in 70% aq. $HClO_4$)

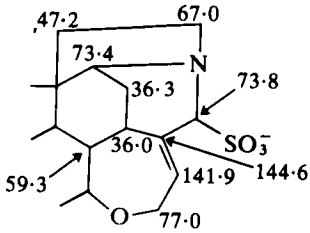

[439] (in 70% aq. $HClO_4$)

The ^{13}C shifts of C(14) (δ 30·5), C(15) (δ 77·4), C(16) (δ 50·4) and C(17) (δ 74·0) in 15-acetoxystrychnine may be compared to those in strychnine [434].[269] ^{1}H NMR parameters for imidazo-, oxazolo- and dioxolo-strychnine derivatives annelated at the 10,11 position of the aromatic nucleus in strychnine are available.[270]

2. *Strychnine derivatives lacking the G ring*

The similarity of the ^{1}H parameters for strychnine [433] and N_a,*O*-diacetyl Wieland Gumlich aldehyde [440] suggests the D ring boat conformation and the similarity of ring conformations is also indicated by the

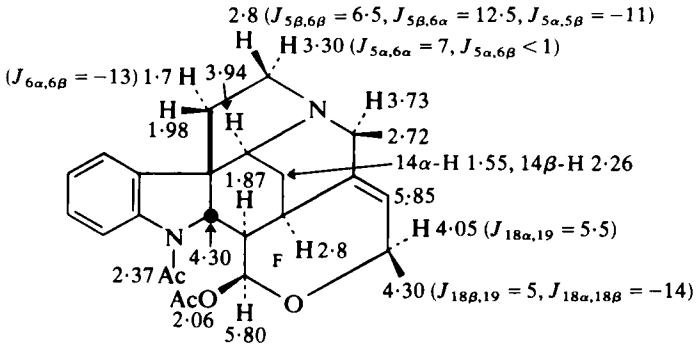

[440] N_a,*O*-Diacetyl Wieland Gumlich aldehyde

similar chemical shifts of the carbon nuclei shown in [441]. C(6) is, however, shielded in [440] (δ 38·1 compared to δ 42·6 in strychnine), indicating some conformational change. The similar shifts also indicate a chair F ring with an equatorial β-acetoxy group in [440].[264]

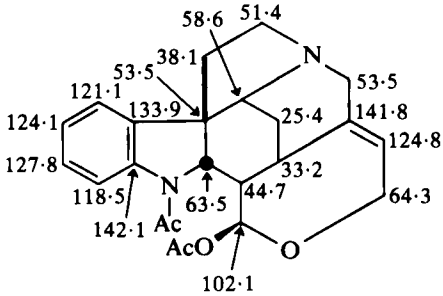

[441] N_a,*O*-Diacetyl Wieland Gumlich aldehyde (in 5 : 1 $CDCl_3$–MeOH)

Comparison of the ^{13}C shifts of C(17), C(15) and C(18) in the Wieland Gumlich aldehyde anomers [442] and [443] with those in strychnine [434]

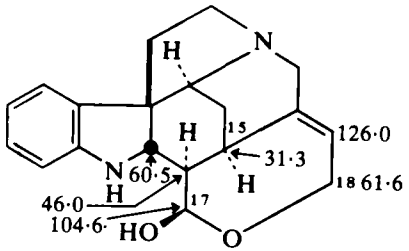

[442] Wieland Gumlich aldehyde

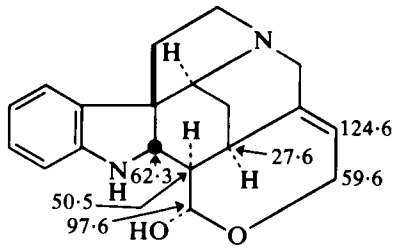

[443] Wieland Gumlich aldehyde

shows the equatorial and axial OH respectively (both in chair F conformations). The shifts in the spectra of the corresponding diaboline anomers [444] and [445] do not, however, accord with the trends observed for [442]

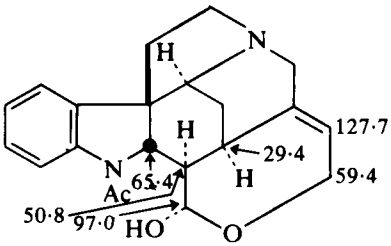

[444] Diaboline

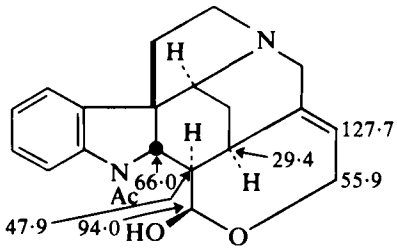

[445] Diaboline

and [443]. The spectra of [444] and [443] are similar, reflecting similar axial hydroxy-substituted chair F ring conformations, whereas the spectrum of [445] shows an unusually shielded C(17) explicable in terms of a boat F ring and a pseudo-axial hydroxy substituent.[264] Data on other related strychnine derivatives are available.[264] Comparison of shifts in isocondensamine [446] with those in [441] shows the effect of changing orientation of the 17-acetoxy substituent.[271]

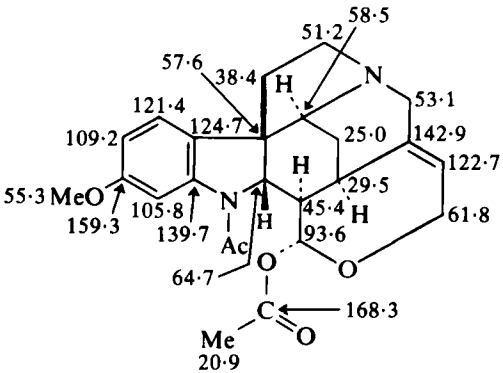

[446] Isocondensamine

3. *Strychnine derivatives lacking the F and G rings*

^{1}H NMR parameters for the two rotamers of retuline are given in [447] and [448] and for a single rotamer of isoretuline in [449].[265] Analysis of the data, particularly of the allylic and homoallylic couplings, suggests a chair ring D conformation for isoretuline [449] and a boat ring D conformation with C(21) in the flagpole position for retuline [447].[265]

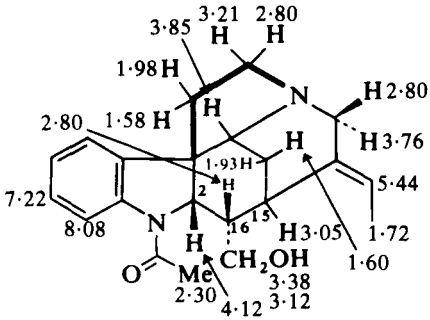

$J_{2,16} = 7{\cdot}2$
$J_{16,15} = c.\ 1$
$J_{21\alpha,18} = 1{\cdot}5$
$J_{21\beta,18} \simeq 0$

[447] Retuline rotamer a

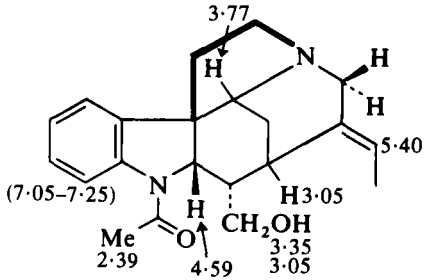

[448] Retuline rotamer b

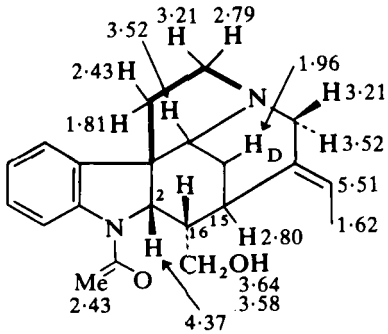

$J_{2,16} = 10{\cdot}4$
$J_{16,15} = c.\ 4$
$J_{21\beta,18} = 2{\cdot}0$
$J_{21\beta,19} = 1{\cdot}8$
$J_{21\alpha,18} = 0$

[449] Isoretuline

These conclusions are supported by comparison of ^{13}C shifts in isoretuline [450] and in Wieland Gumlich aldehyde derivatives (e.g. [441]) which show the deshielding of C(14) and C(21) in the chair D ring of isoretuline [450].[264]

The ^{1}H NMR spectra of the related retulinal, isoretulinal[272] and 16-hydroxyisoretulinal[273] have been described in detail. The spectra of retulinal and isoretulinal recorded in DMSO at 100 °C are given in [451] and [452]

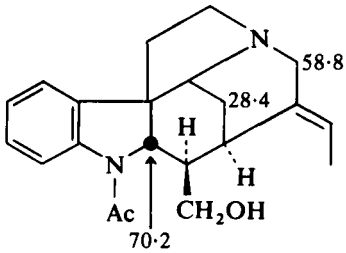

[450] Isoretuline

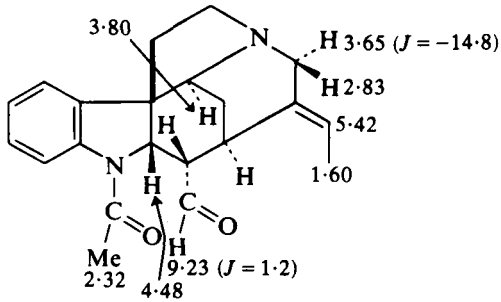

[451] Retulinal (DMSO at 100 °C)

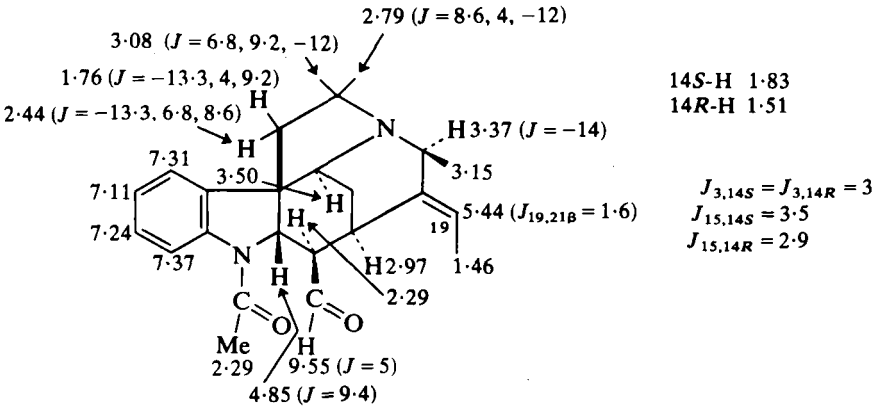

[452] Isoretulinal (DMSO at 100 °C)

and at ambient temperatures the NMR spectrum of retulinal shows absorption for 2-H at δ4·29 (J = 8·4) for rotamer a and at δ4·83 (J = 8·3) for rotamer b (rotameric designations as in [447] and [448]).[272]

In the ^{1}H NMR spectrum of 16-hydroxyisoretulinal [453][273] the magnitude of the allylic coupling ($J_{21\beta,19}$ = 2·0 Hz) and of the homoallylic coupling ($J_{Me,21\beta}$ = 2·0 Hz) suggest the chair D ring (compare isoretuline [449]). In the spectrum of strychnopivotine [454][273] the 21a-proton shows coupling to the 18-Me and indicates the boat D ring (cf. retuline [447]).

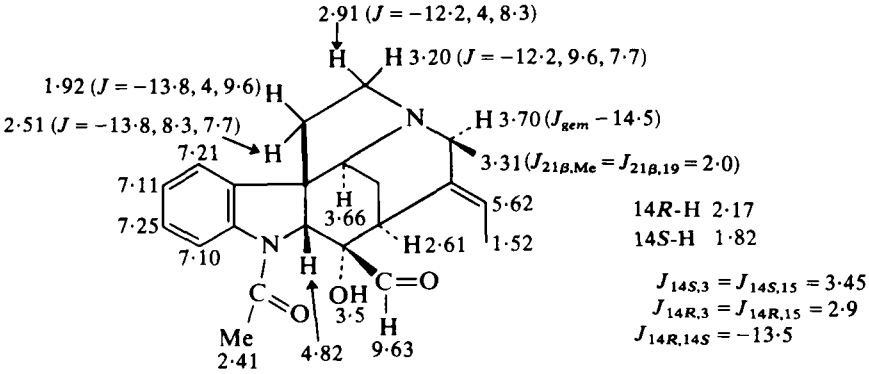

[453] 16-Hydroxyisoretulinal

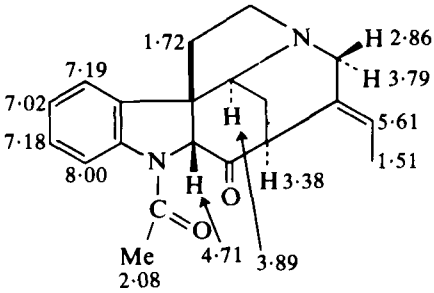

[454] Strychnopivotine (in DMSO)

The ^{1}H NMR of a new strychnos-type alkaloid is shown in [455].[274] The structure of scholarine (12-methoxyechitamidine) [456] is based on a comparison of ^{13}C shifts in alstovine (11-methoxyechitamidine C(9) 120·3, C(10) 105·9, C(11) 159·9 and C(12) 97·2) and in akuammicine (C(9)

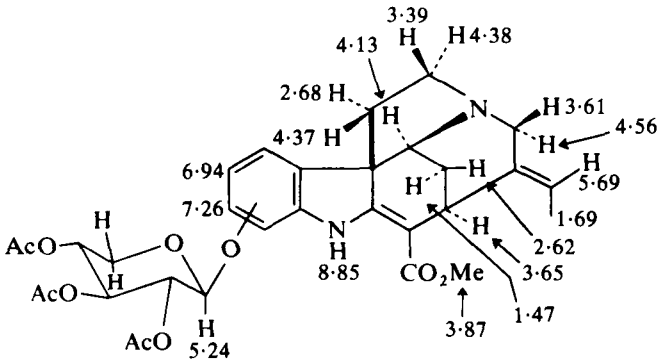

[455]

120·3*, C(10) 120·5*, C(11) 127·3, C(12) 109·1).[275] NMR data for fluorocurarine are summarized in [457] and [458].[276]

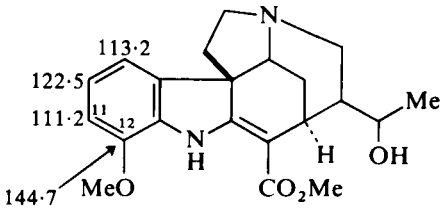

[456] Scholarine

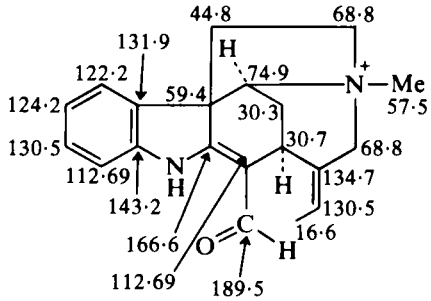

[457] Fluorocurarine (in D_2O)

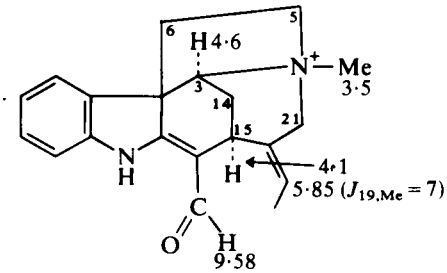

[458] Fluorocurarine (in CD_3OD)

$J_{3,14} \approx 2{\cdot}4$
$J_{21,21'} = -14{\cdot}4$
$J_{5,5'} \approx -13$
$J_{6,6'} \approx -14$
$J_{14,14'} \approx -14{\cdot}8$

21-H	4·29
21-H′	4·17
5-H	4·05
5-H′	3·98
6-H	2·87
14-H	2·81
6′-H	2·14

4. *Other strychnine derivatives*

The ^{1}H NMR spectrum of rosibiline [459],[273] particularly the value of $J_{2,16} = 6{\cdot}3$ Hz and the absence of allylic and homoallylic coupling of 21β-H

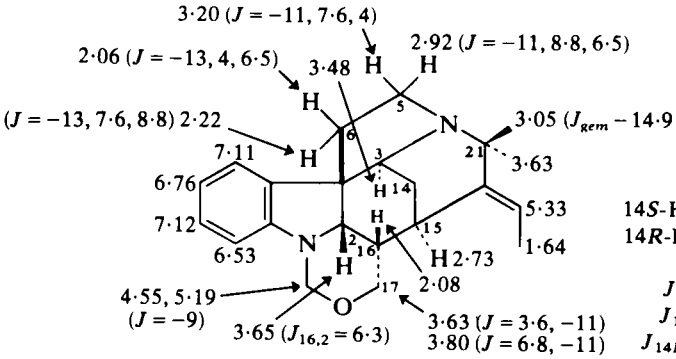

[459] Rosibiline

with 19-H and 18-Me, indicates the retuline-type series [447]. The geminal coupling of the NCH_2O protons (22-methylene) of −9·0 Hz suggests the *trans*-fused A/B ring stereochemistry. In the compound [460] obtained via

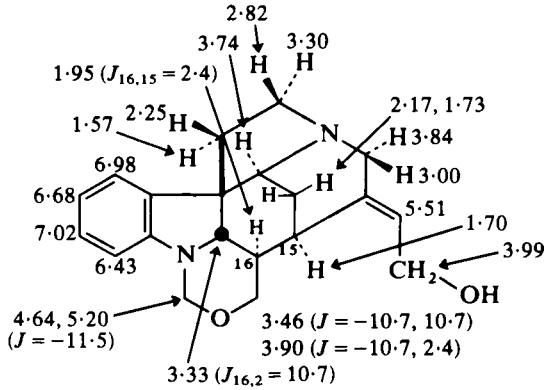

[460]

Wieland Gumlich aldehyde the J_{gem} of −11·4 Hz for the corresponding protons indicates the *O*-inside *cis*-fused A/B conformation.[276] These differing ring fusions are present in the model compounds [461] and [462].[277]

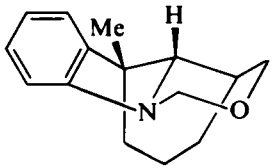

J_{gem} = −8·2

[461]

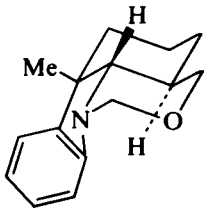

J_{gem} = −11·4

[462]

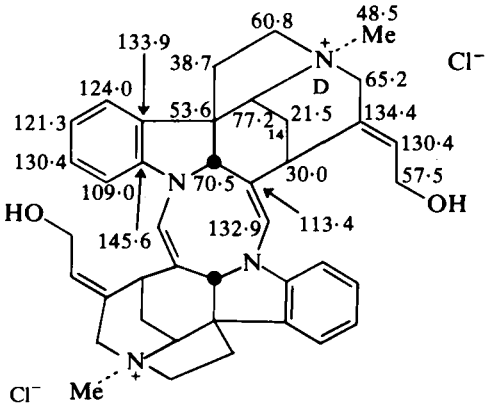

[463] Toxiferine I (in 1 : 5 D_2O–MeOH)

The low frequency shift of C(14) (δ21·5) in the spectrum of toxiferine I [463] indicates a reciprocal γ-effect from the N^+Me.[264] (Compare δ24·0 for C(14) and δ54·4 for N^+Me in strychnine methiodide, which possesses a boat D ring.)

E. Sarpagine, gardneria, ajmaline and vincamine-type alkaloids

In the ^{1}H NMR spectra of N_a-methylgardneral [464] and N_a-methyl-epi-gardneral [465] the aldehyde protons absorb at δ9·07 and δ9·56 respectively. The COO*Me* protons in the corresponding methoxycarbonyl

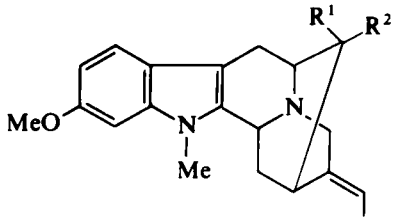

[464] N_a-Methylgardneral (R^1 = CHO, R^2 = H)
[465] N_a-Methyl-epi-gardneral (R^1 = H, R^2 = CHO)
[466] R^1 = COOMe, R^2 = H
[467] R^1 = H, R^2 = COOMe

derivatives [466] and [467] absorb at δ3·07 and δ3·66 respectively. These differences reflect the stereochemistry of the substituent with respect to the indole ring.[278] ^{13}C shifts for *O*-acetylnormacusine B are provided in [468][271] and the double bond geometry in the related [469] and [470] is indicated by the ^{13}C shifts of C(15) and C(21).[279]

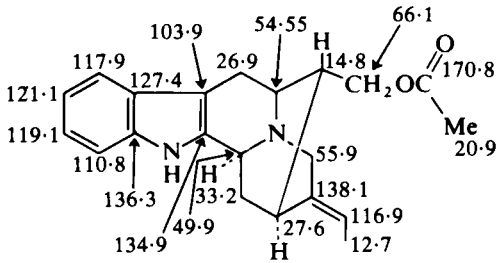

[468] *O*-Acetylnormacusine B

In the ^{13}C NMR spectra of the Gardneria alkaloids [471]–[474][279] the double bond geometry is determined by the γ-effect on the allylic carbons (C(15) or C(21)) of the 18-substituent on the double bond. In the spectra of the *E*-isomers (18-substituent *cis* to C(15)), C(15) absorbs to lower

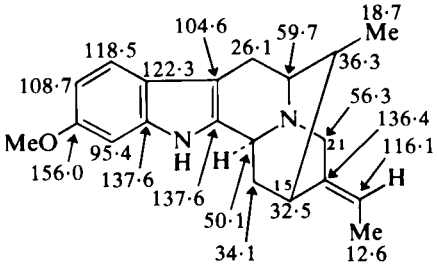

[469]

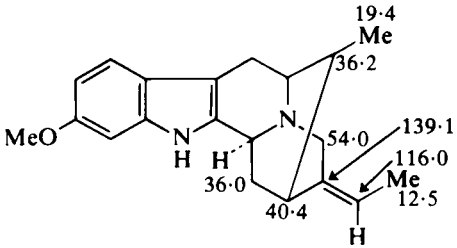

[470]

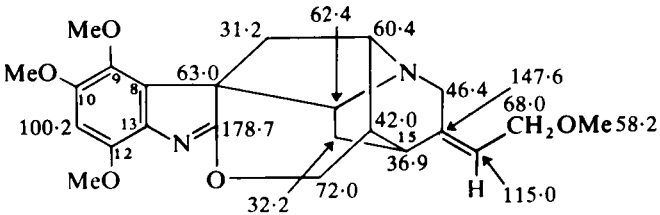

[471] Gardneramine

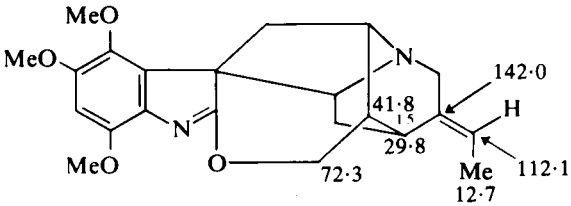

[472]

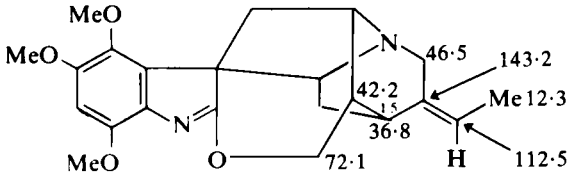

[473]

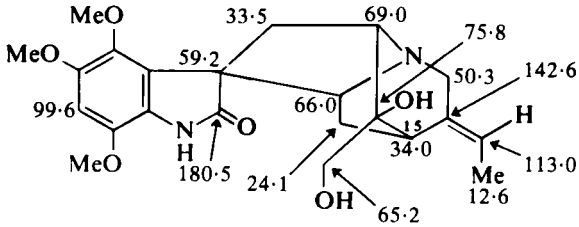

[474] Chitosenine

frequency of the corresponding signal in the *Z*-isomers. The opposite situation holds for the C(21) shifts.[279]

The C(12) absorption at δ 97·5 in rauflexine [475] (cf. δ 109·1 in ajmaline [476] and δ 109·2 in vincamajorenine [477]) indicates its *ortho* relationship

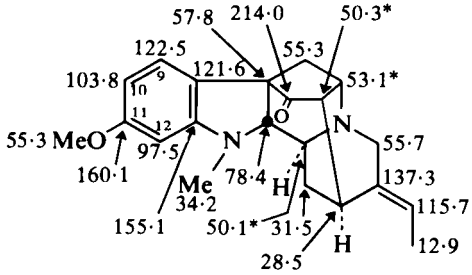

^{1}H NMR:

9-H	7·08	$J = 8$
10-H	6·35	$J = 8, 2$
12-H	6·25	$J = 2$

[475] Rauflexine

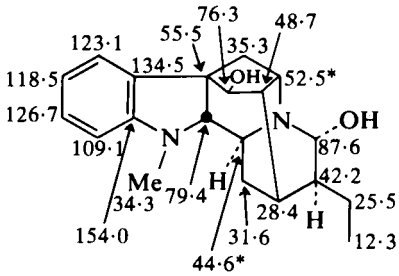

[476] Ajmaline

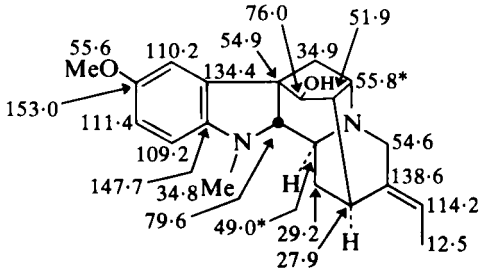

[477] Vincamajoreine (in $CDCl_3$–CD_3OD)

to the methoxy and *N*-methyl groups and locates the methoxy substituent at C(11). This is confirmed by the ^{1}H NMR absorption of the aromatic ring protons.[280]

NMR parameters of compounds obtained in synthetic studies related to eburnamonine are shown in [478]–[480][281] and in [481] and [482].[282]

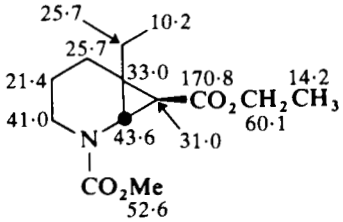

[478]

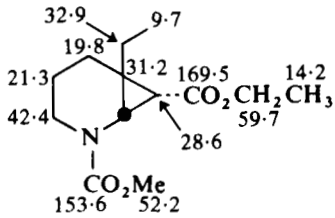

[479]

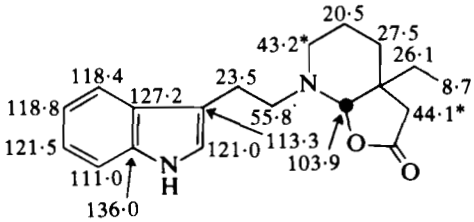

[480]

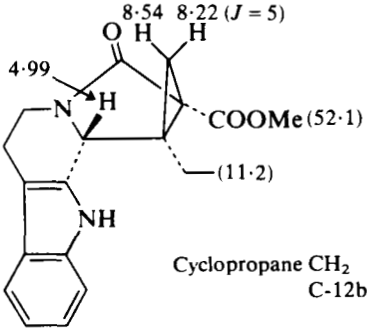

Cyclopropane CH_2 δ 25·11
C-12b 58·4

[481]

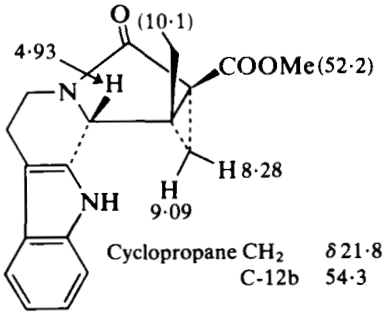

Cyclopropane CH_2 δ 21·8
C-12b 54·3

[482]

F. Aspidospermine, quebrachamine and iboga alkaloids

The larger differences between the C(9), C(15), C(17), C(18) and C(21) shifts in the spectra of ψ-vincadifformine [483] and in 20-epi-ψ-vincadifformine [484] than in the corresponding pandoline epimers (for ^{13}C NMR spectrum of pandoline see structure [447] in reference 2) has been interpreted[283] in terms of a deformed boat conformation for ring D in [483] as compared to a chair D ring in [484].

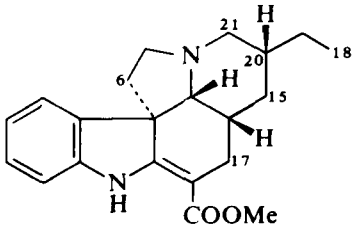

[483] Pseudovincadifformine

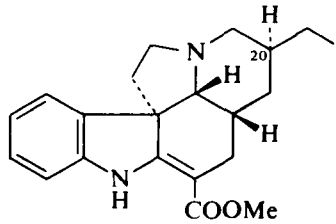

[484] 20-Epipseudovincadifformine

Differences between the ^{1}H NMR chemical shifts of the protons of the methoxycarbonyl group in the 19-aroyloxy-(+)- and 19-aroyloxy-(−)-vincadifformine alkaloids and in (−)-echitoveniline [485] and 19-epi-(+)-echitoveniline [486] have been discussed[284] in terms of the C(19) configuration. Only in the 19*R* configuration of the (+)-vincadifformine does the methoxycarbonyl group lie close to the deshielding zone of the 19-aroyloxy moiety.

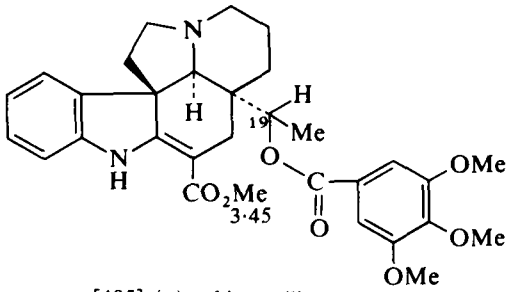

[485] (−)-echitoveniline

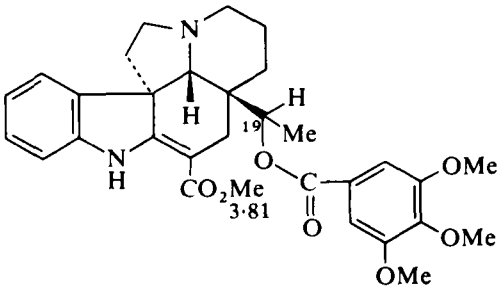

[486] 19-Epi-(+)-echitoveniline

The structures of the nitriles [487] and [488] were assigned[285] from a comparison of ^{13}C NMR data with the ^{13}C NMR spectrum of vincadifformine (see structure [435] in reference 2). The configurations of the nitrile groups are based on the ^{1}H NMR parameters for 3-H and 5-H.

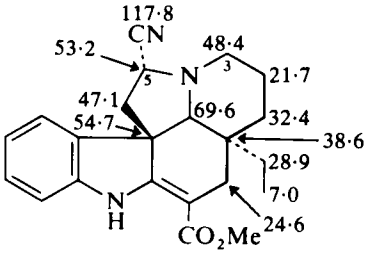

[487]

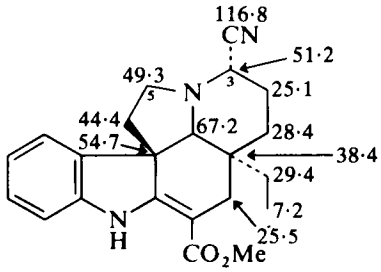

[488]

Assignment of the α-orientation of the N-oxide bond in tabersonine N_b-oxide [489] is based on the deshielding of the 9-proton.[286] The ^{13}C shifts of the aminomethine and of the CH_2CH_3 in tabersonine α- and β-epoxide [490] and [491] are indicative of stereochemistry.[287]

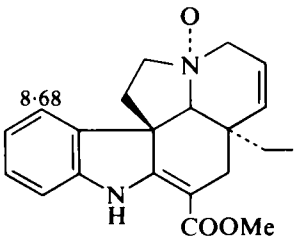

[489] Tabersonine N-oxide

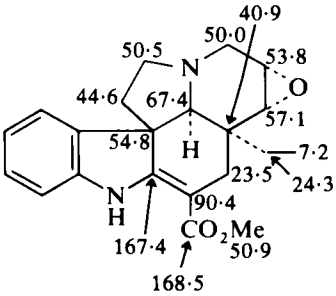

[490] Lochnericine (tabersonine α-epoxide)

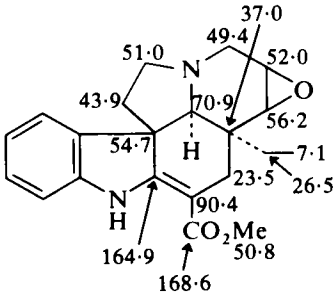

[491] Pachysiphine (tabersonine β-epoxide)

The ^1H NMR spectra of 20-epi-ibophyllidine [492] and desethyl-ibophyllidine [493] are very similar, suggesting similar C and D ring conformations. The change in conformation of these rings in ibophyllidine [494] indicated by the changes in ^1H NMR parameters are presumably caused by the minimization of interactions involving the ethyl substituent.[288]

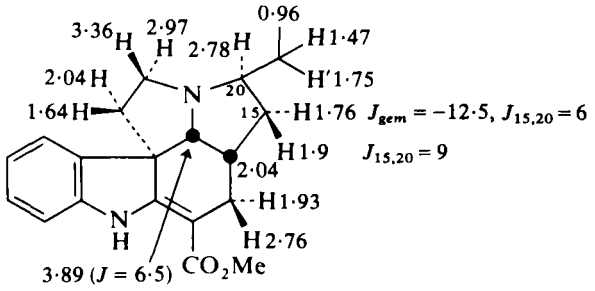

$J_{5\alpha,5\beta} = -12·5$
$J_{5\alpha,6\alpha} = 6$
$J_{5\alpha,6\beta} = 0·5$
$J_{5\beta,6\alpha} = 12·5$
$J_{5\beta,6\beta} = 5·5$
$J_{6\alpha,6\beta} = -12·5$

[492] 20-Epi-ibophyllidine

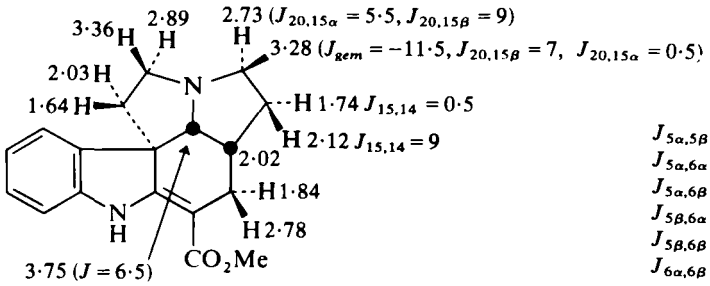

$J_{5\alpha,5\beta} = -12·5$
$J_{5\alpha,6\alpha} = 6$
$J_{5\alpha,6\beta} = 0·5$
$J_{5\beta,6\alpha} = 12·5$
$J_{5\beta,6\beta} = 5·5$
$J_{6\alpha,6\beta} = -12·5$

[493] Desethylibophyllidine

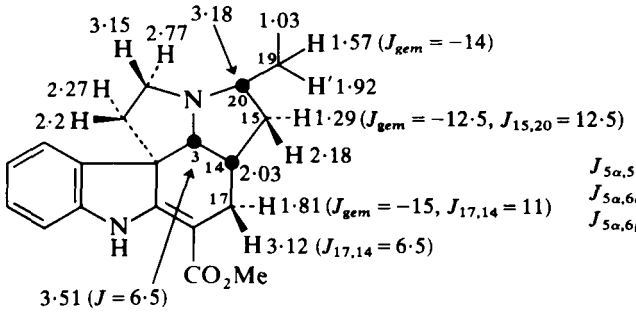

$J_{5\alpha,5\beta} = -10$
$J_{5\alpha,6\alpha} = 7$
$J_{5\alpha,6\beta} = 7$

[494] Ibophyllidine

Changes in ^{1}H NMR parameters in these types of alkaloids caused by differences in 19-configuration are shown by the spectra of 19*R*- and 19*S*-hydroxy-20-epi-ibophyllidine [495] and [496].[289]

The ^{1}H NMR spectra of the epimeric esters [497] and [498] obtained[290] as intermediates in a synthesis of vindoline shows shielding of the N*Me* group protons in the axial methoxycarbonyl derivative [497]. ^{1}H NMR parameters for 14,15-anhydrocapuronidine [499][291] and for [500][292] obtained as an intermediate in synthetic studies related to desethylcatharanthine are displayed.

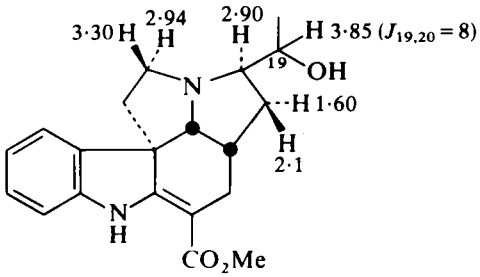

[495] 19*R*-Hydroxy-20-epi-ibophyllidine

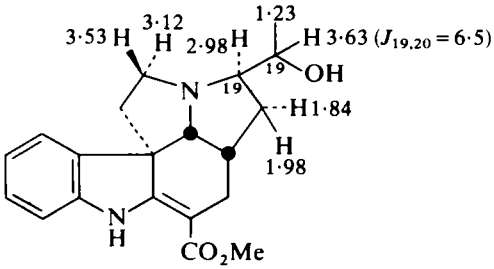

[496] 19*S*-Hydroxy-20-epi-ibophyllidine

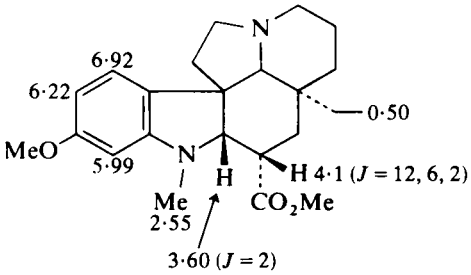

[497]

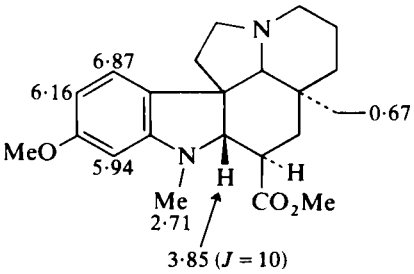

[498]

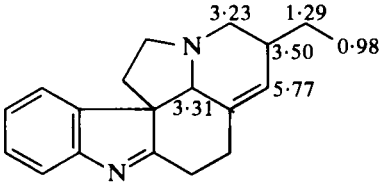

[499] 14,15-Anhydrocapuronidine

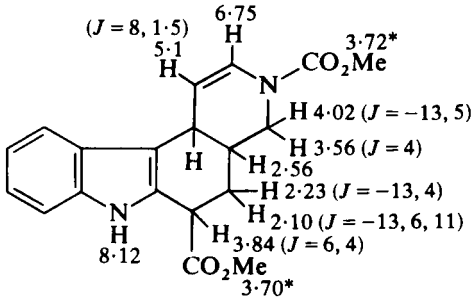

[500] (at 60 °C)

Comparison of the chemical shifts of the 18-Me (δ1·12) and of 19-H (δ4·08) in (−)-heyneatine [501][293] with those in the 19-hydroxycoronaridine series[294] (18-Me: 19*S* δ1·11; 19*R* δ1·28. 19-H: 19*S* δ4·13; 19*R* δ3·81) indicates the 19*S* stereochemistry.

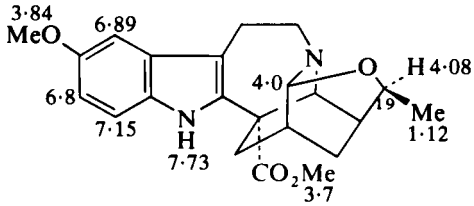

[501] Heyneatine

^{13}C shifts for 5-norcantharanthine [502] show a low frequency shift for C(16) (compare δ55·0 for C(16) in catharanthine – structure [472] in reference 2). ^{1}H NMR shifts for 5-norcantharanthine are given in [503].[295]

The ^{1}H NMR and ^{13}C NMR spectra of the product of hydroxymercuration of catharanthine are summarized in [504] and [505].[296] The ethyl signals in the ^{1}H NMR spectra of the alcohols [506] and [507] (both *trans*-fused C/D stereochemistry) isolated during a synthesis of quebrachamine, undergoes a marked change on intramolecular quaternization

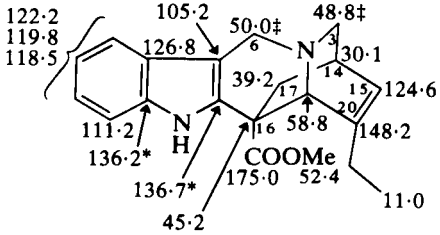

[502] 5-Norcatharanthine

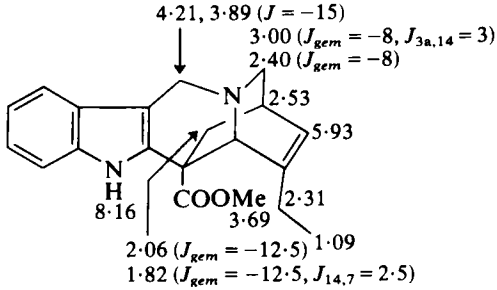

[503] 5-Norcatharanthine

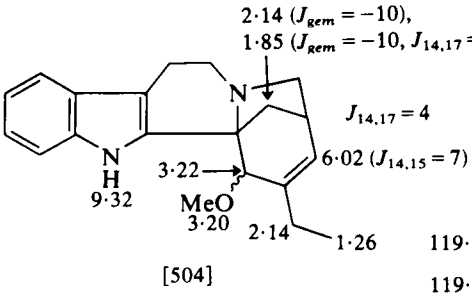

[504]

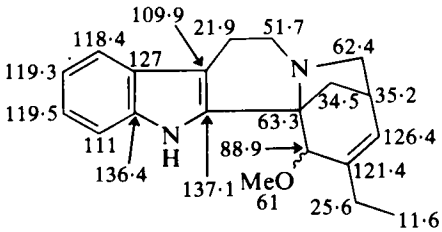

[505]

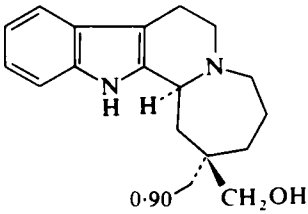

[506] (in DMSO)

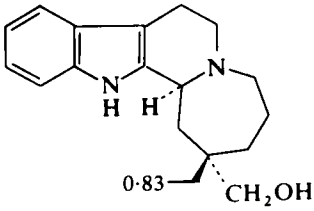

[507] (in DMSO)

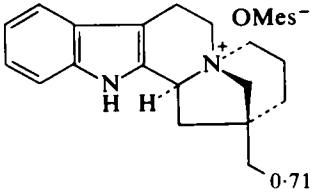

[508] (in D_2O)

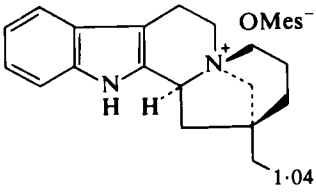

[509] (in D_2O)

to [508] and [509]. In [508] the ethyl group is situated above the plane of the indole ring with resultant shielding of the CH_2CH_3 protons.[297]

G. Other indole alkaloids

The observation of an NOE enhancement for 15-H in the spectrum of 10-hydroxyapparicine on irradiation of the 18-Me signal permits assignment of the *E* configuration for C(19) as shown in [510] for 10-methoxyapparicine.[298]

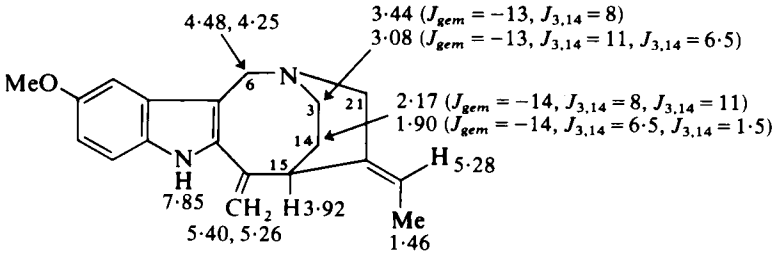

[510] 10-Methoxyapparicine

On the basis of the ^{1}H NMR data summarized in [510], in particular the values of $J_{14,15}$, the piperidine ring in 10-methoxyapparicine is shown to adopt a slightly twisted boat conformation ([511]). This conclusion is supported by ^{1}H relaxation measurements and some discussion of possible conformations of the eight-membered ring consistent with NOEs is available.[299]

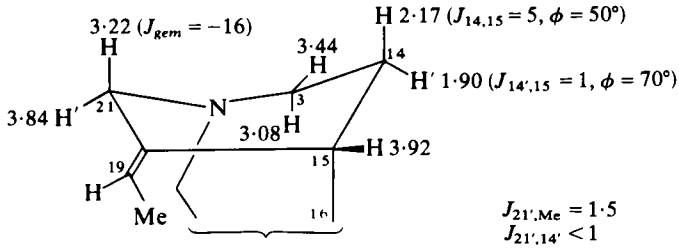

[511]

In the ^{1}H NMR spectrum of 1,4,5,7-tetrahydro-2,5-ethano-2*H*-azocino[4,3-*b*]indol-6(3*H*)-one [512] which possesses the ring skeleton of

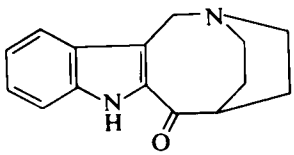

[512]

apparicine the NCH_2 signal (δ 4·54 in $CDCl_3$) is shifted to high frequency by 0·51 ppm on changing solvent from $CDCl_3$ to CD_3CO_2D. Similar high frequency shifts (0·45 and 0·31 ppm) have been noted for the corresponding protons in apparicine.[300]

NMR parameters for 16-decarbomethoxy-20-epiervertamine [513],[301] akagerinelactone [514][302] and koumine [515][303] are provided with the structures.

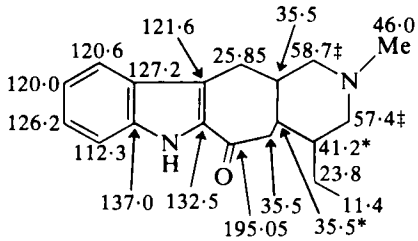

[513] 16-Decarbomethoxy-20-epiervertamine

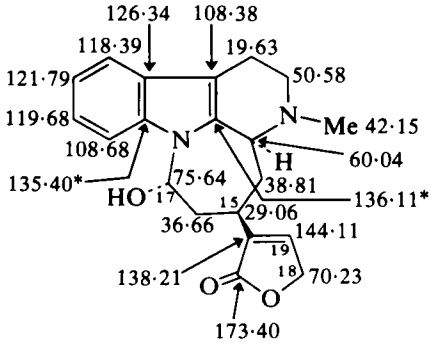

^{1}H NMR:	
15-H	8·45
17-H	6·30
18-H	4·80
19-H	7·12
NMe	2·59

[514] Akagerinelactone (in $CDCl_3$–CD_3OD)

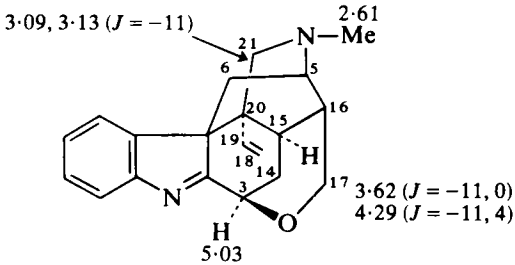

[515] Koumine

The detailed ^{13}C and ^{1}H NMR study of peduncularine summarized in [516] and [517] has led to a revision of the structure of this alkaloid.[304] The NMR spectra of other *Aristotelia* alkaloids have been described – those

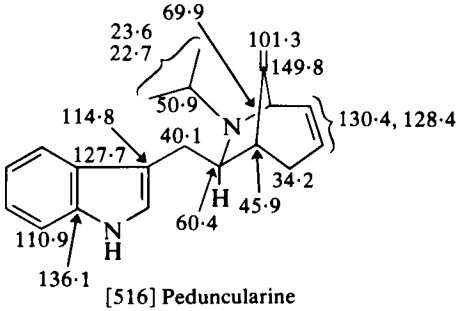

[516] Peduncularine

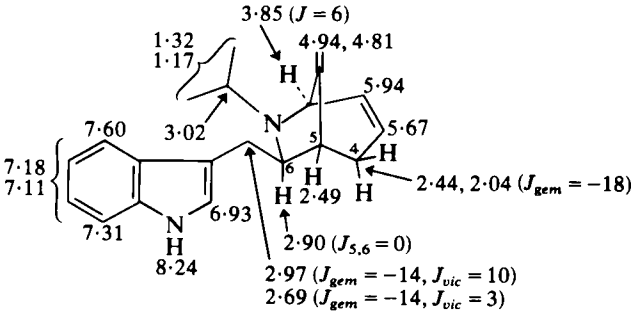

[517] Peduncularine

of sorrelline are summarized in [518] and [519],[305] that of hobartine in [520] and [521][305] and those of aristoserratin in [522] and [523].[306]

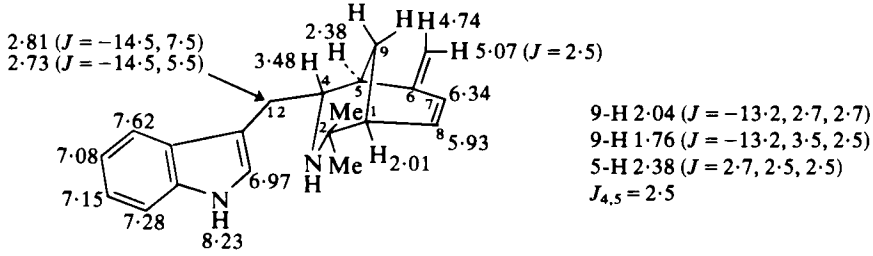

[518] Sorrelline

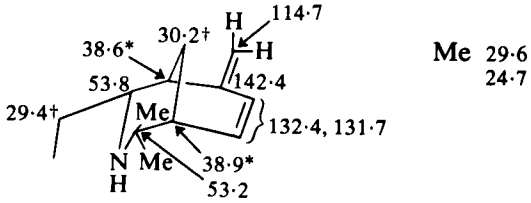

[519] Sorrelline

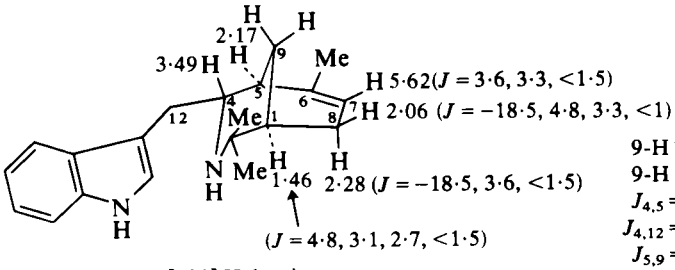

9-H 2·07 (J = −12·5, 2·7)
9-H 1·61 (J = −12·5, 3·1)
$J_{4,5}$ = 2·5
$J_{4,12}$ = 7·7, 6·4
$J_{5,9}$ = 3·1, 2·7

[520] Hobartine

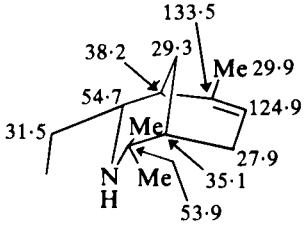

Me 25·83, 25·76

[521] Hobartine

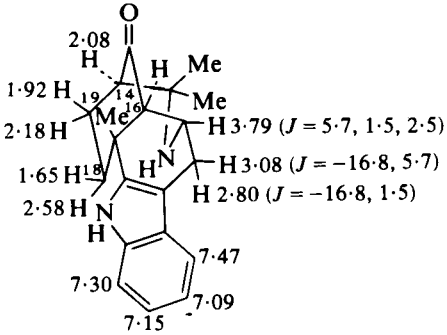

16-H 2·35
$J_{19ax,19eq}$ = −14·2
$J_{18ax,18eq}$ = −13·8
$J_{14,16}$ = 1·3
$J_{19ax,18ax}$ = 13·8
$J_{19ax,14}$ = 3·8
$J_{19eq,14}$ = 2·5
$J_{19ax,18eq}$ = 5·6
$J_{19eq,18eq}$ = 2·0
$J_{19eq,18ax}$ = 5·8

[522] Aristoserratin

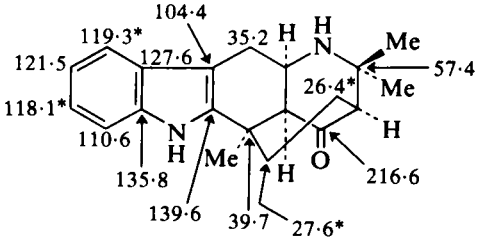

C(11), C(14), C(16)	58·5, 55·5, 51·7
Me	27·6, 27·3, 25·6

[523] Aristoserratin

H. Bisindole alkaloids

1. *Ochrolifuanine, voacamine and related dimers*

Comparison of the ^{13}C NMR spectra of ochrolifuanine C and of ochrolifuanine D [524] and [525] with the spectra of ochrolifuanine A and

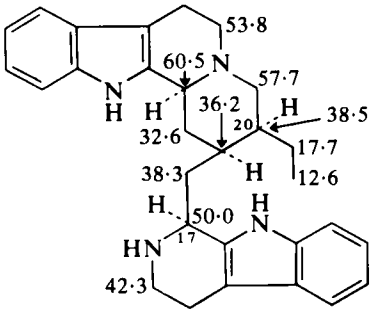

[524] Ochrolifuanine C

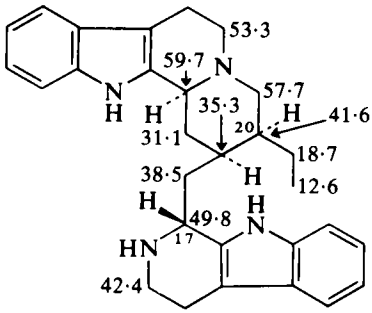

[525] Ochrolifuanine D

B ([546] and [547] in reference 2) shows the effect of changing the C(20) stereochemistry on the chemical shifts.[307] Comparison of the ^{13}C shifts for nigritanin [526] with those of ochrolifuanine B ([547] in reference 2) shows the effects of *N*-methylation.[308] The 18-Me protons in nigritanin [526]

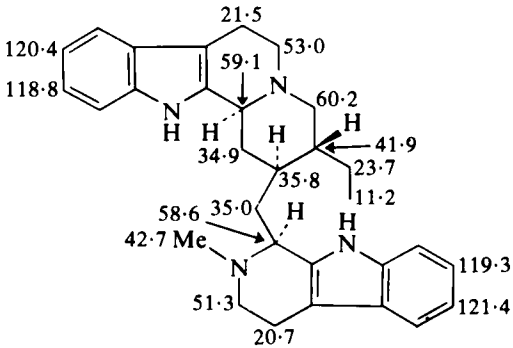

[526] Nigritanin

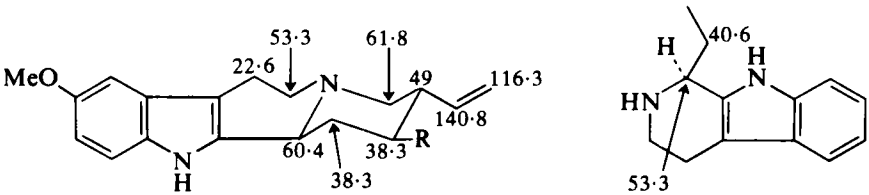

[527] 3α,17α-Cinchophylline (in pyridine-d_5)

absorb at δ 0·93 (cf. δ 0·92 in ochrolifuanine B and δ 0·73 in ochrolifuanine A).[309] The ^{13}C shifts of the four isomeric cincophyllines are given in [527]–[530].[310] The C/D ring fusion may be assigned on the basis of C(3) and C(21) shifts. The C(17) configuration is not so clearly indicated by the spectra but in the 17α-H series [527] and [529] C(17) absorbs at higher frequency than in the 17β-H series. In addition there is a shielding of C(14), C(15), C(16) in the 17β-H series [528] and [530].[310] ^{13}C shifts of

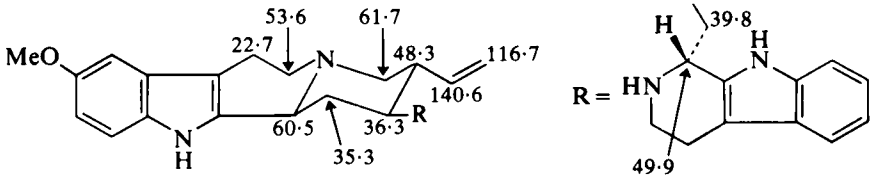

[528] 3α,17β-Cinchophylline (in pyridine-d_5)

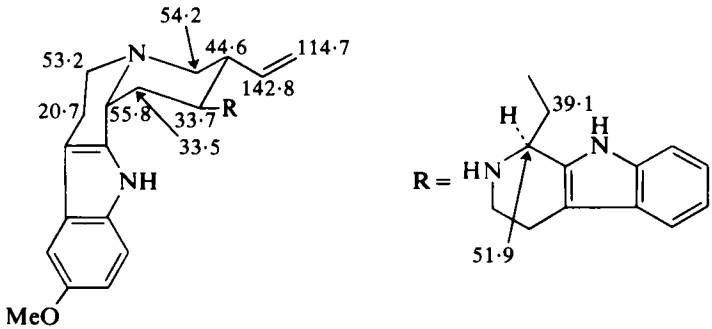

[529] 3β,17α-Cinchophylline (in pyridine-d_5)

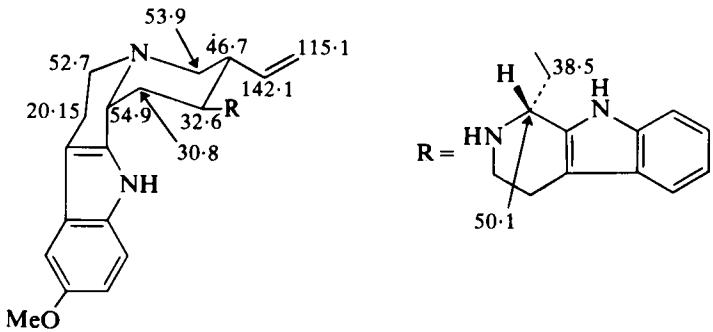

[530] 3β,17β-Cinchophylline (in pyridine-d_5)

the dehydro derivatives of the ochrolifuanines, viz. of tchibangensine[307] and of usamberensine,[231] are given in [531] and [532] respectively. The

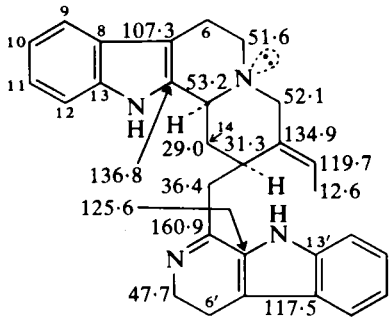

[531] Tchibangensine

C(6), C(6′)	19·3, 17·8
C(8), C(8′)	128·7, 128·0
C(9), C(9′)	119·2, 117·8
C(10), C(10′)	124·6, 121·0
C(11), C(11′)	120·3, 119·9
C(12), C(12′)	111·6, 112·1
C(13), C(13′)	137·4, 137·0

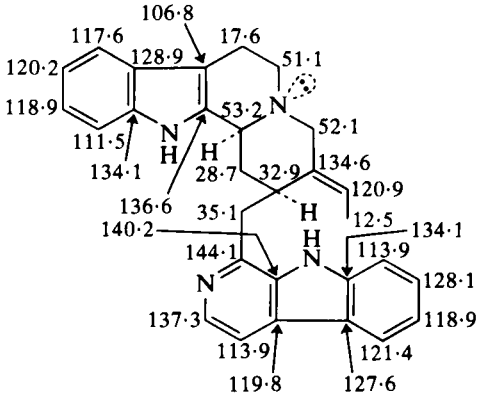

[532] Usamberensine (in DMSO-d_6)

^{13}C shifts of the related pseudotubulosines are summarized in [533]–[536].[311] The 9-proton signal in the spectrum of strychnofoline [537]

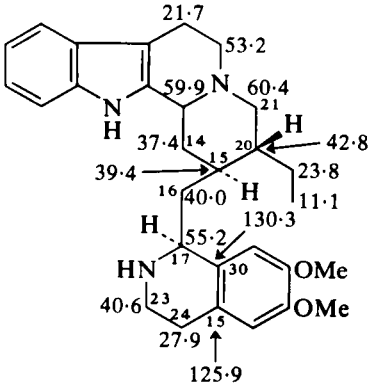

[533]

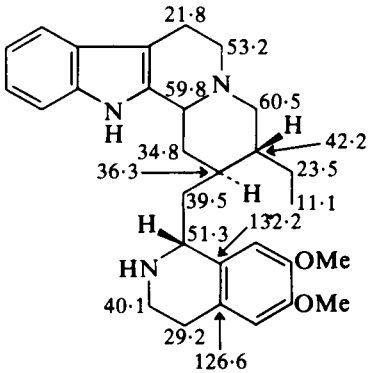

[534]

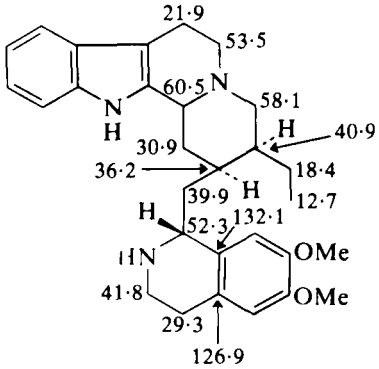

[535]

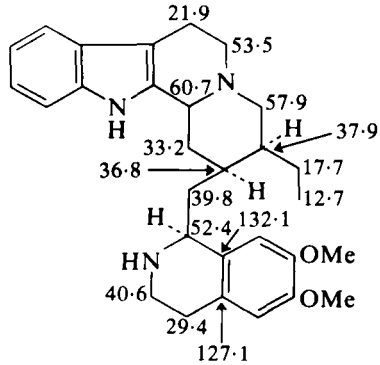

[536]

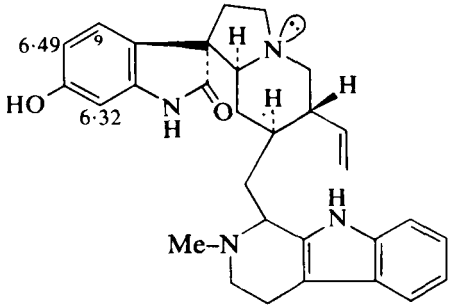

[537] Strychnofoline

absorbs to higher frequency (chemical shifts not obtainable due to masking by aromatic signals from the other half of the dimer) of the corresponding signal in the spectrum of isostrychnofoline [538] as a result of the *cis* relationship between 9-H and the nitrogen lone pair.[312]

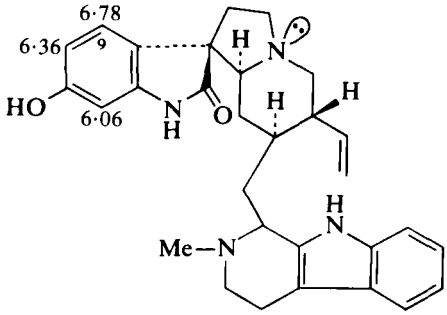

[538] Isostrychnofoline (in $CDCl_3$–CD_3OD)

The position of attachment of the 2-acylindole moiety to the iboga unit in voacamine-type bisindole alkaloids may readily be deduced from the iboga aromatic proton parameters, as illustrated by voacamine [539],

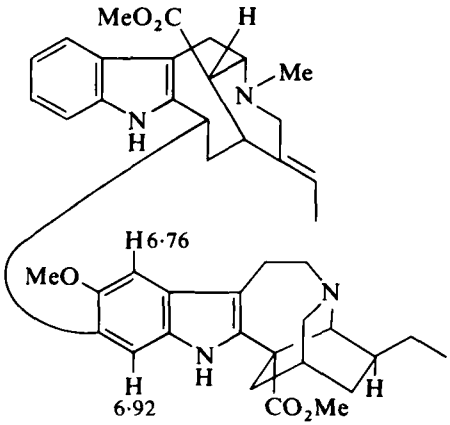

[539] Voacamine

voacamidine [540], conodurine [541] and conoduramine [542].[313] In alkaloids possessing unmethoxylated iboga units the 11-H signal is of diagnostic importance. Thus in ibogamine [543] itself 11-H absorbs at δ 7·50 whereas in tabernamine [544] 11′-H absorbs as a doublet ($J = 8$ Hz)

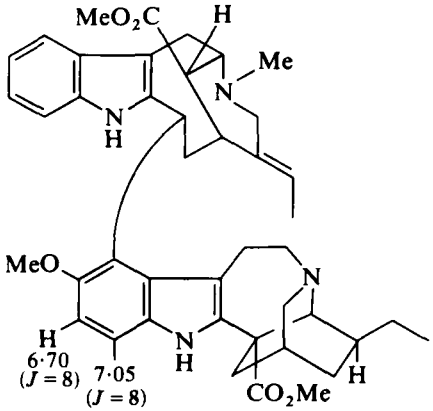

[540] Voacamidine

at δ 7·28 (cf. singlet at δ 7·20 in accedinisine – structure [540] in reference 2). Comparison of the ^{13}C shifts of the aromatic carbon nuclei in

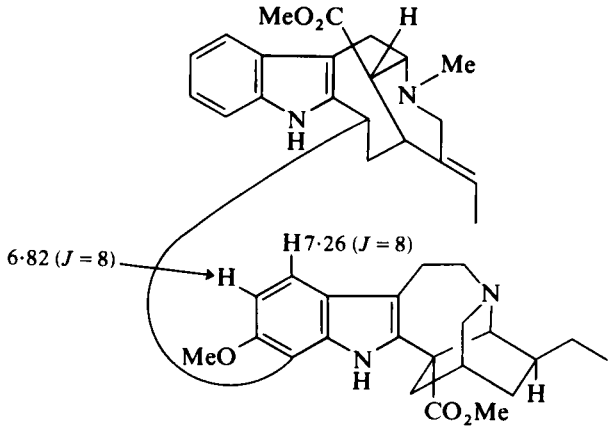

[541] Conodurine

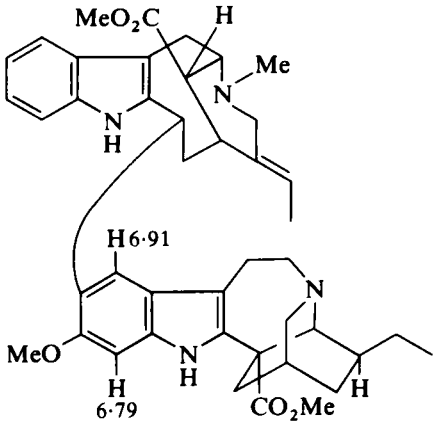

[542] Conoduramine

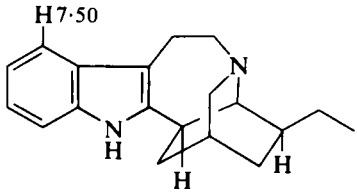

[543] Ibogamine

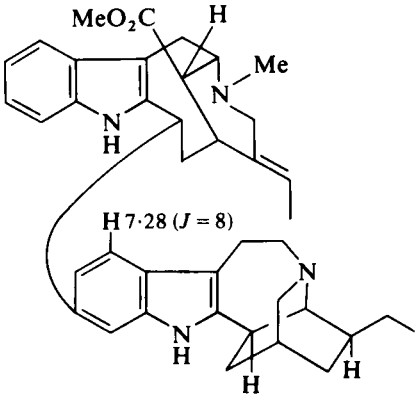

[544] Tabernamine

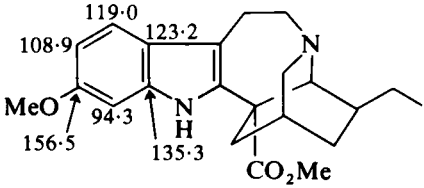

[545] Isovoacangine

isovoacangine [545] with those in tabernaelegantines A and B [546] and [547] provides examples of the use of these shifts in determining the type of dimer linkage.[313]

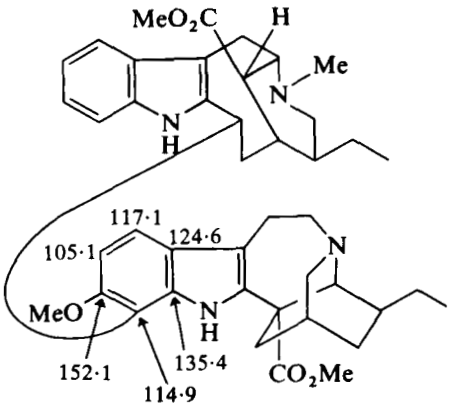

[546] Tabernaelegantine A

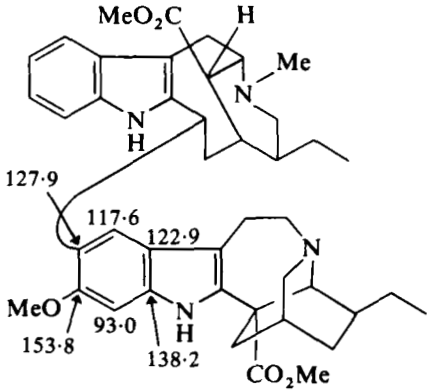

[547] Tabernaelegantine B

The configuration of the cyano group in tabernaelegantinine C [548] is shown to be *S* in particular by the low frequency shift (3·5 ppm) of C(15′) relative to that in the C(3′) unsubstituted parent compound tabernaelegantine C (structure [537] in reference 2). In addition the cyano substituent induces a low frequency shift (1·9 ppm) of C(21′), a high frequency shift (1·8 ppm) of C(3′) and a low frequency shift (1·4 ppm) of C(5′).[314]

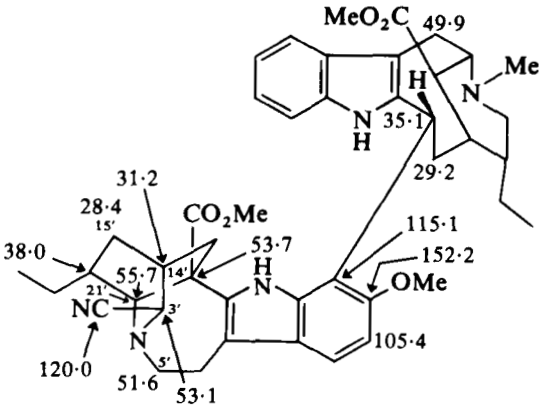

[548] Tabernaelegantinine C

2. *Vincaleucoblastine and related alkaloids*

A detailed study of the 360 MHz ^{1}H NMR spectra of vincaleucoblastine in $CDCl_3$, acetone-d_6 and benzene-d_6 has been published[315] and the data

for the spectrum recorded in $CDCl_3$ solution are summarized in [549] and [550]. The magnitudes of the vicinal coupling constants in the piperidine ring [550] of the catharanthine moiety, particularly of $J_{3'eq,14'eq}$ 1 Hz, $J_{14'eq,15'eq}$ 1 Hz, $J_{14'eq,15'ax}$ 6 Hz, suggest a flattened chair conformation in the C(14′)–C(15′)–C(20′) region.

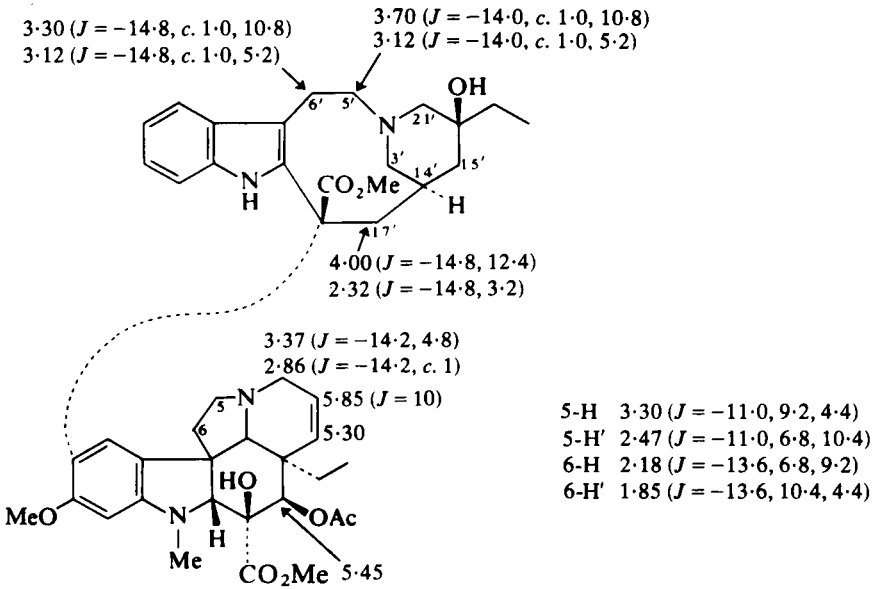

[549] Vincaleucoblastine

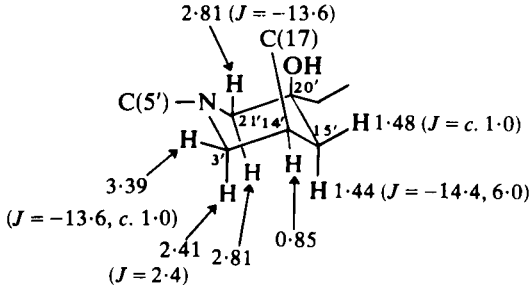

[550]

The couplings between the C(5′) and the C(6′) methylene protons and between the C(17′) and C(14′) protons suggest a boat–chair conformation [551] for the azacyclononene ring.[315] Comparison of the ^{13}C NMR spectrum of 21′-oxoleurosine with that of leurosine (structure [508] in reference 2) permits the assignment of structure [552]. In addition the 5′-equatorial proton in the spectrum of [552] is shifted to δ 4·66 (J = −12, 4, 4).[316]

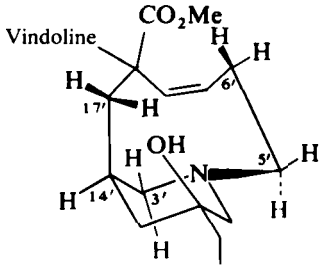

[551]

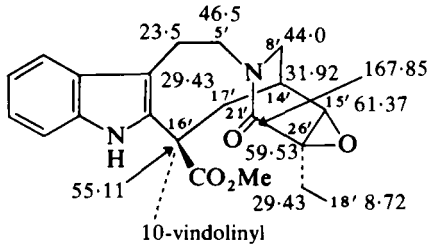

[552] 21'-Oxoleurosine

The ^{13}C NMR spectrum of 5'-noranhydrovinblastine is summarized in [553].[317] In the ^1H NMR spectrum of [553] the 6'-methylene protons absorb at δ 4·58, 4·51 ($J = -14$ Hz) and $J_{3,14} = 3{\cdot}5$, $J_{14,15} = 9{\cdot}5$ Hz (317).

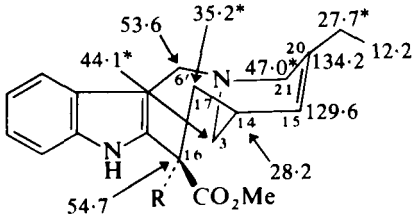

[553] 5'-Noranhydrovinblastine

Comparison of the ^{13}C NMR spectrum of a dimeric vindoline metabolite with that of dihydrovindoline ether [555] permits assignment of the

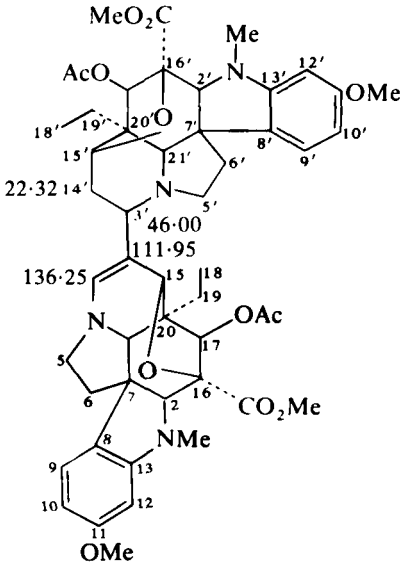

[554]

C(2)	84·76,	83·69
C(5)	52·01,	51·07
C(6)	49·12,	46·00
C(7)	53·31,	51·46
C(8)	130·50,	130·31
C(9)	121·73,	121·05
C(10)	103·67,	103·21
C(11)	161·04,	160·94
C(12)	95·03,	94·67
C(13)	151·72,	150·48
C(15)	79·30,	76·77
C(16)	88·30,	85·80
C(17)	74·79,	74·14
C(18)	9·10,	8·51
C(19)	32·55,	29·66
C(20)	48·50,	46·56
C(21)	67·64,	66·18

^1H NMR:

15-H, 15'-H	4·10, 4·26
3-H	6·11

structure [554]. In the ^{1}H NMR spectrum of the metabolite the 15- (15′-) protons absorb at δ 4·10, 4·26, and the olefinic proton absorbs at δ 6·11.[318]

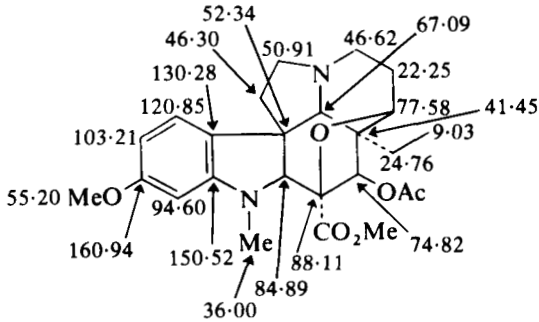

[555] Dihydrovindoline ether

3. *Bisindoles containing the strychnine moiety*

The ^{1}H NMR spectrum of 12′-hydroxyisostrychnobiline [556] shows $J_{2,16}$ 8·75 Hz and $J_{2',16'}$ 10·2 Hz, indicating the 16β-H configuration (retuline) and the 16′α-H configuration (isoretuline). The tetrahydro-1,3-oxazine

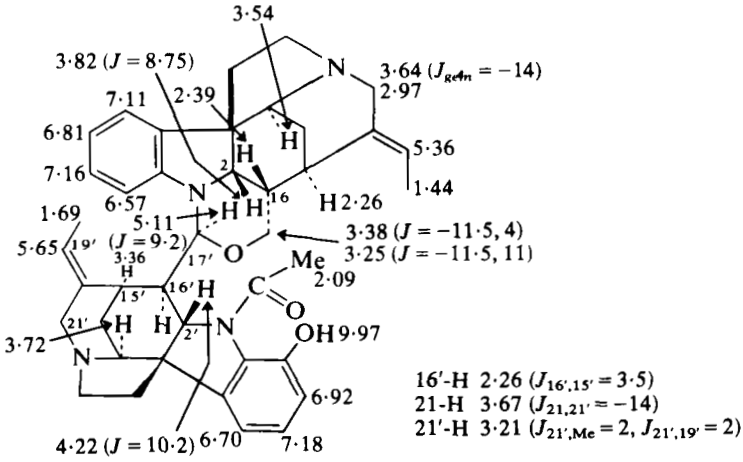

[556] 12′-Hydroxyisostrychnobiline

moiety is clearly indicated by the doublet absorption at δ5·11.[319] Some ^{1}H NMR data for the unsymmetrical dimeric alkaloid sungucine are given in [557].[320] In the ^{13}C NMR spectrum of geissospermine [558] the C(3′) and C(6′) shifts indicate the *cis*-quinolizidine moiety. The C(18′)/(15′)-H γ-interaction indicated by the C(18′) shift suggests the adoption of the conformation [559] for the geissoschizine portion of the alkaloid.[252]

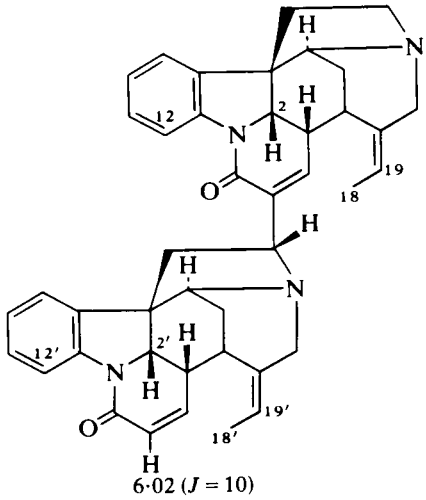

[557] Sungucine

12-H, 12'-H 8·28, 8·03
19-H, 19'-H 5·47, 5·24
2-H, 2'-H 4·38, 4·35
18-H, 18'-H 1·74, 1·65

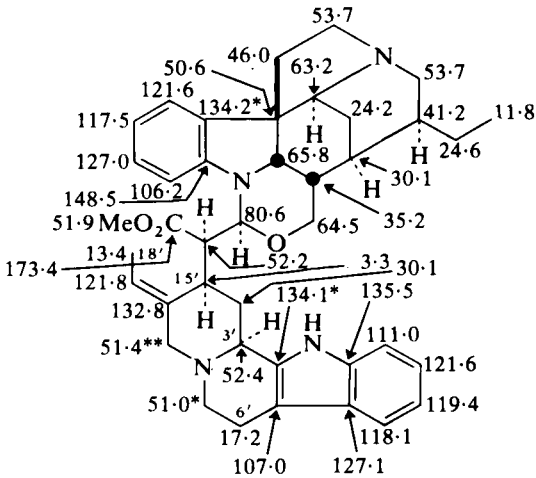

[558] Geissospermine

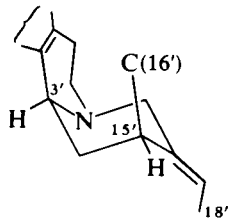

[559]

4. *Other bisindole alkaloids*

The assignment of structure [560] to pleiocraline has been based in part on a comparison with the ^{13}C NMR shifts in pleiocorine (structure [529] in reference 2) and in N_a-methyldeacetyldeformyl-1,2-dihydroakuammiline [561]. The 2β-H configuration of [560] is indicated by the C(2') shift (δ80·3) (cf. δ79·1 in [561] and δ70·6 in the 2α-H compound [562]).[321]

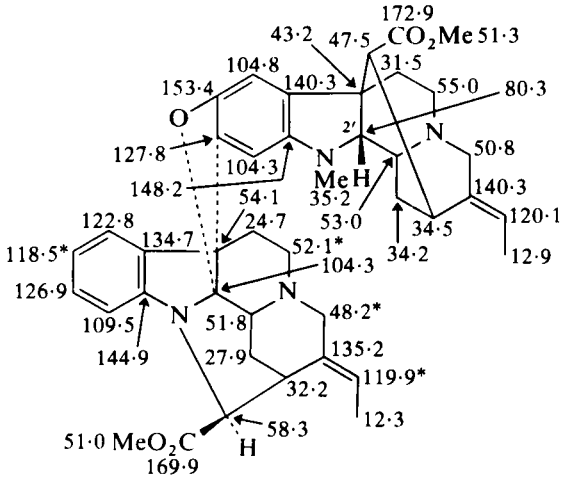

[560] Pleiocraline

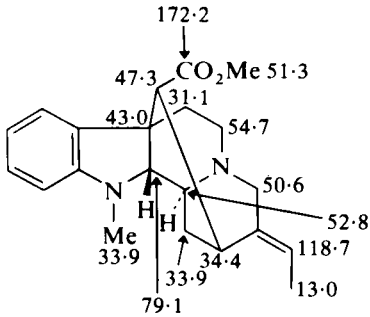

[561] N_a-Methyldeacetyldeformyl-1,2-dihydroakuammiline

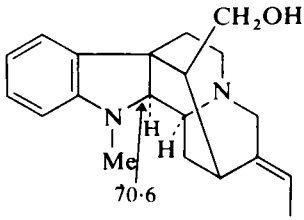

[562]

The ^{13}C NMR spectrum of ervafoline [563][322] and of three alkaloids, peceyline [564], peceylanine [565] and pelankine [566] of a new biphenyl type are summarized in the structures (structures [564]–[565] may require interchange of epoxide and double bond units).[287] The chemical shifts of

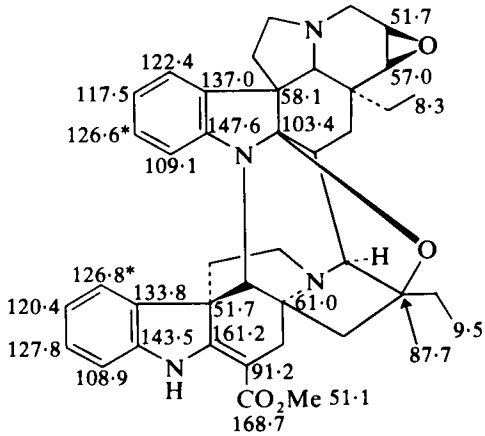

[563] Ervafoline

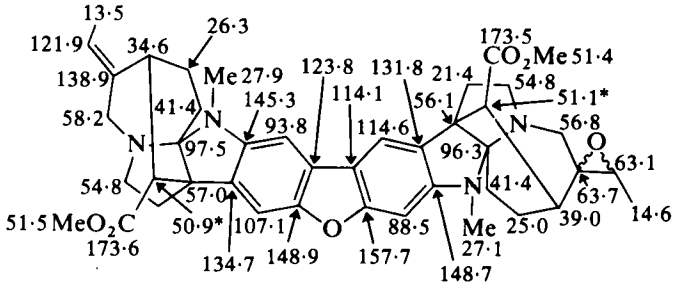

[564] Peceyline

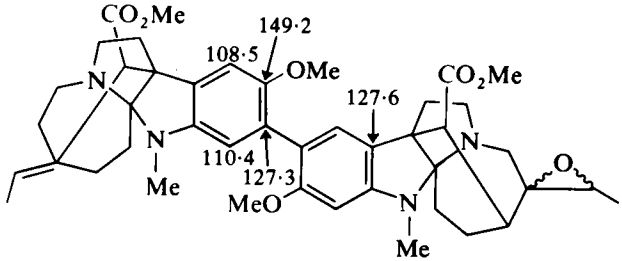

[565] Peceylanine

peceylanine and peceyline are similar except for those noted in [565]. The C(2′) shift of δ 79·3 in pelankine [566] is typical of ajmaline-type alkaloids, and the *N*Me resonance (δ 33·8) in the non-vincorine moiety of [566] is deshielded relative to [564] and [565], indicative of less substitution at C(2′).[287]

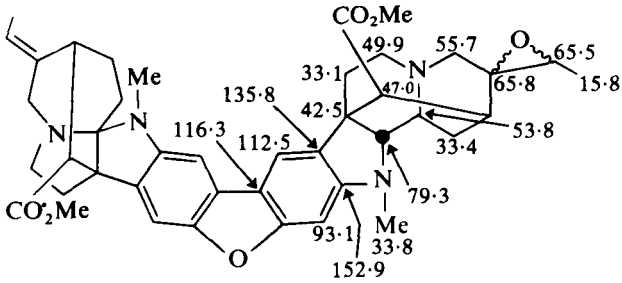

[566] Pelankine

XIII. DITERPENE ALKALOIDS

^{13}C NMR assignments for aconitine-type and lycoctonine-type diterpenoid alkaloids have been reviewed[323] and complete assignments (in some cases correcting published assignments) are given for pseudaconitine, indaconitine, veratroylpseudaconine, falaconitine, mithaconitine, pyrodelphinine, browniine, 14-acetylbrowniine, delphatine, delcosine, 14-acetyldelcosine, delsoline, lycoctonine, tricornine, anthranoyllycoctonine, ajacine, methyllycaconitine and delsemine. ^{13}C NMR assignments for lappaconitine [567], lappaconine, lapaconidine [568], ranaconine, aconine

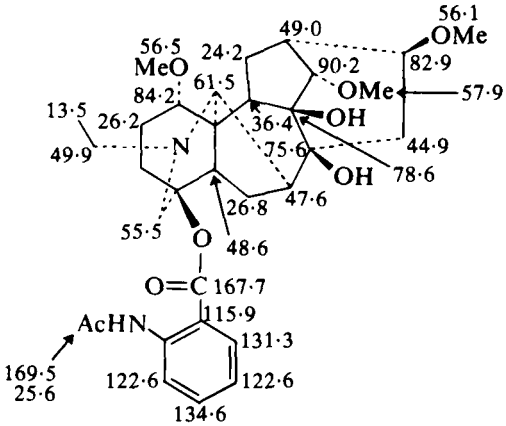

[567] Lappaconitine

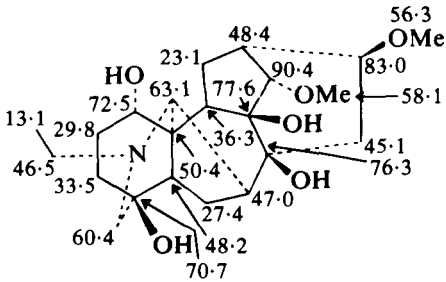

[568] Lapaconidine

[569], pseudoaconine [570], deoxyaconine, hypaconine and 14-dehydrobrowniine [571] have also been published.[324] The presence of the C(15) hydroxy group in aconine [569] is shown by a shift to high frequency of

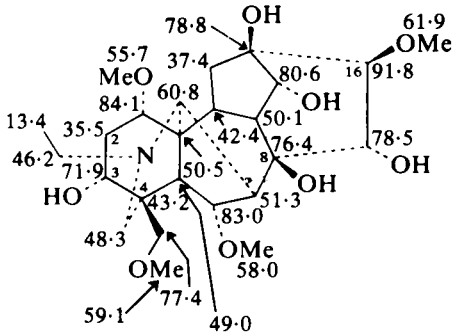

[569] Aconine

^{13}C NMR in pyridine-d_5:

C(2)	38·3
C(3)	69·3
C(4)	44·3

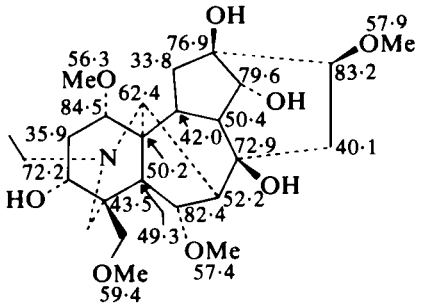

[570] Pseudoaconine

^{13}C NMR in pyridine-d_5

C(2)	38·1
C(3)	69·0
C(4)	44·6

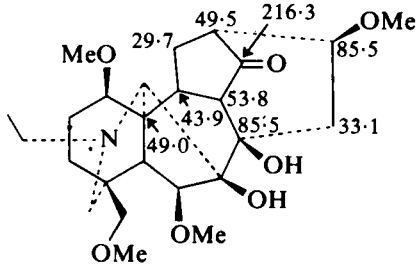

[571] 14-Dehydrobrowniine

C(8) and C(16) relative to the corresponding signals in the spectrum of pseudoaconine [570]. Whereas the spectrum of lapaconidine [568] is insensitive to a change of solvent from $CDCl_3$ to pyridine-d_5, the C(2), C(3) and C(4) shifts in the spectra of aconine [569] and pseudoaconine [570] show a significant solvent dependency. This suggests that in pyridine

solution the 3α-OH forms a hydrogen bond with the solvent which stabilizes the chair conformation of ring A. In $CDCl_3$ solution the hydrogen bond exists between the 3α-OH and the nitrogen lone pair of electrons in the boat ring A conformation.[326]

Comparison of the ^{13}C NMR spectra of 14-dehydrobrowniine [571][324] and browniine [572][323] shows the high frequency shifts of C(8), C(9), C(10), C(11), C(12), C(13) and C(16) in [571] relative to [572].[324] Comparison

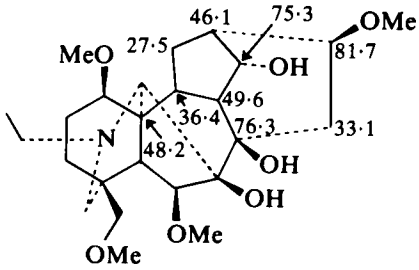

[572] Browniine

of the ^{13}C NMR spectra of ranaconitine and of lappaconitine [567][324] permits the assignment of structure shown in [573].[325] Similarities between the ^{13}C NMR spectra of lycoctonine [574][323] and "delsemine" [575],

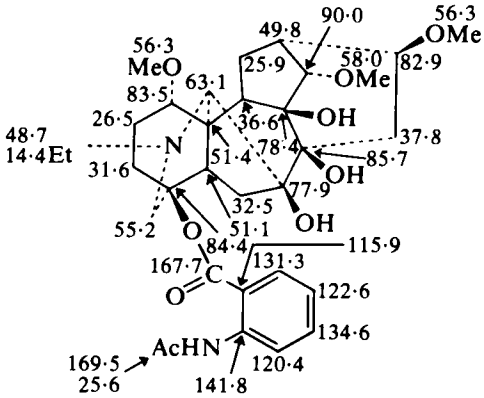

[573] Ranaconitrine

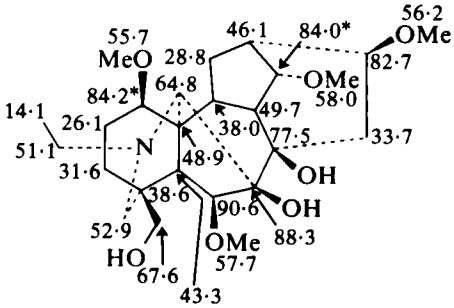

[574] Lycoctonine

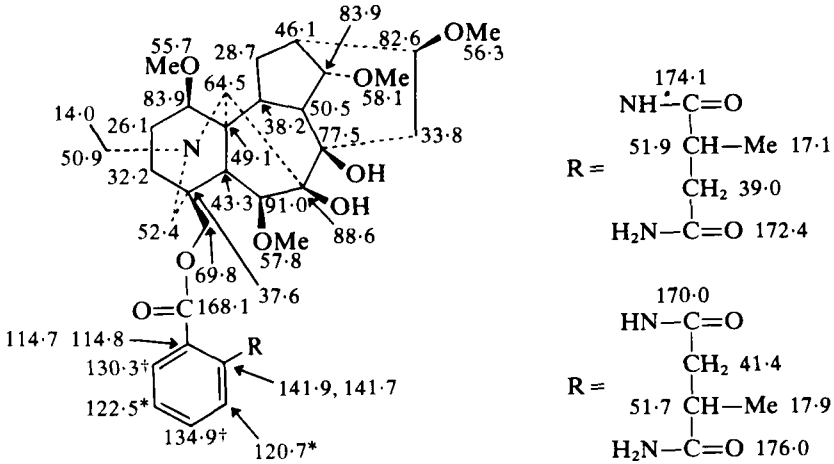

[575] "Delsemine"

together with the presence of twin peaks from side chain nuclei, show "delsemine" to consist of a mixture of two compounds.[326] Shifts for the C(4) side chain carbon nuclei in the related methyllycaconitine are given in [576].[323] The ^{13}C NMR spectrum of tricornine is consistent with it being the C(18) acetate [577] of lycoctonine [574].[327]

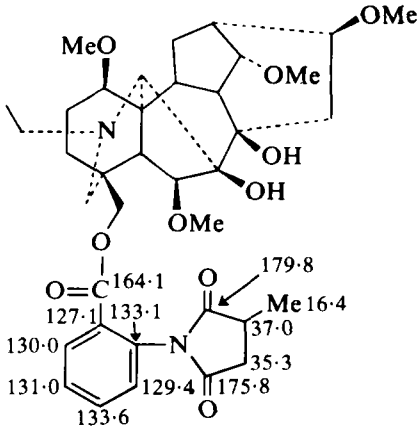

[576] Methyllycaconitine

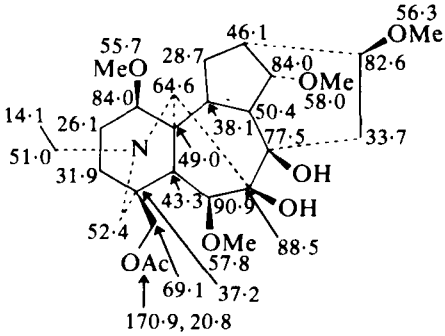

[577] Tricornine

Structural assignments to other diterpenoid alkaloids have been made largely from a comparison of ^{13}C NMR data with that of alkaloids of established structure – sachaconitine [578],[328] foresaconitine [579][329] and ezochasmanine [580][330] (from a comparison with the spectrum of

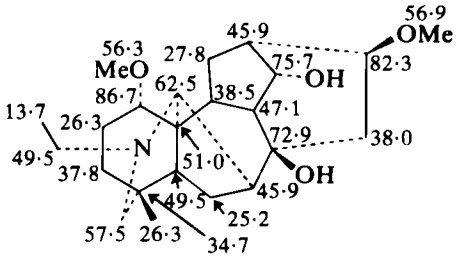

[578] Sachaconitine

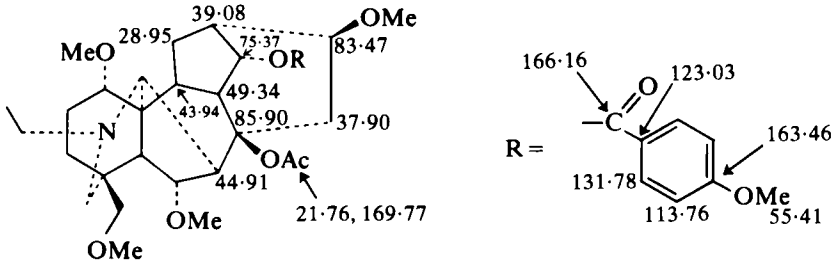

[579] Foresaconitine

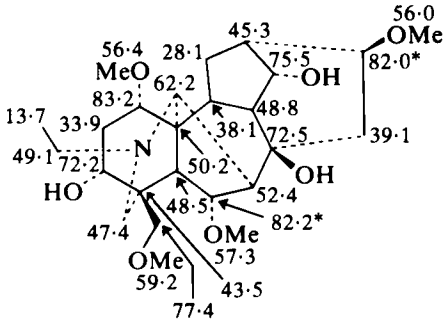

[580] Ezochasmanine

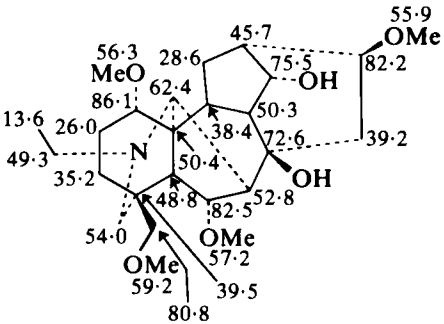

[581] Chasmanine

chasmanine [581]) and isodelphinine [582] (from a comparison with isodelphinine – structure [553] in reference 2).[328]

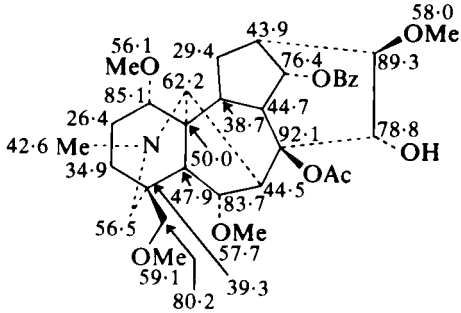

[582] Isodelphinine

The ^{13}C NMR spectrum of takaonine (2,3-dehydro-14-dehydrodelcosine) and of 14-dehydrodelcosine are summarized in [583] and [584] respectively.[331]

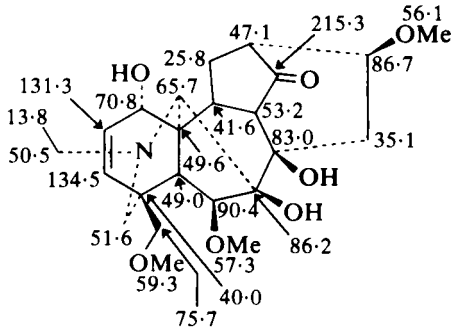

[583] Takaonine

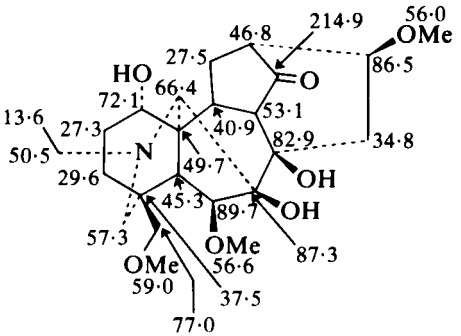

[584] Dehydrodelcosine

Complete ^{13}C NMR assignments for 13 C_{19}-diterpenoid alkaloids containing the methylenedioxy group have been published,[332] e.g. dictyocarpinine [585], 14-dehydrodictyocarpine [586], 14-dehydrodictyocarpinine [587], 6-dehydrodictyocarpinine [588], deltaline [589] and delcorine [590].

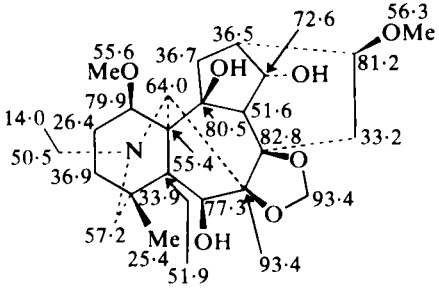

[585] Dyctyocarpinine

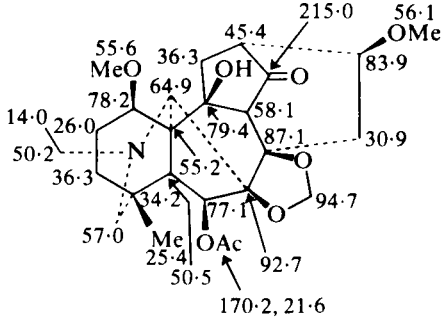

[586] 14-Dehydrodictyocarpine

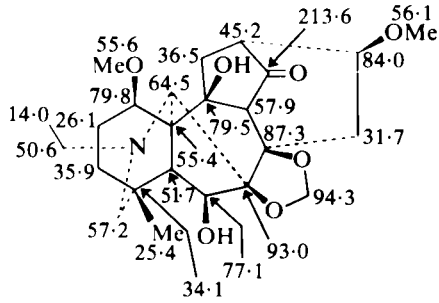

[587] 14-Dehydrodictyocarpinine

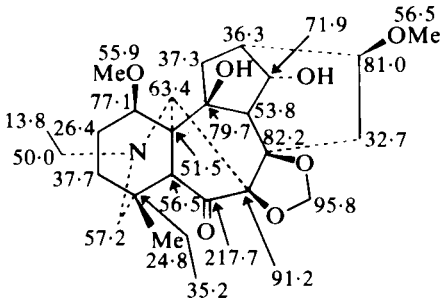

[588] 6-Dehydrodictyocarpinine

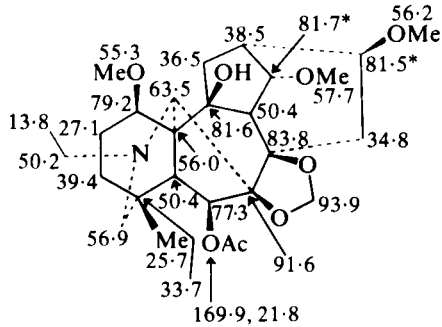

[589] Deltaline

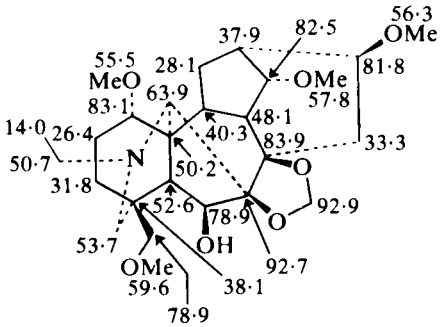

[590] Delcorine

Comparison of the spectra of [585], [586] and [587] permits an evaluation of the shift changes caused by oxidation of the C(14) hydroxy group and

by C(6) acetylation. The low frequency shift of C(14) in the spectrum of dictyocarpinine [585] relative to other lycoctonine alkaloids such as browniine [572] reflects the presence of the C(10) hydroxy group. The low frequency shifts of C(7) and C(11) in the spectrum of 6-dehydrodictyocarpinine [588] relative to dictyocarpinine [585] result from the strained cyclopentanone moiety. The C(14) methoxy group in deltaline [589] causes a high frequency shift of C(13) and C(14) relative to [585] and [588].[332] The ^{13}C NMR spectra of ajaconine and a rearrangement product, 7α-hydroxyisoatisine, are summarized in [591] and [592]. The high frequency shifts of C(7), C(19), C(20), C(21) and C(22) in ajaconine on changing solvent from $CDCl_3$ to ionic solvents suggests ionization of the ether linkage and covalent solvation.[333]

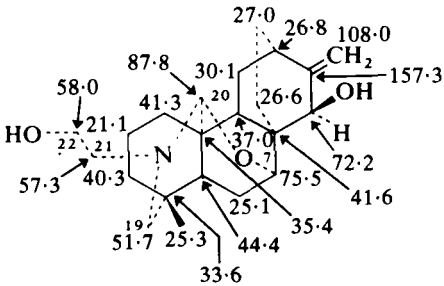

[591] Ajaconine

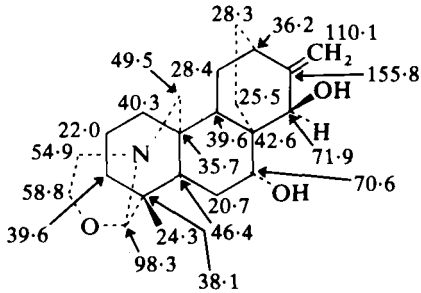

[592] 7α-Hydroxyisoatisine

The ^{1}H NMR spectrum of cuachichine [593] indicates only a single set of signals, showing the absence of C(20) epimers. The C(16)-Me configuration in isocuachichicine [594] and 16-epi-isocuachichicine [595] is assigned

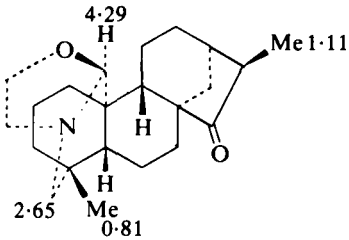

[593] Cuauchichicine

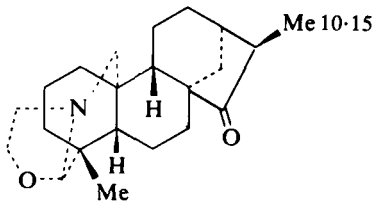

[594] Isocuauchichicine

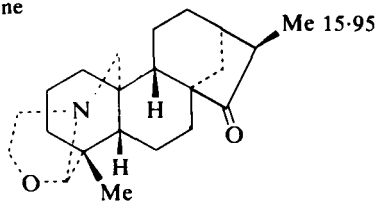

[595] 16-Epi-isocuauchichicine

on the basis of the ^{13}C Me shifts and an examination of molecular models which shows more steric compression for the β-Me group.[334]

XIV. LYCOPODIUM ALKALOIDS

The ^{1}H NMR spectrum of megastachine is summarized in [596].[335] Spectral data on some reduced 2-quinolones obtained as intermediates in a synthesis of luciduline are available.[336] The *cis*- and *trans*-fused isomers

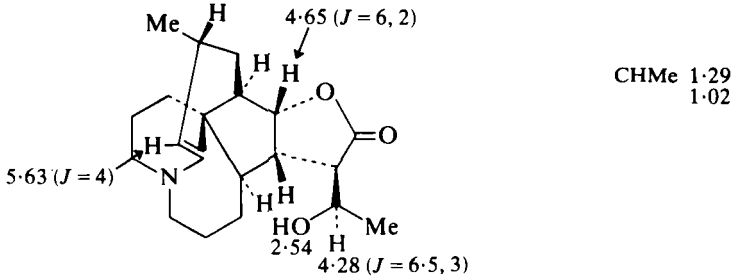

[596] Megastachine

[597] and [598] may be differentiated by the angular 9-H parameters and the *E*-configuration has been assigned to the derived ester [599] from the high frequency absorption of 6-H_{eq} deshielded by the ester function. The *cis* fusion in [597] was confirmed by comparison of the ^{13}C NMR spectrum

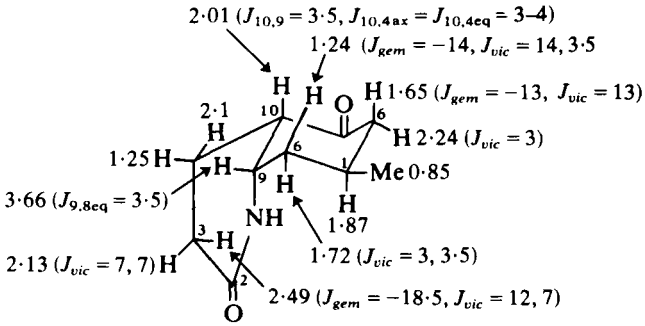

[597] (in $CHCl_3$–C_6H_6 (4 : 3))

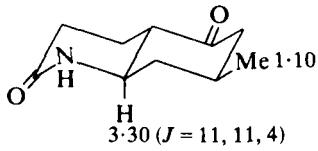

[598]

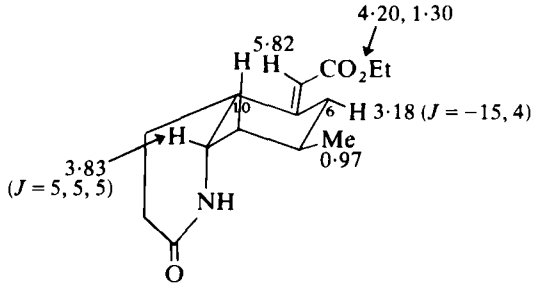

[599]

[600] with that of 3-methylcyclohexanone [601]. The spectrum of the 2-quinolone shows the relative low frequency shift of C(7), indicating the γ-interaction with the C(9) substituent.[336]

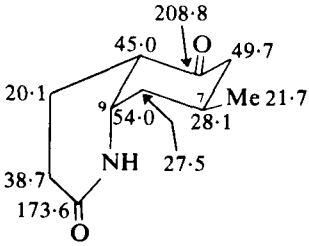

[600]

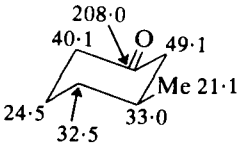

[601]

REFERENCES

1. T. A. Crabb, in *Annual Reports on NMR Spectroscopy*, Vol. 6A (ed. E. F. Mooney), Academic Press, London, 1975, p. 249.
2. T. A. Crabb, in *Annual Reports on NMR Spectroscopy*, Vol. 8 (ed. G. A. Webb), Academic Press, London, 1978, p. 1.
3. M. Shamma and D. M. Hindenlang, *Carbon-13 NMR Shift Assignments of Amines and Alkaloids*, Plenum Press, New York and London, 1979.
4. D. W. Hughes and D. B. MacLean, in *The Alkaloids*, Vol. 18 (ed. R. H. F. Manske and R. G. A. Rodrigo), Academic Press, New York, 1981, Chap. 3.
5. S. R. Johns and R. I. Willing, *Austral. J. Chem.*, 1976, **29**, 1617.
6. D. W. Hughes, H. L. Holland and D. B. Maclean, *Canad. J. Chem.*, 1976, **54**, 2252.
7. R. Mata and J. L. McLaughlin, *Phytochemistry*, 1980, **19**, 673.
8. J. Siwon, R. Verpoorte, T. Van Beek, H. Meerburg and A. B. Svendsen, *Phytochemistry*, 1981, **20**, 323.
9. E. Leete, *Tetrahedron Letters*, 1979, 4527.
10. A. J. Marsaioli, E. A. Ruveda and F. de A. M. Reis, *Phytochemistry*, 1979, **17**, 1655.
11. E. Wenkert, B. L. Buckwalter, I. R. Burfitt, M. J. Gasic, H. E. Gottlieb, E. W. Hagaman, F. M. Schell and P. M. Wovkulich, in *Topics in Carbon-13 NMR Spectroscopy*, Vol. 2 (ed. G. C. Levy), Wiley-Interscience, New York, 1976, p. 81.
12. J. C. Lindon and A. G. Ferrige, *Tetrahedron*, 1980, **36**, 2157.

13. V. A. Mnatsakanyan, V. Preininger, V. Šimaňek, J. Jůrina, A. Klásek, L. Dolejš and F. Santavý, *Collect. Czech. Chem. Commun.*, 1977, **42**, 1421.
14. H. Guinaudeau, M. Leboeuf and A. Cavé, *Lloydia*, 1979, **42**, 325.
15. W. H. Soine, J. E. Hudson, B. A. Shoulders and R. V. Smith, *J. Pharm. Sci.*, 1980, **69**, 1040.
16. A. J. Marsaioli, F. de A. M. Reis, A. F. Magalhães, E. A. Rúveda and A. M. Kuck, *Phytochemistry*, 1979, **18**, 165.
17. S. Kano, Y. Takahagi, E. Komiyama, T. Yokomatsu and S. Shibuya, *Heterocycles*, 1976, **4**, 1013.
18. O. Oshino, M. Ohtani and B. Umezawa, *Chem. Pharm. Bull. (Japan)*, 1979, **27**, 3101.
19. P. K. Bhaumik, B. Mukherjee, J. P. Juneau, N. S. Bhacca and R. Mukherjee, *Phytochemistry*, 1979, **18**, 1584.
20. K. Yakushijin, S. Sugiyama, Y. Mori, H. Murata and H. Furukawa, *Phytochemistry*, 1980, **19**, 161.
21. S. V. Kessar, Y. P. Gupta, V. S. Yadav, M. Narula and T. Mohammad, *Tetrahedron Letters*, 1980, 3307.
22. M. Hamonnière, M. Leboeuf and A. Cavé, *Phytochemistry*, 1977, **16**, 1029.
23. A. Arzúa and B. K. Cassels, *Tetrahedron Letters*, 1978, 2649.
24. W. D. Smolnycki, J. L. Moniot, D. M. Hindenlang, G. A. Miana and M. Shamma, *Tetrahedron Letters*, 1978, 4617.
25. H. Guinaudeau, M. Leboeuf, M. Debray, A. Cavé and R. R. Paris, *Planta Med.*, 1975, **27**, 304.
26. O. Hoshino, H. Hara, M. Ogawa and B. Umezawa, *J. Chem. Soc. Perkin I*, 1980, 1165.
27. A. J. Marsaioli, A. F. Magalhães, E. A. Rúveda and F. de A. M. Reis, *Phytochemistry*, 1980, **19**, 995.
28. O. R. Gottlieb, A. F. Magalhães, E. G. Magalhães, J. G. S. Maia and A. J. Marsaioli, *Phytochemistry*, 1978, **17**, 837.
29. J. W. Skiles, J. M. Saá and M. P. Cava, *Canad. J. Chem.*, 1979, **57**, 1642.
30. J. W. Skiles and M. P. Cava, *J. Org. Chem.*, 1979, **44**, 409.
31. P. D. Senter and C-L. Chen, *Phytochemistry*, 1977, **16**, 2015.
32. L. Castedo, D. Domínguez, J. M. Saá and R. Suau, *Tetrahedron Letters*, 1979, 4589.
33. G. S. Ricca and C. Casagrande, *Org. Magn. Reson.*, 1977, **9**, 8.
34. F. Scheinmann, E. F. V. Scriven and O. N. Ogbeide, *Phytochemistry*, 1980, **19**, 1837.
35. W.-N. Wu, J. L. Beal, E. H. Fairchild and R. W. Doskotch, *J. Org. Chem.*, 1978, **43**, 580.
36. J. Wu, J. L. Beal and R. W. Doskotch, *J. Org. Chem.*, 1980, **45**, 213.
37. R. Ahmad and M. P. Cava, *J. Org. Chem.*, 1977, **42**, 2271.
38. J. Wu, J. L. Beal and R. W. Doskotch, *J. Org. Chem.*, 1980, **45**, 208.
39. S. F. Hussain and M. Shamma, *Tetrahedron Letters*, 1980, 3315.
40. S. F. Hussain, M. Siddiqui and M. Shamma, *Tetrahedron Letters*, 1980, 4575.
41. W.-N. Wu, J. L. Beal and R. W. Doskotch, *Tetrahedron*, 1977, **33**, 2919.
42. J. L. Marshall, D. E. Miller, S. A. Conn, R. Seiwell and A. M. Ihrig, *Accounts Chem. Res.*, 1974, **7**, 333.
43. D. Tourwé and G. Van Binst, *Heterocycles*, 1978, **9**, 507.
44. N. Takao, K. Iwasa, M. Kamigauchi and M. Sugiura, *Chem. Pharm. Bull. (Japan)*, 1977, **25**, 1426.
45. M. Cushman and F. W. Dekow, *J. Org. Chem.*, 1979, **44**, 407.
46. C. Moulis, J. Gleye and E. Stanislas, *Phytochemistry*, 1977, **16**, 1283.
47. H.-C. Chiang and E. Brochmann-Hanssen, *J. Org. Chem.*, 1977, **42**, 3190.
48. M. H. Abu Zarga and M. Shamma, *Tetrahedron Letters*, 1980, 3739.
49. H. Hara, M. Hosaka, O. Hoshino and B. Umezawa, *J. Chem. Soc. Perkin I*, 1980, 1169.
50. P. Chinnasamy, R. D. Minard and M. Shamma, *Tetrahedron*, 1980, **36**, 1515.

51. M. Shamma, J. L. Moniot and D. M. Hindenlang, *Tetrahedron Letters*, 1977, 4273.
52. P. Chinnasamy and H. Shamma, *Canad. J. Chem.*, 1979, **57**, 1647.
53. K. Orito, Y. Kurokawa and M. Itoh, *Tetrahedron*, 1980, **36**, 617.
54. H. G. Kiryakov, D. W. Hughes, B. C. Nalliah and D. B. MacLean, *Canad. J. Chem.*, 1979, **57**, 53.
55. S. F. Hussain and M. Shamma, *Tetrahedron Letters*, 1980, 1909.
56. D. Dime and S. McLean, *Canad. J. Chem.*, 1979, **57**, 1569.
57. H. Ishii, E. Ueda, K. Nakajima, T. Ishida, T. Ishikawa, K.-I. Harada, I. Ninomiya, T. Naito and T. Kiguchi, *Chem. Pharm. Bull. (Japan)*, 1978, **26**, 864.
58. H. Ishii, T. Ishikawa, K. Hosoya and N. Takao, *Chem. Pharm. Bull. (Japan)*, 1978, **26**, 166.
59. L. Castedo, D. Dominguez, J. M. Saá and R. Suau, *Tetrahedron Letters*, 1978, 2923.
60. N. Takao and K. Iwasa, *Chem. Pharm. Bull. (Japan)*, 1979, **27**, 2194.
61. K. Iwasa, N. Takao, G. Nonaka and I. Nishioka, *Phytochemistry*, 1979, **18**, 1725.
62. I. Ninomiya, O. Yamamato and T. Naito, *J. Chem. Soc. Perkin I*, 1980, 212.
63. M. Cushman and T.-C. Choong, *Heterocycles*, 1980, **14**, 1935.
64. H. G. Kiryakov, Z. H. Mardirossian, D. W. Hughes and D. B. MacLean, *Phytochemistry*, 1980, **19**, 2507.
65. B. C. Nalliah, D. B. MacLean, H. L. Holland and R. Rodrigo, *Canad. J. Chem.*, 1979, **57**, 1545.
66. G. Sariyar and J. D. Phillipson, *Phytochemistry*, 1980, **19**, 2189.
67. R. Hohlbrugger and W. Klötzer, *Chem. Ber.*, 1979, **112**, 849.
68. R. Hohlbrugger and W. Klötzer, *Chem. Ber.*, 1979, **112**, 3486.
69. H. Ronsch, *Tetrahedron*, 1981, **37**, 371.
70. A. Bladé-Font, R. Muller, J. Elguero, R. Faure and E.-J. Vincent, *Chemistry Letters*, 1979, 233.
71. C. D. Hufford, C. C. Collins and A. M. Clark, *J. Pharm. Sci.*, 1979, **68**, 1239.
72. S. P. Singh, S. S. Parmar, V. I. Stenberg and S. A. Farnum, *Spectrosc. Letters*, 1977, **10**, 1001.
73. C. D. Hufford, H-G. Capraro and A. Brossi, *Helv. Chim. Acta*, 1980, **63**, 50.
74. H. G. Capraro and A. Brossi, *Helv. Chim. Acta*, 1979, **62**, 965.
75. A. Brossi, M. Rösner, J. V. Silverton, M. A. Iorio and C. D. Hufford, *Helv. Chim. Acta*, 1980, **63**, 406.
76. A. Bladé-Font, *Tetrahedron Letters*, 1977, 2977.
77. T. Kametani, S. A. Surgenor and K. Fukumoto, *J. Chem. Soc. Perkin I*, 1981, 920.
78. T. Fujii, S. Yoshifuji and H. Kogen, *Tetrahedron Letters*, 1977, 3477.
79. T. Fujii, S. Yoshifuji and M. Tai, *Chem. Pharm. Bull. (Japan)*, 1975, **23**, 2094.
80. T. Fujii and S. Yoshifuji, *Tetrahedron*, 1980, **36**, 1539.
81. S. F. Dyke, R. G. Kinsman, P. Warren and A. W. C. White, *Tetrahedron*, 1978, **34**, 241.
82. C.-H. Chen and T. O. Soine, *J. Pharm. Sci.*, 1972, **61**, 56.
83. M. H. Abu Zarga, G. A. Miana and M. Shamma, *Tetrahedron Letters*, 1981, 541.
84. M. Shamma, A. S. Rothenberg, G. S. Jayatilake and S. F. Hussain, *Tetrahedron*, 1978, **34**, 615.
85. K. Yamasaki and K. Fujita, *Chem. Pharm. Bull. (Japan)*, 1979, **27**, 43.
86. S. Kobayashi, H. Ishikawa, E. Sasakawa, M. Kihara, T. Shingu and A. Kato, *Chem. Pharm. Bull. (Japan)*, 1980, **28**, 1827.
87. S. Kobayashi, M. Kihara, T. Shingu and K. Shingu, *Chem. Pharm. Bull. (Japan)*, 1980, **28**, 2924.
88. S. Kobayashi, H. Ishikawa, M. Kihara, T. Shingu and T. Hashimoto, *Chem. Pharm. Bull. (Japan)*, 1977, **25**, 2244.
89. D. J. Morgans, Jr, and G. Stork, *Tetrahedron Letters*, 1979, 1959.

90. P. W. Jeffs and T. M. Capps, *Tetrahedron Letters*, 1979, 131.
91. M. Kihara and S. Kobayashi, *Chem. Pharm. Bull. (Japan)*, 1978, **26**, 155.
92. A. Mondon, H. G. Vilhuber, C. Fischer, M. Epe, B. Epe and C. Wolff, *Chem. Ber.*, 1979, **112**, 1110.
93. A. Mondon, M. Epe, C. Wolff, T. Clausen and H. G. Vilhuber, *Chem. Ber.*, 1979, **112**, 1126.
94. A. Mondon and H. J. Nestler, *Chem. Ber.*, 1979, **112**, 1329.
95. A. Mondon, S. Mohr, C. Fischer and H. G. Vilhuber, *Chem. Ber.*, 1979, **112**, 2472.
96. S. Mohr, C. Fischer, T. Clausen and A. Mondon, *Chem. Ber.*, 1979, **112**, 3110.
97. S. Mohr, T. Clausen, B. Epe, C. Wolff and A. Mondon, *Chem. Ber.*, 1979, **112**, 3795.
98. K. P. Tiwari and M. Masood, *Phytochemistry*, 1979, **18**, 2069.
99. K. P. Tiwari and M. Masood, *Phytochemistry*, 1979, **18**, 704.
100. M. Masood and K. P. Tiwari, *Phytochemistry*, 1980, **19**, 490.
101. M.-F. Séguineau and N. Langlois, *Phytochemistry*, 1980, **19**, 1279.
102. E. McDonald and A. Suksamrarn, *J. Chem. Soc. Perkin I*, 1978, 434.
103. K. Ito and H. Tanaka, *Chem. Pharm. Bull. (Japan)*, 1977, **25**, 3301.
104. D. Weisleder, R. G. Powell and C. R. Smith, Jr, *Org. Magn. Reson.*, 1980, **13**, 114.
105. K. L. Mikolajczak and C. R. Smith, Jr, *J. Org. Chem.*, 1978, **43**, 4762.
106. H. Rönsch and W. Schade, *Phytochemistry*, 1979, **18**, 1089.
107. W. Fleischhacker and B. Richter, *Chem. Ber.*, 1979, **112**, 3054.
108. W. Fleischhacker and B. Richter, *Chem. Ber.*, 1980, **113**, 3866.
109. M. A. Schwartz and R. A. Wallace, *Tetrahedron Letters*, 1979, 3257.
110. J. Minamikawa, K. C. Rice, A. E. Jacobson, A. Brossi, T. H. Williams and J. V. Silverton, *J. Org. Chem.*, 1980, **45**, 1901.
111. V. Vecchietti, C. Casagrande, G. Ferrari, B. Danieli and G. Palmisano, *J. Chem. Soc. Perkin I*, 1981, 578; and personal communication from Dr Vecchietti.
112. P. R. Barkowski, J. S. Horn and H. Rapoport, *J. Amer. Chem. Soc.*, 1978, **100**, 276.
113. R. A. Barnes and O. M. Soeiro, *Phytochemistry*, 1981, **20**, 543.
114. D. L. Leland, J. O. Polazzi and M. P. Kotick, *J. Org. Chem.*, 1980, **45**, 4026.
115. R. D. Gless and H. Rapoport, *J. Org. Chem.*, 1979, **44**, 1324.
116. J. Hartenstein, T. Heigl and G. Satzinger, *Angew. Chem. Int. Ed. Engl.* 1980, **19**, 1018.
117. H. L. Holland, D. W. Hughes, D. B. MacLean and R. G. A. Rodrigo, *Canad. J. Chem.*, 1978, **56**, 2467.
118. E. J. Barreiro, A. de Lima Pereira, L. Nelson, L. F. Gomes and A. J. R. da Silva, *J. Chem. Res. (S)*, 1980, 330.
119. L. H. Zalkow, L. Gelbaum and E. Keinan, *Phytochemistry*, 1978, **17**, 172.
120. N. V. Mody, R. S. Sawhney and S. W. Pelletier, *J. Natural Products*, 1979, **42**, 417.
121. H. Wiedenfeld and E. Röder, *Phytochemistry*, 1979, **18**, 1083.
122. S. E. Drewes, I. Antonowitz, P. T. Kaye and P. C. Coleman, *J. Chem. Soc. Perkin I*, 1981, 287.
123. E. Röder, H. Wiedenfeld and M. Frisse, *Phytochemistry*, 1980, **19**, 1275.
124. J. A. Edgar, N. J. Eggers, A. J. Jones and G. B. Russell, *Tetrahedron Letters*, 1980, **21**, 2657.
125. M. Hikichi, Y. Asada and T. Furuya, *Tetrahedron Letters*, 1979, 1233.
126. K. Yamada, H. Tatematsu, R. Unno, Y. Hirata and I. Hirono, *Tetrahedron Letters*, 1978, 4543.
127. M. Hikichi and T. Furuya, *Tetrahedron Letters*, 1978, 767.
128. E. Röder and H. Wiedenfeld, *Phytochemistry*, 1977, **16**, 1462.
129. F. Bohlmann, W. Klose and K. Nikisch, *Tetrahedron Letters*, 1979, 3699.
130. F. Bohlmann and K.-H. Knoll, *Phytochemistry*, 1978, **17**, 599.
131. F. Bohlmann, C. Zdero and G. Snatzke, *Chem. Ber.*, 1978, **111**, 3009.

132. K. K. Purushothaman, A. Sarada, J. D. Connolly and J. A. Akinniyi, *J. Chem. Soc. Perkin I*, 1979, 3171.
133. D. Shiengthong, A. Ungphakorn, D. E. Lewis and R. A. Massy-Westropp, *Tetrahedron Letters*, 1979, 2247.
134. J. W. Daly, T. Tokuyama, T. Fujiwara, R. J. Highet and I. L. Karle, *J. Amer. Chem. Soc.*, 1980, **102**, 830.
135. E. Leete and R. M. Riddle, *Tetrahedron Letters*, 1978, 5163.
136. R. Ott-Longoni, N. Viswanathan and M. Hesse, *Helv. Chim. Acta*, 1980, **63**, 2119.
137. L. Faber, E.-G. Herrmann, F. F. Perrollaz, U. P. Schlunegger and W. Wiegrebe, *Annalen*, 1979, 1212.
138. M. Suguira, N. Takao, K. Iwasa and Y. Sasaki, *Chem. Pharm. Bull. (Japan)*, 1978, **26**, 1168.
139. M. Suguira, N. Takao, K. Iwasa and Y. Sasaki, *Chem. Pharm. Bull. (Japan)*, 1978, **26**, 1901.
140. M. Suguira, N. Takao, K. Iwasa and Y. Sasaki, *Chem. Pharm. Bull. (Japan)*, 1979, **27**, 3144.
141. J. J. Tufariello and R. C. Gatrone, *Tetrahedron Letters*, 1978, 2753.
142. J. Quick and C. Meltz, *J. Org. Chem.*, 1979, **44**, 573.
143. S. Yasuds, M. Hanaoka and Y. Arata, *Chem. Pharm. Bull. (Japan)*, 1979, **27**, 2456.
144. K. Fuji, T. Yamada, E. Fujita and H. Murata, *Chem. Pharm. Bull. (Japan)*, 1978, **26**, 2515.
145. S. Yasuda, M. Hanaoka and Y. Arata, *Chem. Pharm. Bull. (Japan)*, 1980, **28**, 831.
146. R. T. Lalonde, N. Muhammad, C. F. Wong and E. R. Sturiale, *J. Org. Chem.*, 1980, **45**, 3664.
147. P. Peura and M. Lounasmaa, *Phytochemistry*, 1977, **16**, 1122.
148. P. Slosse and C. Hootelé, *Tetrahedron Letters*, 1979, 4587.
149. P. Slosse and C. Hootelé, *Tetrahedron Letters*, 1978, 397; and personal communication from Dr C. Hootelé.
150. W. Boczoń, G. Pieczonka and M. Wiewiorowski, *Tetrahedron*, 1977, **33**, 2565.
151. A. Daily, H. Dutschewska, N. Mollov and S. Spassov, *Tetrahedron Letters*, 1978, 1453.
152. S. Ohmiya, H. Otomasu, J. Haginiwa and I. Murakoshi, *Phytochemistry*, 1979, **18**, 649.
153. S. Ohmiya, H. Otomasu, J. Haginiwa and I. Murakoshi, *Phytochemistry*, 1978, **17**, 2021.
154. S. Ohmiya, K. Higashiyama, H. Otomasu, I. Murakoshi and J. Haginiwa, *Phytochemistry*, 1979, **18**, 645.
155. F. Bohlmann and R. Zeisberg, *Chem. Ber.*, 1975, **108**, 1043.
156. S. Ohmiya, H. Otamasu, J. Haginiwa and I. Murakoshi, *Chem. Pharm. Bull. (Japan)*, 1980, **28**, 546.
157. K. Morinaga, A. Ueno, S. Fukushima, M. Namakoshi, Y. Iitaka and S. Okuda, *Chem. Pharm. Bull. (Japan)*, 1978, **26**, 2483.
158. J. T. Wróbel, J. Ruszkowska and K. Wojtasiewicz, *J. Mol. Struct.* 1978, **50**, 299.
159. I. Lantos, C. Razgaitis, B. Loev and B. Douglas, *Canad. J. Chem.*, 1980, **58**, 1851.
160. E. Gössinger, *Tetrahedron Letters*, 1980, **21**, 2229.
161. R. H. Mueller and M. E. Thompson, *Tetrahedron Letters*, 1980, **21**, 1097.
162. S. C. Pakrashi, B. Achari, E. Ali, P. P. Ghosh Dastidar and R. R. Sinha, *Tetrahedron Letters*, 1980, **21**, 2667.
163. J. A. Kroll, *J. Forensic Sci.*, 1979, **24**, 303.
164. W. C. Evans and V. A. Woolley, *Phytochemistry*, 1978, **17**, 171.
165. A. S. Martin, J. Rovirosa, V. Gambaro and M. Castillo, *Phytochemistry*, 1980, **19**, 2007.
166. F. Bohlmann and C. Zdero, *Phytochemistry*, 1978, **17**, 1337.
167. H. Ripperger, *Phytochemistry*, 1979, **18**, 717.
168. E. Leete and J. A. McDonell, *J. Amer. Chem. Soc.*, 1981, **103**, 658.

169. V. S. Dimitrov, S. L. Spassov, T. Zh. Radeva and J. A. Ladd, *J. Mol. Struct.*, 1975, **27**, 167.
170. M. Sahai and A. B. Ray, *J. Org. Chem.*, 1980, **45**, 3265.
171. J. J. Tufariello and G. B. Mullen, *J. Amer. Chem. Soc.*, 1978, **100**, 3638.
172. I. Christofidis, A. Welter and J. Jadot, *Tetrahedron*, 1977, **33**, 977.
173. I. Christofidis, A. Welter and J. Jadot, *Tetrahedron*, 1977, **33**, 3005.
174. M. F. Roberts and R. T. Brown, *Phytochemistry*, 1981, **20**, 447.
175. J. J. Tufariello and Sk. A. Ali, *Tetrahedron Letters*, 1978, 4647.
176. S. Linke, J. Kurz and H.-J. Zeiler, *Tetrahedron*, 1978, **34**, 1979.
177. C. K. Sehgal, P. L. Kachroo, R. L. Sharma, S. C. Taneja, K. L. Dhar and C. K. Atal, *Phytochemistry*, 1979, **18**, 1865.
178. R. M. Smith, *Tetrahedron*, 1979, **35**, 437.
179. R. B. Filho, M. P. De Souza and M. E. O. Mattos, *Phytochemistry*, 1981, **20**, 345.
180. A. D. Harmon, U. Weiss and J. V. Silverton, *Tetrahedron Letters*, 1979, 721.
181. T. Imanishi, N. Yagi and M. Hanaoka, *Tetrahedron Letters*, 1981, 667.
182. R. K. Chaudhuri, O. Sticher and T. Winkler, *Helv. Chim. Acta*, 1980, **63**, 1045.
183. R. K. Chaudhuri, O. Sticher and T. Winkler, *Tetrahedron Letters*, 1981, **22**, 559.
184. D. A. Evans, A. M. Golob, N. S. Mandel and G. S. Mandel, *J. Amer. Chem. Soc.*, 1978, **100**, 8170.
185. E. Medina and G. Spiteller, *Chem. Ber.*, 1979, **112**, 376.
186. E. Leete, K. C. Ranbom and R. M. Riddle, *Phytochemistry*, 1979, **18**, 75.
187. E. Leete, *J. Org. Chem.*, 1979, **44**, 165.
188. J. A. Elvidge, J. R. Jones, R. B. Mane and J. M. A. Al-Rawi, *J. Chem. Soc. Perkin Trans. II*, 1979, 386.
189. J. I. Seeman, H. V. Secor, J. F. Whidby and R. L. Bassfield, *Tetrahedron Letters*, 1978, 1901.
190. R. G. Powell, C. R. Smith, Jr, D. Weisleder, D. A. Muthard and J. Clardy, *J. Amer. Chem. Soc.*, 1979, **101**, 2784.
191. A. S. Kende and T. P. Demuth, *Tetrahedron Letters*, 1980, **21**, 715.
192. H. Ripperger, *Phytochemistry*, 1978, **17**, 1069.
193. K. Yamada, Y. Shizuri and Y. Hirata, *Tetrahedron*, 1978, **34**, 1915.
194. R. L. Baxter, L. Crombie, D. J. Simmonds and D. A. Whiting, *J. Chem. Soc. Perkin Trans. I*, 1979, 2972.
195. L. Crombie, W. M. L. Crombie, D. A. Whiting and K. Szendrei, *J. Chem. Soc. Perkin Trans. I*, 1979, 2976.
196. R. L. Baxter, W. M. L. Crombie, L. Crombie, D. J. Simmonds, D. A. Whiting and K. Szendrei, *J. Chem. Soc. Perkin Trans. I*, 1979, 2982.
197. G. Grethe, H. L. Lee, T. Mitt and M. R. Uskoković, *J. Amer. Chem. Soc.*, 1978, **100**, 589.
198. L. E. Overman and P. J. Jessup, *J. Amer. Chem. Soc.*, 1978, **100**, 5179.
199. N. M. D. Brown, M. F. Grundon, D. M. Harrison and S. A. Sugenor, *Tetrahedron*, 1980, **36**, 3579.
200. D. L. Dreyer, *Phytochemistry*, 1980, **19**, 941.
201. M. F. Grundon and H. M. Okely, *Phytochemistry*, 1979, **18**, 1768.
202. C. Kaneko, T. Naito, M. Hashiba, H. Fujii and M. Somei, *Chem. Pharm. Bull. (Japan)*, 1979, **27**, 1813.
203. M. F. Grundon, V. N. Ramachandran and M. E. Donnelly, *J. Chem. Soc. Perkin Trans. I*, 1981, 633.
204. G. J. Kapadia, Y. N. Snukla, S. P. Basak, H. M. Fales and E. A. Sokoloski, *Phytochemistry*, 1978, **17**, 1444.
205. A. Ahond, F. Picot, P. Potier, C. Poupat and T. Sévenet, *Phytochemistry*, 1978, **17**, 166.

206. F. R. Stermitz and I. A. Sharifi, *Phytochemistry*, 1977, **16**, 2003.
207. M. Sarkar, S. Kundu and D. P. Chakraborty, *Phytochemistry*, 1978, **17**, 2145.
208. J. Reisch, I. Mester, J. Körösi and K. Szendrei, *Tetrahedron Letters*, 1978, 3681.
209. A. Ahond, C. Poupat and J. Pusset, *Phytochemistry*, 1979, **18**, 1415.
210. J. F. Ayafor, B. L. Sondengam and B. Ngadjui, *Tetrahedron Letters*, 1980, **21**, 3293.
211. M. S. Hifnawy, J. Vaquette, T. Sévenet, J.-L. Pousset and A. Cavé, *Phytochemistry*, 1977, **16**, 1035.
212. D. Bergenthal, I.M.Zs. Rózsa and J. Reisch, *Phytochemistry*, 1979, **18**, 161.
213. I. H. Bowen, K. P. W. C. Perera and J. R. Lewis, *Phytochemistry*, 1978, **17**, 2125.
214. J. Reisch, I. Mester, S. K. Kapoor, Z. Rózsa and K. Swendrei, *Annalen*, 1981, 85.
215. J. A. Adamovics, J. A. Cina and C. R. Hutchinson, *Phytochemistry*, 1979, **18**, 1085.
216. E. Baxman and E. Winterfeldt, *Chem. Ber.*, 1978, **111**, 3403.
217. D. L. Dreyer and R. C. Brenner, *Phytochemistry*, 1980, **19**, 935.
218. H. Y. Aboul-Enein and R. F. Borne, *Chem. Biomed. Environ. Instrumentation*, 1980, **10**, 231.
219. M. R. Brennan and K. L. Erickson, *Tetrahedron Letters*, 1978, 1637.
220. G. T. Carter and K. L. Rinehart, Jr, *Tetrahedron Letters*, 1978, 4479.
221. J. H. Cardellina II, M. P. Kirkupp, R. E. Moore, J. S. Mynderse, K. Seff and C. J. Simmons, *Tetrahedron Letters*, 1979, 4915.
222. H. Achenbach and B. Raffelsberger, *Tetrahedron Letters*, 1979, 2571.
223. A. Jossang, J.-L. Pousset, H. Jacquemin and A. Cave, *Tetrahedron Letters*, 1977, 4317.
224. G. J. Kapadia, Y. N. Shukla, S. P. Basak, E. A. Sokoloski and H. M. Fales, *Tetrahedron*, 1980, **36**, 2441.
225. G. J. Kapadia, Y. N. Shukla, B. K. Chowdhury, S. P. Basal, H. M. Fales and E. A. Sokoloski, *J. Chem. Soc. Chem. Commun.*, 1977, 535.
226. I. Mester and J. Reisch, *Annalen*, 1977, 1725.
227. S. Michel, F. Tillequin and M. Koch, *Tetrahedron Letters*, 1980, **21**, 4027.
228. J.-Y. Lallemand, P. Lemaitre, L. Beeley, P. Lesca and D. Mansuy, *Tetrahedron Letters*, 1978, 1261.
229. C. A. Coune, L. J. G. Angenot and J. Denoel, *Phytochemistry*, 1980, **19**, 2009.
230. H. Wagner and T. Nestler, *Tetrahedron Letters*, 1978, 2777.
231. M. P. Jain, S. K. Koul, K. L. Dhar and C. K. Atal, *Phytochemistry*, 1980, **19**, 1880.
232. F. Faini, M. Castillo and R. Torres, *Phytochemistry*, 1978, **17**, 338.
233. A. M. Giesbrecht, H. E. Gottlieb, O. R. Gottlieb, M. O. F. Goulart, R. A. De Lima and A. E. G. Santana, *Phytochemistry*, 1980, **19**, 313.
234. J. S. Carlé and C. Christophersen, *J. Amer. Chem. Soc.*, 1979, **101**, 4012; *J. Org. Chem.*, 1980, **45**, 1586.
235. T. Hino, S. Kodato, K. Takahashi, H. Yamaguchi and M. Nakagawa, *Tetrahedron Letters*, 1978, 4913.
236. M. Yamazaki, H. Fujimoto and E. Okuyama, *Chem. Pharm. Bull. (Japan)*, 1977, **25**, 2554.
237. M. Yamazaki, H. Fujimoto and E. Okuyama, *Chem. Pharm. Bull. (Japan)*, 1978, **26**, 111.
238. M. Yamazaki, E. Okuyama and Y. Maebayashi, *Chem. Pharm. Bull. (Japan)*, 1979, **27**, 1611.
239. Y. Konda, M. Onda, A. Hirano and S. Omura, *Chem. Pharm. Bull. (Japan)*, 1980, **28**, 2987.
240. M. Yamazaki, E. Okuyama, M. Kobayashi and H. Inoue, *Tetrahedron Letters*, 1981, **22**, 135.
241. J. P. Springer, G. Büchi and J. Clardy, *Tetrahedron Letters*, 1977, 2403.
242. G. Gatti, R. Cardillo and C. Fuganti, *Tetrahedron Letters*, 1978, 2605.

243. R. T. Gallagher, T. McCabe, K. Hirotsu, J. Clardy, J. Nicholson and B. J. Wilson, *Tetrahedron Letters*, 1980, **21**, 243.
244. R. T. Gallagher, J. Finer, J. Clardy, A. Leutwiler, F. Weibel, W. Acklin and D. Arigoni, *Tetrahedron Letters*, 1980, **21**, 235.
245. R. T. Gallagher, J. Clardy and B. J. Wilson, *Tetrahedron Letters*, 1980, **21**, 239.
246. A. E. De Jesus, P. S. Steyn, F. R. Van Heerden, R. Vlegaar, P. L. Wessels and W. E. Hull, *J. Chem. Soc. Chem. Commun.*, 1981, 289.
247. S. N. Y. Fanso-Free, G. T. Furst, P. R. Srinivasan, R. L. Lichter, R. B. Nelson, J. A. Panetta and G. W. Gribble, *J. Amer. Chem. Soc.*, 1979, **101**, 1549.
248. R. Besselièvre, J.-P. Cosson, B. C. Das and H.-P. Husson, *Tetrahedron Letters*, 1980, **21**, 63.
249. W. R. Ashcroft and J. A. Joule, *Tetrahedron Letters*, 1980, **21**, 2341.
250. G. Rackur and E. Winterfeldt, *Chem. Ber.*, 1976, **109**, 3837.
251. G. Höfle, P. Heinstein, J. Stöckigt and M. H. Zenk, *Planta Med.*, 1980, **40**, 120.
252. R. Goutarel, M. Païs, H. E. Gottlieb and E. Wenkert, *Tetrahedron Letters*, 1978, 1235.
253. E. Wenkert, T. D. J. Halls, G. Kunesch, K. Orito, R. L. Stephens, W. A. Temple and J. S. Yadav, *J. Amer. Chem. Soc.*, 1979, **101**, 5370.
254. M. Lounasmaa and M. Hämeila, *Tetrahedron*, 1978, **34**, 437.
255. M. Lounasmaa and R. Jokela, *Tetrahedron*, 1978, **34**, 1841.
256. R. T. Brown and J. Leonard, *Tetrahedron Letters*, 1979, 1805.
257. M. Lounasmaa and S.-K. Kan, *Tetrahedron*, 1980, **36**, 1607.
258. D. Ponglux, T. Supavita, R. Verpoorte and J. D. Phillipson, *Phytochemistry*, 1980, **19**, 2013.
259. R. T. Brown and J. Leonard, *Tetrahedron Letters*, 1977, 4251.
260. F. Hotellier, P. Delaveau and J.-L. Pousset, *Phytochemistry*, 1980, **19**, 1884.
261. D. Herlem and F. Khuong-Huu, *Tetrahedron*, 1979, **35**, 633.
262. J. Borges, M. T. Manresa, J. L. M. Ramon, C. Pascual and Y. A. Rumbero, *Tetrahedron Letters*, 1979, 3197.
263. R. F. Bond, J. C. A. Boeyens, C. W. Holzapfel and P. S. Steyn, *J. Chem. Soc. Perkin Trans. I*, 1979, 1751.
264. E. Wenkert, H. T. A. Cheung, H. E. Gottlieb, M. C. Koch, A. Rabaron and M. M. Plat, *J. Org. Chem.*, 1978, **43**, 1099.
265. D. Tavernier, M. J. O. Anteunis, M. J. G. Tits and L. J. G. Angenot, *Bull. Soc. Chim. Belg.*, 1978, **87**, 595.
266. J. Leung and A. J. Jones, *Org. Magn. Reson.* 1977, **9**, 333.
267. R. Verpoorte, P. J. Hylands and N. G. Bisset, *Org. Magn. Reson.* 1977, **9**, 567.
268. J. T. Edward, P. G. Farrell, S. A. Samad, R. Wojtowski and S. C. Wong, *Canad. J. Chem.*, 1980, **58**, 2380.
269. C. Galeffi, M. Nicoletti and G. B. Marini Bettolo, *Tetrahedron*, 1979, **35**, 2545.
270. A. Edenhofer and W. Arnold, *Helv. Chim. Acta*, 1979, **62**, 1466.
271. G. B. Marini-Bettolo, C. Galeffi, M. Nicoletti and I. Messana, *Phytochemistry*, 1980, **19**, 992.
272. M. Tits, L. Angenot and D. Tavernier, *Tetrahedron Letters*, 1980, **21**, 2439.
273. M. Tits, D. Tavernier and L. Angenot, *Phytochemistry*, 1980, **19**, 1531.
274. J. P. Kutney, L. S. L. Choi, P. Kolodziejczyk, S. K. Sleigh, K. L. Stuart, B. R. Worth, W. G. W. Kurz, K. B. Chatson and F. Constabel, *Phytochemistry*, 1980, **19**, 2589.
275. A. Banerji and A. K. Siddhanta, *Phytochemistry*, 1981, **20**, 540.
276. M. Caprasse, C. Coune and L. Angenot, *J. Pharm. Belg.*, 1981, **36**, 243.
277. T. A. Crabb and J. Rouse, *Org. Magn. Reson.*, in press.
278. S.-I. Sakai, Y. Yamamoto and S. Hasegawa, *Chem. Pharm. Bull. (Japan)*, 1980, **28**, 3454.
279. N. Aimi, K. Yamaguchi, S.-I. Sakai, J. Haginiwa and A. Kubo, *Chem. Pharm. Bull. (Japan)*, 1978, **26**, 3444.

280. A. Chatterjee, M. Chakrabarty, A. K. Ghosh, E. W. Hagaman and E. Wenkert, *Tetrahedron Letters*, 1978, 3879.
281. E. Wenkert, T. Hudlický and H. D. H. Showalter, *J. Amer. Chem. Soc.*, 1978, **100**, 4893.
282. R. Becker, G. Benz, M. Rösner, U. Rosentreter and E. Winterfeldt, *Chem. Ber.*, 1979, **112**, 1879.
283. M. E. Kuehne, C. L. Kirkemo, T. H. Matsko and J. C. Bohnert, *J. Org. Chem.*, 1980, **45**, 3259.
284. P. L. Majumder, S. Joardar, B. N. Dinda, D. Bandyopadhyay, S. Joardar and A. Basu, *Tetrahedron*, 1981, **37**, 1243.
285. J. Santamaria, D. Herlem and F. Khuong-Huu, *Tetrahedron*, 1977, **33**, 2389.
286. N. Aimi, Y. Asada, S.-I. Sakai and J. Haginiwa, *Chem. Pharm. Bull. (Japan)*, 1978, **26**, 1182.
287. N. Kunesch, A. Cavé, E. W. Hagaman and E. Wenkert, *Tetrahedron Letters*, 1980, **21**, 1727.
288. C. Kan, H.-P. Husson, H. Jacqueimin, S.-K. Kan and M. Lounasmaa, *Tetrahedron Letters*, 1980, **21**, 55.
289. C. Kan, H.-P. Husson, S.-K. Kan and M. Lounasmaa, *Tetrahedron Letters*, 1980, **21**, 3363.
290. J. P. Kutney, U. Bunzli-Trepp, K. K. Chan, J. P. de Souza, Y. Fujise, T. Honda, J. Katsube, F. K. Klein, A. Leutwiler, S. Morehead, M. Rohr and B. R. Worth, *J. Amer. Chem. Soc.*, 1978, **100**, 4220.
291. I. Chardon-Loriaux, M.-M. Debray and H.-P. Husson, *Phytochemistry*, 1978, **17**, 1605.
292. C. Marazano, J.-L. Fourrey and B. C. Das, *J. Chem. Soc. Chem. Commun.*, 1981, 37.
293. S. P. Gunasekera, G. A. Cordell and N. R. Farnsworth, *Phytochemistry*, 1980, **19**, 1213.
294. M. DeBellefon, M. M. Debray, L. Le Men-Olivier and J. Le Men, *Phytochemistry*, 1975, **14**, 1649.
295. R. W. Andriamialisoa, N. Langlois, Y. Langlois, P. Potier and P. Bladon, *Canad. J. Chem.*, 1979, **57**, 2572.
296. P. Mangeney and Y. Langlois, *Tetrahedron Letters*, 1978, 3015.
297. S. Takano, S. Hatakeyama and K. Ogasawara, *J. Amer. Chem. Soc.*, 1979, **101**, 6414.
298. L. Akhter, R. T. Brown and D. Moorcroft, *Tetrahedron Letters*, 1978, 4137.
299. F. Heatley, L. Akhter and R. T. Brown, *J. Chem. Soc. Perkin Trans. II*, 1980, 919.
300. D. I. C. Scopes, M. S. Allen, G. J. Hignett, N. D. V. Wilson, M. Harris and J. A. Joule, *J. Chem. Soc. Perkin Trans. I*, 1977, 2376.
301. V. Vecchietti, G. Ferrari, F. Orsini, F. Pelizzoni and A. Zajotti, *Phytochemistry*, 1978, **17**, 835.
302. A. A. Olaniyi and W. N. A. Rolfsen, *J. Natural Products*, 1980, **43**, 595.
303. F. Khuong-Huu, A. Chiaroni and C. Riche, *Tetrahedron Letters*, 1981, **22**, 733.
304. H.-P. Ros, R. Kyburz, N. W. Preston, R. T. Gallagher, I. R. C. Bick and M. Hesse, *Helv. Chim. Acta*. 1979, **62**, 481.
305. R. Kyburz, E. Schöpp, I. R. C. Bick and M. Hesse, *Helv. Chim. Acta*, 1979, **62**, 2539.
306. M. A. Hai, N. W. Preston, R. Kyburz, E. Schöpp, I. R. C. Bick and M. Hesse, *Helv. Chim. Acta*, 1980, **63**, 2130.
307. C. Richard, C. Delaude, L. Le Men-Olivier and J. Le Men, *Phytochemistry*, 1978, **17**, 539.
308. J. U. Oguakwa, M. Nicoletti, I. Messana, C. Galeffi and G. B. Marini-Bettõlo, *Rend. Sci. Fis. Mat. Nat.*, 1978, **65**, 299.
309. J. U. Oguakwa, C. Galeffi, I. Messana, R. La Bua, M. Nicoletti and G. B. Marini-Bettõlo, *Gazz. Chim. Ital.*, 1978, **108**, 615.
310. M. Zeches, F. Sigaut, L. Le Men-Olivier, J. Lévy and J. Le Men, *Bull. Soc. Chim. Fr.*, 1981, 75.
311. E. Seguin, M. Koch, E. Chenu and M. Hayat, *Helv. Chim. Acta*, 1980, **63**, 1335.

312. L. Angenot, *Plantes Méd. Phytotherap.*, 1978, **12**, 123; and personal comments from Professor Angenot.
313. J. P. Kutney, A. Horinaka, R. S. Ward and B. R. Worth, *Canad. J. Chem.*, 1980, **58**, 1829.
314. B. Danieli, G. Palmisano, B. Gabetta and E. M. Martinelli, *J. Chem. Soc. Perkin Trans. I*, 1980, 601.
315. A. de Bruyn, L. de Taeye and M. J. O. Anteunis, *Bull. Soc. Chim. Belg.*, 1980, **89**, 629.
316. A. El-Sayed, G. A. Handy and G. A. Cordell, *J. Natural Products*, 1980, **43**, 157.
317. P. Mangeney, R. Z. Andriamialisoa, J.-Y. Lallemand, N. Langlois, Y. Langlois and P. Potier, *Tetrahedron*, 1979, **35**, 2176.
318. T. Nabih, L. Youel and J. P. Rosazza, *J. Chem. Soc. Perkin Trans. I*, 1978, 757.
319. M. Tits, D. Tavernier and L. Angenot, *Phytochemistry*, 1979, **18**, 515.
320. J. Lamotte, L. Dupont, O. Dideberg, K. Kambu and L. Angenot, *Tetrahedron Letters*, 1979, 4227.
321. B. C. Das, J.-P. Cosson and G. Lukacs, *J. Org. Chem.*, 1977, **42**, 2785.
322. A. Henriques, C. Kan-Fan, A. Ahond, C. Riche and H.-P. Husson, *Tetrahedron Letters*, 1978, 3707.
323. S. W. Pelletier, N. V. Mody, R. S. Sawhney and J. Bhattacharyya, *Heterocyles*, 1977, **7**, 327.
324. S. W. Pelletier, N. V. Mody and R. S. Sawhney, *Canad. J. Chem.*, 1979, **57**, 1652.
325. S. W. Pelletier, N. V. Mody, A. P. Venkov and N. M. Mollov, *Tetrahedron Letters*, 1978, 5045.
326. S. W. Pelletier and J. Bhattacharyya, *Tetrahedron Letters*, 1977, 2735.
327. S. W. Pelletier and J. Bhattacharyya, *Phytochemistry*, 1977, **16**, 1464.
328. S. W. Pelletier, N. V. Mody and N. Katsui, *Tetrahedron Letters*, 1977, 4027.
329. C. Wei-shin and E. Breitmaier, *Chem. Ber.*, 1981, **114**, 394.
330. H. Takayama, M, Ito, M. Koga, S.-I. Sakai and T. Okamoto, *Heterocycles*, 1981, **15**, 403.
331. S.-I. Sakai, H. Takayama and T. Okamoto, *Yakugaku Zasshi*, 1979, **99**, 647.
332. S. W. Pelletier, N. V. Mody and O. D. Dailey, Jr, *Canad. J. Chem.*, 1980, **58**, 1875.
333. S. W. Pelletier and N. V. Mody, *J. Amer. Chem. Soc.*, 1979, **101**, 492.
334. S. W. Pelletier, H. K. Desai, J. Finer-Moore and N. V. Mody, *J. Amer. Chem. Soc.*, 1979, **101**, 6741.
335. J.-C. Braekman, C. Hootele, N. Miller, J.-P. Declercq, G. Germain and M. Van Meerssche, *Canad. J. Chem.*, 1979, **57**, 1691.
336. J. Szychowski and D. B. MacLean, *Canad. J. Chem.*, 1979, **57**, 1631.

Thallium NMR Spectroscopy

J. F. HINTON, K. R. METZ
AND R. W. BRIGGS

Department of Chemistry, University of Arkansas, Fayetteville, Arkansas 72701, USA

I. INTRODUCTION

The advent of pulsed Fourier transform (FT) nuclear magnetic resonance spectroscopy has opened the periodic table of the elements to investigation in an extraordinary manner. With a few exceptions, any nuclide with spin

can now be observed routinely in the NMR experiment. However, one should not be misled into thinking that were it not for the FT technique the less common or more difficult to observe nuclides could not be studied. In fact, it is important to note that NMR experiments had been performed with about 30 elements in the solid, liquid or gas phase during the decade following the landmark papers of Bloch[1] and Purcell[2] in 1946. The availability of wide bore, high field magnets and pulsed Fourier transform techniques have allowed the "re-discovery" of these same elements and an extension to the remainder of the periodic table.[3]

One element studied during the early period in the history of NMR spectroscopy was thallium. By 1953, solid[4] and liquid[5] state spectra had been obtained for the thallium nucleus. Thallium is particularly well suited for the NMR experiment due to its intrinsic nuclear properties. Thallium has two isotopes, ^{203}Tl (29·5% natural abundance) and ^{205}Tl (70·5% natural abundance), both of which have spin $\frac{1}{2}$. The relative receptivity of the more abundant isotope, ^{205}Tl, is 0·1355 with respect to the proton with a value of 1. This makes the ^{205}Tl nucleus the third most receptive spin $\frac{1}{2}$ nuclide. Thallium-205 is the most receptive heavy metal spin $\frac{1}{2}$ nucleus by a factor of 30 over ^{119}Sn, which is the second most receptive heavy metal. A summary of the pertinent nuclear properties for the ^{203}Tl and ^{205}Tl nuclides is found in Table I.

TABLE I

NMR properties of the ^{203}Tl and ^{205}Tl nuclides.

Isotope	Spin	Natural abundance/%	Magnetogyric ratio, $\gamma/10^7$ rad T^{-1} s^{-1}	Magnetic moment, $\mu/\mu N$	NMR frequency, Ξ/MHz	Standard
203	$\frac{1}{2}$	29·5	15·278	2·7646		
205	$\frac{1}{2}$	70·5	15·438	2·7914	57·683 833[a]	$TlNO_3$ aq.

[a] Scaled such that the ^{1}H resonance of Me_4Si is at exactly 100 MHz. The value quoted is for the resonance of the standard listed in the next column.

Not only do the nuclear properties of the thallium isotopes make them easy to observe in the NMR experiment, but the spectral parameters of chemical shift, coupling constant and spin–lattice relaxation time are exceptionally sensitive to the chemical (i.e. electronic) environment in which the thallium nucleus is placed. Consequently, thallium NMR spectroscopy is a very useful technique for investigating a wide variety of chemical and physical interactions in the solid and the solution states. Furthermore, the Tl(I) ion is a good replacement for the Na(I) and K(I) ions in many biological

systems, thus providing a convenient spectroscopic alternative for the study of such phenomena as ion transport across membranes, activation and regulation of enzymes, etc.

Until recently, the chemist was primarily interested in solution-state applications of NMR. However, new experimental techniques such as the combination of "magic angle" sample spinning (MASS) and cross-polarization (CP) have made it possible to obtain spectra of nuclei in the solid state in a relatively easy manner. The data obtained have provided valuable new information about structure, bonding and dynamics in the solid state. It is becoming clear that, in some cases, one must have solid state information in order to understand certain aspects of data obtained for the solution state. Therefore, we include in this report solution state and solid state results which have been obtained for thallium in order to present an overall view of thallium NMR spectroscopy.

The great extremes found between the spectral parameters for solid and solution state ^{205}Tl NMR spectroscopy can be seen in Fig. 1. The solid state ^{205}Tl spectrum of thallium iodide exhibits a line width of about 56 kHz at half-height. The degassed aqueous solution spectrum of the Tl(I) ion has a line width of about 3 Hz. Each spectrum was obtained under identical conditions in the authors' laboratory, using a spectral width of 250 000 Hz. Each sample was contained in a 5 mm tube placed in the same insert in the magnet.

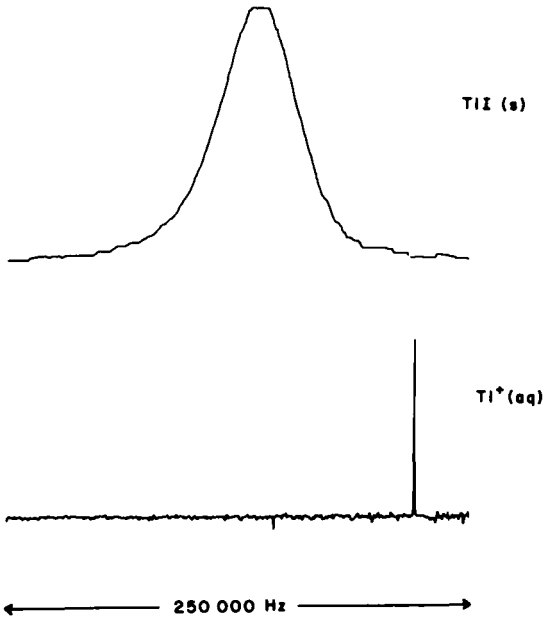

FIG. 1. ^{205}Tl NMR spectra of aqueous $TlNO_3$ and TlI powder.

This report reviews the pertinent literature up to early 1981. The authors have attempted to cover the literature as thoroughly as possible. However, in some instances of the very early solid state literature the journals or technical reports are not available, and in those cases *Chemical Abstracts* is the source of information.

II. Tl(I) SOLUTION STUDIES

A. Chemical shifts

Before discussing the chemical shift of the thallium nucleus, a few brief comments are necessary concerning how the data are presented and some general aspects of heavy metal NMR spectroscopy. Table II summarizes the data on thallium chemical shifts for Tl(I) and Tl(III) in the solid and solution states. Unless stated otherwise, all measurements of chemical shifts are for the ^{205}Tl nucleus, which has a higher receptivity than the ^{203}Tl nucleus. The table contains the chemical shift on the ppm scale and the resonance frequency of each species. It should be noted that for the heavy metal nuclides, such as thallium, which have extremely large chemical shift ranges (e.g. about 7000 ppm for ^{205}Tl), the chemical shift scale can be in error because of the way it is defined. Therefore, we give both the resonance frequency and chemical shift. The control of the sample temperature in heavy metal NMR is extremely important since the chemical shifts of most such nuclides are exceptionally temperature dependent. For example, the authors have observed a 5 ppm per degree dependence of the Tl(I) ion shift in methylamine solutions. The chemical shift table, consequently, contains the temperature, where known, for each entry.

The outer electronic configuration of thallium, $6s^26p^1$, suggests that this element should exist in the +1 and +3 oxidation states. Both oxidation states are well known for thallium, but oxidation potential data indicate the +1 state to be more stable in aqueous solution than the +3 state where extensive hydrolysis and complexation occurs. In general, solution studies involving ion–solvent interactions, ion-pairing, etc., have been performed with Tl(I), and organothallium compounds have been used to study Tl(III). However, some Tl(III) compounds are also good probes for investigating solution phenomena.

The chemical shift range for thallium is extremely large, covering about 7000 ppm for Tl(III) species and over 3400 ppm for Tl(I) species.

The origin of this large chemical shift range lies with the paramagnetic term of the nuclear shielding tensor. The total diamagnetic shielding of the thallium atom is quite appreciable, being about 10 000 ppm. However, in chemical bonding the core electrons are relatively unperturbed, the valence electrons being most affected. Therefore, the important quantity

TABLE II

^{205}Tl resonance frequencies and chemical shifts.

Compound	Conc./M[a]	Solvent	Temp./°C	Ξ/MHz[b]	Chemical shift/ppm[j]	Reference
$Tl_3Fe(CN)_6$		Solid	27	(58·491)	+14000 ± 700	16
$Tl_3Co_{0\cdot934}Fe_{0\cdot066}(CN)_6$		Solid	27	(58·030)	+6000 ± 300	16
				(57·6602)	−410 ± 200	16
				(57·6602)	−410 ± 100	16
$Tl_3Co(CN)_6$		Solid	27	(57·6602)	−410 ± 100	16
$TlFe(SO_4)_2\cdot12H_2O$		Solid	27	(57·6602)	−410 ± 100	16
Me_3Tl		*n*-Pentane	24	(57·977 617)	+5093	121
Me_3Tl		Et_2O	24	(57·958 004)	+4753	121
Me_3Tl	20%	Et_2O		(57·958 12)	+4755 ± 20	64
Me_3Tl	10%	Acetone	−70	57·943 64[c]	+4504[c]	80
Et_3Tl		*n*-Pentane	24	(57·970 118)	+4963	121
Ph_3Tl		Et_2O	24	(57·903 839)	+3814	121
$[Et_4N][Tl(S_2C_2H_2)_2]$		Acetone-d_6	56	(57·918 895)	+4075[c]	91
$(Me_2TlPPh_2)_2$		C_6D_6		(57·912 780)	+3969	118
$Me_2TlSSCNEt_2$		$CDCl_3$	−50	(57·898 878)	+3728[c]	91
$(Me_2TlNMe_2)_2$		C_6D_6	37	(57·916 010)	+4025[c,k]	91
$(Me_2TlNMe_2)_2$		C_6H_6	24	(57·913 876)	+3988	121
$(Me_2TlNMe_2)_2$		Et_2O	24	(57·905 397)	+3841	121
$(Me_2TlOEt)_2$		C_6D_6	37	(57·905 685)	+3846[c,k]	91
$(Me_2TlOEt)_2$		Toluene-d_8	37	(57·905 281)	+3839[c,k]	91
$(Me_2TlOEt)_2$		Toluene-d_8	−60	(57·907 012)	+3869[c]	91
$(Me_2TlOEt)_2$		*n*-Hexane	24	(57·900 320)	+3753	121
Me_2Tl-N 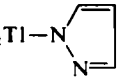		Toluene	54	(57·899 224)	+3734	121

TABLE II (*cont.*)

Compound	Conc./M[a]	Solvent	Temp./°C	Ξ/MHz[b]	Chemical shift/ppm[i]	Reference
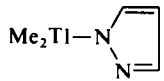		Melt	54	(57·898 994)	+3730	121
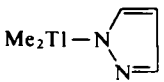		Toluene	24	(57·892 591)	+3619	121
Me_2TlOH		H_2O	24	(57·893 571)	+3636	121
Me_2TlOPh	0·2	CH_2Cl_2	29	57·899 766	+3743	71
Me_2TlOPh	0·8	CH_2Cl_2	29	57·899 560	+3740	71
Me_2TlOPh	0·9	Pyridine	29	57·891 336	+3597	71
Me_2TlOPh	0·2	Pyridine	29	57·891 183	+3595	71
Me_2TlOPh	0·8	DMSO	29	57·889 811	+3571	71
Me_2TlOPh	0·2	DMSO	29	57·889 266	+3561	71
Me_2TlI	0·1	Pyridine	29	57·896 617	+3689	71
Me_2TlI	1·2	DMSO		(57·891 149)	+3594	121
Me_2TlI	0·9	DMSO	29	57·892 660	+3620	71
Me_2TlI	0·2	DMSO	29	57·889 756	+3570	71
Me_2TlBr	Sat'd.	DMSO		(57·890 053)	+3575	121
Me_2TlBr	5%	NH_3(liq.)	−30	57·888 24[c]	+3544[c]	71
Me_2TlF	Sat'd	H_2O		(57·885 669)	+3499	121
Me_2TlF	Sat'd	DMSO		(57·880 708)	+3413	121
Me_2TlClO_4	0·4	en		(57·890 976)	+3591	119
Me_2TlClO_4	0·4	D_2O		(57·887 688)	+3534	119
Me_2TlClO_4	0·4	Pyridine		(57·886 592)	+3515	119
Me_2TlClO_4	0·4	CH_3CN		(57·886 188)	+3508	119
Me_2TlClO_4	0·4	*n*-Butylamine		(57·883 881)	+3468	119
Me_2TlClO_4	0·4	DMSO		(57·883 131)	+3455	119

TABLE II (*cont.*)

Compound	Conc./M[a]	Solvent	Temp./°C	Ξ/MHz[b]	Chemical shift/ppm[i]	Reference
Me_2TlClO_4	0·4	DMF		(57·882 611)	+3446	119
Me_2TlClO_4	0·4	DMA		(57·879 958)	+3400	119
Me_2TlClO_4	0·4	HMPA		(57·879 035)	+3384	119
Me_2TlNO_3	1·2	50% en		(57·894 379)	+3650	121
Me_2TlNO_3	∞-dil. (0·026)	*n*-Butylamine	23	57·890 667	+3586	74
Me_2TlNO_3	1·2	*n*-Butylamine		(57·890 110)	+3576	121
Me_2TlNO_3	0·4	D_2O		(57·887 284)	+3527	119
Me_2TlNO_3	1·0	D_2O		(57·884 457)	+3478	121
Me_2TlNO_3	1·0	H_2O		(57·884 169)	+3473	121
Me_2TlNO_3	0·8	H_2O	29	57·886 757	+3518	71
Me_2TlNO_3	0·5	H_2O	26	(57·886 757)	+3518	40
Me_2TlNO_3	0·2	H_2O	29	57·886 755	+3518	71
Me_2TlNO_3	∞-dil. (0·0005)	H_2O	23	57·886 561	+3514	74
Me_2TlNO_3		D_2O	37	(57·886 76)[c]	+3518	91
Me_2TlNO_3	∞-dil. (0·001)	Formamide	23	57·884 390	+3477	74
Me_2TlNO_3	0·6	CH_3OH		(57·881 977)	+3435	121
Me_2TlNO_3	∞-dil. (0.008)	DMSO	23	57·882 828	+3450	74
Me_2TlNO_3	0·2	DMSO	29	57·881 787	+3432	71
Me_2TlNO_3	0·4	DMSO		(57·881 342)	+3424	119
Me_2TlNO_3	1·0	DMSO	29	57·880 949	+3417	71
Me_2TlNO_3	1·2	DMSO		(57·879 554)	+3393	121
Me_2TlNO_3	∞-dil. (0·001)	NMF	23	57·882 261	+3440	74
Me_2TlNO_3	∞-dil. (0·0025)	NEF	23	57·882 167	+3438	74
Me_2TlNO_3	1·2	Pyridine		(57·879 208)	+3387	121
Me_2TlNO_3	1·0	Pyridine	29	57·889 683	+3569	71
Me_2TlNO_3	0·4	Pyridine		(57·881 862)	+3433	119
Me_2TlNO_3	0·2	Pyridine	29	57·880 456	+3409	71
Me_2TlNO_3	∞-dil. (0·006)	Pyridine	23	57·881 361	+3424	74

TABLE II (*cont.*)

Compound	Conc./M[a]	Solvent	Temp./°C	Ξ/MHz[b]	Chemical shift/ppm[j]	Reference
Me_2TlNO_3	∞-dil. (0·005)	DMF	23	57·882 417	+3443	74
Me_2TlNO_3	0·4	DMF		(57·879 150)	+3386	119
Me_2TlNO_3	1·2	DMF		(57·878 401)	+3373	121
Me_2TlNO_3	0·4	DMA		(57·877 824)	+3363	119
Me_2TlNO_3	∞-dil. (0·011)	HMPA	23	57·876 826	+3346	74
Me_2TlNO_3	0·4	HMPA		(57·875 401)	+3321	119
Me_2TlNO_3	1·2	HMPA		(57·874 478)	+3305	121
$MeTlNO_3$	0·4	0·49 Pyridine/0·51 DMF		(57·879 035)	+3384[l]	119
Me_2TlNO_3	0·4	0·53 pyridine/0·47 DMA		(57·878 170)	+3369[l]	119
Me_2TlNO_3	0·4	0·68 pyridine/0·32 HMPA		(57·876 670)	+3343[l]	119
Me_2TlNO_3	0·4	0·67 DMA/0·33 HMPA		(57·875 343)	+3320[l]	119
Me_2TlOAc	0·4	H_2O	29	57·886 824	+3519	100
Et_2TlBr		DMSO		(57·881 631)	+3429	121
Et_2TlNO_3		DMSO		(57·867 037)	+3176	121
Pr^n_2TlBr		DMSO		(57·883 881)	+3468	121
$Pr^n_2TlNO_3$		DMSO		(57·869 748)	+3223	121
Ph_2TlBr		DMSO		(57·867 556)	+3185	121
Ph_2TlCl	5%	NH_3(liq.)	−20	57·867 5[c]	+3184	80
$PhTlCl_2 \cdot PPh_3$		Pyridine	24	(57·872 921)	+3278	121
$PhTlCl_2 \cdot$dipy		Pyridine	24	(57·862 249)	+3093	121
$PhTlCl_2$		Pyridine	24	(57·861 903)	+3087	121
$PhTlCl_2$		CH_3OH	24	(57·856 250)	+2989	121
$MeTl(OAc)_2$	1·0	MeOH	29	57·864 691	+3135	100
$MeTl(OAc)_2$	0·8	$CHCl_3$	29	57·861 186	+3075	100
2,4,6-$Me_3C_6H_2Tl(TFA)_2$	0·4	CH_3CN	25	57·852 831	+2930	72
2,4,6-$Me_3C_6H_2Tl(TFA)_2$	0·4	THF	25	57·852 013	+2916	72
2,4,6-$Me_3C_6H_2Tl(TFA)_2$	0·4	DMSO	25	57·850 376	+2887	72
2,4-$Me_2C_6H_3Tl(TFA)_2$	0·4	DMSO	25	57·848 509	+2855	72

TABLE II (*cont.*)

Compound	Conc./M[a]	Solvent	Temp./°C	Ξ/MHz[b]	Chemical shift/ppm[i]	Reference
$2,5\text{-}Me_2C_6H_3Tl(TFA)_2$	0·4	DMSO	25	57·847 228	+2833	72
$3,4\text{-}Me_2C_6H_3Tl(TFA)_2$	0·4	THF	25	57·851 579	+2908	72
$3,4\text{-}Me_2C_6H_3Tl(TFA)_2$	0·4	DMSO	25	57·846 961	+2828	72
$2,4,6\text{-}Me_3C_6H_2Tl(TFA)_2$	0·4	MeOH	25	57·851 176	+2901	72
$4\text{-}MeC_6H_4Tl(TFA)_2$	0·4	THF	25	57·851 056	+2899	72
$4\text{-}MeC_6H_4Tl(TFA)_2$	0·4	DMSO	25	57·846 326	+2817	72
$C_6H_5Tl(TFA)_2$	0·4	THF	25	57·849 483	+2872	72
$C_6H_5Tl(TFA)_2$	0·4	DMSO	25	57·844 746	+2790	72
$4\text{-}Bu^tC_6H_4Tl(TFA)_2$	0·4	DMSO	25	57·846 367	+2818	72
$4\text{-}Pr^iC_6H_4Tl(TFA)_2$	0·4	DMSO	25	57·846 679	+2823	72
$4\text{-}Pr^nC_6H_4Tl(TFA)_2$	0·4	DMSO	25	57·846 271	+2816	72
$4\text{-}EtC_6H_4Tl(TFA)_2$	0·4	DMSO	25	57·846 342	+2817	72
$4\text{-}BrC_6H_4Tl(TFA)_2$	0·4	DMSO	25	57·844 119	+2779	72
$4\text{-}FC_6H_4Tl(TFA)_2$	0·4	DNSO	25	57·843 958	+2776	72
$4\text{-}ClC_6H_4Tl(TFA)_2$	0·4	DMSO	25	57·843 577	+2769	72
$Zn(TlCl_4)_4$		Solid		(57·854 58)	+2960	17
$(NH_4)_3(TlCl_6)$		Solid		(57·811 89)	+2220	17
$K_3(TlCl_6)$		Solid		(57·811 89)	+2220	17
$TlCl_3{\cdot}4H_2O$		Solid	27·2	(57·802 14)	+2051	67
$TlCl_3{\cdot}4H_2O$		Solid		(57·854 58)	+2960	
				(57·833 23)	+2590	17
				(57·811 89)	+2220	
$TlCl_3$		Solid	25	(57·827 18)	+2485	184
$TlCl_3$		Melt	25	(57·832 95)	+2585	64
$TlCl_3$		Melt	25	(57·828 91)	+2515	184
$TlCl_3$	8·0	H_2O	24	(57·831 100)	+2553	121
$TlCl_3$	Dilute	H_2O	25±3	(57·819 39)	+2350	5
$TlCl_3$	0·3	H_2O		(57·817 37)	+2315	9

TABLE II (*cont.*)

Compound	Conc./M[a]	Solvent	Temp./°C	Ξ/MHz[b]	Chemical shift/ppm[i]	Reference
$TlCl_3$	∞-dil. (0·1)	H_2O		(57·816 91)	+2307	65
$Tl(ClO_4)_3·6H_2O$		Solid	27·2	(57·809 30)	+2175	67
Me_2TlBr		Solid	35	58·006 50	+5590 (isotropic)	198
$KTlCl_4$		Solid	27·2	(57·840 50)	+2716	67
$Cs_2TlCl_5·H_2O$		Solid	27·2	(57·800 47)	+2022	67
$Na_2TlCl_5·4H_2O$		Solid	27·2	(57·798 28)	+1984	67
$Na_3TlCl_6·12H_2O$		Solid	27·2	(57·797 59)	+1972	67
$K_3TlCl_6·2H_2O$		Solid	27·2	(57·799 60)	+2007	67
$[Co(NH_3)_6]TlCl_6$		Solid	27·2	(57·800 30)	+2019	67
$Cs_3Tl_2Cl_9$		Solid	27·2	(57·794 93)	+1926	67
$KTlBr_4·2H_2O$		Solid	27·2	(57·756 63)	+1262	67
$[Co(NH_3)_6]TlBr_6$		Solid	27·2	(57·610 52)	−1271	67
$Cs_3Tl_2Br_9$		Solid	27·2	(57·614 96)	−1194	67
$[NBu_4]TlI_4$		Solid	27·2	(57·593 85)	−1560	67
Tl_2Cl_4		Melt	*c.* 230	(57·714 41)	+530	20
				(57·849 66)	+2840	
$TlPO_3$	*c.* 298	Glassy		(57·680 95)	−50	197
$TlPO_3$	*c.* 298	Crystalline		(57·661 34)	−390	197
$Tl_{0·3}WO_3$		Solid	27	(57·714 98)	+540	204
$Tl(ClO_4)_3$		Solid		(57·797 18)	+1965	184
$Tl(ClO_4)_3$		Melt	*c.* 100	(57·792 57)	+1885	184
$Tl(NO_3)_3$	1·5	H_2O	25±3	(57·790 55)	+1850	5
$Tl(NO_3)_3$[h]	0·6	H_2O		(57·684 70)	+15	64
$Tl(NO_3)_3$	0·69	1·5 M HNO_3		(57·793 43)	+1900	65
$Tl(NO_3)_3$	0·61	1·5 M HNO_3		(57·791 12)	+1860	65
$Tl(NO_3)_3$	∞-dil. (0·25)	∞-dil. HNO_3(0·125)		(57·833 35)	+2592	65
$TlBr_3·4H_2O$		Solid	27·2	(57·747 17)	+1098	67

TABLE II (*cont.*)

Compound	Conc./M[a]	Solvent	Temp./°C	Ξ/MHz[b]	Chemical shift/ppm[j]	Reference
$TlBr_3$	0·29	H_2O	27·2	(57·755 07)	+1235	65
Tl(III)	0·05	Conc. HCl	27·2	(57·562 93)	+2096	67
Tl(III)	0·05	Conc. HBr	27·2	(57·616 40)	+1169	67
Tl(III)	0·05	Conc. $HClO_4$	27·2	(57·565 24)	+2056	67
$(TlOEt)_4$		Melt		57·852 00[i]	+2915	64
$(TlOEt)_4$		Melt	24	(57·850 712)	+2893	21
$(TlOEt)_4$		C_6H_6	37	(57·852 10)	+2917[k]	91
TlI		Solid	25	57·777 88	+1630	191
TlI		Solid		(57·817 66)	+2320	9
TlI		Solid	24	(57·794 18)	+1913	21
TlI		Solid	20	(57·790 26)	+1845	184
TlI		Melt	430	(57·809 01)	+2170	184
TlBr		Solid	20	(57·747 29)	+1100	184
TlBr		Solid		(57·745 55)	+1070	9
TlBr		Solid	24	(57·732 46)	+843	21
TlBr		Solid		(57·731 13)	+820	192
TlBr		Solid	24	(57·727 27)	+753	185
TlBr		Melt	480	(57·777 28)	+1620	184
TlCl		Solid	20	(57·702 58)	+325	184
TlCl		Solid		(57·718 44)	+600	9
TlCl		Solid	24	(57·706 50)	+393	21
TlCl		Solid		(57·706 93)	+383	193
TlCl		Solid	24	(57·705 93)	+383	185
TlCl		Solid		(57·698 25)	+250	192
TlCl		Melt	430	(57·755 94)	+1250	184
TlF		Solid		(57·728 83)	+780	9
TlF		Solid	20	(57·758 82)	+1300	184
TlF		Solid		(57·723 06)	+680	193

TABLE II (*cont.*)

Compound	Conc./M[a]	Solvent	Temp./°C	Ξ/MHz[b]	Chemical shift/ppm[l]	Reference
TlF		Melt	327	(57·763 44)	+1380	184
Tl_3PO_4		Solid	24	(57·797 07)	+1963	185
Tl_3PO_4		Solid	24	(57·797 07)	+1963	193
TlO_2CH		Solid		(57·747 29)	+1100	9
TlO_2CH		Melt	101	57·724 61	+707	194
$TlOAc^m$		Solid	20	(57·711 23)	+475	184
$TlOAc^m$		Solid	25±3	(57·709 04)	+437	5
$TlOAc^m$		Melt	110 (m.p.)	(57·730 38)	+807	184
$TlOAc^m$		Melt	110 (m.p.)	57·732 11	+837	194
$TlOAc^m$		Melt	132 (m.p.)	57·738 06	+940	194
Tl_2CO_3		Solid	38	57·677 63	−108	195
Tl_2CO_3		Solid	100	57·680 04	−66	195
Tl_2CO_3		Solid		(57·747 86)	+1110	9
Tlcp		Solid	24	(57·707 94)	+418	230
Tl_2SO_4		Solid		(57·688 45)	+80	9
Tl_2SO_4		Solid	20	(57·681 24)	−45	184
Tl_2SO_4		Solid	24	(57·677 66)	−107	193
Tl_2SO_4		Solid	24	(57·677 66)	−107	21
Tl_2SO_4		Solid	32	57·677 46	−110	195
Tl_2SO_4		Melt	632	(57·714 41)	+530	184
$TlNO_3$		Solid		(57·699 41)	+270	9
$TlNO_3$		Solid	32	57·676 07	−135	225
$TlNO_3$		Solid	20	(57·676 05)	−135	184
$TlNO_3$		Solid	24	(57·675 25)	−147	193
$TlNO_3$		Solid	24	(57·675 35)	−147	21
$TlNO_3$		Melt	206	(57·693 06)	+160	184
$TlClO_4$		Solid		(57·661 91)	−380 MHz	9

TABLE II (*cont.*)

Compound	Conc./M[a]	Solvent	Temp./°C	Ξ/HMz[b]	Chemical shift/ppm[i]	Reference
$TlClO_4$		Solid	34	57·653 61	−524 (isotropic)	227
Tl^+/valinomycin(ClO_4^-)		Solid	28	57·652 44	−544 (isotropic)	199 199
Tl^+/gramicidin A(OAc^-)		Solid	61	57·674 00	−160	196
$Tl_2SeAs_2Te_3$				(57·783 05)	+1720	200
$(Tl_2Se)_{0\cdot1}(As_2Se_3)_{0\cdot9}$		Glassy	25	(57·730 56)	+890	201
$(Tl_2Se)_{0\cdot33}(As_2Se_3)_{0\cdot67}$		Glassy	25	(57·775 55)	+1670	201
$(Tl_2Se)_{0\cdot67}(As_2Se_3)_{0\cdot33}$		Glassy	25	(57·793 43)	+1980	201
$(Tl_2O)_{0\cdot35}(B_2O_3)_{0\cdot65}$		Glassy	25	(57·742 67)	+1020	202
$(Tl_2O)_x(SiO_2)_{1-x}$, $0\cdot09 \leqslant x \leqslant 0\cdot40$		Glassy	25	(57·795 16)	+1930	202
$TlClO_4$	∞-dil. (0·2)[e]	en		(57·807 68)	+2147	23
$TlBF_4$	∞-dil. (0·2)	*n*-Butylamine		(57·796 78)	+1958	22
$TlClO_4$	∞-dil. (0·2)	*n*-Butylamine		(57·793 20)	+1896	23
$TlNO_3$	∞-dil. (0·2)	*n*-Butylamine		(57·782 36)	+1708	22
$TlNO_3$	∞-dil. (0·002)	*n*-Butylamine	25	57·790 444	+1848	27
$TlNO_3$	∞-dil. (0·0008)	NH_3(liq.)	25	57·788 767	+1819	30
$TlClO_4$	∞-dil. (0·0016)	NH_3(liq.)	25	57·788 767	+1819	30
$TlClO_4$	∞-dil. (0·2)[e]	Pyrrolidine		(57·785 18)	+1757	23
$TlClO_4$	∞-dil. (0·2)	Et_2NH		(57·729 63)	+794	23
$TlNO_3$	∞-dil. (0·002)	Pyridine	25	57·729 028	+783	25
$TlClO_4$	∞-dil. (0·2)	Pyridine		(57·722 14)	+664	23
$TlNO_3$	∞-dil. (0·002)	DEA	25	57·714 444	+531	25
$TlNO_3$	∞-dil. (0·02)	HMPA	25	57·712 806	+502	27
$TlClO_4$	∞-dil. (0·2)[e,d]	HMPA		(57·709 39)	+443	23
$TlClO_4$	∞-dil. (0·2)	Pyrrole		(57·654 64)	−506	22
$TlNO_3$	∞-dil. (0·002)	Pyrrole	25	57·661 389	−389	27
Tl/2,2,1	*c.* 0·2		25	57·719	+600	41

TABLE II (*cont.*)

Compound	Conc./M[a]	Solvent	Temp./°c	Ξ/MHz[b]	Chemical shift/ppm[i]	Reference
Tl/2,2,28	*c.* 0·2		25	57·687	+62	41
Tl/2,2,2	*c.* 0·2		25	57·686	+62	41
$TlClO_4$/15C5	*c.* 0·2	DMSO	29	(57·696 24)[g]	+215[g]	43
$TlClO_4$/DB18C6	*c.* 0·2	DMSO	29	(57·695 31)[g]	+199[g]	43
$TlClO_4$/DCH18C6	*c.* 0·2	DMSO	29	(57·690 35)[g]	+113[g]	43
$TlClO_4$/C222	*c.* 0·2	DMSO	29	(57·687 41)	+62	43
$TlClO_4$/C222	*c.* 0·2	Pyridine	29	(57·686 37)	+44	43
$TlClO_4$/18C6	*c.* 0·2	DMSO	29	(57·682 28)	−27[g]	43
TlOAc/DB18C6	*c.* 0·3	MeOH	*c.* 29	(57·681 81)[g]	−35[g]	26
TlOAc/18C6	*c.* 0·3	MeOH	*c.* 29	(57·679 80)[g]	−70[g]	26
$TlClO_4$/DB18C	*c.* 0·3	DMF	*c.* 29	(57·677 49)[g]	−110[g]	26
$TlNO_3$/18C6	*c.* 0·01	$CHCl_3$	23	57·674 600	−160	185
$TlClO_4$/18C6	*c.* 0·3	DMF	*c.* 29	(57·673 45)[g]	−180[g]	26
Tl^+/lasalocid	0·1	$CDCl_3$	24	57·700 321	+294·5	52
Tl^+/nigericin$^-$	0·005	$CHCl_3$	23	57·691 727	+137	55
Tl/monensin acid	0·1	$CHCl_3$	23	57·691 572	+134	55
Tl^+/monensin$^-$	0·12	$CHCl_3$	23	57·689 990	+106·7	55
				57·689 409	+96·7	
Tl^+/nigercin$^-$	0·69	$CHCl_3$	23	57·689 661	+101	55
Tl^+/nonactin	0·10	$CHCl_3$	24	57·668 739	−261·7	54
Tl^+/monactin	0·09	$CHCl_3$	24	57·668 728	−261·9	54
Tl^+/dinactin	0·13	$CHCl_3$	24	57·668 706	−262·2	54
Tl^+/valinomycin	0·09	$CHCl_3$	23	57·652 653	−541	53
Tl^+/gramicidin	0·003	Dioxane	50	57·644 397	−675	49
$TlNO_3$	0·3	H_2O		(57·683 43)	−7	8
$TlNO_3$	0·3	H_2O (and 0·15 M OAc^-)		(57·684 87)	+18	8
$TlNO_3$	0·3	H_2O (and 0·15 M citrate)		(57·693 52)	+168	8
$TlNO_3$	0·3	H_2O (and 0·15 M $Fe(CN)_6^{3-}$)		(57·736 79)	+918	8

TABLE II (*cont.*)

Compound	Conc./M[a]	Solvent	Temp./°C	Ξ/MHz[b]	Chemical shift/ppm[i]	Reference
$TlNO_3$	0·5	H_2O	26	(57·683 20)	−11	40
$TlNO_3$	0·5	H_2O (and 0·25 M en)	26	(57·691 16)	+127	40
$TlNO_3$	0·5	H_2O (and 0·5 M en)	26	(57·699 98)	+280	40
$TlNO_3$	0·5	D_2O	26	(57·682 74)	−19	40
$TlNO_3$	0·5	D_2O (and 0·25 M en)	26	(57·694 39)	+183	40
$TlNO_3$	0·5	D_2O (and 0·5 M en)	26	(57·705 35)	+373	40
TlOAc	1·0	H_2O	26	(57·685 91)	+36	40
TlOAc	1·0	H_2O (and 0·25 M en)	26	(57·694 39)	+183	40
TlOAc	*c.* 0·3	MeOH		(57·713 37)	+512	26
$TlClO_4$	∞-dil. (0·2)[e]	MeOH[f]		(57·685 85)[f]	+35[f]	22
$TlClO_4$	∞-dil. (0·2)[e]	DMSO		(57·705 12)	+369	23
$TlNO_3$	∞-dil. (0·002)	DMSO	25	57·704 606	+360	25
$TlNO_3$	∞-dil. (0·002)	NEF	25	57·701 506	+306	25
$TlNO_3$	∞-dil. (0·002)	NEA	25	57·699 961	+280	25
$TlNO_3$	∞-dil. (0·002)	NMF	25	57·693 139	+161	25
$TlNO_3$	∞-dil. (0·002)	DMF	25	57·692 222	+145	27
$TlClO_4$	∞-dil. (0·2)[e]	DMF		(57·690 99)	+124	22
$TlClO_4$	∞-dil. (0·2)[e]	DMA		(57·691 101)	+126	23
$TlNO_3$; $TlClO_4$	∞-dil. (0·2)[e]	Formamide		(57·689 37)	+96	23
$TlNO_3$	∞-dil. (0·002)	Formamide	25	57·688 244	+77	25
$TlNO_3$	∞-dil. (0·002)	H_2O	25	57·683 833	0	25
TlF;TlOAc;TlO_2CH; $TlClO_4$; $TlBF_4$	∞-dil. (0·2)[e]	H_2O		(57·683 83)	0	23
$TlClO_4$	0·2	$(Bu^nO)_3PO$[f]		(57·682 68)[f]	−20[f]	22
$TlClO_4$	0·2	THF[f]		(57·679 22)[f]	−80[f]	22
$TlClO_4$	0·2	Methylacetate[f]		(57·676 33)[f]	−130[f]	22
$TlClO_4$	0·2	*p*-Dioxane[f]		(57·676 33)[f]	−130[f]	22
$TlClO_4$	0·2	DME		(57·674 03)[f]	−170[f]	22

TABLE II (*cont.*)

Compound	Conc./M[a]	Solvent	Temp./°C	Ξ/MHz[b]	Chemical shift/ppm[i]	Reference
$TlClO_4$	0·2	Acetone[f]		(57·669 99)[f]	−240[f]	22
$TlClO_4$	0·2	Propylene carbonate[f]		(57·656 72)[f]	−470[f]	22
TlO_2CH	1·0	H_2O (and 0·5 M en)	26	(57·701 60)	+308	40
TlO_2CH	1·0	D_2O	26	(57·685 62)	+31	40
TlO_2CH	1·0	D_2O (and 0·25 M)	26	(57·695 14)	+196	40
TlO_2CH	1·0	D_2O (and 0·5 M en)	26	(57·705 23)	+371	40

[a] As molarity unless otherwise indicated. Values in parentheses for infinite dilution extrapolations denote lowest concentration measured.

[b] Resonance frequency at magnetic field strength giving a TMS ^1H resonance frequency of exactly 100 MHz. Values in parentheses calculated from chemical shifts.

[c] Measured by $^1H\{^{205}Tl\}$ INDOR.

[d] Two-point extrapolation.

[e] Extrapolated to infinite dilution anion concentration.

[f] Thallium salt insoluble in this solvent; shift and frequency calculated from an iterative extrapolation of mixed solvent data.

[g] Calculated frequency (and shift) of the Tl^+/crown complex; obtained by an iterative fitting procedure, averaged from shifts for different anions and competing cations. These individual shifts often varied largely (*c.* 100 ppm).

[h] Probably $TlNO_3$ rather than $Tl(NO_3)_3$.

[i] Because of the uncertainty of the standard in reference (see preceding footnote, *h*), this frequency was measured in the authors' laboratory at the University of Arkansas.

j Shift values for compounds from each literature reference are internally consistent; uncertainties propagated in calculating chemical shifts (or frequencies) with respect to the single reference of aqueous $TlNO_3$ are ±5–15 ppm, occasionally as great as ±50 ppm, for comparison of shifts from different laboratories.

[k] Reference 133 incorrectly lists the shift of $(TlOEt)_4$ in C_6H_6 as +111 ppm, rather than −599 ppm, with respect to aqueous Me_2TlNO_3. Its listing of chemical shifts with respect to $MeTlNO_3$ for Me_3Tl in acetone at −70 °C and Me_2TlBr in liquid NH_3 at −30 °C, calculated from the (correct) frequencies of reference 130, are also erroneous and should be +986 and +26 ppm, respectively. In reference 133, the frequency ratios for $(Me_2TlNMe_2)_2$ in C_6H_6, and $(Me_2TlOEt)_2$ in C_6H_6 and in toluene (all at 37 °C), are in error and should be 0·579 161 1, 0·579 057 8, and 0·579 053 8.[232]

[l] Reference 247 lists the obviously incorrect values of 3165 ppm (pyridine/DMF), 3150 ppm (pyridine/DMA), 3124 ppm (pyridine/HMPA), and 3101 ppm (DMA/HMPA). The values tabulated here were obtained on the assumption that the wrong modulation side band was detected (upfield rather than downfield), which would result in an error of −218·8 ppm. Note; the shifts corrected in this manner for the pyridine/DMF and DMA/HMPA systems fall outside the range of the pure solvent values.

[m] Exceedingly pure TlOAc melts at 131 °C while slightly impure TlOAc melts sharply at 110 °C.

in determining the chemical shift is not the total shielding, but the shielding per valence electron. For thallium, the diamagnetic contribution per valence electron is of the order of 100–250 ppm. This is small compared to the observed chemical shift range of about 7000 ppm. This means that the paramagnetic term must be responsible for about 95% of the variation observed in thallium chemical shifts.

The direct measurement of the paramagnetic shielding is a rather difficult problem. One method of determining the value of the paramagnetic term for the thallium nucleus would be to obtain the shielding anisotropy from the NMR spectrum of this nucleus in a linear molecule in the solid state. Since the parallel component of the paramagnetic term is zero in the linear molecule, the measured anisotropy gives the value of the paramagnetic term.[6] If the anisotropy in the paramagnetic term must be corrected for the diamagnetic anisotropy, the method of Flygare can be used.[7] For the covalently bonded thallium nucleus, the chemical shielding anisotropy (CSA) is probably several thousand ppm.

1. Ion–solvent interactions

Conceptually, the simplest system to study in solution would be an ion interacting with only one type of solvent molecule. Here one would be interested in relating the resonance frequency of the ion to some property of the solvent, such as basicity, which reflects the strength of interaction between the ion and the solvent molecule. In practice, however, such a study can be rather difficult since it requires one to obtain the "infinite dilution" resonance frequency of the ion (i.e. the resonance frequency in the absence of any effect due to ion pairing). In solvents of low polarity, ion pairing dominates the ionic equilibrium. Consequently, one must obtain the resonance frequency of the nucleus as a function of decreasing salt concentration to define the resonance frequency–salt concentration curve well enough to extrapolate to the "infinite dilution" resonance frequency. The extreme sensitivity of the thallium resonance frequency to its chemical environment (e.g. the difference in thallium chemical shift between the Tl^+–NO_3^- ion pair in liquid ammonia and the Tl^+ ion at infinite dilution is 66 ppm) and the non-linear relationship between the resonancy frequency and salt concentration makes this extrapolation dangerous. It is advisable in such studies to use several salts whose anions are quite different, to approach the "infinite dilution" point from more than one position on the resonance frequency–concentration plot. A computer analysis of the resonance frequency–concentration curve for each salt then yields the "infinite dilution" resonance frequency value for a particular solvent.

The resonance frequency–salt concentration relationship for the association process,

$$Tl^+ + A^- \rightleftharpoons Tl^+A^- \qquad (1)$$

may be described by the equation

$$\delta_{obs} = \chi_f \delta_f + \chi_{ip} \delta_{ip} = (C_f/C_t)(\delta_f - \delta_{ip}) + \delta_{ip} \quad (2)$$

where δ_f and δ_{ip} are the "infinite dilution" resonance frequencies or chemical shifts of the free (solvated) and ion-paired cation, respectively, while χ_f and χ_{ip} are the corresponding mole fractions, and C_f and C_t are the free and total cation concentrations, respectively. For the association process described by equation (1), the ion pair formation constant for the equilibrium may be written as

$$K_{ip} = [Tl^+A^-]/\gamma_\pm^2[Tl^+][A^-] \quad (3)$$

where $\gamma_\pm$ is the mean activity coefficient which can be calculated from the Debye–Hückel equation. Equation (2) may be used to obtain the free cation concentration. From initial estimates of δ_f and δ_{ip} and the experimentally determined values of δ_{obs}, C_f can be calculated for each C_t value and then used to calculate $\gamma_\pm$ for each C_t. Equation (3) then yields a K_{ip} for each point; the average of these ion pair formation constants may be used to calculate a theoretical resonance frequency or chemical shift for each concentration. Computer analysis is then used to determine K_{ip} by varying δ_f and δ_{ip} to minimize variations between calculated and observed shifts. Consequently, this type of analysis not only gives the "infinite dilution" resonance frequency or chemical shift but also the ion pair formation constant and the resonance frequency of the ion pair.

The concentration and anion dependence of the chemical shift of thallous salts in aqueous solutions[8–21] and in non-aqueous solutions[22–31] have been investigated. The anion and concentration dependence of the Tl(I) ions are in the range of 10–100 ppm. "Infinite dilution" resonance frequencies or chemical shifts are found in Table II. A correlation between the "infinite dilution" resonance frequency of the Tl(I) ion and the Gutman donor number,[32] a measure of solvent basicity, has been made for a number of different solvents.[31] This relationship indicates that the more basic the solvent, the higher the resonance frequency of the Tl(I) ion. The increase in resonance frequency with increasing solvent basicity may be viewed as a measure of the strength of interaction between the ion and solvent molecules, with the solvent acting as a Lewis base and interacting electrostatically and covalently with the ion. Transient orbital mixing created by ion–solvent collision-induced polarization of the ion electron cloud may also contribute to the observed resonance frequency changes.

The ion pair association constant and ion pair chemical shift, δ_{ip}, have been determined for a number of solvents using the method described above.[29] As expected, K_{ip} was found to increase with decreasing dielectric constant of the solvent.

In general thallium(I) salts show low solubility in most solvents, even water. However, liquid ammonia is an excellent solvent for $TlNO_3$ and $TlClO_4$. The Tl(I) resonance frequency has been determined for liquid ammonia solution of these salts as a function of electrolyte concentration (0·005–9·8 M) and temperature.[30] The dependence of the resonance frequency on concentration suggests the presence of free, fully solvated thallium ions, ion pairs, and higher order aggregates as the concentration increases. Analysis of the low concentration data between 0 and 30 °C allows the determination of $TlNO_3$ ion pair association constants and thermodynamic parameters ($\Delta H = +6{\cdot}5$ kcal mol^{-1}, $\Delta S = +36$ e.u.). A precipitous decrease in the resonance frequency is observed for NH_3 to $TlNO_3$ mole ratios below 3 : 1, suggesting the formula $(NH_3)_3Tl^+NO_3^-$ for the fully solvated, contact ion pair. It is interesting to note that a change of approximately 2000 ppm occurs in the Tl(I) chemical shift in going from the $TlNO_3$ melt to Tl(I) at "infinite dilution" for $TlNO_3$ dissolved in liquid ammonia. One word of caution seems in order when comparing data on ion pairing obtained by NMR techniques with that from conductance measurements on the same system. Conductance measurements recognize as ion pairs all species in which the component ions are not free to conduct, including contact, solvent-shared, and solvent-separated ion pairs. NMR more easily monitors contact and solvent-separated ion pair equilibria, but differentiates less distinctly between free ions and solvent-separated ion pairs. It may be that in solvents of low dielectric constant, disparities between NMR and conductance data reflect the fact that the magnetic resonance technique monitors the equilibrium between contact and solvent-separated ion pairs, while conductance monitors the equilibrium between free ions and ion pairs.

The exceptional sensitivity of the thallous ion resonance frequency to its solvent environment (e.g. about 2000 ppm change in going from water to liquid ammonia), makes this ion an excellent probe for studying ion–solvent interactions in mixed solvent systems.[22,23,25,31,33,34] Using a model for preferential solvation in mixed solvent systems based upon a non-statistical distribution of solvate species,[35–39] the chemical shift for 0·005M $TlNO_3$ in nine binary solvent systems has been analysed.[34] The theory is used to obtain equilibrium constants and free energies of preferential solvation as one type of solvent molecule replaces another type in the solvation sphere of the ion.

Solvent isotope shifts for H_2O and D_2O have been observed to vary with concentration and anion by as much as 10 ppm and, in the case of the complexation of Tl(I) with ethylenediamine, by 100 ppm.[40]

The interaction between the Tl(I) ion and cryptands[41] and crown ethers[26,42,43] has been investigated using ^{205}Tl NMR. Thallium-205 studies were performed on Tl(I) complexes of the cryptands (2, 2, 1), (2, 2, 2) and

(2, 2, 2B) in a number of non-aqueous solvents and in water.[41] The chemical shift of the ion complexed by a particular cryptand is found to be independent of solvent and anion, suggesting that the Tl(I) ion is completely shielded by the cryptand. It is also found that the ion resonance signal moves to low frequency with an increasing number of oxygen atoms in the ligands. The formation constants for complexes of the crown ethers, dibenzo-21-crown-7 and dibenzo-24-crown-8 with the Tl(I) ion have been determined in several non-aqueous solvents at 30 °C.[42]

B. Biological studies

Because of its similarities to the alkali metal cations Na(I) and K(I), the Tl(I) ion has been used as a probe for studying Na(I) and K(I) functions in biological systems. Arnold and Scholl[44] studied the ^{205}Tl(I) chemical shift of 0·1 M $TlNO_3$ as a function of pH in 0·0125 M and 0·025 M phosphate solutions, observing high frequency shifts of 13·5 ppm and 27 ppm at the second H_3PO_4 dissociation point. They also observed a 5·75 ppm high frequency shift for a D_2O solution of $TlNO_3$ and dipalmitoylphosphatidylcholine (DPPC) as the Tl(I):DPPC ratio decreases and as the temperature is lowered through the thermal phase transition point of DPPC. Reuben and Kayne determined the effect of the presence of pyruvate kinase and its substrates on the chemical shift, T_1 and T_2 of the ^{205}Tl(I) ion.[45,46] Longitudinal relaxation rates of ^{205}Tl(I) were used to show that the monovalent cation binding site in (Na(I)–K(I))-ATPase is very near the divalent cation binding site.[47,48]

The interactions between the Tl(I) ion and antibiotic molecules to form complexes similar to those found in membrane systems and involved in ion transport across the membrane have been studied in non-aqueous solutions and in a model membrane system.[49–55] The chemical shift range of Tl(I) in the antibiotic complexes is approximately 1000 ppm (Table II). There appears to be qualitative agreement between the chemical shift and the basicity of the binding functional groups much the same as found with the Tl(I) ion in solvents of different basicity (i.e. increasing basicity produces high frequency shifts). The association of the Tl(I) ion with gramicidin in 2,2,2-trifluoroethanol has been studied, and the data obtained suggest that the gramicidin dimer has two strong binding sites and possibly one or more weak binding sites. From the temperature dependence of the strong binding site association constant, as determined from the ^{205}Tl(I) chemical shift, values for the association enthalpy and entropy of $-2{\cdot}13$ kcal mol^{-1} and 5·45 e.u., respectively, are obtained.[51] The interaction between the Tl(I) ion and gramicidin dimers incorporated into micelles has been investigated using ^{205}Tl(I) NMR techniques.[50] The chemical shift data are interpreted in terms of a model in which the dimer has only one tight binding site. The binding constant for this site is calculated to be 900 M^{-1} at 30 °C.

C. Relaxation

The spin–lattice relaxation rate for the Tl(I) ion has been shown to be extremely sensitive to environmental effects. The longitudinal relaxation rate of the Tl(I) ion in aqueous solution has been found to increase linearly with added paramagnetic $Fe(CN)_6^{-3}$ up to a concentration of 0·01M.[56] A large, linear increase in the spin–lattice relaxation rate with dissolved oxygen up to an oxygen partial pressure of five atmospheres has been reported.[40,57] As can be seen in Table III, the spin–lattice relaxation time for the ^{205}Tl(I) ion in aqueous solution changes from 0·12 to 1·85 s as the oxygen pressure decreases from 0·2 atm to zero, respectively.[57] At 1 atm oxygen pressure, the spin–lattice relaxation time is 0·024 s (i.e. the relaxation time changes by a factor of 77 compared to a degassed solution). This oxygen dependence can be used to advantage since it normally provides a relaxation mechanism which allows faster pulsing and, hence, more rapid spectral accumulation. It has also been reported that the ^{205}Tl(I) and ^{203}Tl(I) relaxation rates are equal in aqueous solution, i.e. $T_2 = T_1$, and that the relaxation rates are independent of solvent isotopic substitution (D_2O, H_2O), concentration 0·03–2·0 M), anion, and resonance frequency[40,57] (Table III). The spin–lattice relaxation time of the ^{205}Tl(I) ion is solvent dependent, ranging from 0·8 s in *n*-butylamine[58] to 1·85 s in methanol.[40]

Reeves[40,57] suggested that in aqueous solution the Tl(I) spin–lattice relaxation is dominated by the spin–rotation mechanism. The temperature dependence of the spin–lattice relaxation time of the Tl(I) ion in aqueous solution does, indeed, show the dominance of the spin–rotation mechanism.[58] However, in non-aqueous solvent systems the spin–lattice relaxation time of the Tl(I) ion shows a strong dependence on the CSA mechanism. The importance of the transient CSA mechanism is illustrated by a concentration and temperature study of the spin–lattice relaxation time of $TlClO_4$ in DMSO.[59] At low temperature and high concentration the spin–lattice relaxation is obviously dominated by the transient CSA mechanism created by the formation of transient ion pairs. However, with the Tl(I)–antibiotic complexes the spin–lattice relaxation time is determined by contributions from the spin–rotation, dipolar and CSA processes in varying degrees depending upon the temperature and particular antibiotic complex.[52–55] The importance of transient spin–rotation and CSA mechanisms for thallium relaxation has been theoretically described,[60] while other mechanisms have been studied experimentally.[61]

The effect of dissolved oxygen on the spin–lattice relaxation time of the Tl(I) ion provides some very useful information about the solution structure of the Tl(I)–antibiotic complexes. In Table III it is noted that only with actin complexes is there no effect of dissolved oxygen on the spin–lattice

TABLE III

^{205}Tl spin-lattice and spin–spin relaxation rates.

Compound	Conc./M	Solvent	Temp./°C	R_1/s^{-1}	R_2/s^{-1}	Added paramagnetic	Reference
TlOAc	4·0	H_2O		$0{\cdot}57+9{\cdot}2\,P_{O_2}$	$1{\cdot}96+37{\cdot}0\,P_{O_2}$	$P_{O_2}=0$–1 atm	187
TlO_2CH	2·0	H_2O	26	$0{\cdot}54+37{\cdot}0\,P_{O_2}$		$P_{O_2}=0$–5 atm	40
TlO_2CH	2·0	H_2O (and 0·5 M *o*-phen)	26	$2{\cdot}0+37{\cdot}2\,P_{O_2}$		$P_{O_2}=0$–5 atm	40
TlO_2CH	2·0	H_2O (and 0·5 M en)	26	$5{\cdot}1+38{\cdot}5\,P_{O_2}$		$P_{O_2}=0$–5 atm	40
TlO_2CH	1·0	MeOH	26	$1{\cdot}1+148{\cdot}6\,P_{O_2}$		$P_{O_2}=0$–5 atm	40
Me_2TlNO_3	0·8	H_2O	26	$1{\cdot}8+1{\cdot}1\,P_{O_2}$[c]		$P_{O_2}=0$–5 atm	40
$TlNO_3$	0·5	H_2O	26	0·54+2·9[en]		None	40
TlO_2CH	1·0	H_2O	26	0·53+9·7[en]		None	40
TlO_2CH	1·0	H_2O	26	0·53+3·1[*o*-phen]		None	40
$TlNO_3$	0·0803	H_2O	26	0·54	0·83	None	57
$TlNO_3$	0·0803	H_2O	26	8·3	9·6	$P_{O_2}=0{\cdot}2$	57
$TlNO_3$	0·0803	H_2O	26	38·0		$P_{O_2}=1{\cdot}0$	57
$TlNO_3$	0·080	H_2O	26	15·3	13	8×10^{-5} M $Fe(CN)_6^{3-}$	57
$TlNO_3$	0·15	H_2O	26	9·9	19	7×10^{-3} M Cu^{2+}	57
$TlNO_3$	0·0839	D_2O	26	0·44	0·8	None	57
$TlNO_3$	0·0839	D_2O	26	8·3	9·6	$P_{O_2}=0{\cdot}2$ atm	57
$TlNO_3$	0·0839	D_2O	26	41·0		$P_{O_2}=1{\cdot}0$ atm	57
$TlNO_3$	0·3	H_2O		8+54 000[$Fe(CN)_6^{3-}$]		[$Fe(CN)_6^{3-}$] = 0–10^{-2} M	8
$TlNO_3$	0·2	H_2O	22	0·57+105 000·[TANOL][a]	0·75+(2×10^6)·[TANOL][a,b]	[TANOL][a] = 0–10^{-3} M	61
$TlNO_3$	0·2	H_2O	10	5·3	161·0	[TANOL][a] = 5×10^{-5} M	61
$TlNO_3$	0·2	H_2O	18	4·8	139·0	[TANOL][a] = 5×10^{-5} M	61
$TlNO_3$	0·2	H_2O	40	5·2	88·0	[TANOL][a] = 5×10^{-5} M	61

TABLE III (*cont.*)

Compound	Conc./M	Solvent	Temp./°C	R_1/s^{-1}	R_2/s^{-1}	Added paramagnetic	Reference
$TlNO_3$	0·2	H_2O	62	5·4	54·0	[TANOL][a] = 5×10^{-5} M	61
$TlNO_3$	0·2	H_2O	83	5·4	45·0	[TANOL][a] = 5×10^{-5} M	61
$TlNO_3$	*c.* 0·2	H_2O	25	0·56		None	27
$TlNO_3$	*c.* 0·2	Pyrrole	25	0·95		None	27
$TlNO_3$	*c.* 0·2	DMF	25	1·52		None	27
$TlNO_3$	*c.* 0·2	Formamide	25	1·47		None	27
$TlNO_3$	*c.* 0·2	NEF	25	2·50		None	27
$TlNO_3$	*c.* 0·2	DMSO	25	5·56		None	27
$TlNO_3$	*c.* 0·2	HMPA	25	1·64		None	27
$TlNO_3$	*c.* 0·1	Pyridine	25	11·1		None	27
$TlNO_3$	*c.* 0·2	*n*-Butylamine	25	12·5		None	27
$TlNO_3$	*c.* 0·2	H_2O	70	0·69		None	27
$TlNO_3$	*c.* 0·2	HMPA	110	0·90		None	27
Tl/monensin acid	≤0·1	$CHCl_3$	23	2·5		None	55
Tl/monensin acid	≤0·1	$CHCl_3$	23	6·7		P_{O_2} = 0·2 atm	55
Tl^+/monensin$^-$	*c.* 0·2	$CHCl_3$	−20	2·1		None	55
Tl^+/monensin$^-$	*c.* 0·2	$CHCl_3$	23	2·0		None	55
Tl^+/monensin$^-$	*c.* 0·2	$CHCl_3$	23	7·1		P_{O_2} = 0·2 atm	55
Tl^+/monensin$^-$	*c.* 0·2	$CHCl_3$	45	1·9		None	55
Tl^+/nigericin$^-$	*c.* 0·1	$CHCl_3$	23	3·0		None	55
Tl^+/nigericin$^-$	*c.* 0·1	$CHCl_3$	23	12·5		P_{O_2} = 0·2 atm	55
Tl^+/nonactin	*c.* 0·10	$CHCl_3$	24	0·41		None	54
Tl^+/nonactin	*c.* 0·10	$CHCl_3$	24	0·49		P_{O_2} = 0·2 atm	54
Tl^+/monactin	*c.* 0·09	$CHCl_3$	0	0·52		None	54
Tl^+/monactin	*c.* 0·09	$CHCl_3$	24	0·47		None	54
Tl^+/monactin	*c.* 0·09	$CHCl_3$	24	0·50		P_{O_2} = 0·2 atm	54
Tl^+/monactin	*c.* 0·09	$CHCl_3$	40	0·47		None	54
Tl^+/monactin	*c.* 0·09	$CHCl_3$	50	0·52		None	54

TABLE III (*cont.*)

Compound	Conc./M	Solvent	Temp./°C	R_1/s^{-1}	R_2/s^{-1}	Added paramagnetic	Reference
Tl^+/dinactin	*c.* 0·13	$CHCl_3$	24	0·48		None	54
Tl^+/dinactin	*c.* 0·13	$CHCl_3$	24	0·48		$P_{O_2} = 0·2$ atm	54
Tl^+/valinomycin	*c.* 0·09	$CHCl_3$	0	0·53		None	53
Tl^+/valinomycin	*c.* 0·09	$CHCl_3$	23	0·44		None	53
Tl^+/valinomycin	*c.* 0·09	$CHCl_3$	23	2·5		$P_{O_2} = 0·2$ atm	53
Tl^+/valinomycin	*c.* 0·09	$CHCl_3$	38	0·37		None	53

[a] TANOL is the radical 4-hydroxy-2,2,6,6-tetramethylpiperidine-1-oxyl.
[b] The slope is not constant, but increases with TANOL concentration.
[c] The slope is non-linear in the 0–1 atm range of P_{O_2}, being 3·5 up to $P_{O_2} = 0·2$ atm.

relaxation time of Tl(I). This suggests that the actins have a molecular framework that surrounds the Tl(I) ion in such a manner as to shield it from collisions with the dissolved oxygen molecules. With the other antibiotics, the structures are more open and permit collisions with oxygen molecules, thereby decreasing the spin–lattice relaxation time. These solution results are consistent with the structures of the complexes determined by X-ray crystallographic techniques.

D. Coupling constants

Because of the highly ionic nature of Tl(I) complexes, few spin–spin couplings have been found. A proton NMR study of the thallium complex of the cryptand ($N[(CH_2)_2O(CH_2)_2O(CH_2)_2]_3N$) gave a ^{205}Tl, ^{1}H coupling of 11·5 Hz to the *N*-methylene protons and 14·5 Hz to the *O*-methylene protons.[62a] A ^{15}N study of Tl(I) complexes with cryptands also revealed Tl coupling to the nitrogen nuclei.[62b] A reduced coupling of 850 Hz is reported. A ^{13}C investigation of the Tl(I)–valinomycin complex in $CDCl_3$ shows thallium–carbon spin–spin couplings of 96 Hz and 101 Hz, which are assigned to the carbonyl carbons of the D- and L-valine residues.[63] These couplings are also found in the ^{205}Tl study of the valinomycin complex.[53]

III. Tl(III) SOLUTION STUDIES

A. Chemical shifts

Because Tl(III) salts tend to hydrolyse in aqueous solution, only a few investigations of the $^{205}Tl(III)$ NMR of these systems have been made.[5,21,64–67] The concentration dependence of the chemical shift of the Tl(III) ion for $Tl(NO_3)_3$ in HNO_3 and for dilute $TlCl_3$ in varying ratios of $HCl:HNO_3$ has been investigated.[5] Chemical shifts for the $TlCl_3$, $TlBr_3$ and $Tl(NO_3)_3$ salts as a function of increasing concentration of their respective acid was studied by Figgis,[65] as was the shift of $Tl(NO_3)_3$ with added H_2SO_4, HF, $HClO_4$, HBr and HCl. The chemical shift range for the concentration, anion and pH of the Tl(III) ion is approximately 2000 ppm (Table II).

Glaser and Henriksson[67] have used a combination of solution and solid state ^{205}Tl NMR experiments to study the formation and geometry of $TlX_n^{(3-n)-}$ complexes (X = Cl, Br). The chemical shifts for the individual species and their respective stability constants are determined for dilute (0·05 M) and concentrated (1·0–2·6 M) Tl(III) aqueous solutions. The existence of such species as $TlCl_5^{2-}$, $TlCl_6^{3-}$ and $TlBr_4^{-}$ is verified in these studies. This study clearly emphasizes the importance of using solid state

NMR data to better understand solution state results. For example, it is found that the species $TlCl_3$ is 300–400 ppm less shielded in aqueous solution than in the solid state, indicating a significant structural difference.

The solvent dependence of the Tl(III) chemical shift has still not been adequately investigated.

B. Relaxation

No explicit relaxation studies have been performed on the Tl(III) ion in solution, although some line widths have been reported for non-degassed solutions.[65,67] These range from 30 Hz for Tl(III) in concentrated $HClO_4$ and 10 Hz for $TlCl_3$ in HCl to approximately 5000 Hz for $Tl(NO_3)_3$ in HBr at Br^- : Tl(III) ratios of about 1·5.

C. Coupling constants

A proton NMR study of the Tl(III) complex with the nitrilotriacetate ion in D_2O at pH ≤ 3 has revealed spin–spin coupling of the methylene protons to ^{205}Tl of 387 Hz and to ^{203}Tl of 384 Hz.[68]

IV. ALKYLTHALLIUM (III) COMPOUNDS IN SOLUTION

A. Chemical shifts

Shortly after the discovery of the element thallium, the first organothallium compound was synthesized.[69] This compound, diethylthallium chloride, is sufficiently stable in water and air that it served as the parent compound for the synthesis of a large number of other dialkylthallium compounds by simple anionic replacement of the chlorine. These compounds are convenient models for the pseudothallium(I) cations.

The ^{205}Tl chemical shifts (Table II) have been determined for solutions of the alkylthallium(III) compounds, $(CH_3)_3Tl$,[21,64,70] $(C_2H_5)_3Tl$,[21] $(CH_3)_2Tl^+$,[21,40] and CH_3Tl^{2+},[75] as well as for the complex bis(*cis*-1,2-dithioethene)thallate anion[73] and of the ethoxide, *N,N*-dimethylamine, pyrazole, and *N,N*-diethyldithiocarbamate derivatives of dimethylthallium.[20,73] The temperature, concentration, anion and solvent dependencies of the dimethyl and monomethyl cations have been investigated.[72,75–77] In general, it is found that the temperature dependence of the chemical shift is greater than that resulting from changes in anion or concentration for the compounds $(CH_3)_2TlX$ ($X = NO_3, BF_4, O_2CCH_3$).[77] For several dimethylthallium(III) derivatives in a number of solvents, a linear correlation is found[76] to exist between the ^{205}Tl chemical shift and the Drago base parameters.

The trialkyls resonate at the highest frequency while the dialkyl and monoalkyl signals come at about 1000–1500 ppm and 1500–2000 ppm, respectively, to low frequency.

Solvent isotope shifts for dimethylthallium in H_2O and D_2O are found to be concentration dependent, amounting to approximately 5 ppm.[40]

B. Relaxation

The spin–lattice relaxation time of $(CH_3)_2Tl^+$ is 0·56 s for a degassed solution and it is independent of anion, concentration, resonance frequency, solvent isotope composition, and thallium isotope.[40] The decrease in relaxation time with increasing dissolved oxygen concentration is found to be very significant but not as large as is observed with the Tl(I) ion.[40] The dominance of the contribution from the CSA mechanism to the spin–lattice relaxation of ^{205}Tl in some dialkylthallium(III) derivatives has been demonstrated by measurements at two different magnetic field strengths and is also reflected in the line widths of coupled protons.[78] The effect upon the proton line widths suggests a new method for monitoring changes in the spin–lattice relaxation of the ^{205}Tl nucleus in spin–spin coupled systems. The ^{205}Tl dynamic nuclear polarization of $(CH_3)_3Tl$ in solution with an organic radical has been measured.[79]

C. Coupling constants

Many spin–spin couplings involving the ^{205}Tl and ^{203}Tl nuclides have been measured. Most of the reported couplings have been determined without direct observation of the thallium nucleus but rather through the observation of other nuclei such as ^{1}H, ^{13}C, ^{19}F and ^{31}P. This being the case, and in view of the extensive literature on thallium compounds, the authors apologize if some couplings are omitted due to unintentional oversight. However, couplings representative of a large variety of compounds are presented so that trends may be adequately detected. It is immediately obvious from a perusal of the coupling data found in Tables IV–XV that the magnitudes of the couplings are large, with coupling through five and six bonds being observable. Couplings to ^{1}H in trialkyls,[80–90] mixed trialkyls,[80,81,88,90–98] mixed alkyl–vinyl,[83] alkyl–alkynyl,[93] and mixed alkyl–cyclopentadienyl[93,99,100] compounds have been observed and are summarized in Table IV. It is seen that the two-bond couplings with protons have negative signs. Couplings of ^{205}Tl with ^{13}C in Me_3Tl ($^{1}J = +1930$ Hz) and in $[(Me_3Si)_2N]_3Tl$ ($^{3}J = 83$ Hz) and with ^{19}F in $Tl(O_2CCF_3)$ ($^{4}J = 85·2$ Hz) have been reported. Also reported are $^{2}J(^{205}Tl, ^{205}Tl) = 536·2$ Hz in $(Me_2TlNMe_2)_2$ and 1037 Hz and 971 Hz in the *cis* and *trans* conformers of $(Me_2TlNHMe)_2$, respectively. The value of $^{2}J(^{205}Tl, ^{203}Tl) = 1200$ Hz in $(Me_2TlOEt)_2$ has also been observed.

TABLE IV

Representative coupling constants for triorganothallium(III) compounds.[b]

Compound	Solvent	Temp./ °C	$^{2}J(^{205}Tl-^{1}H)$/ Hz	$^{3}J(^{205}Tl-^{1}H)$/ Hz	$^{4}J(^{205}Tl-^{1}H)$/ Hz	Other $^{n}J(^{205}Tl-^{Z}X)$/Hz	Reference
Me_3Tl	Acetone	−70	−268·8[a]			$^{1}J(^{205}Tl-^{13}C)$ =+1930[a]	80
Me_3Tl	CH_2Cl_2	−85	−251[a]				81
Me_3Tl	CH_2Cl_2	−50	−243[a]				81
Me_3Tl	CH_2Cl_2	−30	−232[a]				81
Me_3Tl	CH_2Cl_2	−70	−250·8[a]				81, 82
							87
Me_3Tl	Me_2O	−60	−269·6				83
Me_3Tl	NMe_3	−60	−270·3				83
Me_3Tl	DME	−70	−266				84, 85
Et_3Tl	CH_2Cl_2	−85	−198·2	+396·1			81, 82
Ph_3Tl	NMe_3			+259·4 (*o*-H)[a]	+80±5 (*m*-H)[a]	$^{5}J(^{205}Tl-^{1}H)$ =+35±5[a] (*p*-H)	82, 83
							122
Me_2EtTl	CH_2Cl_2	−85	−223·0 (Me)	+472·4			81
			−242·4 (Et)				
Et_2MeTl	CH_2Cl_2	−85	−186·9 (Me)	+441·5			81
			−218·8 (Et)				
$Me_2Tl-(-CONPh-)_2NMe_2$	Toluene-d_8		−392				98
$Me_2Tl-(-CONPh-)_3NMe_2$	Toluene-d_8		−391				98
$Me_2Tl-(-CONPh-)_4NMe_2$	Toluene-d_8		−393				98
Me_2cpTl	Monoglyme	39	−372 (Me)				99

TABLE IV (*cont.*)

Compound	Solvent	Temp./ °C	$^{2}J(^{205}Tl-^{1}H)$/ Hz	$^{3}J(^{205}Tl-^{1}H)$/ Hz	$^{4}J(^{205}Tl-^{1}H)$/ Hz	Other $^{n}J(^{205}Tl-^{Z}X)$/Hz	Reference
Me_2cpTl	Pyridine	39	−379 (Me)				93
Me_2cpTl	SO_2(liq.)	60	−378 (Me)				100
$Me_2(SeCF_3)Tl$	Pyridine		−383 (Me)				94
$Me_2(MeS)Tl$	Pyridine	39	−372 (Me)				93
$Me_2(MeS)Tl$	CH_2Cl_2	39	−371 (Me)				93
$Me_2(PhC{\equiv}C)Tl$	Pyridine	39	−393 (Me)				93
$Me_2(CH_2{=}CH)Tl$	NMe_3	−60	−295·5 (Me)				83
$Me_2(CH_2{=}CH)Tl$	Me_2O	−60	−294·6 (Me)				83
$(CH_2{=}CH)_2MeTl$	NMe_3	−60	−317·4 (Me)				83
$(CH_2{=}CH)_2MeTl$	Me_2O	−60	−316·8 (Me)				83
$(Me_2TlNMe_2)_2$	C_6D_6	37	−343·8 (Me)	94·5 (NMe)	−2·2 (Me)	$^{2}J(^{205}Tl-^{205}Tl)$ =536·2	91, 95
$(Et_2TlNMe_2)_2$	C_6H_6		−381·8 (Et)	81·1 (NMe) +612·4 (Et)			95
$(Et_2TlNMe_2)_2$	C_6D_6		−382 (CH_2-CH_3)	+613 (CH_2CH_3) 80 (NMe)			97
$(Me_2TlNEt_2)_2$	C_6D_6		−340 (Me) (NCH_2CH_3)	101 or 36	8·5 (Me)		97
$(Me_2TlNMet)_2$	C_6D_6		−342 (Me)	94 (*cis*, NMe) 99 (*trans*, NMe)			97
$(Me_2TlNHMe)_2$	C_6D_6		−360 (*cis*, Me) −359 (*trans*, Me)	90 (*cis*, NMe) 92 (*trans*, NMe)	0 (*cis*, Me) 1 (*trans*, Me)	$^{2}J(^{205}Tl-^{205}Tl)$= 1037 (*cis*) 971 (*trans*)	97
$(Me_2TlNHEt)_2$	C_6D_6		−361 (Me)				97
$(Pr^{n}_2TlNMe_2)_2$	C_6D_6		−388 ($CH_2CH_2CH_3$)	+566 ($CH_2CH_2CH_3$) 81 (NMe)			97

TABLE IV (*cont.*)

Compound	Solvent	Temp./ °C	$^{2}J(^{205}Tl-^{1}H)$/ Hz	$^{3}J(^{205}Tl-^{1}H)$/ Hz	$^{4}J(^{205}Tl-^{1}H)$/ Hz	Other $^{n}J(^{205}Tl-^{Z}X)$/Hz	Reference
$(Pr^{n}_{2}TlNEt_{2})_{2}$	C_6D_6		−382 ($CH_2CH_2CH_3$)	+518 ($CH_2CH_2CH_3$) 117 (NCH_2CH_3)	8·5 (NCH_2CH_3)		97
	C_6D_6		−355 (Me)				97
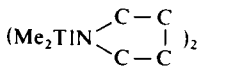	C_6D_6		−347 (Me)				97
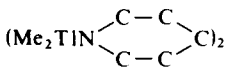	C_6D_6		−343 (Me)				97
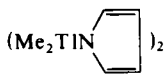	Pyridine-d_5 H_2O		−404 (Me) −402 (Me)				97
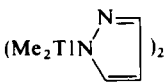	C_6D_6		−376 (Me)				97
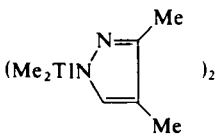	C_6D_6		−375 (Me)				97
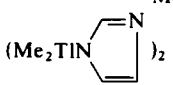	Pyridine-d_5		−402 (Me)				97
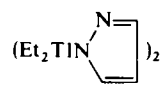	C_6D_6		−302 (CH_2CH_3)	+605 (CH_2CH_3)			97

TABLE IV (*cont.*)

Compound	Solvent	Temp./ °C	$^{2}J(^{205}Tl-^{1}H)$/ Hz	$^{3}J(^{205}Tl-^{1}H)$/ Hz	$^{4}J(^{205}Tl-^{1}H)$/ Hz	Other $^{n}J(^{205}Tl-^{Z}X)$/Hz	Reference
$(Me_2TlOEt)_2$	Toluene	−60	−371 (Me)			$^{2}J(^{205}Tl-^{203}Tl)$ =1200±20	91
$Tl(O_2CCF_3)_3$	THF	−110				$^{4}J(^{205}Tl-^{19}F)$ =85·2	86
$Tl(O_2CCH_3)_3$	CD_3OD	−85			26·3		86
$(Me_3Si)_3Tl$	CH_2Cl_2	−60		102·1			88
$(Me_3Si)_3Tl$	Toluene	−60		101·5			88
$(Me_3Si)_3Tl$	Monoglyme	−60		106·2			88
$(Me_3Si)_3Tl$	NMe_3[c]	−60		112·9			88
$N(CH_2CO_2)_3Tl$	D_2O[d]			387[e]			68
$[(Me_3Si)_2N]_3Tl$	Toluene				5	$^{3}J(^{205}Tl-^{13}C)$ =83	90
$Me_2TlN(SiMe_3)_2$	C_6D_6		−324				90

[a] Coupling constant sign was determined experimentally.
[b] Couplings involving ^{203}Tl usually 1–2% less than those involving ^{205}Tl.
[c] 1 : 1 $(Me_3Si)_3Tl:NMe_3$ adduct formed.
[d] pH ≤ 3.
[e] Possibly ^{4}J rather than ^{3}J.

There are a large number of thallium–proton couplings reported in the literature for dialkylthallium(III) compounds, as shown in Tables V and VI. Many studies have been conducted of the effect of solvent and anion[40,71,80,82,91–94,96,98,100–119] on the coupling found in Me_2Tl^+. Burke *et al.*[76] for example, have correlated $^2J(^{205}Tl, ^1H)$ and $^1J(^{205}Tl, ^{13}C)$ with solvent basicity parameters for a number of dimethylthallium derivatives in a number of solvents. Couplings for diethyl,[82,92,101,105,120] dipropyl (*n,i-*)[82,121,122] and dibutyl[82] compounds have been observed, as have those for $(Me_3SiCH_2)_2Tl^+$[123] and $(Me_3Si)_2Tl^+$.[124] Thallium coupling with ^{13}C in the Me_2Tl^+ ion has been reported as a function of solvent and anion.[71,80,91,100,117,119] Thallium–proton couplings in mixed dialkylthallium,[82,111,123,125–128] alkylvinyl,[129] alkyl–aryl,[111,125,129,130] alkyl–alkyl[111,125] and alkyl–cyclopentadienyl[129] organothallium compounds have also been recorded.

Monoalkylthallium(III) couplings in the literature include thallium–proton values for $MeTl^{2+}$,[100,102,105,111,131,132] $ETTl^{2+}$,[105,132] and others.[123,128,133–135] For $MeTl(OAc)_2$, $^1J(^{205}Tl, ^{13}C)$ has been reported to be 5631 Hz in $CDCl_3$ and 5976 Hz in CH_3OH.[100]

Thallium–proton couplings have been obtained for a number of substituted vinyl[82,122,136–140] and divinyl[82,122,141] thallium(III) derivatives.

V. ARYLTHALLIUM (III) COMPOUNDS IN SOLUTION

A. Chemical shifts

Thallium chemical shifts have been determined for phenylthallium(III) dichloride and its complexes with PPh_3 and dipyridine in methanol and pyridine,[121] diphenylthallium(III) chloride in liquid ammonia,[80] diphenylthallium(III) bromide in DMSO,[121] a series of substituted arylthallium(III) bis(trifluoroacetates) in a number of solvents,[72] and triphenylthallium(III) in ether.[121]

In general, it appears that the diaryls resonate about 200 ppm to high frequency of the monoaryls and about 600 ppm to low frequency of the triaryls (see Table II).

B. Coupling constants

Couplings between thallium and protons have been measured in Ph_3Tl[82,83] and are listed in Table IV. A large five-bond coupling of about 35 Hz is observed in this compound.

Thallium–proton couplings in mixed aryl–alkyl diorganothallium compounds have been determined.[111,125,129,130] These couplings are found in Table IV. Thallium–proton couplings have been reported in a number of

TABLE V

Thallium–carbon and thallium–proton coupling constants for dialkylthallium compounds R_2TlY.[a]

R	Solvent	$^1J(^{205}Tl-^{13}C)$/Hz	$^2J(^{205}Tl-^1H)$/Hz	$^3J(^{205}Tl-^1H)$/Hz	Reference
Me	D_2O	+2459[b], +2478[c] (NO_3) +2503·2[d] (ClO_4) +2513[d] (OAc)	−408±1·5% (NO_3, ClO_4, OAc, OH, F, SCN, CO_3, O_2CCF_3, MnO_4, PO_4 SO_4, CrO_4, S_2O_3, malonate, succinate, maleate, fumarate, lactate, acac, Oph, OC_6H_4Cl-*o*, $OC_6H_4(CHO)$-*o*, O_2CCHMe_2, CN_2, O_2CNMe_2, O_2SNMe_2, O_3SNMe_2)		40, 71, 100, 82, 101–107, 98, 119
	Pyridine	+3018[c], +3080[c] (NO_3) +3053·7[d] (ClO_4) +3012[f] (I) +2897[g], +2918[c] (OPh)	−429±2% (NO_3, O_2PF_2, O_2CCF_3, lactate, O_2SEt, SCN, O_2SMe, acac, CO_3, MnO_4, OH, CN, $CH(COPh)_2$, oxinate, PO_4) −412±1·7% (OAc, BF_4, I, ClO_4, BPh_4, CN_2)		71, 100, 93 94, 101, 103, 107, 108, 113 96, 116, 119
	CH_3CN		−412±0·2% (ClO_4) −404·8 (NO_3) −398 (oxinate)		92, 119 119 108
	Sulpholane		−408 (ClO_4)		92
	CH_3OH		−417±1% (acac, OAc, NO_3, ClO_4)		100, 92, 110
	2,6-Lutidine		−416 (ClO_4)		92
	2-Picoline		−416 (ClO_4) −408 (oxinate)		92 108
	3-Picoline		−426 (ClO_4)		92
	4-Picoline		−424 (oxinate)		108

TABLE V (*cont.*)

R	Solvent	$^{1}J(^{205}Tl-^{13}C)$/Hz	$^{2}J(^{205}Tl-^{1}H)$/Hz	$^{3}J(^{205}Tl-^{1}H)$/Hz	Reference
Me	NH_3 (liq.)	+3456[i,k,h] (Br)	−448·9[h,k,l] (Br)		80
	Acetone		−401 ($B_{10}H_{13}$)		109
	TMG		−421 (ClO_4)		92
	eh		−427·5±0·2% (ClO_4)		92, 119
	TMU		−426 (ClO_4)		92
	DMF		−435±1·6% (acac, NO_3, ClO_4, oxinate)		92,107, 108 110, 119
			−420 (CN_2)		
	DMSO	+2918·2[d] (ClO_4) +2905,[e] +2903[c] (NO_3) +2928[g], +2934[c] (I) +2928,[b,i] +2971[c,i] (OPh)	−438±2·7 (OPh, acac, oxinate, CN_2, $CH(COPh)_2$, NO_3, ClO_4, I, OAc, BF_4)		71, 100, 92 107, 108, 110 119
	DMA		−446±1·5% (ClO_4)		92, 119
			−445·6 (NO_3)		119
	HMPA		−464±2% (ClO_4)		92, 108, 110
			−472±0·7% (NO_3)		119
			−445 (acac, oxinate)		
			−464 (BF_4)		
	Tetramethylene sulphoxide		−457 (ClO_4)		92
	CH_2Cl_2	+2487,[b,i] +2475[c,i] (OPh)	−400±1% (SO_4, $CH(COPh)_2$, $CH(COMe)_2$, oxinate)		40, 82, 92, 108
			−371[i] (SMe, OPh)		
	$CDCl_3$		−385±1% (oxinate, hydroxamate)		91, 100, 104,
			−375±1% (acac, O_2CCHMe_2, OAc)		105, 108, 111,
			−360±1·7% (Sat, Aat, S_2CNMe_2, S_2CNEt_2)		114, 115

TABLE V (*cont.*)

R	Solvent	$^{1}J(^{205}Tl-^{13}C)$/Hz	$^{2}J(^{205}Tl-^{1}H)$/Hz	$^{3}J(^{205}Tl-^{1}H)$/Hz	Reference
Me	CCl_4		−365±1·4% (OSiMe, OpH, OC_6H_4Cl-*o*)		103, 112
	Bu^nNH_2		−418·0[d] (ClO_4)		119
	Toluene	+2556[c,j] (OPh) +2516[j] (OC_6H_4Cl-*o*)	−372±2·2% (OC_6H_4Cl-*o*, OEt, OBu^t, OPh, $SC(O)NME_2$, $SC(NMe_2)NMe$) −385±0·5% (OC(OEt)NPh, OC_6H_4Cl-*o*) −391 ($OC(NMe_2)NPh$) −355 (SPh)		71, 91, 93, 98 103, 111, 117
	C_6D_6		−375±1·3% (OPh, acac, S_2COEt) −364±1·1% ($SC(S)NMe_2$, $SC(NMe_2)NPh$, SC(OEt)NPh, $SP(S)Ph_2$) −395, −371 ($SC(PPh_2)NPh$)		103, 104, 111, 113, 98, 118
	CCl_2CHCl		−396 (oxinate)		108
	TFAA		−362 (NO_3, ClO_4, acac)		110
	HCO_2H		−389 (ClO_4, NO_3)		110
	TMP		−437 (ClO_4, NO_3)		110
	DMSO+H_2O		−429 (Cl) −408±1% (Sat, Aat)		114
	$SbCl_5$+SO_2		−336 (Cl)		114
	65% $HClO_4$		−372 (NO_3) −362 (ClO_4, acac)		114
	60% $HClO_4$		−373 (acac, ClO_4) −362 (NO_3)		114
	40% $HClO_4$		−391 (NO_3)		114

TABLE V (*cont.*)

R	Solvent	$^{1}J(^{205}Tl-^{13}C)$/Hz	$^{2}J(^{205}Tl-^{1}H)$/Hz	$^{3}J(^{205}Tl-^{1}H)$/Hz	Reference
Me	20% $HClO_4$		−400 (NO_3)		114
	60% HNO_3		−385±0·6% (acac, ClO_4, NO_3)		114
Et	D_2O		−338±0·6%[k] (NO_3, ClO_4, SCN, lactate, CO_3, SO_4)	+623 (NO_3, ClO_4, SCN, lactate, CO_3) +634 (ClO_4) +628 (SO_4)[k]	82, 92, 101, 120
	Pyridine		−373 (NO_3) −365 (ClO_4) −360±0·6% (SCN, CO_3, lactate) −332 (I)	+629 (NO_3, SCN) +639 (ClO_4) +620 (lactate)	92, 101
	CH_3CN		−344 (ClO_4)	+624 (ClO_4)	92
	Sulpholane		−338 (ClO_4)	+630 (ClO_4)	92
	CH_3OH		−377 (ClO_4)	+644 (ClO_4)	92
	2-Picoline		−356 (ClO_4)	+626 (ClO_4)	92
	Acetone		−353 (ClO_4)	+631 (ClO_4)	92
	TMG		−360 (ClO_4)	+637 (ClO_4)	92
	en		−390 (ClO_4)	+659 (ClO_4)	92
	TMU		−378 (ClO_4)	+630 (ClO_4)	92
	DMF		−387 (ClO_4)	+641 (ClO_4)	92
			−376 (Br)	+639 (Br)	121
			−393 (NO_3)	+633 (NO_3)	121
	DMSO		−384 (ClO_4)	+633 (ClO_4)	92
	DMA		−394 (ClO_4)	+642 (ClO_4)	92
	HMPA		−399 (ClO_4)	+628 (ClO_4)	92
	$CDCl_3$		−306 (O_2CCHMe_2)	+612 (O_2CCHMe_2)	105
Pr^n	D_2O[m]		−341[k] (SO_4)	+469[k] (SO_4)	82, 122

TABLE V (*cont.*)

R	Solvent	$^1J(^{205}Tl-^{13}C)$/Hz	$^2J(^{205}Tl-^1H)$/Hz	$^3J(^{205}Tl-^1H)$/Hz	Reference
Pr^n	DMSO[o]		−380 (Br)	+478 (Br)	121
			−390 (NO_3)	+432 (NO_3)	
Pr^i	D_2O		−259 (SO_4)	+574 (SO_4)	82
Bu^n	D_2O		−320 (SO_4)	+452 (SO_4)	82
Bu^i	D_2O[n]		−356[k] (SO_4)	+494[k] (SO_4)	82
Me_3SiCH_2	$CDCl_3$		−537 (Cl, Br)		123
			−566 (O_2CCHMe_2)		
Me_3Si	Monoglyme			143·4 (Cl)	124

[a] The Y moieties are in parentheses after the coupling constants.
[b] 0·8 M.
[c] 0·4 M.
[d] 0·4 M.
[e] 1·0 M.
[f] 0·1 M.
[g] 0·9 M.
[h] 5%, −30 °C.
[i] $^1J(^{203}Tl-^{13}C)=+3422$ Hz.
[j] Average of unresolved $^{203,205}Tl$ couplings.
[k] Coupling constant sign was determined experimentally.
[l] $^2J(^{203}Tl-^1H)=444·3$ Hz
[m] $^4J(^{205}Tl-^1H)=+20·5$ Hz[k] (SO_4).
[n] $^4J(^{205}Tl-^1H)=+16·4$ Hz[k] (SO_4).
[o] $^4J(^{205}Tl-^1H)=+24$ Hz (Br) and +30 Hz (NO_3).

TABLE VI

Thallium–proton coupling constants for mixed diorganothallium(III) compounds RR'TlY.

R	R'	Y	Solvent	$^{2}J(^{205}Tl-^{1}H)$	$^{3}J(^{205}Tl-^{1}H)$	$^{4}J(^{205}Tl-^{1}H)$	$^{6}J(^{205}Tl-^{1}H)$	Reference
Me	Et	OAc	D_2O	−354 (Me)				111, 125
		SMe	$CDCl_3$	−304 (Me)				126
		SPh	$CDCl_3$	−294 (Me)				126
		S_2CNMe_2	$CDCl_3$	−301 (Me)				126
		Oxinate	$CDCl_3$	−345 (Me)				126
		D_2CCHMe_2	$CDCl_3$	−331 (Me)				126
		Tropolonate	$CDCl_3$	−338 (Me)				126
		Salicylaldehydate	$CDCl_3$	−334 (Me)				126
		SO_4	D_2O	−359 (Me)				82
				−399 ($-CH_2CH_3$)	+680 ($-CH_2CH_3$)			
Me	Me_3SiCH_2	Br	$CDCl_3$	−342 (Me)				123
				−539 ($-CH_2SiMe_3$)				123
		O_2CCHMe_2	$CDCl_3$	−376 (Me)				
				−562 ($-CH_2SiMe_3$)				
Me	$CH_2=CH-$	O_2CCHMe_2	$CDCl_3$	−412 (Me)				129
Me	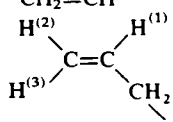	OAc	$CDCl_3$	−364 (Me)	198 (H-1)	226 (H-3)		127
				−533 ($-CH_2CHCH_2$)		205 (H-2)		
		O_2CEt	$CDCl_3$	−369 (Me)	195 (H-1)	223 (H-3)		127
				−534 ($-CH_2CHCH_2$)		205 (H-2)		
		O_2CCHMe_2	$CDCl_3$	−365 (Me)	197 (H-1)	222 (H-3)		127
				−532 ($-CH_2CHCH_2$)		198 (H-2)		
		S_2CNMe_2	$CDCl_3$	−334 (Me)	195 (H-1)	234 (H-3)		127
				−491 ($-CH_2CHCH_2$)		220 (H-2)		
		Tropolonate	$CDCl_3$	−359 (Me)				127
		Cl	DMSO-d_6	−369 (Me)	195 (H-1)	223 (H-3)		127
				−534 ($-CH_2CHCH_2$)		205 (H-2)		

TABLE VI (*cont.*)

R	R′	Y	Solvent	$^2J(^{205}Tl-^1H)$	$^3J(^{205}Tl-^1H)$	$^4J(^{205}Tl-^1H)$	$^6J(^{205}Tl-^1H)$	Reference
Me	$PhCH(OMe)CH_2$	OAc	$CDCl_3$	−360, −520 ($-CH_2-$) −380 (Me)				128
		S_2CNMe_2	$CDCl_3$	−275, −460 ($-CH_2-$)[d] +420[e] −360 (Me)[f]				128
Me	$MeCH(OMe)CH_2$	OAc	$CDCl_3$	−435, −485 ($-CH_2-$) −377 (Me)		36 (R′Me)		128
Me	n-$C_6H_{13}CH(OMe)CH_2$	OAc	$CDCl_3$	−440, −485 ($-CH_2-$)	128			
Me	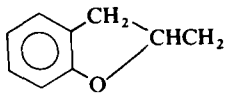	Cl	$CDCl_3$	−400, −430 ($-CH_2-$) −360 (Me)	+680 ($-CH_2CH<$)			128
Me	Ph	OAc	D_2O	−455 (Me)				111, 125
		O_2CCHMe_2	$CDCl_3$	−426 (Me)				129
Me	$PhC\equiv C$	OAc	D_2O	−672 (Me)				111, 125
Me	$N\equiv C$	OAc	D_2O	−828 (Me)				111, 125
Me	cp	OAc	$CDCl_3$	−451 (Me), 219 (cp)				129
		O_2CEt	$CDCl_3$	−454 (Me), 220 (cp)				129
		O_2CCHMe_2	$CDCl_3$	−456 (Me), 217 (cp)[a]				129
		O_2CCHMe_2	CD_3OD	−491 (Me), 225 (cp)[b]				129
		O_2CCHMe_2	CD_3OH	−492 (Me), 210 (cp)[c]				129
Me	cp	4-pr^i-tropolonate	$CDCl_3$	−445 (Me), 216 (cp)				129
Ph	$Me_2NCS_2CH_2$	OAc	$CDCl_3$	−360 ($-CH_2-$)			7·5 (Me), 7·5 (Me′)	130
		S_2CNPh_2	$CDCl_3$	−320 ($-CH_2-$)			6·4 (Me), 7·9 (Me′)	130
		S_2CNMe_2	$CDCl_3$	−316 ($-CH_2-$)			6·8 (Me), 9·7 (Me′)	130
4-MeC_6H_4	Me_2NCSCH_2	OAc	$CDCl_3$	−346 ($-CH_2-$)			6·4 (Me), 6·4 (Me′)	130
		S_2CNPh_2	$CDCl_3$	−318 ($-CH_2-$)			5·0 (Me), 8·0 (Me′)	130
		S_2CNMe_2	$CDCl_3$	−312 ($-CH_2-$)			5·4 (Me), 9·7 (Me′)	130

[a] Also at −40 °C. [b] 12 °C. [c] −72 °C. [d] At 23 °C; −180±30, −470 at −50 °C; −296, −455 at 50 °C. [e] At 23 °C; +380±30 at −50 °C; +435 at 50 °C. [f] At 23 °C; −356 at −50 °C; −361 at 50 °C.

TABLE VII

Thallium–carbon and thallium–proton coupling constants for monoalkylthallium(III) species $RTlY_2$.[a]

R	Solvent	$^1J(^{205}Tl-^{13}C)$/Hz	$^2J(^{205}Tl-^1H)$/Hz	$^3J(^{205}Tl-^1H)$/Hz	$^4J(^{205}Tl-^1H)$/Hz	Reference
Me	D_2O		−936			102, 105, 131
			−931 (O_2CCHMe_2)			
	$CDCl_3$	+5631[b] (O_2CMe)	−892, −911[b]			100, 105, 131
			−676±2 (S_2CNMe_2 S_2CNEt_2)			132, 111
			−790 (oxinate)			105, 132
			−835 (tropolonate)			
	CH_3OH	+5976[c] (O_2CMe)	−921, −939[c]			100, 105, 131
	CH_3CN		−911[d]			100
	CH_2Cl_2		−890[d]			100
	Acetone		−914[d]			100
	Pyridine		−890[e]			100
	DMSO		−928[f]			100
Et	$CDCl_3$		−822 (O_2CCHMe_2)	+1626 (O_2CCHMe_2)		105
			−769 (oxinate)	+1398 (oxinate)		132
			−793 (tropolonate)	+1485 (tropolonate)		132
			−631 (S_2CNMe_2)	+1370 (S_2CNMe_2)		132
			−631 (S_2CNEt_2)	+1355 (S_2CNEt_2)		132
Me_3SiCh_2	$CDCl_3$		−1121 (O_2CCHMe_2)			123
$(HO)Me_2CCH_2$	DMSO-d_6		−864, −871·5		101	135
PhCH-(OCH_2CH_2OH)CH_2	Pyridine		−732, −875	+739		134
$PhCH(OMe)CH_2$	CD_3OD or $CDCl_3$		−760, −920	+748		133
	CD_3OD or $CDCl_3$		−758, −906 (O_2CCHMe_2)	+752 (O_2CCHMe_2)		133
	$CDCl_3$		−534, 670 (S_2CNMe_2)[g]	+545±20(S_2CNMe_2)[h]		128

TABLE VII (*cont.*)

R	Solvent	$^{1}J(^{205}Tl-^{13}C)$/Hz	$^{2}J(^{205}Tl-^{1}H)$/Hz	$^{3}J(^{205}Tl-^{1}H)$/Hz	$^{4}J(^{205}Tl-^{1}H)$/Hz	Reference
$PhCH(OEt)CH_2$	CD_3OD or $CDCl_3$		−768, −921	+737		133
$PhCH(OEt)CH_2$	CD_3OD or $CDCl_3$		−759, −904 (O_2CCHMe_2)	+716 (O_2CCHMe_2)		133
$PhCH(OPr^n)CH_2$	CD_3OD or $CDCl_3$		−768, −929	+751		133
$PhCH(OPr^i)CH_2$	CD_3OD or $CDCl_3$		−786, −921	+818		133
$PhCH(OBu^n)CH_2$	CD_3OD or $CDCl_3$		−774, −934	+757		133
$PhCH(OBu^i)CH_2$	CD_3OD or $CDCl_3$		−772, −917	+828		133
$PhCMe(OMe)CH_2$	CD_3OD or $CDCl_3$		−810, −892		29	133
$PhCMe(OEt)CH_2$	CD_3OD or $CDCl_3$		−822, −890		29	133
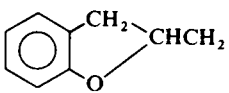	$CDCl_3$		−635, −670 (S_2CNMe_2)[i]	+685 (S_2CNMe_2)[j]		128

[a] Y=OAc unless otherwise indicated in parentheses after the coupling constant.
[b] 0·8 M.
[c] 1·0 M.
[d] Saturated solution, 29 °C.
[e] 0·1 M.
[f] 0·2 M.
[g] 23 °C; −487, −665 at −50 °C; −550, −675 at 50 °C.
[h] +23 °C; +460 at −50 °C; +590 at 50 °C.
[i] at 23 °C; −635, −660 at −50 °C.
[j] at 23 °C; +605 at −50 °C.

TABLE VIII

Coupling constants of selected vinyl and divinyl thallium(III) derivatives.

Compound	Solvent	$^3J(^{205}Tl-^1H\ trans)$/Hz	$^3J(^{205}Tl-^1H\ cis)$/Hz	$^2J(^{205}Tl-^1H\ gem)$/Hz	Reference
$(CH_2{=}CH)_2TlClO_4$	D_2O	$+1618\pm5^a$	$+805\pm5^a$	$+842\pm5^a$	82, 122
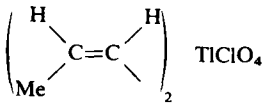 $TlClO_4$	D_2O	$+1485\pm5^a$	$-94{\cdot}0$ (^4J,$-CH_3$)^a	-637 ± 5^a	82
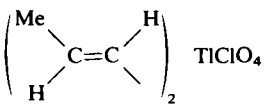 $TlClO_4$	D_2O	$-47{\cdot}1$ (^4J, $-CH_3$)^a	$+809\pm10^a$	$+640\pm10^a$	82
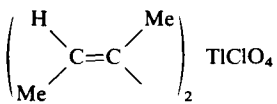 $TlClO_4$	D_2O	$+1348\pm5^a$	$-98{\cdot}0$ (^4J,$-CH_3$)^a	398 (^3J,$-CH_3$)	82
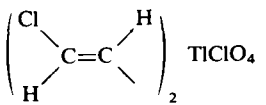 $TlClO_4$	D_2O		+511 or +486	+453 or +477	82
			+1650		137
$CH_2{=}CHTlCl_2$ $CH_2{=}CHTl(ClO_4)_2$	D_2O	$+3750\pm10^a$	$+1806\pm10^a$	$+2004\pm10^a$	82, 122
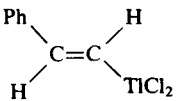			+1600		137

TABLE VIII (*cont.*)

Compound	Solvent	$^3J(^{205}Tl-^1H\ trans)$/Hz	$^3J(^{205}Tl-^1H\ cis)$/Hz	$^2J(^{205}Tl-^1H\ gem)$/Hz	Reference
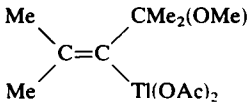	D_2O	−107 (^4J, $-CH_3$)	−187 (^4J, $-CH_3$)	80 (^4J, $-CCH_3$) 4 (^5J, $-COCH_3$)	136
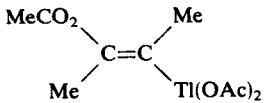	$CDCl_3$		−144 (^4J, $-CH_3$)	997 (^3J, $-CH_3$)	139
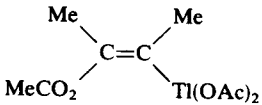	$CDCl_3$	−66 (^4J, $-CH_3$)		1078 (^3J, $-CH_3$)	139
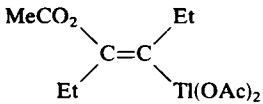	$CDCl_3$		−126 (^4J, $-CH_2CH_3$)	1338 (^3J, $-CH_2CH_3$)	139
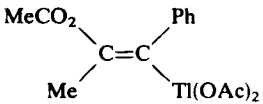		13 (^6J, $-OCCH_3$)	−142 (^4J, $-CH_3$)	125·5 (^4J, *o*-H) 64 (^5J, *m*-H)	138, 140
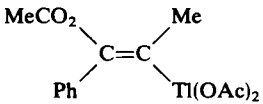	CD_3OD	13 (^6J, $-OCCH_3$)		985·5 (^3J, $-CH_3$)	138, 140
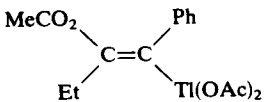	CD_3OD	13 (^6J, $-OCCH_3$)	−116 (^4J, $-CH_2CH_3$)	126 (^4J, *o*-H) 64 (^5J, *m*-H)	138, 140

TABLE VIII (*cont.*)

Compound	Solvent	$^3J(^{205}Tl-^1H\ trans)$/Hz	$^3J(^{205}Tl-^1H\ cis)$/Hz	$^2J(^{205}Tl-^1H\ gem)$/Hz	Reference
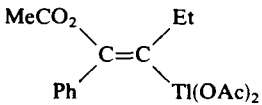	CD_3OD	13 (^6J, $-OCCH_3$)		1299 (^3J, $-CH_2CH_2CH_3$) 20 (^4J, $-CH_2CH_3$)	138, 140
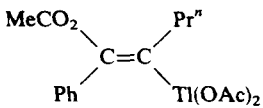	CD_3OD			1311 (^3J, $-CH_2CH_2CH_3$)	138, 140
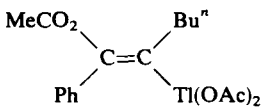	CD_3OD			1316 (^3J, $-CH_2CH_2CH_2CH_3$)	138, 140

[a] Coupling constant sign was determined experimentally.

TABLE IX

Thallium–proton and thallium–fluorine coupling constants for diarylthallium(III) compounds ϕ_2TlY.

ϕ	Y	Solvent	H-2 (^3J)/Hz	H-3 (^4J)/Hz	H-4 (^5J)/Hz	H-5 (^4J)/Hz	H-6 (^3J)/Hz	Reference
Ph	ClO_4	D_2O	+451[b]	+139[b]	+51·7[b]	+139[b]	+451[b]	122, 82
Ph	Br	DMSO	+437	+131	+63	+131	+437	121
	TFA	DMSO-d_6	+455	+117	+55	+117	−455	142
	$S(S)P(OMe)_2$	DMSO-d_6	+447·4	+132·5	+54·5	+132·5	+447·4	143
	L'[a]	Pyridine-d_5	+445·0	+137·0	+47·0	+137·0	+445·0	144
	L'[a]	$CDCl_3$	+438·0	+134·0	+46·5	+134·0	+438·0	144
	Cl	NH_3(liq.)	+461·3±2[b]	+140·5±2[b]	+51·7±2[b]	+140·5±2[b]	+461·3±2[b]	80
C_6F_5	Br	C_6H_6	799 (^{205}Tl–^{19}F)[c]	343 (^{205}Tl–^{19}F)[c]	99 (^{205}Tl–^{19}F)[c]	343 (^{205}Tl–^{19}F)[c]	799 (^{205}Tl–^{19}F)[c]	147
3-FC_6H_4	Br	DMSO-d_6	+512		+21±2	+180	+448	145
4-FC_6H_4	TFA	Pyridine			113 (^{205}Tl–^{19}F)			148
	TFA	THF			112 (^{205}Tl–^{19}F)			148
	TFA	DMSO-d_6	+448	+104		+104	+448	142
4-ClC_6H_4	TFA	DMSO-d_6	+456	+113		+113	+456	142
4-BrC_6H_4	TFA	DMSO-d_6	+455	+115		+115	+455	142
4-(OMe)C_6H_4	TFA	DMSO-d_6	+433	+106		+106	+433	142
4-EtC_6H_4	TFA	DMSO-d_6	+455	+128	^6J=21 (—CH_2CH_3)	+128	+455	142
4-MeC_6H_4	TFA	DMSO-d_6	+448	+128	^6J=24 (Me)	+128	+448	142
	L'[a]	Pyridine-d_5	+435·0	+127·0	^6J=28·0 (Me)	+127·0	+435·0	144
	L'[a]	$CDCl_3$	+431·8	+127·0	^6J=27·0 (Me)	+127·0	+431·8	144
4-ClC_6H_4	L'[a]	Pyridine-d_5	+442·0	+112·0		+112·0	+442·0	144
	L'[a]	$CDCl_3$	+429·5	+109·5		+109·5	+429·5	144
2,4-$Me_2C_6H_3$	TFA	DMSO-d_6	^4J=46·7 (Me)	+206 (?)	^6J=25·3 (Me)	+206 (?)	+441	142
2,5-$Me_2C_6H_3$	TFA	DMSO-d_6	^4J=48 (Me)	+208	+40	^5J=17·6 (Me)	+454	142
3,4-$Me_2C_6H_3$	TFA	DMSO-d_6	+456 (?)	^5J=23 (Me)	^6J=27·6 (Me)	+141·2	+456 (?)	142

TABLE IX (*cont.*)

ϕ	Y	Solvent	H-2 (^3J)/Hz	H-3 (^4J)/Hz	H-4 (^5J)/Hz	H-5 (^4J)/Hz	H-6 (^3J)/Hz	Reference
2,4,6-$Me_3C_6H_2$	TFA	DMSO-d_6	^4J=49 (Me)	+168	^6J=36 (Me)	+168	^4J=49 (Me)	142
	L'[a]	Pyridine-d_5	^4J=53·0 (Me)	+170·0	^6J=26·0 (Me)	+170·0	^4J=53·0 (Me)	144
	L'[a]	$CDCl_3$	^4J=53·0 (Me)	+170·5	^6J=27·0 (Me)	+170·5	^4J=53·0 (Me)	144
	I^-	$CDCl_3$	^4J=41 (Me)	+165	^6J=22 (Me)	+165	^4J=41 (Me)	146

[a] L' = 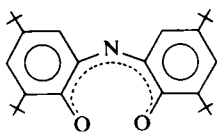

[b] Coupling constant sign was determined experimentally.
[c] ±5 Hz.

diarylthallium compounds[80,82,121,122,142–146] as well as some thallium–fluorine couplings for the same type of compound.[147–148] Again large couplings are observed. For example, the compound $(C_6F_5)_2TlBr$ has thallium–fluorine couplings of $^3J = 799$ Hz, $^4J = 343$ Hz and $^5J = 99$ Hz (see Table IV).

A number of thallium–proton couplings have been measured for monoarylthallium compounds (see Table X)[72,82,122,142–146,149–156] and for two dithallated monoaryl compounds.[155,156] Thallium–fluorine[148] (Table X) and thallium–carbon couplings[148,157–160] have also been determined for the monoarylthallium compounds (Table XI). The one-bond thallium–carbon couplings are extremely large, $^1J(^{205}Tl, ^{13}C) = 10\,000$ Hz!

VI. MISCELLANEOUS COMPOUNDS

A. Thallous ethoxide

Thallous ethoxide exists as a tetramer both in solution and as the neat liquid. The tetrameric structure was determined from the ^{205}Tl and ^{203}Tl spectra of the pure liquid.[64] The thallium spectra show ^{205}Tl–^{203}Tl coupling, $J = 2560$ Hz, and no thallium–proton coupling, thus indicating the polymeric nature of the system. The ^{205}Tl chemical shift is found to be 2914 ppm to high frequency of aqueous $TlNO_3$.[64,121]

B. Miscellaneous Tl(III) compounds (coupling constants)

Values of $^nJ(^{205}Tl–^1H)$ have been determined for a series of thallated naphthyl, phenanthryl, and other fused-ring aromatic systems,[82,145] for a series of dichloropyridiomethylthallium and chloro-bis(pyridiomethyl)thallium cations,[161] and for the bis(*cis*-1,2-dithioethene)thallate anion,[162] and the closely related 1,2-diothio-1,2-dicyanoethanedimethylthallate anion[163] (Table XV).

A one-bond thallium–proton coupling of 6144 Hz is proposed for the unstable hydride TlH_4^-.[164]

Thallium–proton couplings for norbornyl and norbornenyl thallium compounds[165] and thallium norbornyl lactones[166] have been bound. Thallium–carbon couplings for norbornyl, norbornenyl, benzonorbornyl, and norbornyl lactones have also been measured[167,168] (Tables XV, XVI).

Thallium–proton couplings[169–174] and thallium–carbon couplings[174–177] for Tl(III) porphyrins and a related dimethylthallium(III) dipyrromethene[178] have been determined. Evidence has recently been revealed to suggest that thallium in these porphyrins may be five-coordinate[174] rather than six-coordinate as previously assumed[169–177] (Tables XII, XIII).

TABLE

Thallium–proton and thallium–fluorine coupling

ϕ	Y	Solvent	H-2(^3J)/Hz	H-3(^4J)/Hz
Ph	ClO_4	D_2O	+948[b]	+365[b]
	ClO_4, OAc	D_2O	+912	+350
	TFA	DMSO-d_6	+1035	+396
		MeOH	+670	+270
	Cl	MeOH	+850	+323
		Pyridine	+812	+306
3-$(CF_3)C_6H_4$	SO_4	DMSO-d_6	+1000 ± 20	
4-FC_6H_4	TFA	TFAA		
		Pyridine		
		DMSO		
		THF		
		p-Dioxane		
Ph	$S(S)P(OMe)_2$	DMSO-d_6	+805·5	+315
	$S(O)P(OMe)_2$	DMSO-d_6	+77·5	+295·5
	TFA	95 : 5 $CDCl_3$: CD_3OD[c]	+1057	+428
	Cl, L'[a]	C_6D_6	+754	+292
		$CDCl_3$	+738·5	+297 or 292·8
2-MeC_6H_4	ClO_4	D_2O	^4J = 104·2 (Me)	
	ClO_4, OAc		^4J = 106 (Me)	
	TFA	95 : 5 $CDCl_3$: CD_3OD[c]	^4J = 114 (Me)	+537
	Cl	DMSO-d_6		+492
3-MeC_6H_4	ClO_4	D_2O		^5J = 50·1 (Me)
	ClO_4, OAc	D_2O		^5J = 50 (Me)
	TFA	95 : 5 $CDCl_3$: CD_3OD[c]	+1102	^5J = 57 (Me)
	Cl	DMSO-d_5	+986	
4-MeC_5H_4	ClO_4	D_2O		
	ClO_4, OAc	D_2O		
	TFA	DMSO-d_6	+1025	+376
	Cl	DMSO-d_6	+927	+339
	Cl, L'[a]	$CDCl_3$	+765	+280
2,4-$Me_2C_6H_3$	TFA	DMSO-d_6	^4J = 111 (Me)	+496(?)
	ClO_4, OAc	D_2O	^4J = 103 (Me)	
3,4-$Me_2C_6H_3$	TFA	DNSO-d_6	+1040(?)	^5J = 60 (Me)
	ClO_4, OAc	D_2O		^5J = 58 (Me)
4-$Ph^2C_6H_4$	TFA	95 : 5 $CDCl_3$: CD_3OD[c]	+1013	+379
2,5-$Me_2C_6H_3$	TFA	DMSO-d_6	^4J = 113 (Me)	+559
	ClO_4, OAc	D_2O	^4J = 103 (Me)	
2,6-$Me_2C_6H_3$	Cl	DMSO-d_6		+403
2,4,6-$Me_3C_6H_2$	TFA	DMSO-d_6	^4J = 114 (Me)	+460
	Cl	$(CD_3)_2CO$	^4J = 99 (Me)	+381
	Cl, L'	$CDCl_3$	^4J = 96·0 (Me)	+350

X

constants for monoarylthallium(III) compounds ϕTlY_2.

H-4(^5J)/Hz	H-5(^4J)/Hz	H-6(^3J)/Hz	Reference
+123[b]	+365[b]	+948[b]	122, 82
+110	+350	+912	149
+115	+396	+1035	150, 151, 142
+ 80	+270	+674	152
+110	+323	+(850)	152
+105·5	+306	+812	152
(+)90	+320	+930 ± 20	145
240 (^{205}Tl–^{19}F)			148
230 (^{205}Tl–^{19}F)			148
240 (^{205}Tl–^{19}F)			148
233 (^{205}Tl–^{19}F)			148
226 (^{205}Tl–^{19}F)			148
+112·8	+315	+805·5	143
+104·3	+295·5	+775·5	143
+142	+428	+1057	153
+ 94	+292	+754	144
+96·5	+297 or 292·8	+738·5	144
			122, 82
			149
+124	+372	+1071	153
+121	+327	+968	82
			122, 82
			149
+117	+474	+1054	153
+108	+397	+942	82
^6J = +61·0 ± 0·5 (Me)			122, 82
^6J = +61 (Me)			149
^6J = +66 (Me)	+376	+1025	150, 151, 142
	+339	+927	82
^6J = +53·0 (Me)	+280	+765	144
^6J = +65 (Me)	+496(?)	+1065	150, 151, 142
^6J = +60 (Me)			149
^6J = +66 (Me)	+420	+1040 (?)	150, 151, 142
^6J = +51 (Me)			149
^7J = 7·5 (Ph'*o*-H)	+379	+1013	153
+115	^5J = 55 (Me)	+1109	150, 151, 142
	^5J = 50 (Me)		149
+112	+403		145
^6J = +64 (Me)	+460	^4J = 114 (Me)	150, 151, 142
^6J = +54 (Me)	+381	^4J = 99 (Me)	146
^6J = +52·0 (Me)	+350	^4J = 96·0 (Me)	144

TABLE

ϕ	Y	Solvent	H-2(^3J)/Hz	H-3(^4J)/Hz
Ph	Br, L′	$CDCl_3$	+770	+290·0
4-EtC_5H_4	TFA	DMSO-d_6	+1059	+394
4-FC_6H_4	TFA	DMSO-d_6	+960	+280
4-$(CF_3)C_6H_4$	TFA	95:5 $CDCl_3$: CD_3OD[c]	+1015	+353
4-ClC_6H_4	TFA	DMSO-d_6	+965	+296
2-$(CO_2H)C_6H_4$	TFA	DMSO-d_6		+430
2-FC_2H_4	TFA	95:5 $CDCl_3$: CD_3OD[c]		+570
2-ClC_6H_4	TFA	95:5 $CDCl_3$: CD_3OD[6]		+504
2-(CH_2OMe)-C_6H_4	TFA	$CDCl_3$	$^4J = 115$ (—CH_2OMe)	−460?
4-$(OMe)C_6H_4$	ClO_4, OAc	D_2O	+874	+264
3-$(OMe)C_6H_4$	TFA	95:5 $CDCl_3$: CD_3OD[c]	+1228	
3-FC_6H_4	TFA	95:5 $CDCl_3$: CD_3OD[c]	+1143	
3-ClC_6H_4	TFA	95:5 $CDCl_3$: CD_3OD[c]	+1088	
3-BrC_6H_4	TFA	95:5 $CDCl_3$: CD_3OD[c]	+1070	
3-$(CF_3)C_6H_4$	TFA	95:5 $CDCl_3$: CD_3OD[c]	+1076	
3-$[Tl(TFA)_2]$-4-$(OMe)C_6H_3$	TFA	DMSO-d_6	+999	
3-$Tl(TFA)_2$-4-$(OEt)C_6H_3$.	TFA	DMSO-d_6	+992	

[a] L′ = 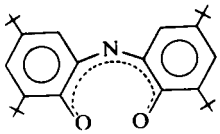

[b] Coupling constant sign was determined experimentally.
[c] Also a trace of CF_3CO_2D.

X (*cont.*)

H-4(^4J)/Hz	H-5(^4J)/Hz	H-6(^3J)/Hz	Reference
+98·0	+290·0	+770	144
^6J = +49 (—CH_2CH_3)	+394	+1059	150, 151, 142
	+280	+960	150, 151, 142
	+353	+1015	153
	+296	+965	150, 151, 142
+124	+430	+1010	150, 151, 142
+54	+314	+1114	153
+89	+329	+1082	153
+141	+460	+554	154
	+264	+874	149
+72	+552	+1018	153
+57	+503	+976	153
+76	+476	+1004	153
+82	+468	+1013	153
+108	+388	+1016	153
	+430	+980, ^5J = +67	155, 156
	+420	+915, ^5J = +67	156

TABLE

Thallium–carbon coupling constants for

ϕ	Solvent	$^1J(^{205}Tl-^{13}C-1)$/ Hz	$^2J(^{205}Tl-^{13}C\text{-}2)$/ Hz	$^3J(^{205}Tl-^{13}C\text{-}3)$/ Hz
Ph	DMSO-d_6		+500	+1010
		10 718	+527·3	+1047·4
Ph	THF	9902	+676	+878
Ph	6:4 CD_3OD: TFAA		+547	+1047
4-MeC_6H_4	DMSO-d_6		+562	+1084
4-MeC_5H_4	THF	9756	+756	+895
4-MeC_6H_4	7:3 THF: $(CD_3)_2CO$		+589	+1065
4-EtC_6H_4	DMSO-d_6		+556	+1066
4-$Pr^iC_6H_4$	DMSO-d_6		+563	+1072
4-$Pr^nC_5H_4$	DMSO-d_6		+562	+1075
4-$Bu^tC_6H_4$	DMSO-d_6		+560	+1062
2,4-$Me_2C_6H_3$	DMSO-d_6		+567[a] ^3J = 444 (Me)	+1017[a]
2,4-$Me_2C_6H_3$	THF	9329	+646[c] ^3J = 402 (Me)	+793
3,4-$Me_2C_6H_3$	THF	9634	+565	+800
3,4-$Me_2C_5H_3$	DMSO-d_6		+552[a]	+1071[a] ^4J = 76 (Me)
2,5-$Me_2C_6H_3$	DMSO-d_6		+520[a] ^3J = 445 (Me)	+1047[a]
2,4,6-$Me_3C_6H_2$	DMSO-d_6		+509 ^3J = 454 (Me)	+996
2,4,6-$Me_3C_6H_2$	THF	8841	+512 ^4J = 459 (Me)	+968
2,4,6-$Et_3C_6H_2$	DMSO-d_6		+557 ^3J = 437 ($-CH_2CH_3$) ^4J = 61 ± 3 ($-CH_2CH_3$)	+987

[a] Coupling constant sign was determined experimentally.
[b] Y is trifluoroacetate.
[c] Assignments incorrectly switched in reference 190; correctly listed in reference 201.

XI

monoarylthallium(III) compounds ϕTlY_2[b]

$^4J(^{205}Tl-^{13}C\text{-}4)$/ Hz	$^3J(^{205}Tl-^{13}C\text{-}5)$/ Hz	$^2J(^{205}Tl-^{13}C\text{-}6)$/ Hz	Reference
−185	+1010	+500	157, 158
−202·2	+1047·4	+527·3	159
−183	+878	+676	148, 160
	+1047	+547	157, 158
−209	+1084	+562	157, 158
$^5J = +114$ (Me)			
−195	+895	+756	148, 160
$^5J = +110$ (Me)			
	+1065	+589	157, 158
−199	+1066	+556	157, 158
−206	+1072	+563	157, 158
−204	+1075	+562	157, 158
$^5J = +94$ (—$CH_2CH_2CH_3$)			
$^6J = 47$ (—$CH_2CH_2CH_3$)			
$^7J < 1$ (—$CH_2CH_2CH_3$)			
−211	+1062	+560	157, 158
$^5J = +79$ (—CMe_3)			
$^6J = 23$ (—$C(CH_3)_3$)			
−191[a]	+1048[a]	+505[a]	157, 158
$^5J = +112$ (Me)[a]			
c. −140	+849	+549[c]	148, 160
−183	+820	c. +500	148, 160
−217[a]	+1101[a]	+515[a]	157, 158
$^5J = +92$ (Me)[a]			
−196	+1015[a]	+461[a]	157, 158
	$^4J = 92$ (Me)		
−174	+996	+509	157, 158
$^5J = +115$ (Me)		$^3J = 454$ (Me)	
−166	+968	+512	148, 160
$^5J = +107$ (Me)		$^3J = 459$ (Me)	
−173	+987	+557	157, 158
$^5J = +104$ (—CH_2CH_3)		$^3J = 437$ (—CH_2CH_3)	
$^6J = 38 \pm 10$ (—CH_2CH_3)		$^4J = 61 \pm 3$ (—CH_2CH_3)	

TABLE XII

Thallium–proton coupling constants for Tl(III) porphyrin derivatives.[a]

Porphyrin	L	L′	^4J(H-1–H-8)	^4J(H-α–H-δ)	^5J(H-R^1–H-R^8)	Other	Reference
Copro-I	Cl^-	[b]		45·5	8·4		169
	O_2CMe^-	H_2O		46·5	8·0		170
Copro-II	Cl^-	[b]		44·9, 45·3	8·3		169
Copro-III	Cl^-	[b]		44·9, 45·0, 45·3	8·3, 8·1, 8·1		169
Copro-IV	Cl^-	[b]		44·8, 45·1, 45·4	8·0, 8·2		169
OEP	Cl^-	[b]		44·4	6·1, 18·1 ($-CH_2CH_3$)	^6J=7·5 ($-CH_2CH_3$)	170–172
	CH_3			7·8		^2J(Tl, CH_3)=715±3	174
	O_2CMe^-	H_2O		46·0			170
	I^-	I^-		45·0			170
	CN^-	CN^-		32·0			170
OEP	$O_2CCF_3^-$	$O_2CCF_3^-$		49·0			170
Aetio-I	Cl^-	[b]		46·2	8·0 (Me); 11·8 ($-CH_2CH_3$)		170
	Cl^-	[b]		45	8·2 (Me); 10, 14 ($-CH_2CH_3$)	^6J=1·4 ($-CH_2CH_3$)	173
Aetio-I	$O_2CCF_3^-$	$O_2CCF_3^-$		51·0	9·0 (Me)		170
Aetio-II	Cl^-	[b]		45·5	8·5 (Me)		170
Aetio-IV	Cl^-	[b]		45·0, 46·0, 45·0	8·0 (Me)		170
TPP	Cl^-	[b]	65·4				170
	O_2CMe^-	H_2O	64·0				170
	CH_3		16·4			^2J (Tl, CH_3)=724±2	174
Pyrro-XV	Cl^-	[b]	70·0	44·6, 44·0, 47·0, 46·8	8·5, 9·5, 9·0 (Me)		170, 172
γ-Phyllo-XV	Cl	[b]		45		^5J=28 (γ-Me)	170, 172
α, γ-Dioxo-OEP	Cl^-	[b]			20 ($-CH_2CH_3$)		172

[a] Solvent was $CDCl$

[b] These ligands were originally reported, in the references cited, as OH^- and H_2O. But NMR and X-ray crystallography data reported in references showed, for the TPP and OEP complexes, that Cl^- (presumably from the $CHCl_3$ solvent) was the only ligand. It is highly likely that all thallium(III) porphyrins are five-coordinate, rather than six-coordinate, because the thallium atom is markedly displaced out of the porphyrin plane, by 0·69 Å (Cl–OEP) and 1·11 Å (Me–TPP), for example.

TABLE XIII

Thallium–carbon coupling constants for Tl^{I}(III) porphyrin derivatives.[a]

Porphyrin	L	L′	^{2}J(C-1′-C-8′)	^{3}J(C-1-C-8)	^{3}J(C-α-C-γ)	^{4}J(C-R^{1}-C-R^{8})	^{5}J(C′-R^{1}-C′-R^{8})	Reference
Copro-I	Cl^-	[c]	18, 20	109 (C-1, 3, 5, 7) 106 (C-2, 4, 6, 8)	147	15 (−CH_3) 12 (−$CH_2CH_2CO_2Me$)		175, 176
Copro-II	Cl^-	[c]	18, 20	107 (C-1, 3, 5, 7) 106 (C-2, 4, 6, 8)	145	15 (−CH_3) 15 (−$CH_2CH_2CO_2Me$)		176
Copro-III	Cl^-	[c]	18, 18, 18, 15	108, 108(C-1, 3, 5, 7) 106, 106(C-2, 4, 6, 8)	147	15 (−CH_3) 13 (−$CH_2CH_2CO_2Me$)		176
Copro-IV	Cl^-	[c]	17, 17, 18, 19	108, 108(C-1, 3, 5, 7) 105, 106, (C-2, 4, 6, 8)	147 (C-β, γ, δ) 145 (C-α)	15 (−CH_3) 13 (−$CH_2CH_2CO_2Me$)		176
Deut-IX	Cl^-	[c]		110(C-1 · · · C-8)	150 (C-γ, C-δ) 143 (C-α, C-β)	12, 10(−CH_3) 12 (−$CH_2CH_2CO_2H$)		176
TPP	CH_3		33·5	27·6	56·4			174
TPP	Cl^-	[c]	13	119	141	25 (C-1″)	19, 20 (C-2″)	177
OEP	CH_3 [b]		29·4	24·4	52			174
OEP	Cl^-	[c]	18	104	147	13 (−CH_2CH_3)		176
TPP	O_2CMe^-	H_2O	7	110	115	17 (C-1″)	20, 13 (C-2″)	177
TOP	Cl^-	[c]	21	116		17	26, 17 (C-2″) 25, 17 (C-6″)	177

[a] Solvent was $CDCl_3$,

[b] ^{1}J(Tl, CH_3)=5835±3 Hz.

[c] These ligands were originally reported, in the references cited, as OH^- and H_2O. But NMR and X-ray crystallography data reported in the reference showed, for the TPP and OEP complexes, that Cl^- (presumably from the $CHCl_3$ solvent) was the only ligand. It is highly likely that all thallium (III) porphyrins are five-coordinate, rather than six-coordinate, because the thallium atom is markedly displaced out of the porphyrin plane, by 0·69 Å (Cl–OEP) and 1·11 Å (Me–TPP), for example.

Thallium–proton couplings in $Me_3TlCH_2PMe_3$[179] and $(Me_2TlPPh_2)_2$, $(Me_2TlPHPh)_2$, $(Et_2TlPPh_2)_2$, and $(Me_2TlAsPh_2)_2$[118] have been measured. Thallium–carbon couplings in $Me_3TlCH_2PMe_3$[179] and $(Me_2TlPPh_2)_2$,[118] and thallium–phosphorus and thallium–thallium couplings in $(Me_2TlPPh_2)_2$[118] have also been reported (Table XVI).

Weibel and Oliver measured thallium–proton couplings in the series $Li[(Me_3Sn)_xTlMe_{4-x}]$, with $x = 0, 1, 2, 3, 4$.[484–85,180] Thallium–phosphorus coupling was recently noted in a series of novel thallium–iridium bonded organometallic compounds[181] (Table XV).

Thallium–proton couplings for the bimetallic $Tl[Co(CO)_3P(CH_2SiMe_3)_3]$[182] and $R_2TlM(CO)_3cp$, where R = Me and Et and M = Mo and W[183] have been observed. Thallium–proton couplings to the cyclopentadienyl protons were detected for the methylcylcopentadienylthallium[129] and dicyclopentadienylthallium[82] compounds, in the range 214–225 Hz (Table XV).

Finally, ^{205}Tl–^{1}H and ^{205}Tl–^{11}B couplings for the metallocarboranes $(Me_2Tl)^+(B_{10}H_{12}TlMe_2)^-$ and $(Ph_3PMe)^+(B_{10}B_{12}TlMe_2)^-$ have been obtained by $^{1}H(^{11}B)$ and $^{11}B(^{1}H)$ NMR[109] (Table XV).

VII. SOLID STATE AND MELT STUDIES

A. Introduction

It is widely recognized that NMR spectra exhibited by solid samples are usually quite different from spectra of the same materials in solution. This is partly due to the averaging of shielding anisotropies by rapid molecular tumbling in solution. In addition, the processes which dominate relaxation are usually different in solution than in a rigid solid. Spin–spin relaxation is particularly inefficient in solution. The result is simplification of the broad, complex spectra usually observed with solids to yield the familiar high resolution spectra of solutions. It is important to recognize that this simplification is achieved only at a cost and that fundamentally interesting information which is lost in spectra of solutions may, at least in principle, be obtained from solid state spectra. Properties of solution spectra such as the chemical shift are strongly influenced by parameters like the CSA, which are averaged, but not *eliminated*, in solution. One of the primary motives for studying NMR spectra in solids is therefore to better understand spectra in solution. In addition, solids and melts are often of interest in themselves so their spectra are useful quite aside from any insight they may provide concerning solutions.

In this section, the NMR properties of ^{203}Tl and ^{205}Tl in solids and melts are examined. Prior to discussing experimental shift and relaxation data for specific systems, a few general comments are provided concerning the special features of spectra from solids and melts containing thallium. The

reader is referred to several excellent monographs[231-236] for detailed discussions of solid state NMR spectroscopy.

The primary factors which govern the chemical shift of thallium are its oxidation state and its electronic interactions with the surroundings. In solids, the presence of greater covalency might be expected to result in large high frequency shifts of solvated, ionic thallium species, and this is indeed observed in many cases. However, this is by no means an inviolable rule as the thallium resonance in a crystalline salt may be shifted to low frequency from that in a solution by hundreds of parts per million. The relative shifts are, of course, determined by the strengths of the electronic interactions in the solid compared with those in solution (which may be substantial, as shown previously). Within a series of solids, the highly ionic systems exhibit low frequency shifts while more covalent compounds will resonate at higher frequencies. Chemical shifts for solids and melts are included in Table II, and Knight shifts for various systems containing thallium are listed in Table XVII. Thallium shifts are often highly temperature dependent (Table XIX), and phase transitions are normally accompanied by shift discontinuities (Table XX).

One spectral parameter which is seldom encountered in solution (except in relaxation studies) is the anisotropy of the shielding tensor. Its influence may usually be observed directly in the spectra of solids either through its contribution to the spectral line width or by means of characteristic "powder patterns" in polycrystalline or amorphous samples. In single crystals, the dependence of the shielding on the crystal orientation relative to the applied magnetic field is a manifestation of the shielding anisotropy. The amount of anisotropy exhibited depends largely on the covalency in the system. In highly ionic solids, thallium ions do not experience strong electronic interactions with surrounding species in any direction, thus limiting the total CSA. On the other hand, thallium ions in covalent systems may potentially exhibit large shielding anisotropies provided that the electronic interactions are strongly directional. In other words, ionic character in a solid limits the potential magnitude of the shift anisotropy while strong covalency is a necessary, but not a sufficient, requirement for large anisotropy. This effect may be observed very clearly in the thallium CSA data given in Table XVIII.

Compared with solution spectra, the thallium NMR spectra of solid samples usually contain extremely broad resonance lines (line widths have been compiled in Table XXI). These broad lines are often described in the literature in terms of moments, where the nth moment of a line shape $f(x)$ about x_0 along an NMR field or frequency axis x is defined by

$$M_n = \frac{\int_0^\infty (x - x_0)^n f(x)\,\mathrm{d}x}{\int_0^\infty f(x)\,\mathrm{d}x}$$

TABLE XIV

Key for nomenclature of porphyrin derivatives.[a,b]

Porphyrin	R^1	R^2	R^3	R^4	R^5	R^6	R^7	R^8	R^9
Copro-I	Me	P	Me	P	Me	P	Me	P	H
Copro-II	Me	P	P	Me	Me	P	P	Me	H
Copro-III	Me	P	Me	P	Me	P	P	Me	H
Copro-IV	Me	P	P	Me	P	Me	Me	P	H
OEP	Et	Et	Et	Et	Et	Et	Et	Et	H
α,γ-Dioxo-OEP	Et	Et	Et	Et	Et	Et	Et	Et	H(α, γ := 0)
TPP	H	H	H	H	H	H	H	H	Ph
γ-Phyllo-XV	Me	Et	Me	Et	Me	H	P	Me	H(γ : Me)
Deut-IX	Me	H	Me	H	Me	P	P	Me	H
Pyrro-XV	Me	Et	Me	Et	Me	H	P	Me	H
TOP	H	H	H	H	H	H	H	H	2-MeC_6H_4
Aetio-II	Me	Et	Et	Me	Me	Et	Et	Me	H
Aetio-I	Me	Et	Me	Et	Me	Et	Me	Et	H
Aetio-III	Me	Et	Me	Et	Me	Et	Et	Me	H
Aetio-IV	Me	Et	Et	Me	Et	Me	Me	Et	H

Structural numbering system for the porphyrins

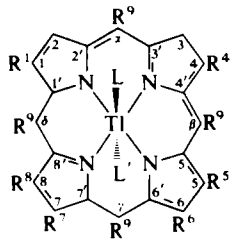

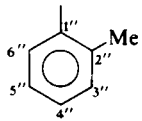

1′–8′: α positions
1–8: β positions
α–δ: *meso* positions

[a] Abbreviations: OEP, octaethylporphyrin; TPP, tetraphenylporphyrin; TOP, tetra(*ortho*-methylphenyl)porphyrin.
[b] P = $CH_2CH_2CO_2Me$.

The second moment ($n = 2$) is simply the mean square line width which takes values depending strongly on the amount of Lorentzian or Gaussian character in $f(x)$. In principle, a line may be completely described by specification of its moments, and in practice the second moment is most often encountered.

A number of factors influence thallium NMR line widths and second moments in solids, most of which are treated in detail in the classic paper of Van Vleck.[237] The most important mechanisms are

(1) chemical shielding anisotropy
(2) direct, through-space dipolar interactions
(3) indirect spin–spin interactions
  (a) pseudodipolar interactions
  (b) exchange interactions
(4) quadrupolar interactions
(5) motional averaging.

In favourable cases, CSA is significantly larger than the total line broadening from all other sources. In these cases, NMR studies of powders or glasses yield highly characteristic "powder patterns" from which the magnitude of the CSA and the values of the principle elements of the shielding tensor may be determined via computer fitting techniques or by inspection.[4,203,234] If the line broadening due to CSA is smaller than that resulting from other factors, then broad, symmetrical lines result. The magnitude of the CSA may still often be determined in these cases from the slope of a plot of M_2 against B_0^2, where M_2 is the second moment and B_0 is the applied magnetic field strength.[238,239]

In view of the large magnetogyric ratios of ^{205}Tl and ^{203}Tl, direct dipole–dipole interactions might be expected to contribute importantly to experimental thallium line widths. If the structure of the sample is known, the contribution of direct dipolar interactions to the second moment can be calculated with excellent accuracy using the method of Van Vleck.[237] In cases where structural details are unknown, the absence of an orientation dependence of the line width of a single crystal suggests the absence of dipolar (and pseudodipolar) broadening. Dipolar line broadening is independent of the magnetic field strength.

The spectra of thallium in solid samples often show line broadening due to indirect spin–spin coupling. These interactions are field-strength independent and depend on the transmission of nuclear spin information indirectly through intervening electrons. The electrons couple with the nuclear spins via dipolar or hyperfine interactions, and correlation between the electrons then results in the indirect nuclear interactions. While the magnitude of indirect coupling may be insignificant for light nuclides, the large thallium hyperfine interaction causes this to be a very important source of line broadening in this case.

TABLE

Miscellaneous thallium–proton

Compound	Solvent	$^2J(^{205}Tl-^1H)$/Hz
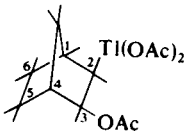		−797 (H-2)[a]
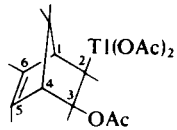		−581 (H-2)
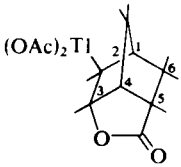		−1200 (H-2)
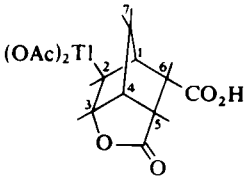		−1197 (H-2)
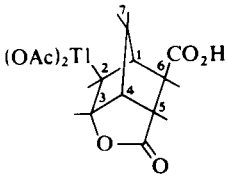		−1204 (H-2)
TlH_4^-		$^1J(^{205}Tl-^1H) = 6144$[b]
$(TlOEt)_4$	neat	$^2J(^{205}Tl-^{203}Tl) = 2560$
$(Me_2Tl)^+(B_{10}H_{12}TlMe_2)^-$	acetone-d_6	−404 (cation Me)
		−354, −338 (anion Me, Me′)
$(Ph_3PMe)^+(B_{10}H_{12}TlMe_2)^-$	$CDCl_3$	−346, −328 (anion Me, Me′)
$Tl[Co(CO)_3P(CH_2SiMe_3)_3]$	C_6H_6	$^nJ = 40{\cdot}1$ (−CH_2−)
$Me_3PCH_2TlMe_3$	C_6H_6	−267 (Me)
		−101 (−CH_2P−)
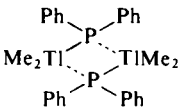	C_6H_6	−319
		$^2J(Tl-Tl) = 155$ Hz

XV

coupling constants.

$^{3}J(^{205}Tl-^{1}H)$/Hz	$^{4}J(^{205}Tl-^{1}H)$/Hz	$^{5}J(^{205}Tl-^{1}H)$/Hz	Reference
+649 (H-1)[a] +624 (H-3)[a]	+817 (H-6 *exo*)[a] 263 (H-4)		165
+410 (H-1)	112 (H-4)	$^{5,4}J$ = 76, 92 (H-5, H-6)	165
+909 (H-3) +630 (H-1)	208 (H-6 *exo*)		166
+911 (H-3) +515 (H-1)	+223 (H-6 *exo*)		166
+898 (H-3) +545 (H-1)			166
			164 64
^{n}J = 66(?) (bridge H)[c]	$^{n}J(^{205}Tl-^{11}B)$ = 70		109
^{n}J = 66(?) (bridge H)[c] ^{n}J = 3·0 (−$SiCH_3$)			109 182 179
^{1}J(Tl–P) = 3203, 3144 Hz			118

TABLE

Compound	Solvent	$^2J(^{205}Tl-^1H)$/Hz
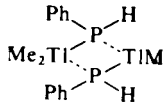	Pyridine-d_5	−273[x] (Me)
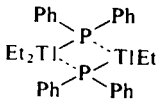	C_6D_6	−325 ($-CH_2CH_3$)
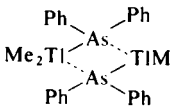	C_6D_5	−310 (Me)
Cyclo[$-Tl(Me)_2CH_2P(Me)_2CH_2-$]$_2$	C_6H_6	−305·5($-Tl-CH_3$) −152·0 ($-CH_2-$)
$Li(TlMe_4)$	DME[e]	−220·8,[f] −224·1[g]
$Li[Me_3SnTlMe_3]$	DME[e]	−223·1[f], −227·8[g]
$Li[(Me_3Sn)_2TlMe_2]$	DME[e]	−214·8,[f] −220·2[g]
$Li[(Me_3Sn)_3TlMe]$	DME[e]	−213·8[g]
$Li[(Me_3Sn)_4Tl]$	DME[e]	
$[(cp)_2Tl]_2SO_4$	D_2O	−214 (cp)
$Me_2TlMo(CO)_3cp$	CH_2Cl_2[d]	−273·0 (Me)
$Me_2TlMo(CO)_3cp$	$CDCl_3$	−272[o], −271[d], −264[p], −259[q], −242[r] (Me)
$Et_2TlMo(CO)_3cp$	$CDCl_3$	−249[s] ($-CH_2CH_3$)
$Me_2TlW(CO)_3cp$	CH_2Cl_2[d]	−265·0 (Me)
$Me_2TlW(CO)_3cp$	$CDCl_3$	−274,[t,u] −272,[v] −268,[i] −264[w] (Me)
$Et_2TlW(CO)_3cp$	$CDCl_3$	−310[w] ($-CH_2CH_3$)
$(Ph_3P)_2(CO)OAc)_2IrTl(OAc)_2$		1134 (^2J(Tl–P))
$(Ph_3P)_2(CO)(O_2CCF_3)_2IrTl(O_2CCF_3)_2$		1081 (^2J(Tl–P))
$(Ph_3P)_2(CO)$ $(O_2CEt)_2IrTl(O_2CEt)_2$		1119 (^2J(Tl–P))
$(Ph_3P)_2(CO)$ $(O_2CCHMe_2)_2IrTl(O_2CCHMe_2)_2$		1112 (^2J(Tl–P))
$(Ph_3P)_2(CO)$ $(O_2CCHMe_2)_2(OAc)IrTl(OAc)_2$		1131, 1113, 1056 (^2J(Tl–P))
$(Ph_3P)_2(CO)Cl(OAc)IrTl(OAc)_2$		1148, 1099 (^2J(Tl–P))
$(Ph_3P)_2(CO)(OH)(O_2CEt)IrTl(O_2CEt)_2$		1121 (^2J(Tl–P))
$(PhMe_2P)_2(CO)(OAc)_2IrTl(OAc)_2$		1202 (^2J(Tl–P))
$(PhMe_2P)_2(CO)$ $(O_2CCF_3)_2IrTl(O_2CCF_3)_2$		1140 (^2J(Tl–P))
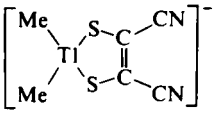		−373

XV (*cont.*)

$^3J(^{205}Tl-^1H)$/Hz	$^4J(^{205}Tl-^1H)$/Hz	$^5J(^{205}Tl-^1H)$/Hz	Reference
			118
+621 ($-CH_2CH_3$)			118
			118
$^2J(Tl-P) = 295{\cdot}0$	3·4 ($-P-CH_3$)		188
			84, 85, 180
32·0[g]			84, 85, 180
39·0[g]			84, 85, 180
44·0[g]			84, 85, 180
47·4[g]			84, 85, 180
−214 or 466 (cp)			82
			183
			189
+529[s] ($-CH_2CH_3$)			189
			183
			183
+627[w] ($-CH_2CH_3$)			183
			181
			181
			181
			181
			181
			181
			181
			181
			163

TABLE

Compound	Solvent	$^2J(^{205}Tl-^1H)$/Hz
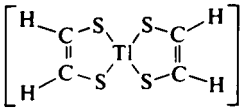	Acetone	
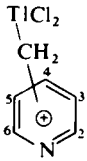	DMSO	−1136 (−CH_2−) −1236 (−CH_2−)[h] −1234 (−CH_2−)[i] −1086 (−CH_2−)[j] −694 (−CH_2−)[k]
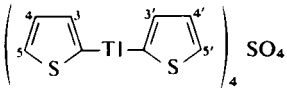	D_2O	
TlCl : C222[v]	D_2O[l]	^nJ = 11·5 (N−CH_2CH_2−)
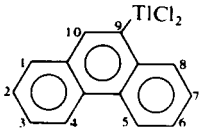	DMSO-d_6	
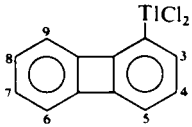	DMSO-d_6	
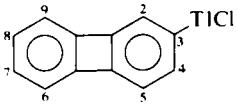	DMSO-d_6	
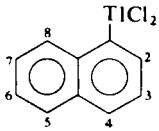	DMSO-d_6	
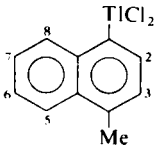	DMSO-d_6	
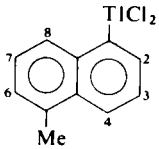	DMSO-d_6	

XV (*cont.*)

$^3J(^{205}Tl-^1H)$/Hz	$^4J(^{205}Tl-^1H)$/Hz	$^5J(^{205}Tl-^1H)$/Hz	Reference
578			162
	? (H-3)	? (H-4, 6), ? (^6J, H-5)	161
	196 (H-3, 5)[h]	49 (H-2, 6)[h]	
J = 166 (N—CH_3)[l]	197 (H-3, 5)[i]	50 (H-2, 5)[i]	
	216 (H-2), 198(H-4)[i]	^6J = 204 (H-6)[i]	
	106 (H-3, 5)[k]	26 (H-2, 6)[k]	
+304 (H-3, 3')[a]	+105 (H-4, 4')[a]		82
	+197 (H-5, 5')[a]		
^nJ = 14·5 (—OCH_2CH_2O—)			62a
+1077 (H-10)			82
+674 (H-3)	+225 (H-4)	+208 (H-5)	145
+710 (H-2)	+215 (H-5)		145
+950 (H-4)			
+984 (H-2)	+287 (H-3)	+118 (H-4)	82
	50 (H-8)	181 (H-5)	
+992 (H-2)	+277 (H-3)	209 (H-5)	82
	54 (H-8)		
+984 (H-2)	+287 (H-3)	+118 (H-4)	82
	50 (H-8)	^6J < 12 (Me)	

TABLE

Compound	Solvent	$^2J(^{205}Tl-^1H)$/Hz
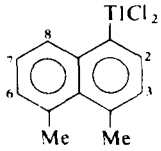	DMSO-d_6	
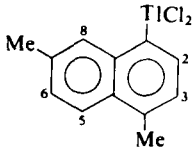	DMSO-d_6	
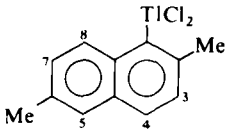	DMSO-d_6	
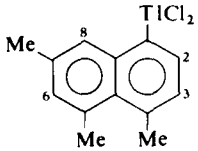	DMSO-d_6	
Tl^{I} : nonactin	$CDCl_3$	
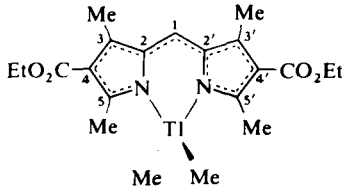	$CDCl_3$	−371·6 (Me)

[a] Coupling constant sign was determined experimentally.
[b] Calculated.
[c] Possibly two singlets from two non-equivalent bridge H atoms.
[d] −70 °C.
[e] DME = 1,2-dimethoxyethane.
[f] −60 °C.
[g] 38 °C.
[h] 4-CH_2TlCl_2.
[i] 4-CH_2TlCl_2; *N*-methyl derivative.
[j] 3-CH_2TlCl_2.
[k] $(4\text{-}CH_2C_5H_5N)_2TlCl$.
[l] 12 °C; same *J* values for $TlNO_3$: C222 in $CDCl_3$ at −32 °C.
[m] Ester C-α protons.

XV (*cont.*)

$^3J(^{205}Tl-^1H)$/Hz	$^4J(^{205}Tl-^1H)$/Hz	$^5J(^{205}Tl-^1H)$/Hz	Reference
+992 (H-2)	+277 (H-3) 54 (H-8)	$^6J < 12$ (5-Me)	82
+994 (H-2)	+277 (H-3)	210 (H-5) $^6J = 19{\cdot}4$ (7-Me) $^6J = +58$ (4-Me) $^6J = 15$ (H-6)	82
+388 (H-3) 125 (2-Me) 44·7 or 36·3 (H-8)	+122 (H-4) 183 (H-5) 21·5 or 29·9 (H-7) $^7J = 12{\cdot}5$ (6-Me)	82	
+994 (H-2)	+277 (H-3)	$^6J = 58$ (4-Me) $^6J < 12$ (5-Me) $^6J = 15$ (H-6) $^6J = 19{\cdot}4$ (7-Me)	82
11·5, 16·0,[n] 3·5[m]			59
	9·2 (5, 5′-Me)		178

[n] C-α protons of the furan rings.
[o] −92 °C.
[p] −48 °C.
[q] −28°C.
[r] −3 °C.
[s] −80 °C.
[t] −89 °C.
[u] −74 °C.
[v] −50 °C.
[w] −10 °C.
[x] −20 °C.
[y] Cryptand, $N[(CH_2)_2O(CH_2)O(CH_2)_2]_3N$.

TABLE XVI

Miscellaneous thallium–carbon coupling constants.

Compound	Solvent	$^{1}J(^{205}Tl-^{13}C)$/Hz	$^{2}J(^{205}Tl-^{13}C)$/Hz	$^{3}J(^{205}Tl-^{13}C)$/Hz	$^{4}J(^{205}Tl-^{13}C)$/Hz	Reference
$Me_3PCH_2TlMe_3$	Toluene-d_8	+2155 (Me) 352 (—CH_2P—)				179
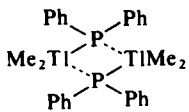	C_6D_5	+2447				118
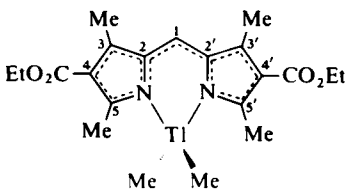	$CDCl_3$	−2808	15·8 (C-2, 2′) 22·6 (C-5, 5′)	72·2 (Me: C-5, 5′) 31·7 (C-4, 4′) 20·4 (C-3, 3′) 13·5 (C-1)		178
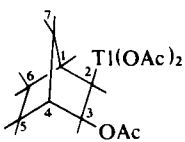	$CDCl_3$	+5754 (C-2)[a]	322·3 (C-1) 683·6 (C-3)	29·3 (C-4) 1303·7 (C-6) 31·8 (C-7)	80·6 (C-5)	167
		5750 (C-2)[b]	320 (C-1) 681 (C-3)	27 (C-4) 1301 (C-6) 32 (C-7)	64 (C-5) 66 (C = 0, 3-OAc) ^{5}J = 59 (Me, 3-OAc)	168
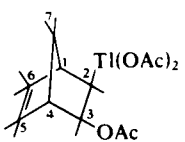	$CDCl_3$	+5764 (C-2)[c]	239·3 (C-1) 427·3 (C-3)	17·1 (C-4) 1069 (C-6) −0 (C-7)	119·7 (C-5)	167
		+5471 (C-2)	244 (C-1) 420 (C-3)	<3 (C-4) 1057 (C-6) 17 (C-7)	120 (C-5) ^{5}J = 49 (Me, 3-OAc)	168

TABLE XVI (*cont.*)

Compound	Solvent	$^{1}J(^{205}Tl-^{13}C)$/Hz	$^{2}J(^{205}Tl-^{13}C)$/Hz	$^{3}J(^{205}Tl-^{13}C)$/Hz	$^{4}J(^{205}Tl-^{13}C)$/Hz	Reference
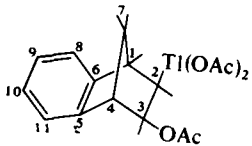	$CDCl_3$	+5645 (C-2)[d]	244 (C-1) 569 (C-6)	45 (C-4) 1149 (C-6) 7 (C-7)	51 (C=O, 3-OAc) 86 (C-8) ^{5}J = 18 (C-11) ^{5}J = 65 (C-9) ^{6}J = 77 (C-10)	168
	Pyridine-d_5	+6321 (C-2)[e]	215 (C-1) 554 (C-3)	59 (C-4) 1101 (C-6) 5 (C-7)	46 (C=O, 3-OAc) 15 (C-5) 78 (C-8) ^{5}J = 17 (C-11) ^{5}J = 59 (C-9) ^{6}J = 71 (C-10)	168
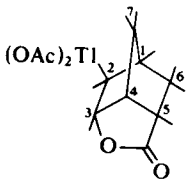	Pyridine	+6655 (C-2)[f]	219·7 (C-1) 61·0 (C-3)	75·7 (C-4) 1289 (C-6) 131·8 (C-7)	70·8 (C-5)	167
Tl^{+} : valinomycin	$CDCl_3$		103·2 (L-Val C=O) 96·4 (D-Val C=O)		8·1 (L-Lac C-α) 3·7 (D-Hiv C-α)	190

[a] $^{1}J(^{203}Tl-^{13}C)$ = +5701 Hz.
[b] $^{1}J(^{203}Tl-^{13}C)$ = +5696 Hz.
[c] $^{1}J(^{203}Tl-^{13}C)$ = +5711 Hz.
[d] $^{1}J(^{203}Tl-^{13}C)$ = +5593 Hz.
[e] $^{1}J(^{203}Tl-^{13}C)$ = +6262 Hz.
[f] $^{1}J(^{203}Tl-^{13}C)$ = +6592 Hz.

TABLE XVII

Knight shifts for thallium metal, alloys and intermetallic compounds.

System	Form	Temperature/K	Isotope	K_s/%[a]	Field strength/T	Reference
Tl metal	Solid	77	205	+1·56		203
Tl metal			205	+1·54 ± 0·05[b]	0·1993 to 0·6495	4
Tl metal			203	+1·0[b]	0·1993	4
Tl metal			203	+1·3[b]	0·6490	4
Tl metal	Solid	298	205	+1·42		206
Tl metal	Single crystal	1·2	205	+1·629	1·00	207
Tl metal	Single crystal	77	205	+1·597	1·00	207
Tl metal	Single crystal	195	205	+1·549	1·00	207
Tl metal	Single crystal	295	205	+1·533	1·00	207
Tl metal	Single crystal	1·2	205	+1·522 to 1·666[c]	1·00	208
Tl metal	Melt	*c.* 576	205	+1·50		209
Tl metal	Melt	593	205	+1·48		210
LiTl	Solid	298	205	+1·415[b]	0·6270	212
NaTl			205	−0·92		213
NaTl			205	−0·5		214
NaTl	Solid		205	−1·03[b]		4
Na_2Tl	Solid		205	+0·68[b]		4
FrTl			205	+0·89 ± 0·09		215
MgTl	Solid		205	+2·12[b]		4
CaTl	Solid		205	+1·67[b]		216
CaTl	Solid		205	+1·670 ± 0·011[b]	0·6349	217
La_3Tl	Solid	295	205	+0·305 ± 0·005	0·4	218
La_3Tl	Solid	295	203	+0·307 ± 0·005	0·4	218
La_3Tl	Solid	200	203	+0·206 ± 0·005	0·4	218
La_3Tl	Solid	200	203	+0·222 ± 0·005	0·4	218
La_3Tl	Solid	118	205	+0·075 ± 0·005	0·4	218
La_3Tl	Solid	118	203	+0·083 ± 0·005	0·4	218

TABLE XVII (*cont.*)

System	Form	Temperature/K	Isotope	K_s/%[a]	Field strength/T	Reference
La_3Tl	Solid	77	205	−0·005 ± 0·005	0·4	218
La_3Tl	Solid	77	203	−0·010 ± 0·005	0·4	218
La_3Tl	Solid	34	205	−0·115 ± 0·005	0·4	218
La_3Tl	Solid	34	203	−0·115 ± 0·005	0·4	218
La_3Tl	Solid	20	205	−0·188 ± 0·005	0·4	218
La_3Tl	Solid	20	203	−0·181 ± 0·005	0·4	218
La_3Tl	Solid	11	205	−0·225 ± 0·010	0·4	218
La_3Tl	Solid	11	203	−0·225 ± 0·010	0·4	218
La_3Tl	Solid	8·3	205	−0·273 ± 0·010	0·4	218
La_3Tl	Solid	8·3	203	−0·256 ± 0·010	0·4	218
La_3TlC	Solid	295	205	+0·755	0·4	218
La_3TlC	Solid	10	205	+0·74	0·4	218
$La_3Tl_{0·5}In_{0·5}$	Solid	295	205	+0·260	0·4	218
$La_3Tl_{0·5}In_{0·5}$	Solid	10	205	−0·40	0·4	218
$La_3Tl_{0·8}Pb_{0·2}$	Solid	295	205	+0·274	0·4	218
$La_3Tl_{0·8}Pb_{0·2}$	Solid	10	205	−0·08	0·4	218
Tl (trace) in Pb	Solid	298	205	+1·93		211
$Pb_{0·34}Tl_{0·66}$	Solid		205	+1·39[b]		4
$Pb_{0·90}Tl_{0·10}$	Solid		205	+1·90[b]		4
$Sn_{0·1}Tl_{0·9}$				+1·9		219
$Sn_{0·25}Tl_{0·75}$	Solid		205	+1·97[b]		4
$In_{0·5}Tl_{0·5}$	Solid		205	+1·68[b]		4
$Hg_{0·13}Tl_{0·87}$	Solid		205	+1·71[b]		4
$Hg_{0·60}Tl_{0·40}$	Liquid		205	+1·49[b]		4
$Hg_{0·72}Tl_{0·28}$	Solid		205	+1·01[b]		4
$Hg_{0·92}Tl_{0·08}$	Liquid	298	205	+1·18[b]		4
$Bi_{0·06}Tl_{0·94}$	Solid		205	+1·71[b]		4
$Bi_{0·19}Tl_{0·81}$	Solid		205	+1·74[b]		4

TABLE XVII (*cont.*)

System	Form	Temperature/K	Isotope	K_s/%[a]	Field strength/T	Reference
$Bi_{0\cdot59}Tl_{0\cdot41}$	Solid		205	+1·1[b]		4
$Tl_{0\cdot680}Tl_{0\cdot320}$	Liquid	700	205	+0·611 ± 0·010	0·97	220
$Tl_{0\cdot680}Tl_{0\cdot320}$	Liquid	800	205	+0·681 ± 0·020	0·97	220
$Tl_{0\cdot674}Tl_{0\cdot326}$	Liquid	700	205	+0·632 ± 0·010	0·97	220
$Tl_{0\cdot674}Tl_{0\cdot326}$	Liquid	800	205	+0·690 ± 0·020	0·97	220
$Tl_{0\cdot662}Tl_{0\cdot338}7$	Liquid	700	205	+0·156 ± 0·015	0·97	220
$Tl_{0\cdot662}Tl_{0\cdot338}$	Liquid	800	205	+0·166 ± 0·020	0·97	220
$LiCd_{0\cdot95}Tl_{0\cdot05}$		298	205	+1·005 ± 0·015[b]	0·6270	212
$LiCd_{0\cdot875}Tl_{0\cdot125}$		298	205	+1·082 ± 0·015[b]	0·6270	212
$LiCd_{0\cdot75}Tl_{0\cdot25}$		298	205	+1·115 ± 0·010[b]	0·6270	212
$LiCd_{0\cdot69}Tl_{0\cdot31}$		298	205	+1·133 ± 0·015[b]	0·6270	212
$LiCd_{0\cdot625}Tl_{0\cdot375}$		298	205	+1·160 ± 0·006[b]	0·6270	212
$LiCd_{0\cdot55}Tl_{0\cdot45}$[d]		298	205	+1·501 ± 0·020[b]	0·6270	212
				+1·198 ± 0·008[b]		
$LiCd_{0\cdot50}Tl_{0\cdot50}$[d]		298	205	+1·510 ± 0·015[b]	0·6270	212
				+1·196 ± 0·020[b]		
$LiCd_{0\cdot45}Tl_{0\cdot55}$[d]		298	205	+1·516 ± 0·015[b]	0·6270	212
				+1·187 ± 0·020[b]		
$LiCd_{0\cdot375}Tl_{0\cdot625}$[d]		298	205	+1·500 ± 0·027[b]	0·6270	212
				+1·180 ± 0·020[b]		
$LiCd_{0\cdot25}Tl_{0\cdot75}$		298	205	+1·455 ± 0·015[b]	0·6270	212
$LiCd_{0\cdot15}Tl_{0\cdot85}$		298	205	+1·420 ± 0·030[b]	0·6270	212
$CaCd_{0\cdot80}Tl_{0\cdot20}$	Solid		205	+0·90[b]		216
$CaCd_{0\cdot80}Tl_{0\cdot20}$	Solid		205	+0·899 ± 0·11[b]	0·6349	217
$CaCd_{0\cdot70}Tl_{0\cdot30}$	Solid		205	+0·96[b]		216
$CaCd_{0\cdot70}Tl_{0\cdot30}$	Solid		205	+0·958 ± 0·011[b]	0·6349	217
$CaCd_{0\cdot60}Tl_{0\cdot40}$	Solid		205	+0·99[b]		216

TABLE XVII (*cont.*)

System	Form	Temperature/K	Isotope	K_s/%[a]	Field strength/T	Reference
$CaCd_{0\cdot60}Tl_{0\cdot40}$	Solid		205	$+0\cdot984\pm0\cdot011$[c]	0·6349	217
$CaCd_{0\cdot55}Tl_{0\cdot45}$	Solid		205	$+1\cdot04$[b]		216
$CaCd_{0\cdot50}Tl_{0\cdot50}$	Solid		205	$+1\cdot08$[b]		216
$CaCd_{0\cdot50}Tl_{0\cdot50}$	Solid		205	$+1\cdot072\pm0\cdot011$[b]	0·6349	217
$CaCd_{0\cdot45}Tl_{0\cdot55}$	Solid		205	$+1\cdot14$[b]		216
$CaCd_{0\cdot40}Tl_{0\cdot60}$	Solid		205	$+1\cdot25$[b]		216
$CaCd_{0\cdot40}Tl_{0\cdot60}$	Solid		205	$+1\cdot251\pm0\cdot011$[b]	0·6349	217
$CaCd_{0\cdot20}Tl_{0\cdot80}$	Solid		205	$+1\cdot44$[b]		216
$CaCd_{0\cdot20}Tl_{0\cdot80}$	Solid		205	$+1\cdot444\pm0\cdot011$[b]	0·6349	217

[a] Knight shifts are references to Tl^+ (aq.) at infinite dilution.

[b] These values are calculated using $K_s = (B_{reference} - B_{sample})/B_{reference}$.

[c] The orientation θ of the crystal [0001] symmetry axis relative to the applied field determines the value of K_s: $K_s = K + \frac{1}{2}K'(3\cos^2\theta - 1)$, where $K = 1\cdot618\%$ and $K' = -0\cdot096\%$.[208]

[d] Two phases exist in these systems so two ^{205}Tl NMR signals are observed.

TABLE XVIII

^{205}Tl chemical shielding anisotropies.

Substance	Temperature/K	$\sigma_{isotropic}$/ppm[a]	σ_{11}/ppm[a]	σ_{22}/ppm[a]	σ_{33}/ppm[a]	$\sigma_{33}-\sigma_{11}$/ppm[a]	Method[b]	Reference
Tl^+/valinomycin (ClO_4^-)	301	−545	−595	−595	−445	150	PP	199
$TlClO_4$	307	−524	−602	−485	−485	117	PP	227
$TlClO_4$	307	−524				≥95	SCR	227
7·5% $TlNO_3$ in KNO_3	305	−304	−341	−286	−286	55	PP	225
7·5% $TlNO_3$ in KNO_3	410	−208	−253	−208	−163	90	PP	225
$TlNO_3$	305	c. −135				≥95	SCR	195
$TlPO_3$ (glass)	c. 298	−50				560	M_2 vs. H_0^2	197
TlI	401	+1190	+500	+1530	1530	1030	PP	191
TlI	298					≤730	M_2 vs. H_0^2	18
$(Tl_2Se)_x(As_2Se_3)_{1-x}$ (glass), $0{\cdot}33 \leq x \leq 0{\cdot}67$		+1670 to +1980				c. 500	M_2 vs. H_0^2	201
Tl_2O_3	77	+5500				1870	M_2 vs. H_0^2	203
Me_2TlBr	308	+5590	+5430	+5430	+5915	485	PP	198
TlCN	210					c. 1000	M_2 vs. H_0^2	228
Tl metal	77	+15600[c]				2500[d]	M_2 vs. H_0^2	203
Tl metal	1·2	+16140[c]				1440[d]	SCR	208

[a] Relative to infinite dilution aqueous ^{205}Tl(I).

[b] Methods used to determine chemical shift anisotropies: PP = theoretical fit to an experimental powder pattern; SCR = single crystal rotation study; M_2 vs. H_0^2 = calculated from slope of a plot of second moment against squared applied field strength.

[c] Isotropic Knight shift.

[d] Knight shift anisotropy.

TABLE XIX

Temperature dependence of the ^{205}Tl shift in solids and melts.

Compound	Form	Approximate temperature range/K[a]	Temperature dependence/ppm K^{-1} [b]	Reference
$TlNO_3$	Solid	323–463	*c.* 0	184
$TlNO_3$	Melt	478–598	0·70 ± 0·05	184
TlF	Melt	533–593	0·77 ± 0·05	184
TlCl	Solid	553–683	0·86 ± 0·05	184
TlCl	Melt	693–813	0·78 ± 0·05	184
TlBr	Solid	543–743	0·60 ± 0·05	184
TlBr	Melt	753–833	0·73 ± 0·05	184
TlI	Solid	573–713	<0·2	184
TlI	Solid	298–423	*c.* 0·2	18
TlI	Solid	433–533	*c.* 0	18
TlI	Melt	723–793	1·4 ± 0·1	184
TlOAc[c]	Solid	293–383	4·2 ± 0·1	184
TlOAc[c]	Solid	313–383	5·2 ± 0·5 (slight curvature)	194
TlOAc[c]	Melt	373–443	0·56 ± 0·05	184
TlOAc[c]	Melt	383–433	0·43 ± 0·05	194
TlOAc[d]	Solid	<403	Non-linear	194
TlOAc[d]	Melt	404–433	0·28 ± 0·04	194
$TlHCO_2$	Solid	<373	Non-linear	194
$TlHCO_2$	Melt	374–433	0·20 ± 0·03	194
$TlMnCl_3$	Solid	130–500	*c.* 0	223
$TlNiCl_3$	Solid	130–500	*c.* 0	223
$TlCoCl_3$	Solid	130–500	*c.* 0	223
Tl_2SO_4	Solid	773–898	0·48 ± 0·05	184
Tl_2SO_4	Melt	933–983	0·43 ± 0·05	184
$TlCl_3$	Solid	293–333	*c.* 0	184
$TlCl_3$	Melt	343–513	0·06	184
$Tl(ClO_4)_3$	Solid	293–343	*c.* 0	184
$Tl(ClO_4)_3$	Melt	398–443	*c.* 0	184
Tl_2Cl_2[Tl(III)]	Melt	503–723	*c.* 0	20
Tl_2Cl_2[Tl(I)]	Melt	523–613	*c.* 0·8	20

[a] Temperature range of experimental measurement. Linear temperature dependence may extend beyond this range.

[b] Positive values signify downfield shift with increasing temperature.

[c] These samples of TlOAc melted at *c.* 110 °C, suggesting slight impurity.

[d] These samples of TlOAc melted at *c.* 130 °C, indicating high purity.

TABLE XX

^{205}Tl chemical shift discontinuities resulting from phase transitions.

Compound	Transition temperature/K	Type of transition	$\Delta\delta$/ppm[a]	Reference
$TlNO_3$	479	Fusion	+170	184
$TlNO_3$	479	Fusion	+132	221
TlCl	703	Fusion	+560	184
TlCl	703	Fusion	+596	221
TlBr	753	Fusion	+550[b]	222
TlBr	753	Fusion	+560	184
TlBr	753	Fusion	+572	221
TlI	713	Fusion	+310	184
TlI	*c.* 430	Orthorhombic to cubic	0 to +400[c]	18
TlOAc	383[d]	Fusion	$<\pm 2$	184
TlOAc	383[d]	Fusion	*c.* 0	194
TlOAc	404[d]	Fusion	*c.* 0	194
$TlHCO_2$	374	Fusion	*c.* 0	194
Tl_2SO_4	905	Fusion	+260	184
$Tl(ClO_4)_3$	*c.* 380	Fusion	−80	184
$TlCl_3$	298	Fusion	+2	184
$Tl_2SeAs_2Tl_3$	359	Glass to liquid	0	200
$(Tl_2Se)_x(As_2Se_3)_{1-x}$, $0{\cdot}33 \leq x \leq 0{\cdot}66$		Fusion	0	201
Tl metal	577	Fusion	*c.* 0[e]	210

[a] Positive value denotes a shift of the resonance line to higher frequency upon transition from the low temperature form to the high temperature form.

[b] Reference 222 indicates that this value represents a refinement of the +560 ppm value given in reference 184.

[c] The magnitude of the solid phase transition shift discontinuity of TlI is field-dependent, with a value of +400 ppm at 0·641 T.

[d] The melting point of rigourously pure TlOAc is 404 K, while samples of slightly lower purity melt sharply at 383 K.

[e] Knight shift discontinuity.

TABLE XXI

Thallium NMR line widths and second moments.

Compound[a]	Form	Temperature/K	Isotope	Line width[b] KHz	Line width[b] 10^{-4} T	Second moment/10^{-8} T^2 [b]	Field strength/T	Reference
Tl metal	Solid or melt	77–400	205	33	(13)		0·1993–0·6495	4
Tl metal	Solid or melt	77–400	203	17	(6·9)		0·1993	4
Tl metal	Solid or melt	77–400	203	33	(13)		0·6490	4
Tl metal (98·7% ^{205}Tl)	Solid	77–300	205	20	(8·1)	(47·9)	0·5560	203
Tl metal (90·5% ^{205}Tl)	Solid	77–300	205	23	(9·4)	(66·3)	0·5560	203
Tl metal (70·5% ^{205}Tl)	Solid	77–300	205	33	(13)	(97·2)	0·5560	203
Tl metal (52·1% ^{205}Tl)	Solid	77–300	205	54	(22)	(135)	0·5560	203
Tl metal (14·0% ^{205}Tl)	Solid	77–300	205	>60	(>24)	(180·6)	0·5560	203
Tl metal (70·5% ^{205}Tl)	Solid	77–300	203	>60	(>24)		0·5560	203
Tl metal (52·1% ^{205}Tl)	Solid	77–300	203	54	(22)		0·5560	203
Tl metal (14·0% ^{205}Tl)	Solid	77–300	203	27	(11)		0·5560	203
Tl metal (14·0% ^{205}Tl)	Solid	77–300	203	25	(10)		0·3288	203
Tl metal	Single crystal	1·2	203	30–36[d]	(12–15)[d]		1·00	208
Tl metal	Melt	593	205	(43·0)	17·5			210
LiTl	Solid	298	205	(6·51)	2·65		0·6270	212
NaTl	Solid		205	50	(20)			4
Na_2Tl	Solid		205	38	(15)			4
MgTl	Solid		205	40	(16)			4
$Ca_{0·5}Tl_{0·5}$	Solid		205	(37·8)	15·4		0·6349	217
$In_{0·5}Tl_{0·5}$	Solid		205	38	(15)			4
$Hg_{0·13}Tl_{0·87}$	Solid		205	34	(14)			4
$Hg_{0·60}Tl_{0·40}$	Melt		205	20	(8·1)			4
$Hg_{0·72}Tl_{0·28}$	Solid		205	33	(13)			4
$Hg_{0·92}Tl_{0·08}$	Melt	298	205	30	(12)			4
$Pb_{0·34}Tl_{0·66}$	Solid		205	34	(14)			4

TABLE XXI (*cont.*)

Compound[a]	Form	Temperature/K	Isotope	Line width[b] KHz	Line width[b] 10^{-4} T	Second moment/10^{-8} T^2 [b]	Field strength/T	Reference
$Pb_{0.90}Tl_{0.10}$	Solid		205	33	(13)			4
$Bi_{0.06}Tl_{0.94}$	Solid		205	75	(31)			4
$Bi_{0.19}Tl_{0.81}$	Solid		205	110	(44·8)			4
$Bi_{0.59}Tl_{0.41}$	Solid		205	110	(44·8)			4
$Sn_{0.25}Tl_{0.75}$	Solid		205	64	(26)			4
$LiCd_{0.95}Tl_{0.05}$	Solid	298	205	(3·24)	1·32		0·6270	212
$LiCd_{0.875}Tl_{0.125}$	Solid	298	205	(2·70)	1·10		0·6270	212
$LiCd_{0.75}Tl_{0.25}$	Solid	298	205	(2·70)	1·10		0·6270	212
$LiCd_{0.69}Tl_{0.31}$	Solid	298	205	(3·12	1·27		0·6270	212
$LiCd_{0.625}Tl_{0.375}$	Solid	298	205	(3·05)	1·24		0·6270	212
$LiCd_{0.55}Tl_{0.45}$	Solid	298	205	(4·54)	1·85		0·6270	212
		298	205	(3·73)	1·52		0·6270	212
$LiCd_{0.50}$	Solid	298	205	(4·42)	1·80		0·6270	212
		298	205	(4·42)	1·80		0·6270	212
$LiCd_{0.45}Tl_{0.55}$	Solid	298	205	(5·03)	2·05		0·6270	212
		298	205	(3·88)	1·58		0·6270	212
$LiCd_{0.375}Tl_{0.625}$	Solid	298	205	(5·53)	2·25		0·6270	212
		298	205	(3·71)	1·51		0·6270	212
$LiCd_{0.25}Tl_{0.75}$	Solid	298	205	(5·40)	2·20		0·6270	212
$LiCd_{0.15}Tl_{0.85}$	Solid	298	205	(7·00)	2·85		0·6270	212
$Ca_{0.50}Cd_{0.40}Tl_{0.10}$	Solid		205	(39·3)	16·0		0·6349	217
$Ca_{0.50}Cd_{0.35}Tl_{0.15}$	Solid		205	(42·8)	17·4		0·6349	217
$Ca_{0.50}Cd_{0.30}Tl_{0.20}$	Solid		205	(48·4)	19·7		0·6349	217
$Ca_{0.50}Cd_{0.25}Tl_{0.25}$	Solid		205	(54·8)	22·3		0·6349	217
$Ca_{0.50}Cd_{0.20}Tl_{0.30}$	Solid		205	(66·8)	27·2		0·6249	217
$Ca_{0.50}Cd_{0.10}Tl_{0.40}$	Solid		205	(48·4)	19·4		0·6349	217

TABLE XXI (*cont.*)

Compound[a]	Form	Temperature/K	Isotope	Line width[b] KHz	Line width[b] 10^{-4} T	Second moment/10^{-8} T^2 [b]	Field strength/T	Reference
$TlNO_3$	Solid		205			2	0·4371	17
$TlNO_3$	Solid		203			7	0·4371	17
$TlNO_3$	Solid (γ)	297	205	(5·2)	2·1	2·0	0·855	193
$TlNO_3$	Solid (γ)	298–343	205	(5·77)	2·35			224
$TlNO_3$	Solid (β)	363–403	205	(3·4)	1·4			224
$TlNO_3$	Solid (α)	418–493	205	(0·2)	0·1			224
$TlNO_3$	Solid (γ)	305	205	7·1	(2·9)		2·114	225
$TlNO_3$	Solid (γ)	205–335	203	11·6	4(4·7)		2·114	225
$TlNO_3$	Solid (γ)	333	205	7·0	(2·8)		2·114	225
$TlNO_3$	Solid (β)	356–410	205	4·1	(1·7)		2·114	225
$TlNO_3$	Solid (β)	372	203	9·3	(3·8)		2·114	225
$TlNO_3$	Solid (α)	425–435	205	0·22	(0·09)		2·114	225
$TlNO_3$	Single crystal (γ)	305	205	3·8 ± 0·5[e]	(1·5 ± 0·2)		2·114	195
TlF	Solid		205			12	0·4371	17
TlF	Solid		205			3·1		226
TlCl	Solid	297	205	(4·9)	2·0	2·7	0·855	193
TlCl	Solid		205			2	0·4371	17
TlCl	Solid		203			4	0·4371	17
TlCl	Solid		205	(6·4 ± 0·5)	2·6 ± 0·2	1·7 ± 0·3	0·395	192
TlCl	Solid		203	(8·1 ± 1)	3·3 ± 0·4	2·7 ± 0·7	0·395	192
TlBr	Solid	297	205	(18)	7·3	17	0·855	193
TlBr	Solid		205			13	0·4371	17
TlBr	Solid		203			31	0·4371	17
TlBr	Solid		205	(26·7 ± 2·5)	10·9 ± 1·0	29·7 ± 5·5	0·395	192
TlBr	Solid		203	(30·2 ± 3·7)	12·3 ± 1·5	28 ± 10	0·395	192
TlBr	Solid		205			20·4		226

TABLE XXI (*cont.*)

Compound[a]	Form	Temperature/K	Isotope	Line width[b] KHz	Line width[b] 10^{-4} T	Second moment/10^{-8} T^2 [b]	Field strength/T	Reference
TlI	Solid	298	205	55·7	(22·7)		2·114	191
TlI	Solid	401	205	36[f]	(15)		2·114	191
TlI	Solid		205			18	0·4371	17
TlI	Solid		203			28	0·4371	17
TlI[g]	Solid (orthorhombic)	298	205	(31·6)	12·9	40	0·641	18
TlI[g]	Solid (orthorhombic)	*c.* 433	205	(25·7)	10·5	26	0·641	18
TlI[g]	Solid (cubic)	*c.* 433	205	(8·20)	3·33	2·5	0·641	18
TlI[g]	Solid (cubic)	*c.* 533	205	(1·2)	0·48		0·641	18
TlOAc	Melt	405–434	205	0·015	(0·006)		2·114	194
$TlHCO_2$	Solid		205			6	0·4371	17
$TlHCO_2$	Solid		203			10	0·4371	17
$TlHCO_2$	Melt	373–413	205	0·175	(0·071)		2·114	194
$TlClO_4$	Solid					1		17
$TlClO_4$	Solid					1		17
$TlClO_4$	Solid	307	205	2·3	(0·94)		2·114	227
$TlClO_4$	Solid	207	203	2·4	(0·98)		2·114	227
$TlClO_4$	Single crystal	307	205	1·5–3·3[d]	(0·61–1·4)[d]		2·114	227
TlCN[h]	Solid	248	205			8	0·432	228
TlCN[h]	Solid	298	205			2	0·432	228
$TlBO_2 \cdot \frac{1}{2}H_2O$	Solid	298	205	(6·1)	2·5		0·5656	229
$TlBO_2 \cdot \frac{1}{2}H_2O$	Solid	398	205	(1·2)	0·5		0·5656	229
$TlPO_3$	Glassy		205	(1·5)	6·2		1·079	197
$TlPO_3$	Glassy		205	(5·4)	2·2		0·326	197
$TlPO_3$	Glassy	298	205	8·6	(3·5)		0·652	197

TABLE XXI (*cont.*)

Compound[a]	Form	Temperature/K	Isotope	Line width[b] KHz	Line width[b] 10^{-4} T	Second moment/10^{-8} T^2 [b]	Field strength/T	Reference
$TlPO_3$	Glassy	443	205	1·9	(0·8)		0·652	197
$TlPO_3$	Crystalline		205	(4·4)	1·8		0·326	197
$TlPO_3$	Crystalline		205	(4·4)	1·8		1·079	197
Tl_2CO_3	Solid		205			8	0·4371	17
Tl_2CO_3	Solid	311	205	6·8±0·8	(2·8±0·3)		2·114	195
Tl_2CO_3	Solid	398	205	6·9±0·8	(2·8±0·3)		2·114	195
Tl_2SO_4	Solid	305	205	6·3±0·5	(2·6±0·2)		2·114	195
Tl_2SO_4	Solid	297	205	(5·6)	2·3	3·3	0·855	193
Tl_2SO_4	Solid		205			3	0·4371	17
Tl_2SO_4	Solid		203			9	0·4371	17
Tl_3PO_4	Solid	297	205	(36·4)	14·8	120	0·855	193
$Tl_3Co(CN)_6$	Solid	300	205	(2·4)	1·0		0·652	16
$Tl_3Fe(CN)_6$	Solid	300	205	(74)	30		0·652	16
$TlFe(SO_4)_2 \cdot 12H_2O$	Solid	300	205	(2·4)	1·0		0·652	16
Tl^+/valinomycin (ClO_4^-)	Solid	301	205	(5·1)[f]	(2·1)		2·114	199
$K_3(TlCl_6)$	Solid		205			1	0·4371	17
$(NH_4)_3(TlCl_6)$	Solid		205			2	0·4371	17
$Zn(TlCl_6)_2$	Solid	300	205			4	0·4371	17
$Tl(ClO_4)_3 \cdot 6H_2O$	Solid	300	205	6·8	(2·8)		2·114	67
$TlCl_3 \cdot 4H_2O$	Solid	300	205	8·0	(3·3)		2·114	67
$TlBr_3 \cdot 4H_2O$	Solid	300	205	14·0	(5·70)		2·114	67
$KTlCl_4$	Solid	300	205	6·0	(2·4)		2·114	67
$KTlBr_4 \cdot 2H_2O$	Solid	300	205	15·5	(6·31)		2·114	67
$K_3TlCl_6 \cdot 2H_2O$	Solid	300	305	6·0	(2·4)		2·114	67
$Na_2TlCl_5 \cdot 4H_2O$	Solid	300	205	5·0	(2·0)		2·114	67
$Na_3TlCl_6 \cdot 12H_2O$	Solid	300	205	5·0	(2·0)		2·114	67

TABLE XXI (*cont.*)

Compound[a]	Form	Temperature/K	Isotope	Line width[b] KHz	Line width[b] 10^{-4} T	Second moment/10^{-8} T^2 [b]	Field strength/T	Reference
$Cs_2TlCl_5 \cdot H_2O$	Solid	300	205	5·1	(2·1)		2·114	67
$Cs_3Tl_2Cl_9$	Solid	300	205	9·0	(3·7)		2·114	67
$Cs_3Tl_2Br_9$	Solid	300	205	12·0	(4·89)		2·114	67
$[NBu_4]TlI_4$	Solid	300	205	20	(8·1)		2·114	67
$[Co(NH_3)_6]TlCl_6$	Solid	300	205	3·3	(1·3)		2·114	67
$[Co(NH_3)_6]TlBr_6$	Solid	300	205	19·0	(7·74)		2·114	67
Tl_2O_3(98·7% ^{205}Tl)	Solid	77–300	205	8·3	(3·4)	(12)	0·5560	203
Tl_2O_3(98·7% ^{205}Tl)	Solid	77–300	205	5·6	(2·3)	(5·8)	0·3288	203
Tl_2O_3(90·5% ^{205}Tl)	Solid	77–300	205	10·5	(4·28)	(15)	0·5560	203
Tl_2O_3(90·5% ^{205}Tl)	Solid	77–300	205	7·4	(3·0)	(9·3)	0·3288	203
Tl_2O_3(70·5% ^{205}Tl)	Solid	77–300	205	20	(8·1)	(32)	0·5660	203
Tl_2O_3(70·5% ^{205}Tl)	Solid	77–300	205	18·0	(7·33)	(32·5)	0·3288	203
Tl_2O_3(52·1% ^{205}Tl)	Solid	77–300	205	32	(13)	(48)	0·5560	203
Tl_2O_3(14·0% ^{205}Tl)	Solid	77–300	205	>60	(>24)	(>66)	0·5560	203
Tl_2O_3(70·5% ^{205}Tl)[c]	Solid	77–300	203	48	(20)	(60)	0·5560	203
Tl_2O_3(52·1% ^{205}Tl)[c]	Solid	77–300	203	33	(13)	(50·8)	0·5560	203
Tl_2O_3(14·0% ^{205}Tl)[c]	Solid	77–300	203	14	(5·7)	(20)	0·5560	203
Tl_2O_3(14·0% ^{205}Tl)[c]	Solid	77–300	203	11	(4·5)	(17)	0·3288	203
$(Tl_2O)_{0\cdot09}(SiO_2)_{0\cdot91}$	Glassy	298	205	(91)	37		1·0	202
$(Tl_2O)_{0\cdot22}(SiO_2)_{0\cdot78}$	Glassy	298	205	(70·0)	28·5		1·0	202
$(Tl_2O)_{0\cdot35}(B_2O)_{0\cdot65}$	Glassy	298	205	(59)	24		1·0	202
$(Tl_2Se)(As_2Se_3)_2$	Glassy		205	(12)	5·0		0[i]	201
$(Tl_2Se)(As_2Te_3)_2$	Glassy		205	23·1	(9·41)		0·756	230
$(Tl_2Se)(As_2Te_3)_2$	Glassy		203	33·9	(13·8)		0·756	230
$Tl_2SeAs_2Te_3$	Glassy		205	22·8	(9·28)	(34·3)	0·756	230
$Tl_2SeAs_2Te_3$	Glassy		205	*c.* 20	*c.* 8		0·65	200

TABLE XXI (*cont.*)

Compound[a]	Form	Temperature/K	Isotope	Line width[b] KHz	Line width[b] 10^{-4} T	Second moment/10^{-8} T^2 [b]	Field strength/T	Reference
$Tl_2SeAs_2Te_3$	Glassy		205	(9·8 ± 1)	(4·0 ± 0·5)		0[i]	200
$Tl_2SeAs_2Te_3$	Glassy		203	34·2	(13·9)	(54·9)	0·756	230
$Tl_{0\cdot3}WO_3$	Solid	77	205	(5·10 ± 0·74)	2·08 ± 0·30		0·6000	204
$Tl_{0\cdot3}WO_3$	Solid	298	205	(4·27 ± 0·20)	1·74 ± 0·08		0·6000	204
$Tl_{0\cdot3}WO_3$	Solid	298	203	(6·95 ± 0·74)	2·83 ± 0·30		0·6000	204

[a] All samples natural abundance (70·5% ^{205}Tl, 29·5% ^{203}Tl) unless otherwise noted.

[b] Line widths measured at half-height for absorption lines or between maximum and minimum extremes of dispersion lines. Values in parentheses have been calculated from data in alternative units.

[c] Table III of reference 203 gives ^{203}Tl line widths versus "percentage abundance ^{203}Tl". From discussion in this reference and from the theory of nuclear spin exchange broadening it is clear that this is a misprint and should read "percentage abundance ^{205}Tl". This has been assumed in compiling the data in Table XXI.

[d] Line width varied with orientation of the crystal axis relative to the applied magnetic field direction.

[e] Independent of orientation relative to the magnetic field direction.

[f] Gaussian line broadening which yields a good fit to the experimental powder pattern.

[g] ^{203}Tl line width was equal to that of ^{205}Tl in orthorhombic TlI but was about 50% greater than the ^{205}Tl line width in the cubic form.[18]

[h] TlCN undergoes a solid state phase transition at about 266 K.[228]

[i] Extrapolated value from measurements at higher fields.

Two types of indirect interactions are possible. When only s electrons transmit nuclear spin information, the interaction is of the scalar exchange type. When s and p electrons are involved, the interaction becomes a tensor quantity and is the pseudodipolar type. When both electrons are in p orbitals, both exchange and pseudodipolar interactions exist.[192] The pseudodipolar interaction is so-named because its directional characteristics are identical to those of the direct dipolar type. In the single crystal rotation experiment mentioned above, it is not possible directly to separate an orientation dependence of the second moment into dipolar and pseudodipolar contributions. However, since the total orientation dependence represents the sum of these, calculation of the dipolar second moment using Van Vleck's approach[237] allows the pseudodipolar contribution to be estimated. Scalar exchange broadening is, of course, independent of orientation.

In 1955, Bloembergen and Rowland[203] examined the ^{205}Tl and ^{203}Tl line widths of Tl_2O_3 and thallium metal as a function of the percentage abundance of ^{205}Tl. It was shown that the ^{205}Tl line was relatively narrow in highly ^{205}Tl-enriched samples, while the ^{203}Tl line was quite broad. The reverse effect resulted from enrichment of samples with ^{203}Tl. From these results, the authors conclude that spin exchange between unlike nuclei (^{205}Tl–^{203}Tl) contributes to the second moment while spin exchange between like nuclei (^{205}Tl–^{205}Tl, ^{203}Tl–^{203}Tl) does not affect the second moment. This provides an excellent method for detecting line broadening contributions from exchange interactions in natural-abundance thallium-containing samples. Since ^{203}Tl, at 29·5% abundance, is surrounded primarily by (unlike) ^{205}Tl in the solid, exchange interactions, when present, broaden this line more than the line of ^{205}Tl which is surrounded mainly by other (like) ^{205}Tl. Equal widths of both lines in natural-abundance samples demonstrates the absence of exchange broadening. The favourable natural abundance and magnetogyric ratio of ^{203}Tl make this a uniquely simple and effective method for investigating exchange broadening. The pulsed FT NMR technique even allows simultaneous detection of ^{205}Tl and ^{203}Tl specifically for the purpose of examining relative line widths, as illustrated in Fig. 2 where the lines from $TlNO_3$ powder are shown. This is clearly a case where exchange interactions cause substantial broadening.

The effect of quadrupole coupling on the line width of a spin $\frac{1}{2}$ nuclide in the solid state has been studied.[240] As expected, the line width of ^{205}Tl or ^{203}Tl in the proximity of a nuclide with a quadrupole moment may increase, and calculations[240] have shown that quadrupole broadening may add a factor of up to 1·84 times the dipolar contribution to the second moment. The lines of ^{205}Tl and ^{203}Tl should be affected equally by quadrupolar interactions.

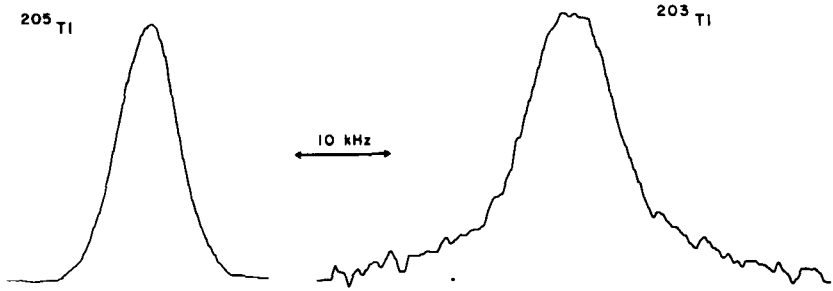

FIG. 2. ^{205}Tl and ^{203}Tl resonance lines in $TlNO_3$ powder at 62 °C.

Finally, motional narrowing can occur in solids and, especially, melts containing thallium. CSA is averaged by fast rotational reorientation, as are dipolar and pseudodipolar interactions. Exchange-broadened lines may also be narrowed with the onset of molecular motion. In this case, the narrowing results from modulation of the distance between interacting nuclei rather than from angular motion. The abrupt narrowing of thallium NMR lines is usually taken as strong evidence for a phase transition in a solid and nearly always accompanies fusion of thallium compounds.

Having considered the basic principles governing the thallium chemical shift and line width in the solid state, experimental results are now considered. These have been divided into several groups according to the type of chemical system investigated.

B. Thallium metal, alloys and intermetallic compounds

The NMR properties of metals are determined largely by the interactions of nuclei with conduction electrons. For example, the chemical shift in a diamagnetic insulator is a manifestation of nuclear couplings to the magnetic fields which result from motions of nearby electrons. In contrast, the NMR shift of thallium in a metallic sample arises from the coupling with the magnetic moments due to the spins of the conduction electrons themselves. This special type of NMR shift found in metals is known as the Knight shift K_s after W. D. Knight who first observed it in metallic copper.[241] The Knight shift has been defined in two basic ways:

$$K_s = (B_{\text{reference}} - B_{\text{sample}})/B_{\text{sample}} \quad (1)$$

$$K_s = (B_{\text{reference}} - B_{\text{sample}})/B_{\text{reference}} \quad (2)$$

$B_{\text{reference}}$ is the field-producing resonance of a thallium salt (aqueous TlOAc is often used). Further definitions can be written in terms of resonance frequencies instead of fields. Definition (2) above is preferable but many values, especially in the early literature, are reported using definition (1).

Table XVII contains values of the Knight shift for thallium in a variety of metallic systems. It will be noted that these shifts are quite large, of the order of 1% (i.e. 10 000 ppm), and generally positive (i.e. resonance signal in the metal is to high frequency of that in the reference compound). Where stated explicitly by the authors, the use of definition (2) above has been clearly indicated. If different definitions are used to calculate K_s values for the same system, a difference of the order of K_s itself could be expected. For example, if $K_s = 1{\cdot}00\%$ as calculated using definition (2), the use of definition (1) would yield a value of about $1{\cdot}00\% \times 1{\cdot}00\% + 1{\cdot}00\% = 1{\cdot}01\%$. Thus, in general, choice of a definition is expected to alter values only in the fourth, and sometimes in the third, significant figure. The K_s values in Table XVII have been corrected to a reference of aqueous Tl(I) at infinite dilution.

Spin–lattice relaxation in metals and alloys is usually the result of mutual spin-flips between nuclear magnetic dipole moments and the magnetic moments of conduction electrons at the Fermi level. When these electrons are highly delocalized, the relaxation time T_1 is related to the Knight shift K_s by the Korringa equation,[242]

$$K_s T_1 = \frac{\hbar}{4\pi k T}\left(\frac{\gamma_e}{\gamma_n}\right)^2$$

where the subscripts e and n on the magnetogyric ratios, γ, refer to the electron and the nucleus (^{205}Tl or ^{203}Tl in the present case). In cases where conduction electrons tend to localize on a particular thallium site, the relaxation rate $1/T_1$ increases proportionally above the value predicted by the Korringa relation.[220] Comparison of experimental T_1 values with those predicted from this relation thus provide useful information concerning the internal electronic structure in the metal or alloy. Further details regarding the Korringa relation, including important refinements, may be found in the monographs of Abragam[231] and Slichter.[232]

The Knight shift for thallium metal was first found by Bloembergen and Rowland[4] to be $+1{\cdot}54 \pm 0{\cdot}05\%$ for ^{205}Tl. (This paper is especially significant because it also contains the first derivation of NMR powder line shapes for molecular systems of non-cubic symmetry, in this case white tin.) The ^{205}Tl line width of 33 kHz and K_s are found to be field- and temperature-independent, but the ^{203}Tl line width exhibits a "baffling" increase from 17 to 33 kHz as the field strength increases from 0·2 to 0·6 T. The K_s value also increases from 1 to 1·5% over the same range. This behaviour remained unexplained until 1955 when the same authors demonstrated the presence of exchange broadening in thallium metal.[203] Since the magnetogyric ratios of ^{205}Tl and ^{203}Tl differ only slightly, the difference between their Zeeman frequencies can be made smaller than their indirect exchange interaction simply by decreasing the applied magnetic field. This results in

the anomalies observed. The transition from separate, comparatively narrow ^{205}Tl and ^{203}Tl signals through a broad intermediate peak to a narrow single line has been observed[243] as the applied field is decreased. Additional determinations of K_s in thallium metal have been reported in the solid[206] and the melt,[209,210] and the temperature dependence of K_s has been successfully correlated with the pressure dependence of the thallium superconducting transition temperature.[207] Several theoretical studies of the Knight shift in liquid thallium metal have appeared.[249-251]

Just as the chemical shift can show an orientation dependence, so too can the Knight shift exhibit anisotropy. The anisotropy in the K_s of thallium metal has been studied using line shape fitting[203] and single-crystal rotation experiments.[208,244] These latter studies have shown that, for a thallium crystal of hexagonal symmetry, $K_s = K + \frac{1}{2}K'(3\cos^2\theta - 1)$, where θ is the angle between the applied field direction and the [0001] symmetry axis, $K = +1{\cdot}618\%$ and $K' = -0{\cdot}096\%$. The finding that the isotropic part K of the Knight shift is much larger than the anisotropic part K' is not surprising. The isotropic part arises from nuclear coupling with s electrons via strong hyperfine interactions while the source of the anisotropic part K' involves weaker interactions with other electrons.[231]

All investigators agree that exchange interactions contribute substantially to the line width in solid thallium metal at high fields.[203,208,244-246] At low fields, where the difference between the Zeeman frequencies of ^{205}Tl and ^{203}Tl becomes small, all thallium spins become effectively identical and spin exchange interactions no longer contribute to the line width.[243,246] The Van Vleck dipolar contribution has been calculated[203] but is small compared to the orientation-dependent pseudodipolar contribution.[203,244-246]

The spin–lattice relaxation time in thallium metal powder has been measured using the inversion-recovery pulse sequence.[247] T_1 is found to be field-independent and $T_1 \times \text{Temperature} = (2{\cdot}0 \pm 0{\cdot}3) \times 10^{-3}$ s K at 77 K while $T_1 \times \text{Temperature} = (2{\cdot}3 \pm 0{\cdot}1) \times 10^{-3}$ s K between 1·5 and 4·2 K.

NMR spectra of thallium in a variety of alloys and intermetallic compounds have been reported. Baden *et al.* have reported Knight shifts and line widths for ^{205}Tl at 25 °C in the $LiCd_{1-x}Tl_x$ ($0{\cdot}05 \leq x \leq 1$) system and observed multiple signals in the region of heterogeneous phase.[212] The Knight shifts for both ^{203}Tl and ^{205}Tl in the superconductor La_3Tl, as well as T_1 values for ^{205}Tl ($T_1 \times \text{Temperature} = 4{\cdot}6 \times 10^{-3}$ s K at 34 K, $3{\cdot}8 \times 10^{-3}$ s K at 20 K, and $3{\cdot}3 \times 10^{-3}$ s K at 11 K), have been determined.[218] The same study determined Knight shifts for La_3TlC, $La_3Tl_{0{\cdot}5}In_{0{\cdot}5}$ and $La_3Tl_{0{\cdot}8}Pb_{0{\cdot}2}$. Related systems have also been investigated.[248]

The Knight shifts and line widths of ^{205}Tl in the $CaCd_{1-x}Tl_x$ ($0 \leq x \leq 1$) system have been determined[216,217] and discussed theoretically.[216,252,253] The semiconducting liquid alloys $Tl_{1-x}Te_x$ have been studied in the region

$x = c.\ 0{\cdot}33$. From the behaviour of the Knight shift in this region, the authors conclude that the system is composed mainly of Tl_2Te clusters.[220] In addition, it is found that $T_1 = T_2^* = 5{\cdot}1 \pm 0{\cdot}5$ μs in $Tl_{0{\cdot}68}Te_{0{\cdot}32}$.

The experimental Knight shift of $In_{0{\cdot}5}Tl_{0{\cdot}5}$ has been reported,[4] as has a theoretical study of K_s in this system.[254] Bloembergen and Rowland[4] have reported values of K_s and line width for various mixtures of thallium metals with bismuth, tin, lead, mercury, magnesium and sodium. Alloys of thallium with mercury,[255] tin,[219] lead[211,256] and francium[215] have also been investigated.

The NMR properties of both ^{205}Tl and ^{203}Tl have been studied[204] in the thallium tungsten bronze $Tl_{0{\cdot}3}WO_3$. Although this bronze conducts readily, the small shifts of $+570 \pm 70$ ppm for ^{203}Tl and $+540 \pm 40$ ppm for ^{205}Tl indicate that little interaction occurs between thallium nuclei and conduction electrons. Shifts are shown to be temperature- and field-independent, and the ^{203}Tl line width is about 50% greater than that of ^{205}Tl. This indicates the importance of exchange broadening and the absence of significant broadening due to CSA. Magnitudes of the direct dipolar contributions to the line widths are calculated using the Van Vleck[237] approach; these are only a fraction of the observed line widths. It has been shown[205] that incorrect structural parameters were used in the calculation of reference 204, but the correct dipolar line width contributions are still substantially smaller than experimental line widths.

A very interesting system is that of sodium thallide, NaTl, as is that of the related compound disodium thallide, Na_2Tl. The first reported ^{205}Tl Knight shifts[4] are $-1{\cdot}03\%$ for NaTl and $-0{\cdot}68\%$ for Na_2Tl. However, a later study[214] found $K_s = -0{\cdot}50\%$ for NaTl. Still later a value of $-0{\cdot}92\%$ was determined for NaTl.[213] It has been suggested[257] that NaTl exhibits a Knight shift of about -1% while $K_s = 0{\cdot}5\%$ for Na_2Tl, and this appears to be the best explanation for the data currently available. The negative values for the Knight shifts of NaTl and Na_2Tl are unusual, and despite efforts by a number of investigators[213,258,259] these negative values are still not well understood. Sodium thallide has been used as a reference material for the determination of performance specifications in a spectrometer design.[260]

C. Thallium salts and organometallic compounds

The NMR properties of thallium in most of the common thallium(I) salts have been investigated, and data are often available for both the solid and melt. Thallium(III) compounds have been much less thoroughly studied, and with rare exceptions only data for solids are available. A few thallium NMR studies of solid or liquid organothallium compounds have been published. A great deal remains to be done, however, before even the

general thallium NMR properties of these solids or melts will be understood.

The effect of temperature on thallium shifts in solids and melts is often pronounced. The ^{205}Tl chemical shift may vary by as much as 5 ppm K^{-1} (solid thallium(I) acetate) or may be temperature-independent within experimental error, as shown by Table XIX. It is highly significant that, among the substantial number of compounds studied, none exhibit a negative dependence of shift on temperature. At first sight this seems remarkable, since an increase in temperature is expected to weaken the thallium–anion interactions which presumably cause most salts to resonate at high frequency. In an excellent study, Hafner and Nachtrieb[184] have shown that this is probably not the dominant effect. Instead, the positive dependence of the chemical shift on temperature almost certainly arises from enhanced vibrational overlap of thallium–anion wave functions, resulting in additional paramagnetic shielding with increasing temperature.

In view of the extreme sensitivity of the thallium chemical shift to variations in the chemical environment, a change in the shift might be expected at the temperature of a phase transition. In fact, a shift discontinuity of several hundred ppm may accompany a phase change (Table XX). In most systems investigated so far, fusion results in a high frequency shift of the ^{205}Tl resonance relative to that in the solid. It is well known that interionic distances in most salts decrease upon melting, this is consistent with observed paramagnetic thallium shifts which result from increased cation–anion electronic overlap.[184]

When sufficient data are available, the shift discontinuity and its temperature-dependence may be used to calculate the distance of closest approach of ions in ionic melts.[264] In the general case, the magnitude of the shift discontinuity may be used as a qualitative measure of overall differences in the two phases, where large discontinuities are associated with the greatest dissimilarities. For this reason it appears that the thallium environments in melts of thallium(III) salts (e.g. $TlCl_3$, $Tl(ClO_4)_3$) may be rather like those in the solids, although additional studies would be helpful. It seems likely that strong cation–anion interactions in these salts (indicated by their chemical shifts) persist upon fusion, and that the basic units in the melt may be comparatively covalent. Thallium(I) carboxylates (e.g. formate and acetate) also exhibit little or no shift discontinuity at the melting point.[184,194] In fact the only effect of fusion on the chemical shifts of these compounds is an abrupt decrease in the temperature dependence $d\delta/dT$ (Table XIX). It seems reasonable to speculate that carboxylate anions bind tightly with thallium cations in these crystals and that the melts contain mainly tight $RCOO^-Tl^+$ units. The absence of line-width discontinuities at the melting points also suggests great similarities between the structures in the solids and melts.[194] Unfortunately, no X-ray crystallographic study of a thallium carboxylate has so far been published.

Thallium NMR line widths are usually quite sensitive to phase changes. An excellent example is that of thallium(I) nitrate. As shown in Table XXI, the ^{205}Tl line width in this compound is essentially independent of temperature for a given phase α, β or γ. However, a sudden narrowing of the line occurs at the transition from orthorhombic γ to hexagonal β and again at the transition from β to cubic α.[193,224,225] The latter phase transition is accompanied by a 100-fold increase in electrical conductivity and must almost certainly mark the onset of thallium(I) diffusion in the solid.[224] This conclusion is supported by other excellent studies of relaxation in $TlNO_3$[261,262] which explain T_2 in terms of both indirect scalar exchange interactions and diffusion, T_1 via indirect coupling modulated by lattice vibrations, and $T_{1\rho}$ by means of diffusion (α), exchange interactions (γ), or both (β). Relaxation in liquid $TlNO_3$ at 485 K has also been studied[263] and shown to occur at equal rates for both ^{205}Tl and ^{203}Tl ($T_1^{203,205}$ = 0·72 ms; $T_2^{205} = T_2^{203}$). It is clear from these studies that thallium NMR line widths, and relaxation in general, can be extremely informative in studies of phase transitions.

Line broadening resulting mainly from exchange interactions effectively prevents the direct observation of CSA in powder spectra of thallium(I) nitrate. The shielding is quite anisotropic in this case, as shown by a preliminary single crystal rotation study,[195] and very slight asymmetry in the powder spectrum also suggests contributions from this source (Fig. 3). In order to learn more about the magnitude of thallium CSA, a study of $TlNO_3/KNO_3$ mixtures has been conducted.[225] Since the primary source of relaxation line broadening in pure $TlNO_3$ arises from spin exchange among Tl(I) ions, dilution in a matrix of KNO_3 should produce considerable narrowing of the thallium lines due to the small magnetic moments of potassium nuclides. A further advantage of KNO_3 as a matrix material is that it has a well known crystal structure which is also different from that of $TlNO_3$. Figure 3 presents ^{205}Tl NMR spectra of powders prepared from melts containing various amounts of $TlNO_3$ in KNO_3. Upon dilution, thallium clearly occupies axially symmetric KNO_3 matrix sites which are different from those in pure $TlNO_3$. Furthermore, the decrease in thallium–thallium exchange interactions apparent from the line narrowing of Fig. 3 suggests a high degree of isolation. The demonstrated equality of the ^{205}Tl and ^{203}Tl line widths in the dilute systems reinforces this conclusion.[225] The ^{205}Tl line shape and shielding tensor elements depend strongly on the KNO_3 crystal structure, and rather different spectra are obtained from systems above and below the KNO_3 orthorhombic $\rightleftharpoons$ trigonal phase transition at 128 °C (Table XVIII).

Attempts to isolate Tl(I) ions in $LiNO_3$, $NaNO_3$ and $AgNO_3$ failed, as shown by the similarities between ^{205}Tl NMR properties of pure $TlNO_3$ and these mixtures. This may be attributed in part to differences in cation

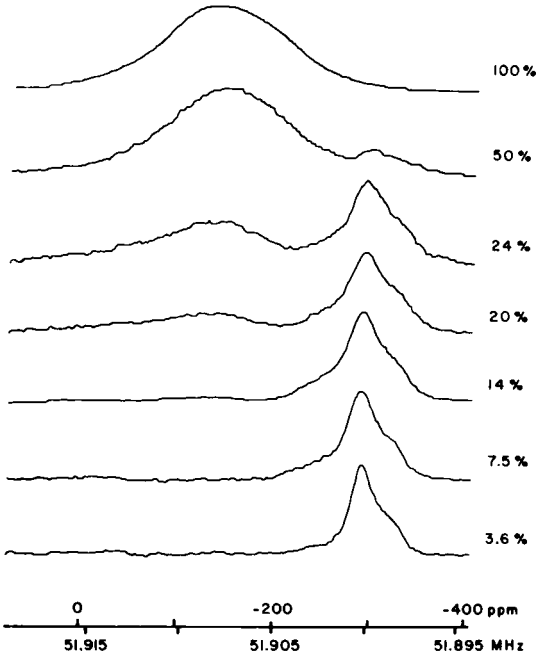

FIG. 3. ^{205}Tl NMR spectra of $TlNO_3/KNO_3$ mixtures at 32 °C. Percentages on right indicate amount of $TlNO_3$ present in mixture.

radii which prevent incorporation of Tl(I) ions into Li(I) or Na(I) lattice sites. $AgNO_3$ has a unique crystal structure[265] rather unlike that of $TlNO_3$, so this may underlie the failure in this instance.

The dilution technique described above has been applied in the case of Tl_2SO_4.[195] The ^{205}Tl NMR powder spectrum of this compound consists of a single, broad, symmetrical line (in fields of 2·1 T or less) with a shift of about 100 ppm to low frequency of aqueous thallium ion (Table II). Since the presence of strong exchange interactions in this compound have been demonstrated[17] by second moment measurements of both ^{205}Tl and ^{203}Tl signals (Table XXI), dilution by isostructural K_2SO_4 yields narrow line shapes which reflect the symmetry properties of the K_2SO_4 (and Tl_2SO_4) lattice sites. Preliminary line shape analysis shows that at least two distinct sites must exist, in agreement with X-ray crystallographic data.

A number of thallium NMR studies of thallium(I) halides have appeared. In addition to determinations of the ^{205}Tl chemical shift in TlF,[17,184] several studies have shown that ^{205}Tl line broadening in this compund is due mainly to direct dipolar interactions between ^{205}Tl and ^{19}F.[192,226,266] Contributions from indirect spin–spin interactions are approximately four times smaller than those from direct dipolar interactions in this compound.[266]

Chemical shifts for thallium(I) chloride have been measured by a number of authors (Table II). It is generally agreed that the thallium NMR line width in this compound results principally from scalar exchange interactions between thallium nuclei.[192,267] However, the relative importance of contributions from other relaxation mechanisms remains unclear. The orientation independence of the line width in the single crystal has been taken as evidence for the lack of significant dipolar or pseudodipolar couplings.[192] This same study found important contributions from Tl–Cl exchange interactions. On the other hand, Clough and Goldburg[267] found immeasurably small Tl–Cl exchange interactions but significant dipolar and pseudodipolar couplings. The latter are found to be approximately equal in magnitude but opposite in sign, which may account for the apparent absence of orientation dependence of the single-crystal line width.

Rotating-frame spin–lattice relaxation times ($T_1\rho$) have been determined for thallium(I) chloride in studies of vacancy diffusion in this compound.[268] Both spin–lattice and spin–spin relaxation have been investigated in molten TlCl from about 450 to 620 °C.[269] At 0·28T, T_1 and T_2 are nearly the same and isotope independent. Values range from about 250 μs at 450 °C to 75 μs at 620 °C; this rapid relaxation is attributed to hyperfine contact interactions with transient unpaired electrons originating from thermal dissociation of Tl(I).

As in the case of TlCl, a number of chemical shift determinations have been published for TlBr (Table II). The thallium NMR line width in this compound is significantly larger than that of TlCl (Table XXI). Dipolar and pseudodipolar contributions may be small, as suggested by the orientation independence of the single-crystal TlBr line width,[192] but indirect spin exchange has been shown to be a very important line-broadening mechanism. By means of decoupling experiments, Saito[192,226] has found large Tl–Tl interactions and, to a lesser degree, Tl–Br interactions in this salt. Further results are reported by Mathur.[270]

The chemical shift and line width in solid TlBr are essentially constant at pressures up to 8000 kg cm^{-1},[192] probably due to the low compressibility of this salt. Relaxation in molten TlBr between 510–610 °C is apparently dominated by transient interactions of thallium(I) with unpaired electrons and paramagnetic Tl(II) generated from the thermal dissociation of Tl(I).[269] The same study has demonstrated that doping liquid TlBr with paramagnetic thallium metal yields the expected enhancement in both spin–spin and spin–lattice relaxation rates.

The thallium NMR properties of thallium(I) iodide have been investigated extensively, in part because this salt exhibits a phase transition from the yellow orthorhombic form below about 160 °C to the red cubic form above this temperature. NMR spectra of the two forms are rather different. The ^{205}Tl resonances in both modifications are shifted by a large amount

to high frequency of aqueous Tl(I), with the cubic form being shifted to highest frequency.[18] The chemical shift of the orthorhombic form is field dependent. When the difference between the ^{205}Tl and ^{203}Tl Zeeman energies approaches the ^{203}Tl–^{205}Tl spin exchange energy, a field dependence of the chemical shift may result.[203,243] However, this explanation does not seem to be entirely adequate in the case of orthorhombic TlI.[18] Transition from the orthorhombic to the cubic form is accompanied by a slight increase in the Tl—I bond length, but more favourable crystal packing results in greater crystal density. This, in turn, causes an effective 4% increase in the covalent character of thallium[271] which is reflected in a positive shift discontinuity at the transition temperature.

The thallium NMR line widths of orthorhombic and cubic TlI are quite different. Upon transition to the cubic phase, the ^{205}Tl line narrows abruptly to approximately 30% of its width in the orthorhombic form and further narrowing occurs with increasing temperature.[18] In the orthorhombic phase, the ^{203}Tl line width equals that of ^{205}Tl, but in the cubic form the ^{203}Tl line is about 50% broader than that of ^{205}Tl. This suggests an important contribution from Tl–Tl exchange interactions in cubic TlI but little in the orthorhombic form.[18,272] Indirect Tl–I spin exchange has been suggested as a major source of line broadening in both forms of solid TlI, in addition to quadrupole broadening and CSA.[18] The upper limit for the latter in orthorhombic TlI was estimated from plots of second moment against B_0^2, but a direct ^{205}Tl shielding anisotropy measurement[191] gives a somewhat larger value (Table XVIII).

^{205}Tl chemical shifts have been determined for molten Tl_2Cl_4 [20,221] and Tl_2Br_2.[221] In both cases, two signals have been observed which have been attributed to equal quantities of TlX and TlX_3. The compound Tl_2Cl_3 has been studied,[17] and the spectrum of this solid also contains two signals but in a 3 : 1 intensity ratio. A possible explanation for this is the presence of $Tl_3(TlCl_6)$ structural units.

Two ^{205}Tl NMR studies of mixed salt solids and melts have appeared. ^{205}Tl shifts in melts containing various proportions of TlX with MX (X = Cl, Br, I; M = Li, Na, K, Rb, Cs, Ag) are found to be linearly dependent on the mole fraction of MX.[20] The direction of the shift depends on M, and for a given mole fraction the shift is linear with the radius of M. These results are interpreted as effects of MX on the TlX covalency. A similar study of TlX/CsX mixtures (X = Cl, Br) reveals a linear dependence of shift on mole fraction in the melt but not in the solid.[222] These effects are again attributed to the influence of CsX on the TlX covalency.

The chemical shift of ^{205}Tl in thallium(I) carbonate has been determined by several investigators (Table II). The line width has been studied less extensively (Table XXI). The ^{205}Tl second moment has been reported to be $8 \times 10^{-8}\ T^2$ [17] and the line width appears to be temperature

independent.[195] An attempt to observe the ^{203}Tl line was unsuccessful, probably due to its width.[17] It is therefore likely that indirect Tl–Tl scalar exchange contributes to the line width. Studies of molten Tl_2CO_3 at 278 °C have shown that $T_1 = T_2 = 38{\cdot}5$ ms and that the relaxation rates are the same for ^{203}Tl and ^{205}Tl.[263]

The thallium chemical shift and second moments for ^{203}Tl and ^{205}Tl in thallium(I) formate at room temperature have been reported.[17] The second moments demonstrate that spin exchange interactions between thallium nuclei contribute substantially to the line width in the solid. Despite the suggestion[273] that no phase transitions occur in solid $TlHCO_2$ between room temperature and the melting point, a plot of ^{205}Tl chemical shift against temperature exhibits regions attributable to distinct phases.[194] Rapid narrowing of the ^{205}Tl line with increasing temperature also indicates motional narrowing. Upon fusion, no shift or line width discontinuities are exhibited and the temperature dependence of these parameters moderates.

Similar behaviour has been observed for thallium(I) acetate. In the rigorously pure salt, fusion occurs at about 130 °C while very slight impurities result in deceptively sharp melting at 110 °C. It has been shown[194] that the purity strongly influences both the chemical shift and the ^{205}Tl line width in this compound. Unfortunately, all of the early results were apparently obtained using the form melting at 110 °C, so NMR parameters determined in this work need verification. A plot of chemical shift against temperature for rigorously pure thallium(I) acetate suggests the presence of distinct solid state phase transitions, in analogy with thallium(I) formate.[194] The line width behaviour of the acetate is also similar to that of the formate, suggesting a smooth microscopic transition from solid to melt. Values of $T_1 = 33$ ms and $T_2 = 18$ ms have been determined for the thallium(I) acetate melt at 137 °C, but the sample used melts at 110 °C.[263]

The line width and second moment of the ^{205}Tl resonance line in thallium(I) cyanide has been studied[228] as a function of field strength and temperature. Clear evidence of multiphase behaviour below room temperature is found, and the dependence of the second moment on B_0^2 suggests a CSA of about 1000 ppm for this compound at 210 K. At room temperature, however, the second moment is field independent so CSA contributes little to the line width at this temperature.

A study of polycrystalline and glassy $TlPO_3$ has revealed a ^{205}Tl CSA of 560 ppm in the glass but little or none in the polycrystalline form.[197] While thallium is quite ionic in both systems, the chemical shift indicates slightly greater ionic character in the polycrystal. The shift of Tl_3PO_4, on the other hand, suggests substantial covalent character.[193]

Thallium(I) perchlorate displays very interesting NMR properties. The isotropic ^{205}Tl shielding is large (Table II), showing that this is a highly ionic salt. Nevertheless, polycrystalline $TlClO_4$ presents a classic powder

spectrum characteristic of axial symmetry with a CSA, $\sigma_{\perp}-\sigma_{\parallel}=$ 117 ppm.[227] That a salt with such ionic character can still exhibit a CSA of this magnitude is remarkable and testifies to the extreme sensitivity of the thallium chemical shift to small electronic effects. In a single crystal, the ^{205}Tl shift depends on the orientation θ as $1-3\cos^2\theta$, and the line width is also quite orientation-dependent (Fig. 4). Freeman *et al.*[17] have pointed out that the ^{205}Tl line width is approximately that predicted from direct dipolar interactions, and the orientation-dependence in the single crystal verifies that this is the primary source of line broadening. Possible contributions from thallium–thallium spin exchange are eliminated by the virtual equality of the ^{205}Tl and ^{203}Tl line widths and second moments in this compound.[17,227] Measurements of spin–lattice relaxation times for ^{205}Tl at various temperatures suggest the dominance of the dipolar relaxation mechanism at long correlation times in the solid.[227]

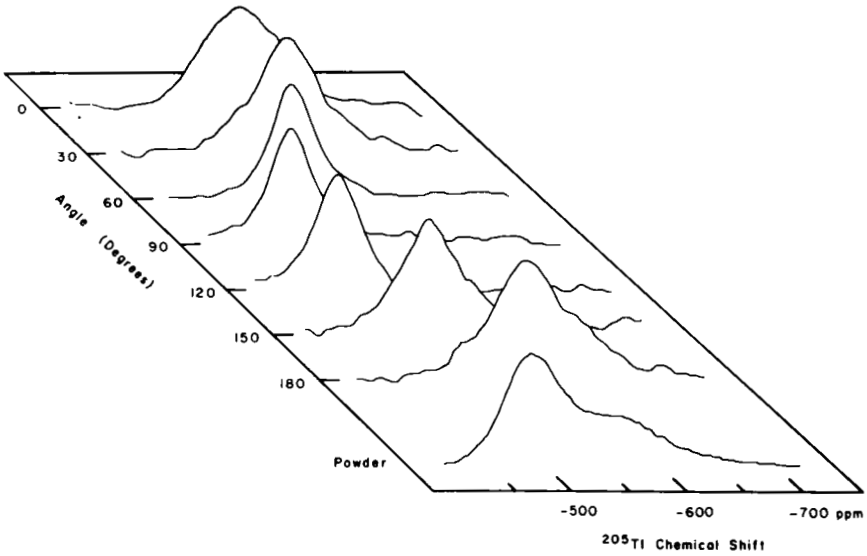

FIG. 4. ^{205}Tl NMR spectra of $TlClO_4$ powder and a single crystal at various orientations and at 34 °C.

^{205}Tl chemical shifts at various temperatures have been determined for melts of the binary mixtures $TlClO_4{\cdot}TlNO_3$ and $TlClO_4{\cdot}AgNO_3$.[184] Mixtures are studied due to the instability of pure $TlClO_4$ in the melt.

The classic paper by Bloembergen and Rowland[203] contains a rather complete study of line widths in solid Tl_2O_3. The importance of scalar spin exchange effects in spectra of this compound has already been discussed. This paper also cites a ^{205}Tl chemical shift of +5500 ppm and a large Tl_2O_3 CSA of 1870 ppm.

^{205}Tl spectra of two solid Tl(I)–antibiotic complexes have been studied. From the spectrum of the valinomycin complex, a value of $\sigma_{\parallel}-\sigma_{\perp}=$ 150 ppm for Tl is found.[199] Within the uncertainty imposed by the 5 kHz line width, Tl(I) ion appears to occupy a site of approximate axial symmetry in agreement with the X-ray crystal structure of the potassium complex. The observed isotropic shift of −545 ppm is to low frequency of any other known Tl(I) system and attests to the highly ionic character of thallium in this complex. The solid state ^{205}Tl chemical shift in the Tl(I)–gramicidin A complex, with acetate as the counteranion, is approximately −160 ppm. This shift suggests somewhat greater thallium covalency in gramicidin than in valinomycin, and it may also reflect solid state interactions with the acetate anion.

Thallium NMR properties of a number of paramagnetic compounds have been investigated. These include $TlCoF_3$ [274] and $TlMnF_3$,[275,276] as well as $TlMnCl_3$, $TlCoCl_3$ and $TlNiCl_3$.[223] In each of these cases, unpaired electron spin density on thallium causes extreme shifts to high frequency in addition to line broadening. Another excellent example is the semiconductor $Tl_3Fe(CN)_6$ which exhibits an extraordinary ^{205}Tl chemical shift of $+14\,000\pm700$ ppm and a line width of 74 ± 25 kHz.[16] These effects are not simply due to the local field of paramagnetic Fe(III), since $TlFe(SO_4)_2\cdot12H_2O$ exhibits a shift of -400 ± 100 ppm and a line width of $2{\cdot}5\pm1{\cdot}2$ kHz. $Tl_3Co(CN)_6$ behaves in a similar manner with a shift of -400 ± 100 ppm and a line width of $2{\cdot}5\pm0{\cdot}7$ kHz.[16]

A variety of thallium(III) salts have been investigated as solids or melts, but few of these have been studied in detail. The lack of published information is demonstrated by the fact that ^{205}Tl NMR data for two-thirds of all the thallium(III) salts ever investigated have recently been reported in a single paper.[67] Furthermore, while chemical shifts in these compounds are reasonably well understood (with certain exceptions discussed below), no systematic experimental investigations of relaxation have been conducted. A great deal remains to be done before the thallium NMR properties in thallium(III) compounds are fully characterized.

The chemical shift of $Tl(ClO_4)_3$ in both the solid and the melt has been studied as a function of temperature.[184] This salt exhibits the only known negative change in shift upon fusion, implying decreased covalency in the melt. The solid hydrate $Tl(ClO_4)_3\cdot6H_2O$ has also been studied.[67] The ^{205}Tl chemical shift of $TlCl_3$ in both the solid[64,184] and the melt[64] has been determined, and both the shift and the line width of $TlCl_3\cdot4H_2O$ are known.[67] A previous study of the tetrahydrate[17] revealed a complex ^{205}Tl spectrum of at least three overlapping lines. The shift of $TlBr_3\cdot4H_2O$ is not greatly different from that of $TlCl_3\cdot4H_2O$, but the line width of 14·0 kHz is nearly twice as large.

Spectra for several solids containing TlX_4^- and TlX_5^{2-} have been determined. These include $Zn(TlCl_4)_2$,[17] as well as $KTlCl_4$, $KTlBr_4 \cdot 2H_2O$ and $[NBu_4]TlI_4$.[67] In this case the ^{205}Tl line width is greatest in the iodide and smallest in the chloride. $[NBu_4]TlI_4$ exhibits a remarkable chemical shift of −1560 ppm, approximately 1000 ppm to low frequency of the nearest thallium(I) salt! The ^{205}Tl chemical shifts and line widths of $Na_2TlCl_5 \cdot 4H_2O$ and $Cs_2TlCl_5 \cdot H_2O$ are similar.[67]

Compounds containing TlX_6^{3-} and $Tl_2X_9^{3-}$ have been studied. The hydrates $Na_3TlCl_6 \cdot 12H_2O$ and $K_3TlCl_6 \cdot 2H_2O$ are similar in both shift (+1972 and +2007 ppm) and line width.[67] The anhydrous salts K_3TlCl_6 and $(NH_4)_3TlCl_6$ exhibit identical shifts of +2220 ppm,[17] but the difference between this value and the more recent figures for the above salts may not be experimentally significant. The shift and line width of $[Co(NH_3)_6]TlCl_6$ are +2019 ppm and 3·3 kHz, respectively, while for $[Co(NH_3)_6]TlBr_6$ they are −1194 ppm and 19·0 kHz.[67] A similar result is obtained with $Cs_2Tl_2Cl_9$ (δ = +1926 ppm, line width = 9·0 kHz) and $Cs_3Tl_2Br_9$ (δ = −1194 ppm, line width = 12·0 kHz).

The results reported so far suggest that the thallium chemical shift in a thallium(III) salt depends largely on the particular halogen involved. In every series where data are available (Table II), $\delta_{Cl} > \delta_{Br} > \delta_I$. The reason for this apparent trend is unclear, and additional compounds must be studied before such a trend is definitely established. Certain salts would be especially interesting. For example, thallium shifts are known for the compounds $MTlX \cdot nH_2O$ (M = NBu_4, K; X = I, Br, Cl; n = 0, 2) so the shift for an analogue with X = F would be very interesting. Likewise, it would be extremely useful to determine the shifts in $[Co(NH_3)_6]TlF_6$ and $[Co(NH_3)_6]TlI_6$. The extraordinary chemical shifts determined for $[NBu_4]_3TlI_4$, $[Co(NH_3)_6]TlBr_6$ and $Cs_3Tl_2Br_9$ merit additional study. Elucidation of the mechanism which shifts the thallium resonance in these salts over 3000 ppm to low frequency of the usual thallium(III) chemical shift range would be of great interest.

The ^{205}Tl(III) line width also seems to depend on the type of halogen present in the compound. The limited data available (Table XXI) indicate that salts containing iodide exhibit broader lines than analogues containing bromide, and these have larger line widths than corresponding chloride compounds. The relative contributions from various line broadening mechanisms are totally unknown for Tl(III) compounds and are worthy of investigation.

The thallium NMR properties of only a few solid or liquid organothallium compounds have been determined. Despite a large number of studies in various solvents (Table II), the ^{205}Tl spectrum in solid dimethylthallium(I) bromide has only recently been observed.[198] The shielding is anisotropic

with $\sigma_{\parallel}-\sigma_{\perp}=485$ ppm, and the isotropic shift is +5590 ppm. By comparison, Tl_2O_3 exhibits an isotropic shift of +5500 ppm and a shielding anisotropy of 1870 ppm. The large isotropic shift of Me_2TlBr presumably results from covalent thallium–methyl interactions in this compound, yet the CSA is smaller than might have been predicted. This probably reflects covalent interactions between thallium and its surrounding bromines, yielding greater than expected electronic symmetry about thallium. Other salts such as the cyanide, perchlorate, tetrafluoroborate and nitrate are believed to be quite ionic[277–280] and might therefore show much larger shielding anisotropies. In addition to Me_2TlBr, chemical shifts have been reported for thallium ethoxide[21,64] and a pyrazole derivative.[21]

D. Glasses and semiconductors

The previous sections have shown that the thallium chemical shift and CSA are highly sensitive to small electronic perturbations which accompany changes in covalency, local symmetry, etc. The line width can also be used to measure thallium interactions with the environment. These properties have been utilized extensively in studies of internal structure in glasses and semiconductors. Several reviews of thallium NMR in glasses[281–285] and semiconductors[286–287] are available.

The structures of thallium silicate glasses of varying thallium contents have been studied using both thallium shifts and line widths.[202,288,289] Large Tl–Tl scalar exchange interactions suggested the presence of thallium clusters in these systems. Thallium germanate glasses have also been investigated.[288,289]

Thallium borate glasses have been studied by several investigators. At least two basic thallium-containing subunits apparently exist in these systems. One is a relatively ionic, spherically symmetric unit while the other is more covalent and less symmetric.[290,291] As the thallium content is varied, the proportions of these subunits change, with low thallium concentrations favouring the more ionic type.[288–291] A CSA of 500–1000 ppm has been found for the low symmetry subunit.[288,289] The ^{205}Tl line width also appears to be composition-dependent with large values at high concentrations suggesting Tl–Tl exchange interactions.[202] The effect of temperature on the thallium chemical shift has been measured and explained in terms of thermally induced overlap of cation and anion wave functions.[19,229]

Various thallium phosphate glasses have been studied. As in the thallium borate glasses, a shielding decrease with increasing thallium content suggests greater covalency in these systems. This effect can be dramatic, as in Tl_2O/P_2O_5 glasses.[193] In glassy $TlPO_3$, thallium sites are moderately ionic, but not as ionic as in the polycrystalline form.[197] The thallium CSA in $TlPO_3$ glass has been determined to be 560 ppm even though the isotropic shift appears at −50 ppm.

Semiconducting chalcogenides of several types have been studied by thallium NMR. Shifts and line widths have been determined for TlSe and Tl_2Se_3,[292] as well as $TlAsSe_2$.[230,292–295] In all cases, line width contributions from CSA are found, and additional line broadening results from Tl–Tl exchange interactions. Systems of thallium metal in As_2Se_3 have been investigated,[296] as have $PSe_{2.5}Tl$ and PSe_4Tl.[297]

NMR studies of As/Se/Tl/Te systems have been reported. These include As_2Se_3–Tl_2Se_3,[295] $(Tl_2Se)_x$–$(As_2Se_3)_{1-x}$[201] and $Tl_2SeAs_2Te_3$, for which spin–lattice relaxation has been studied extensively.[200,230,298,299] A series of defect thallium pyrochlores of the type $Tl_xNbO_{2+x}F_{1-x}$ have been studied at various temperatures in order to characterize the structure and motion of thallium.[300] $Tl_{3.5}TaO_{2.5}F_{0.5}$ was also studied. As discussed previously, the semiconductor $Tl_3Fe(CN)_6$ exhibits a large chemical shift of +14 000 ppm and line width of 74 ± 25 kHz.[16] This may be taken as evidence for transfer of electron spin density onto the thallium.

A theoretical study of chemical shifts in A^{III}–B^{V} semiconductors has appeared.[301]

E. Zeolite and surface studies

The favourable NMR properties of thallium have permitted several investigations of thallium ions adsorbed on surfaces and thallium contained in zeolites. These studies, along with the NMR properties of thallium in solution, have been reviewed fairly recently.[302]

The first published report in this area concerned thallium shifts and spin–spin relaxation times in the zeolite $Tl_3HGe_7O_{16}\cdot nH_2O$.[303] It is found that thallium diffusion is rapid in the completely hydrated zeolite. In fact, the rate of thallium diffusion is essentially the same as that of water at room temperature. The thallium shielding is highly dependent on the amount of water present, suggesting major changes in the thallium environment upon hydration. These same conclusions were reached in another study of this system,[304] which also found more rapid thallium diffusion near room temperature than at liquid nitrogen temperatures.

^{205}Tl NMR properties in silicon/aluminium zeolites have been investigated.[305,306] Evidence for the existence of several thallium sites is found. In addition, the determination of correlation times allow the detailed description of thallium motion as a function of temperature and water content.

The chemical shift and spin–lattice relaxation time of ^{205}Tl(I) ions adsorbed on hydrated silica have been studied.[307] A prolonged equilibration period is required before NMR properties stabilize. The shielding of adsorbed Tl(I) is found to be about 80 ppm greater than in aqueous thallium(I) acetate in the bulk solution (about −40 ppm with respect to infinitely dilute aqueous Tl(I) at zero). The low frequency shift is attributed to dissociation

of ion pairs with acetate upon binding to the surface. Inversion recovery T_1 measurements suggest the dominance of the dipolar relaxation mechanism for adsorbed $^{205}Tl(I)$.

ABBREVIATIONS

The following abbreviations are used in Tables I–XXI in this review:

Aat

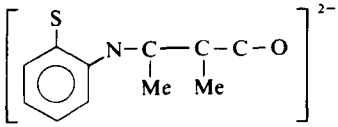

acac	acetylacetonate
Bu^i	isobutyl
Bu^n	*N*-butyl
cp	cyclopentadienyl
C222	cryptand 222, $N[(CH_2)_2O(CH_2)_2O(CH_2)_2]_3N$
DB18C6	dibenzo-18-crown-6
DCH18C6	dicyclohexyl-18-crown-6
DEA	*N,N*-diethylacetamide
dipy	dipyridyl
DMA	*N,N*-dimethylacetamide
DME	1,2-dimethoxyethane
DMF	*N,N*-dimethylformamide
DMSO	dimethylsulphoxide
en	ethylenediamine
Et	ethyl
Hiv	hydroxyisovalerate
HMPA	hexamethylphosphorotriamide, $OP[N(CH_3)_2]_3$
Lac	lactate
liq.	liquid
Me	methyl
NEA	*N,N*-diethylacetamide
NEF	*N*-ethylformamide
NMF	*N*-methylformamide
OAc	acetate
OEP	octaethylporphyrin
o-phen	*o*-phenanthroline
Ph	phenyl
Pr^i	isotropyl
Pr^n	*n*-propyl

Sat

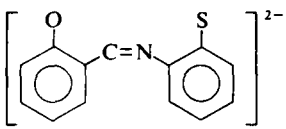

sat'd	saturated solution
TFA	trifluoroacetate
TFAA	trifluoroacetic acid
THF	tetrahydrofuran
TMG	tetramethylguanidine
TMP	trimethylphosphate, $OP(OCH_3)_3$
TMU	tetramethylurea
TOP	tetra(*o*-methylphenyl)porphyrin
TPP	tetraphenylporphyrin
Val	valine
∞-dil.	infinite dilution
15C5	15-crown-5
18C6	18-crown-6

ACKNOWLEDGMENT

Part of this work was supported by a grant from the NSF (PCM-78-27037).

REFERENCES

1. F. Bloch, W. W. Hansen and M. Packard, *Phys. Rev.*, 1946, **69**, 127.
2. E. M. Purcell, H. C. Torrey and R. V. Pound, *Phys. Rev.*, 1946, **69**, 37.
3. R. K. Harris and B. E. Mann (eds), *NMR and the Periodic Table*, Academic Press, London, 1978.
4. N. Bloembergen and T. J. Rowland, *Acta Metal.*, 1953, **1**, 731.
5. H. S. Gutowsky and B. R. McGarvey, *Phys. Rev.*, 1953, **91**, 81.
6. J. Mason, *Advances in Inorganic Chemistry and Radiochemistry*, Vol. 18 (ed. H. J. Emeleus and A. G. Sharpe), Academic Press, New York, 1976, p. 197.
7. T. D. Gierke and W. H. Flygare, *J. Amer. Chem. Soc.*, 1972, **94**, 7277.
8. R. P. H. Gasser and R. E. Richards, *Mol. Phys.*, 1959, **2**, 357.
9. R. Freeman, R. P. H. Gasser, R. E. Richards and D. H. Wheeler, *Mol. Phys.*, 1959, **2**, 75.
10. E. B. Baker and L. W. Burd, *Rev. Sci. Instr.*, 1963, **34**, 238.
11. R. E. Sheriff and D. Williams, *Phys. Rev.*, 1951, **82**, 651.
12. H. L. Poss, *Phys. Rev.*, 1947, **72**, 637.
13. H. L. Poss, *Phys. Rev.*, 1949, **75**, 600.
14. W. G. Proctor, *Phys. Rev.*, 1949, **75**, 522.
15. H. S. Gutowsky and B. R. McGarvey, *Phys. Rev.*, 1953, **91**, 81.
16. D. Herbison-Evans, P. B. P. Phipps and R. J. P. Williams, *J. Chem. Soc.*, 1965, 6170.
17. R. Freeman, R. P. H. Gasser and R. E. Richards, *Mol. Phys.*, 1959, **2**, 301.
18. R. W. Vaughan and D. H. Anderson, *J. Chem. Phys.*, 1970, **52**, 5287.
19. N. H. Nachtrieb and R. K. Momii, in *Reactive Solids, Proceedings of the 6th International Symposium* (ed. J. W. Mitchell), Wiley–Interscience, New York, 1969, p. 675.
20. S. Hafner and N. H. Nachtrieb, *J. Chem. Phys.*, 1965, **42**, 631.
21. H. Koppel, J. Dallorso, G. Hoffman and B. Walther, *Zeit. Anorg. Allg. Chem.*, 1976, **427**, 24.
22. J. J. Dechter and J. I. Zink, *Inorg. Chem.*, 1976, **15**, 1690.

23. J. J. Dechter and J. I. Zink, *J. Amer. Chem. Soc.*, 1975, **97**, 2937.
24. J. J. Dechter and J. I. Zink, *J. Chem. Soc. Chem. Commun.*, 1974, 96.
25. J. F. Hinton and R. W. Briggs, *J. Magn. Reson.*, 1975, **19**, 393.
26. J. J. Dechter and J. I. Zink, *J. Amer. Chem. Soc.*, 1976, **98**, 845.
27. J. F. Hinton and R. W. Briggs, *J. Magn. Reson.*, 1977, **25**, 379.
28. J. J. Dechter, *Diss. Abstr. Int. B*, 1976, **36**, 3944.
29. R. W. Briggs, K. R. Metz and J. F. Hinton, J. *Solution Chem.*, 1979, **8**, 479.
30. J. F. Hinton and K. R. Metz, *J. Solution Chem.*, 1980, **9**, 197.
31. R. W. Briggs and J. F. Hinton, J. *Solution Chem.*, 1977, **6**, 827.
32. V. Gutmann, *Coord. Chem. Rev.*, 1976, **18**, 225.
33. R. W. Briggs and J. F. Hinton, J. *Solution Chem.*, 1978, **7**, 1.
34. R. W. Briggs and J. F. Hinton, *J. Solution Chem.*, 1979, **8**, 519.
35. A. K. Covington, T. H. Lilley, K. E. Newman and G. A. Porthouse, *J. Chem. Soc. Faraday Trans.*, 1973, **69**, 963.
36. A. K. Covington, K. E. Newman and T. H. Lilley, *J. Chem. Soc. Faraday Trans.*, 1973, **69**, 973.
37. A. K. Covington, I. R. Lantzke and J. M. Thain, *J. Chem. Soc. Faraday Trans.*, 1974, **70**, 1869.
38. A. K. Covington and J. M. Thain, *J. Chem. Soc. Faraday Trans.*, 1974, **70**, 1879.
39. A. K. Covington and K. E. Newman, in *Advances in Chemistry Series* no. 155 (ed. W. F. Furter), American Chemical Society, New York, 1976, p. 153.
40. S. O. Chan and L. W. Reeves, *J. Amer. Chem. Soc.*, 1974, **96**, 404.
41. D. Gudlin and H. Schneider, *Inorg. Chim. Acta*, 1979, **33**, 205.
42. M. Shamsipur, G. Rounaghi and A. Popov, *J. Solution Chem.*, 1980, **9**, 701.
43. C. Srivanavit, J. I. Zink and J. J. Dechter, *J. Amer. Chem. Soc.*, 1977, **99**, 5876.
44. K. Arnold and R. Scholl, *Stud. Biophys.*, 1976, **59**, 47.
45. J. Reuben and G. J. Kayne, *J. Biol. Chem.*, 1971, **246**, 6227.
46. F. J. Kayne and J. Reuben, *J. Amer. Chem. Soc.*, 1970, **92**, 220.
47. C. M. Grisham, R. K. Gupta, R. E. Barnett and A. S. Mildvan, *J. Biol. Chem.*, 1974, **249**, 6738.
48. C. M. Grisham and A. S. Mildvan, *Fed. Proc.*, 1974, **23**, 1331.
49. J. F. Hinton, G. L. Turner and F. S. Millett, *J. Magn. Reson.*, 1981, **45**, 42.
50. J. F. Hinton, G. Young and F. S. Millett, *Biochemistry*, 1982, **21**, 651.
51. G. L. Turner, F. J. Hinton and F. S. Millett, *Biochemistry*, 1982, **21**, 646.
52. R. W. Briggs, F. A. Etzkorn and J. F. Hinton, *J. Magn. Reson.*, 1980, **37**, 523.
53. R. W. Briggs and J. F. Hinton, *J. Magn. Reson.*, 1978, **32**, 155.
54. R. W. Briggs and J. F. Hinton, *J. Magn. Reson.*, 1979, **43**, 363.
55. R. W. Briggs and J. F. Hinton, *Biochemistry*, 1978, **17**, 5576.
56. R. P. H. Gasser and R. E. Richards, *Mol. Phys.*, 1959, **2**, 357.
57. M. Bacon and L. W. Reeves, *J. Amer. Chem. Soc.*, 1973, **95**, 272.
58. J. F. Hinton and R. W. Briggs, *J. Magn. Reson.*, 1977, **25**, 379.
59. J. F. Hinton and K. H. Ladner, *J. Magn. Reson.*, 1978, **32**, 303.
60. R. N. Schwartz, *J. Magn. Reson.*, 1976, **24**, 205.
61. B. W. Bangerter and R. N. Schwartz, *J. Chem. Phys.*, 1974, **60**, 333.
62a. J. M. Lehn, J. P. Sauvage and B. Dietrich, *J. Amer. Chem. Soc.*, 1970, **92**, 2916.
62b. H. G. Forster and J. D. Roberts, *J. Amer. Chem. Soc.*, 1980, **102**, 6984.
63. V. F. Bystrov, Y. D. Gavrilov, V. T. Ivanov and Y. A. Ovchinnikov, *Europ. J. Biochem.*, 1977, **78**, 63.
64. W. G. Schneider and A. D. Buckingham, *Disc. Faraday Soc.*, 1962, **34**, 147.
65. B. N. Figgis, *Trans. Faraday. Soc.*, 1959, **55**, 1075.
66. T. Sidei, S. Yano and S. Sasaki, *Oyo Butsuri*, 1958, **27**, 513.

67. J. Glaser and U. Henriksson, *J. Amer. Chem. Soc.*, 1981, **103**, 6642.
68. M. G. Voronkov, V. A. Pestunovich, S. V. M. Khailova, J. Popelis and E. Leipins, *Khim. Geterotsikl. Soedin*, 1973, **3**, 312.
69. C. Hansen, *Chem. Ber.*, 1870, **3**, 9.
70. K. Hildenbrand and H. Dreeskamp, *Zeit. Phys. Chem.*, 1970, **69**, 171.
71. P. J. Burke, R. W. Matthews and D. G. Gillies, *J. Organometal. Chem.*, 1976, **118**, 129.
72. J. F. Hinton and R. W. Briggs, *J. Magn. Reson.*, 1976, **22**, 447.
73. G. M. Sheldrick and J. P. Yesinowski, *J. Chem. Soc., Dalton*, 1975, 870.
74. J. F. Hinton and R. W. Briggs, *J. Magn. Reson.*, 1977, **25**, 555.
75. C. S. Hoad, R. W. Matthews, M. M. Thakur and D. G. Gillies, *J. Organometal. Chem.*, 1977, **124**, C31.
76. P. J. Burke, D. G. Gillies and R. W. Matthews, *J. Chem. Res. (S)*, 1981, 124.
77. P. J. Burke, R. W. Matthews, I. D. Cresshull and D. G. Gillies, *J. Chem. Soc. Dalton*, 1981, **1**, 132.
78. F. Brady, R. W. Matthews, M. J. Forster and D. G. Gillies, *Inorg. Nucl. Chem. Letters*, 1981, **17**, 155.
79. W. Mueller-Warmuth and R. Vilhjalmsson, *Zeit. Phys. Chem.* 1974, **93**, 283.
80. K. Hildenbrand and H. Dreeskamp, *Zeit. Phys. Chem.*, 1970, **69**, 171.
81. J. P. Maher and D. F. Evans, *Proc. Chem. Soc.*, 1961, 208.
82. J. P. Maher and D. F. Evans, *J. Chem. Soc.*, 1965, 637.
83. J. P. Maher and D. F. Evans, *J. Chem. Soc.*, 1963, 5534.
84. A T. Weibel and J. P. Oliver, *J. Amer. Chem. Soc.*, 1972, **94**, 8590.
85. A. T. Weibel and J. P. Oliver, *J. Organometal. Chem.*, 1974, **74**, 155.
86. R. J. Abraham, G. E. Hawkes and K. M. Smith, *Tetrahedron Letters*, 1975, 1999.
87. M. L. Maddox, S. L. Stafford and H. D. Kaesz, *Adv. Organometal. Chem.*, 1966, **3**, 1.
88. A. G. Lee, and G. M. Sheldrick, *J. Chem. Soc. A*, 1969, 1055.
89. F. Schindler and H. Schmidbaur, *Chem. Ber.*, 1967, **100**, 3655.
90. P. Krommes and J. Lorberth, *J. Organometall. Chem.* 1977, **131**, 415.
91. G. M. Sheldrick and J. P. Yesinowski, *J. Chem. Soc. Dalton*, 1975, 870.
92. G. D. Shier and R. S. Drago, *J. Organometal. Chem.*, 1966, **5**, 330.
93. A. G. Lee and G. M. Sheldrick, *Trans. Faraday Soc.*, 1971, **67**, 1.
94. C. J. Marsden, *J. Fluorine Chem.*, 1975, **5**, 423.
95. B. Walther and K. Thiede, *J. Organometal. Chem.*, 1971, **32**, C7.
96. A. G. Lee, *J. Chem. Soc. Chem. Commun.*, 1968, 1614.
97. B. Walther, A. Zschunke, B. Adler, A. Kolbe and S. Bauer, *Zeit. Anorg. Allg. Chem.*, 1976, **427**, 137.
98. B. Walther, R. Mahrwald, C. Jahn and W. Klar, *Zeit. Anorg. Allg. Chem.*, 1976, **423**, 144.
99. A. G. Lee and G. M. Sheldrick, *J. Chem. Soc. Chem. Commun.*, 1969, 441.
100. A. G. Lee, *J. Chem. Soc. A*, 1970, 2157.
101. J. V. Hatton, *J. Chem. Phys.*, 1964, **40**, 933.
102. H. Kurosawa and R. Okawara, *Inorg. Nucl. Chem. Letters*, 1967, **3**, 21.
103. H. Kurosawa, K. Yasuda and R. Okawara, *Bull. Chem. Soc. Japan*, 1967, **40**, 861.
104. H. Kurosawa, K. Yasuda and R. Okawara, *Inorg. Nucl. Chem. Letters*, 1965, **1**, 131.
105. J. Kurosawa and R. Okawara, *J. Organometal. Chem.*, 1967, **10**, 211.
106. U. Knips and F. Huber, *J. Organometal. Chem.*, 1976, **107**, 9.
107. P. Krommes and J. Lorberth, *J. Organometal. Chem.*, 1976, **120**, 131.
108. M. Aritomi and Y. Kawasaki, *J. Organometal. Chem.*, 1975, **90**, 185.
109. N. N. Greenwood, B. S. Thomas and D. W. Waite, *J. Chem. Soc. Dalton*, 1975, 299.
110. Y. Kawasaki and M. Aritomi, *J. Organometal. Chem.*, 1976, **104**, 39.
111. H. Kurosawa and R. Okawara, *Trans. N.Y. Acad. Sci., Ser. II*, 1968, **30**, 962.

112. H. Schmidbaur and F. Schindler, *Angew. Chem.*, 1965, **77**, 865; *Angew. Chem. Int. Ed. Engl.*, 1965, **4**, 876.
113. A. G. Lee, *J. Chem. Soc. A*, 1970, 467.
114. L. Pellerito, R. Cefalu and G. Ruisi, *J. Organometal. Chem.*, 1973, **63**, 41.
115. H.-U. Schwering and J. Weidlein, *J. Organometal. Chem.*, 1975, **99**, 223.
116. B. Schaible, W. Haubold and J. Weidlein, *Zeit. Anorg. Allg. Chem.*, 1974, **403**, 289.
117. P. J. Burke, L. A. Gray, P. J. C. Hayward, R. W. Matthews, M. McPartlin and D. G. Gillies, *J. Organometal. Chem.*, 1977, **136**, C7.
118. B. Walther and S Bauer, *J. Organometal. Chem.*, 1977, **142**, 177.
119. C. Schramm and J. I. Zink, *J. Magn. Reson.*, 1977, **26**, 513.
120. D. W. Turner, *J. Chem. Soc.*, 1962, 847.
121. H. Koppel, J. Dallorso, G. Hoffman and B. Walther, *Zeit. Anorg. Allg. Chem.*, 1976, **427**, 24.
122. J. P. Maher and D. F. Evans, *Proc. Chem. Soc.*, 1963, 176.
123. S. Numata, H. Kurosawa and R. Okawara, *J. Organometal. Chem.*, 1974, **70**, C21.
124. E. A. V. Ebsworth, A. G. Lee and G. M. Sheldrick, *J. Chem. Soc. A*, 1969, 1052.
125. H. Kurosawa, M. Tanaka and R. Okawara, *J. Organometal. Chem.*, 1968, **12**, 241.
126. M. Tanaka, H. Kurosawa and R. Okawara, *J. Organometal. Chem.*, 1970, **21**, 41.
127. T. Abe, H. Kurosawa and R. Okawara, *J. Organometal. Chem.*, 1970, **25**, 353.
128. H. Kurosawa, R. Kitano and T. Sasaki, *J. Chem. Soc. Dalton*, 1978, 234.
129. T. Abe and R. Okawara, *J. Organometal. Chem.*, 1972, **35**, 27.
130. T. Abe, S. Numata and R. Okawara, *Inorg. Nucl. Chem. Letters*, 1972, **8**, 909.
131. H. Kurosawa and R. Okawara, *Inorg. Nucl. Chem. Letters*, 1967, **3**, 93.
132. H. Kurosawa and R. Okawara, *J. Organometal. Chem.*, 1968, **14**, 225.
133. S. Uemura, K. Zushi, A. Tabata, A. Toshimitsu and M. Okano, *Bull. Chem. Soc. Japan*, 1974, **47**, 920.
134. S. Uemura, H. Miyoshi, A. Toshimitsu and M. Okano, *Bull. Chem. Soc. Japan*, 1976, **49**, 3285.
135. W. Kruse and T. M. Bednarski, *J. Org. Chem.*, 1971, **36**, 1154.
136. R. K. Sharma and E. D. Martinez, *J. Chem. Soc. Chem. Commun.*, 1972, 1129.
137. J. P. Maher, PhD thesis, University of London, 1963.
138. S. Uemura, K. Sohma, H. Tara and M. Okano, *Chem. Letters*, 1973, 545.
139. R. K. Sharma and N. H. Fellers, *J. Organometal. Chem.*, 1973, **49**, C69.
140. S. Uemura, H. Tara, M. Okano and K. Ishikawa, *Bull. Chem. Soc. Japan*, 1974, **47**, 2663.
141. A. N. Nesmeyanov, A. E. Borisov, N. V. Novikova and E. I. Fedin, *Dokl. Akad. Nauk SSSR*, 1968, **183**, 118.
142. A. McKillop, J. D. Hunt and E. C. Taylor, *J. Organometal. Chem.*, 1970, **24**, 77.
143. B. Walther, *Zeit. Anorg. Allg. Chem.*, 1973, **395**, 112.
144. H. B. Stegmann, K. B. Ulmschneider and K. Scheffler, *J. Organometal. Chem.*, 1974, **72**, 41.
145. J. P. Maher, M. Evans and M. Harrison, *J. Chem. Soc. Dalton*, 1972, 188.
146. G. B. Deacon and I. K. Johnson, *J. Organometal. Chem.*, 1976, **112**, 123.
147. D. E. Fenton, G. D. Gillies, A. G. Massey and E. W. Randall, *Nature*, 1964, **201**, 818.
148. W. Kitching, D. Praeger, C. J. Moore, D. Doddrell and W. Adcock, *J. Organometal. Chem.*, 1974, **70**, 339.
149. K. Ichikawa, S. Uemura, T. Nakano and E. Uegaki, *Bull. Chem. Soc. Japan*, 1971, **44**, 545.
150. A. McKillop, J. S. Fowler, M. J. Zelesko, J. D. Hunt, E. C. Taylor and G. McGillivray, *Tetrahedron Letters*, 1969, 2423.
151. E. C. Taylor and A. McKillop, *Accounts Chem. Res.*, 1970, **3**, 338.
152. A. G. Lee, *J. Organometal. Chem.*, 1970, **22**, 537.

153. H. C. Bell, J. R. Kalman, J. T. Pinhey and S. Sternhell, *Tetrahedron Letters*, 1974, 3391.
154. B. Davies and C. B. Thomas, *J. Chem. Soc. Perkin I*, 1975, 65.
155. G. B. Deacon, R. N. M. Smith and D. Tunaley, *J. Organometal. Chem.*, 1976, **114**, C1.
156. G. B. Deacon, D. Tunaley and R. N. M. Smith, *J. Organometal. Chem.*, 1978, **144**, 111.
157. L. Ernst, *J. Organometal. Chem.*, 1974, **82**, 319.
158. L. Ernst, *Org. Magn. Reson.* 1974, **6**, 540.
159. J. Y. Lallemand and M. Duteil, *Org. Magn. Reson.*, 1976, **8**, 328.
160. W. Kitching, C. J. Moore, D. Doddrell and W. Adcock, *J. Organometal. Chem.*, 1975, **94**, 469.
161. R. G. Coombes, M. D. Johnson and D. Vamplew, *J. Chem. Soc. A*, 1969, 1055.
162. E. Hoyer, W. Dietzsch, H. Muller, A. Zschunke and W. Schroth, *Inorg. Nucl. Chem. Letters*, 1976, **3**, 457.
162. G. C. Stocco, *Inorg. Chim. Acta*, 1977, **24**, L65.
164. V. P. Tarasov and S. I. Bakum, *J. Magn. Reson.*, 1975, **18**, 64.
165. F. A. L. Anet, *Tetrahedron Letters*, 1964, 3399.
166. A. McKillop, M. E. Ford and E. C. Taylor, *J. Org. Chem.*, 1974, **39**, 2434.
167. P. F. Barron, D. Doddrell and W. Kitching, *J. Organometal. Chem.*, 1977, **132**, 351.
168. I. Morishima, T. Inubushi, S. Uemura and H. Miyoshi, *J. Amer. Chem. Soc.*, 1978, **100**, 354.
169. R. J. Abraham, G. H. Barnett, E. S. Bretschneider and K. M. Smith, *Tetrahedron*, 1973, **29**, 553.
170. R. J. Abraham, G. H. Barnett and K. M. Smith, *J. Chem. Soc. Perkin I*, 1973, 2142.
171. R. J. Abraham and K. M. Smith, *Tetrahedron Letters*, 171, 3335.
172. K M. Smith, *J. Chem. Soc. Chem. Commun.*, 1971, 540.
173. C. A. Busby and D. Dolphin, *J. Magn. Reson.*, 1976, **24**, 211.
174. K Henrick, R. W. Matthews and P. A. Tasker, *Inorg. Chem.*, 1977, **16**, 3293.
175. R. J. Abraham, G. E. Hawkes and K. M. Smith, *J. Chem. Soc. Chem. Commun.*, 1973, 401.
176. R. J. Abraham, G. E. Hawkes and K. M. Smith, *J. Chem. Soc. Perkin II*, 1974, 627.
177. R. J. Abraham, G. E. Hawkes, M. F. Hudson and K. M. Smith, *J. Chem. Soc. Perkin II*, 1975, 204.
178. A. T. T. Hsieh, C. A. Rogers and B. O. West, *Austral. J. Chem.*, 1976, **29**, 49.
179. H. Schmidbaur, H.-J. Fuller and F. H. Kohler, *J. Organometal. Chem.*, 1975, **99**, 353.
180. A. T. Weibel and J. P. Oliver, *J. Organometal. Chem.*, 1973, **57**, 313.
181. P. I. Van Vliet and K. Vrieze, *J. Organometal. Chem.*, 1977, **139**, 337.
182. A. T. T. Hsieh and G. Wilkinson, *J. Chem. Soc. Dalton*, 1973, 867.
183. B. Walther and C. Rockstroh, *J. Organometal. Chem.*, 1972, **44**, C4.
184. S. Hafner and N. H. Nachtrieb, *J. Chem. Phys.*, 1964, **40**, 2891.
185. J. F. Hinton and R. W. Briggs, in *NMR and the Periodic Table* (ed. R. K. Harris and B. E. Mann), Academic Press, London, 1978.
186. Dr James P. Yesinowski, private communication.
187. B. W. Bangerter, *J. Magn. Reson.*, 1977, **28**, 141.
188. H. Schmidbaur and H.-J. Fuller, *Chem. Ber.*, 1974, **107**, 3674.
189. B. Walther, R. Mahrwald, C. Jahn and W. Klar, *Zeit. Anorg. Allg. Chem.*, 1976, **423**, 144.
190. V. F. Bystrov, Yu. D. Gavrilov, V. T. Ivanov and Yu. A. Ovchinnikov, *Europ. J. Biochem.*, 1977, **78**, 63 (cited by V. F. Bystrov in *Progr. NMR Spectr.*, 1976, **10**, 41).
191. K. R. Metz and J. F. Hinton, submitted for publication.
192. Y. Saito, *J. Phys. Soc. Japan*, 1966, **21**, 1072.
193. L. Kolditz and E. Wahner, *Zeit. Anorg. Allg. Chem.*, 1973, **400**, 161.
194. J. F. Hinton and K. R. Metz, submitted for publication.

195. J. F. Hinton and K. R. Metz, unpublished data.
196. K. R. Metz and J. F. Hinton, submitted for publication.
197. L. W. Panek, G. J. Exarhos, P. J. Bray and W. M. Risen, *J. Non-cryst. Solids*, 1977, **24**, 51.
198. J. F. Hinton and K. R. Metz, submitted for publication.
199. J. F. Hinton, K. R. Metz and F. S. Millett, *J. Magn. Reson.*, 1981, **44**, 217.
200. S. G. Bishop, P. C. Taylor and D. L. Mitchell, *J. Non-cryst. Solids*, 1972, **8–10**, 106.
201. S. G. Bishop and P. C. Taylor, *Phys. Rev. B*, 1973, **7**, 5177.
202. K. Otto and M. E. Milberg, *J. Amer. Ceram. Soc.*, 1967, **50**, 513.
203. N. Bloembergen and T. J. Rowland, *Phys. Rev.*, 1955, **97**, 1679.
204. W. H. Jones, E. A. Garbaty and R. G. Barnes, *J. Chem. Phys.*, 1962, **36**, 494.
205. M. S. Whittingham and L. D. Clark, *J. Chem. Phys.*, 1970, **53**, 4114.
206. G. C. Carter, L. H. Bennett and D. J. Kahan, *Progr. Mater. Sci.*, 1977, **20**, 357.
207. J. Schratter and D. L. Williams, *Canad. J. Phys.*, 1974, **52**, 678.
208. J. J. Schratter and D. L. Williams, *Phys. Letters*, 1967, **26A**, 79.
209. W. D. Knight, *Solid State Phys.*, 1956, **2**, 93.
210. D. J. Moulson and E. F. W. Seymour, *Adv. Phys.*, 1967, **16**, 449.
211. L. H. Bennett, R. M. Cotts and R. J. Snodgrass, *Proc. Colloq. AMPERE* (*Atomes Mol. Etudes Radio Elec.*), 1964, **13**, 171.
212. W. Baden, P. C. Schmidt and A. Weiss, *Phys. Status Solidi A*, 1979, **51**, 183.
213. R. E. Watson, L. H. Bennett, G. C. Carter and I. D. Weisman, *Phys. Rev. B*, 1971, **3**, 222.
214. H. E. Shone and W. P. Knight, *Acta Metal.*, 1963, **11**, 179.
215. J. Beene, O. Haeusser, A. B. McDonald, T. K. Alexander, A. J. Ferguson and B. Herskind, *Hyperfine Interact.*, 1977, **3**, 397.
216. P. C. Schmidt and A. Weiss, *Zeit. Naturforsch. A*, 1974, **29**, 477.
217. J. D. Marcoll, P. C. Schmidt and A. Weiss, *Zeit. Naturforsch. A*, 1974, **29**, 473.
218. P. Descouts, B. Perrin, A. Dupanloup and A. Treyvaud, *J. Phys. Chem. Solids*, 1978, **39**, 161.
219. J. Freidel, *J. Phys. Radium*, 1955, **16**, 444.
220. W. W. Warren, *J. Non-cryst. Solids*, 1972, **8–10**, 241.
221. T. J. Rowland and J. P. Bromberg, *J. Chem. Phys.*, 1958, **29**, 626.
222. S. Hafner, *J. Phys. Chem. Solids*, 1966, **27**, 1881.
223. V. M. Buznik, N. A. Porozov, E. A. Vopilov, B. V. Beznosikov and E. P. Zeer, *Fiz. Tverd. Tela* (*Leningrad*), 1978, **20**, 627.
224. P. C. Bury and A. C. McLaren, *Phys. Status Solidi*, 1969, **31**, K5.
225. K. R. Metz and J. F. Hinton, submitted for publication.
226. Y. Saito, *J. Phys. Soc. Japan*, 1958, **13**, 72.
227. J. F. Hinton and K. R. Metz, submitted for publication.
228. T. Matsuo, M. Sugisaki, H. Suga and S. Seki, *Bull. Chem. Soc. Japan*, 1969, **42**, 1271.
229. R. K. Momii and N. H. Nachtrieb, *J. Phys. Chem.*, 1968, **72**, 3416.
230. G. E. Jellison and S. G. Bishop, *Phys. Rev. B*, 1979, **19**, 6418.
231. A. Abragam, *The Principles of Nuclear Magnetism*, Oxford University Press, Oxford, 1961.
232. C. P. Slichter, *Principles of Magnetic Resonance*, 2nd edn, Springer-Verlag, Berlin, 1980.
233. L. Van Gerven (ed.), *Nuclear Magnetic Resonance in Solids*, Plenum Press, New York, 1977.
234. U. Haeberlen, *High Resolution NMR in Solids, Selective Averaging*, Supplement 1 of *Advances in Magnetic Resonance* (ed. J. S. Waugh), Academic Press, New York, 1976.
235. M. Mehring, *High Resolution NMR Spectroscopy in Solids*, Springer-Verlag, Berlin, 1976.
236. E. Fukushima and S. B. W. Roeder, *Experimental Pulse NMR*, Addison-Wesley, Reading, Mass., 1981, Chap. 4.

237. J. H. Van Vleck, *Phys. Rev.*, 1948, **74**, 1168.
238. E. R. Andrew and D. P. Tunstall, *Proc. Phys. Soc. (London)*, 1963, **71**, 986.
239. R. Blinc, E. Pirkmajer, J. Slivnik and I. Zupancic, *J. Chem. Phys.*, 1966, **45**, 1488.
240. D. L. Vanderhart, H. S. Gutowsky and T. C. Farrar, *J. Amer. Chem. Soc.*, 1967, **89**, 5056.
241. W. D. Knight, *Phys. Rev.*, 1949, **76**, 1259.
242. J. Korringa, *Physica*, 1950, **16**, 601.
243. Y. S. Karimov and I. F. Schegolev, *Soviet Phys. JETP*, 1962, **14**, 772.
244. J. Schratter, *Diss. Abstr. Int. B*, 1974, **34**, 6170.
245. J. Schratter and D. L. Williams, *Canad. J. Phys.*, 1974, **52**, 687.
246. Y. S. Karimov and I. F. Shchegolev, *Zhur. Eksptl. Teoret. Fiz.*, 1961, **41**, 1082.
247. N. Karnezos and L. B. Welsh, *Phys. Rev. B*, 1975, **12**, 4790.
248. P. Descouts, B. Perrin and A. Dupanloup, in *Proceedings of the 18th AMPERE Congress on Magnetic Resonance and Related Phenomena*, Vol. 2, 1974, p. 335.
249. N. C. Halder, *J. Chem. Phys.*, 1970, **52**, 5450.
250. J. Heighway and E. F. W. Seymour, *Phys. Kondens. Mater.*, 1971, **13**, 1.
251. G. A. Styles and G. Tranfield, *J. Phys. F*, 1978, **8**, 2035.
252. P. C. Schmidt and A. Weiss, *Zeit. Naturforsch. A*, 1974, **29**, 477.
253. P. C. Schmidt, *Ber. Bunsenges. Phys. Chem.*, 1975, **79**, 1064.
254. N. C. Halder, *Phys. Rev.*, 1969, **177**, 471.
255. J. E. Enderby, R. L. Havill and J. M. Titman, *Proc. Colloq. AMPERE (Atomes Mol. Etudes. Radio Elec.)*, 1966, **14**, 1072.
256. H. Alloul and C. Froidevaux, *Comptes Rend. Acad. Sci. (Paris), B*, 1967, **265**, 881.
257. L. H. Bennett, *Acta Metal.* 1966, **14**, 997.
258. G. C. Carter, L. H. Bennett and D. J. Kahan, *Progr. Mater. Sci.*, 1977, **20**, 3.
259. G. C. Carter, L. H. Bennett and D. J. Kahan, *Progr. Mater. Sci.*, 1977, **20**, 1742.
260. H. Klever and M. Schlaak, *Rev. Sci. Instr.*, 1973, **44**, 25.
261. M. Villa and A. Avogadro, *Phys. Status Solidi B*, 1976, **75**, 179.
262. A. Avogadro, M Villa and G. Chiodelli, *Gazz. Chim. Ital.*, 1976, **106**, 413.
263. M. Hanabusa and N. Bloembergen, *J. Phys. Chem. Solids*, 1966, **27**, 363.
264. N. H. Nachtrieb and S. Hafner, *Zeit. Naturforsch. A*, 1965, **20**, 321.
265. P. F. Lindley and P. Woodward, *J. Chem. Soc. A*, 1966, 123.
266. J. S. Blicharski, *Zeit. Naturforsch. A*, 1972, **27**, 1355.
267. S. Clough and W. I. Goldberg, *J. Chem. Phys.*, 1966, **45**, 4080.
268. G. L. Samuelson, *Diss. Abstr. Int. B*, 1971, **32**, 3591.
269. V. G. I. Deshmukh, E. F. W. Seymour and G. A. Styles, *Phys. Letters A*, 1979, **74**, 432.
270. J. P. Mathur, *Diss. Abstr. Int. B*, 1972, **32**, 7219.
271. S. K. Novoselov, L. A. Baidakov and L. P. Strakhov, *Vestn. Leningrad Univ., Fiz., Khim.*, 1971, 54.
272. S. K. Novoselov, L. A. Baidakov and L. P. Strakhov, *Fiz. Tverd. Tela (Leningrad)*, 1970, **12**, 1173.
273. N. M. Sokolov, *Zhur. Neorg. Khim.*, 1979, **24**, 3125.
274. V. M. Buznik, E. A. Vopilov and V. N. Voronov, *Fiz. Tverd. Tela (Leningrad)*, 1979, **21**, 1593.
275. M. P. Petrov and G. A. Smolenskii, Fiz. *Tverd. Tela (Leningrad)*, 1965, **7**, 2156.
276. D. A. Zhogolev, *Fiz. Tverd. Tela (Leningrad)*, 1966, **8**, 2798.
277. G. E. Coats and R. N. Mukherjee, *J. Chem. Soc.*, 1963, 229.
278. G. B. Deacon, J. H. S. Green and R. S. Nyholm, *J. Chem. Soc.*, 1965, 3411.
279. G. D. Shier and R. S. Drago, *J. Organometal. Chem.*, 1966, **5**, 330.
280. G. B. Deacon and J. H. S. Green, *Spectrochim. Acta*, 1968, **24A**, 885.
281. P. J. Bray, *Silikattechnik*, 1968, **19**, 350.
282. N. H. Nachtrieb, *U.S. Clearinghouse Fed. Sci. Tech. Inform.*, 1970, No. 705676.

283. P. J. Bray, *U.S. Clearinghouse Fed. Sci. Tech. Inform.*, 1970, No. 715463.
284. P. J. Bray, *Stekloobrazh. Sostoyanie*, 1971, **191–3**, 264.
285. P. J. Bray, *10th Int. Congr. Glass*, [*Pap.*], 1974, **13**, 1.
286. J. M. Delrieu, Report FRNC-TH-515, 1974.
287. S. Grande, S. Wartewig and K. Werner, *Wiss. Zeit. Karl-Marx-Univ. Leipzig, Math.-Naturwiss. Reihe*, 1971, **20**, 171.
288. L. W. Panek and P. J. Bray, *J. Chem. Phys.*, 1977, **66**, 3822.
289. L. W. Panek, *Diss. Abstr. Int. B*, 1978, **38**, 6019.
290. J. F. Baugher and P. J. Bray, *Phys. Chem. Glasses*, 1969, **10**, 77.
291. J. F. Baugher, *Diss. Abstr. Int. B*, 1970, **31**, 347.
292. L. A. Baidakov and A. N. Kudryavtsev, *Izv. Akad. Nauk SSSR, Neorg. Mater.*, 1973, **9**, 1055.
293. L. A. Baidakov and Z. U. Borisova, in *Proceedings of the 5th International Congress on Amorphous Liquid Semiconductors*, Vol. 2, 1973, p. 1035.
294. L. A. Baidakov, A. N. Kudryavtsev and S. K. Novoselov, *Izv. Akad. Nauk SSSR, Neorg. Mater.*, 1973, **9**, 1640.
295. L. A. Baidakov and A. N. Kudryavtsev, *Vestn. Leningrad Univ., Fiz. Khim.*, 1973, 114.
296. S. Ueda and T. Shimizu, *Phys. Status Solidi B*, 1979, **95**, 279.
297. L. A. Baidakov, A. N. Katruzov and Kh. M. El Labani, *Izv. Akad. Nauk SSSR, Neorg. Mater.*, 1978, **14**, 1810.
298. G. E. Jellison and S. G. Bishop, *Phys. Rev. Letters*, 1978, **40**, 1204.
299. G. E. Jellison and S. G. Bishop, in *Proceedings of the 7th International Conference on Amorphous Liquid Semiconductors*, 1977, p. 607.
300. A. D. English, A. W. Sleight, J. L. Fourquet and R. De Pape, *Mater. Res. Bull.*, 1980, **15**, 1727.
301. K. Huebner, *Phys. Status Solidi B*, 1971, **45**, 619.
302. V. V. Morariu and A. Chifu, *Stud. Cercet. Fiz.*, 1979, **31**, 391.
303. T. Wada and J. P. Cohen-Addad, *Bull. Soc. Fr. Mineral. Crystallogr.*, 1969, **92**, 238.
304. H. Bittner and E. Hauser, *Monatsh. Chem.*, 1970, **101**, 1471.
305. D. Freude, A. Hauser, H. Pankau and H. Schmiedel, *Zeit. Phys. Chem.* (*Leipzig*), 1972, **251**, 13.
306. D. Freude, U. Lohse, H. Pfeifer, W. Schirmer, H. Schmiedel and H. Stach, *Zeit. Phys. Chem.* (*Leipzig*), 1974, **255**, 443.
307. V. V. Morariu, *Chem. Phys. Lett.*, 1978, **56**, 272.

Rotational Correlation Times in Nuclear Magnetic Relaxation

RENÉ T. BOERÉ AND R. GARTH KIDD

Department of Chemistry, The University of Western Ontario, London, Canada

I. INTRODUCTION

A theoretical model with which we can picture at the microscopic level the behaviour of matter in the liquid state still represents one of the major challenges faced by today's physical chemist. Experimental observations based largely upon X-ray diffraction have provided us with a spongy sphere model for atoms and molecules in the solid state, and bond lengths and bond angles can now be predicted with reasonable confidence. The liquid state, however, represents molecules in motion, and a satisfactory way in which to describe this motion still proves elusive. The names that loom large in bringing us to our present level of understanding are Bernal,[1] Debye[2] and Staudinger,[3] while in bringing the NMR technique to bear on the problem, the experiments and insight of Hertz[4] have provided new avenues to understanding the microdynamical features of the liquid state.

The rotational motion of molecules in the gas phase is well represented by the equipartition of energy theorem and the laws of statistical mechanics, both of which are premised on the view that, except during instantaneous collisions, the molecules move independently of one another. Between collisions, the angular velocity is uniform and is determined solely by the molecule's moment of inertia and the temperature. In the liquid phase, however, the picture is rather more complex. Separations are small, intermolecular forces which are molecule specific come into play, and the macroscopic manifestation of these uniquely liquid phase characteristics is the bulk *viscosity* of the system. For most molecules in the liquid phase, the rotation rate depends upon the viscosity and is independent of the moment of inertia, indicating that intermolecular frictional forces rather than inertial factors are paramount. During its brief lifespan, NMR spectroscopy has quickly become the most powerful method for investigating the intimate details of this relationship.

A. The relaxing nucleus

Spectroscopic relaxation, like money, only becómes a problem when the amount is inadequate. Optical and infrared spectroscopists are seldom concerned with relaxation. The reason for this happy state of bliss lies in the Einstein theory of transition probabilities,[6] according to which the probability for spontaneous emission is proportional to the cube of the frequency, while the probability for induced absorption is proportional to the radiation density and independent of frequency. Relaxation is therefore a much slower process at radio frequencies than at optical frequencies, and the magnetic resonance spectroscopist's concern about saturation is well founded. While relaxation times in optical spectroscopy are typically of the order of 10^{-8} s, the shortest NMR relaxation times are of the order of 10^{-6} s and relaxation times in the range $1\ \mathrm{s} \leqslant T_1 \leqslant 10\ \mathrm{s}$ are common. The blissful state can also represent the ignorant state, and while the optical spectroscopist doesn't have to worry about saturation, his spectra do not yield relaxation times which in turn provide information about molecular dynamics.

The need to ensure adequate relaxation was recognized at an early date by NMR spectroscopists, and in 1948 Bloembergen presented to the University of Leiden a thesis on nuclear magnetic relaxation[24] in which the relationship between theory and experiment was established and some of the relaxation mechanisms were outlined. For liquid samples, whose spectra showed the deleterious effects of RF saturation, it was standard practice at this time to facilitate relaxation by addition of paramagnetic ions; thus enabling the determination of otherwise unobservable line positions but vitiating any attempt to determine intrinsic relaxation times. Although there has been some interest in nuclear spin relaxation times since the advent of NMR spectroscopy, the first few generations of commercial spectrometers were of the continuous wave variety, which made difficult or uncertain the routine measurement of relaxation times, and chemical interest centred upon the determination of shieldings and coupling constants.

The swing from continuous wave to pulsed spectrometers in recent years, primarily to achieve the sensitivity enhancement available through Fourier transformation (FT), has brought with it the routine capability for measuring relaxation times.[8] This is reflected in the NMR literature, which shows a significant increase over the past few years of papers in which structural information of chemical interest has been extracted from relaxation times.

B. The rotating molecule

The first requirement for spontaneous relaxation is that the nucleus be coupled to its surroundings, and in the rate equations for relaxation by

each of the different mechanisms, the strength of this coupling is represented by a term having units of (frequency)^2. Relaxation results when this coupling is modulated at the appropriate frequency by molecular tumbling, and the other variable in each equation is a time constant related to the rate of molecular rotation. The rate equation for nuclear relaxation contains these two variables, neither of which is directly measureable in an NMR experiment.

The first 35 years of nuclear magnetic relaxation studies can be characterized as the period in which independently determined values for a coupling constant were combined with a measured relaxation rate to yield information about molecular rotation in the form of a correlation time τ_c. It was evident to Bloembergen even in 1948[24] that while the classical Stokes–Einstein–Debye (SED) model for the rotational diffusion of a sphere in a viscous fluid would yield a theoretical value for τ_c, this only approximated the molecular reality to within one or two orders of magnitude. With increasing vigour during the past 15 years, relaxation measurements have been brought to bear on the microdynamic behaviour of liquids and in the process, the SED model has undergone several improvements, each adapting the original model to reflect the rotational behaviour of molecules increasingly diverse in both their size and shape.

A comprehensive review of this field was provided by Hertz in 1967,[4] and in 1970 Huntress[26] provided the theoretical basis for evaluating the individual components of the rotational diffusion tensor for molecules undergoing anisotropic reorientation. As part of a general review of pressure effects on nuclear relaxation, Jonas in 1973[9] drew together the definitive results from rotational diffusion studies up to that time. Great strides have been made since 1973 and, as Section VII of this review indicates, the Hu–Zwanzig and the Youngren–Acrivos improvements provide us with theoretical models for calculating τ_c, the reliability of which have been tested on a variety of molecules containing nuclei which are relaxed by a variety of mechanisms.

C. The coupling constant evaluated

Four different types of coupling constant, when modulated by molecular rotation, contribute to nuclear magnetic relaxation. Nuclear quadrupole coupling constants are measured on solid samples by NQR spectroscopy and on gaseous samples using molecular beam methods.[10] No convenient method for determining this constant on liquid samples is currently available. Spin–rotation coupling constants needed to establish absolute shielding scales for various nuclei are only available from molecular beam measurements on gaseous samples.[7] Dipole–dipole coupling constants depend only upon the gyromagnetic ratios of the coupled nuclei and their

separation, and are calculated whenever the dipole–dipole distance is known with sufficient precision. Shielding anisotropies are obtained from chemical shift measurements on oriented molecules and the product of the anisotropy and the magnetic field strength yields the associated coupling constant. Each of these four coupling constants provides valuable insight into some aspect of molecular structure and yet, with the exception of the nuclear quadrupole coupling constant, the experimental complexity associated with their determination means that few have been measured.

With the advent of FT NMR spectrometers, instrumentation for measuring nuclear relaxation rates is more widely available than is the instrumentation for the direct measurement of any of the four coupling constants listed above. This being so, coupling constants can be obtained from measured relaxation rates if one can calculate with confidence the rotational correlation time for the molecule.

This study represents a critical analysis of the theoretical models presently available for carrying out the calculation of τ_c in which calculated and observed values are compared for several hundred molecules. While in some cases the comparison is not as gratifying as one might wish, the overall results provide a realistic basis for the evaluation of nuclear quadrupole coupling constants and spin–rotation constants from nuclear magnetic relaxation times.

II. THE MECHANICS OF MOLECULAR ROTATION

The simplest example of molecular rotation that we can visualize is that of a spherical molecule rotating freely in space. The rate of rotation increases with increasing thermal energy, kT, and decreases with increasing rotational inertia, I. When considering relaxation processes, the rotation rate is a less convenient property with which to work than its reciprocal, and the free rotation time, τ_{FR}, defined as the time taken for a molecule to rotate through an angle of one radian, is adopted as one of the reference variables.

The moment of inertia, I, for an object describes its intrinsic rotational characteristics, and classical mechanics defines the angular momentum, J, for the object by

$$J = I \cdot \omega \qquad (\text{dimensions } \mathcal{M}\mathcal{L}^2\mathcal{T}^{-1}), \tag{1}$$

where ω is angular velocity in radians per second. Because a dimensional analysis incorporating specific units does not reveal whether angular velocity is measured in radians per second or in hertz, it is not uncommon to encounter in the literature dealing with relaxation phenomena discrepancy factors of $2\pi = 6{\cdot}3$ and $(2\pi)^2 = 39$, the source of which is difficult to track

down. When dealing with angular velocity in this context, pedantry is preferable to confusion. In the case of a spherical object, I is a scalar while ω and J are vectors. In the more general anisotropic case, I, ω and J are all tensors.

In characterizing rotational correlation, a time scale based upon the rotation period for a freely rotating molecule is commonly used, and rotation period is directly related to rotational energy. Classically, an object can rotate with any angular velocity and can therefore have any rotational kinetic energy.

$$E_{\text{rot}} = \tfrac{1}{2} I \omega^2 \tag{2}$$

Molecules obeying the quantum restrictions will have, using the Bohr postulate, angular momenta

$$I \cdot \omega = J \cdot \hbar \qquad (J = 0, 1, 2, \ldots) \tag{3}$$

and rotational energies

$$E_{\text{rot}} = \frac{1}{2} \frac{(I \cdot \omega)^2}{I} = \frac{J^2 \cdot \hbar^2}{2I} \tag{4}$$

For a molecule whose rotational energy corresponds with the equipartition value of $(3/2)\,kT$, $\langle J^2 \rangle \hbar = 3I \cdot kT$ and the period of rotation

$$\tau_\theta = \frac{1}{\omega} = 0{\cdot}58 \left(\frac{I}{kT}\right)^{1/2} \text{ s rad}^{-1} \tag{5}$$

Defined in this way, τ_θ is the time required for the freely rotating molecule to rotate through an angle of 1 radian. For angular displacement θ measured in radians, the time required to rotate through any specific angle is

$$\tau = \theta \left(\frac{I}{3kT}\right)^{1/2} \tag{6}$$

A molecule whose rotation time depends only upon I and T is said to be in the *inertial region*.

A. The free rotation time

This review is concerned with liquid phase molecular rotation in which viscous drag slows down the rate of rotation and causes τ_{rot} to become longer than for the freely rotating molecule. The free rotation time, however, occupies a central position in all discussions of liquid phase rotation since it is regarded as the limit approached by the actual τ_θ as the viscosity approaches zero. Because there are various ways in which the "average" rotational energy for a single molecule can be defined, different

authors have found it convenient to designate this property in slightly different ways, each of which yields a different value for the numerical constant in equation (5). Wallach and Huntress[11] adopt the equipartitioning of energy approach and obtain the factor 3/5 which has subsequently been incorporated into the χ-test (*q.v.*) used to distinguish the diffusion from the inertial regions of molecular rotation.[11,12] Maryott *et al.*,[13] in their classic study on the rotational diffusion of liquid ClO_3F, choose a freely rotating molecule with the Boltzmann r.m.s. angular velocity and obtain the factor 1·0.† Wasylishen and Pettit[14] use a Maxwellian distribution of energies which yields a factor of 4/5. Where the experimental τ_{FR} value under analysis is obtained by a long extrapolation out of the diffusion region towards the inertial limit; coefficient variations of this magnitude, particularly when applied to relatively short τ-values, are insignificant.

Free rotation times needed in this review have been calculated using the definition

$$\tau_{FR} = (I/kT)^{1/2} \tag{7}$$

In doing so, it is recognized that variations of up to ±20% are encompassed by the definitional range for angular velocity which is available. Benchmark values for molecules spanning a range of I values at some typical temperatures are given in Table I.

TABLE I

Representative free rotation times at different temperatures.

Molecule	$I_{Av}/10^{-40}$ g cm^2 [a]	$(I/kT)^{1/2}$/ps rad^{-1} 150 K	300 K	400 K
CH_4	5·3	0·16	0·11	0·098
CF_4	149	0·85	0·60	0·52
ClO_3F	156	0·87	0·61	0·53
CCl_4	490	1·5	1·1	0·94
$SnCl_4$	858	2·0	1·4	1·2
$PbCl_4$	928	2·1	1·5	1·3
SnI_4	4270	4·5	3·2	2·8

[a] $I_{Av} = \frac{1}{3}(2I_{\perp} + I_{\parallel})$.

B. The rotational diffusion region

The diffusion concept originated in an attempt to describe the spontaneous translational motion of small particles and carries with it implications of continuous motion and a retarding force. The translational diffusion

† A denominator inversion is required to correct the defining equation in reference 13.

coefficient, D_{tr}, with dimensions $(\mathscr{L}^2\mathscr{T}^{-1})$ relates a material flux per unit area, F mol cm^{-2} s^{-1}, to a concentration gradient, $\partial C/\partial x$; mol cm^{-2}, according to the equation

$$F = -D_{tr}\frac{\partial C}{\partial x} \tag{8}$$

The rotational diffusion model of a liquid views the reorientational motion of a molecule as being impeded by a viscosity-related frictional force where, again, continuous motion is implied. If the rotational friction coefficient operating at the surface of the molecule regarded as a sphere is that represented by the macroscopic viscosity, η, then the rotational friction coefficient has the Stokes value[15,16]

$$\xi = 8\pi a^3\eta \qquad (\mathscr{M}\,\mathscr{L}^2\,\mathscr{T}^{-1}) \tag{9}$$

and the rotational diffusion rate is given by

$$D_{rot} = \frac{kT}{8\pi a^3\eta} \qquad (\mathscr{T}^{-1}) \tag{10}$$

in rad s^{-1} when the other variables are expressed in coherent units.

In the hydrodynamical view of molecules rotating within a continuous fluid, it is assumed that the molecule undergoes small random jumps characterized by a rotational diffusion tensor **D** in which the three elements D_i of the diagonalized tensor are defined in such a way that the molecule rotates or diffuses through r.m.s. angles[17,18]

$$\langle\Delta\theta_i^2\rangle^{1/2} = (2D_i\,\Delta t)^{1/2}\ \text{rad} \tag{11}$$

in a time Δt. The value of Δt required for $\langle\Delta\theta_i^2\rangle^{1/2}$ to reach 1 rad has been defined as τ_θ and for typical systems this time is observed to be in the picosecond range. Although the jump nature of the motion makes it incremental, it is regarded as continuous because many jumps are required to achieve a diffusion angle of 1 rad.

The model has received extensive use in the characterization of Brownian motion,[19] and the diffusion rates involved in the motion have been measured by dielectric relaxation.[20] Since the rotation is perceived as occurring in small steps, the initiation of each step is associated with a "collision". Collison number, Z, defined as the average number of steps required to rotate through 1 rad, and collision frequency represented by Z/τ_θ are both used to characterize the motion when one wishes to emphasize its incremental features. In the classical diffusion model, a time period τ_J is formally identified with the average time between instantaneous collisions and this time interval is given by τ_θ/Z. In summary, there are two time constants associated with the classical diffusion picture of molecular rotation. The

angular time constant τ_θ represents the time required for the average molecule to rotate through an angle $\theta = 1$ rad. The *velocity* (or angular *momentum*) time constant τ_J, so named because velocity/momentum remains constant between collisions and changes during collisions, is the average time between collisions. The diffusion view requires τ_J to be shorter than τ_θ. When molecular rotation is viewed as a random walk process, these time constants characterize the rates at which *angular* correlation and *velocity* correlation are lost. Their definitions in this role are discussed in Section III dealing with rotational correlation.

While it is fluctuations in molecular *orientation* that modulate nuclear quadrupole, dipole–dipole and chemical shielding anisotropy interactions leading to nuclear relaxation, it is fluctuations in the *velocity* of molecular rotation that modulates the spin–rotation coupling constant leading to nuclear relaxation by this mechanism. The characteristic time associated with the spin–rotation component of the total relaxation rate is τ_J, and independent access to this parameter is thus available through measurements of spin–rotation relaxation rates. Although τ_J, as a correlation time, is formally and more generally defined as the time constant describing the rate of fluctuation of angular momentum, in the small-step diffusion region it corresponds with the average collision interval τ_θ/Z.

1. The Hubbard relationship

The angular velocity of a rotating molecule and its angular orientation are clearly not independent of one another. The time features of the small-step diffusion picture are contained in the two time constants discussed above, and Hubbard[21] has shown that they are inversely related to one another by the equation

$$\tau_\theta \cdot \tau_J = I/6kT \tag{12}$$

This relationship is valid only in the diffusion region where $\tau_J \ll \tau_\theta$, but in this region the inverse dependence is readily understood in terms of the model. The "random walk" feature of the process describes the random torque exerted on the molecule at each collision, and as the collision frequency increases, the time required for the molecule to reorient through 1 rad becomes longer. Increasing collision frequency corresponds to decreasing τ_J which occasions increased τ_θ. As for the dependence of τ_θ upon the molecular properties, the rotation becomes more sluggish as I increases and as T decreases, requiring longer time periods to rotate through a fixed angle.

The independent determination of τ_J from spin–rotation relaxation rates requires knowledge of the spin–rotation constant, a parameter which is not readily available for most molecules. Because τ_θ is easily measured in a

number of different ways, it is common practice for rotation in the diffusion region to rely on τ_J values calculated using the Hubbard relationship. While the τ_J values so obtained generally appear to be reasonable, caution should be exercised when drawing extended conclusions. In critical studies of $SnCl_4$ and $PbCl_4$ that involve a test of the Hubbard relationship, Sharp has shown[22,23] that the $\tau_\theta \cdot \tau_J \cdot T$ product is *not* independent of temperature as required by equation (12) and that the τ_J values yielded by the equation are in the range 10^{-14}–10^{-13} s, significantly shorter than can be rationalized on the basis of any reasonable microdynamic process.

2. The χ-test

Diffusion theories assume that the duration of a collision is short relative to the period between collisions, τ_J. When τ_J becomes shorter than the half-period of a typical bending vibration (c. 5×10^{-14} s), then the opposite inequality holds and diffusion-model assumptions no longer hold. It is convenient to have a simple test for determining when a particular rotation can safely be regarded as satisfying the diffusion assumptions, and the χ-test introduced by Wallach and Huntress[11] meets this need. The test is based on a comparison of the observed rotation time τ_θ with the theoretical reorientation time of the free gas molecule, judged to be in the inertial region, at the same temperature.

The period for rotation through one radian of a free gas molecule unhindered by viscous drag is $(3/5)(I/kT)^{1/2}$ s. This also represents the time in which the tensor correlation function for a free spherical rotor decays to $1/e$ of its initial value. The extent to which molecular rotation is hindered by viscous drag is related to a constant χ of the motion representing the ratio of the rotation rates in the gas and in the liquid:

$$\chi = \frac{\tau_\theta}{\tau_{F_R}} = \frac{5\tau_\theta}{3}\left(\frac{kT}{I}\right)^{1/2} \tag{13}$$

In the case of anisotropic rotation, the rotation time for the ith component of the diffusion process is $\tau_i = (1/6)D_i$ and the χ-test can be applied to the individual components using

$$\chi_i = \frac{5}{18\,D_i}\left(\frac{kT}{I}\right)^{1/2} \tag{14}$$

Gillen and Noggle[12] have applied the χ-test to a variety of symmetric top molecules in the liquid state and in the process have established the following more or less arbitrary boundary conditions:

$\chi < 3$,	inertial region;
$3 < \chi < 5$,	intermediate region;
$\chi > 5$,	diffusion region.

By these criteria, $D_\perp$ for $VOCl_3$, CCl_3CN and $CDCl_3$ is in the diffusion region at 300 K, and the other molecules studied reach the diffusion region on cooling to the following temperatures: CD_3CN at 270 K, NH_3 at 260 K, CD_3CCD at 220 K, and BCl_3 at 200 K. For $D_\parallel$, only $VOCl_3$ is in the diffusion region at 300 K, CCl_3CN reaches it on cooling to 240 K, BCl_3 at 215 K, while for $CDCl_3$, CD_3CN and CD_3CCD $D_\parallel$ remains in the inertial region down to 180 K.

C. Models for calculating τ_c

The phenomenological approach to rotational correlation times begins with a relaxation-measured value for τ_c followed by the establishment of its dependence upon the bulk or macroscopic properties of the material undergoing relaxation. This approach has led early[24] and lately[14,17] to the recognition that viscosity and temperature are the determining variables. Molecular rotation in the liquid phase is assumed to be hindered by viscous drag, and gas-phase rotation which is relatively unhindered represents the limiting condition in which the viscous drag approaches zero. According to this picture, τ_c is a linear function of viscosity and the model, illustrated in Fig. 1, is represented by the equation

$$\tau_c = \tau_0 + \eta\tau_{red} \tag{15}$$

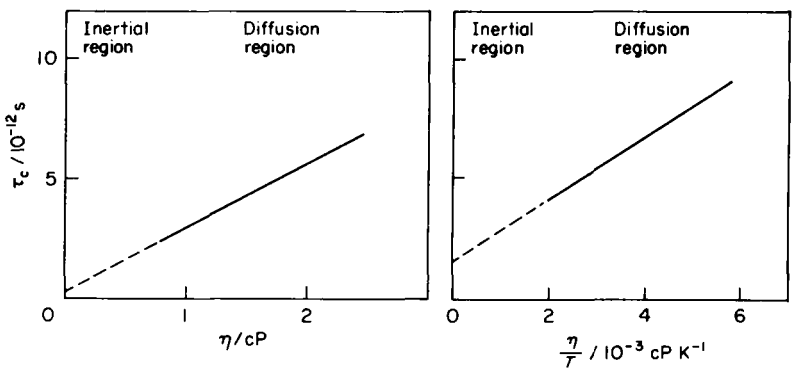

FIG. 1. Viscosity dependence of τ_c. The slope represents τ_{red} in each case.

when viscosity is varied at constant temperature by changing the solvent, or by the equation

$$\tau_c = \tau_0 + \frac{\eta\tau_{red}}{T} \tag{16}$$

when viscosity variation is achieved solely by varying the temperature. In the latter case, the intercept at $\eta/T = 0$ represents an ambiguous condition.[25] If it corresponds to finite viscosity and infinite temperature, then

one expects $\tau_0 = 0$. If it corresponds to zero viscosity and finite temperature then one expects a small but non-zero τ_0 representative of the free rotation time at the unknown temperature. Since most studies yield positive intercepts,[25,17] τ_0 is usually interpreted as a free rotation time and comparisons with $\tau_{FR} = (I/kT)^{1/2}$ are made.

The sequence of models discussed below for describing liquid-phase molecular rotation all treat the motion as a diffusion process and therefore deal only with the viscosity-dependent term in equations (15) and (16). The slopes of the lines in Fig. 1, represented by τ_{red} in equations (15) and (16), are reduced correlation times from which the viscosity dependence has been removed and which therefore depend only upon the size and shape of the molecule. The theoretical models which follow use molecular size and shape as input parameters to calculate a rotational friction coefficient which, when substituted in the appropriate equation from Table V, yields a calculated τ_{red} with which to compare the experimentally determined slope.

The number of studies in which τ_c has been measured over a range of viscosities or temperatures is small. Much more numerous are the compounds for which a single τ_c has been measured. Since these represent the largest body of experimental data available on the subject, the primary objective of this review is to use these data in testing the available theoretical models. Unfortunately, the models all yield values for τ_{red}, not for τ_c, and single datum points do not give the slopes that represent τ_{red}. Two palliatives are available which circumvent, but do not by any means eliminate, this problem. In cases where τ_c exceeds 10 ps, τ_0 as estimated from τ_{FR} may be less than 1 ps, in which case the assumption $\tau_0 = 0$ yields a slope having error limits within $\pm 10\%$. In cases where $\tau_c < 10$ ps, it may be possible using τ_{FR} and chemical intuition to estimate a value for τ_0 which, together with the single datum point, will again yield a slope. Both of these palliatives have been used where necessary to obtain τ_{red} values tabulated in Sections V and VI.

1. *The Stokes–Einstein–Debye (SED) model*

The hydrodynamic basis for determining the rotational friction coefficient, ξ, for a sphere of radius a rotating in a medium of viscosity η is the equation introduced by Stokes[16] in 1856 to describe the resistance to rotation of a macroscopic sphere rotating in a viscous liquid:

$$\xi = \frac{\text{torque}}{\text{Angular momentum}} = 8\,\pi\,a^3\,\eta \tag{17}$$

Einstein[19] subsequently showed that the same relationship can be used to characterize the Brownian motion of micrometre-sized particles, and

Debye[20] extended its application to the molecular level in the description of dielectric relaxation.

In the case of spherical molecules, the rotational diffusion rate is given by

$$D = kT/\xi \tag{18}$$

and in the general case of anisotropic rotation, the individual components of the diagonalized diffusion tensor are given by $D_i = kT/\xi_i$.[26] The rotational correlation governing NMR relaxation is related to D_i by

$$\tau_i = \frac{1}{6D_i} \tag{19}$$

and a spherical molecule obeying classical mechanics exhibits a rotational correlation time, given by

$$\tau_{\mathrm{SED}} = \frac{\xi}{6\,kT} = \frac{V\eta}{kT} \tag{20}$$

where V is the molecular volume determined by the Stokes radius a. For $\eta = 1$ cP, $a = 1$ Å and $T = 300$ K, equation (20) fortuitously gives $\tau_{\mathrm{SED}} =$ 1 ps and using this convenient reference value, the τ_{SED} for any molecule which can be regarded as a sphere is readily obtained in picoseconds from the cube of the Stokes radius in ångstroms. For a molecule such as CCl_4 with $a = 2{\cdot}75$ Å this gives 21 ps, a value roughly 10 times greater than that observed by NMR relaxation.[27] The body of τ_c data which has been built up over the past 15 years all indicate that the rotational correlation time for a molecule in the diffusion region where viscous drag limits the rotation rate is a factor of 5 or 6 shorter than is predicted using the classical SED model. In other words, the rate of rotation is faster than predicted, indicating that the frictional restraint must be lower than that represented by the Stokes coefficient. This discrepancy suggests that the effective viscosity at the surface of a molecule is not well represented by the bulk viscosity η, and Gierer and Wirtz[28] have introduced the idea of a *microviscosity factor* as a dimensionless index applied to the viscosity variable in the SED model.

2. The Gierer–Wirtz (GW) model

The classical view of a perfect sphere rotating in a *continuous* medium characterized by a bulk viscosity is clearly a gross oversimplification of the quantum-mechanical reality of molecular rotation. Where the radius of the molecule is much larger than the radius of the solvent molecules and the ratio $a_s/a \ll 1$, the medium will appear reasonably continuous to the rotating molecule and classical behaviour is likely to be approached. Where the solvent radius approaches or exceeds that of the rotating molecule, the medium will appear discrete, reducing the effective contact at the rotating

surface and occasioning an apparent reduction in viscosity. Gierer and Wirtz[28] have introduced an elaboration to the SED model whereby all of the discrepancy between observed and calculated τ_c values is contained in a rotational *microviscosity* correction factor f whose radius ratio dependence is given by

$$f = [6(a_s/a) + (1 + a_s/a)^{-3}]^{-1} \tag{21}$$

The functional dependence of f upon a_s/a is given in Table II: (i) where the solvent molecule is very small or the solute molecule is very large, little correction is introduced; (ii) for neat liquids where $a_s/a = 1$, the correction factor is $0{\cdot}16 \simeq 1/6$, a value that is observed experimentally in a surprisingly large number of instances; and (iii) where the solvent molecule is very large or the solute molecule is very small, the solute molecules "rattle" in the interstices between solvent molecules and the frictional resistance to rotation is very small.

TABLE II

Microviscosity factor dependence upon solute/solvent radius ratio.

a_s/a	=	0·01	0·1	0·5	0·7	1·0	2·0	10
f	=	0·97	0·74	0·30	0·23	0·16	0·08	0·02

Subsequent authors writing about the boundary conditions for the rotational friction coefficient adopt the "slip" and "stick" terminology, and it is useful to recognize that the $a_s/a \ll 1$ limit corresponds to their "slip" boundary condition in which the rotating molecule slips through the solvent with $\xi = 0$ provided that the rotation can occur without solvent displacement. The $a_s/a \ll 1$ limit (classical behaviour) corresponds to the "stick" boundary condition where the solvent at the surface of the rotating molecule has the same velocity as the surface and $\xi = 8\pi\eta a^3$. Using slip/stick terminology, the $a_s/a = 1$ condition, where the microviscosity factor has the value $f = 0{\cdot}16$, represents a friction coefficient with 16% of the stick value.

3. *The Hu–Zwanzig (HZ) model*

For molecules that can be regarded as spherical, the Gierer and Wirtz elaboration adjusts the classical model to accommodate the observation that molecular rotational friction coefficients are less than the Stokes value of $8\pi\eta a^3$ and for neat liquids lie closer to the slip rather than the stick boundary condition. Many of the molecules with which chemists are vitally concerned are not spherical; they can, however, be regarded as prolate (cigar-shaped; $a = b < c$) or oblate (pancake-shaped; $a < b = c$) spheroids whose rotational motion is thus anisotropic. While the microviscosity

approach is adequate for describing rotation *about* the symmetry axis, rotation *of* the symmetry axis requires displacement of solvent molecules, thereby introducing viscous drag even in the slip limit. Hu and Zwanzig[15] have calculated the magnitude of the rotational friction coefficient for the slipping boundary limit for both prolate and oblate spheroids over a range of a/c values. These provide rotational correlation times in good agreement with those obtained from NMR (±40%) relaxation measurements on a number of prolate and oblate examples. Again the τ_c value is significantly shorter than the τ_{SED} classical value calculated for a sphere of radius equal to the longer semi-axis of the spheroid, indicating that the effective friction coefficient is smaller than $8\pi\eta(\max)^3$. As was done for the Gierer and Wirtz adjustment, this correction can also be represented as a viscosity adjustment and in Table III are listed the friction coefficients calculated by Hu and Zwanzig for the slip boundary condition, and the microviscosity factors $f_{HZ(slip)}$ to which they give rise. The corresponding $f_{HZ(stick)}$ factors are provided for comparison. Rotational correlation times τ_{HZ} predicted according to this model are obtained by substituting the appropriate values from Table III into the appropriate equation in Table V.

Several features of the data in Table III are worthy of note. In the slip boundary limit, the only frictional resistance to rotation results from solvent displacement, and for a sphere this is zero. Since oblate spheroids displace more solvent on rotation than do prolate spheroids, the oblate values are

TABLE III

Rotational friction coefficients and microviscosity factors for prolate and oblate spheroids.[15]

	Prolate			Oblate		
ρ [a]	ξ^*_{slip} [b]	f_{slip}	f_{stick}	ξ^*_{slip} [b]	f_{slip}	f_{stick}
1·00	0·0	0·0	1·00	0·0	0·0	1·00
0·90	0·0468	0·0059	0·84	0·0505	0·0063	0·88
0·80	0·169	0·021	0·68	0·199	0·025	0·79
0·70	0·341	0·043	0·57	0·441	0·055	0·70
0·60	0·534	0·067	0·46	0·771	0·096	0·62
0·50	0·723	0·090	0·38	1·18	0·15	0·58
0·40	0·880	0·11	0·31	1·66	0·21	0·52
0·30	0·976	0·12	0·24	2·18	0·27	0·47
0·25	0·991	0·12	0·21	2·45	0·31	0·46
0·20	0·980	0·12	0·18	2·71	0·34	0·45
0·10	0·853	0·11	0·14	3·16	0·40	0·44
0·05	0·715	0·089	0·10	3·32	0·42	0·43
0·01	0·503	0·063	0·07	3·39	0·42	0·42

[a] ρ = min. axis/max. axis.
[b] Dimensionless $\xi^* = \xi/\pi\eta(\max)^3$ values tabulated.

all higher than the corresponding prolate ones. As an oblate spheroid becomes flatter, its friction coefficient becomes uniformly greater, consistent with the greater volume of solvent displaced on rotation. For prolate spheroids, however, the friction coefficient increases with increasing departures from sphericity up to a (max)/(min) ratio of 4, beyond which, as the molecule becomes more needle-like, the friction coefficient diminishes.

The Hu–Zwanzig elaboration has been tested with both prolate and oblate examples, and agreement with the experimental values has been gratifying. Vold *et al.*[25] have measured the ^{33}S relaxation in CS_2 over a range of temperature and obtain a linear η/T plot for τ_c. The 1 cP, 300 K value is 2·1 ps, this value being calculated for a prolate spheroid with semi-axes of 3·25 and 1·70 Å. Bauer *et al.*[29] observe for benzene a value of 3·5 ps compared with a calculated 5·0 ps, and for larger oblate examples they obtain even better observed (calculated) agreement with 9·5 ps (10·3 ps) for hexafluorobenzene and 10·6 ps (11·3 ps) for mesitylene. For triphenylene in a range of solvents, Wasylishen *et al.*[17] obtain an average $\tau_{red} = 21$ ps as compared with the value of 46 ps calculated for an oblate spheroid of "radius" 5·8 Å.

4. *The Youngren–Acrivos (YA) model*

Youngren and Acrivos[18] have extended the HZ model to the more general case of ellipsoidal molecules in which all three axes have different lengths. Using the same slip boundary condition as in the HZ model, they have calculated three friction coefficients for each axis ratio and their data are reproduced in Table IV. The authors demonstrate the superiority of their model by obtaining observed (calculated) agreement of 3·5 ps (3·8 ps) for τ_{red} of benzene,[18] as compared with the 3·5 ps (5·1 ps) agreement obtained by Bauer *et al.*[29] using the HZ model.

Because both Hu and Zwanzig[15] and Youngren and Acrivos[18] tabulate their friction coefficients as dimensionless indices multiplied by a (volume × viscosity) factor, some controversy among subsequent workers has arisen[31] because the volume factor used by HZ is the *volume of the smallest sphere* that will contain the spheroidal molecule, while that used by YA is the *actual volume* of the ellipsoidal molecule. The latter will always be smaller than the former. Thus, although the numerical indices for spheroidal cases which appear in the YA tabulation are virtually identical with those in the HZ tabulation, the YA *friction coefficients* are in fact *lower* than the others.

Several workers,[30,32] by using the YA index λ_i in an equation of the form

$$\tau_{red} = \lambda_i V_w / 8\,\rho_1 \rho_2\, kT \tag{22}$$

where ρ_1 and ρ_2 are the axis ratios a/c and b/c respectively ($a \leq b \leq c$) and V_w is the actual volume of the ellipsoid, have systematically increased the YA friction coefficients, bringing them into coincidence with those

calculated by Hu and Zwanzig. In order to maintain consistency with the interpretation given by subsequent workers to the YA λ_i indices, all correlation times which we have calculated using the YA model have been done in accordance with equation (22).

The YA model promises considerable improvement in calculated τ_c values for molecules of complex shape. Testing of the results, however, requires the experimental determination of three independent correlation times for reorientation about each of the *a*, *b*, *c*, axes of the molecule. To date, only a limited number of relaxation studies have been conducted at this level of sophistication.

TABLE IV

Rotational friction coefficients for ellipsoids.[18]

	ρ_1								
ρ_2	1·0	0·9	0·8	0·7	0·6	0·5	0·4	0·3	0·2
1·0	$\lambda_a = 0$	0·00	0·00	0·00	0·00	0·00	0·00	0·00	0·00
	$\lambda_b = 0$	0·05	0·20	0·44	0·77	1·18	1·67	2·18	2·70
	$\lambda_c = 0$	0·05	0·20	0·44	0·77	1·18	1·67	2·18	2·70
0·9	0·05	0·00	0·04	0·04	0·04	0·04	0·03	0·03	0·03
	0·05	0·05	0·19	0·41	0·71	1·08	1·53	2·00	2·49
	0·00	0·05	0·05	0·19	0·41	0·73	1·16	1·60	2·05
0·8	0·20	0·05	0·00	0·16	0·15	0·14	0·12	0·10	0·08
	0·20	0·19	0·17	0·38	0·65	0·99	1·39	1·82	2·28
	0·00	0·04	0·17	0·05	0·18	0·40	0·72	1·10	1·50
0·7	0·44	0·19	0·05	0·00	0·32	0·29	0·25	0·21	0·17
	0·44	0·41	0·38	0·35	0·60	0·91	1·26	1·65	2·06
	0·00	0·04	0·16	0·35	0·05	0·17	0·39	0·69	1·03
0·6	0·77	0·41	0·18	0·05	0·00	0·50	0·45	0·38	0·30
	0·77	0·71	0·65	0·60	0·54	0·83	1·13	1·49	1·86
	0·00	0·04	0·15	0·32	0·54	0·04	0·17	0·38	0·66
0·5	1·18	0·73	0·40	0·17	0·04	0·00	0·66	0·56	0·46
	1·18	1·08	0·99	0·91	0·83	0·75	1·01	1·32	1·64
	0·00	0·04	0·14	0·29	0·50	0·75	0·04	0·17	0·36
0·4	1·67	1·16	0·72	0·39	0·17	0·04	0·00	0·77	0·63
	1·67	1·53	1·39	1·26	1·13	1·01	0·89	1·15	1·43
	0·00	0·03	0·12	0·25	0·45	0·66	0·89	0·04	0·16
0·3	2·18	1·60	1·10	0·69	0·38	0·17	0·04	0·00	0·80
	2·18	2·00	1·82	1·65	1·49	1·32	1·15	0·98	1·22
	0·00	0·03	0·10	0·21	0·38	0·56	0·77	0·98	0·04
0·2	2·70	2·05	1·50	1·03	0·66	0·36	0·16	0·04	0·00
	2·70	2·49	2·28	2·06	1·86	1·64	1·43	1·22	0·99
	0·00	0·03	0·08	0·17	0·30	0·46	0·63	0·80	0·99

TABLE V

Theoretical models for rotational friction coefficients and the derived rotational correlation times.

Model	Rotational correlation time		τ_{red} at 300 K/ps cP^{-1} [a]
Classical	Rotational friction coefficient (sphere) $= \frac{\text{Torque}}{\text{Angular momentum}}$		
		$= \xi_{stick} = 8\pi a^3 \eta$	
Stokes–Einstein–Debye	$\tau_{SED} = \frac{\xi_{stick}}{6kT}$	$= \frac{V_{sphere}\eta}{kT}$	$\tau^*_{SED} = 0{\cdot}242\ V_w$
Gierer–Wirtz	$\tau_{GW} = \frac{f_{GW}\xi_{stick}}{6\,kT}$	$= \frac{f_{GW}V_{sphere}\eta}{kT}$	$\tau^*_{GW} = 0{\cdot}242\, f_{GW} V_w$
Hu–Zwanzig	$\tau_{HZ} = \frac{\xi^*\pi a^3_{max}\eta}{6\,kT}$	$= \frac{\xi^* V_{sphere}\,\eta}{8\,kT}$	$\tau^*_{prolate} = \frac{0{\cdot}0302\xi^* V_w}{\rho^2}$
			$\tau^*_{oblate} = \frac{0{\cdot}0302\xi^* V_w}{\rho}$
Youngren–Acrivos	τ_{YA}	$= \frac{\lambda_i V_{ellipsoid}\eta}{6\,kT}$	$\tau_i^* = \frac{0{\cdot}0302\lambda_i V_w}{\rho_1\rho_2}$

[a] V_w calculated in Å^3 by atomic increment method.[70]

III. THE ENSEMBLE PROPERTY OF ROTATIONAL CORRELATION

The subject matter of Section II has been restricted to the rotational properties that can be ascribed to a single molecule. In particular, the time constants τ_θ and τ_J have been interpreted as the period for 1 rad rotation and the average intercollision period, respectively. Nuclear relaxation, however, is a co-operative phenomenon which must necessarily be described using parameters characteristic of a molecular ensemble. The temporal characteristics of an ensemble are described by the time periods in which various properties remain *correlated* in the face of ceaseless, random particle motions which cause the rapid decay of any particular, instantaneous arrangement perceived using a "fast shutter" spectroscopic technique. These characteristic time periods are referred to as *correlation times*, and their definition as ensemble parameters is presented below.

The rotational correlation time that one measures in a nuclear magnetic relaxation experiment is an ensemble property which, when used in a precise sense, has validity only with respect to the ensemble. A particular τ value so regarded cannot be used to characterize the motion of a single molecule. There is, however, a rough correspondence between the τ_θ and

τ_J parameters measured as ensemble time constants, and the single molecule τ_θ and τ_J parameters defined in Section II as properties of the ensemble constituents. Since most chemists who measure relaxation times are motivated by a desire to characterize molecules rather than ensembles, rotational correlation time interpretations are generally discussed in terms of single molecule properties such as size, shape and intermolecular bonding characteristics. Throughout this review we will conform with practice in the current NMR literature and regard single molecule time constants as equivalent to ensemble time constants. In doing so, however, it must be borne in mind that the time period in which the "average" molecule rotates through 1 rad may not be precisely the same as the time period in which the angular correlation function decays to 1/e of its initial value.[33]

A. The correlation function in the time domain

Bloembergen,[5,24] in his classic study on nuclear magnetic relaxation, first showed that the energy transfer essential to relaxation will occur if the position vectors $\vec{r}_{ij}$ which determine the instantaneous magnetic dipolar or electric quadrupolar coupling of the ith nucleus with its surroundings are functions of time. In a liquid, the functions of the nuclear position coordinates which contain this time dependence, $F(t)$, vary with time in a random fashion as the molecules containing the magnetic nuclei execute their Brownian motions. While the random nature of the motion is reduced to zero, the value of $F(t)$, being a measure of magnetic or electric coupling, is non-zero, and it is the *differences* between $F(t)$ values over short intervals of time τ that are characterized by the *correlation function* of $F(t)$:

$$F(t)\cdot F^*(t+\tau)=k(\tau) \tag{23}$$

This function represents the decay in correlation as the time interval τ becomes longer. For small τ, F^* at $(t+\tau)$ is highly correlated with the initial value of F, while for large τ, F and F^* are independent variables which are not correlated.

For the molecular processes that presently concern us, $k(\tau)$ takes the form

$$k(\tau)=\overline{F(t)\,F^*(t+\tau)}\times e^{-\tau/\tau_c} \tag{24}$$

In general, $k(\tau)$ is a function that goes rapidly to zero when τ exceeds a characteristic value τ_c known as the *correlation time*. This equation thus defines τ_c for the ensemble as the length of time required by the kT randomizing force to reduce $F(t)$ to 1/e or 37% of its initial value. Since the independent variable in this equation is time, the exponentially decaying curve one obtains by plotting $k(\tau)$ against τ is known as the correlation function in the *time domain*.

It is a magnetic field fluctuating at the Larmor frequency that promotes relaxation, and in order to recognize the frequencies hidden within the continuously decaying $k(\tau)$ function, it is subjected to a mathematical device known as a Fourier transformation which converts it from a time function into a frequency function.

B. The spectral density and the frequency domain

The randomizing force driving the rotational and translational motion of the molecules brings about the exponential reduction in the correlation function with time and for the rotational contribution we can readily perceive that there will be *frequencies* associated with the cyclical nature of rotations. Less readily perceived are the frequencies associated with translations, but a Fourier transformation of the correlation function

$$J(\omega) = \int_{-\infty}^{+\infty} k(\tau)\, e^{i\omega\tau}\, d\tau \tag{25}$$

casts it into the *frequency domain* and yields a spectrum of frequencies in which the value of $J(\omega)$ at each frequency is known as the *spectral density*. The intensity of the fluctuation in $F(t)$ at a particular frequency is obtained by substituting (24) into (25) and yields

$$J(\omega) = \overline{2\, F(t)\, F^*(t)} \times \frac{\tau_c}{1 + (\omega\tau_c)^2} \tag{26}$$

The independent variable ω in this equation is the label designating the individual frequency components of the Fourier spectrum. These frequencies modulate the approach to zero of $F(t)$ the $F^*(t)$ and provide an oscillating magnetic field at the ith nucleus, one component of which has the Larmor frequency and makes a contribution to the relaxation proportional to its spectral density $J(\omega_0)$.

A representation of equation (26) in the frequency domain is obtained by plotting $J(\omega)$ against ω for an ensemble with a particular τ_c. Figure 2 contains these plots for ensembles having three different correlation times. The three curves are normalized to equal kinetic energy in each ensemble by maintaining equal areas under each curve. This has the effect of raising the height of the low frequency plateau as the horizontal extension of the curve is reduced through selecting ensembles with progressively longer τ_c. The character of each Fourier spectrum is such that the intensity of the individual frequency components remains constant for low frequencies below τ_c^{-1}, falling off rapidly to zero at high frequencies. The half-intensity point on each curve occurs for that component whose frequency is τ_c^{-1} and Fig. 2 shows that for the ω_0 frequency component that promotes relaxation, $J(\omega_0)$ is maximized in that ensemble whose $\tau_c = \omega_0^{-1}$. Curve B

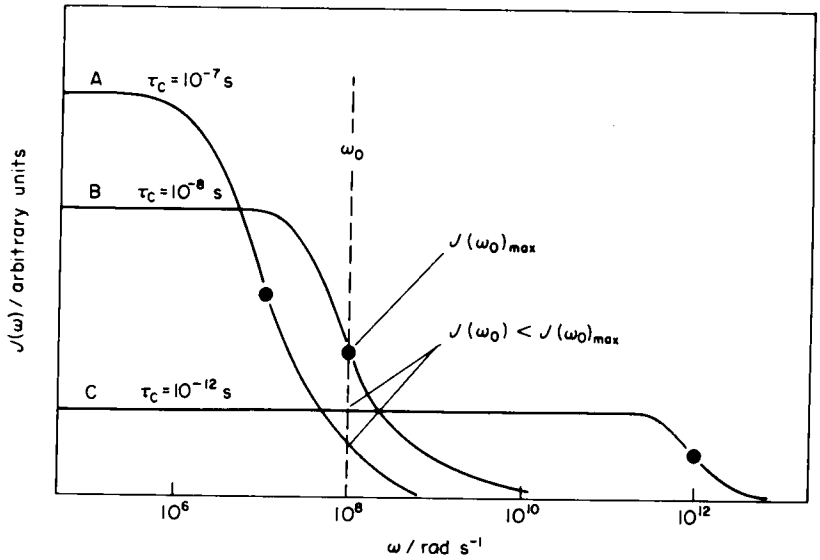

FIG. 2. Fourier spectra in the frequency domain for molecular ensembles with different correlation times.

represents the ensemble with $\tau_c = 10^{-8}$ s. If the nucleus undergoing relaxation in this ensemble has a Larmor frequency $\omega_0 = 10^8$ rad s^{-1}, then the spectral density at this frequency is that designated $J(\omega_0)_{max}$ in Fig. 2. Curves A and C representing ensembles having τ_c values longer and shorter, respectively, than that represented by curve B both have spectral densities at ω_0 which are less than $J(\omega_0)_{max}$, as shown. While the spectral density for ensemble B will be higher than $J(\omega_0)_{max}$ at frequencies lower than ω_0, the resonance nature of the phenomenon makes these higher intensities less effective at promoting relaxation.

An alternative representation of equation (26) is the familiar Lorentz curve shown in Fig. 3. Here the intensity of the ω_0 frequency component is plotted as a function of τ_c for the ensemble, and again we see that spectral density at the Larmor frequency is maximized when τ_c for the ensemble coincides with ω_0^{-1}. Correlation times above and below this value are both less effective. Since τ_c in the picosecond range is much shorter than the shortest Larmor period ω^{-1} experimentally achievable, changes such as viscosity increases and temperature decreases which lengthen τ_c for the ensemble will increase the intensity of that spectral component with frequency ω_0, increasing the relaxation rate and broadening the spectral line.

In summary, we have seen how the random Brownian motion of molecules can generate a fluctuating magnetic field with specific frequency

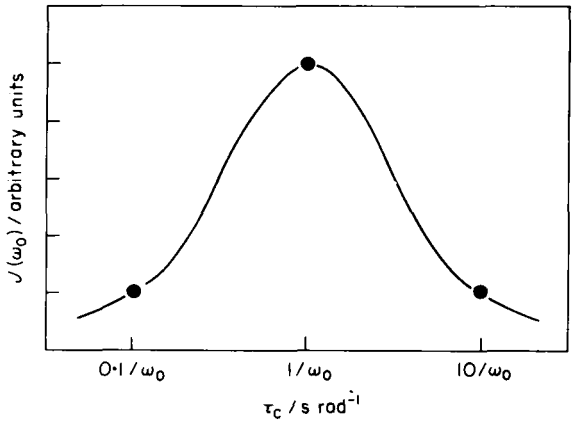

FIG. 3. Spectral density of the ω_0 Fourier component for ensembles with different τ_c.

components, and how the spectral density of these components is related to τ_c for the particular ensemble. It is now time to see how τ_c affects the relaxation rate achieved by each of the five mechanisms under consideration.

IV. RELAXATION INTERACTIONS MODULATED BY MOLECULAR ROTATION

The classical or phenomenological view of an NMR experiment pictures an ensemble of identical nuclei precessing randomly about the external field direction such that the macroscopic magnetization vector given by the ensemble vector sum lies coincident with the direction of the external magnetic field. Application of an r.f. field that satisfies the resonance condition introduces phase coherence to the Larmor precession cone and tilts the magnetization vector away from the external field, giving it a transverse component. Following removal of the r.f. field, the transverse component decays to zero according to a first-order rate law as the magnetization vector reassumes coincidence with the external field. The process is designated transverse relaxation and characterized by a rate constant $R_2 = 1/T_2$, where T_2 is known as the transverse relaxation time. Thermodynamically, the process represents a redistribution of energy within the ensemble and for this reason T_2 is also referred to as the spin–spin relaxation time. In those situations, particularly solids, where molecular reorientation is restricted, the transfer of energy from the ensemble to its surroundings (the "lattice") is characterized by another first-order rate constant R_1 which for restricted rotation is less than R_2. Under these circumstances it is possible to measure independently a spin–lattice or longitudinal relaxation

time T_1. In the region of rapid molecular motion, provided that τ_c is shorter than the reciprocal of the r.f. frequency, ω_0^{-1}, R_1 and R_2 become equal and remain equal as τ_c becomes shorter.[24] For operating frequencies of 100 MHz and less, R_1 remains equal to R_2 for rotational correlation times up to about 1500 ps. This is an order of magnitude greater than the τ_c values encountered in this review, and for this reason R_1 and R_2, and their corresponding relaxation times T_1 and T_2, have not been differentiated with a subscript. Molecular behaviour in which $R_1 = R_2$ lies within the region of "motional narrowing" where an increase in either ω_0 or the rate of molecular rotation causes narrowing of the resonance line width.

In the liquid phase, relaxation rates as slow as $10^{-2}\,s^{-1}$ and as fast as $10^7\,s^{-1}$ are encountered. Five independent mechanisms may contribute to the total relaxation process and the relaxation rate for a particular nucleus in a specific chemical environment will depend upon which mechanisms contribute and the effectiveness of each. The quadrupole mechanism is four or five orders of magnitude more effective than any of the others in promoting relaxation, and where present it accounts for essentially all of the relaxation. For this reason, the problem of estimating the relative importance of the other mechanisms only arises with spin $I = 1/2$ nuclei and those $I > 1/2$ nuclei whose quadrupole moments are extremely small, e.g. ^{6}Li,[34] as given in Table VI.

Each of the five mechanisms is discussed, taken in diminishing order of potential capability for contributing to relaxation. It is seen that each of the relaxation rate equations contains three factors: (i) a numerical constant

TABLE VI

Constants and molecular parameters determining relaxation rates for quadrupolar nuclei.

Nucleus	I	$Q/10^{-28}\,m^2$	$\left(\frac{3\pi^2}{10}\right)\frac{2I+3}{I^2(2I-1)}$	Max NQCC/MHz	Max R^Q for $\tau_c =$ 10 ps/s^{-1}	Min. T/ms
^{2}H	1	2.7×10^{-3}	14·8	0·24	8	100
^{6}Li	1	$4{\cdot}6\times10^{-4}$	14·8			
^{9}Be	3/2	$5{\cdot}2\times10^{-2}$	3·95	0·35	5	200
^{11}B	3/2	$3{\cdot}6\times10^{-2}$	3·95	3·0	360	3
^{14}N	1	$1{\cdot}6\times10^{-2}$	14·8	6·0	5300	0·2
^{17}O	5/2	$-2{\cdot}6\times10^{-2}$	0·947	14·0	2000	0·5
^{23}Na	3/2	0·14	3·95	2·1	175	5
^{25}Mg	5/2	0·22	0·947			
^{27}Al	5/2	0·15	0·947			
^{33}S	3/2	$-6{\cdot}4\times10^{-2}$	3·95	15	9000	0·1
^{35}Cl	3/2	$-7{\cdot}9\times10^{-2}$	3·95	150	9×10^5	1×10^{-3}

which contains the spin number I of the relaxing nucleus; (ii) an interaction constant with dimensions of (frequency)^2 which designates the degree to which the relaxing nucleus is coupled to its surroundings by the mechanism in question; and (iii) a rotational correlation time τ_c which describes the frequency components of the coupling modulation produced by molecular rotation. The focus of the discussion is the evaluation of τ_c from an experimentally determined R in cases where the coupling constant is independently available. With reliable τ_c data for a variety of molecules at hand, several models for the semi-empirical calculation of τ_c are tested to ascertain the reliability of calculated τ_c values. With uncertainty limits of ±25% or better, the use of relaxation measurements to determine coupling constants for systems where they are not independently available becomes a real possibility. Of particular significance is the fact that in each relaxation equation, the coupling constant occurs as a squared term, while τ_c occurs to the first power. As a consequence the uncertainty in the coupling constant evaluated using an independently evaluated τ_c is the square root of the uncertainty in τ_c.

A. The quadrupole (Q) mechanism

Coupling between a nuclear electric quadrupole moment and an electric field gradient generated by the molecular environment in which the nucleus is situated can provide the most effective route to relaxation wherein the spin system dissipates energy to the lattice. For nuclei such as ^{181}Ta with large quadrupole moments of around 3×10^{-28} m^2, quadrupole relaxation limits the lifetime of the excited state to such an extent that uncertainty broadening makes the NMR signal unobservable even in highly symmetric environments having minimum electric field gradients.[35] The general expression for the rate of quadrupole relaxation is given by

$$R^Q=\frac{1}{T^Q}=\frac{3\pi^2}{10}\times\frac{2I+3}{I^2(2I-1)}\times\chi^2\cdot\left(1+\frac{\eta^2}{3}\right)\tau_c \tag{27}$$

where $\chi=e^2qQ/h$, which is the nuclear quadrupole coupling constant (NQCC).

The numerical coefficient which contains the spin factor varies from 14·8 to 0·112 with variation in spin number I; the values for particular nuclei are given in Table VI. Some authors,[23,36,37] by incorporating $\hbar$ rather than h into the denominator, express χ in radians per second rather than the customary hertz. In these instances, the NQCC is numerically greater by a factor of 2π, and the numerical coefficient must be reduced in compensation by the factor $(2\pi)^{-2}$.

The NQCC can be evaluated on solids by NQR spectroscopy and in the gas phase by molecular beam methods, and where a reliable NQCC value

is available, the measured relaxation rate can be used to determine τ_c. The NQCC is a tensor property, and the extent to which it departs from cylindrical symmetry is described by the asymmetry parameter η. Reference 38 contains a large list of asymmetry parameters for ^{14}N NQCCs in a wide variety of molecules, and shows that in most cases $\eta < 0.2$. Since $\eta = 0.2$ affects R by just over 1%, the asymmetry correction is customarily ignored unless the molecular structure suggests that $\eta > 0.2$.

The ranges of NQCCs observed for quadrupolar nuclei in typical covalently bonded environments are given in Table VI. When combined with a representative τ_c of 10 ps, they yield maximum quadrupolar relaxation rates up to $10^6\ s^{-1}$ for ^{35}Cl; for ^2H, with its lower quadrupole moment, the maximum rate is about $10\ s^{-1}$. This is still an order of magnitude greater than the fastest relaxation achievable by the dipole–dipole mechanism and two orders of magnitude faster than can be achieved through chemical shielding anisotropy. Only the spin–rotation mechanism, which in favourable cases can achieve rates of $10^2\ s^{-1}$, can compete with the quadrupolar mechanism, and then only in those instances where the NQCC is less than about 3 MHz, either because of a low quadrupole moment or a low electric field gradient. In all other cases, the quadrupole mechanism dominates to such an extent that the contribution from any other mechanism is immeasurably small.

B. The spin–rotation (SR) mechanism

Molecules in which the electric charge distribution is not spherically symmetric possess a *molecular* magnetic moment under rotation of this asymmetric charge distribution. The interaction between a nuclear magnetic moment and the molecular magnetic field produced at the position of the nucleus is designated the spin–rotation coupling constant, C, and is measured in hertz. Modulation of this interaction by changes in the *rate* of molecular rotation causes nuclear magnetic relaxation at a rate[39] given by

$$R^{SR} = \frac{1}{T^{SR}} = \frac{2IkT}{\hbar^2} \times C^2 \times \tau_J \tag{28}$$

Unlike the time constants appearing in the relaxation rate equations for the other mechanisms, the correlation time τ_J in equation (28) refers to changes in the magnitude of the molecular angular momentum vector rather than to changes in the orientation of the molecule that are characterized by τ_θ. The spin–rotation relaxation rate thus provides access to an independent correlation time and only where the Hubbard relationship (equation (12)) is applicable can it be used to measure or corroborate τ_θ.

The coupling constant, C, is a tensor property of the molecule and in the anisotropic case of a symmetric top, the diagonalized tensor has $C_\perp$

and $C_{\parallel}$ components. Relaxation time measurements give the r.m.s. value $(\overline{C^2})^{1/2}$ of this tensor while molecular beam and magnetic shielding determinations yield $C_{av} = (2C_{\perp} + C_{\parallel})/3$. These are related by

$$\overline{C^2} = C_{av}{}^2 + \tfrac{2}{9}(C_{\perp} - C_{\parallel})^2 \tag{29}$$

and $\overline{C^2} \geqslant C_{av}{}^2$, depending upon the degree of anisotropy.[40] Only where $C_{\perp}$ and $C_{\parallel}$ are of opposite sign do C_{av} and $(\overline{C^2})^{1/2}$ differ by more than about 30%.

For a given temperature, rapid molecular rotation occurs about axes relative to which I is small, and large spin–rotation constants occur for small molecules with low moments of inertia. Typical values for C_{av} range from 0·5 kHz for CCl_4 to 116 kHz for PH_3, while individual component values for C can run as high as 150 kHz for rotations in which only hydrogen atoms move.[40–42]

At room temperature (300 K) and in the diffusion region where the Hubbard relationship $\tau_\theta \tau_J = I/6kT$ holds,

$$R^{SR} = \frac{2I^2}{6\hbar^2} C^2 \frac{1}{\tau_\theta} \tag{30}$$

and the maximum spin–rotation relaxation rates possible occur around $5\ s^{-1}$ for molecular parameters $I \simeq 160 \times 10^{-40}$ g cm^2; $C \simeq 140$ kHz; $\tau_\theta \simeq$ 0·5 ps. A value in this range has been observed[13] for ^{19}F relaxation in ClO_3F. This room temperature R^{SR} is unusually high because the low, 0·18 cP viscosity results in a very short τ_θ for a molecule of this size. A more typical maximum is the $R^{SR} = 0{\cdot}9^{-1}$ rate observed[42] for the ^{199}Hg relaxation in Me_2Hg ($I_{av} = 164 \times 10^{-40}$ g cm^2; $C_{av} = 97$ kHz; $\tau_\theta = 6{\cdot}7$ ps; viscosity = 1·0 cP). Because a rough inverse proportionality exists between I and C, a search for higher R^{SR} rates by seeking out molecules having larger I or larger C is unlikely to be successful. Higher values for R^{SR} can be achieved, but only at elevated temperatures, as reflected in equation (28).

1. *Absolute shielding scales from spin–rotation constants*

The non-spherical part of the electric charge distribution in a molecule which generates the molecular magnetic moment also generates that portion of the nuclear shielding designated by the second-order paramagnetic term, σ_p, in Ramsay's[43] general screening equation,

$$\sigma = \sigma_d + \sigma_p \tag{31}$$

Using Flygare's "atom in a molecule" approximation,[44] the proportionality between σ_p and the $C.I$ product takes the form

$$\sigma_p = \left(\frac{\mu_0 e^2}{8\pi m_e}\right)\left(\frac{\pi}{m_p \mu_n \gamma}\right) C.I \tag{32}$$

for molecules with cubic symmetry in which both the spin–rotation constant and the moment of inertia are scalars; for symmetric top molecules, in which these molecular parameters are tensors, the relationship is

$$\sigma_p = \left(\frac{\mu_0 e^2}{8\pi m_e}\right)\left(\frac{\pi}{m_p \mu_n \gamma}\right)\tfrac{1}{3}(2C_\perp I_\perp + C_\parallel I_\parallel) \tag{33}$$

Agreement between C values determined experimentally from molecular beam measurements and those calculated from σ_p using equations (32) and (33) is within 5%.[45] Extensive use of this correlation has been made to establish absolute nuclear shielding scales for ^{31}P,[45,46] ^{19}F,[45] ^{119}Sn,[23] ^{207}Pb[22] and ^{199}Hg.[42] A plot of chemical shift, δ_{ref}, relative to an arbitrarily chosen reference versus the $C.I$ product for a series of compounds containing the same spin 1/2 nucleus gives the straight line

$$\delta_{ref} = \left(\frac{5{\cdot}23 \times 10^{34}}{\gamma}\right) C.I + \sigma_d \tag{34}$$

where γ is the nuclear magnetogyric ratio in radians per tesla per second. The intercept on the δ_{ref} axis where $\sigma_p = 0$ gives the absolute value of σ_d representing the extent to which the bare nucleus is shielded by the spherically disposed electronic charge. The resonance frequency for the bare nucleus can then be determined from a calculated listing of atomic σ_d values provided by Dickenson,[47] Ramsey[48] or Malli,[49] and the bare nucleus can be used as a shielding reference if so desired. Since there are few molecular beam determinations of spin–rotation constants, more reliable τ_J values emerging from this review in conjunction with spin–rotation relaxation rates and equation (28) will provide spin–rotation constants for the establishment of absolute shielding scales.

C. The dipole–dipole (DD) mechanism

The magnetic coupling between a relaxing nucleus and the other magnetic nuclei in the same molecule provides another interaction whose modulation by molecular rotation causes relaxation. Where the coupling is between identical isotopes, the relaxation rate[39] is given by

$$R^{DD} = \frac{1}{T^{DD}} = \frac{\mu_0{}^2 \gamma_I{}^4 \hbar^2 I(I+1)\tau_c}{8\pi^2 r^6} \tag{35}$$

in which I is the spin number of the nucleus and r is the dipole–dipole separation. Where the coupling is between different isotopes, the relaxation rate[39] is given by

$$R^{DD} = \frac{1}{T^{DD}} = \frac{\mu_0{}^2 \gamma_I{}^2 \gamma_S{}^2 \hbar^2 S(S+1)\tau_c}{12\pi^2 r_6} \tag{36}$$

in which S is the spin number of the other nucleus. A comparison of equations (35) and (36) reveals that, even after variations in γ and spin number have been accounted for, coupling between like spins is more effective in promoting relaxation than coupling between unlike spins. Abragam[39] has dubbed this "the 3/2 effect" because of the ratio $R^{DD}_{like}/R^{DD}_{unlike} = 3/2$.

The r^{-6} dependence of the dipolar relaxation rate makes this an effective mechanism only when the two dipoles are in close proximity, and in operational terms this means about 2 Å or less. A number of consequences limiting the incidence of dipole–dipole relaxation follow from the 2 Å distance:

(i) Only *intra*molecular couplings to directly bonded atoms are generally effective. *Inter*molecular couplings are significant only in the special cases of dissolved paramagnetic impurities and solvent protons in van der Waals contact with other protons. In both these cases, translational motion mediates the coupling and a different relaxation equation containing a translational correlation time governs.

(ii) The larger the covalent radius of the target atom, the less effective is the dipolar mechanism and beyond the first row of the periodic table the dipolar contribution to the total relaxation rate is small. Comparing ^{29}Si and ^{13}C, their radius ratio raised to the sixth power is a factor of 13.

(iii) Compared with the hydrogen covalent radius of 0·37 Å, all other bonded atoms have covalent radii that put the bond length outside the 2 Å limit and make their dipolar contribution to the relaxation minimal.

The ^{13}C atom to which protons are covalently bonded provides the most favourable case for dipolar relaxation, and examples of relaxation rates in the range $0{\cdot}1 \simeq 1{\cdot}0\ s^{-1}$ have been observed. Since the rate of quadrupolar relaxation, where present, is several orders of magnitude greater than this, the dipolar mechanism makes a significant contribution to the total relaxation process only for $I = 1/2$ nuclei which have no quadrupole moment. In addition, the atom to which the $I = 1/2$ nucleus is bonded must have a non-zero magnetic moment, and in this context it must be recalled that fewer than 2% of all carbon and oxygen atoms have a nuclear magnetic moment. For purposes of studying dipolar relaxation in molecules having a variety of shapes and sizes, ^{13}C and ^{15}N bearing one or more hydrogen atoms provide data whose interpretation is open to the least ambiguity, while ^{29}Si and ^{31}P in certain environments derive a significant portion of their relaxation from dipolar interactions and could be potentially useful. At the present stage of development, carbon-13 provides most of our data.

For $I = 1/2$ nuclei bonded to hydrogen atoms equation (36) takes the form

$$R^{D} = \frac{n\mu_0{}^2\gamma_I{}^2\gamma_H{}^2\hbar^2\tau_c}{16\pi^2 r^6_{C-H}} \tag{37}$$

where n is the number of hydrogen atoms bonded to the ith atom. The constants used to extract rotational correlation times from this equation are listed in Table VII. Before τ_c values can be extracted, however, the dipolar component must be separated from any other contributions to the total relaxation process, and this is accomplished by measuring through proton decoupling the nuclear Overhauser enhancement (NOE), a property whose magnitude is proportional to the fraction of total relaxation that occurs by the dipole–dipole mechanism. The theoretical maximum NOE for a particular nucleus, observable when 100% of the relaxation is dipolar, is calculated from the $\gamma_H/2\gamma_I$ values given in Table VII. The experimentally

TABLE VII

Constants used to extract rotational correlation times from dipolar relaxation rates of $I = 1/2$ nuclei bonded to protons.

Nucleus	$\gamma/10^7$ rad T^{-1} s^{-1}	$\gamma_H/2\gamma_I$	$r_{I-H}/10^{-10}$ m	$\left(\frac{\mu_0}{4\pi}\right)^2 \hbar^2\gamma_I^2\gamma_H^2 r^{-6}/s^{-2}$
^1H	26·75	0·5	0·74	$4{\cdot}76\times10^{12}$ [a]
^{13}C	6·73	1·988	1·107	$1{\cdot}94\times10^{10}$
^{15}N	−2·71	−4·94	1·01	$5{\cdot}46\times10^{9}$
^{29}Si	−5·31	−2·52	1·48	$2{\cdot}12\times10^{9}$
^{31}P	10·83	1·24	1·40	$1{\cdot}23\times10^{10}$
^{77}Se	5·10	2·62	1·47	$2{\cdot}03\times10^{9}$
^{119}Sn	−9·97	−1·34	1·70	$3{\cdot}25\times10^{9}$
^{195}Pt	5·75	2·32	c. 1·7	$1{\cdot}1\times10^{9}$

[a] Corrected for 3/2 effect.

observed NOE_{exp}, defined as (double resonance intensity/single resonance intensity − 1), yields the dipolar component of the total relaxation rate from the equation

$$R^D = \frac{NOE_{exp}}{\gamma_H/2\gamma_I} R^{total} \tag{38}$$

Experimental NOE values can routinely be measured with a precision of ±15%, and ±5% can be achieved in favourable cases.

The r^{-6} factor in the dipolar relaxation equation makes derived τ_c values particularly sensitive to the dipole separation used in the derivation, and it is the uncertainty in r that determines the precision with which τ_c can be evaluated using this method. The conventional C—H distance of 1·09 Å for an sp^3 carbon has been used by most investigators, but Vold and coworkers[50] favour a vibrationally averaged value of 1·107 Å which yields τ_c values that are 10% larger than those obtained using 1·09 Å.

D. The shielding anisotropy (SA) mechanism

That portion of the external magnetic field B_0 imposed on a molecule by an NMR spectrometer which is actually experienced by the nucleus is

determined by the shielding constant according to the equation

$$B_{loc} = B_0 - \sigma B_0 = B_0(1-\sigma) \tag{39}$$

If the molecule is anisotropic, σ will vary with direction and different chemical shifts will be observed along different molecular axes if the molecule remains static relative to the B_0 direction. Since the rate of molecular rotation in mobile liquids, in the range 10^{10}–$10^{12}\,s^{-1}$, is several orders of magnitude greater than typical observation frequencies of $10^8\,s^{-1}$, the individual components are mixed and only the average value $\sigma_{av} = (2\sigma_\perp + \sigma_\parallel)/3$ or $\sigma_{av} = (\sigma_{xx} + \sigma_{yy} + \sigma_{zz})/3$ is observed experimentally. Because the instantaneous B_{loc} is orientation dependent due to the anisotropy in σ, however, the magnetic coupling between B_0 and the relaxing nucleus is modulated by the molecular rotation at frequencies determined by τ_c. The intensities of the frequency components that promote nuclear relaxation are again given by functions similar to those represented in Figs 1 and 2, and in the region of motional narrowing where $\omega\tau_c < 1$, relaxation rates are given[39] by

$$R_1^{Sa} = \frac{\mu_0}{30\pi}\gamma_I^2 B_0^2(\sigma_\parallel - \sigma_\perp)^2\tau_c \tag{40}$$

$$R_2^{SA} = \frac{7\mu_0}{180\pi}\gamma_I^2 B_0^2(\sigma_\parallel - \sigma_\perp)^2\tau_c \tag{41}$$

In this particular instance, R_1^{SA} and R_2^{SA} are differentiated because even in the motional narrowing region, the nature of the correlation function is such that R_1^{SA} and R_2^{SA} differ by about 15%. It should be borne in mind, however, that this difference is probably less than the experimental uncertainty in most R^{SA} determinations.

Shielding anisotropy can only make a measureable contribution to relaxation if the anisotropy term $(\sigma_\parallel - \sigma_\perp)$ exceeds some threshold value which is only achieved in practice for atoms that experience a large range of chemical shifts. Typical values of 5×10^7 rad $T^{-1}\,s^{-1}$ for γ; 2·4 T for B_0; and 10^{-11} s for τ_c require $(\sigma_\parallel - \sigma_\perp)$ to be at least 1600 ppm if an R^{SA} of $0{\cdot}05\,s^{-1}$ is to be achieved. Lassigne and Wells[42] have studied the ^{199}Hg relaxation in dimethyl mercury and find that with an anisotropy of 4600 ppm, the shielding anisotropy contributes 10% of the total $0{\cdot}88\,s^{-1}$ relaxation rate at 300 K. Since the remaining 90% comes from the spin–rotation mechanism, the shielding anisotropy fraction increases with decreasing temperature.

The presence of B_0 in equations (40) and (41) makes the shielding anisotropy relaxation rate field/frequency dependent. Not only does this provide an experimental criterion for identifying the presence of a shielding anisotropy contribution to the total relaxation rate; it means that molecules

whose anisotropy is not sufficiently large to yield a measureable R^{SA} at conventional field strengths may display one at the elevated fields coming more generally into use.

E. The scalar coupling (SC) mechanism

Where spin–spin (scalar) coupling between two nuclei in the same molecule exists, the strength of this interaction is represented by the familiar spin–spin coupling constant $J_{I\text{-}S}$ measured in hertz, and can be expressed as $A = 2\pi J$ rad s^{-1}. When the relaxation rate of nucleus S is low and $T_{1(S)}$ is long, a multiplet is observed in the NMR spectrum of nucleus I and there is no fluctuation of the local field generated at I by S. If the relaxation rate of nucleus S is greater than the coupling constant, A, as frequently occurs for quadrupole-relaxed nuclei, the local field produced at I by S fluctuates with a correlation time $\tau_S = T_{1(S)}$ and causes relaxation of I at a rate proportional to the square of the coupling constant.

Under these circumstances, the relaxation rates for nucleus I by this mechanism[39] are

$$R_1^{SC} = \frac{2A^2}{3} S(S+1) \frac{\tau_S}{1+(\omega_I - \omega_S)^2 \tau_S^2} \tag{42}$$

$$R_2^{SC} = \frac{A^2}{3} S(S+1) \left\{ \tau_S + \frac{\tau_S}{1+(\omega_I - \omega_S)^2 \tau_S^2} \right\} \tag{43}$$

Differences in Larmor frequencies for the coupled nuclei represented by $(\omega_I - \omega_S)$ are typically 10^7–10^8 rad s^{-1} while the shortest τ_S values occur for ^{35}Cl, ^{79,81}Br, ^{127}I and are typically longer than 10^{-6} s. The $[1+(\omega_I - \omega_S)^2 \tau_S^2]$ denominator in equations (42) and (43) is therefore much greater than unity and scalar coupling contributes significantly only to transverse relaxation represented by equation (43).

Although the maximum strength of scalar coupling A, at *c.* 10^4 s^{-1}, is several orders of magnitude weaker than the other coupling interactions that promote relaxation, the correlation time τ_S is much larger than typical τ_c values of 10^{-11}–10^{-12} s, and SC contributions to the relaxation process have been well documented for a number of systems where favourable combinations of A and τ_S obtain. Sharp[22,23] has shown that the transverse relaxation of ^{207}Pb in $PbCl_4$ is dominated by scalar coupling, and that it also makes a significant contribution to ^{119}Sn relaxation in $SnCl_4$ and SnI_4. Lassigne and Wells[51] have measured the SC contribution to the ^{1}H and ^{13}C relaxation in CH_3Br and use the information to evaluate the unresolved couplings to ^{79,81}Br.

While this relaxation mechanism is similar to the other four discussed above in that the rate expression contains a coupling constant and a

correlation time, in the case of the scalar coupling mechanism, the correlation time tells us nothing about the molecular motion which is the focal point of this review. For this reason, the quantitative aspects of relaxation by scalar coupling will not be further pursued.

V. RELAXATION PARAMETERS FOR QUADRUPOLAR NUCLEI

The interpretation of relaxation data for quadrupolar nuclei is relatively straightforward and is considered first. The nuclei for which data are tabulated in this section have quadrupole moments in the range $0{\cdot}0027 \times 10^{-28}\,\mathrm{m}^2$ (^{2}H) $\leq Q \leq 2{\cdot}6 \times 10^{-28}\,\mathrm{m}^2$ (^{187}Re), all of which are sufficiently large that relaxation from mechanisms other than quadrupole coupling is at least an order of magnitude smaller and makes no measurable contribution to the total relaxation rate. Equation (27) provides the theoretical base for interpreting the relaxation and, in cases for which the NQCC is independently available, τ_c is obtained directly from a measured R^Q.

Equation (16) and Fig. 1 show τ_c to be a linear function of sample viscosity and temperature. It is τ_{red} represented by the *slopes* in Fig. 1 that should correlate with molecular size and shape if an adequate theoretical model has been developed, and τ_{red} is independent of viscosity and temperature. The most reliable τ_{red} measures are obtained by observing τ_c over a range of viscosities. Few such studies have been carried out, however, and most of the 300 K τ_{red} values tabulated are obtained from $\tau_{red} \simeq \tau_c/\eta$ on the assumption that the τ_0 intercept is close to zero. Values based upon a measured slope, or for which an estimate of τ_0 has been made, are tabulated in bold-faced type in the tables which follow. Most single temperature data in the literature have been measured within ±5 K of 300 K and only where the measured value lies outside this range has τ_{red} been temperature-adjusted to 300 K.

Symmetric molecules for which rotation is isotropic yield a single τ_c which is directly related to the rotational diffusion coefficient by

$$\tau_c = 1/6D \tag{44}$$

By measuring τ_c for several different nuclei in the same molecule, it is possible to evaluate the individual components of the rotational diffusion tensor for a molecule whose rotation is anisotropic, and a number of elegant studies where this objective has been achieved are included in the tables that follow. In these instances, it is generally the components of **D** which are reported in the literature, and for ease of comparison these are converted to correlation times using

$$\tau_i = 1/6D_i \tag{45}$$

and tabulated as such.

For symmetric top molecules, two diffusion constants $D_{\parallel}$ and $D_{\perp}$ representing rotation about axes parallel and perpendicular to the principle symmetry axis describe the anisotropic rotation, and τ_c is given[26] by

$$\tau_c = \frac{(1/4)(3\cos^2\theta - 1)^2}{6D_{\perp}} + \frac{3\sin^2\theta\cos^2\theta}{5D_{\perp}+D_{\parallel}} + \frac{(3/4)\sin^4\theta}{2D_{\perp}+4D_{\parallel}} \tag{46}$$

where θ is the angle between the symmetry axis of the molecule and the z-axis of the molecular coordinate system that diagonalizes the electric field gradient tensor at the nucleus. In most cases this can be taken as the bond axis to the quadrupolar nucleus. Although the complexity of equation (46) would appear to complicate the interpretation of τ_c, the weighting factors for each of its three terms shown in Table VIII lead one to the following general conclusions for C_{3v} molecules with a long symmetry axis (e.g. CD_3CN; CD_3CCD):

TABLE VIII

Weighting factors for equation (46) terms.

θ/deg	$(1/4)(3\cos^2\theta - 1)^2$	$3\sin^2\theta\cos^2\theta$	$(3/4)\sin^4\theta$
0	1·0	0	0
90	0·25	0	0·75
109·5	0·1	0·3	0·6

(i) Only $D_{\perp}$ contributes to the relaxation of atoms lying on the figure axis, and since $D_{\perp}$ is slower than $D_{\parallel}$ their relaxation is likely to lie in the diffusion region and τ_{red} should correspond with that calculated using one of the diffusion models.

(ii) For an atom lying off the figure axis at the tetrahedral angle, in molecules where $D_{\parallel}/D_{\perp} \approx 10$, each term contributes about equally to τ_c, whose value is about one-third of that in (i) because the angle θ is more effective in reducing correlation.

A. Deuterium

The field of deuterium NMR was thoroughly reviewed in 1977[52] and most of the existing data on ^2H relaxation were drawn together at that time. Since then, definitive studies aimed at resolving individual diffusion components for specific molecules whose rotation is anisotropic have been carried out and, in most of these, ^2H has provided one of the two or three τ_c values needed to achieve a separation. For these, the ^2H relaxation data are presented in Table IX and the derived rotational diffusion components are presented in Table XIX.

The NQCCs that are required to calculate τ_c are obtained in a number of different ways, all of them involving some degree of approximation since no routine method provides this parameter for the liquid state. Where both solid- and gas-phase values for a particular molecule are available, a suitable intermediate average for the liquid is adopted.[53] Where measured values for typical organic molecules are lacking, use has been made of the correlation with hybridization of the carbon atom to which the ^2H is bonded and 170 kHz for sp^3, 180 kHz for sp^2 and 25 kHz for sp are adopted as fairly typical.[36]

B. Nitrogen-14

^{14}N relaxation data and quadrupole coupling constants have been compiled by Lehn and Kintzinger.[38] Thus by 1973 both these parameters had been measured for over 50 nitrogen-containing molecules, so that an effective correlation time, τ_c, could be calculated. Relaxation times for many other covalent as well as a number of quaternary nitrogen compounds are included in reference 38.

Table X presents a tabulation of ^{14}N relaxation times for those compounds for which τ_c and viscosities are known, arranged in order of increasing molecular volume. The scope and experimental method backing up such data have been discussed by Lehn and Kintzinger.[38]

C. Chlorine-35

In 1963 O'Reilly and Schacher[109] published a ^{35}Cl relaxation study of CCl_4, $CHCl_3$, C_6H_5Cl, $TiCl_4$ and ClO_3^-, and by 1976 R^O/NQCC data enabling the determination of τ_c was available for over 30 molecules. These have been tabulated by Lindman and Forsen,[27] who discuss the scope, limitations and experimental aspects of halogen relaxation rates and correlation times. Table VI, containing the nuclear properties for quadrupolar nuclei, shows that the quadrupole coupling constants experienced by ^{35}Cl in typical molecular environments are an order of magnitude greater than those experienced by the others. As a consequence contributions to ^{35}Cl relaxation by mechanisms other than the quadrupolar one are insignificant, making the interpretation of chlorine relaxation rates particularly straightforward. Table XI contains the relaxation parameters and reduced rotational correlation times for chlorine-containing molecules.

The τ_{red} values assembled in Table XI illustrate better than any of the other data sets the correlation that exists with molecular size. Although the τ_c column shows little regularity, τ_{red} is seen to increase with the size of the molecule, the trend being most pronounced for those with large central atoms such as Ti, Sn and Pb, which have τ_{red} in excess of 5 ps.

D. Beryllium-9, boron-11, oxygen-17, sodium-23, sulphur-33, vanadium-51, bromine-81 and iodine-127

There are some quadrupolar nuclei for which only a limited number of relaxation studies have been conducted. There is another set for which a rather more extensive body of relaxation data is available but which lack the quadrupole coupling constants required to extract τ_c from the relaxation rates. Table XII contains what data are available for both these sets of nuclei.

The study by Kintzinger and Lehn[81] of relaxation in the sodium cryptates is particularly valuable as it was one of the first to utilize the double spin probe technique for determining τ_c, and it is unfortunate that reliable viscosities for these solutions are unavailable.

Oxygen-17 is the leading example of the second category identified above. The early work on this nucleus by Diehl and his coworkers[120,121] provides a rich variety of line width-based relaxation rates, but very few ^{17}O quadrupole coupling constants are available with which to compare these. Since these coupling constants are so difficult to obtain by standard means, oxygen-17 provides a leading example of the value of theoretically based τ_c values for the indirect evaluation of coupling constants.

VI. RELAXATION PARAMETERS FOR $I = 1/2$ NUCLEI

Nuclei having only $1/2\hbar$ of spin angular momentum have zero quadrupole moments and are cut off from the most effective route for nuclear magnetic relaxation. The most efficient relaxation mechanism available to these nuclei is dipolar coupling to a near neighbour nucleus of large magnetic moment and this, in practice, means a covalently bonded proton. Carbon shows a higher incidence of covalently bonded protons than any other atom, and carbon-13 spectra provide the largest variety of dipolar-relaxed nuclei. By comparison, all other $I = 1/2$ nuclei provide only a few examples each of molecules whose rotational dynamics can be deduced from relaxation rates.

A. Carbon-13

Table XIII contains the relaxation rates and rotational correlation times obtained from carbon-13 spectra, along with the viscosities necessary to obtain reduced correlation times. In each case, the dipolar component has been separated from the total relaxation rate using the nuclear Overhauser enhancement ratio given in Table VII, and the dipole–dipole coupling constant has been calculated using the proton–carbon distance given in Table VII.

TABLE IX

Rotational correlation times from ^{2}H relaxation.

Compound	Condition	R^Q/s^{-1}	$\frac{e^2qQ}{h}$/kHz	τ_c/ps	η/cP[b]	τ_{red}/ps cP^{-1} [c]	Ref.
D_2O	Neat; 298 K	2·3[a]	237	2·9	1·1	2·6	54
D_2O	Neat; 303 K	0·143	230	2·6	0·98	**1·8**	55
D_2O	Neat; 298 K	2·3[a]	258	2·3	1·1	2·1	56
ND_3	Liquid; 293 K	0·15	282	0·13	0·16	0·8	112
CD_4	Liquid; 90 K	0·10	185	0·20	0·21	0·95	56
CH_3OD	Neat; 298 K	3·3	245	3·6	0·55	6·5	56
CD_3F	Neat	0·15	159	0·4	—	—	57
CD_3Br	Neat; 301 K	0·135	171	0·31	0·17	1·8	51
CD_3I	Neat; 303 K	0·19	180	0·40	0·46	0·86	58
CD_3CN	Neat; 298 K	0·14	148	0·43	0·35	1·2	53, 59
CD_3NH_2	D_2O	0·46	177	1·0	(3·3)	(0·30)	37
CD_2Cl_2	Neat	0·31	170	0·73	0·42	1·7	56, 60
CD_2Br_2	Neat; 298 K	0·72	181	1·5	0·97	1·5	61
CD_2I_2	Neat; 298 K	1·7	175	3·8	2·6	1·5	62
$CDCl_3$	Neat; 304 K	0·63	168	1·5	0·59	2·5	53, 63
$CDBr_3$	Neat	1·3	(175)	2·9	1·74	1·7	103
DCOOD	Neat	2·2	166	5·4	1·6	3·4	102
CD_3COOD	H_2O; 20% v/v	0·56	170	1·3	1·25	1·0	102
CD_3COO^-	D_2O; 4·7 mol%	0·61	184	1·2	(2·5)	(0·48)	37
CH_3CH_2OD	Neat; 298 K	9·1	245	10·0	1·1	9·1	56
$(CD_3)_2CO$	Neat; 304 K	0·21	(165)	0·52	0·29	1·8	53
$(CD_3)_2SO$	Neat; 304 K	1·4	(165)	3·5	1·8	1·9	53
$(CD_3)_2SO_4$	Neat; 304 K	0·42	(165)	1·0	1·7	0·59	53
$CD_3CD_2COO^-$	D_2O; 4·7 mol%	1·7	223	2·3	(2·5)	(0·92)	37
$(CH_3)_2CHOD$	Neat; 298 K	19·2	245	22	2·1	10·5	56

TABLE IX (*cont.*)

Compound	Condition	R^Q/s^{-1}	$\frac{e^2qQ}{h}$/kHz	τ_c/ps	η/cP[b]	τ_{red}/ps cP^{-1} [c]	Ref.
CD_3CCH	Neat; 243 K	0·16	162	0·41	0·28	1·5	64
CH_3CCD	Neat; 243 K	0·83	187	1·6	0·28	5·7	64
$(CH_3)_3COD$	Neat; 298 K	45·5	245	56	4·7	11·9	56
$(CH_3)_3CCl$	Neat; 300 K	0·48	174	1·07	0·47	2·3	65
$(CD_3)_2Hg$	Neat	0·46	165	1·1	1·03	1·1	42
$(CD_3)_4C$	Neat						107
$(CD_3)_4Sn$	Neat; 300 K	0·368	(165)	0·91	0·40	2·3	66
$(CD_2)_6(CD)_4$	CCl_4 (0·1 M)	0·96	174	2·1	0·92	**2·3**	14
C_5D_5N	Neat; 298 K	0·85	193	1·6	0·83	1·9	67
C_5D_5N	Trace H_2O	0·94	193	1·7	1·67	1·0	68
C_6D_6	Neat; 304 K	0·69	194	1·2	0·56	2·1	53
$C_6D_3F_3$	Chlorocarbon	2·0	181	4·5	—	—	69
C_5D_{10}	Neat; 304 K	0·28	(174)	0·62	0·39	1·6	53
C_6D_{12}	Neat; 304 K	0·68	174	1·5	0·83	1·8	53
$C_6D_5CH_3$	Neat; 304 K	0·93	(194)	1·7	0·53	3·2	53
$C_6D_5NO_2$	Neat	4·1	190	7·7	1·83	4·2	50
$C_6(C_4D_4)_3$	CCl_4; 0·1 M	11·8	187	23	0·9	**25**	17

[a] Relaxation rates containing an intermolecular dipolar component.
[b] Values in parentheses are estimated.
[c] Bold-face values obtained from definitive studies.

TABLE X

Rotational correlation times from ^{14}N relaxation.

Compound	Condition	$R^{Q}/10^{2}\,s^{-1}$	$\frac{e^2qQ}{h}$/MHz	τ_c/ps	η/cP	τ_{red}/ps cP^{-1} [b]	Ref.
NH_3	[a]	0·26	3·12	0·18	0·14	1·3	112
N_2	Liquid, 106 K	0·67	4·64	0·21	0·074	2·8	38
CH_3CN	[a]			1·1	0·35	3·1	12, 59
CH_3NC	[a]	0·0083	0·26	0·8	—	—	38
$HC{\equiv}CCN$	Hydrocarbon to ∞-dil.				—	**0·83**	71
CH_3NO_2	[a]	0·51	1·63	1·3	0·63	2·1	38
C_2H_5CN	[a]	3·57	3·77	1·7	0·41	4·1	38
C_2H_5NC	[a]	0·010	0·27	0·9	—	—	38
$HOC_2H_4NH_2$				20	12	1·7	86
CH_3SCN	[a]	5·0	3·54	2·7	0·72	3·8	38
$NCCH_2CN$	[a]	12·5	3·92	5·5	7·6	0·73	38
C_4H_5N	[a]	0·50	0·65	8·0	1·2	6·8	38
$C_2H_5NO_2$	[a]	0·34	1·13	1·8	0·72	2·5	38
$NCC{\equiv}CCN$				—	—	**3·5 ± 0·1**	
$N(CH_3)_3$	[a]	2·4	5·20	0·6	0·18	3·3	38
C_5H_5N	[a]	6·06	4·88	1·7	0·89	1·9	38, 67
C_4H_9N	[a]	8·33	4·33	3·0	0·80	3·7	38
NCC_2H_4CN	(m.p. 57 °C)	11·6	3·88	5·2	—	—	38
$O_2NC_2H_4NO_2$	[a]	1·67	1·46	5·3	—	—	38
CCl_3CN	[a]	6·67	4·09	2·7	0·75	3·6	27, 38
$(C_2H_5)_2NH$			4·48		0·35		73
C_6H_7N	[a]	41·7	3·93	18·2	3·7	4·9	38

TABLE X (*cont.*)

Compound	Condition	$R^Q/10^2\,s^{-1}$	$\frac{e^2qQ}{h}$/MHz	τ_c/ps	η/cP	τ_{red}/ps cP^{-1} [b]	Ref.
NCC_3H_6CN	[a]	12·5	3·82	5·8	6·2	0·94	38
$C_6H_5NO_2$	[a]	2·99	1·76	6·5	1·83	3·6	38, 50
$C_6H_{11}NH_2$	[a]	6·67	3·28	4·2	2·0	2·1	38
C_9H_7N (quinoline)	[a]	24·0	4·45	8·2	3·3	2·5	38
C_9H_7N (isoquinoline)	[a]	30·3	4·13	12·0	3·7	3·2	38
$N(C_2H_5)_3$	[a]	8·0	5·07	2·1	0·34	6·2	38
$(CH_2)_6N_4$	∞-dil. $CDCl_3$			12·3	0·53	23·2	74
$O_2N(CH_2)_6NO_2$	[a]	1·67	1·46	5·3	—	—	38

[a] Neat liquid, approximately 298 K.
[b] Bold-face values obtained from definitive studies.

TABLE XI

Rotational correlation times from ^{35}Cl relaxation.

Compound	Condition	$R^Q/10^4\ s^{-1}$	$\frac{e^2qQ}{h}$/MHz	τ_c/ps[a]	η/cP[b]	τ_{red}/ps cP^{-1}	Ref.
CH_3Cl	Neat; RT	1·00	68·0	0·55	0·18	3·1	27
ClO_3F	Neat; 300 K	0·070	19·2	0·48	0·17	2·8	13
CH_2Cl_2	Neat; RT	—	72·0	1·14 ± 0·09 (4)	0·43	2·7	27
CF_2Cl_2	Neat; 293 K	2·5	76·0	1·1	0·24	4·6	27
$SOCl_2$	Neat; 299 K	2·63	64·0	1·62	(0·60)	(2·7)	27
BCl_3	Neat; 298 K	—	43·0	1·19 ± 0·11 (2)	1·17	1·0	27
$CHCl_3$	Neat; RT	—	77·0	1·81 ± 0·41 (9)	0·59	3·1	27
SO_2Cl_2	Neat; 298 K	3·33	75·4	1·48	(0·77)	(2·0)	27
CrO_2Cl_2	Neat; RT	—	31·4	2·8 ± 0·4 (3)	0·88	3·2	27
$CFCl_3$	Neat; RT	—	79·6	1·13 ± 0·15(3)	0·43	2·7	27
S_2Cl_2	Neat; 299 K	4·55	71·6	2·25	0·92	2·4	27
PCl_3	Neat; RT	—	52·3	2·2 ± 0·37 (6)	0·6	3·7	27
$PBrCl_2$	50:50 PCl_3:PBr_3; 298 K	2·86	52·3	2·7	(1·2)	(2·3)	94
$AsCl_3$	Neat; RT	—	50·3	5·15 ± 1·1 (2)	1·2	4·3	27
$POCl_3$	Neat; 299 K	3·70	57·9	2·8	1·05	2·6	27
$SiHCl_3$	Neat; 303 K	0·83	38·0	1·5	(0·5)	(3·0)	36
PBr_2Cl	50:50 PCl_3:PBr_3; 298 K	2·87	52·3	2·7	(1·2)	(2·2)	94
$VOCl_3$	Neat; RT	—	23·1	3·37 ± 0·46 (4)	0·73	4·6	27
CCl_4	Neat; RT	—	81·3	1·76 ± 0·16 (7)	0·88	2·0	27
CH_3CCl_3	Neat; 300 K	4·65	75·8	2·05	0·75	2·7	27
CCl_3CN	Neat; 298 K	7·41	83·3	2·70	0·75	3·6	27
$(CH_3)_3CCl$	Neat; 300 K	2·35	62·4	1·53	0·54	2·8	65
C_6H_5Cl	Neat; RT	—	69·2	4·07 ± 0·06 (3)	0·76	4·4	27
$SiCl_4$	Neat; RT	—	40·8	2·66 ± 0·58 (4)	0·46	5·	27
$GeCl_4$	Neat; 299 K	2·44	51·4	2·33	(0·8)	(2·9)	27

TABLE XI (*cont.*)

Compound	Condition	$R^{O}/10^{4}\,s^{-1}$	$\frac{e^2qQ}{h}$/MHz	τ_c/ps[a]	η/cP[b]	τ_{red}/ps cP^{-1}	Ref.
$TiCl_4$	Neat; RT	—	12·2	4·53 ± 0·55 (6)	0·77	5·9	27
$SnCl_4$	Neat; RT	—	48·3	4·43 ± 1·53 (3)	0·92	5·5	27
$PbCl_4$	Neat; 298 K	14·0	45·4	17·2	(3·0)	(5·7)	27
$SbCl_5$	Neat; 299 K	6·25	57·2	4·8	2·1	2·3	27
ClO_3^- (aq.)	298 K	6·4	59·8	4·5	—	—	27
ClO_3^- (aq.)	6 M; 298 K	4·2	59·6	3·0	(1·8)	(2·5)	27
ClO_4^- (aq.)	301 K		—	(6·1)	—	—	27
Cl_3^- (aq.)	298 K	—	—	6·4 ± 0·2 (2)	—	—	27

[a] Parenthetical numbers indicate number of independent determinations; uncertainty limits are standard deviations.
[b] Values in parentheses are estimates.

TABLE XII

Rotational correlation times from ^{9}Be, ^{11}B, ^{17}O, ^{23}Na, ^{33}S, ^{51}V, ^{81}Br, and ^{127}I relaxation.

Compound	Nucleus	R^{Q}/s^{-1}	$\frac{e^2qQ}{h}$/MHz	τ_c/ps	η/cP[a]	τ_{red}/ps cP^{-1} [b]	Ref.
$Be(acac)_2$	^{9}Be	$1{\cdot}16\times10^{1}$	0·35	24	(2·1)	(11)	34
BCl_3	^{11}B			1·2	1·17	1·0	12
H_2O	^{17}O	$1{\cdot}43\times10^{2}$	7·7	2·5	0·81	3·1	101
D_2O	^{17}O	$1{\cdot}49\times10^{2}$	7·7	2·6	1·04	2·5	101
ClO_3F	^{17}O	$4{\cdot}3\times10^{1}$	14	0·23	0·18	1·3	100
Na^+ solvates	^{23}Na						118
$Na(N_2O_4$ cryptate$)^+$	^{23}Na	$4{\cdot}15\times10^{2}$	2·1	24	(1·8)	(13)	81
$Na(N_2O_5$ cryptate$)^+$	^{23}Na	$1{\cdot}45\times10^{2}$	1·3	21	(1·8)	(12)	81
$Na(N_2O_6$ cryptate$)^+$	^{23}Na	$9{\cdot}1\times10^{1}$	0·9	26	(1·8)	(14)	81
$Na(N_2O_2S_2$ cryptate$)^+$	^{23}Na	$1{\cdot}54\times10^{2}$	1·3	23	(1·8)	(13)	81
CS_2	^{33}S	$1{\cdot}09\times10^{3}$	14·87	1·3	0·35	**2·13**	25
$VOCl_3$	^{51}V				0·68		12
$PBrCl_2$	^{81}Br	$1{\cdot}4\times10^{6}$	373	2·6	(1·2)	(2·2)	94
PBr_2Cl	^{81}Br	$1{\cdot}5\times10^{6}$	373	2·65	(1·2)	(2·2)	94
PBr_3	^{81}Br	$1{\cdot}5\times10^{6}$	373	2·7	(1·2)	(2·2)	94
PBr_3	^{81}Br			5·8	1·82	3·2	27
$SnICl_3$	^{127}I	$6{\cdot}3\times10^{6}$	1355	3·6	—	—	82
SnI_3Cl	^{127}I	$8{\cdot}1\times10^{6}$	1355	4·6	—	—	82
SnI_4	^{127}I	$6{\cdot}7\times10^{6}$	1390	3·67	—	—	23
HgI_4^{2-} (aq.)	^{127}I	$9{\cdot}1\times10^{6}$	(840)	14			119

[a] Values in parentheses are estimates.
[b] Bold-faced values obtained from definitive studies.

B. Nitrogen-15

Nitrogen is particularly valuable for relaxation studies because it has both a quadrupole and a dipolar relaxed isotope. The relaxation rates observed for the quadrupolar ^{14}N, and listed in Table X, are three to four orders of magnitude greater than those for the dipolar ^{15}N listed in Table XIV, and this difference highlights the aspect of ^{15}N relaxation studies which is particularly troublesome.

Nitrogen bases have a strong affinity for metal cations, and any metal atoms in a solution containing such bases will spend most of their time in close proximity to a nitrogen atom. If the metal cation happens to be paramagnetic, as many of them are, its magnetic coupling to a ^{15}N nucleus provides a relaxation path roughly a thousand times more effective than that provided by dipolar coupling to a proton. While trace amounts of paramagnetic impurity in solution will not compete with the quadrupolar mechanism in relaxing ^{14}N, they will compete effectively in relaxing ^{15}N because the regular mechanisms for relaxing this nucleus are relatively inefficient. Levy and coworkers[85-87] have recognized this problem and have taken precautions to eliminate the effects of paramagnetic impurities from their ^{15}N relaxation studies. Results of ^{15}N studies where this precaution has not been taken have been excluded from Table XIV.

C. Hydrogen-1, fluorine-19, silicon-29, phosphorus-31, tin-119, mercury-199 and lead-207

After carbon-13 and nitrogen-15, the remaining $I = 1/2$ nuclei provide relatively little data that can be used to characterize rotational diffusion. Many studies of ^{1}H and ^{19}F relaxation have been carried out and most of the relaxation observed results from dipole–dipole coupling, but in all of these instances a significant portion of the relaxation is attributable to *intermolecular* couplings in which the distance factor cannot be specified with sufficient precision to quantify the coupling constant.

Table XV contains the relaxation parameters that provide information about rotational correlation times for a selection of other nuclei. For some of the nuclei, data on only one or two compounds are available.

VII. TESTS OF THE THEORETICAL MODELS FOR CALCULATING τ_c

The theoretical models in current use by NMR spectroscopists for discussing observed values of rotational correlation times are described in section II.C. Input variables required for each model are some measure of molecular size, and in addition, for the Hu–Zwanzig and Youngren–Acrivos

TABLE XIII

Rotational correlation times from ^{13}C relaxation.

Compound	Conditions	$R^{Q}/10^{-2}\,s^{-1}$	$R^{SR}/10^{-2}\,s^{-1}$	τ_θ/ps	τ_J/ps	η/cp[f]	τ^*_θ/ps cP^{-1}	Ref.
CH_4	Liquid; 174 K	2·08	3·54	0·26	0·25	0·21	1·2	77
CH_3OH	$X = 0·86$ in C_6D_6	2·92	—	0·50	—	0·62	0·81	37
CH_3NH_2	$X = 0·17$ in D_2O	6·02	—	1·03	—	(3)	(0·33)	37
CH_3Br	Neat; 278 K	1·8	4·8	0·31	—	0·20	1·6	51
C_3H_6[a]	50% $CDCl_3$	1·4	1·4	0·33	—	—	—	76
CS_2	Neat; 293 K	—	—	1·4	0·087	0·35	4·0	126
CH_3I	Neat	7·7	5·6	1·4		0·46	3·0	58
CH_3CONH_2	5·3 M D_2O in H_2O	Using ^{15}N, ^{13}C data from three atoms, $\tau_{ceff} = 7·5$ ps						77
C_4H_8[a]	50% $CDCl_3$; 303 K	2·0	0·8	0·47		—	—	76
$CHCl_3$	0·05 M CS_2	$\tau_\parallel = 0·8$ ps, $\tau_\perp = 1·1$ ps						75
C_6H_6	Along with Raleigh scattering $\tau^*_\parallel = 0·0$ ps, $\tau^*_\perp = 3·5 \pm 0·1$ ps							29
C_5H_{10}[a]	50% $CDCl_3$; 302 K	2·6	0·8	0·61		—	—	76
CH_2I_2	33% in C_6D_6	1·3	1·5	0·31	—	—	—	83
CCl_4	Neat enriched; 303 K	0·44 ± 0·01	0·39	1·72	0·133	—	—	127
$CFBr_3$	Neat; 298 K	0·76	—	1·75	—	1·4	1·3	80
CH_3COO^-	4·7 mol% D_2O	7·58	—	1·19	—	~2·5	~4·8	37
$CH_3CON(CH_3)_2$	Using ^{13}C and ^{15}N data from four atoms, $\tau_{ceff} = 11·1$ ps							77
C_6H_{12}[a]	50% $CDCl_3$; 303 K	5·0	0·2	1·2	—	—	—	76
C_8H_7N[c]	4 M acetone-d_6, 311 K	17	—	8·1	—	~1·4	~5·8	84
CHI_3	Neat; 303 K	7·7	5·6	1·4	—	0·46	3·0	58
$C_2H_5COO^-$	4·7 mol% D_2O	14·5	—	2·27	—	~2·5	~0·91	37
$(CH_3)_4Sn$	Neat; 293 K	7·3		1·1	—	0·43	2·6	66
C_7H_{14}[a]	50% $CDCl_3$; 303 K	6·3	0	1·5	—	—	—	76
$(CH_2)_6N_4$	0·5 M $CDCl_3$	53	—	13·7	—	0·53	25·8	14
C_8H_{16}[a]	50% $CDCl_3$; 303 K	9·7	0	2·3	—	—	—	76

TABLE XIII (*cont.*)

Compound	Conditions	$R^{O}/10^{-2}\,s^{-1}$	$R^{SR}/10^{-2}\,s^{-1}$	τ_θ/ps	τ_J/ps	η/cp[f]	τ^*_θ/ps cP^{-1}	Ref.
$(CH_2)_6(CH)_4$	0·5 M $CDCl_3$	7·7	—	2·0	—	0·53	3·8	14
$C_{10}H_{20}$[a]	50% $CDCl_3$; 303 K	2·1	0	4·9	—	—	—	76
$Be(acac)_2$	3 M $CDCl_3$	58	—	24·1	—	>1·0	<24	34
$C_{18}H_{12}$[d]	0·045 M CCl_4	47	—	21	—	0·9	23	17
$C_{20}H_{14}$[e]	0·5 M $CDCl_3$			$\tau_\perp = 16 \pm 1$ ps, $\tau_\parallel = 48 \pm 8$ ps		0·47		32
$Na(N_2O_4)^{+}$[b]	0·25M in 5% D_2O/95% MeOH	95		21·5 ± 15%		—	—	81
$Na(N_2O_5)^{+}$[b]		80		18·0 ± 15%		—	—	81
$Na(N_2O_6)^{+}$[b]		100		22·5 ± 15%		—	—	81
$Na(N_2O_2S_2)^{+}$[b]		91		20·5 ± 15%		—	—	81

[a] Cycloalkanes.
[b] Bicyclic cryptate complexes with the indicated numbers of N, O and S donor atoms.
[c] Indole; carbon-12 relaxation data given.
[d] Triphenylene, $C_6(C_4H_4)_3$.
[e] Triptycene, $(C_6H_4)_3(CH)_2$.
[f] Values in parentheses are estimates.

TABLE XIV

Rotational correlation times from ^{15}N relaxation.

Compound	Conditions	$R^D/10^{-2}\,s^{-1}$	τ_c/ps	η/cP	τ_c^*/ps cP^{-1}	Ref.
$HCONH_2$	90% in acetone-d_6	69	—	3·22	—	86
CH_3CONH_2	5·3 M in D_2O, H_2O	Using ^{15}N, ^{13}C data from three atoms, $\tau_{ceff} = 7·5$				77
$C_3H_4N_2$ [a]	8 M DMSO; 299 K	13	—	5·12	—	85
$HOC_2H_5NH_2$	Neat liquid; 303 K	22	20	12	1·7	86
C_4H_5N [b]	Neat; 299 K	2·5	—	1·18	—	85
C_5H_5N [c]	Neat; 299 K	1·2	—	0·9	—	85
$HOC_3H_6NH_2$	Neat liquid; 303 K	27	24	17	1·4	86
C_4H_9N [d]	Neat; 299 K	1·7	—	0·80	—	85
n-$C_4H_9NH_2$	Neat; 299 K	1·4	—	0·55	—	85
$C_6H_5NH_2$	Neat; 299 K	7·7	—	3·71	—	85
$C_6H_5NH_2$	1 M $CDCl_3$	2·9	2·7	—	—	87
$C_6H_5NH_3^+$	1 M $CDCl_3$	63	38	—	—	87
n-C_4H_9ONO	Neat liquid; 303 K	4·1 ± 0·2	—	—	—	78
C_8H_7N [e]	8 N DMSO; 299 K	33	—	11·5	—	85
$(C_6H_5)_2N_2$ [f]	2·7 M $CDCl_3$; 301 K	1·8 ± 0·1	—	—	—	78

[a] Imidazole.
[b] Pyrrole.
[c] Pyridine.
[d] Pyrrolidine.
[e] Indole.
[f] *trans*-Azobenzene.

models, some measure of molecular shape is required. Since the chemist has some latitude in assigning size and shape parameters to a specific molecule, the testing of a particular model using data from a single molecule can yield agreement between observed and calculated values for τ_c that is misleadingly good. A more severe test is the assignment of size/shape parameters to a set of molecules spanning a reasonable range of size and shape, *adopting the same size/shape assumptions and criteria for all members of the set.* It is this test that is here applied using those molecules for which τ_c values are included in the tabulations of Section V and VI.

The aim of this testing has been threefold: (i) to develop a uniform and unambiguous method for assigning size and shape parameters to simple molecules; (ii) to select the most reliable τ_c model using the size/shape parameters obtained; (iii) to assess the reliability of τ_c calculated using this model and hence the reliability of a coupling constant obtained from a measured relaxation rate in combination with the calculated τ_c. The results provide a good deal of confidence for those people who must estimate a τ_c value in order to obtain a badly needed nuclear quadrupole or spin–rotation coupling constant.

A. Uniform assignment of molecular size and shape

The time-dependent molecular property that emerges from measurements of NMR relaxation times is a reduced correlation time τ_{red} which is shown in Section II.C to have units of ps K cp^{-1}. The functional relationship between τ_{red} and τ_c calculated using each of the theoretical models is given in Table V. At the heart of each calculated τ_c lies an accurate and unambiguous molecular volume. Edward has argued persuasively in favour of the van der Waals (V_w) volume concept, and has demonstrated its validity for electrolytic conductivity and translational diffusion of small molecules.[105,106] The definition for V_w and the atomic radii required for its determination are given in a comprehensive paper by Bondi.[70]

Once V_w for a particular molecule is calculated, the next step is to decide on a shape factor for those where departures from spherical symmetry are significant. These factors are axis ratios for the ellipsoids which best represent the real molecules. Shape factors in turn yield friction coefficients which are tabulated for each model in Tables II–IV.

1. *Molecular volumes*

Van der Waals radii taken from Bondi[70] have been used for volume determinations and are presented in Table XVI. Clearly there are many omissions, particularly for the heavy main group elements and most metals. The scope and limitations of these values are fully discussed by Bondi,[70] but it should be noted that any error resulting from unjustified assumptions

TABLE XV

Rotational correlation times from ^{1}H, ^{19}F, ^{29}Si, ^{31}P, ^{119}Sn, ^{119}Hg and ^{207}Pb relaxation.

Compound	Condition	Relaxation data	Reference
		Hydrogen-1	
H_2O	Liquid; 298 K	$\tau_c = 2{\cdot}7$ ps, $\eta = 0{\cdot}89$, $\tau^* = 3{\cdot}0$	54
H_2O	1 bar, 303 K	$R_1 = 0{\cdot}24\ s^{-1}$, $\tau_\theta = 2{\cdot}07$ ps, $\eta = 0{\cdot}801$, $\tau^* = 2{\cdot}6$	55
$CHCl_3$	0·05 M CS_2; 303 K	Various R give $\tau_\parallel = 0{\cdot}8 \pm 0{\cdot}1$ ps, $\tau_\perp = 1{\cdot}1 \pm 0{\cdot}2$ ps	75
$(CH_3)_2Hg$	Liquid; 296 K	$R_1 = 0{\cdot}139\ s^{-1}$; used with ^{2}H data to get $D_\parallel$ and $D_\perp$	42
$(CH_2)_6N_4$	Infinite dilution $CHCl_3$; 298 K	$\tau_2 = 12{\cdot}3 \pm 0{\cdot}6$ ps, $\eta = 0{\cdot}53$, $\tau_2^* = 23 \pm 1$ ps cP^{-1}	74
CH_3Br	Neat; 315 K	$R_1 = 0{\cdot}073\ s^{-1}$; with Br data, $\tau_\parallel = 0{\cdot}128$, $\tau_\perp = 0{\cdot}83$ ps	51
CH_3I		$R = 0{\cdot}81\ s^{-1}$ for pure liquid at 293 K; $R_1 = 0{\cdot}068\ s^{-1}$ in 68·5% CD_3I	58
CH_2Cl_2	Liquid; 298 K	$\tau_c = 0{\cdot}82$ ps using several nuclei	60
CH_2Br_2	Liquid; 298 K	$\tau_c = 1{\cdot}5 \pm 0{\cdot}1$ ps using several nuclei	61
CH_2I_1	Liquid; 298 K	$\tau_c = 4{\cdot}3 \pm 0{\cdot}3$ ps using several nuclei	62
$CHBr_3$	Neat; 294 K	$R_1^{d} = 0{\cdot}058\ s^{-1}$ (46% DD inter, 36% SR, 18% DD intra)	103
		Fluorine-19	
$CFCl_3$	Neat; 294 K	$R_1 = 0{\cdot}32\ s^{-1}$, $C_\sigma = -3{\cdot}30$ Hz, $\tau = 1{\cdot}1$ ps, $\eta \simeq 0{\cdot}42$, $\tau^* \simeq 2{\cdot}6$	89
ClO_3F	Neat; 300 K	$R_1^{SR} = 4{\cdot}4\ s^{-1}$, $\tau = 0{\cdot}48$ ps, $\eta = 0{\cdot}17$, $\tau^* = 2{\cdot}8$ ps cP^{-1}	13
SF_6	Liquid; 303 K	$R_1 = 2{\cdot}4\ s^{-1}$, $\tau = 1{\cdot}33$ ps	122, 123
$C_6D_3F_3$	310 K	$R_1 \simeq 0{\cdot}03\ s^{-1}$ (molecular fraction = 0·33 in hexachlorobuta-1,3-diene)	69
CDF_3	Liquid; 182 K	$R_1 \simeq 0{\cdot}23\ s^{-1}$, $\tau_c \simeq 1{\cdot}0$ ps	57
$CFBr_3$	Neat; 293 K	$R_1^{SR} = 0{\cdot}119\ s^{-1}$, $C_\sigma = -1{\cdot}4$ kHz, $\tau_\sigma \simeq 0{\cdot}16$ ps, $\eta = 1{\cdot}56$, $\tau^* = 0{\cdot}10$	80
		Silicon-29	
$(C_6H_5)_2SiH_2$	Neat; 311 K	$R_1 = 0{\cdot}038\ s^{-1}$, $\tau_c = 9{\cdot}0$ ps	90
$C_6H_5SiH(CH_3)_2$	Neat; 311 K	$R_1 = 0{\cdot}0053\ s^{-1}$, $\tau_c = 2{\cdot}5$ ps	90
$(CH_3)_3SiSCH_3$	88 vol% in C_6D_6	$R_1 = 0{\cdot}022\ s^{-1}$	91
$N(Si(CH_3)_3)_3$	$X = 0{\cdot}5$ in C_6H_6/C_6D_6	$R_1 = 0{\cdot}013\ s^{-1}$	91
$Si(CH_3)_4$	85% in acetone-d_6; 298 K	$R_1 = 0{\cdot}052$, $R_1^{d} = 0{\cdot}002$, $R_1^{SR} = 0{\cdot}051\ s^{-1}$	90
$Si(OC_2H_5)_4$	Neat; 311 K	$R_1 = 0{\cdot}0074\ s^{-1}$	90

TABLE XV (*cont.*)

Compound	Condition	Relaxation data	Reference
		Phosphorus-31	
PCl_3	50:50 molar mixture of PCl_3 and PBr_3; 298 K	$R_1^{SR} = 0{\cdot}300\ s^{-1}$, $C_{eff} = 5{\cdot}55$ kHz	94
PCl_2Br		$R_1^{SR} = 0{\cdot}201\ s^{-1}$, $C_{eff} = 3{\cdot}66$ kHz	94
$PClBr_2$		$R_1^{SR} = 0{\cdot}152\ s^{-1}$, $C_{eff} = 2{\cdot}28$ kHz	94
PBr_3		$R_1^{SR} = 0{\cdot}128\ s^{-1}$, $C_{eff} = 1{\cdot}60$ kHz	94
$P(C_2H_5)_3$	0·7 M $CDCl_3$; 302 K	$R_1^d = 0{\cdot}016\ s^{-1}$	95
$P(C_6H_5)_3$	0·7 M $CDCl_3$; 302 K	$R_1^d = 0{\cdot}011\ s^{-1}$	95
$OP(C_6H_5)_3$	1·0 M $CDCl_3$; 302 K	$R_1^d = 0{\cdot}016\ s^{-1}$	95
$(C_6H_5)PH_2$	Neat; 300 K	$R_1 \simeq 0{\cdot}8\ s^{-1}$, $\eta \simeq 0{\cdot}67$ (largely SR mechanism)	96
$(C_6H_5)PCl_2$	Neat; 300 K	$R_1 \simeq 0{\cdot}1\ s^{-1}$	97
$(C_6H_5)_2PCl$	Neat; 300 K	$R_1 \simeq 0{\cdot}25\ s^{-1}$	97
PH_3	Liquid, 300 K	$R_1 \simeq 5\ s^{-1}$	124
PD_3	Liquid, 300 K	$R_1 \simeq 3\ s^{-1}$	124
		Tin-119	
$Sn(CH_3)_4$	Neat; 300 K	$R_1^{SR} = 1{\cdot}67\ s^{-1}$, $C_{eff} = 17{\cdot}7$ kHz, $\tau_J = 0{\cdot}049$ ps	66
$SnCl_4$	Neat; 298 K	$R_1^{SR} = 0{\cdot}63\ s^{-1}$ $C_{eff} = 6{\cdot}1$ kHz $\tau_\sigma = 5{\cdot}0$ ps	23
$SnCl_3I$		Scalar relaxation of the second kind	82
$SnClI_3$		Scalar relaxation of the second kind	82
SnI_4	Neat; 423 K	$R_1 = 2{\cdot}0\ s^{-1}$, $R_2 = 62{\cdot}5\ s^{-1}$, $\tau_\sigma = 3{\cdot}67$ ps, $\tau_J = 0{\cdot}37$ ps	23
$SnBr_4$		Scalar relaxation of the second kind	25
		Mercury-199	
$(CH_3)_2Hg$	Liquid; 298 K	$R_1 = 0{\cdot}459\ s^{-1}$	42
		Lead-207	
$PbCl_4$	Neat; 298 K	$C_{eff} = 4{\cdot}5$–$7{\cdot}8$ kHz, $\tau_J = 1 \times 10^{-15}$–$10 \times 10^{-15}$ s	22

TABLE XVI

Van der Waals radii of the elements.[a]

Element	r/Å	Element	r/Å	Element	r/Å	Element	r/Å
H	1·2	Mg	1·7	Ga	1·9	Sb[c]	2·2
He[b]	1·8	Al[c]	2·1	Ge[c]	2·0	Te	2·1
Li	1·8	Si	2·1	As[c]	2·0	F	1·96
Be[d]	1·7	P	1·85	Se	1·9	Xe[b]	2·2
B[d]	1·7	S	1·8	Br	1·85	Pt	1·75
C	1·7	Cl	1·76	Kr[b]	2·0	Au	1·7
N	1·55	Ar[b]	1·9	Pd	1·6	Hg	1·5
O	1·5	K	2·8	Ag	1·7	Tl	2·0
F	1·55	Ni	1·6	Cd	1·6	Pb	2·0
Ne[b]	1·6	Cu	1·4	In	1·9	U	1·9
Na	2·3	Zn	1·4	Sn	2·2		

Atomic volume increments for carbon compounds.[a]

Compound type	$V/Å^3$	Compound type	$V/Å^3$
C, aliphatic	5·53	OH, alcohol	13·35
C, olefin	8·32	Hydrogen bonds, various	−1·74 (e.g.)
Conjugated double bond	− 0·42	CO, carbonyl	19·43
C, cumulative double bond (central)	11·56	Decrement per carboxyl, amide	−0·37
C, acetylenic	13·37	S, sulphide	17·9
C, conjugated acetylenic (central)	12·99	SH, thiol	24·6
C, aromatic	9·20	NH_2, primary amine	17·5
C, aromatic condensed	7·87	NH, secondary amine	13·42
H, aliphatic hydrocarbon	5·73	N, tertiary amine	7·19
H, olefinic hydrocarbon	5·76	CN, nitrile	24·41
H, acetylenic hydrocarbon	5·81	NO_2, nitrate	27·90
H, aromatic hydrocarbon	4·18	P, tertiary phosphines	17·34
Cyclohexyl and pentyl ring	−1·89	F, average	9·9
Methylene condensed to aromatics	−2·76	Cl, average	19·8
O, cyclic ether	8·64	Br, average	24·5
O, acyclic ether	6·1	I, average	32·8
O, aromatic ether	5·3		

[a] All values from reference 70, unless otherwise indicated. Consult reference 70 for assumptions and explanations.

[b] G. A. Cook, *Argon, Helium and the Rare Gases* Wiley, New York, 1961, Vol. I, p. 13.

[c] L. Pauling, *The Nature of the Chemical Bond*, 3rd edn, Cornell University Press, Ithaca, N.Y., 1960.

[d] Interpolated.

in the volume determination directly affects all calculations of τ_{red} in this study. Where necessary, van der Waals radii estimated using the Pauling rule[128] are included in Table XVI.

For organic compounds, where the range and type of interatomic distance are fairly regular, Bondi has produced the series of atomic volume increments included in Table XVI, and these are used in our calculations. Such generalizations are not valid for inorganic compounds where greater variation in bond length is encountered. For most of the main group inorganic compounds included here, V_w has been calculated using the radii from Table XVI along with published bond lengths according to the method outlined in Fig. 3 of reference 70.

Molecular volume can also be obtained from the molar volume, V_m, if a suitable packing factor, R, can be obtained. R, defined as $6{\cdot}0 \times 10^{23}\ V_w/V_m$, has been calculated for most of the compounds presented in Tables XVII–XIX, and has been found to range from 0·46 to 0·87 (mean $R = 0{\cdot}58 \pm 0{\cdot}07$ S.D.) and for similar chemical species packing factors tend to be highly uniform. This method has been used to estimate molecular volumes of several transition element compounds for which suitable radii are unavailable.

2. *The shape parameter*

Friction coefficients for both slip models are listed as a function of ρ, where ρ is an appropriately defined axial ratio. The Hu–Zwanzig model approximates the shape of the molecule by an ellipsoid of revolution or a spheroid. The Youngren–Acrivos model allows for general ellipsoidal shape and thus contains an additional degree of freedom.

As is shown below, τ_{red} for the slip models is quite sensitive to the magnitude of the shape factor chosen. For this reason, its evaluation must be realistic and generally applicable, and must above all eschew the temptation to make individual adjustments to accommodate the recognized idiosyncracies of particular molecules. Only a method meeting these criteria yields calculated values of τ_c suitable for deriving coupling constants from relaxation times.

The method which has been adopted is to construct the smallest right-angled box that will accommodate the molecule's van der Waals surface, with the centre of the box lying somewhere on the highest symmetry axis of the molecule. By letting the dimensions of this box be $2a < 2b < 2c$, the radial semi-axes of the molecule regarded as an ellipsoid are $a < b < c$. For molecules with cylindrical symmetry, two of the three dimensions are automatically equal and, because both slip models become unrealistic in the limit of small ρ, molecules for which a, b and c are within $\approx 10\%$ of each other are deemed "nearly spherical" and are analysed using the Gierer–Wirtz model only.

Where the Hu–Zwanzig model is applied, the two closest dimensions are averaged to give a shape factor defined as one of

$$\rho_{\text{prolate}} = \frac{a+b}{2c} \quad \text{or} \quad \rho_{\text{oblate}} = \frac{2a}{b+c} \tag{46}$$

For pear-shaped molecules which emerge from this treatment as prolate spheroids, a further averaging is applied to yield a shape factor given by ρ = (average width)/length. Whenever the HZ shape factors are thus calculated for molecules with less than cylindrical symmetry a gross oversimplification is of course being made, and, as might be expected, this sometimes leads to anomalous results. For example, in estimating the axes for thionyl chloride we find $(b-a) \simeq (c-b)$, leaving no obvious choice between a prolate or oblate description. What is more disconcerting is to discover that τ_{red} for the former description comes to 0·21 ps cP^{-1} while the latter gives 1·7 ps cP^{-1}, an order of magnitude different!

Clearly, for molecules such as $SOCl_2$ the Youngren–Acrivos approximation to a general ellipsoid represents a vast improvement. For this model the shape parameters (two *per molecule*) are defined by

$$\rho_1 = a/c \quad \text{and} \quad \rho_2 = b/c \tag{47}$$

We find the above method to give acceptable results for most small or rigid molecules; where substituents longer than ethyl or propyl are encountered it is found to break down. Whenever the most stable conformation of a molecule is not immediately obvious, molecular models must be used. Careful measurements on sophisticated models are needed to extend the above method to molecules larger or less rigid than those which are considered here.

3. *Viscosities*

Accurate viscosity data are essential to the testing of any hydrodynamic model. Unfortunately the reliability and availability of published viscosities varies enormously from compound to compound. Most reliable are those values where the NMR experimenters have determined the viscosity of the samples used in the actual relaxation studies. This is especially true for solutions of arbitrary concentration. The importance of providing viscosities was realized by the earliest reporters of relaxation data,[24] and it is surprising in view of the widespread use and discussion of hydrodynamic models that more workers do not measure and report their sample viscosities. If we sound irritable on this point, it results from encountering in the literature dozens of careful and highly detailed relaxation studies the results of which are rendered useless for *any* theoretical analysis through lack of a viscosity parameter.

By far the most accurate τ_{red} measurements are those where the slope of a τ_c versus viscosity plot is reported (i.e. a variety of solvents has been used.) This has the added safeguard of identifying by non-linearity all systems which are not hydrodynamic in behaviour. Also helpful are infinite dilution relaxation times so that the pure solvent viscosity (usually the most accurately measured) can be used.

However, for the great majority of molecules studied here, viscosities are taken from the standard tabulations of physicochemical data.

Every attempt has been made to match the viscosity to the conditions of the NMR measurement since viscosity and τ_{red} frequently have different temperature dependences.[27] In many instances, however, this attempt was frustrated by the many experiments reported without a full description of conditions. Wherever estimates of viscosities have been made, this is noted in the tabulation.

B. Testing of the models

Three hydrodynamic models for molecular rotation are in current use by NMR spectroscopists for discussing the results of nuclear relaxation measurements. The Gierer–Wirtz model utilizes a spherical representation for molecules and the Hu–Zwanzig and Youngren–Acrivos models are based upon spheroidal and ellipsoidal representations, respectively. Using the methods described above for evaluating molecular size and shape, reduced correlation times are calculated for some 75 molecules and compared with experimentally determined τ_{red} values.

Two difficulties complicate the direct comparison of models: one relates to the models and the other to the molecules. The slip models assume a zero friction coefficient and hence inertial rotation in the limit where ρ approaches 1·0, but experimental reality indicates considerably more viscous drag than these models predict. Thus for pure liquids the microviscosity factor of Gierer and Wirtz for spherical molecules is 0·16, larger than the microviscosity factors for all prolate cases in the Hu–Zwanzig model, and equal to that for oblate cases with ρ of about 0·5. In consequence, all near-spherical molecules are treated by the GW model; the others by one of the slip models.

The second difficulty centres around molecules whose rotation is highly anisotropic. For those with cylindrical symmetry, rotational correlation times $\tau_{\parallel}$ and $\tau_{\perp}$ are required to characterize the motion parallel and perpendicular to the figure axis, while most experimental determinations provide only a single $\tau_{effective}$ to which both $\tau_{\parallel}$ and $\tau_{\perp}$ contribute according to equation (46). As a result of the slip limit assumption that applies to the HZ model for spheroidal molecules, rotation about the figure axis is assumed to be in the inertial region and the correlation time which one

calculates is effectively $\tau_\perp$. In the comparison testing of the HZ model which follows, experimental $\tau_\perp$ values are used when available. Otherwise effective τ_c values which may be close to but are not necessarily identical with $\tau_\perp$ are used.

The YA model, on the other hand, can only be applied when the three components of the diagonalized rotational diffusion tensor are separated out, so that τ_a, τ_b and τ_c about well defined axes a, b and c are available. At the present time full separations have been made for only a handful of molecules; the result is that the Hu–Zwanzig model has had to be used for many molecules possessing less than cylindrical symmetry which undoubtedly reorient anisotropically. Only one side-by-side comparison of the three models has been reported.[115]

1. *Hydrodynamic models applied to near-spherical molecules*

Table XVII contains reduced rotational correlation times for 16 near-spherical molecules calculated according to the Stokes–Einstein–Debye and the Gierer–Wirtz models, along with experimental τ_{red} values for comparison. Examples giving good coverage of the size range 30–200 Å^3 have been found. The microviscosity model of Gierer and Wirtz is clearly superior to the rudimentary SED model for the majority of molecules; the only exception is hexamethylene tetramine, for which the viscous drag is very much greater than is predicted by the GW microviscosity factor. Of similar size and shape is adamantane whose rotation lies in the other extreme, near the inertial limit of zero viscous drag. Chemical effects to explain both of these anomalies have been provided by Wasylishen and coworkers.[14]

Figures 4 and 5 contain correlation plots of the data in Table XVII. The first is a simple correlation plot for the Gierer–Wirtz model in which all of the data are included. The best regression line, with slope and correlation coefficient, is obtained for data with reliability indices A and D. τ^*_{SED} has been plotted against τ^*_{expt} for pure liquids which comprise the bulk of our data. This gives an "empirical microviscosity factor" of 0·15 for pure liquids, in excellent agreement with the theoretical value of 0·16.

2. *The Hu–Zwanzig model*

This earliest of the slip models has been previously tested for a select 15 compounds by Bauer *et al.*[29] Both ^{13}C and light-scattering data are employed, and the range of volumes and τ^* reported go well beyond those which we have examined. This early study was very promising, and was based on reliable τ^* data obtained by fitting equation (15). A correlation curve using data given in reference 29 is presented in Fig. 6. The least squares line has a slope of 0·93 and a correlation coefficient of 0·997.

TABLE XVII

Testing of hydrodynamic models for near-spherical molecules.

Compound	V/Å^3	τ^*_{SED}/ps	τ^*_{GW}/ps	τ^*_{expt}/ps	RI[b]	Details	Ref.
CH_4	28·4	6·86	1·12	1·2	*A*	^{13}C; 174 K; liquid	77
ClO_3F	53·5	12·9	2·1	2·9	*A*	^{35}Cl	13
$CFCl_3$	76·5	18·5	3·0	2·7	*A*	^{35}Cl	27
CCl_4	86·9	21·0	3·4	2·0	*A*	^{35}Cl	27
$CFBr_3$	88·2	21·3	3·5	1·3	*A*	^{19}F	80
CH_3CCl_3	89·2	21·5	3·5	2·7	*A*	^{35}Cl	27
$(CH_3)_3CCl$	94·0	22·7	3·7	2·8	*A*	^{35}Cl	65
$SiCl_4$	96·2	23·2	3·8	5·8	*A*	^{35}Cl	27
$GeCl_4$	97·3	23·5	3·8	2·9±0·6	*D*	^{35}Cl	27
$TiCl_4$	(100)	(24·2)	(3·9)	5·9	*A*	Volume estimated using $R = 0·55$; ^{35}Cl	27
$PbCl_4$	106·6	25·7	4·2	5·7±0·8	*D*	^{35}Cl	22
$SnCl_4$	108·1	26·1	4·3	5·5	*A*	^{35}Cl	27
$Sn(CH_3)_4$	118·6	28·6	4·7	2·35	*A*	^{119}Sn and ^{2}H	66
$(CH_2)_6N_4$[a]	126·9	30·6	7·7	23·2	*E*	^{1}H, ^{13}C, ^{14}N; strong interaction postulated	14, 74
$(CH_2)_6(CH)_4$[a]	143·2	34·6	8·7	2·75	*E*	Average ^{2}H and ^{13}C; inertial rotation	14
$Be(acac)_2$[a]	196·9	47·6	11	~12	*D*	3 M $CDCl_3$ solution; ^{9}Be and ^{13}C	34

[a] Solutions other than neat liquids.
[b] Reliability index for the data used in the comparison, as follows: *A*, best data; *D*, uncertain viscosity data used; *E*, some anomaly evident.

The results of our calculations for over 50 molecules are presented in Table XVIII. Only compounds for which NMR relaxation data are presented elsewhere in this review are used. The data are assigned by letter as an indication of reliability. These are incorporated in Fig. 7(a), which presents the comparison as a regression line similar to Fig. 6. The best fit is obtained using class *A*, *B*, *C* and *D* data where only points with ρ values $<0·70$ are included. The slope of the line is 0·47 and the correlation coefficient 0·91. If all ρ values are allowed, the fit reduces to a slope of 0·44 and a correlation coefficient of 0·88. Visual inspection confirms that *all* points with large ρ values ($>0·70$) have abnormally small τ^*_{model} results.

In Fig. 7(b) the best data from Fig. 7(a) are divided between prolate and oblate molecules. No obvious bias for either shape can be found, and although the scatter is larger for oblate cases, in this subset the number of oblate molecules is approximately twice the number of prolates.

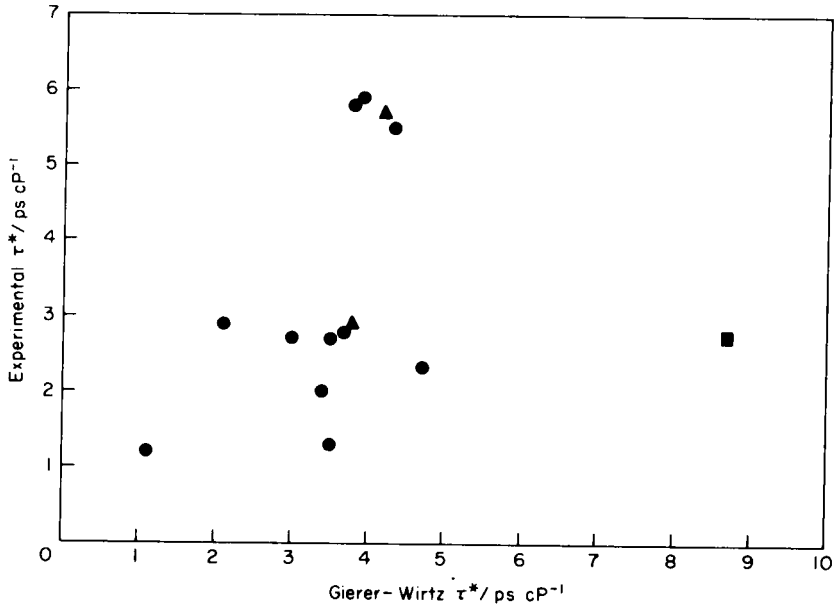

FIG. 4. Correlation of the Gierer–Wirtz model with experimental data. Data from Table XVII with reliability indices as follows: ●, *A* data; ▲, *B* data; ■, *C* data.

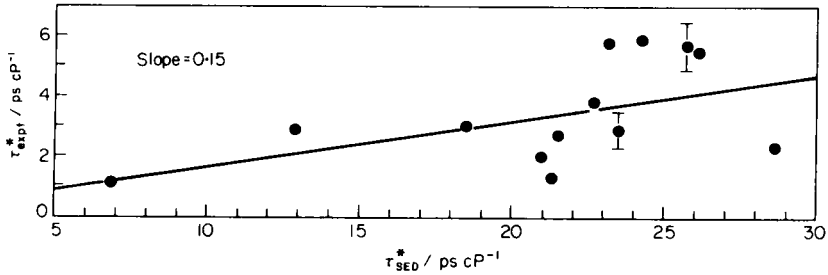

FIG. 5. Empirical microviscosity factor for pure liquids. Reliability index *A* data from Table XVII.

Class *E* data, for which rough shape parameter estimates only are available, reduce the accuracy of the correlation. This would seen to emphasize the importance of accurate ρ estimations. The anomalously low τ^*_{model} for large ρ suggests that the limitations of the slip model are greater than was initially supposed. The model simply becomes unreliable in the limit of large ρ; the unreliability setting in for $\rho > 0{\cdot}65$–$0{\cdot}70$.

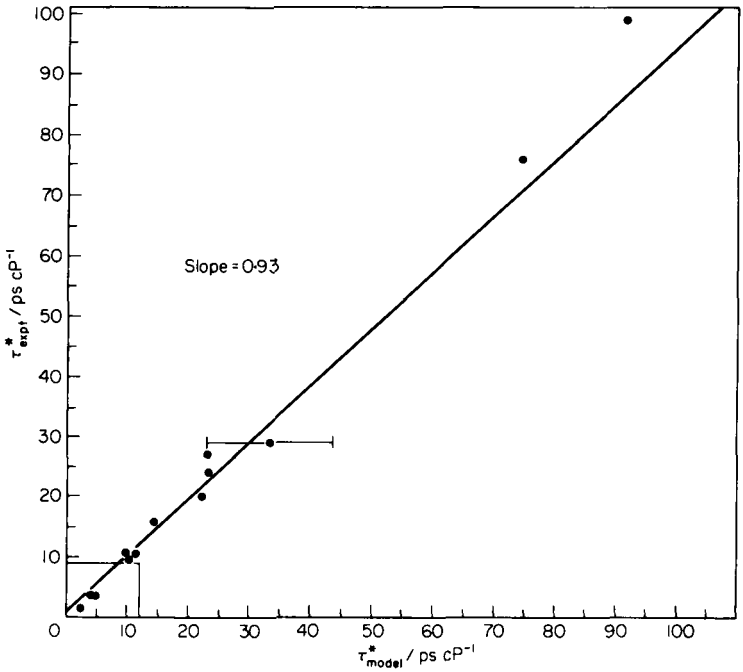

FIG. 6. Correlation curve for ^{13}C and depolarized light scattering data of Pecora *et al.*[29]

3. *The Youngren–Acrivos model*

Since the publication of the general ellipsoid model[18] over 40 references to it have been made in the chemical literature to date; nevertheless, there have been only two published applications![32,115] Together with data for nitrobenzene[29,50] and toluene,[29] these give four systems where sufficient data are available to test the YA model. Unfortunately, reports of D_a, D_b and D_c values for eight further compounds include insufficient solvent, temperature or viscosity information for analysis in this review.

The results for toluene, *trans*-decalin, nitrobenzene and fluorene are given in Table XIX. The regression line shown in Fig. 8 has a slope of 1·3 and a correlation coefficient of 0·98. The improvement over Fig. 7 is of course substantial. Nevertheless, it must be born in mind that the YA data are all taken from very careful studies in which the authors have separated the individual components of the rotational diffusion tensor and have themselves corrected for the effects of viscosity and temperature. This agreement is probably due as much to the fact that it is medium sized molecules in small molecule solvents (usually $CHCl_3$) that are being studied rather than to any intrinsic superiority of the YA model. Comparable agreement is observed with the HZ model (Fig. 6) when similar care in recognizing all of the variables is exercised.

TABLE XVIII

Testing of the Hu–Zwanzig model.

Compound	Volume[a]	Shape factor[b]	τ^*_{model}/ps cP^{-1} [c]	τ_{expt}/ps cP^{-1} [d]	RI[e]	Details	Ref.
H_2O	19·0	0·18 Pr	0·14	2·5	*C*	^2H, ^{17}O	55, 101
N_2	23·5	0·74 Pr	0·35	2·8	*C*	^{14}N	38
CH_3OH	36·1	0·86 Pr	0·13	0·9	*C*	^{13}C, in benzene, τ^*_{neat} = 6·6	37, 56
CH_3NH_2	40·2	0·86 Pr	0·15	0·35	*D*	^2H, ^{13}C	37
CH_3Cl	42·0	0·73 Pr	0·68	3·2	*C*	^{35}Cl	27
CH_3Br	46·6	0·71 Pr	0·90	1·75	*C*	Average of ^2H and ^{13}C	51
CH_3CN	47·1	0·66 Pr	1·4	3·4	*B*	^{14}N, ^2H	12, 65
ClO_3^-	47·4	0·72 Ob	0·77	2·5	*D*	^{35}Cl	109
HCCCN	50·3	0·48 Pr	5·0	0·83	*F*	Solvent larger than solute	71
CH_3NO_2	50·6	0·79 Ob	0·43	2·1	*C*	^{14}N	38
CS_2	51·8	0·54 Pr	3·5	2·1	*A*	Slope $<\tau^* = 3·85$	25
CH_3I	54·6	0·69 Pr	1·2	2·2	*B*	^2H	58
CH_3CCH	55·3	0·58 Pr	2·8	4·6	*B*	^2H on and off axis	64, 86
CH_2Cl_2	57·7	0·67 Pr	1·5	2·7	*B*	^{35}Cl	27, 36, 60
C_2H_5CN	64·1	0·56 Pr	3·8	4·1	*E*	^{14}N	38
$HOC_2H_4NH_2$	64·8	0·56 Pr	3·8	1·7	*E*	^{15}N	86
CH_3SCN	65·0	0·62 Pr	2·5	3·8	*C*	^{14}N	38
CH_2Br_2	65·5	0·64 Pr	2·2	3·4	*B*	^2H	61
$NCCH_2CN$	65·8	0·60 Pr	2·9	0·57	*D*	^{14}N	38
CF_2Cl_2	66·1	0·81 Pr	0·47	4·6	*C*	^{35}Cl	27
$SOCl_2$	66·5	0·66 Ob	1·7	2·7	*F*	^{35}Cl; could be prolate	27
Pyrrole, C_4H_5N	66·9	0·51 Ob	4·5	6·8	*C*	^{14}N	38
$C_2H_5NO_2$	67·6	0·75 Pr	0·91	2·5	*E*	^{14}N	38
BCl_3	68·8	0·54 Ob	3·9	1·0	*C*	^{11}B, ^{35}Cl	12, 27
$CHCl_3$	72·3	0·74 Ob	0·99	3·1	*C*	^{35}Cl	27

TABLE XVIII (*cont.*)

Compound	Volume[a]	Shape factor[b]	τ^*_{model}/ps cP^{-1} [c]	τ_{expt}/ps cP^{-1} [d]	RI[e]	Details	Ref.
SO_2Cl_2	72·5	0·78 Pr	0·72	2·0	*D*	^{35}Cl	12
CrO_2Cl_2	(74·0)	0·77 Pr	0·82	3·2	*C*	^{35}Cl	27
$NCC{\equiv}CCN$	74·8	0·40 Pr	12·4	3·5	*F*	Solvent > solute	114
$(CH_3)_3N$	75·3	0·64 Ob	2·2	3·3	*C*	^{14}N	38
Pyridine, C_5H_5N	75·5	0·51 Ob	5·1	2·0	*C*	^{2}H, ^{14}N; neat	38, 67
$HOC_3H_6NH_2$	76·5	0·43 Pr	10·5	1·4	*E*	^{15}N, volume reduced by three hydrogen bonds	86
S_2Cl_2	77·0	0·67 Pr	2·2	2·4	*C*	^{35}Cl	27
PCl_3	77·1	0·69 Ob	1·6	3·7	*C*	^{35}Cl	27
Pyrrolidine, C_4H_9N	79·5	0·7 Ob	1·5	3·7	*E*	^{14}N	38
Benzene, C_6H_6	80·3	0·50 Ob	5·7	3·5	*A*	^{13}C; simple; $\tau^* = 2·1$	29
$PBrCl_2$	81·2	0·69 Ob	1·7	3·1	*D*	^{35}Cl, ^{81}Br	94
$AsCl_3$	82·7	0·74 Ob	1·1	4·3	*C*	^{35}Cl	27
$POCl_3$	82·8	0·86 Ob	0·29	2·6	*C*	^{35}Cl	27
$SiHCl_3$	83·4	0·74 Ob	1·1	3·0	*D*	^{35}Cl	36
CH_2I_2	84·6	0·55 Pr	5·3	3·8	*B*	^{2}H	62, 83
PBr_2Cl	85·3	0·68 Ob	1·9	3·2	*D*	^{35}Cl, ^{81}Br	94
$VOCl_3$	(86)	0·80 Ob	0·65	4·6	*C*	^{35}Cl	12, 27
PBr_3	89·3	0·68 Ob	2·0	3·2	*C*	^{81}Br; neat liquid	27
$Cl_3CC{\equiv}N$	90·9	0·74 Pr	1·3	5·1	*B*	^{14}N, ^{35}Cl	12
CH_3COO^-	(93·3)	0·74 Ob	1·3	4·6	*D*	^{2}H, ^{13}C; aqueous solution	37
$C_6H_5NH_2$	93·6	0·49 Ob	7·1	4·9	*C*	^{14}N; neat liquid	38
$NC(CH_2)_3CN$	94·1	0·46 Pr	11·2	0·94	*E*	^{14}N; uncertain conditions	38
C_6H_5Cl	96·1	0·44 Ob	9·6	5·4	*C*	^{35}Cl	27, 109
Indole, C_8H_7N	109·4	0·42 Ob	12	5·8	*D*	^{13}C; acetone solution	84
$CH_3CH_2COO^-$	(110·7)	0·69 Ob	2·3	1·3	*D*	^{2}H, ^{13}C; aqueous solution	37
$C_6H_{11}NH_2$, cyclohexylamine	117·6	0·65 Ob	3·3	2·1	*C*	^{14}N; neat liquid	38

TABLE XVIII (*cont.*)

Compound	Volume[a]	Shape factor[b]		τ_{expt}/ps cP^{-1} [d]	RI[e]	Details	Ref.
Isoquinoline, C_9H_7N	118·0	0·41 Ob	12	3·2	*C*	^{14}N; uncertain conditions	38
Quinoline	118·0	0·41 Ob	12	2·5	*C*	^{14}N; uncertain conditions	38
$SbCl_5$	125·0	0·87 Pr	0·39	2·4	*C*	^{35}Cl	27
$(C_2H_5)_3N$	126·3	0·57 Ob	5·9	6·2	*C*	^{14}N	38
Triphenylene, $C_{18}H_{12}$	207·8	0·31 Ob	43	24	*C*	^{2}H, ^{13}C	17
Triptycene, $C_{20}H_{14}$	235·3	0·65 Ob	6·5	34	*F*	$\tau^*_{\perp}$; but $\tau^*_{\parallel} = 104$!	32

[a] Volume in cubic ångstroms calculated by method of atomic increments. Values in parentheses represent estimates (for metal compounds) or hydration volumes (ionic compounds).

[b] Given as a ratio ρ, defined in equation (46).

[c] Calculated from V and ρ by equation in Table V.

[d] In picoseconds per centipoise, either by dividing τ_c by η or by using slope as indicated.

[e] Reliability index for the data used in the comparison, as follows: *A*, best data, where τ^*_{expt} comes from a slope of τ_c versus η; *B*, $\tau^*_{\perp}$ has been used, in agreement with the assumptions of the model; *C*, a single τ_c value available; *D*, uncertain viscosity data used; *E*, some ambiguity in shape factor; *F*, omitted from correlations and plots for specific experimental reasons.

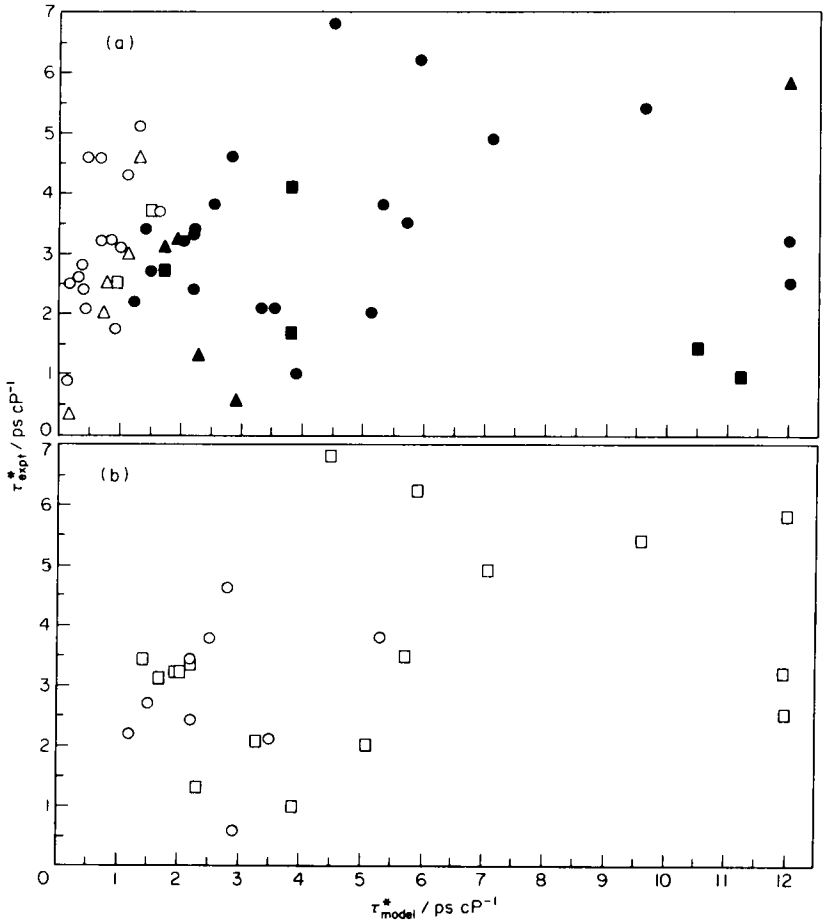

FIG. 7. (a) Correlation of experimental data with the Hu–Zwanzig model. Data from Table XVIII with reliability indices *A*, *B* and *C* represented by circles, that with RI *D* represented by triangles, and that with RI *E* represented by squares. Open symbols represent compounds for which $\rho > 0{\cdot}70$. (b) Correlation with Hu–Zwanzig model differentiated by shape: ○ are prolate examples; □ are oblate examples.

VIII. A SUMMING UP AND FUTURE CONSIDERATIONS

The rotational correlation times that provide the data base for the analysis contained in this review have been generated by groups of research workers over a period of about 20 years. If one adopts the pessimistic stance, it could be argued that except for a few definitive studies of recent origin, no coherent pattern upon which a theoretical model might rest can be

TABLE XIX

Testing of the Youngren–Acrivos model

Compound	Volume/Å^3	ρ_1 [a]	ρ_2 [a]		τ^*_{model} [b]	τ^*_{expt} [b]
Toluene[c]	98·8	0·44	0·79	τ_1^*	1·2	0·0±0·3
				τ_2^*	10·3	12·5±1·5
				τ_3^*	4·8	3·2±0·4
Nitrobenzene[d]	104·0	0·39	0·77	τ_1^*	1·3	0·7±0·3
				τ_2^*	14·5	17±3
				τ_3^*	7·5	2·75±0·3
trans-Decalin[e]	155·0	0·57	0·80	τ_1^*	1·5	0·3±0·2
				τ_2^*	7·7	7·1±0·7
				τ_3^*	2·5	1·2±0·4
Fluorene[f]	155·3	0·30	0·64	τ_1^*	7·6	13±2
				τ_2^*	38	49±9
				τ_3^*	12·3	17±2

[a] $\rho_1 = a/c$, $\rho_2 = b/c$; where $a \leq b \leq c$.
[b] Reported in picoseconds per centipoise; consult reference for residual τ_0.
[c] Reference 29. ^{13}C and light-scattering data measured as slopes.
[d] References 29, 50. ^{2}H, ^{13}C and ^{14}N data measured as slopes.
[e] Reference 115. ^{13}C data measured as slopes.
[f] Reference 32. ^{13}C data for 1 M $CDCl_3$ solution.

discerned. One could rationalize this stance by pointing out that most of the τ_c determinations make no attempt to accommodate anisotropy in the rotation by separating out the rotations about specific molecular axes. Largely ignored are those interactions between molecules not reflected in the bulk viscosity but which in some instances must have a significant effect upon τ_c.

After reviewing all of the pertinent literature in this area we are drawn to a rather more optimistic position. For molecules that can be approximated by spheres, the Gierer–Wirtz model provides a good description of the motion for solutions in solvents of smaller molecular size; for neat liquids the description is not as good because non-viscous intermolecular forces affecting τ_c are more likely to be present.

For molecules with cylindrical (spheroidal) symmetry, values for $\tau_\perp$ calculated using the Hu–Zwanzig model are invariably more reliable than are calculated values of $\tau_\parallel$. Realistic uncertainty limits would be ±25% for $\tau_\perp$ and ±75% for $\tau_\parallel$. The HZ model is a diffusion model and since rotation *of* the figure axis displaces solvent while rotation *about* the figure axis does

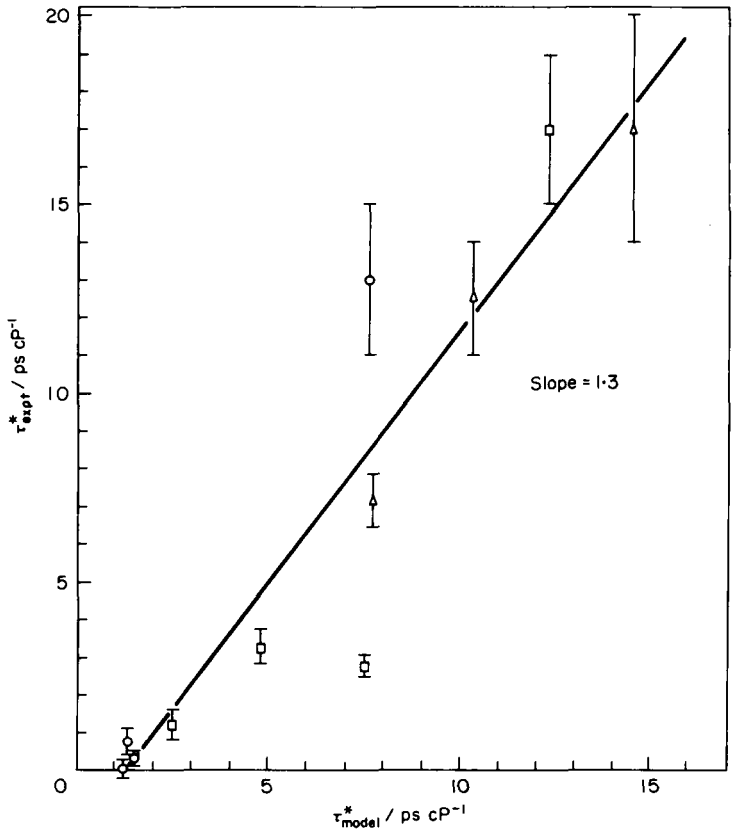

FIG. 8. Correlation of experimental data with the Youngren–Acrivos model. Data from Table XIX with circles indicating τ^*_a, triangles representing $\tau_b{}^*$, and squares indicating τ^*_c.

not, the $\tau_\perp$ motion is likely to be in the diffusion region while the $\tau_\parallel$ motion can be close to the inertial limit. This same consideration applied to ellipsoidal molecules makes τ_b more reliable than either τ_a or τ_c.

For ellipsoidal molecules with their less than cylindrical symmetry, reliable values for τ_c can only be expected when one allows for the full anisotropy of the motion, and this requires use of the Youngren–Acrivos model. The HZ model will invariably prove unreliable in these cases because it was not designed to accommodate a second degree of shape variation. Molecules in this category need a second shape parameter to satisfy the input requirements of the YA model. Although it is more versatile than the HZ model, the YA model still requires that the molecule have a set of three axes relative to which the rotational diffusion tensor can be diagonalized, making the off-diagonal elements zero. In practice this

requirement is probably not quite as rigid as has been stated and rotational motion for which the off-diagonal elements, while not zero, are small relative to the diagonal elements of the tensor can be adequately represented by the YA model.

In the final analysis, the judgment one makes on the theoretical state of a subject depends on what one expects to learn by using the theories. Today, with relaxation times for nuclei in many different chemical environments increasingly available, the only barrier to nuclear quadrupole coupling constants and spin–rotation constants for these environments derived from the relaxation time is the absence of an appropriate correlation time. In recognizing that these desirable coupling constants may be completely unknown in the absence of this correlation time, one appreciates the motivation behind the search for its theoretical representation. With the coupling constants occurring as squared terms in the relaxation equations, uncertainty limits of ±75% in the correlation time propagate ±32% uncertainty limits for the coupling constant, while the more precise ±25% limits for τ yield a very acceptable ±12% for the coupling constant. Viewed in this light the current state of theoretical development, while leaving some room for improvement, not only opens the door but goes a considerable distance down the path of relaxation-determined coupling constants.

What does the future hold for theoretical developments in this area? The microviscosity factor contained in the Gierer–Wirtz model for spherical molecules is an adjustable parameter which allows the theoretician to achieve any degree of surface adhesion between the stick and the slip limits. Both the Hu–Zwanzig and the Youngren–Acrivos models, as presently formulated, lack this element of adjustability, and it is conceivable that some improvement may be achieved in this direction. We are inclined to agree with Harris and Newman,[32] however, in the belief that major improvements lie in the direction of numerical solutions to the friction coefficient equation that are not limited to the two shape parameters of the YA model and that span shapes having lower symmetry than an ellipsoid. These must await computer programs capable of dealing with more generalized shapes and a higher level of agreement than presently exists on the quantitative specification of molecular shape.

REFERENCES

1. J. D. Bernal, *Nature*, 1960, **185**, 68.
2. P. J. W. Debye, *J. Appl. Phys.*, 1944, **15**, 338.
3. *Dictionary of Scientific Biography* (ed. C. C. Gillispie), Charles Scribner's Sons, New York, 1976, Vol. XIII, p. 1.
4. H. G. Hertz, in *Progress in NMR Spectroscopy*, Vol. 3 (ed. J. W. Emsley, J. Feeney and L. H. Sutcliffe), Pergamon Press, Oxford, 1967, p. 159.
5. N. Bloembergen, E. M. Purcell and R. V. Pound, *Nature*, 1947, **160**, 475.

6. A. Einstein, *Phys. Zeit.*, 1917, **18**, 121.
7. M. R. Baker, C. H. Anderson and N. F. Ramsey, *Phys. Rev.*, 1964, **133A**, 1533.
8. T. C. Farrar and E. D. Becker, *Pulse and Fourier Transform NMR*, Academic Press, New York, 1971, Chap. 5.
9. J. Jonas, in *Advances in Magnetic Resonance*, Vol. 6 (ed. J. S. Waugh), Academic Press, New York, 1973, p. 73.
10. E. A. C. Lucken, *Nuclear Quadrupole Coupling Constants*, Academic Press, New York, 1969.
11. D. Wallach and W. T. Huntress, *J. Chem. Phys.*, 1969, **50**, 1219.
12. K. T. Gillen and J. H. Noggle, *J. Chem. Phys.*, 1970, **53**, 801.
13. A. A. Maryott, T. C. Farrar and M. S. Malmberg, *J. Chem. Phys.*, 1971, **54**, 64.
14. R. E. Wasylishen and B. A. Pettitt, *Canad. J. Chem.*, 1977, **55**, 2564.
15. C. M. Hu and R. Zwanzig, *J. Chem. Phys.*, 1974, **60**, 4354.
16. G. Stokes, *Trans. Cambridge Philos. Soc.*, 1856, **9**, 5.
17. R. E. Wasylishen, B. A. Pettitt and W. Danchura, *Canad. J. Chem.*, 1977, **55**, 3602.
18. G. K. Youngren and A. Acrivos, *J. Chem. Phys.*, 1975, **63**, 3846.
19. A. Einstein, *Investigations on the Theory of the Brownian Movement*, Dover, New York, 1956, pp. 19–34.
20. P. Debye, *Polar Molecules*, Dover, New York, 1929.
21. P. S. Hubbard, *Phys. Rev.*, 1963, **131**, 1155.
22. R. M. Hawk and R. R. Sharp, *J. Chem. Phys.*, 1974, **60**, 1009.
23. R. R. Sharp, *J. Chem. Phys.*, 1972, **57**, 5321.
24. N. Bloembergen, *Nuclear Magnetic Relaxation*, W. A. Benjamin, New York, 1961.
25. R. R. Vold, S. W. Sparks and R. L. Vold, *J. Magn. Reson.*, 1978, **30**, 497.
26. W. T. Huntress, in *Advances in Magnetic Resonance*, Vol. 4 (ed. J. S. Waugh), Academic Press, New York, 1970, p. 1.
27. B. Lindman and S. Forsén, in *NMR Basic Principles and Progress*, Vol. 12 (ed. P. Diehl, E. Fluck and R. Kosfeld), Springer-Verlag, Berlin, 1976, Chap. 2.
28. A. Gierer and K. Wirtz, *Zeit. Naturforsch.*, 1953, **A8**, 532.
29. D. R. Bauer, J. I. Brauman and R. Pecora, *J. Amer. Chem. Soc.*, 1974, **96**, 6840.
30. G. R. Alms, T. D. Gierke and G. D. Patterson, *J. Chem. Phys.*, 1977, **67**, 5779.
31. G. R. Alms and G. D. Patterson, *J. Chem. Phys.*, 1979, **71**, 563;
S. L. Whittenburg and C. H. Wang, *J. Chem. Phys.*, 1979, **71**, 561.
32. R. K. Harris and R. H. Newman, *Mol. Phys.*, 1979, **38**, 1315.
33. D. Kivelson and P. A. Maddon, *Ann. Rev. Phys. Chem.*, 1980, **31**, 533.
34. F. W. Wehrli, *J. Magn. Reson.*, 1978, **30**, 193.
35. L. C. Erich, A. C. Gossard and R. L. Hartless, *J. Chem. Phys.*, 1973, **59**, 3911.
36. H. Saito, H. H. Mantsch and I. C. P. Smith, *J. Amer. Chem. Soc.*, 1973, **95**, 8453.
37. J. P. Jacobsen and K. Schaumburg, *J. Magn. Reson.*, 1977, **28**, 191.
38. J. M. Lehn and J. P. Kintzinger, in *Nitrogen NMR* (ed. M. Witanowski and G. A. Webb), Plenum Press, London, 1973, p. 86.
39. A. Abragam, *The Principles of Nuclear Magnetism*, Oxford University Press, London, 1961, Chap. 8.
40. C. Deverell, *Mol. Phys.*, 1970, **18**, 319.
41. A. A. Maryott, M. S. Malmberg and K. T. Gillen, *Chem. Phys. Letters*, 1974, **25**, 169.
42. C. R. Lassigne and E. J. Wells, *Canad. J. Chem.*, 1977, **55**, 1303.
43. N. F. Ramsey, *Phys. Rev.*, 1950, **78**, 699.
44. W. H. Flygare, *J. Chem. Phys.*, 1964, **41**, 793.
45. C. Deverall, *Mol. Phys.*, 1970, **18**, 323.
46. K. T. Gillen, *J. Chem. Phys.*, 1972, **56**, 1573.
47. W. C. Dickenson, *Phys. Rev.*, 1950, **80**, 563.

48. N. F. Ramsey, *Molecular Beams*, Oxford Press, London, 1956.
49. G. Malli and C. Froese, *Int. J. Quant. Chem.*, 1967, Symposium 1, 95.
50. R. E. Stark, R. L. Vold and R. R. Vold, *Chem. Phys.*, 1977, **20**, 337.
51. C. R. Lassigne and E. J. Wells, *J. Magn. Reson.*, 1977, **27**, 215.
52. H. H. Mantsch, H. Saito and I. C. P. Smith, in *Progress in NMR Spectroscopy*, Vol. 11 (ed. J. W. Emsley; J. Feeney and L. H. Sutcliffe), Pergamon Press, Oxford, 1978, p. 211.
53. J. A. Glasel, *J. Amer. Chem. Soc.*, 1969, **91**, 4569.
54. H. G. Hertz, in *Progress in NMR Spectroscopy*, Vol. 3 (ed. J. W. Emsley, J. Feeney and L. H. Sutcliffe), Pergamon Press, Oxford, 1967, p. 192.
55. J. Jonas, T. De Fries and D. J. Wilbur, *J. Chem. Phys.*, 1976, **65**, 582; 1976, **65**, 1783.
56. B. M. Fung and T. W. McGaughy, *J. Chem. Phys.*, 1976, **65**, 2970.
57. J. W. Harrell, *J. Magn. Reson.*, 1976, **23**, 335.
58. K. T. Gillen, M. Schwartz and J. H. Noggle, *Mol. Phys.*, 1971, **20**, 899.
59. T. E. Bull and J. Jonas, *J. Chem. Phys.*, 1970, **53**, 3315.
60. H. S. Sandhu, *J. Magn. Reson.*, 1978, **29**, 563.
61. H. S. Sandhu, *J. Magn. Reson.*, 1977, **26**, 7.
62. H. S. Sandhu and H. Peemoeller, *J. Magn. Reson.*, 1976, **21**, 349.
63. W. T. Huntress, *J. Chem. Phys.*, 1968, **48**, 3524.
64. J. Jonas and T. M. DiGennaro, *J. Chem. Phys.*, 1969, **50**, 2392.
65. D. E. O'Reilly, E. M. Peterson, C. E. Scheie and E. Seyfarth, *J. Chem. Phys.*, 1973, **59**, 3576.
66. C. R. Lassigne and E. J. Wells, *J. Magn. Reson.*, 1977, **26**, 55.
67. J. P. Kintzinger and J. M. Lehn, *Mol. Phys.*, 1971, **22**, 273.
68. J. P. Kintzinger, *Mol. Phys.*, 1975, **30**, 673.
69. T. E. Bull, *J. Chem. Phys.*, 1973, **59**, 6173.
70. A. Bondi, *J. Phys. Chem.*, 1964, **68**, 441.
71. N. M. Szeverenyi, R. R. Vold and R. L. Vold, *Chem. Phys.*, 1976, **18**, 31; 1976, **18**, 23.
72. H. Versmold, *Ber. Bunsenges. Phys. Chem.*, 1974, **78**, 1318.
73. T. J. Rowland, *J. Chem. Phys.*, 1975, **63**, 608.
74. D. E. O'Reilly and E. M. Peterson, *J. Chem. Phys.*, 1973, **59**, 1551.
75. A. Briguet, J. Charriére, G. Tétu, J. C. Duplan and J. Delmau, *J. Phys. Lettres*, 1977, **38**, L73.
76. S. Berger, F. R. Kreissl and J. D. Roberts, *J. Amer. Chem. Soc.*, 1974, **96**, 4348.
77. D. D. Giannini, I. M. Armitage, H. Pearson, D. M. Grant and J. D. Roberts, *J. Amer. Chem. Soc.*, 1975, **97**, 3416.
78. J. B. Lambert and D. A. Netzel, *J. Magn. Reson.*, 1977, **25**, 531.
79. W. T. Huntress, *J. Phys. Chem.*, 1969, **73**, 103.
80. S. G. Huang and M. T. Rogers, *J. Chem. Phys.*, 1978, **68**, 5601.
81. J. P. Kintzinger and J. M. Lehn, *J. Amer. Chem. Soc.*, 1974, **96**, 3313.
82. R. R. Sharp and J. W. Tolan, *J. Chem. Phys.*, 1976, **65**, 522.
83. C. L. Mayne, D. M. Grant and D. W. Alderman, *J. Chem. Phys.*, 1976, **65**, 1684.
84. G. C. Levy and U. Edlund, *J. Amer. Chem. Soc.*, 1975, **97**, 5031.
85. G. C. Levy, J. J. Dechter and J. Kowalewski, *J. Amer. Chem. Soc.*, 1978, **100**, 2308.
86. G. C. Levy, C. E. Holloway, R. C. Rosanske and J. M. Hewitt, *Org. Magn. Reson.*, 1976, **8**, 643.
87. G. C. Levy, A. D. Godwin, J. M. Hewitt and C. Sutcliffe, *J. Magn. Reson.*, 1978, **29**, 553.
88. L. M. Ishol, T. A. Scott and M. Goldblatt, *J. Magn. Reson.*, 1976, **23**, 313.
89. K. T. Gillen, D. G. Douglass, M. S. Malmberg and A. A. Maryott, *J. Chem. Phys.*, 1972, **57**, 5170.
90. G. C. Levy, J. D. Cargioli, P. C. Juliano and T. D. Mitchell, *J. Amer. Chem. Soc.*, 1973, **95**, 3445.

91. R. K. Harris and B. Lemarié, *J. Magn. Reson.*, 1976, **23**, 371.
92. R. K. Harris and B. J. Kimber, *J. Magn. Reson.*, 1975, **17**, 174.
93. R. K. Harris and B. J. Kimber, *Advan. Mol. Relaxation Processes*, 1975, **8**, 23.
94. T. K. Leipert, W. J. Freeman and J. H. Noggle, *J. Chem. Phys.*, 1975, **63**, 4177.
95. N. J. Koole, A. J. DeKoning and M. J. A. DeBis, *J. Magn. Reson.*, 1977, **25**, 375.
96. S. J. Seymour and J. Jonas, *J. Magn. Reson.*, 1972, **8**, 376.
97. S. J. Seymour and J. Jonas, *J. Chem. Phys.*, 1971, **54**, 487.
98. R. K. Harris and E. M. McVicker, *J. Chem. Soc. Faraday II*, 1976, **72**, 2291.
99. C. R. Lassigne and E. J. Wells, *Canad. J. Chem.*, 1977, **55**, 927.
100. J. Virlet and G. Tantot, *Chem. Phys. Letters*, 1976, **44**, 296.
101. B. B. Garrett, A. B. Denison and S. W. Rabideau, *J. Phys. Chem.*, 1967, **71**, 2606.
102. T. Bjorholm and J. P. Jacobson, *J. Magn. Reson.*, 1980, **39**, 237.
103. H. S. Sandhu, *J. Magn. Reson.*, 1979, **34**, 141.
104. H. W. Spiess, D. Schweitzer, U. Haeberlen and K. H. Hausser, *J. Magn. Reson.*, 1971, **5**, 101.
105. J. T. Edward, *Chem. Ind.*, 1956, 774.
106. J. T. Edward, *J. Chem. Educ.*, 1970, **47**, 261.
107. B. A. Pettitt, R. E. Wasylishen, R. Y. Dong and T. P. Pitner, *Canad. J. Chem.*, 1978, **56**, 2576.
108. R. E. Wasylishen and B. A. Pettitt, *Canad. J. Chem.*, 1979, **57**, 1274.
109. D. E. O'Reilly and G. E. Schacher, *J. Chem. Phys.*, 1963, **39**, 1768.
110. D. G. Gillies, L. P. Blaauw, G. R. Hays, R. Huis and A. D. H. Clague, *J. Magn. Reson.*, 1981, **42**, 420.
111. J. R. Lyerla, D. M. Grant and C. H. Wang, *J. Chem. Phys.*, 1971, **55**, 4676.
112. P. W. Atkins, A. Loewenstein and Y. Margolit, *Mol. Phys.*, 1969, **17**, 329.
113. H. W. Spiess, D. Schweitzer, U. Haeberlen and K. H. Hausser, *J. Magn. Reson.*, 1971, **5**, 101.
114. R. R. Vold, R. L. Vold and N. M. Szeverenyi, *J. Chem. Phys.*, 1979, **70**, 5213.
115. M. E. Moseley, *Chem. Scripta*, 1981, **16**, 28.
116. D. M. Grant, R. J. Pugmire, E. P. Black and K. A. Christensen, *J. Amer. Chem. Soc.*, 1973, **95**, 8465.
117. S. Berger, F. R. Kreissl, D. M. Grant and J. D. Roberts, *J. Amer. Chem. Soc.*, 1975, **97**, 1805.
118. A. Delville, C. Detellier, A. Gerstmans and P. Laszlo, *J. Magn. Reson.*, 1981, **42**, 14.
119. D. E. O'Reilly, G. E. Schacher and K. Schug, *J. Chem. Phys.*, 1963, **39**, 1756.
120. H. A. Christ, P. Diehl, H. R. Schneider and H. Dahn, *Helv. Chim. Acta*, 1961, **44**, 865.
121. H. A. Christ and P. Diehl, in *Proceedings of the 11th Colloque AMPERE, Eindhoven, 1962*, p. 224.
122. W. R. Hackleman and P. S. Hubbard, *J. Chem. Phys.*, 1963, **39**, 2688.
123. J. K. Tison and E. R. Hunt, *J. Chem. Phys.*, 1971, **54**, 1526.
124. D. W. Sawyer and J. G. Powles, *Mol. Phys.*, 1971, **21**, 83.
125. R. R. Sharp, *J. Chem. Phys.*, 1974, **60**, 1149.
126. H. W. Spiess, D. Schweitzer, U. Haeberlen and K. H. Hauser, *J. Magn. Reson.*, 1971, **5**, 101.
127. K. T. Gillen, J. H. Noggle and T. K. Leipert, *Chem. Phys. Letters*, 1972, **17**, 505.
128. L. Pauling, *The Nature of the Chemical Bond*, 3rd edn, Cornell University Press, Ithaca, N.Y., 1960, Chap. 7.

This Page Intentionally Left Blank

SUBJECT INDEX

A

D

H

I

J

K

L

M

Q

T

U

V

This Page Intentionally Left Blank